SHEAR STRENGTH AND DEFORMABILITY OF ROCK JOINTS

by
CHEE-KUEN YIP

B.S., Columbia University
(1977)

Submitted in partial fulfillment
of the requirements for the
degree of

Master of Science

at the

Massachusetts Institute of Technology

March, 1979

Signature of Author. .....
Department of Civil Engineering, March 30, 1979

Certified by.....
Thesis Supervisor

Accepted by.....
Chairman, Department Committee

SHEAR STRENGTH AND DEFORMABILITY OF ROCK JOINTS

by
CHEE-KUEN YIP

Submitted to the Department of Civil Engineering
on March 30, 1979 in partial fulfillment of the requirements
for the Degree of Master of Science

ABSTRACT

This thesis is concerned with the shear strength and deformability of rock joints. An extensive set of data was supplied by Dames & Moore, Goldberg, Zoino & Dunicliff Bureau of Reclamation and Waterways Experiment Station as well as a collection of data was extracted from published literature. A model was developed to describe the stress-displacement behavior of rock joints in terms of descriptive parameters. Data management and statistical analysis of these paramters using a computer system were employed to determine relations between shear strength and deformability of rock joints. On the other hand, the relations were also determined from data published in literature.

Peak and residual friction angles of the available rock types were investigated. The peak friction angles for all rock types lie in a range of extremely low and high values. The low values are due to high cohesion, while the high values represent a limiting condition at extremely low normal stress. Friction angles of the sedimentary rocks, metamorphic rocks and igneous rocks, and each individual rock type, were investigated. Metamorphic rocks have the lowest and highest values of friction angles. Sedimentary rocks have the lowest residual angles, while igneous rocks have the highest. Among all rock types, gneiss, marble, phyllite, basalt and monzonite (quartz) often have peak angles lower than the residual angles.

The effect of water can either reduce or increase the shear strength. Reduction of shear strength is due to surface cleanliness. Increase of shear strength may be due to the adverse effect of water on the tensile and compressive strength of brittle material. Joint type affects the strength that rough surfaces give higher friction angles than the smooth surfaces. Increase in normal stress may increase or decrease in friction angle.

The data for deformability of rock joints in this thesis is limited. The limit amount of shear stiffness and normal stiffness indicates that for a certain rock type, the variation in the values are due to the joint type, test methods and filler material.

Thesis Supervisor — Herbert H. Einstein

Title — Associate Professor of Civil Engineering

ACKNOWLEDGEMENTS

Professor Herbert H. Einstein receives my sincere appreciation for the guidance which he has provided in the completion of this thesis. His generous contribution of time and personal interest are a credit to himself. I have received financial support for this research from his grant. This support is gratefully acknowledged.

Credit and thanks are also due to William Roberds, who developed the flow-chart described in Appendix A, and to Mark Chan, who performed the data reduction.

Finally, acknowledgement is given to Dames & Moore, Goldberg, Zoino & Dunicliff, the Bureau of Reclamation, and Waterways Experiment Station, who supplied data for this thesis, and Fred Zelt, who collected the data.

TABLE OF CONTENTS

LIST OF FIGURES

LIST OF TABLES

LIST OF NOTATION

A	area of joint surface
a_s	proportion of the joint area sheared through the asperities
C_p	peak cohesion
C_r	residual cohesion
d_n	dilation angle
H	height of asperities
h	dilatancy
h_0	maximum dilatancy at zero normal load
i, i_s	inclination of asperities in the direction of shearing
i_p	inclination of asperities in the direction perpendicular to that of shearing
k	reduction coefficient of dilatancy
u	constant defining τ-δ_s hyperbolic function having the dimension of force per length squared
t	constant defining τ-δ_s hyperbolic function having the dimension of force per length
τ_p	peak shear stress
τ_r	residual shear stress
τ_i	shear strength of intact material
τ_y	shear stress at yield point
$(\sigma_n)_p$	peak normal stress
σ_c	unconfined compressive strength

σ_t	uniaxial tensile strength
$(\sigma_n)_L$	low limit of normal stress
$(\sigma_n)_H$	upper limit of normal stress
σ_T	transition pressure
σ_1	axial stress at failure
σ_3	effective confining pressure
$(\delta_s)_p$	relative peak shear displacement
$(\delta_s)_r$	relative residual shear displacement
$(\delta_s)_e$	shear displacement in the elastic range
δ_{s0}	reference shear displacement (initial state)
δ_n	relative normal displacement
δ_{n0}	reference normal displacement (initial state)
δ_{rs}	base width of asperities in the direction perpendicular to that of shearing
δ_{mc}	maximum joint closure
$\delta_{s,y}$	shear displacement at yield point
δ'_s	shear degradation distance
δ'_n	normal dilation distance
$\dot{\delta}_s$	shear displacement rate
$(\delta_n/\delta_s)_p$, $\dot{v}$	peak dilation rate
$(k_s)_e$	elastic shear stiffness
$k_{s,y}$	shear stiffness at yield point
$(k_s)_{50\%}$	shear stiffness at 50% peak point of τ-δ_s curve
k_n	secant normal stiffness
ϕ	inclination of Mohr envelope at point of tangency
ϕ_p	peak friction angle

ϕ_r, ϕ_ν	residual friction angle
β	angle fault makes with principal stress σ_1
β_1	orientation of anisotropic fractures
β_2	orientation of joint surface
ξ	seating pressure defining the initial condition for measuring the normal deformation
$(k_s)_p$	peak shear stiffness

CHAPTER 1

INTRODUCTION

The understanding of the rock mass behavior is very important in many rock engineering problems. An in-situ rock mass derives its strength and deformation characteristics from both the physical properties of the competent intact material and the properties of discontinuities: such as joints, faults, foliation surfaces or bedding planes. In general, the discontinuities have properties of strength and deformability which are quite different from those of the intact rock, and in many cases, the discontinuities completely dominate the performance of the in-situ rock mass.

Results from laboratory or in-situ tests on rock joint are essential in the analysis of rock mass. Numerous tests have been run; they are not conviently assembled to the potential uses. The purpose of this thesis is to develop a model which describes the stress-displacement behavior of rock joints in a unified manner and to store the values of the descriptive parameters in a large segmented data base. A computer system is used to retrieve subsets of the data base conditional on various characteristics, e.g. rock types, and to then derive the conditional statistics of the descriptive parameters in these subsets, e.g. the statistics of ϕ_ν for all tests on granite.

The structure of the thesis reflects the approach described above. In Chapter 2, analytical models of shear strength of discontinuities, and important factors which influence the shear strength are discussed. In addition, a description of deformability of discontinuities in terms of

normal stiffness and shear stiffness, and factors that influence these stiffnesses are discussed. Descriptions of the model for the stress-displacement behavior of rock joints and of the data storage and management structure constitute Chapter 3. Chapter 4 discusses results of data management, i.e. the statistics of the descriptive parameters conditional on various rock-mass characteristics.

CHAPTER 2

SHEAR STRENGTH AND DEFORMABILITY OF ROCK JOINTS

Many research efforts on the variables which control the shearing resistance along discontinuities have been made. This chapter reviews some available models which attempt to describe the factors that influence the shear strength. In addition, deformability of rock joints in terms of the stiffness properties, the shear stiffness and normal stiffness, is described.

2.1 Description of Shear Strength of Discontinuities

Model Description

Several models are available which attempt to describe the shear strength of rock discontinuities. These models are discussed here.

Bilinear (Patton) Model

Patton (1966) identified two different mechanisms of peak shear resistance. By performing direct shear tests on models of discontinuities with regularly shaped asperities, he found that these mechanisms of peak shear resistance were dependent on the level of normal stress acting on the discontinuity. At low normal stresses, peak resistance was mobilized, while the upper block was riding up and over surface asperities of the lower block. The shear resistance can be defined as

$$s = n \tan(\phi_v + i) \qquad (2\text{-}1)$$

where s = shear force parallel to the general shear surface required to sustain sliding

n = force normal to the place of sliding

ϕ_v = angle of frictional sliding resistance on flat, smooth surface

i = the angle of inclination of the asperities upon which sliding takes place, measured with respect to the average plane of the discontinuity.

At high normal stresses, the mode of failure changes and the asperities are sheared off. The shear resistance is represented as

$$s = c + n \tan \phi_r \qquad (2\text{-}2)$$

where c = cohesion mobilized in shearing off the asperities

ϕ_r = the residual angle of friction active on flat surfaces after large displacements, and approximately equal to ϕ_v

The relationship between the two modes of failure and residual sliding friction is shown in Fig. 2-1.

Equation 2-1 represents the lower portion of the strength envelope, while Eq. 2-2 represents the upper portion. These two modes of failure, therefore, form the bilinear envelope. The vertical distance between the bilinear envelope and the residual envelope represents the geometrical component of the shear strength which includes both the geometry of the surface and the internal strength of the rock asperities. In real rock discontinuities, asperities have many different sizes and shapes, with the result that the two mechanisms of shear resistance occur simultaneously

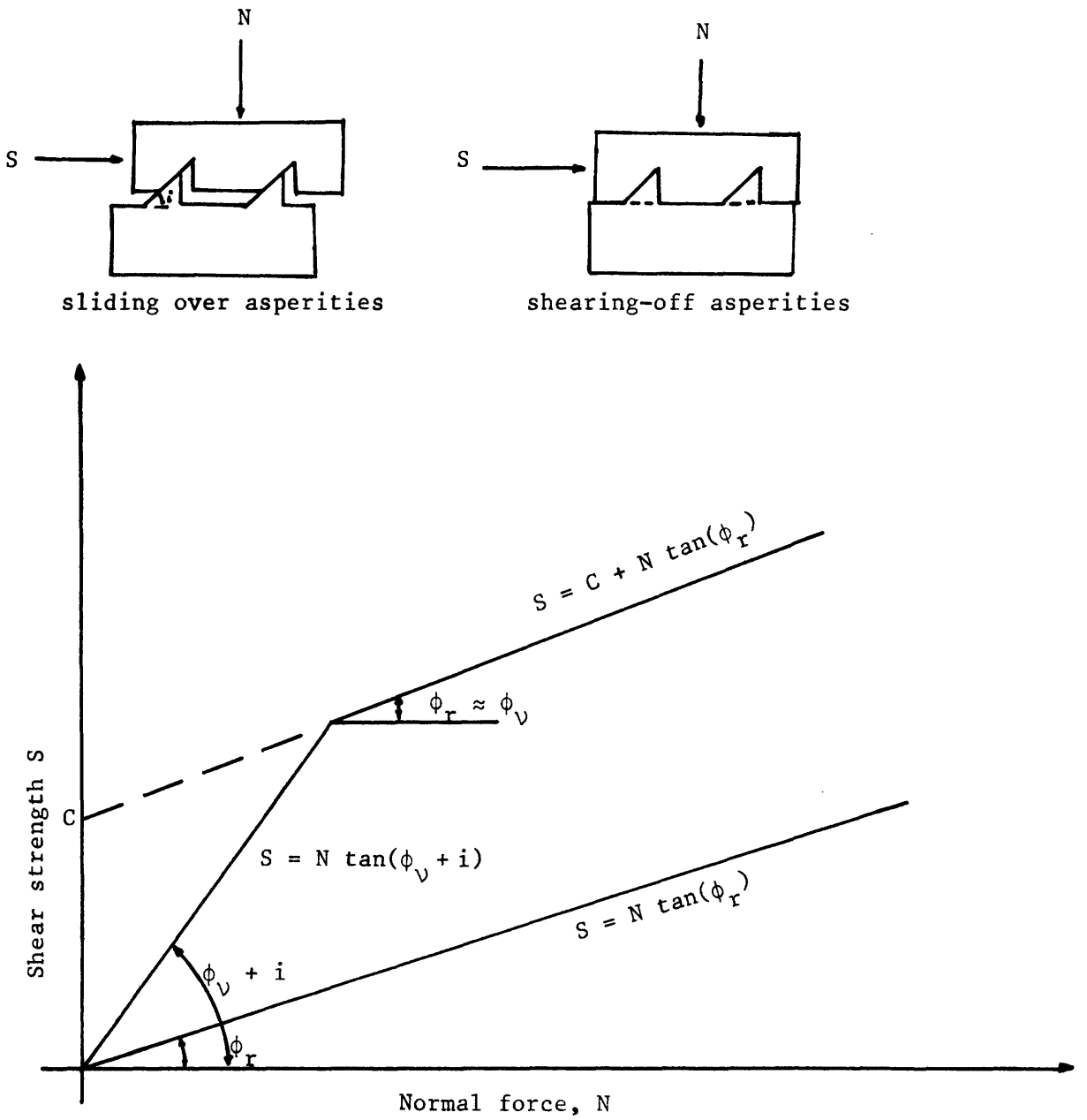

Figure 2-1 Idealized bilinear envelope by Patton (1966)

on different asperities. This causes the failure envelope to be curved rather than bilinear for actual discontinuities.

Ladanyi and Archambault Model

Ladanyi and Archambault (1970) developed a criterion to describe the shear strength of rock discontinuities using an energy approach. They combined friction, dilatancy, and interlock strength contributions in a conceptually derived peak strength equation which has proved accurate in their model studies. The peak strength is given by:

$$\tau_p = \frac{\sigma(1-a_s)\ (\dot{v} + \tan \phi_\nu) + a_s \tau_i}{1 - (1-a_s)\ \dot{v} \tan \phi_\nu} \qquad (2\text{-}3)$$

where a_s, $\dot{v}$ and τ_i are the following functions of σ

a_s is the proportion of the joint area sheared through the asperities

$\dot{v}$ is the secant dilation rate at peak shear stress

τ_i is the shear strength of the intact material; Fairhurst's parabolic criterion (Fairhurst, 1964) was used and was given as

$$\tau_i = \sigma_c \left(\frac{(n+1)^{1/2} - 1}{n} \right) \left(1 + \frac{n\sigma}{\sigma_c} \right)^{1/2} \qquad (2\text{-}4)$$

$$\text{where } n = \frac{\sigma_c}{-\sigma_t}$$

Power laws were suggested for the first two parameters.

$$a_s = 1 - \left(1 - \frac{\sigma}{\sigma_T}\right)^{k_1} \qquad (2\text{-}5)$$

$$\dot{v} = (1 - \frac{\sigma}{\sigma_T})^{k_2} \tan i \qquad (2\text{-}6)$$

For sliding of continuous rough surfaces, the suggested values of the exponents are $k_1 = 1.5$ and $k_2 = 4$; a_s increases from 0 at $\sigma = 0$ to 1 at $\sigma = \sigma_T$ while $\dot{v}$ decreases from tan i when $\sigma = 0$ to 0 at $\sigma = \sigma_T$. The "transition pressure" σ_T is the normal stress above which the joints cease to be weak elements in the rock mass. It can be approximated by $\sigma_T = \sigma_c$, the unconfined compressive strength of the wall rack (which may be substantially lower than the unconfined strength for intact rock due to weathering along the joints). With these conditions Eq. 2-3 will define a curved peak strength criterion as shown in Fig. 2-2.

The most serious limitation to the practical use of Eq. 2-3 is the determination of $\dot{v}$ and a_s. It is not known whether the relationships given by Eqs. 2-5 and 2-6 are generally applicable to rock discontinuities. The measurement of $\dot{v}$ in shear tests is an increasingly common procedure, so that $\dot{v}$ data is available to compare with Eq. 2-6. However, the direct measurement of a_s is seldom done, so there is very little information on a_s.

Barton's Model

Barton developed a model to describe the shear strength of rock discontinuities under low stresses and high stresses.

Low Stress Levels

Barton (1971a) employed an empirical approach in the development of an equation to describe the shear strength of rock discontinuities. Fig. 2-3 shows the results of direct shear tests performed on a variety

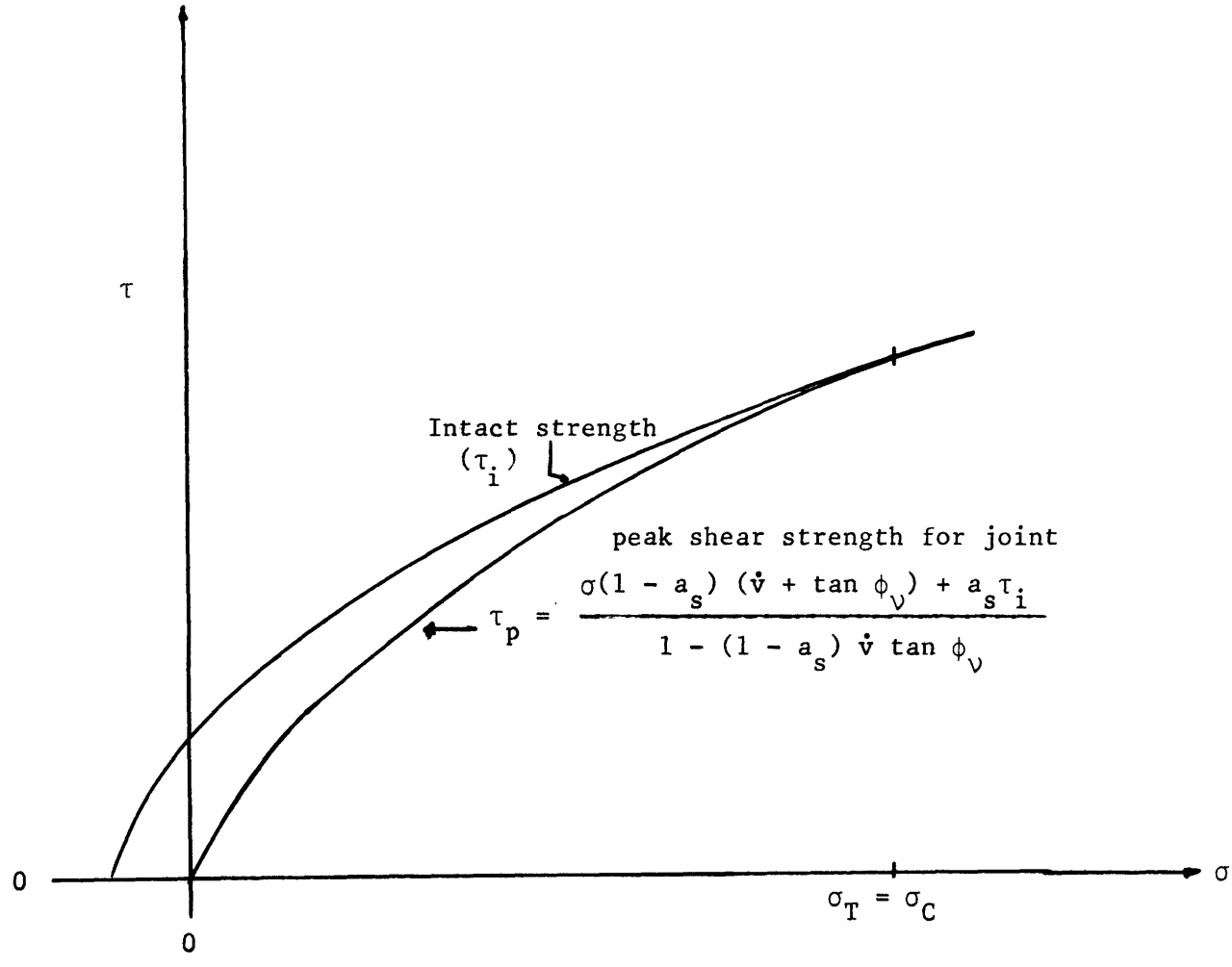

Figure 2-2 Ladanyi and Archambault's shear strength relation for rough joints

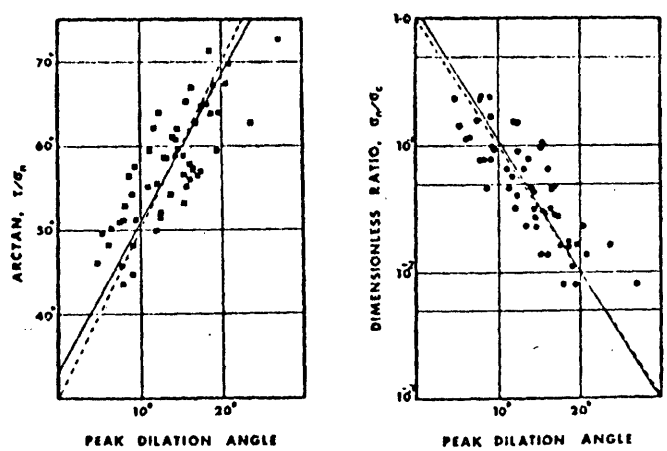

Figure 2-3 Peak shear strength of direct shear tests on tension fractures (from Barton, 1973

of artificial tension fractures generated through realistic brittle model materials. Analyzing the data from these tests, Barton observed that the following relationships could be approximated:

$$\tau/\sigma_n = \tan (2d_n + 30^o) \tag{2-7}$$

$$d_n = 10 \log_{10} (\sigma_c/\sigma_n) \tag{2-8}$$

where τ = peak shear strength

σ_n = effective normal stress

d_n = dilation angle at peak resistance

σ_c = the uniaxial compression strength of the material

The approximate peak shear strength envelope for the model tension fractures is obtained by eliminating d_n between Eqs. 2-7 and 2-8.

$$\tau/\sigma_n = \tan \left(20 \log_{10} \left(\frac{\sigma_c}{\sigma_n} \right) + 30^o \right) \tag{2-9}$$

For low and medium stress levels this equation gives a close approximation to the peak shear strength of interlocking rough-surfaced joints, tension fractures and artificial faults, as shown in Fig. 2-4.

Barton (1973) modified Eq. 2-9 to incorporate different degrees of surface roughness and different angle of frictional sliding resistance ϕ_v, and proposed a generalized form of Eq. 2-9 as

$$\tau/\sigma_n = \tan \left(JRC \log_{10} \left(\frac{JCS}{\sigma_n} \right) + \phi_v \right) \tag{2-10}$$

where JRC = Joint roughness coefficient

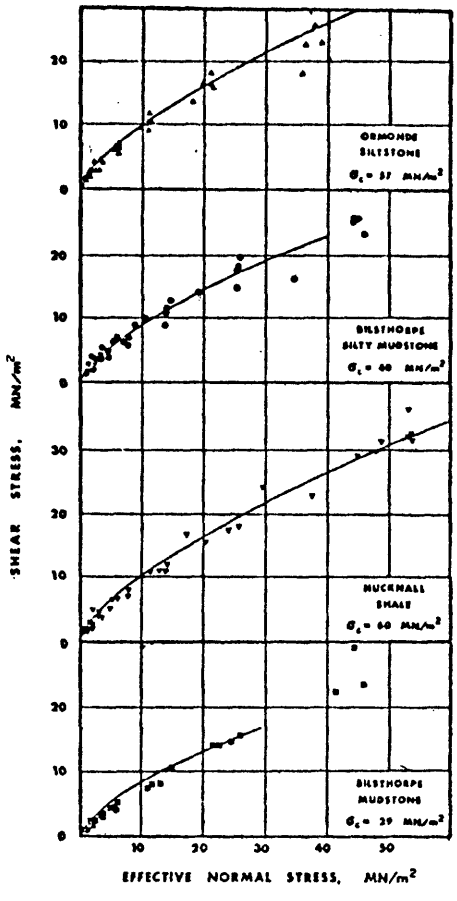

Figure 2-4 Experimental results and the predicted peak shear strength envelopes (from Barton, 1973)

JCS = Joint wall compressive strength

ϕ_v = angle of frictional sliding resistance on flate smooth surfaces.

JRC represents a sliding scale of roughness which varies from 0 for smooth planar discontinuities to 20 for rough undulating discontinuities. JCS is a measure of the strength of the surface irregularities, and is equal to the unconfined compression strength σ_c of the rock if the joint is unweathered, but may reduce to approximately 1/4 σ_c if the joint walls are weathered. ϕ_v can be determined from sliding tests on samples of the wall rock. The large amount of experimental data reported in the literature for sandblasted and sawn surfaces, as shown in Table 2-1, suggests that most rocks have basic angles of friction the same as the residual angle for natural joints, and lying between approximately 25^o and 35^o, at least at medium stress levels, σ_n = 0.1-10 MN/m^2(1-100 kg/m^2). The physical appearance of Eq. 2-10 for different values of the joint roughness coefficient is seen from Fig. 2-5. From Fig. 2-5, it can be seen that the strong influence of surface roughness JRC and variable rock strength JCS affect rock joints to exhibit a wide spectrum of shear strength under low effective normal stress levels as shown in Fig. 2-6. The experimental data shown in Fig. 2-6 shows several plotted points with values of arctan (τ/σ_n) of about 80^o when the effective normal stress is below 0.5 MN/m^2 (5 kg/m^2). Some of the other high values reported in the literature are shown in Table 2-2. A shear strength envelope for rough joints formed from these high values of arctan (τ/σ_n) having a vertical

Rock	Moisture	σ_n(MN/m^2)	ϕ_b^o	References[a]
Amphibolite	dry	0.1–4.2	32	a
Basalt	dry	0.1–8.5	35–38	b
	wet	0.1–7.9	31–36	b
Conglomerate	dry	0.3–3.4	35	c
Chalk	wet	0–0.4	30	d
Dolomite	dry	0.1–7.2	31–37	b
	wet	0.1–7.2	27–35	b
Gneiss (schistose)	dry	0.1–8.1	26–29	b
	wet	0.1–7.9	23–26	b
Granite (f.g.)	dry	0.1–7.5	31–35	b
	wet	0.1–7.4	29–31	b
Granite (c.g.)	dry	0.1–7.3	31–35	b
	wet	0.1–7.5	31–33	b
Limestone	dry	0–0.5	33–39	e
	wet	0–0.5	33–36	e
	dry	0.1–7.1	37–40	b
	wet	0.1–7.1	35–38	b
	dry	0.1–8.3	37–39	b
	wet	0.1–8.3	35	b
Porphyry	dry	0–1.0	31	f
	dry	4.1–13.3	31	f
Sandstone	dry	0–0.5	26–35	e
	wet	0–0.5	25–33	e
	wet	0–0.3	29	g
	dry	0.3–3.0	31–33	c
	dry	0.1–7.0	32–34	b
	wet	0.1–7.3	31–34	b
Shale	wet	0–0.3	27	g
Siltstone	wet	0–0.3	31	g
	dry	0.1–7.5	31–33	b
	wet	0.1–7.2	27–31	b
Slate	dry	0–1.1	25–30	f

(a) Wallace et al. (1970)
(b) Coulson (1972)
(c) Krsmanovic (1967)
(d) Hutchinson (1972)
(e) Patton (1966a)
(f) Barton (1971b)
(g) Ripley & Lee (1962)

Table 2-1 Basic friction angle for rocks with sandblasted, rough-sawn and residual surfaces (from Barton, 1973)

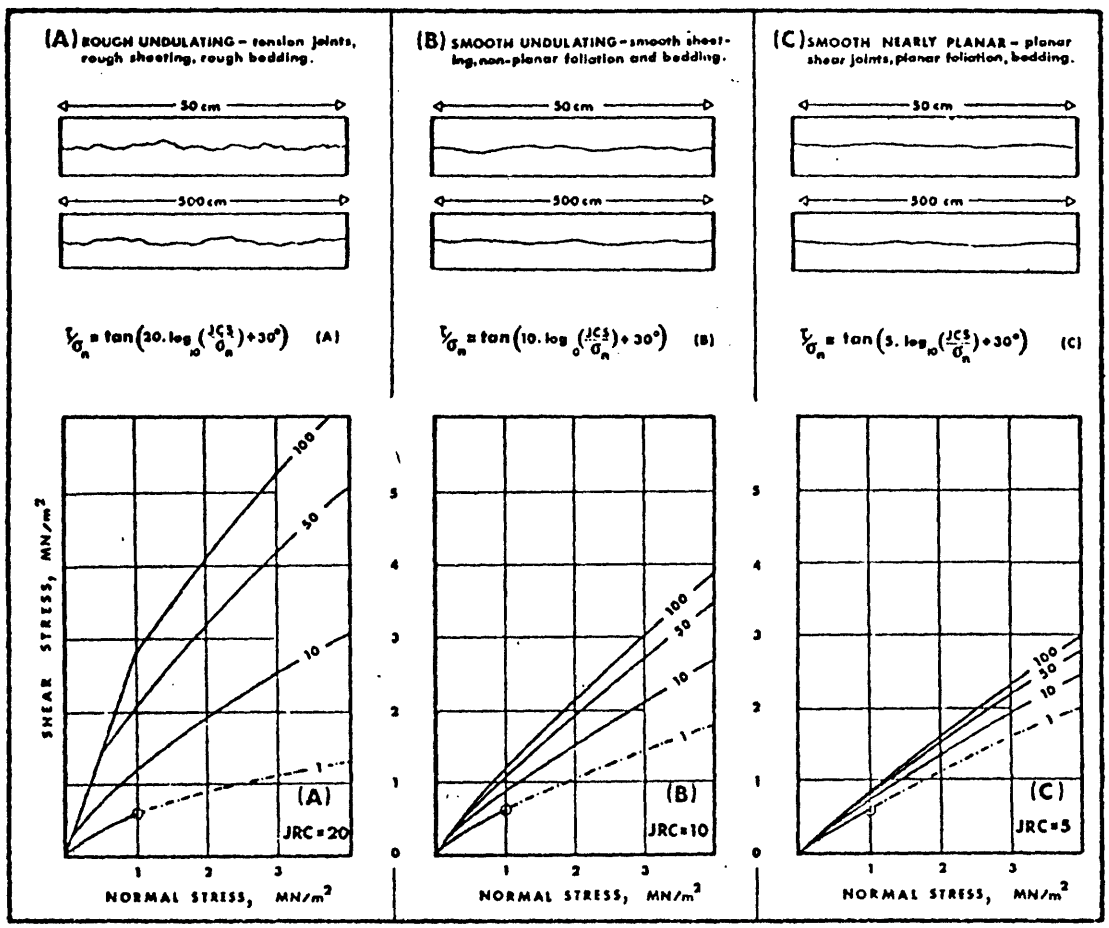

Figure 2-5 Classification of roughness and prediction of shear strength for non-planar rock joints. Each curve is numbered with the appropriate values of (JCS) (from Barton, 1973)

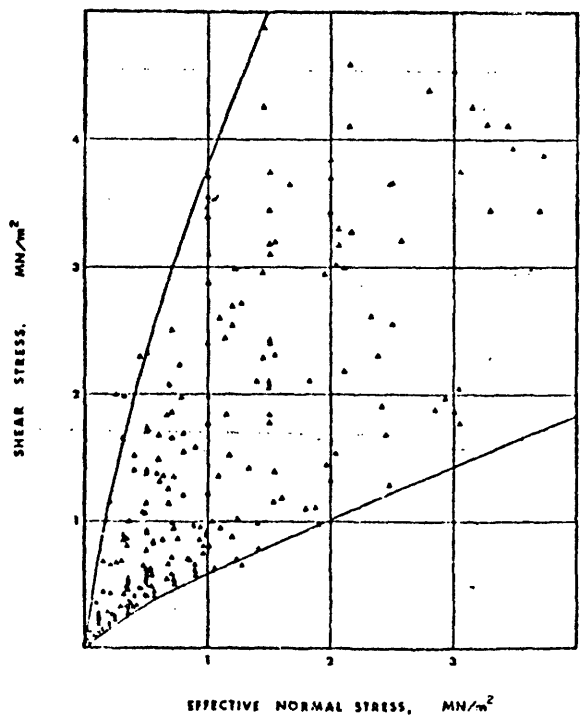

Figure 2-6 Wide spectrum of strength envelope of tests in laboratory and in-situ under low normal stress (from Barton, 1976)

Description of discontinuity	τ/σ_n (MN/m^2)	arctan (τ/σ_n)	Reference
Limestone: slightly rough bedding surface	0.68/0.16	77°	a
	0.66/0.21	72°	
	1.68/0.60	71°	
Limestone: rough bedding surface	0.68/0.31	66°	a
	2.07/0.68	72°	
Shale: closely jointed seam in limestone	0.06/0.02	71°	a
	0.06/0.02	70°	
Quartzite, gneiss and amphibolite discontinuities beneath natural slopes:	—	80°	b
discontinuities beneath excavated slopes:	—	75°	
Granite: rough, undulating, artificial extension fractures	0.45/0.15	72°	c
	0.92/0.35	69°	

(a) Goodman (1970) (b) Paulding (1970) c(c) Rengers (1970)

Table 2-2 Maximum values of peak (τ/σ_n) at low normal stress (from Barton, 1973)

tangent at or close to the shear stress axis is inherently satisfying as a limiting condition at extremely low normal stress.

High Stress Levels

Barton (1976) attempted to fit Eq. 2-10 to the results of triaxial shearing tests on artificial faults performed at stress levels of several hundred MN/m^2. There was an increasing error between prediction and test results, if the effective normal stress σ_n exceeds the rock's unconfined compressive strength σ_c. He reasoned that the discrepancy was due to the effect of confinement on the compressive strength of rock asperities. When the differential stress $(\sigma_1 - \sigma_2)$ approached the value of JCS in Eq. 2-10, Barton generalized Eq. 2-10 as follows:

$$\tau/\sigma_n = \tan\left(\text{JRC}\ \log_{10}\left(\frac{\sigma_1-\sigma_3}{\sigma_n}\right) + \phi_v\right) \qquad (2\text{-}11)$$

where σ_1 = axial stress at failure

σ_3 = effective confining pressure

σ_n can be calculated from the following equations:

$$\tau = 1/2\ (\sigma_1 - \sigma_3)\ \sin 2\beta \qquad (2\text{-}12)$$

$$\sigma_n = 1/2\ (\sigma_1 + \sigma_3) - 1/2\ (\sigma_1 - \sigma_3)\ \cos 2\beta \qquad (2\text{-}13)$$

$$\beta = 45^o - \phi/2 \qquad (2\text{-}14)$$

where β = angle of fault makes with major effective principal stress σ_1

ϕ = inclination of the Mohr envelope at point of tangency.

Barton showed experimental evidence for the validity of Eq. 2-11. He gathered the results of triaxial compression tests performed on intact cylinders of Weber sandstone by Byerlee (1975) as shown in Fig. 2-7A, and an ideal set of experimental data provided by Raleigh and Paterson (1965), Mogi (1966), Byerlee (1967) and Byerlee (1968) as shown in Fig. 2-8A. These experimental values of $(\sigma_1 - \sigma_3)$ and the values of (σ_n) as estimated above together with assumed values of JRC = 20, $\phi_\nu = 30$, $\beta = 30$ were substituted in Eq. 2-11. The experimental and predicted peak shear strength of the faults were shown in Figs. 2-7B, 2-7C, 2-8B, 2-8C. There is remarkable agreement between prediction and experiment in Fig. 2-7B and Fig. 2-7C. The predicted data in Fig. 2-8C are scattered more widely than the experimental data in Fig. 2-8B and also are a little low. The reasons are due to missing data points for Solenhofen limestone above an effective normal stress of about 120 MN/m^2 in Fig. 2-8B and the use of the assumed value $\phi_\nu = 30^o$ for limestone. If the corresponding data point for Solenhofen limestone above an effective axial stress about 120 MN/m^2 are excluded in Fig. 2-8C and the mean value of $\phi_\nu = 37^o$ for limestone in place of 30^o is used, the predicted envelope would be close to the experimental values.

Eq. 2-11 gives a good prediction of peak shear strength envelope at high stress levels. Since Eq. 2-11 depends on JRC, ϕ_ν and σ_n which is a function of β, the prediction depends for its accuracy on correct assumptions regarding the values of JRC, ϕ_ν and β. At high levels of

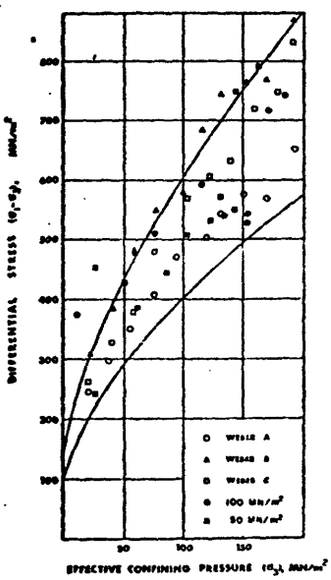

Differential stress at failure as a function of effective confining pressure for Weber sandstones A, B and C

(A)

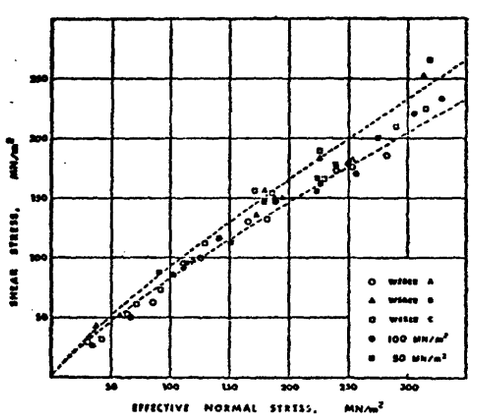

Shear stress as a function of effective normal stress for sliding on the fault surfaces produced by failure of the Weber sandstones

(B)

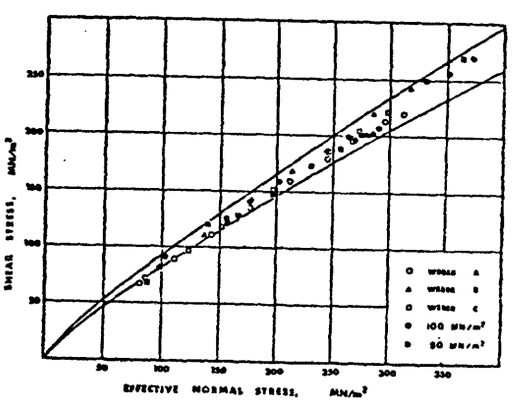

Predicted peak shear strength of the faults in Weber sandstones

(C)

Figure 2-7 Comparison of experimental results (weber sandstone) and prediction using friction law for high normal stress (from Barton, 1976)

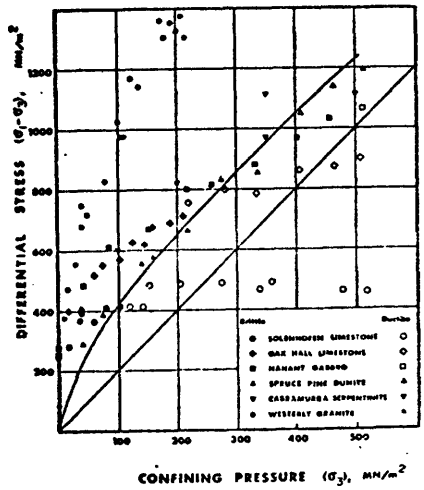

Differential stress vs confining pressure at fracture, or at 5% strain if specimen was ductile. Closed symbols indicate brittle behaviour, open symbols, ductile.

(A)

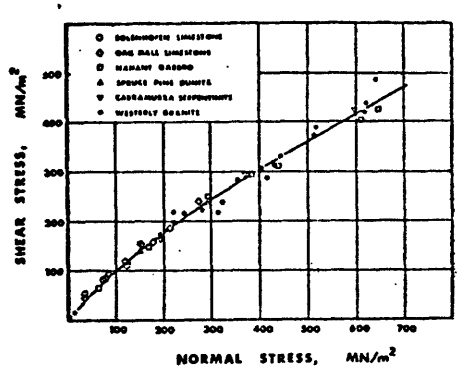

Shear stress vs normal stress for frictional sliding on the faults developed in the triaxial tests

(B)

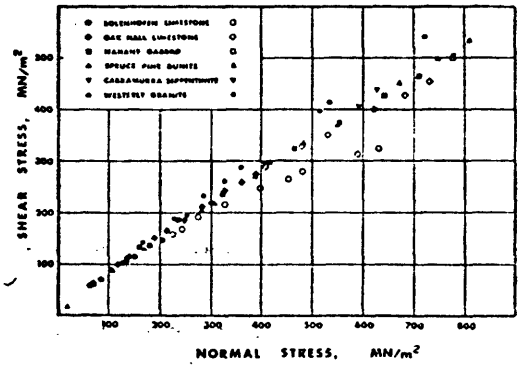

Predicted peak shear strength of the faults developed in the triaxial tests

(C)

Figure 2-8 Comparison of experimental results (limestone, gabbro, dunite, serpertinite, granite) and prediction using friction law for high normal stress (from Barton, 1976)

effective normal stress the frictional strength is related to the confined compression strength which is represented by the differential stress ($\sigma_1 - \sigma_3$) at fracture. The dimensionless ratio ($\sigma_1 - \sigma_3$)/ σ_n, which relates directly to τ/σ_n in Eq. 2-11, varies relatively little over a wide range of σ_3 and results in a limited range of frictional strength at high stress levels as shown in Fig. 2-9 compared to the wide range of frictional strength exhibited at low stress levels in Fig. 2-6.

Schneider Model

Schneider (1976) developed a friction law, which would take into account the variation of the friction force and the dilatancy of the joints with increasing movements. He ran friction tests on models with natural joint morphology of a tension joint in granite, sandstone and limestone. The dilation-shear displacement behavior was investigated. Comparing the maximum dilatancy of a single model type at different normal stresses as shown in Fig. 2-10, it can be seen that the dilatancy decreases with increasing normal load; the dilatancy decreases according to the function

$$h = h_o e^{-k\sigma} \tag{2-15}$$

where h = dilatancy

h_o = maximum dilatancy at zero normal load

k = reduction coefficient of dilatancy

k is different for each joint and material type as shown in Fig. 2-11. k can be related to the tensile strength of the material for each joint

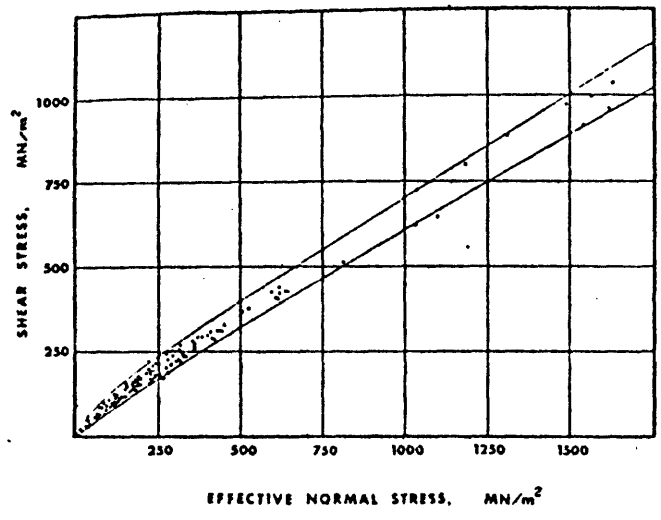

Figure 2-9 Shear strength of faults and tension fractures at high normal stress (from Barton, 1976)

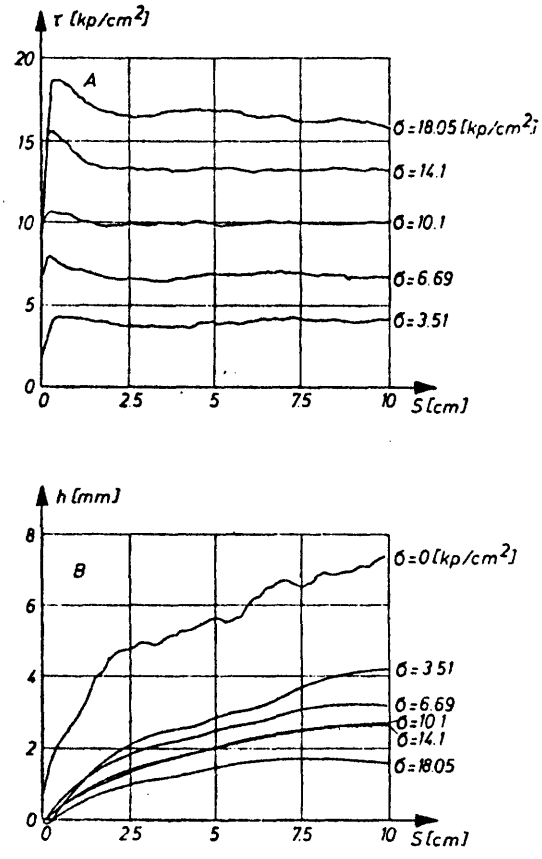

Shear stress – shear displacement diagrams (*A*), dilatation-shear displacement diagrams (*B*) of friction tests on models with granite joint morphology (model material Hartformengips)

Figure 2-10 Shear stress-shear displacement curves for different material type and normal loads (from Schneider, 1976)

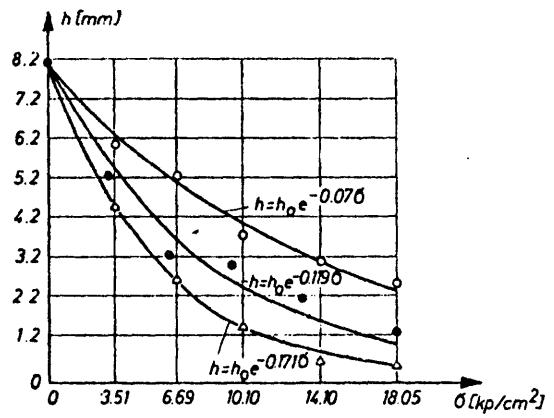

Decrease of maximum dilatation with normal stress in the friction test on models with sandstone joint morphology. Model material: Hartformengips (○), Moldano (△) and Alabasterformengips (●)

Figure 2-11 Effect of joint type and material type on k values (from Schneider, 1976)

type by the function

$$k = a\,(\sigma_t d)^{-b} \qquad d = [1\ \frac{cm^2}{kp}\ ] \tag{2-16}$$

where a and b are coefficients for each joint type with a special number as shown in Fig. 2-12. According to Eq. 2-16, k decreases with increasing material strength. That means that at high material strength only a few asperities are sheared through which influences both dilatancy and friction resistance. At low material strength the influence of the joint roughness upon the friction behavior decreases. Since dilatancy is maximum at zero normal stress, it is related to the angle of inclination of asperities. He took angle of inclination of asperities as the dilation angle which is defined as:

$$\tan i = \frac{\Delta h}{\Delta s} \tag{2-17}$$

With Eqs. 2-15 and 2-17, he modified Eq. 2-1 to develop a function relating the peak friction to the dilation angle as:

$$\tau = \sigma \tan (\phi_\nu + \arctan \frac{\Delta h_o e^{-k\sigma}}{\Delta s}) \tag{2-18}$$

The validity of the friction law in tests on natural rock samples could be demonstrated only for sandstone. For granite and limestone samples, its applicability is limited. The validity of this friction law needs to be further demonstrated.

2.2 Factors Influencing Shear Strength

It is important to identify and discuss those factors which influence

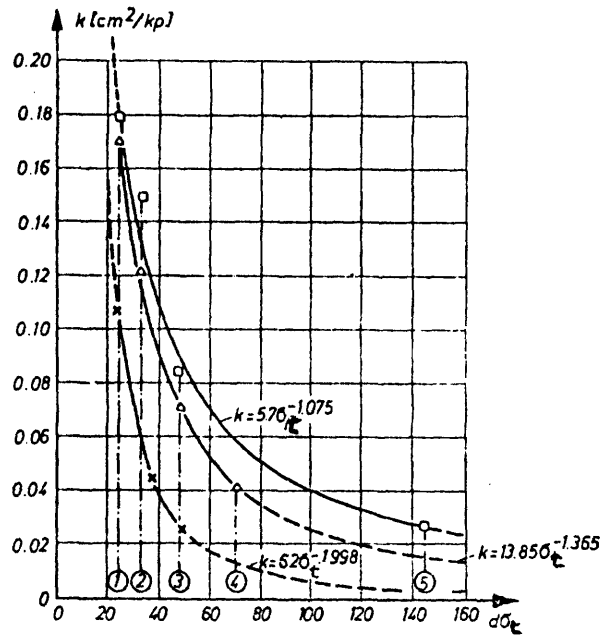

Reduction coefficients of the dilatation as a function of the tensile strength from Alabasterformengips (*1*), Moldano (*2*), Hartformengips (*3*), Sandstone (*4*) and Granite(*5*) for the joint types of Granite (□), Sandstone (△) and Limestone (×)

Figure 2-12 Effect of a and b on k values (from Schneider, 1976)

the shearing mechanism of rock joints. These factors are: rock type, weathering, surface geometry, water, over-closure, scale effect, test method and filler material.

Rock Type

Rock type influences the shear strength of rock joints through its texture, mineralogy and fabric, which contribute to the strength of surface irregularities and friction between planar joint surfaces.

Weathering

Weathering affects shear strength of rock joint to a great extent. As discussed in connection with Barton Model, the compressive strength of the joint wall is an important component of the shear strength, weathering that causes a reduction in this compressive strength should result in reduced shear strength. The depth of penetration of weathering into joint walls depends largely on the rock type, and in particular on its permeability. Barton (1973) indicated the mechanical effects of weathering is that slight alteration of the fresh rock may cause a much more severe drop in mechanical strength than subsequent steps in the alteration of the weathered rock. However, Dearman et al. (1978) showed that compressive strength decreases linearly with increasing degree of weathering.

Surface Geometry

The geometry of the joint surface (roughness) has an important effect on shear behavior, and is particularly significant in determining dilation and the effect of asperities in general. Schneider (1976) tested model samples of granite, sandstone and limestone with the same

material strength and different joint surface roughness. The shear stress-shear deformation curves of the test are shown in Fig. 2-13. The distinct differences in these curves are due to various roughness geometries.

Water

The presence of water in a rock joint leads to several mechanical and some chemical effects, the most important of which will probably be the reduction in effective stress. The water will also tend to reduce surface energy and crystal strength, with the result that the mechanical strength of the rock is lowered. This has the subsequent effect of lowering the shear strength. However, some types of rock joints appear to be little affected by water (besides the effective stress effect) and may have a slightly higher shear strength when wet. Table 2-3 shows the effect of water on shear strength of rock joints. Most of the smooth polished surfaces are unaffected or increase in strength slightly when wet. Most of the natural or rough joint surfaces reduce in strength when wet. Brownell (1966) and Dickey (1966) explained that the effect of water on smooth surfaces is due to surface cleanliness. The presence of water has no effect on smooth, clean surfaces. However, if smooth surfaces are unclean, then water causes an increase in strength from the dry condition. Barton (1973) explained that the reduction in strength due to water on rough surface is related to the reduction in tensile and compressive strength of brittle material due to adverse effect of water.

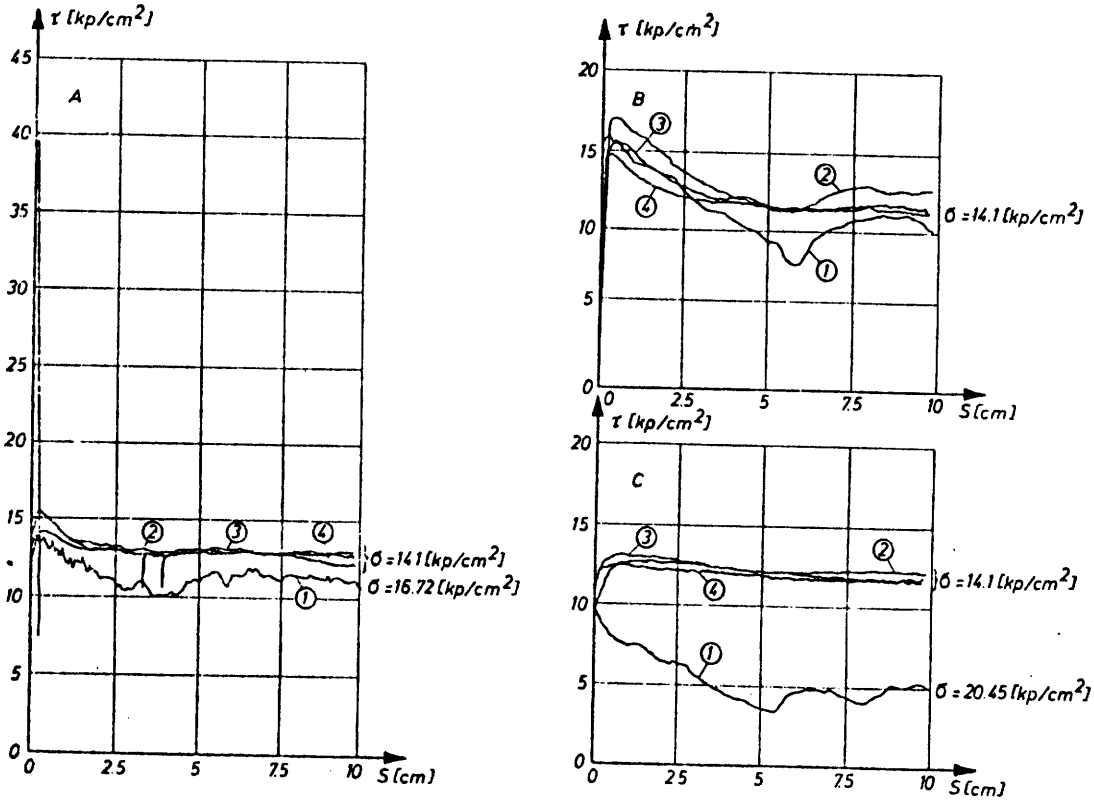

Shear stress – shear displacement curves of friction tests in Granite (*A1*), Sandstone (*B1*) and Limestone (*C1*), in models with identical joint morphology of Hartformengips (*2*), Moldano (*3*) and Alabasterformengips (the limestone and its models had only similar (*4*) joint morphologies)

Figure 2-13 Effect of surface roughness on shear stress-shear displacement curves (from Schneider, 1976)

Rock type	Description of discontinuity	Dry		Wet		Reference
		Φ°	μ	Φ°	μ	
Quartzite	artificial, planar, polished (σ_n: 30—400 kg/cm²)					Jaeger and Rosengren (1968)
				no change		
Shales, siltstones and slates	minor faults; smooth, polished or slickensided, graphite coated			*in*		Rosengren (1968)
				general		
Shales, siltstones and slates	extension fractures; coated with limonite, pyrite, quartz					Rosengren (1968)
				reduction		
Granite, gneiss, sandstone	shear fractures from failure of intact specimens (σ_n: 100—2,500 kg/cm²)		0.71 0.52		0.61 0.47	Jaeger (1959)
		Φ_r		Φ_r		
Sandstones, carbonates	artificial, rough sawn, equivalent to residual	25—34 33—39		24—33 32—36		Patton (1966a)
Shales, siltstones and slates	minor fault, smooth, polished, chlorite coated		0.49		0.40	Rosengren (1968)
Dolerite	joint	52		37		Duncan (1969)
Granite	artificial surface	38		31		
Gneiss	natural schistose plane, "keyed"	49		44		
Phyllite	schistose plane	40		32		
Shale	joint	37		27		
Quartzite	joint	44		34—37		Duncan and Scheerman-Chase (1965—66)
Marble	joint	49		42		
				increase		
		Φ_r		Φ_r		
Sandstone	artificial, planar, polished (equivalent to slickenside)	27—32		30—38		Patton (1966a)
Gabbro	joint	47		48		
Oolitic limestone	joint	44		48		Duncan (1969)
Chalk (2 of 3 types)	joint	40		41		
Quartzite	artificial, planar, polished	23		30		Duncan and Scheerman-Chase (1965—66)
Basalt	artificial, planar, polished	33		35		
Schistose gneiss, granite, sandstone	artificial, planar, polished with increasing polish during shear	—	—	—	—	Coulson (1970)

Table 2-3 Effect of water on the frictional strength of rock joints (from Barton, 1973)

Over-closure

Barton (1973) indicated that non-planar joints intersecting the rock may be pre-loaded or over-closed, as shown in Fig. 2-14. The methods of obtaining or exposing rock joints for shear testing involve such a degree of disturbance that any potential over-closure effect will be destroyed, and the strength measured therefore rather conservative. The only way of recovering the effect is to pre-consolidate the joints, before shear testing.

Scale Effect

Scale effect of specimens on the compression strength and frictional strength of rocks has been demonstrated in rock mechanics. Pratt et al. (1972) indicated that compressive strength decreases with increase in specimen length, but the scale effect appears to die out when specimen sizes exceed about 1 m. Pratt et al. (1974) showed that shear strength of joints decreases with increase in joint length, as shown in Fig. 2-15, but the scale effect appears to die out for joint length in excess of 2 to 3 m. However, literature on scale effect is scarce, and the scale effect needs therefore to be further investigated.

Test Methods

Shear strength of rock joints can be investigated in the laboratory with triaxial tests or direct shear tests or others. The results of these two methods on the same rock type basically agree well as shown in Fig. 2-16. Because of changes of geometry during sliding, the triaxial method is not well suited to the study of continued sliding. In addition, it is not good for testing seams, or joints of shear origin.

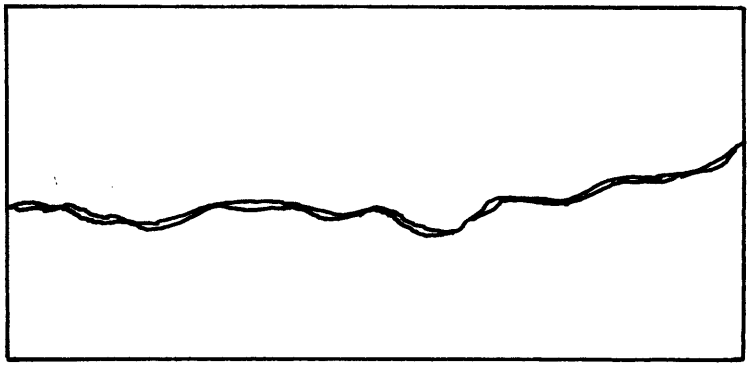

over-closed joint
before sampling

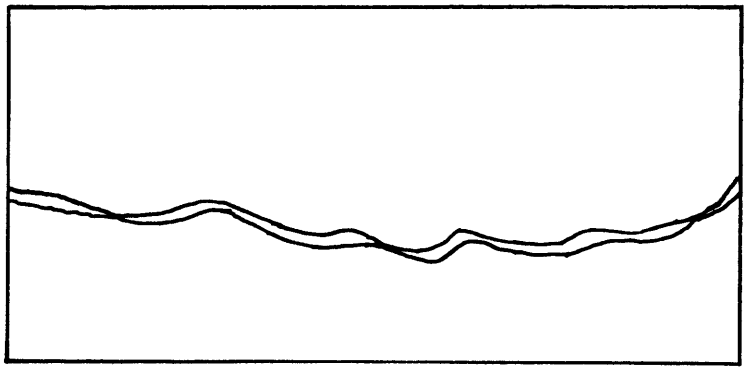

disturbed joint
after sampling

Figure 2-14 Joint over-closure

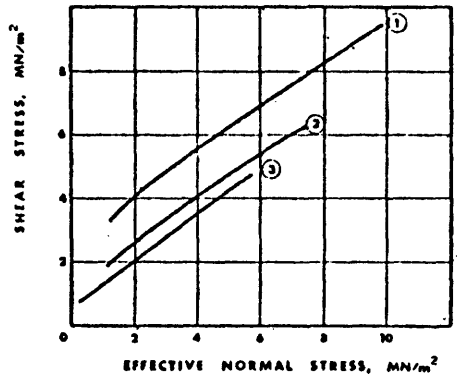

Results of *in situ* shear tests on joints in quartz diorite, Envelope (1) represents specimens with an average area of approx 200 cm², (2) an average area of 1500 cm², and (3) an average of 5000 cm².

Figure 2-15 Scale effect of joint length on shear strength (from Barton, 1976)

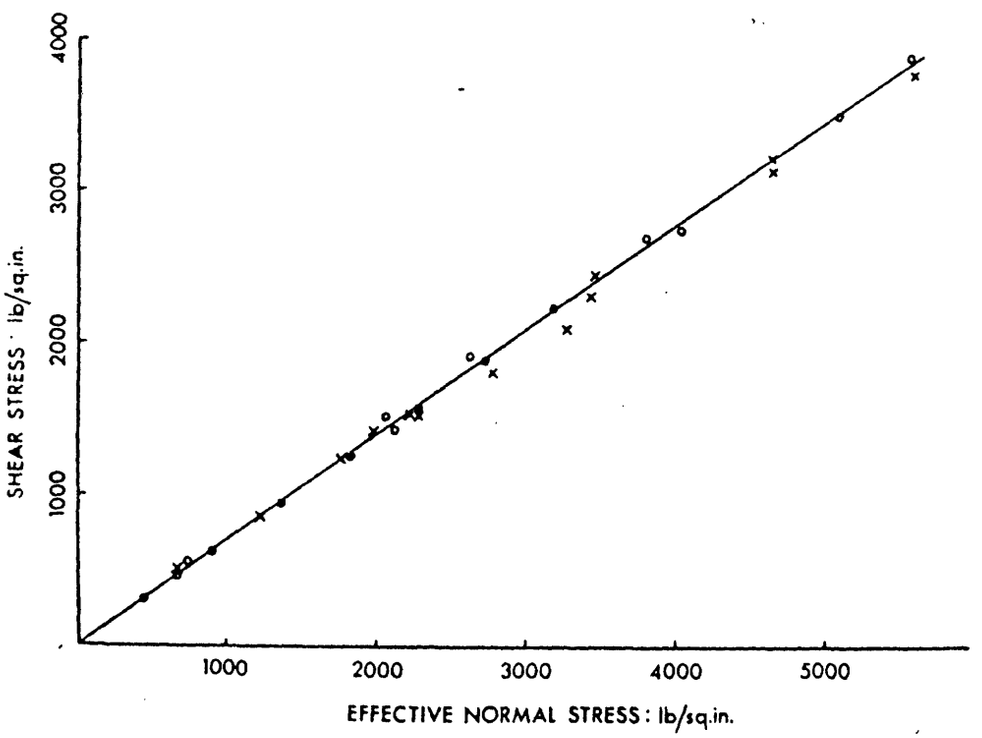

Sliding of Narrandera quartzite under various conditions. Filled dots: direct shear, dry. Open circles: triaxial test, dry Crosses: triaxial test with fluid pressure in the joint.

Figure 2-16 Comparison of shear strength for direct shear tests and triaxial test (from Jaeger and Rosengren, 1968)

Because of the large size of the shear box, the direct shear test has the advantage that comparatively large surfaces may be used and thus a better simulation of natural conditions obtained. However, it is not a simple matter to produce a reasonably uniform stress distribution inside a direct shear box, and there is the problem of direct shear tests concerning the lateral boundary conditions. Fortunately, different elaborate direct shear machines like the direct shear machine by Hoek and Pentz (1968), the shear machine by Krsmanovic (1967), etc. were developed to solve the above mentioned problems.

Filler Materials

For sliding of a filled joint, there will be an initial failure corresponding to shear failure of the filling material, and subsequently there will be sliding on this surface of failure. If the filler material thickness is greater than the height of surface irregularities, the characteristics of the filler can completely dominate the behavior of the discontinuity. If the filler thickness is less than that height, then the filler material and the irregularities will interact in the some way. Goodman (1974) indicated that the behavior of filled joints is different from that of unfilled joints, as shown in Fig. 2-17. The convex upward stress-deformation curve of the filled joint resembles that of a clay with a poorly defined peak and continuous curvature. Ladanyi and Archambault (1975) indicated that the strength of a filled joint is located between that of the filling alone and that of the same type of joint when unfilled. The strength decreases steadily with the filling thickness to approach that of the filler when the thickness exceeds the height of the irregularities by about 50 percent.

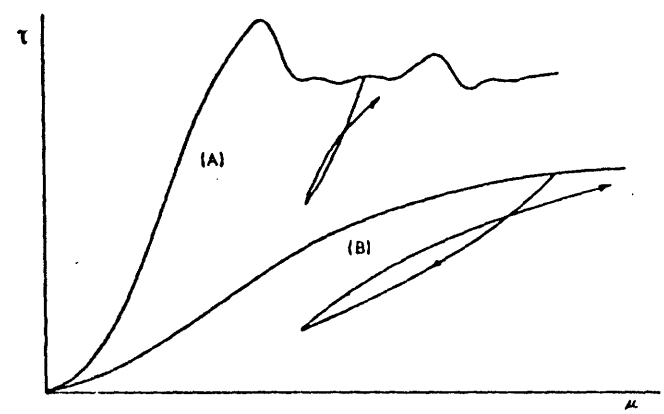

(A) unfilled joints
(B) filled joints

Figure 2-17 $\tau - \delta_s$ curves for unfilled joints and filled joints (from Goodman, 1974)

2.3 Description of Deformability of Discontinuities

With the advent of finite-element and finite difference computer methods, the stiffness properties, shear stiffness k_s and normal stiffness k_n, which describe stress-deformation response, have been introduced into the determination of rock mass behavior together with values for peak and residual shear displacements and maximum joint closure values. These stiffness properties make possible the computation of the contribution of joints to the total displacements of structures in rock. The stiffness properties for a joint or fracture are determined experimentally by measuring the loads and displacement on a rock specimen in both the shear and normal directions.

Normal Stiffness

Normal stiffness k_n refers to the rate of change of normal stress with respect to normal displacement. If average normal stress and average normal displacement are taken, the 'secant' normal stiffness k_n is

$$k_n = \frac{(\sigma_n)_a}{(\delta_n)_a} \tag{2-19}$$

In this thesis, the secant normal stiffness is defined (see Fig. 2-18) as the change in normal stress over the change in relative normal displacement, i.e.

$$k_n = \frac{\Delta\sigma_n}{\Delta\delta_n} \tag{2-20}$$

If instantaneous change of normal stress with respect to shear displacement is considered, "tangent" normal stress can be used:

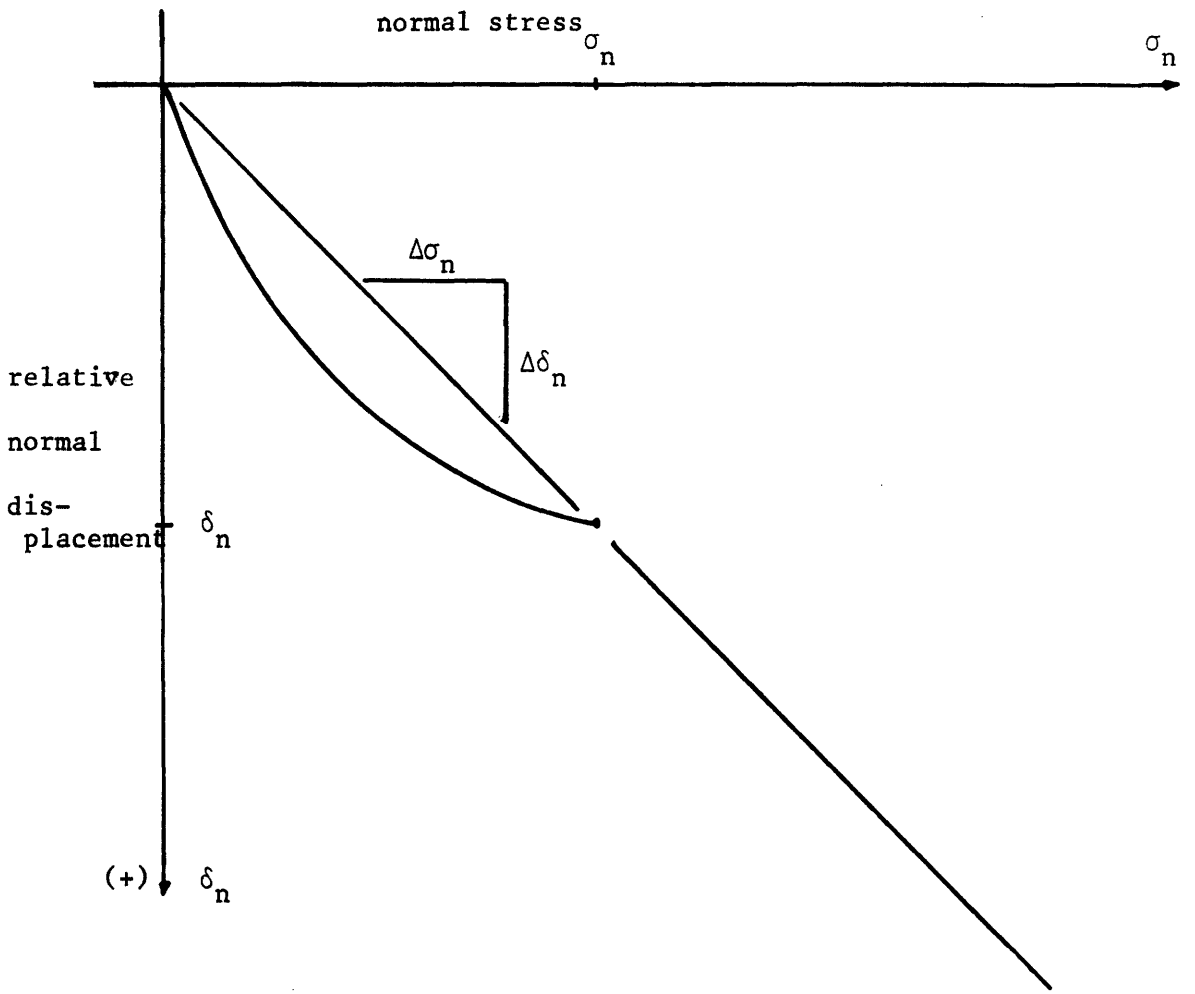

Figure 2-18 Normal stress-relative normal displacement diagram

$$k_n = \frac{d\delta_n}{d\delta_n} \tag{2-21}$$

The normal stiffness, which depends exclusively on the joint characteristics, i.e. initial aperture, roughness, type and character of filling, etc., is zero under tensile leading; it increases under compressive loading to a very large number as the joint approaches a fully closed condition. Values of normal stiffness from published literature are summarized in Table 2-4. Goodman (1974) suggested a hyperbolic variation between normal stress σ and normal displacement δ_n given by

$$\sigma = \frac{\Delta\delta_n}{\delta_{mc} - \Delta\delta_n} \xi + \xi \tag{2-22}$$

where ξ = the seating pressure defining the initial condition for measuring the normal deformation

$\Delta\delta_n$ = the change in joint thickness corresponding to an increase in normal stress from the initial seating pressure ξ to an value of σ.

δ_{mc} = the maximum joint closure, which is smaller than or equal to the joint thickness e as shown in Fig. 2-19(a).

δ_{mc} can be determined from a σ-δ_n plot by sketching the asymptote to the deformation curve as shown in Fig. 2-19(b), or rewriting Eq. 2-22 as

$$\Delta\delta_n = \delta_{mc} - (\xi\ \delta_{mc})\ 1/\sigma \tag{2-23a}$$

$$\delta_{mc} - \Delta\delta_n = \frac{\xi\delta_{mc}}{\sigma} \tag{2-23b}$$

Test designation (1)	Specimen description (2)	Discontinuity: Area, in square meters (3)	Discontinuity: Thickness, in millimeters (4)	Joint face roughness, in millimeters (5)	Normal stiffness, K_n, in giganewton per cubic meter (6)	Modulus of rock, E_r, in giganewton per cubic meter (7)	E_r/K_n, in meters (8)	Reference (9)
QP2	Boise sandstone with dry, rough sawed joint	5×10^{-4}	—	—	35.1	7.46	0.21	a
Vouglans Dam	Marly sand filled joint	4.4	1-2	—	1.96	—	—	b
SLL Khajuri Dam	Closely jointed shale zone in limestone	5	2-5	—	0.24	—	—	b
SLS Khajuri Dam	Shale interbed—wet	5	2-5	—	0.26	—	—	b
25	Lyon's sandstone with clay joint*	1.45×10^{-3}	2.26	1.91	5.59	2.48	0.44	c
26	"	"	1.88	1.42	5.40	"	0.46	c
28	"	"	0.25	0.20	5.40	"	0.46	c
47	"	"	0.53	0.21	5.43	"	0.46	c
69	Sierra White Granite with clay joint*	"	1.47	1.33	5.21	22.06	4.23	c
70	"	"	1.37	1.51	16.91	"	1.30	c
71	"	"	1.22	2.27	67.59	"	0.33	c
72	"	"	1.07	0.06	7.22	"	3.06	c

*Clay filled joint is saturated and has the following properties: 100% < 2μ, w_L = 57%, PI = 27.
Note: 1 GN/m³ = 3,684 lb/cu in.

(a) Mahtab (1970) (b) Goodman (1968) (c) Goodman (1972)

Table 2-4 Summary of Normal Stiffness Values (from Kulhaway, 1978)

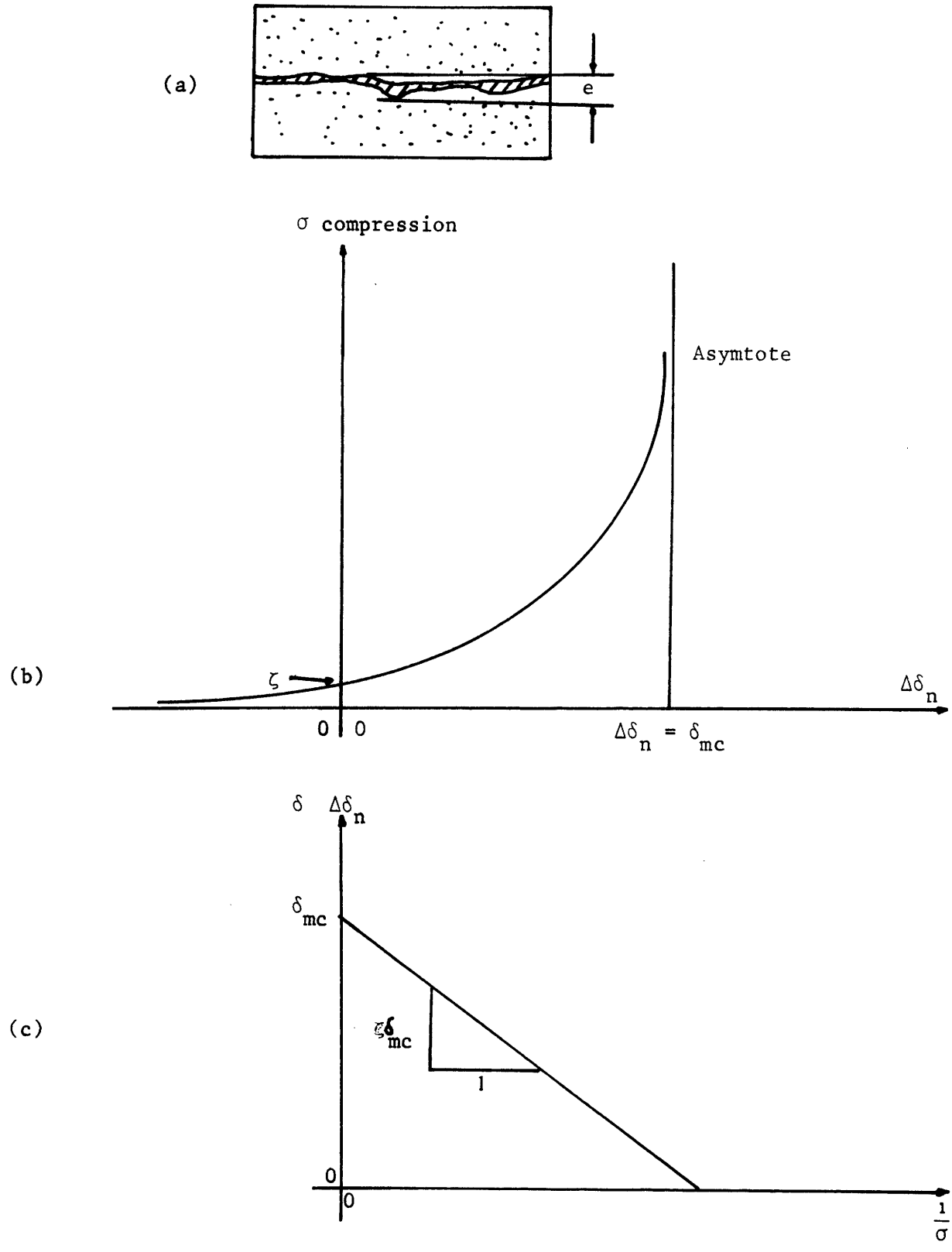

Figure 2-19 Joint compression

to get a plot of $\Delta\delta_n$ against $1/\sigma$ as shown in Fig. 2-19(c) from which δ_{mc} and $-\xi\delta_{mc}$ are obtained. Differentiation of Eq. 2-22 and substitution of Eq. 2-23 give

$$k_n = \frac{d\sigma}{d(\Delta\delta_n)} = \frac{\sigma^2}{\xi\delta_{mc}} \qquad (2\text{-}24)$$

Since the relationship, Eq. 2-22, is hyperbolic rather than linear, k_n is not a constant but a variable equal to Eq. 2-24. Hungr and Coates (1978) showed in Fig. 2-20 that the normal stress-displacement curves of precompressed samples, limestone and sandstone, did not exhibit a hyperbolic relationship as proposed by Eq. 2-22. The relationship, Eq. 2-22, may be valid only for joints that are not precompressed.

Shear Stiffness

Shear stiffness refers to the rate of change of shear stress with respect to shearing displacement. If average shear stress and average shear displacement are used, the "secant" shear stiffness k_s is

$$k_s = \frac{(\tau)_a}{(\delta_s)_a} \qquad (2\text{-}25)$$

In this thesis, the "secant" shear stiffness can be defined either as the elastic shear stiffness $(k_s)_e$, which is the change in elastic relative shear displacement (see Fig. 2-21), or as the peak shear stiffness $(k_s)_p$, which is the change in shear stress over the change in

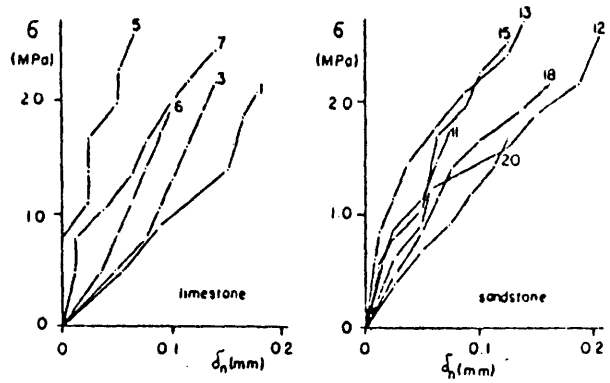

Figure 2-20 Normal stress-displacement curves obtained from the joint closure tests (from Hungr and Coates, 1978)

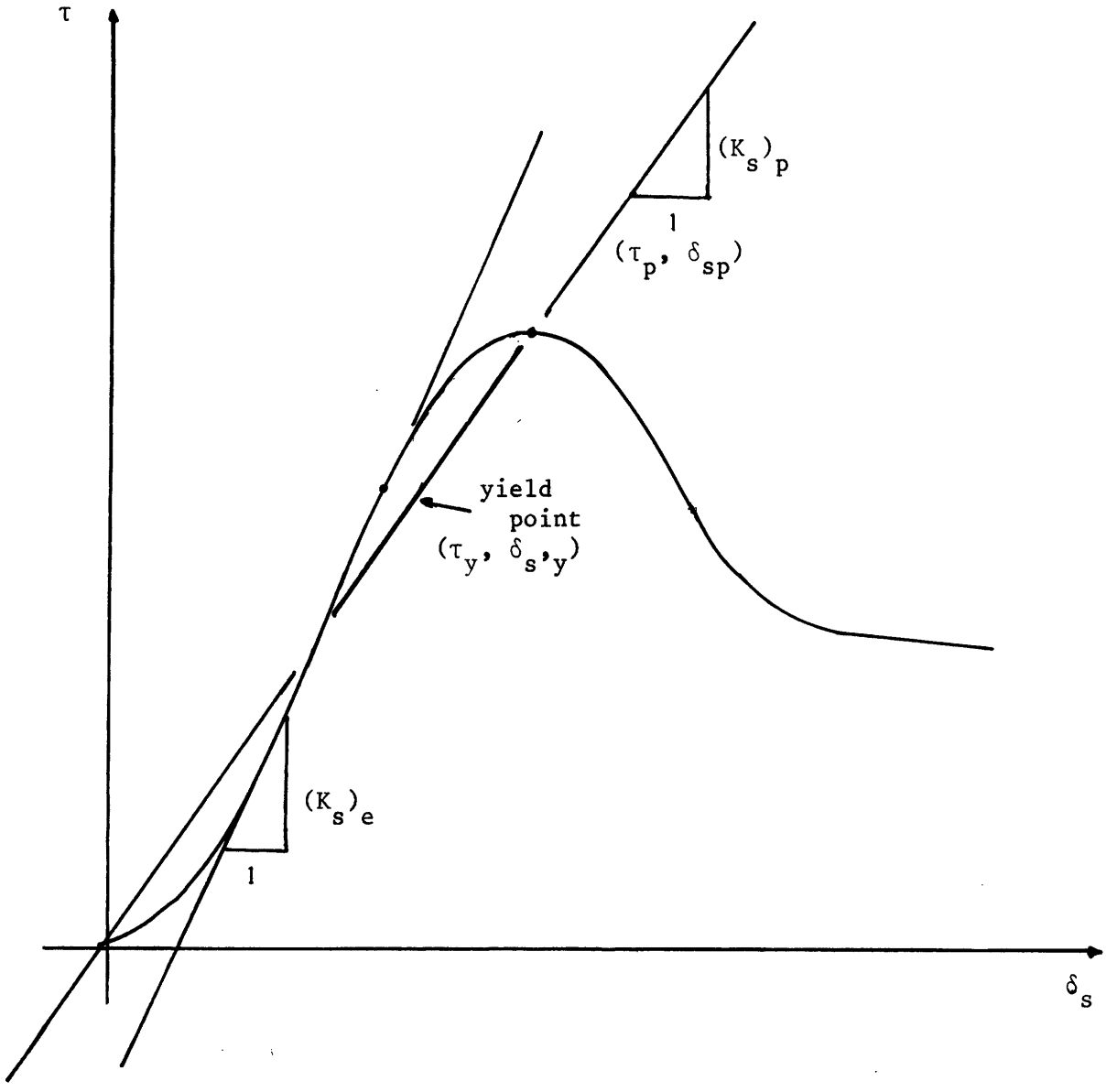

Figure 2-21 Shear stress-relative shear displacement diagram

relative shear displacement from beginning to peak (see Fig. 2-21), i.e.

$$(k_s)_e = \frac{\Delta\tau}{\Delta(\delta_s)_e} \tag{2-26}$$

$$(k_s)_p = \frac{\tau_p}{(\delta_s)_p} \tag{2-27}$$

If the shear stress and shear displacement are taken as those at yield point or at 50% peak point of τ-δ_s curve (see Fig. 2-21), these give

$$k_{s,y} = \frac{\tau_y}{\delta_{s,y}} \tag{2-28}$$

$$(k_s)_{50\%} = \frac{(\tau_p)_{50\%}}{(\delta_{s,p})_{50\%}} \tag{2-29}$$

If instantaneous change of shear stress with respect to shear displacement is considered, the tangent stiffness is used:

$$k_s = \frac{d\tau}{d\delta_s} \tag{2-30}$$

Table 2-5 summarizes shear stiffness at yield point and peak point from published literature. Shear stiffness coefficients are not constants, but vary with both normal stress σ and shear stress τ or shear displacement δ_s. According to the shape of the shear stress-displace-

Properties of discontinuities under direct shear conditions

Discontinuity number	Test designation	Specimen description	Discontinuity thickness (cm)	Discontinuity area (cm^2)	Range of initial normal stress (MN/m^2)	Secant shear stiffness K_s (GN/m^3) Yield Range	Yield Avg.	Peak Range	Peak Avg.	Cohesion, C (MN/m^2) Maximum C	Cohesion, C (MN/m^2) Residual C_r	Angle of friction ϕ Maximum ϕ	Angle of friction ϕ Residual ϕ_r	Curve type	Reference
DLL-1	10-14.6 run 3 — U. Illinois	Berea sandstone — dry, sawed joint	—	82	0.28	—	—	—	29.80	—	—	—	—	2a	Goodman (1968)
DLL-2	6-14.7 run 7 — U. Illinois	Limestone — dry, sawed joint	—	82	10.40	—	—	—	8.73	—	—	—	—	2a	Goodman (1968)
DLL-3	QP2 — U. C., Berkeley	Boise sandstone — dry, rough saw cut	—	5	2.43	—	—	—	1.29	—	—	—	—	2b	Mahtab (1969)
DLL-4	Blackingstone — Imperial Col.	Granite — dry, rough joint from breaking beam	—	144—205	1.18— 1.42	1.26— 1.57	1.42	0.99— 1.57	1.32	—	—	—	—	3a	Goodman (1968)
DLL-5	Delgado — Imperial Col.	Slate — dry, natural cleavage surface	—	500	4.37	—	0.88	—	0.79	—	—	—	—	3b	Goodman (1968)
DLL-6	Vouglans Dam	Limestone — oolitic, compact to stylolitic	—	575	0.49	—	6.08	1.68— 4.61	2.78	—	—	—	—	4a	Goodman (1968)
DLL-7	Larouviere — 1965	Marl layers in limestone — sat.	0.1—0.3	605—730	0.47— 0.56	2.16— 3.73	2.84	0.51— 3.73	2.13	—	—	—	—	1.4a	Goodman (1968)
DL- 1	Larouviere — 1964	Marly partings in limestone — sat.	0.1—5.0	51—63	0.24— 0.77	2.16— 3.34	2.74	0.85— 5.69	2.89	—[A]	0	—[A]	38.4	1	Goodman (1968)
DL- 2	Vouglans Dam	Limestone with marly joints — dry	0.025—2.0	28—47	0.49— 1.47	—	—	2.26—23.55	9.75	0.92	0.11	46.6	37.8	1	Goodman (1968)
DL- 3	L'Aquila Meridional Apennine	Sandstone — marl contact	—	—	0.10— 0.98	0.33— 2.08	0.84	0.11— 0.17	0.15	0.20	0.15	45.0	38.0	3	Baldovin (1970)
DL- 4	Brescia Meridional Prealps	Phyllitic schist fractures	—	—	9.20— 1.47	0.41— 0.97	0.65	0.14— 0.40	0.22	0	0	45.0	40.0	3	Baldovin (1970)
DL- 5	B-2 Sarajevo	Limestone — slightly rough bedding	—	1600	0.15— 3.63	0.83— 4.12	2.17	0.20— 1.37	0.84	1.23	0.67	36.9	29.8	3a	Goodman (1968)
DL- 6	B-3 Sarajevo	Limestone — rough bedding surfaces	—	1600	0.30— 3.36	0.33—14.90	5.93	0.25— 7.35	3.06	0.89	0.23	53.5	43.2	3a	Goodman (1968)
DL- 7	D-2 Sarajevo	Limestone — rough unfilled fractures	—	1600	1.52— 4.00	0.24—13.80	8.46	1.26— 2.61	1.98	2.69	0.88	19.0	31.8	3a	Goodman (1968)
DL- 8	Malpasset MIII6	Foliated gneiss and mylonite	4.0—5.0	10.6—24.5	0.39— 2.94	1.46— 4.71	2.56	0.69— 3.69	2.36	1.17	0	53.0	46.3	3a	Goodman (1968)
DL- 9	Delgado — Imperial Col.	Porphyry — dry, natural joint surface	—	500	3.24—10.10	0.96— 1.64	1.30	0.26— 1.94	1.02	0.74	0	39.0	35.5	3b	Goodman (1968)
DL-10	B-1 Sarajevo	Limestone — mylonite along bedding	—	1500	0.21— 2.38	1.04— 8.04	3.90	0.28— 5.69	1.25	0.51	0.29	37.3	35.5	4a	Goodman (1968)
DL-11	Vouglans Dam	Moist marly joint in limestone	1.5—3.0	980—1243	0.53— 2.99	1.18— 3.33	2.65	0.41— 4.71	1.70	0.36	0.08	26.0	25.2	4a	Goodman (1968)
DL-12	B-1 Sarajevo	Limestone — thin shale seams along bedding	—	1500	1.23— 2.80	1.55—13.90	5.96	0.32— 5.33	3.08	0.49	0.49	30.6	30.6	4b	Goodman (1968)
DL-13	Vouglans Dam	Marly joint — sat.	1.3—3.2	1030—1240	0.49— 2.94	0.09— 2.74	1.41	0.02— 1.86	0.78	0	0	23.4	23.4	4b	Goodman (1968)
DL-14	D-1 Sarajevo	Limestone — smooth unfilled fractures	—	1600	0.88— 2.40	0.41— 2.36	1.07	0.20— 1.28	0.51	0	0	38.4	36.3	4c	Goodman (1968)
DL-15	Torino Gran Paradiso Massiccio	Granitic gneiss fractures	—	—	0.20— 0.78	0.29— 0.38	0.33	0.09— 0.12	0.11	0	0	40.0	40.0	4c	Baldovin (1970)
DL-16	Vouglans Dam	Limestone with marly joints — sat.	0.025—0.2	24—40	0.49— 1.47	—	1.47	0.14—31.60	7.41	0	0	55.8	39.6	1.3a 4a,b,c	Goodman (1968)
DIS- 1	1P Krivoklat	Bedding plane in greywacke	0.5—0.8	2265	1.24	—	—	—	0.23	—	—	—	—	4b	Goodman (1968)
DIS- 2	2P Krivoklat	Bedding plane in greywacke	>0.1	3510	1.01	—	—	—	1.21	—	—	—	—	4b	Goodman (1968)
DIS- 3	3P Krivoklat	Bedding plane in greywacke	Closed, clean	3660	0.43	—	—	—	2.26	—	—	—	—	4b	Goodman (1968)
DIS- 4	Vouglans Dam	Marly sand filled joint	0.1—0.2	44000	0.98	—	—	—	2.34	—	—	—	—	4b	Goodman (1968)
DIS- 5	K1 Kurobe IV Dam	Vertical fault	Thick, uneven	—	0.37— 1.07	—	—	0.17— 0.23	0.20	—	—	—	—	4c	Goodman (1968)
DIS- 6	SLL Khajuri Dam	Closely jointed shale zone in limestone	0.2—0.5	50000	0.02[2]	—	—	0.01— 0.02	0.02	—	—	—	—	4c	Goodman (1968)
DIS- 7	SLS Khajuri Dam	Shale interbed — wet	0.2—0.5	50000	0.02— 0.03	—	—	0.01— 0.02	0.02	—	—	—	—	4c	Goodman (1968)
DIS- 8	C-2 Dolesice Dam	Schistosity plane in amphibolite	—	5000	0.12	—	—	—	0.59	—	—	—	—	—	Goodman (1968)
DIS- 9	Jupia Dam	Unbonded basalt — sandstone contact	—	307900	0.13	—	—	—	0.11	—	—	—	—	—	Goodman (1968)
Overall summary or average			Closed — 5.0	5—307900	0.02—10.40	0.09 -14.90	3.02	0.01—31.60	2.82	0.61	0.18	39.3	35.7		

DLL series — laboratory direct shear tests over limited stress range.
DL series — laboratory direct shear tests.
DIS series — in-situ block direct shear tests.

A — data too scattered and/or too little spread.

Avg. Normal stiffnesses, K_n (in GN/m^3) are:
35.1 for DLL-3, 1.98 for DIS-4, 0.24 for DIS-6,
6.26 for DIS-7.

Table 2-5 Summary of values of shear stiffness
(from Kulhway, 1975)

ment curves at constant σ, Hungr and Coates (1978) suggested the possibility of using a hyperbolic function to depict the pre-peak shear behavior of joint. The function must pass through the origin and can therefore be written as

$$\tau = ut/(t-\delta_s) - u \tag{2-31}$$

where u = constant having the dimension of force per length squared

t = constant having the dimension of force per length

δ_s = shear displacement

To define the hyperbola, they selected two additional conditions: a) the function must pass through the yield point, and b) the function must attain its maximum curvature at the yield point. Condition (a), as shown in Fig. 2-22A, yields:

$$\tau_y = ut/(t-\delta_{s,y}) - u \tag{2-32}$$

where τ_y = shear stress at yield point

$\delta_{s,y}$ = shear displacement at yield point

Condition (b), as shown in Fig. 2-22A, can be written as:

$$\frac{d}{d\delta_s}\left[\frac{d^2\tau/d\delta_s^2}{\{1 + (d\tau/d\delta s)^2\}^{3/2}}\right] = 0 \text{ at } \tau = \tau_y \text{ and } \delta_s = b\delta_{s,y} \tag{2-33}$$

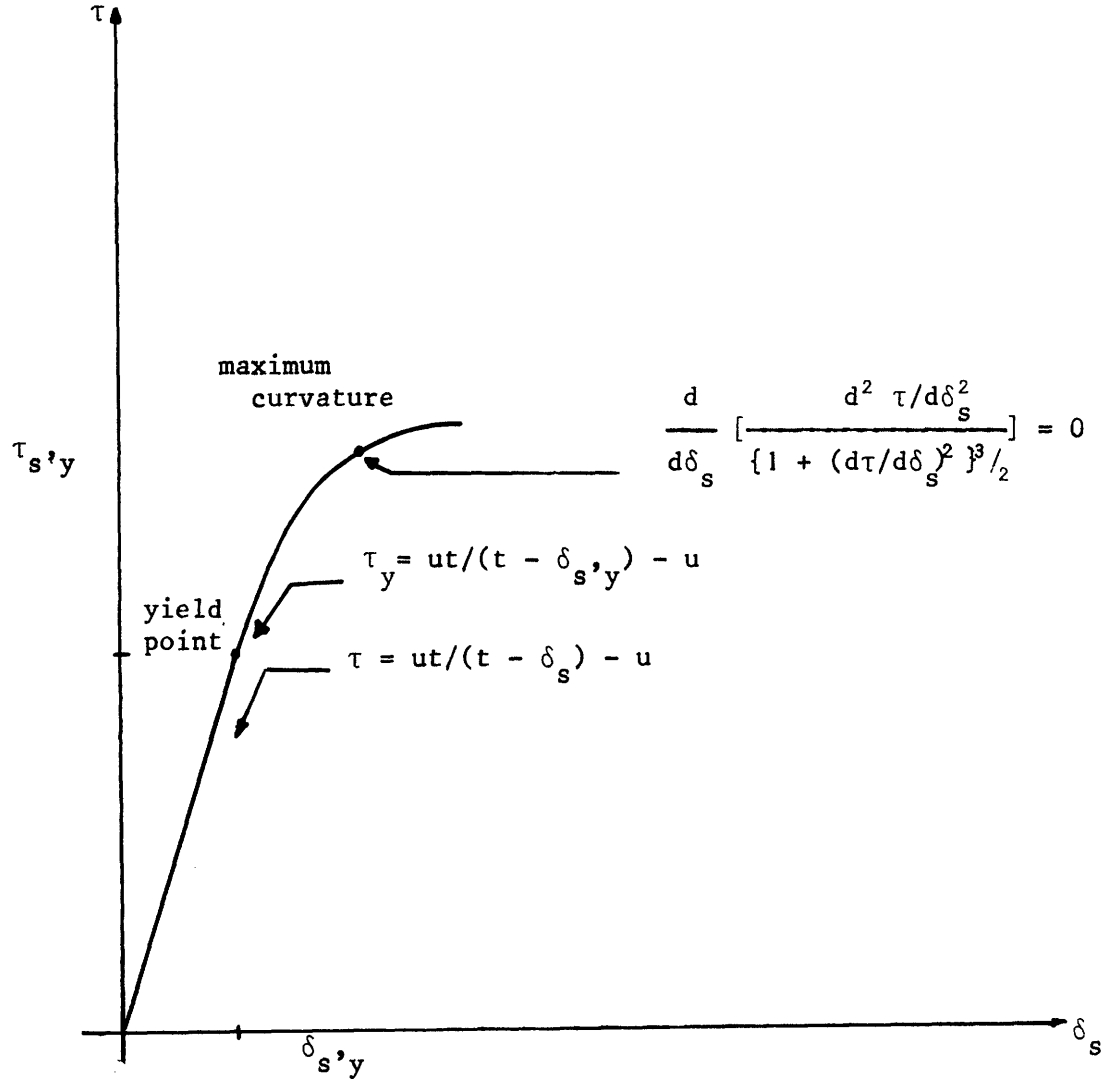

Figure 2-22A Hyperbolic function of $\tau - \delta_s$ curve with conditions (a) at yield point (b) at maximum curvature

where b = scale coefficient equal to the ratio of unit length on stress axis to the unit length on the displacement axis of the test plot.

Solving Eq. 2-32 and Eq. 2-33 give u and t as follows:

$$u = \frac{-\tau_y^2}{\delta_{s,y}\left(\frac{\tau_y}{\delta_{s,y}} - b\right)} \tag{2-34}$$

$$t = \frac{-\tau_y b}{\frac{\tau_y}{\delta_{s,y}}\left(\frac{\tau_y}{\delta_{s,y}} - b\right)} \tag{2-35}$$

τ_y and $\delta_{s,y}$ are dependent variables whose magnitudes are influenced by the applied normal stress σ. It is possible to write

$$k_{s,y} = \tau_y/\delta_{s,y} = a\sigma \tag{2-36a}$$

The relationship of $k_{s,y}$ and σ is shown in Fig. 2-22B, such that

$$\delta_{s,y} = \frac{\tau_y}{a\sigma} \tag{2-36b}$$

a = a coefficient with dimension of length^{-1}

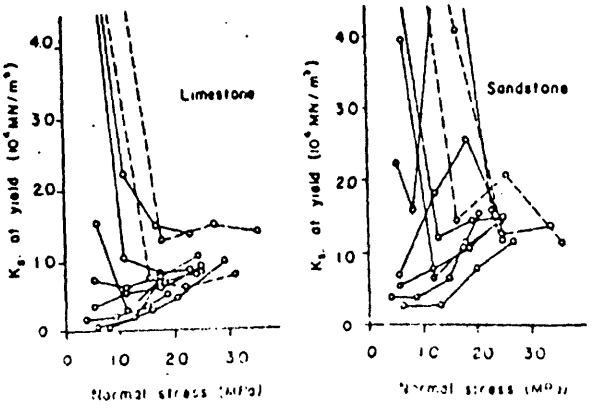

Figure 2-22B Relation between k_s at yield point and σ (from Hungr and Coates, 1978)

Since yield stress τ_y is always lower than the peak stress τ_p, τ_y can be approximated as

$$\tau_y = 0.9\ \tau_p \tag{2-37}$$

τ_p can be approximated as

$$\tau_p = f\sigma \tag{2-38}$$

where f = friction coefficient for certain type of rock

Equation 2-38 can be replaced by any non-linear strength equation. Combining Eq. 2-36, 2-37, 2-38 and substituting into Eqs. 2-34 and 2-35 yields

$$u = -0.9\ af\sigma^2/(a\sigma - b) \tag{2-39}$$

$$t = -0.9\ fb/a\ (a\sigma - b) \tag{2-40}$$

u and t can be substituted into Eq. 2-32. The functional variation of the k_s in relation to either δ_s or τ may be established from Eq. 2-32 as

$$k_s = \frac{\tau}{\delta_s} = \frac{1}{\delta_s}\left(\frac{ut}{t-\delta_s} - u\right) \tag{2-41}$$

Using the above equations, an unique function describing the shear stiffness coefficient k_s of a certain type of joint can be established.

To obtain this unique function, the following procedures can be used:

(1) Get the τ-δ_s plots from direct shear test and establish the point of maximum curvature of the plots. Calculate k_s using Eq. 2-25

(2) Produce plots of $k_{s,y}$ versus σ, as shown in Fig. 2-22B to determine coefficient a

(3) Establish a coefficient of friction or introduce another shear strength criterion into Eq. 2-38

(4) For a given σ, calculate u and t using Eqs. 2-39 and 2-40

(5) Substitute u and t into Eq. 2-32 to obtain the stress-displacement function from which k_s can be determined for any value of τ or δ_s.

The hyperbolic curves given by Eq. 2-32 represent only the pre-peak portion of the stress-displacement relationship. To simulate the post-peak behavior of joints in shear, they must be supplemented by other functions which have to be developed.

2.4 Factors Influence Deformability

In the last section, two functions that describe the normal stiffness and shear stiffness were discussed. This section presents a brief discussion of the important factors that influence the deformability: joint type, test methods, and filler material. These factors affect the shear stiffness more than the normal stiffness.

Joint Type

Goodman (1970) generalized the characteristics of the shear-stress displacement curves for different types of weakness surfaces. The

generalizations are shown in Fig. 2-23. Type 1 curves rise steeply to peak stress at very low deformations and then quickly fall to a residual value. Type 2 curves develop peak stress at very low deformations but do not fall so sharply to the residual value. Type 3 curves show lower stiffness and numerous secondary peaks. The irregularities in the load-deformation curve result from overriding of successive asperities. In types 1-3 it mattered little whether the surfaces are dry or wet. In type 4 curve show the behavior is modified by a change in the water content. Water content reduces stiffness to a great extent. Thin seams show hardening behavior and the ultimate strength is greater than the peak point. Thick seams may have ideal elastio-plastic behavior. Shear stress-displacement curves from laboratory tests may deviate from these generalizations.

Test Methods

The stiffness properties for a joint can be determined experimentally. The problem which arises in all experimental programs is the development of independent experimental laboratory techniques which produce results comparable to each other and are repeatable. Rosso (1976) generated comparable stiffness values for direct shear test and triaxial test for a similar shale. He also ran in-situ test on quartz diorite. The laboratory test results are also compared with those of in-situ test. Table 2-6 shows the comparison of these values for direct shear test, triaxial test and in-situ test. The results of these three experimental methods compare quite well.

The shear stiffnesses presented in Table 2-6 not only vary due to

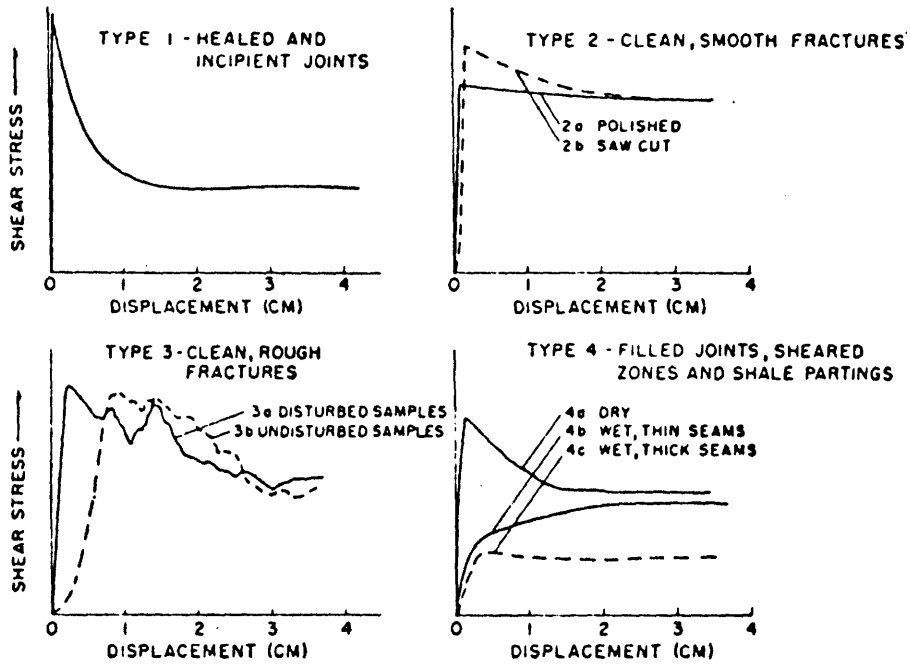

Type	Type of Surfaces Typically Exhibiting Behavior in This Class
1	Healed joints and incipient joints
2	Clean, smooth fractures
	2a polished
	2b unpolished (rough saw cut)
3	Clean, rough fractures
	3a artificial extension fractures and disturbed samples
	3b undisturbed samples
4	Filled joints, sheared zones, shale partings, and smooth bedding
	4a dry or slightly moist
	4b wet; thin seam
	4c wet; thick seam

Figure 2-23 Effect of joint type on deformation of rock joints (from Goodman, 1970)

SHEAR STIFFNESS					
Direct Shear		Jointed Triaxial		*In Situ*	
σ_n bars	K_s Kb/cm	σ_n bars	K_s Kb/cm	σ_n bars	K_s Kb/cm
35	4.3±.5	10-27	2.2±1	0-12	1.6±1
70	4.9±.5	35-85	3.3±1.5	0-28	1.2±1
105	7.6±.5	70-180	9.5±3	0-63	4.8±1.5

Table 2-6 Comparison of shear stiffness for direct shear test, triaxial test, in-situ test (from Rosso, 1976)

the parameters such as rock type, joint type, roughness, etc., but also due to differences between testing techniques. The stress paths were not the same for all three methods because of the loading technique used in the jointed triaxial and in-situ tests. During the direct shear test normal stress σ_n across the joint surface is held constant throughout the test. For the other two tests, σ_n increased along with τ until slip occured. The other differences include the difference between joints in quartz diorite tested in-situ and the joints in shale tested in the laboratory.

Filler Material

The effect of filler material on shear strength of rock joints has been discussed earlier; filler also affects the deformability of a rock joint. Goodman (1920) carried out studies on the effect of joint filling thickness on the joint deformability. The results, as shown in Fig. 2-24, indicate that, for the type of joint tested, the stiffness of the filled joint was twice that of the filling material alone. Ladanyi and Archambault (1975) ran tests on model (concrete bricks) material with clay filling. They showed that for thickness of clay filling up to 60 percent, which is the ratio of thickness of filling material to the height of asperities, the joints of the model materials show a locking character in shear, i.e. their rigidity increases with the displacement. For medium filling thickness (30 to 60%), clay filled joints show first a distinct yield point in shear at a small displacement, and the peak strength at a much larger displacement, (see Fig. 2-25).

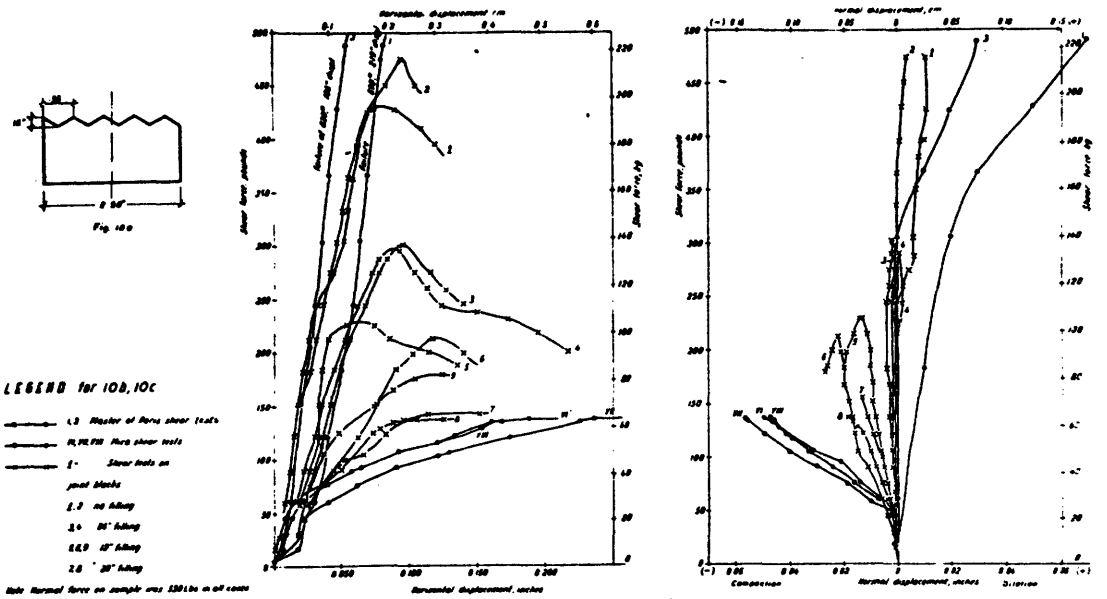

Load-deformation curves for direct shear tests on mica-filled joints.

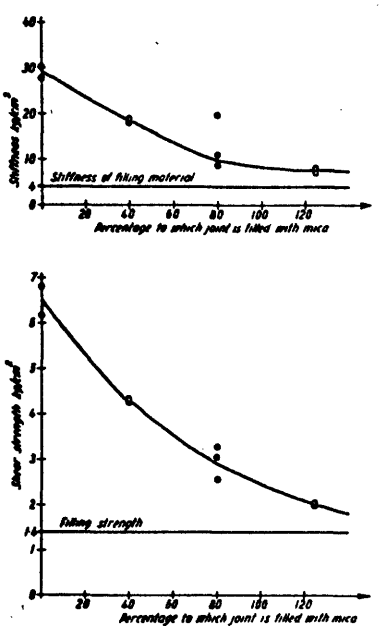

Effect of thickness of joint filling on stiffness and strength.

Figure 2-24 Effect of joint filling on rock joint behavior (from Goodman, 1970)

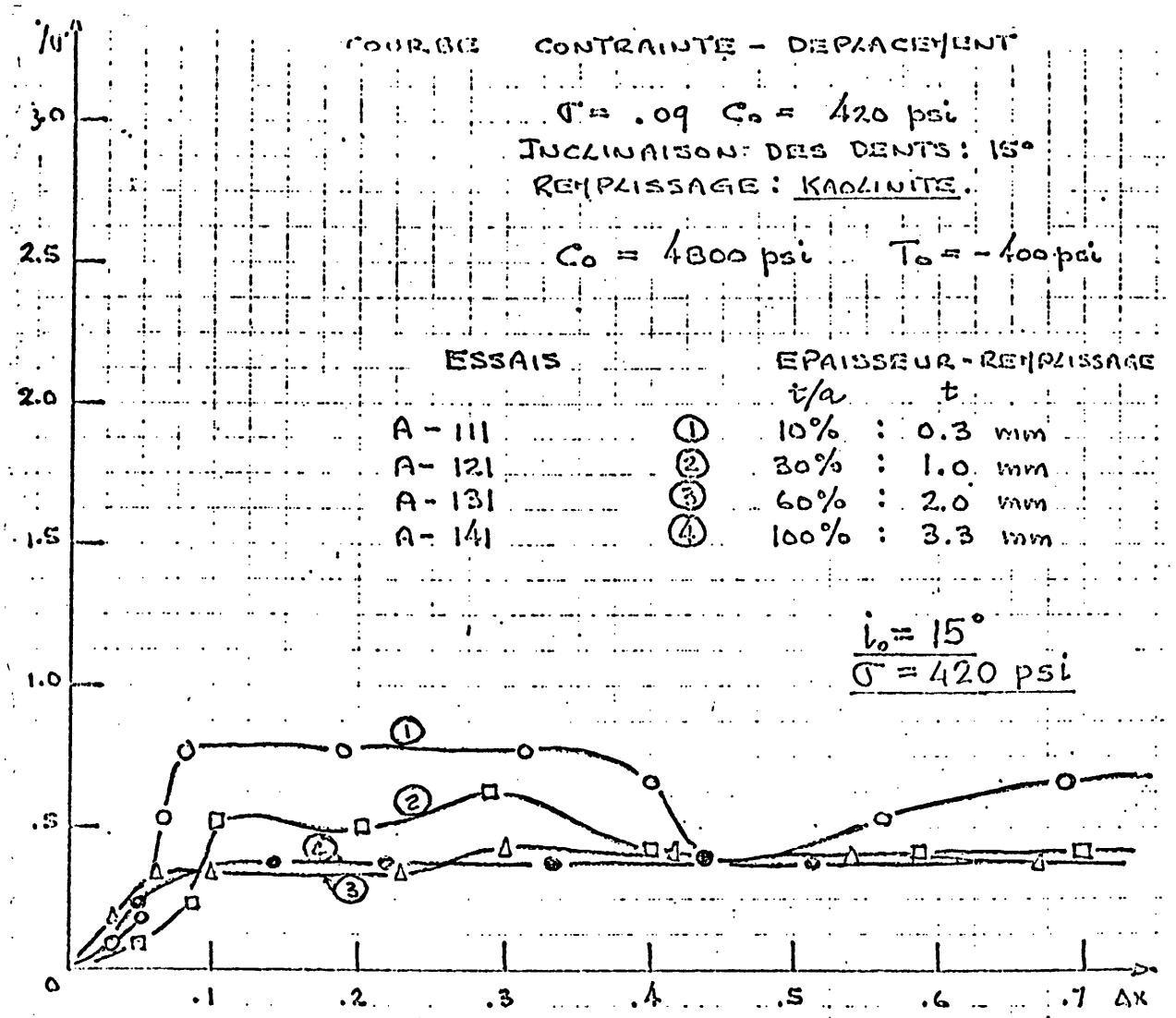

Figure 2-25 Deformation curves for clay filled joint (from Ladanyi and Archambault, 1975)

Description of shear strength and deformability of rock joints in this chapter provides background to develop the model for the stress-displacement behavior. This model is presented in Chapter 3.

CHAPTER 3

MODEL DESCRIPTION AND DATA MANAGEMENT

An extensive set of stress-displacement test data on rock joints was collected from a variety of sources. A model for the stress-displacement behavior was then developed; the model reduces these test data to a group of descriptive parameters for storage using a computer program; the computer system then retrieves these parameters for statistical analysis conditional on a variety of rock-mass characteristics.

3.1 Model Description

The behavior of rock joints may be described in terms of stresses and relative displacements, normal and tangential, to a joint plane. Descriptive parameters used to model this behavior are defined and illustrated in this section.

There are three modes of stress-displacement behavior. The first mode of behavior is relative shear displacement due to changes in shear stress only. The second mode of behavior is relative normal displacement due to changes in normal stress only. The third mode of behavior is relative normal displacement due to relative shear displacement.

Some modes--especially the second--are not always recorded. Moreover, the measurements are usually not continuous, but occur at discrete points. Smooth curves are drawn through these discrete data points, from which the descriptive parameters are then derived.

Mode of Shear Stress-Shear Displacement

From a complete shear stress-relative shear displacement diagram (see Fig. 3-1), the following descriptive parameters can be derived.

τ_p = peak maximum shear stress at a given normal stress, $(\sigma_n)_p$, at small relative shear displacement, $(\delta_s)_p$.

τ_r = residual shear stress at a given normal stress $(\sigma_n)_r$, constant or mean value of shear stress at large relative shear displacement; i.e. $(\delta_s)_r$. In order to estimate a mean residual shear stress, in case of varying shear stress τ at large relative shear displacements, it is assumed that this variation approximates a sine curve. One must be able to identify at least one trough and one peak, otherwise it is not possible to estimate the mean residual shear stress τ_r. (See Fig. 3-2.)

$(k_s)_e$ = elastic shear stiffness, defined as the change in shear stress over the change in elastic relative shear displacement:

$$(k_s)_e = \frac{\Delta\tau}{\Delta(\delta_s)_e} \qquad (3\text{-}1)$$

where the behavior is assumed to be in the elastic range prior to the peak and can be identified in general as the steepest straight-line portion of the τ-δ_s curve.

$(k_s)_p$ = peak shear stiffness, defined as the change in shear stress over the change in relative shear displacement from

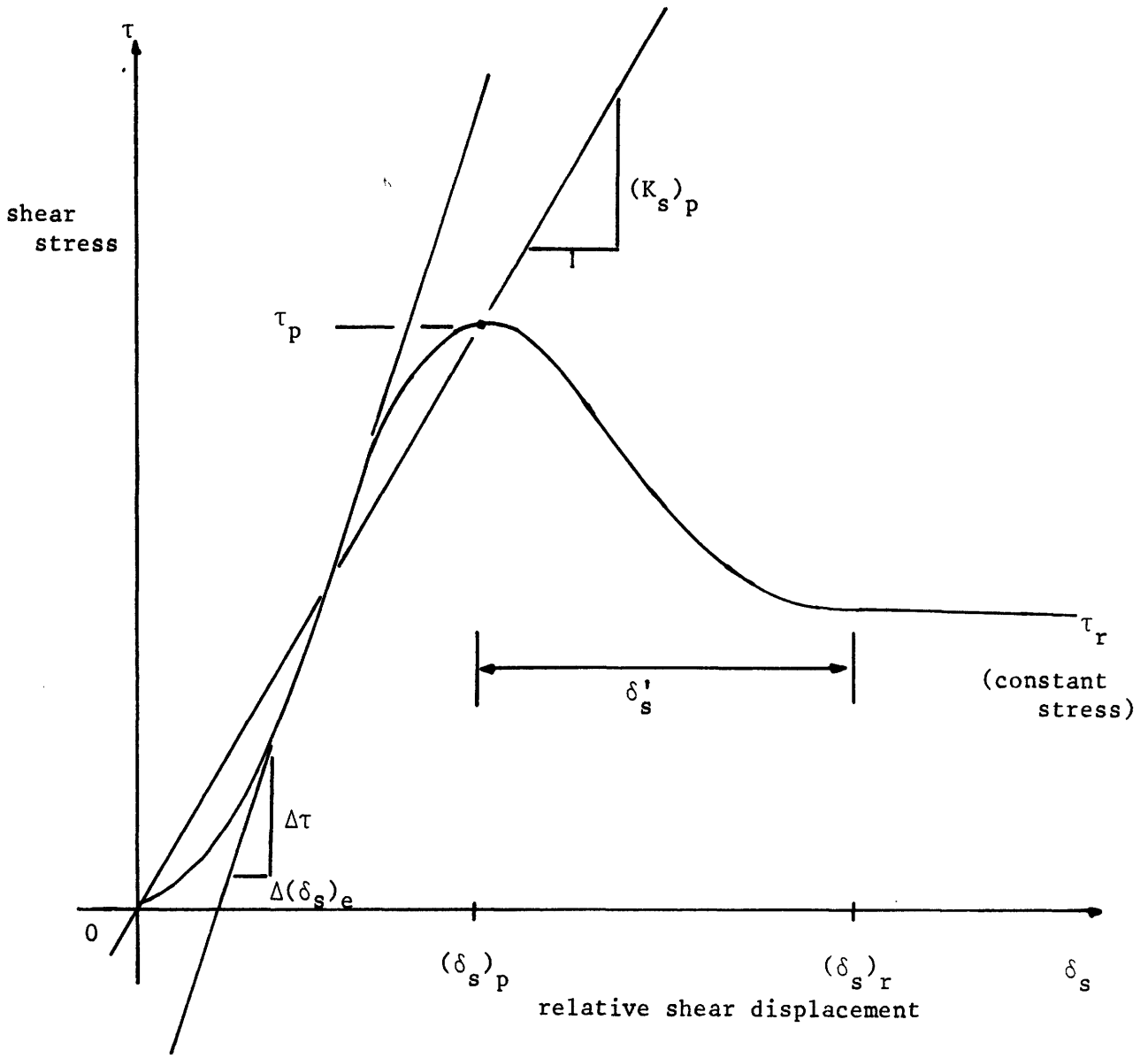

Figure 3-1 Shear stress-relative shear displacement diagram with constant residual value

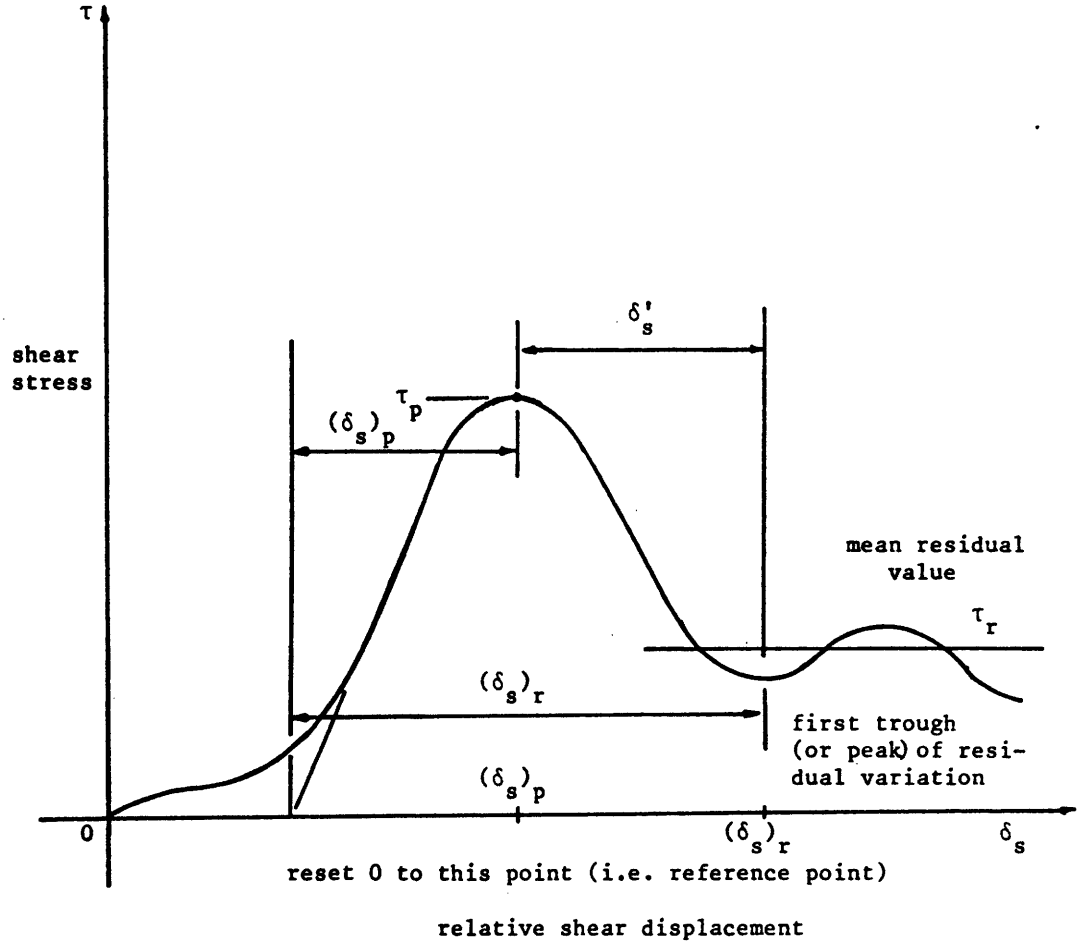

Figure 3-2 Shear stress-relative shear displacment diagram with oscillating residual value

beginning to peak:

$$(k_s)_p = \frac{\tau_p}{(\delta_s)_p} \tag{3-2}$$

Since displacements are relative to an initial state, i.e. δ_{so} at $\tau = 0$, the zero point--or reference displacement δ_{so}--may have to be adjusted for excessive prior relative shear displacements; see Fig. 3-2.

δ_s' = shear degradation distance, defined as the change in relative shear displacement from peak to residual conditions:

$$\delta_s' = (\delta_s)_r - (\delta_s)_p \tag{3-3}$$

Here the residual condition is identified as the constant or mean shear stress at large relative shear displacements; if the mean residual shear stress is used, it is assumed that $(\delta_s)_r$ corresponds to the first peak or trough of the residual variation; see Fig. 3-2.

$(\sigma_n)_p$ = normal stress occurring at peak conditions

$(\sigma_n)_r$ = normal stress occurring at residual conditions

Note that $(\sigma_n)_r$ can be equal to $(\sigma_n)_p$.

Mode of Normal Stress - Normal Displacement

The following descriptive parameters can be evaluated from a complete normal stress-relative normal displacement diagram, as in Fig. 3-3:

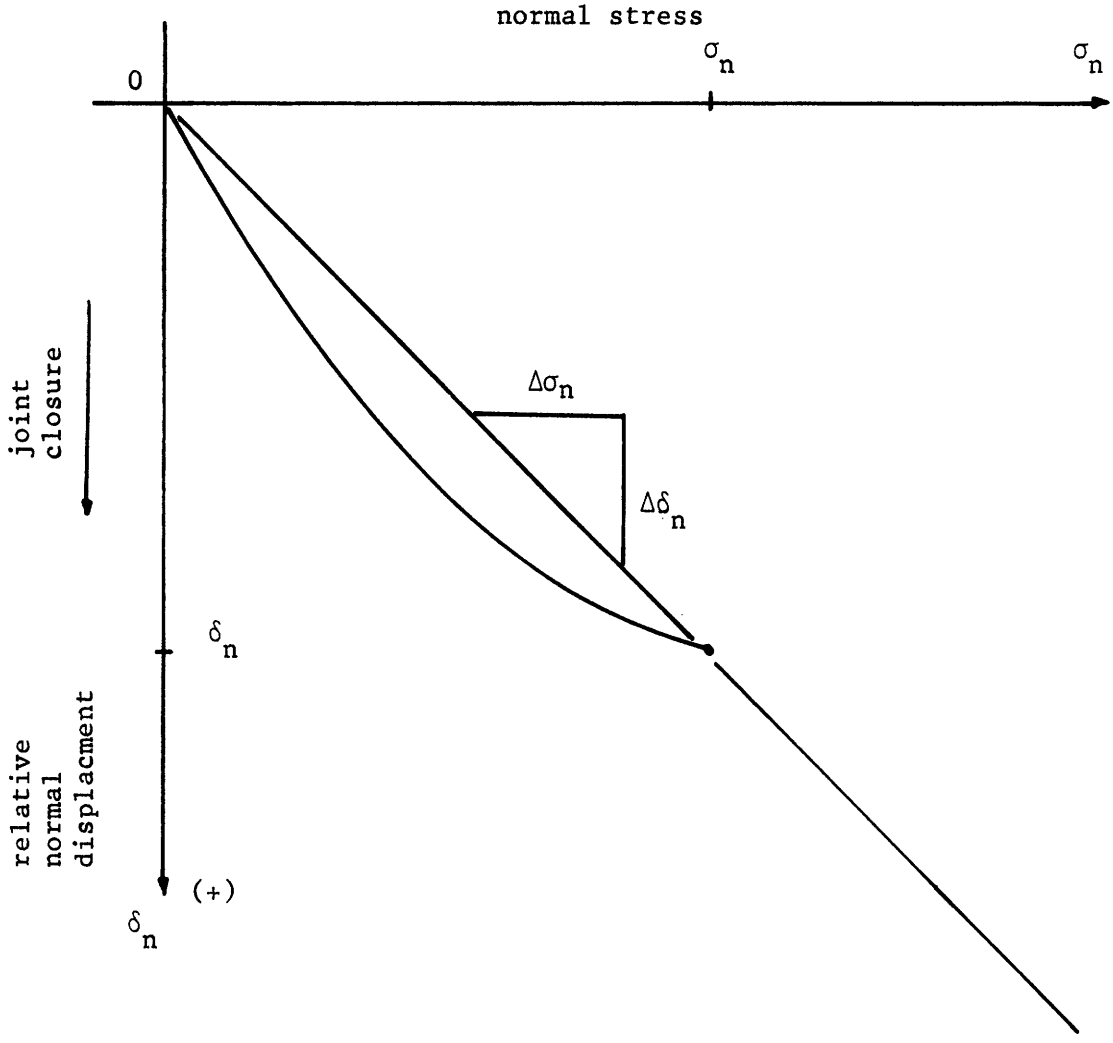

Figure 3-3 Normal stress-relative normal displacement diagram

k_n = secant normal stiffness at a given normal stress, defined as the change in normal stress, i.e. $\Delta\sigma_n = \sigma_n$, over the change in relative normal displacement, i.e. $\Delta\delta_n = \delta_n$, (where joint closure is positive) from beginning to end:

$$k_n = \frac{\Delta\sigma_n}{\Delta\delta_n} = \frac{\sigma_n}{\delta_n} \tag{3-4}$$

Since displacements are relative to an initial state, i.e. δ_{no} at $\sigma_n = 0$, the zero point--or reference displacement, δ_{no}--may have to be adjusted for excess prior relative normal displacements; it is analagous to shear behavior as depicted in Fig. 3-2. Note that joint closure is positive.

Mode of Shear-Normal Displacement (Dilation)

From a complete relative shear-normal displacement diagram as in Fig. 3-4, the following descriptive parameters can be derived.

δ_n' = normal dilation distance, defined as the change in relative normal displacement, i.e. $\Delta\delta_n = \delta_n'$, where joint openning is negative, which occurs when the shear stress τ changes from its initial state to residual condition as depicted in Fig. 3-1, and is not due to changes in normal stress, i.e. $\Delta\sigma_n = 0$:

$$\delta_n' = \delta_n - (\delta_n)_r \tag{3-5}$$

The residual conditions, $(\delta_n)_r$, occurs as does residual stress, where the mean residual value α_r of the $\delta_n - \delta_s$

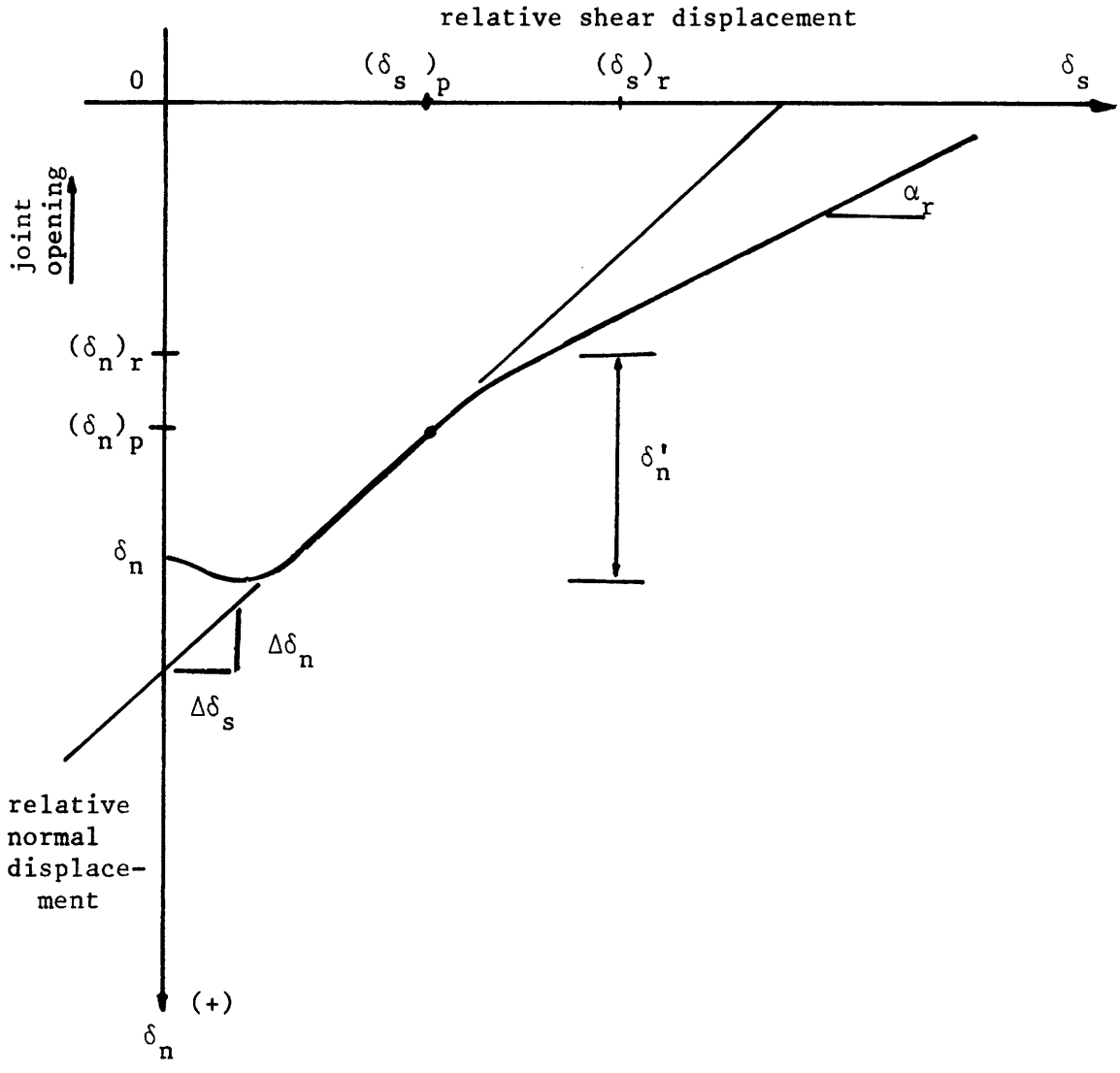

Figure 3-4 Relative shear-normal displacement (dilation)

curve becomes parallel to the inclination α of the joint plane, i.e. at $\delta_s = (\delta_s)_r$ as shown in Fig. 3-5A.

$(\delta_n/\delta_s)_p$ = peak dilation rate defined as the ratio of the change in relative normal displacement, i.e. $\Delta\delta_n$, not due to changes in normal stress, i.e. $\Delta\sigma_n = 0$, to the change in relative shear displacement, i.e. $\Delta\delta_s$, at peak conditions:

$$(\delta_n/\delta_s)_p = \frac{\Delta\delta_n}{\Delta\delta_n} \tag{3-6}$$

where the ratio is obtained by measuring the slope of the curve at peak conditions, i.e., $(\delta_s)_p$, $(\delta_n)_p$. Note that positive ratio indicates closing; negative ratio indicates opening.

In addition to all the parameters discussed above, the characteristics of the intact material, joint geometry, filler material and test are also defined.

Test Conditions

The following information is needed to describe testing.

The TEST TYPE is defined as the type of test: for example, the direct shear test.

The MODIFICATION OF TEST is defined as the additional information about the test run, such as the use of the portable shear box.

A is the area of joint surface tested.

$\dot{\delta}_s$ is shear displacement rate of test.

T is temperature ($T^{o}F$) at which the test is run.

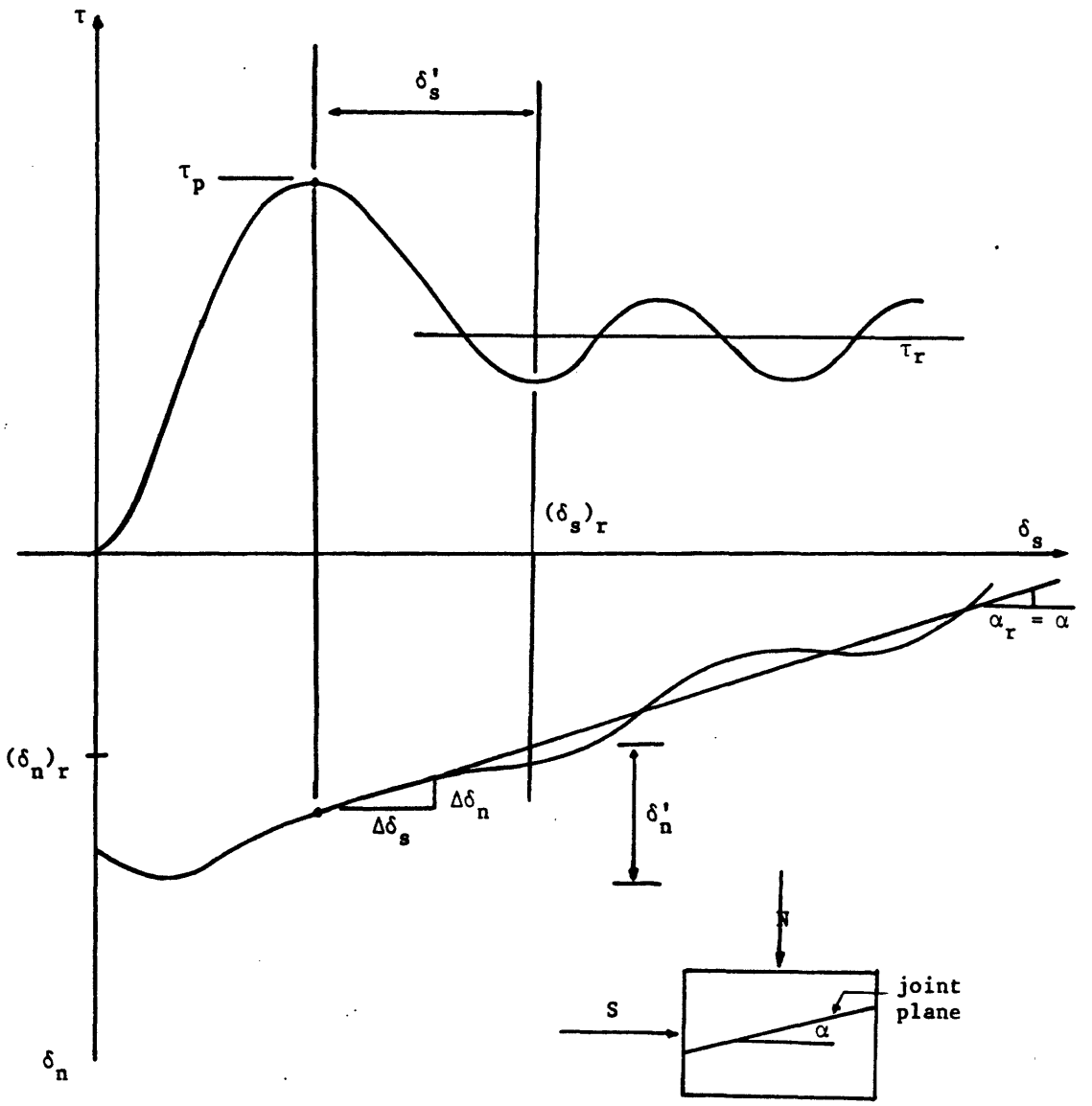

Figure 3-5A Variant normal-shear behavior

Test Rock Specimen Information

Test rock samples can be described by using the following information.

BLOCK is defined as the top or bottom test specimen block for which the description of intact rock and anisotropic features is obtained.

The VOLUME OF BLOCK (%) is defined as the volume of the block (top or bottom) as a percentage of the volume of the entire test rock specimen.

The INTACT ROCK DESCRIPTION is represented by a characterization of its basic composition and of less prominent parts, e.g. Gneiss, Hornblende, Biotite, Garnet. Gneiss is the basic composition, the other three are less prominent ones.

FORMATION is the location from where the test specimen is obtained.

ANISOTROPIC FEATURES is defined as those features like bedding, banding, or foliation in rock sample.

$\beta 1$ defines the orientation of the anisotropic features with respect to the test direction as shown in Fig. 3-5B.

Material Properties of Intact Rock or Joint Filler Material

The following parameters are required to describe the material properties of intact rock or filler material.

E = Young's modulus of elasticity

G = shear modulus of elasticity

V = Poisson's ratio

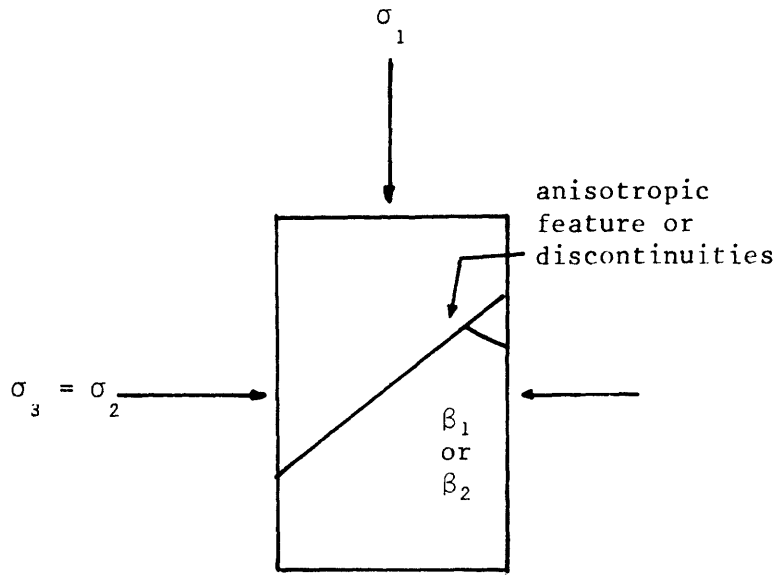

β_1 with respect to longitudinal axis for triaxal test

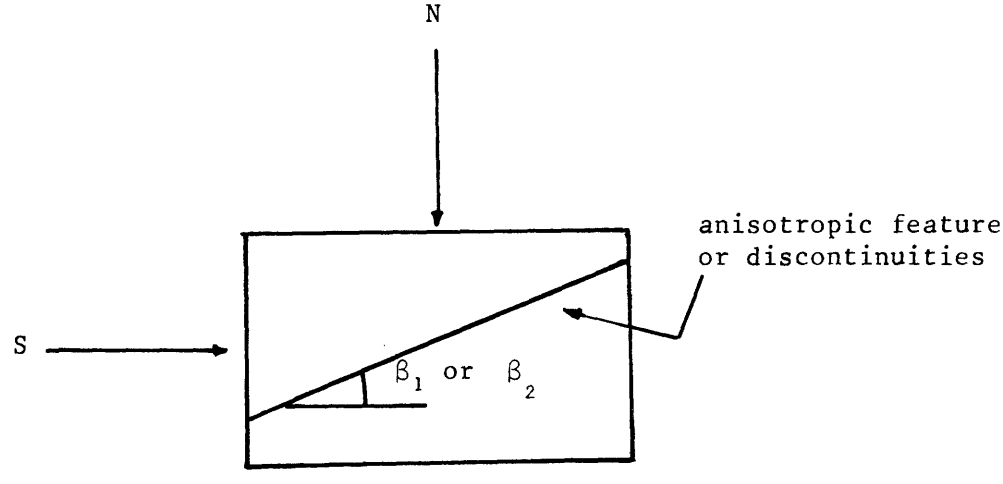

β_1 with respect to horizontal axial for direct shear test

Figure 3-5B Orientations of anisotropic features and discontinuities

γ = density (dry or wet)

σ_c = unconfined compressive strength

σ_t = uniaxial tensile strength

Discontinuity Information

Discontinuity description is furnished by the following information.

$\beta 2$ is the orientation of joint with respect to test condition as shown in Fig. 3-5B.

PERSISTENCE indicates the degree of separation of intact rock in a discontinuity or "the continuity of discontinuities" as represented in Fig. 3-6 and is defined as:

$$\text{persistence} = \sum_{i=1}^{n} \frac{\ell_i}{\ell}$$

$$= \sum_{i=1}^{n} \frac{a_i}{A} \qquad (3\text{-}7)$$

where n is the total number of individual joints elements

Persistence indicates whether the joint plane is continuous or not.

JOINT WIDTH is defined as the distance between the joint surfaces. Its numerical values denote the tightness ("open or closed") of the joint.

The CORRELATION OF JOINT SURFACES is defined as the degree of matching or degree of contact area of joint surface as shown in Fig. 3-7. It is expressed as the ratio of matched area to the total joint surface area.

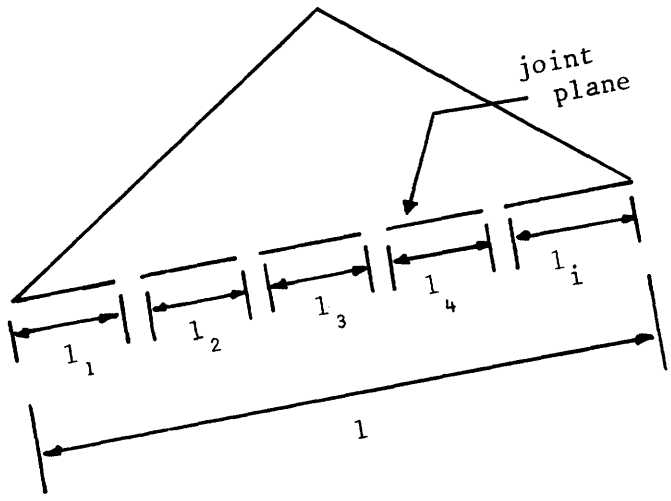

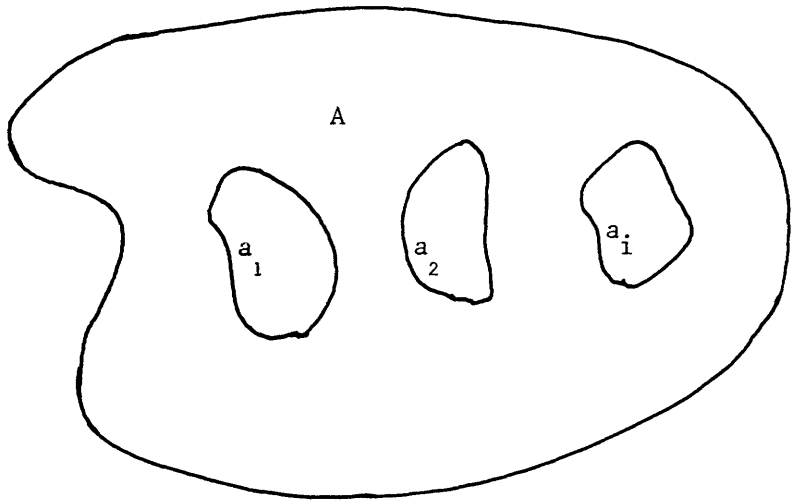

l_i - length of individual joint
l - length of joint plane
a_i - area of individual joint
A - area of joint plane

Figure 3-6 Diagram of persistence.

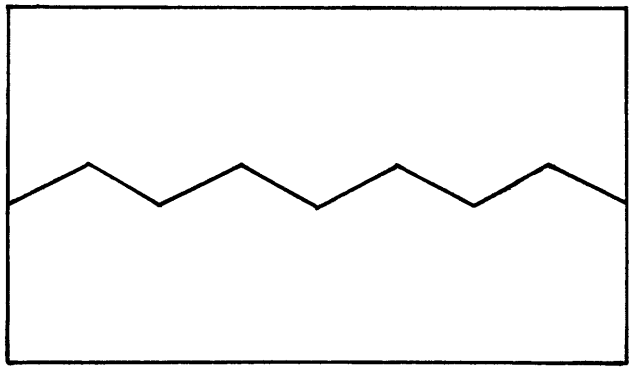

joint surfaces matched (100%)

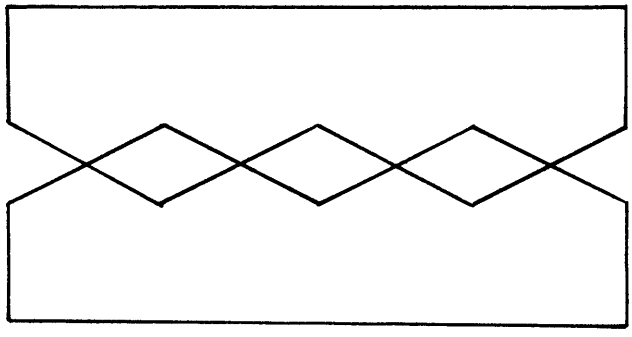

joint surfaces not matched (0%)

Figure 3-7 Correlation of joint surfaces

The UPPER OR LOWER SURFACE DESCRIPTION describes the joint surfaces in a qualitative sense, i.e. rough, polished, clean, etc.

MOISTURE is defined as wetness of the joint surfaces. It is expressed as dry or wet.

Surface Material

Surface material can be described by the following information.

BLOCK is defined as the top or bottom test specimen block for which surface material is described

The AREA OF BLOCK (%) is defined as the joint surface area of the block (top or bottom) as a percentage of the total joint surface area of the test rock specimen.

The SURFACE MATERIAL DESCRIPTION is represented a characteristic of its basic mineral composition and of the less prominent parts, e.g. quartz, chlorite, muscovite, or epidote. Quartz is the basic composition, the other three are less prominent ones.

Surface Geometry Description

The surface geometry may be characterized by these parameters:

H = height of asperities

i_s = inclination of asperities in the direction of shearing

i_p = inclination of asperities in the direction perpendicular to that of shearing

δ_{rs} = base width of asperities in the direction of shearing

δ_{rp} = base width of asperities in the direction perpendicular to that of shearing

Joint Filler Material

The VOLUME OF FILLER MATERIAL (%) is defined as the amount of volume of filler material as a percentage of the whole volume of test block.

The FILLER MATERIAL is represented by its composition from basic one to the less prominent ones, e.g. clay, sand, silt. Clay is the basic composition, the rest are the less prominent ones.

Compiled Test Results

They are the data from a series of strength tests as depicted in a Mohr diagram, as in Fig. 3-8B. Fig. 3-8B represents the dotted line portion in Fig. 3-8A.

$(\sigma_n)_L$ = lower limit of normal stress for which the cohesion (c), friction angle (ϕ) characterizing the Mohr envelope are applicable.

$(\sigma_n)_H$ = upper limit of normal stress for which the c, ϕ parameters characterizing the Mohr envelope are applicable.

C_p = cohesion, or shear intercept, of peak Mohr envelope

ϕ_p = friction angle or inclination of peak Mohr envelope

C_r = cohesion, or shear intercept of residual (or ultimate) Mohr envelope

ϕ_r = friction angle, or inclination of residual (or ultimate) Mohr envelope

$(\delta_n/\delta_s)_{pave}$ = average value of the dilation rate corresponding to each of the data points in Fig. 3-8.

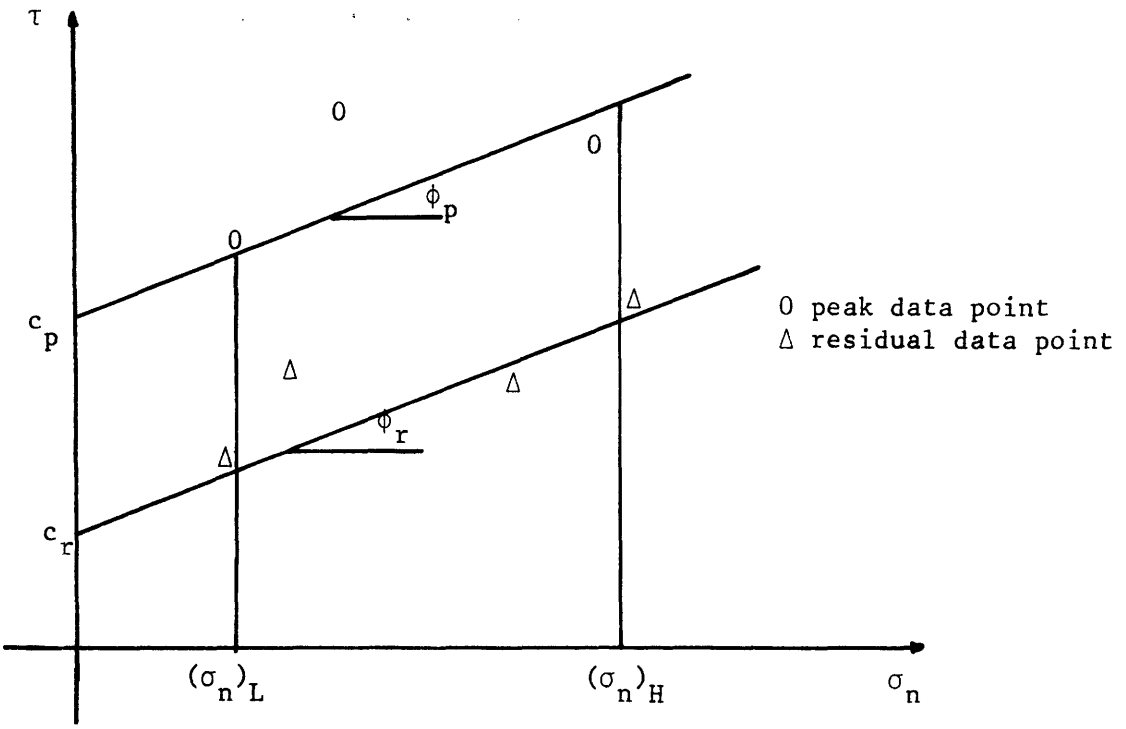

Figure 3-8B Compiled test data diagram (Mohr diagram) for a certain range of normal stress

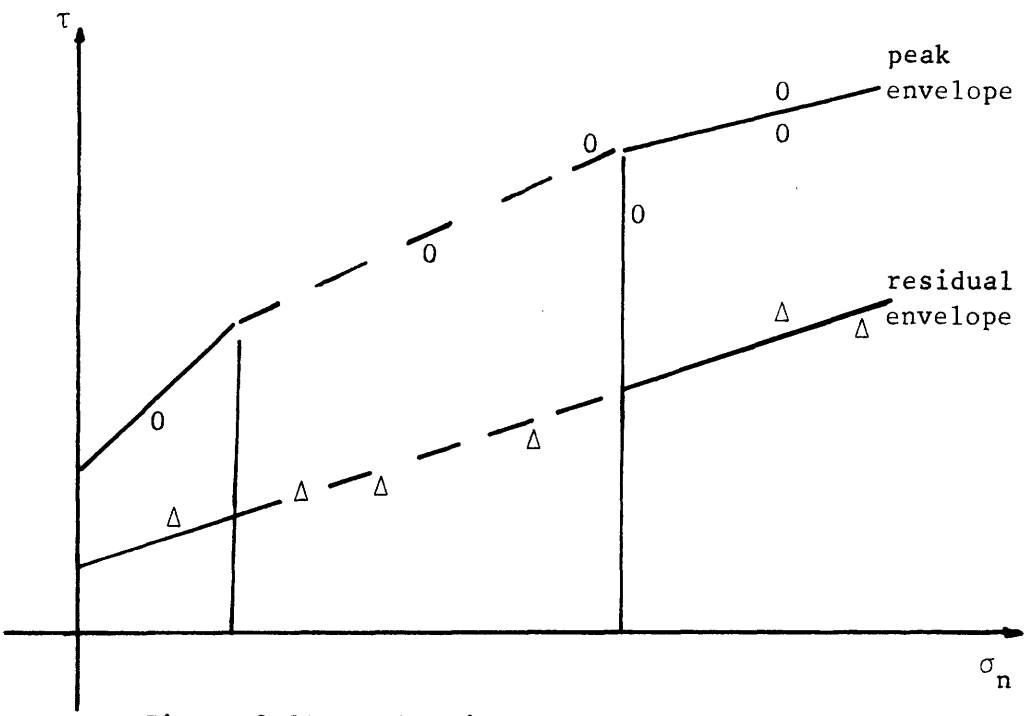

Figure 3-8A Mohr diagram for all stress ranges

3.2 File Description

All the parameters and information discussed in the previous section can be assembled into matrix form or files. These parameters and information are stored in the appropriate files by a developed program. The structure of the program is described in the next section. The formate of these files with appropriate parameters and information are listed in Fig. 3-9.

Each row of parameters or information is identified by the name of source, series number, test number and miscellaneous number, which are stored in the first four columns of each file. If there are more parameters or information to be stored than the available storage space in one row in a file, these additional parameters have to be stored in the next row. In order to identify this row of information as the continuation of the previous one, an identification number called the described number is created automatically by the program to serve this purpose, and is stored in the fifth column of the file.

There are twelve files to store the data; these are names files A, B, C, D, I, L, N, P, Q, R, S, T. An extra File K is created to keep track of how many times each file has been stored. File A is used to store information of joint filler material. File B is used to store information on material properties of joint filler material. Several pairs of columns are available for name of material property and its numerical value. Compile test results are stored in File C. Discontinuity information is stored in File D. All the parameters that describe the stress displacement of rock joints are stored in File I.

File A

Identification						Joint Filler Material Description			
Source	Series No.	Test No.	Misc. No.	Described No.	% Vol.	Basc Comp.	1st	2nd	3rd
1	2	3	4	5	6	7	8	9	10

NOTE: Numbers in each file represent the column number

File B

Identification					Filler Material Properties							
Source	Series No.	Test No.	Misc. No.	Described No.	Name of Proper.	Value	Name of Proper.	Value	Name of Proper.	Value	Name of Proper.	Value
1	2	3	4	5	6	7	8	9	10	11	12	13

File C

Identification				Compiled Test Results							
Source	Series No.	Test No.	Descr. No.	$(\sigma_n)L$	$(\sigma_n)H$	C_p	ϕ_p	C_r	ϕ_r	$(\delta_n/\delta_s)p$ ave.	Joint Type
1	2	3	4	5	6	7	8	9	10	11	12

File D

Identification					Discontinuity Description												
					Persistence		Joint Width		Corr. Bet. Surf.		Upper Surf. Descrp.			Low Surf. Descrp.			
Source	Series No.	Test No.	Misc. No.	Joint Orient w.r.t. Test β_2	Cont. Descr.	Value	Tight-ness Descr.	Val.	Match Descr.	Val.	Basic	1st	2nd	Basic	1st	2nd	Moisture
1	2	3	4	5	6	7	8	9	10	11	12	13	14	15	16	17	18

Figure 3.9 Format of Files

File I

Identification				Individual Test Results (Stress-Displacement Parameters)										Joint
Source	Series No.	Test No.	Misc. No.	$(\sigma_n)_p$	τ_p	$(\sigma_n)_r$	τ_r	$(k_s)_e$	$(k_s)_p$	δ'_s	k_n	δ'_n	$(\delta_n/\delta_s)_p$	Joint Type
1	2	3	4	5	6	7	8	9	10	11	12	13	14	15

File K

No. of times each file is stored											
File I	File C	File L	File N	File T	File R	File P	File D	File S	File Q	File A	File B
1	2	3	4	5	6	7	8	9	10	11	12

File L

Identification				List of Individual Test			
Source	Series No.	Test No.	Descr. No.	Misc. No.			
				Misc.1	Misc. 2	Misc. 3	Misc. 4
1	2	3	4	5	6	7	8

File N

Identification				Ident. of the Previous Test			
Source	Series No.	Test No.	Misc. No.	Source	Series No.	Test No.	Misc. No.
1	2	3	4	5	6	7	8

Figure 3.9 (Cont'd) Format of Files

File P

Identification					Material Properties of Intact Rock							
Source	Series No.	Test No.	Misc. No.	Descr. No.	Name of Prop.	Value	Name of Prop.	Value	Name of Prop.	Value	Name of Prop.	Value
1	2	3	4	5	6	7	8	9	10	11	12	13

File Q

Identification					Quantified Surface Geometry				
Source	Series No.	Test No.	Misc. No.	Descr. No.	H	Direction of Shear		Perpen. to Shear Dire.	
						i_s	δ_{rs}	i_p	δ_{rp}
1	2	3	4	5	6	7	8	9	10

File R

Identification							Testing Rock Block Description						Anistp. Feat.	
Source	Series	Test	Misc.	Descr.	Block	% Vol.	Basic Comp.	1st Comp.	2nd Comp.	3rd Comp.	4th Comp.	Form.	Anis. Feat.	Orient wrt test
1	2	3	4	5	6	7	8	9	10	11	12	13	14	15

File S

Identification							Surface Material Description				
Source	Series No.	Test No.	Misc. No.	Descr. No.	Block	% Area	Basic Comp.	1st Comp.	2nd Comp.	3rd Comp.	4th Comp.
1	2	3	4	5	6	7	8	9	10	11	12

Figure 3.9 (Cont'd) Format of Files

File T

				Test Condition Parameters				
Source	Series No.	Test No.	Misc. No.	Test Type: Basic Type	Test Type: Modif.	Surf. Area A	Shear-Disp. Rate $\dot{\delta}_s$	Temp T
1	2	3	4	5	6	7	8	9

Figure 3.9 (Cont'd) Format of Files

In File L, columns five to eight are used to store the "miscellaneous number" of each individual test, which form the compiled test results, as shown in Fig. 3-8. When the information of an individual test has already been described by a previous test, the identification of this previous test is stored in File N, columns five through eight. File P is used to store the material properties of intact rock. Several pairs of columns are available for name of material property and its numerical value in this file. Information on joint surface geometry is stored in File Q. Information on test rock specimen is stored in File R. Joint surface material and test condition are stored in File S and File T, respectively. Examples of these stored files are listed in Appendix A.

3.3 Structure of Program

The parameters and information described before are derived from the data supplied by different sources, e.g. Dames & Moore, Goldberg, Zoino & Dunnicliff, etc. A computer program was developed to direct different parameters, which are typed in from a computer terminal, to be stored in the appropriate file. A simplified flow-chart is listed on Fig. 3-10.

Program Structure

The computer program is developed to store either individual test results or compiled test results, as shown in Fig. 3-10. For the compiled test results, information on these results and the miscellaneous numbers of each individual test which form the compiled test results are stored, respectively. For individual test data, the program is

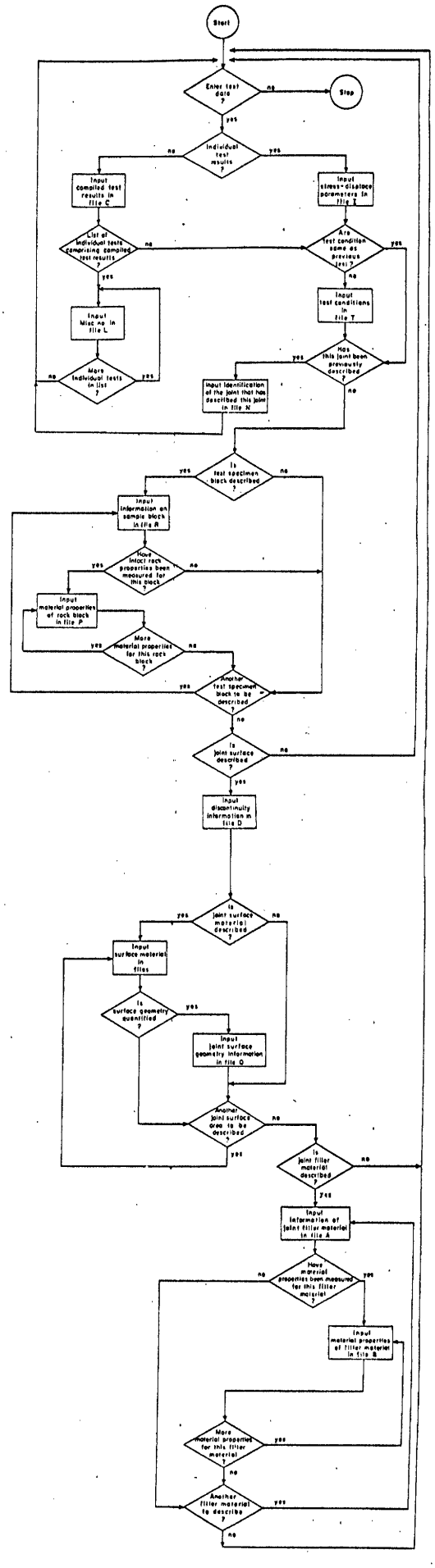

Fig. 3.10 Simplified flow-chart

structured to store, in order, information on stress-displacement behavior, test conditions, test specimen block, joint surface, joint surface material, joint surface geometry, and joint filler material.

A. Structure of Compiled Test Results Segment

All the information on compiled test results are stored in File C, as shown in Fig. 3-9 and Fig. 3-11. If there is a list of individual test results that comprise the compiled test results, the miscellaneous number of each individual test is stored in File L.

B. Individual Test Results

Structure of Parameters of Stress-Displacement Behavior and Test Condition Segment

For individual test results, as represented in Fig. 3-12, the parameters which describe the stress-displacement behavior of an individual joint are stored in File I. Next, the test condition of the joint is considered. If the test condition of the joint is different from that of the previous joint, information of the test condition of this joint is stored in File I. In addition, it is necessary to check if this joint has been previously described by another joint. If so, identification of the previous joint are stored in File N. Otherwise, description of the test specimen block has to be checked.

Structure of Test Specimen Block Segment

If the description of a test specimen block and the material properties of the intact rock are available, they are stored in File R and File P, respectively, as shown in Fig. 3-13. If not,

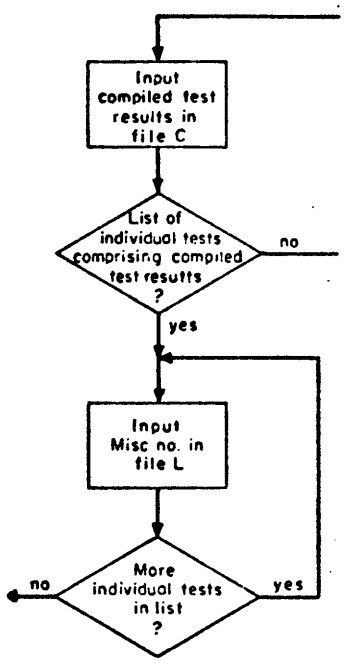

Figure 3-11 Structure of Compiled Test Results segment

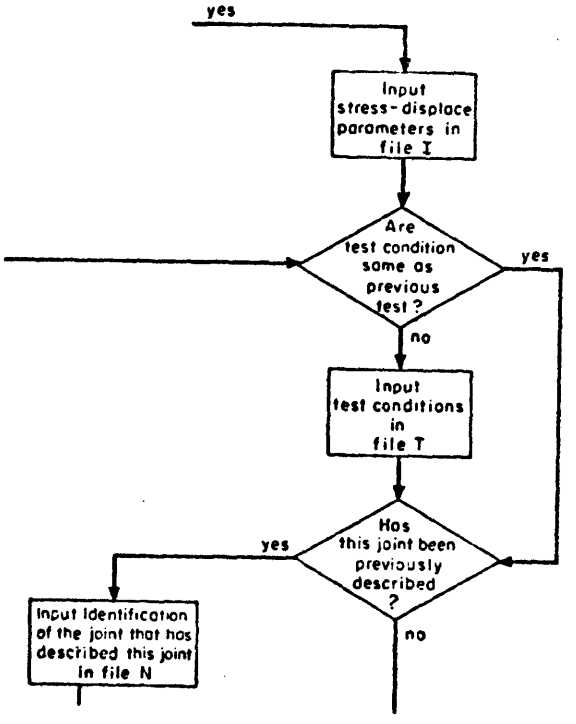

Figure 3-12 Structure of Stress-displacement Behavior and Test Condition Segment

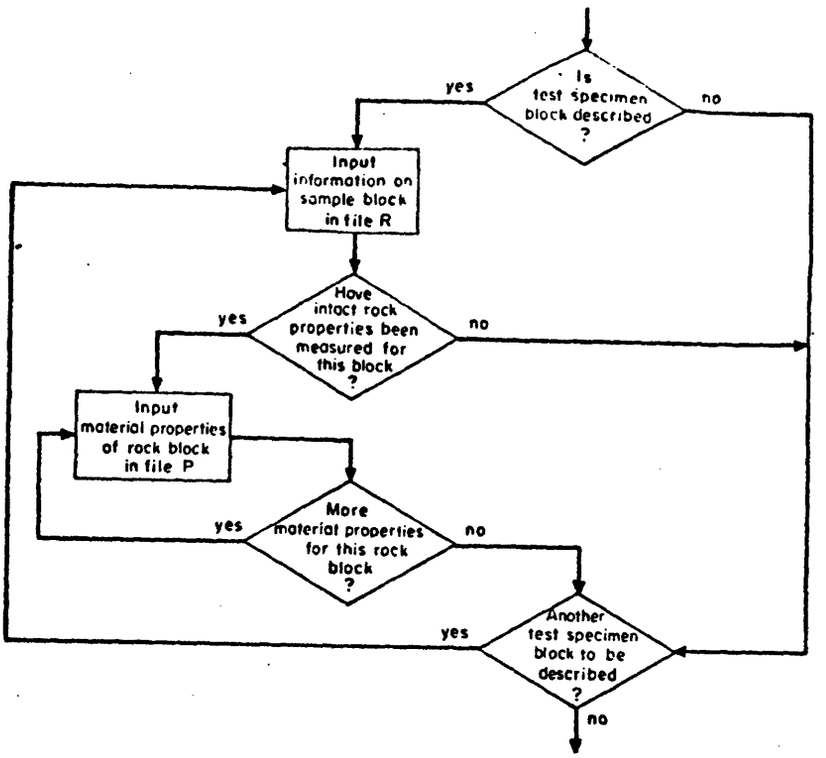

Figure 3-13 Structure of Test Specimen Block segment

it is necessary to obtain this information from another test specimen block.

Structure of Joint Surface Segment

If the joint surface is described, the description is stored in File D. Otherwise, storing is terminated, as shown in Fig. 3-14.

Structure of Joint Surface Material and Surface Geometry

If the descriptions of joint surface material and surface geometry are available, they are stored in File S and File Q. Additional joint surfaces are also checked for this information, as shown in Fig. 3-15.

Structure of Joint Filler Material Segment

If there is joint filler material, information on this material is stored in File A, as shown in Fig. 3-16; otherwise, storing is terminated here. Also, material properties of the filler material are considered. These filler material properties are stored in File B. After these properties are stored, it is necessary to obtain information on the second filler material, if this filler material is present. A detailed flow-chart and the list of the entire program are given in Appendix A.

3.4 Data Storage

Feature of Multics

Multics is the computer system used to store the developed program and all files of data. It is a general purpose computer system to support transaction-oriented application, word processing, and applica-

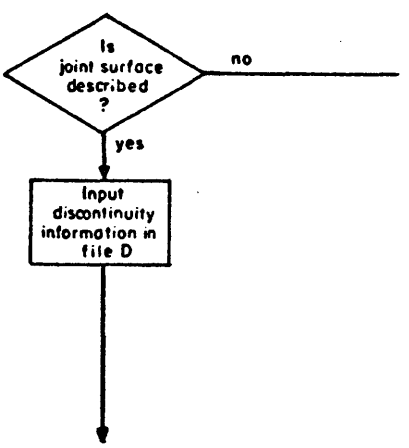

Figure 3-14 Structure of Joint Surface segment

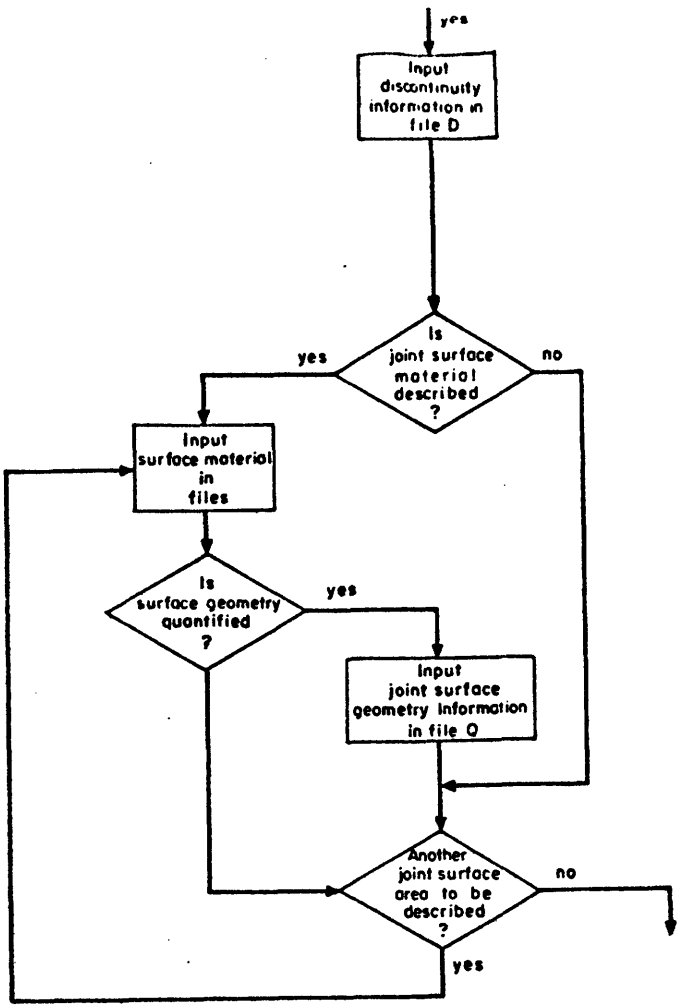

Figure 3-15 Structure of Joint Surface Material and Surface Geometry segment

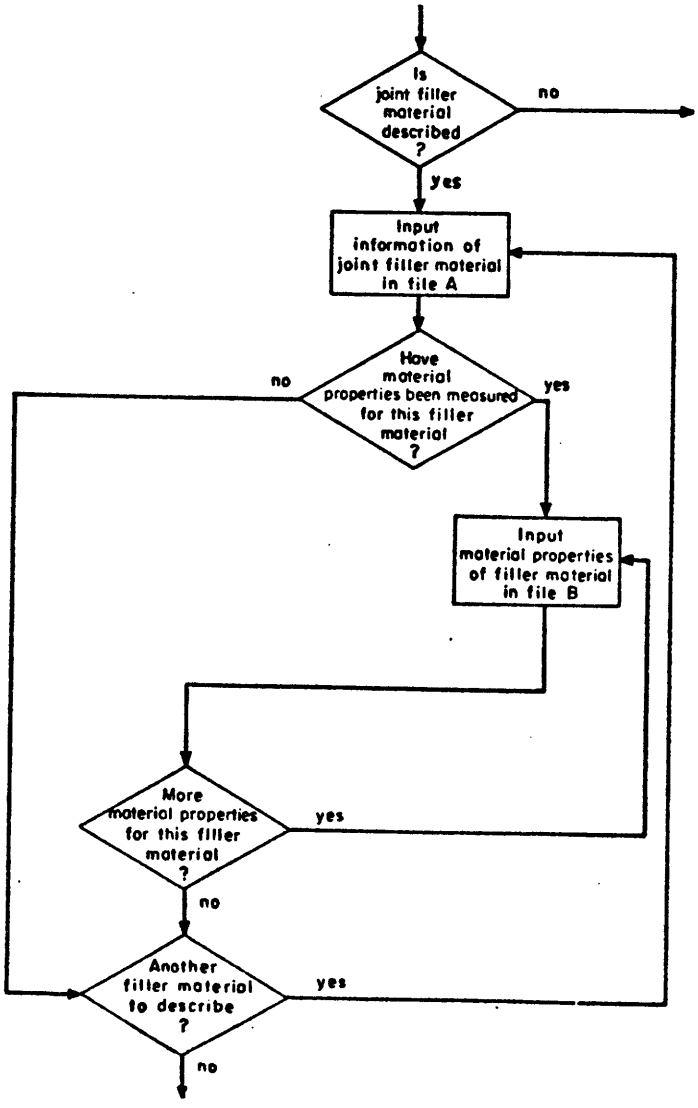

Figure 3-16 Structure of Filler Material segment

tion and system programming developement. It supports a wide variety of languages, most notably PL/1, COBOL, FORTRAN, BASIC and APL. The Multics system multiplexes a central computer among the jobs of many users, each of whom accesses Multics from a terminal. With Multics, users have facilities that allow them to edit, compile, debug, and run programs in one continuous, interactive session. Each Multics user can structure information, manipulate it, and simultaneously share it with other users. But Multics is more than a mere time-sharing system. It supports diverse subsystems, such as the consistent system and graphics system (see below).

Login Procedure

Before users can gain access to Multics, they must be registered on the system by the site system administrator, and allowed access to particular project by the administrator of that project. The system administrator assigns each user a person identification and a project identification. In addition, the system administrator assigns a special password to each user. After the user has dialed the appropriate telephone number and a connection has been established between Multics and the user's terminal, Multics prints a message giving the number of the current system, the location of the system, the actual number of users logged in, and the number of users the system is currently accepting.

```
Multics 33.16: MIT, Cambridge, Mass.
Load = 19.0 out of 85.0 units: users = 19
```

At this point, the user issues the login command and his personal identification, separated by a blank.

```
login PKYip
Password:
```

After the user has typed his password, the system responds with information as following:

```
You are protected from preemption.
PKYip USBM logged in 10/29/78  1212.5 est Sun from ASCII terminal
                                                        "none".
Last login 10/28/78  1641.9 est Sat from ASCII terminal "none".

Month-to-Date: $   137.36; Limit: $     open; Total: $   464.30;
No mail.
r $0.01 $0.01 1212.7
```

The last line is the ready message. At this point program and files can be printed, executed and edited.

Listing of Program and Files

To have a listing of the developed program, the following has to be typed on the terminal:

```
Print InputR
```

"InputR" is the name of the developed program that is stored in the Multics system.

In order to print the contents of the files, the following command is issued:

```
Print fileR
```

"fileR" is the name of the individual file.

Program Execution

To run the developed program which is stored in the Multics system, it is necessary to type in the name of the program.

```
InputR
```

After this is typed, the program is executed, and data inputting can be started. An example of the program execution and data inputting is listed in Appendix A.

Editing of Program or File

Since typing errors are quite frequent, editing the files and program is necessary. Before editing, the editor facility of the system has to be invoked. In order to do so, the following is typed:

```
QX
```

Editing the appropriate file or the developed program can be done with:

```
r fileI
```

"fileI" is the name of the file that needs editing. If the program needs to be edited, "InputR" should be typed instead of "fileI". At this point, editing can start.

If it is necessary to change a word or numerical value in a particular line, this line must be printed out before any correction is made. This can be achieved by typing the word or numerical value characterized the line, e.g.:

```
/DM/
```

The line that contains the word DM will then be printed out. If there are more than one line that contain the specific word or numerical value, the first line that contains this word is printed out. The other lines can be printed out using the same procedure.

If it is the line number that needs to be known, this can be achieved with:

```
/DM/=
36
```

The system will then print out the line number "36".

To change a numerical value or word in a specific line, this can be done by the following:

```
s/FOw/FO/p
```

The word "FOw" is substituted by "FO". The last word "p" is to print out the corrected line. After the line has been printed out and to make correction take effect, the following has to be typed:

```
w
```

The correction is temporarily done in the buffer of the system. This command "w" is to transfer whatever the correction is from the buffer into the file.

A line can be added before or after a specific line. This can be achieved by first printing out the specific line, then adding a line

before or after that line with a format such as:

```
$
DM     2     9     1     15.00    -    -1.00    -    -1.00

a (i)

DM     3     1     1      3.50    -    -1.00    -    -1.00
\f

w
```

"$" is the command to print out the last line in the file. If it is not the last line to which a line is appended, the line number, e.g. "36", is issued instead of "$". Adding a line before or after a specific line can be done through the command "a" or "i" respectively. After issuing "a" or "i", text of a line is inputted, and then followed by "\f". "\f" is a signal to the system that the inputting of text is finished. The "w" command is to transfer the text into the file. After editing, returning to the ready message can be done by typing:

```
Q
```

All the commands that are described above are generally employed in this thesis to edit the files and program before doing any data management. Other commands can be obtained from the Multics Introductory User's Guide.

3.5 Data Management and Statistical Analysis

Data management and statistical analysis can be done in Consistent System (CS).

Features of the Consistent System

The Consistent System is a system within Multics. Basically, the Consistent System is a collection of programs for analyzing and manipulating data, and for building and analyzing models. The system is primarily intended for "online" interactive use by non-programming analysts or behavioral scientists. The programs are invoked by commands issued by user and can be combined in arbitrary ways to perform different types of analysis. Janus is a data-management and analysis system that is developed within the Consistent System in Multics. It contains the capabilities usually found in a relational database management system together with elementary summary statistics and a powerful and integrated report manager.

Entering Consistent System (CS) and Janus System

To enter the Consistent System, the following command has to be issued after the Multics ready message:

```
cs -create
```

This creates the CS directory for the user (for the first time). Next time, the user just types:

```
cs
```

The system responds with the following:

```
add_search_rules: Name duplication, >libraries>imsl already in search
R                                                                  path
```

"R" is the CS ready message.

After entering the CS system, the following has to be done

```
dpub j
```

This creates access to Janus directory, where Janus resides. This is not needed again next time unless a new CS directory is created. To enter the Janus, the following has to be done:

```
Janus : j -create
```

This is to enter Janus for the first time, and to start a new database. The following time, just typing Janus without "-create" is sufficient. The Janus ready message is

```
j
```

The entire data management is done within Janus.

Dataset Creating

Before doing any data management, all the Multics files have to be transferred to Janus database. After transferral, each file is called dataset. Each dataset contains attributes as shown in Fig. 3-17A. The contents in each attribute are the corresponding values of those in a column of a Multics file. To create a dataset and its attributes in Janus database, the following can be done:

```
J
dfdr fileN line_marked with clp1  =82
J
dfar sourcel as text clm 1 for 3
J
dfar seriesl as integer clm 13 for 4
```

Dataset File C

Source	Series	Test	ϕ_p
SWS	1	1	30
SWS	1	2	40
SWS	1	3	50
DM	2	1	20
BR	3	1	35
DM	2	2	42

Dataset File R

Source	Series	Test	Rock
SWS	1	2	SS
DM	2	1	MO
BR	3	1	AM
SWS	1	3	CS
DM	2	2	GR
SWS	1	1	GN

Source	Series	Test	ϕ_p	Rock
SWS	1	1	30	GN
SWS	1	2	40	SS
SWS	1	3	50	CS
DM	2	1	20	MO
BR	3	1	35	AM
DM	2	2	42	GR

Dataset File C

Figure 3.17B Principle of Data Management

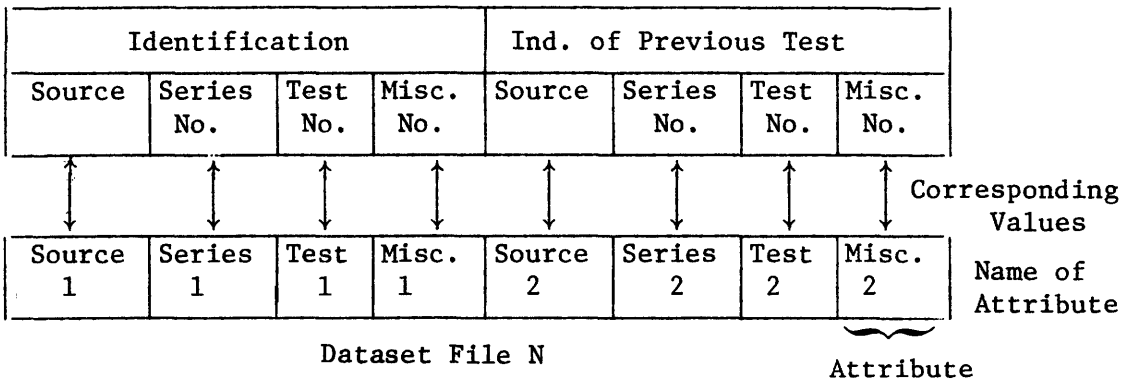

Fig. 3-17A Dataset and Its Attribute

```
J
dfar testl as integer clm 23 for 4
J
dfar miscl as integer clm 33 for 4
J
dfar source2 as text clm 44 for 3
J
dfar series2 as integer clm 56 for 4
J
dfar test2 as integer clm 66 for 4
J
dfar misc2 as integer clm 76 for 4
J
```

The first line is to define dataset File N from the Multics File N into Janus database with eighty-two columns per line. The second line is to define the attribute "source1" in the dataset File N from the corresponding column information in Multics File N as text starting from column one with length of three columns. "Source1" is the name given to the attribute. The rest of the lines are to define all the other attributes in the dataset.

After dataset definition, the following command has to be issued.

```
crar source1,series1,test1,misc1,source2,series2,test2,misc2
```

The purpose of this command is to report any error when the attributes are defined. Dataset creation for other Multics files are the same except for File I. Since File I has too many columns, the following has to be done before creating this dataset.

```
link >nbdd>cs>janus>card
```

This command is given after the Multics ready message before entering Janus.

The command that is used to define dataset File I is

multics card fileI 131

This command is given after the Janus ready message.

Afterwords, the attribute can be defined and created as described above.

Principle of Data Management

The basic principle is: when an attribute of information is not contained in a dataset, say dataset A, but appears in another dataset, say dataset B, this attribute of information can be retrieved from dataset B and stored in the corresponding rows in dataset A, or vice versa, providing that there are identifications for every row in each dataset, and these identifications of one dataset must relate to those of another. This basic principle of data management in Janus employed in this thesis is illustrated in Fig. 3-17B. Dataset File C contains identification and ϕ_p in each row; dataset File R contains identification and rock type. The identification in dataset C is related to those in dataset R by using the relation facility in the Janus system.

The arrows in the diagram show how the identification in dataset File K are matched to those in dataset File C through the relation facility. After matching, the attribute, "rock" is retrieved from dataset File R and stored in the corresponding rows in dataset File C by using the attribute-creating facility in the system. The relation and attribute-creating facilities in the system are discussed in the next section.

Data Management

After datasets are created, data management can now start. The basic principle of data management described before is employed here; datasets in this section are analagous to datasets A and B. In datasets File C and File I, there is no information about rock type; only dataset FileR has this information. It is, therefore, necessary to create attributes of rock type in datasets File C and File I. To create attributes of rock type and formation in File C, the following commands have to be issued.

```
crr member2 := match(source,series,test in fileC to source,series,
                                                    test in fileR)

cra rock1 in fileC := infer(rock thru member2)

cra formation1 in fileC := infer(formation thru member2)
```

"Source," "series" and "test" are the identification of each row in datasets File C and File R. "crr" is the relation facility called "member 2" to do the identification matching. "cra" is the attribute-creating facility which creates attributes "rock1 and "formation1" in dataset File C from the information contained in attributes, "rock" and "formation", respectively, in dataset File R through the relation, "member2". The identification of each row of information is therefore very important for data management.

To create an attribute of rock type in File I, the following commands are issued.

```
crr member1 := match(source2,series2,test2,misc2 in fileN to
                     source4,series4,test4,misc4 in fileR)

cra rock in fileN := infer(rock thru member1)

crr member1 := match(source,series,test,misc in fileI to source1,
                     series1,test1,misc1 in fileN)

cra rock1 in fileI := infer(rock thru member1)
```

An attribute of rock type, "rock1", is created in File I. Information of an attribute or of a subset of an attribute can be printed out through the display command.

```
ds nhigh,shigh in fileI

ds nhigh,shigh,rock1 in fileI for rock1 = "AM"

ds nhigh,shigh,rock1 in fileI for rock1 = "AM" & shigh <= 1500
```

These subsets of an attribute can be put into a dataset for statistical analysis. This can be done by the following command.

```
crdc NHIGH SHIGH in STRESS := nhigh,shigh in fileI for rock1 =
                                        "AM" & shigh <= 1500
```

where "NHIGH" and "SHIGH" are the names of the attributes in the newly created dataset "STRESS".

Statistical Analysis

Linear Regression Analysis (Best-Fit Line Plot)

The specific commands that are needed to get the linear regression plots and histograms are discussed here.

To get the best-fit line of the scatter plot for a specific rock type, the following commands are very important.

```
crdc NHIGH,SHIGH in STRESS := nhigh,shigh in fileI for rock 1 = "AM"

crg stress1 := NHIGH

crg stress2 := SHIGH

cs eval rgattr(stress1,stress2 save(res := residuals))

cs eval linear := extract_attr(res with attr(fitted))

cs grp_vect stress1 stress2 -vec_sw 3 -grid_sw 0 -eq_scale_sw 1
                                                    -symbol "."

cs grp_connect stress1 linear -noerase
```

The first command is to create new dataset, a subset corresponding to rock type "AM". The second and third commands are to create genarray "stress1" and "stress2" in CS to store information corresponding to "NHIGH" and "SHIGH", respectively. The fourth and fifth commands are to invoke the programs "rgattr" and "extract_attr" in CS for linear regression evaluation. "CS" is a means to provide an interface between Janus and the Consistent System. The last two commands are for the scatter plot and the best-fit line, respectively. Everytime the plot is finished, stress1 and stress2 are deleted in order to minimize dataset storage by the following commands

```
cs delete stress1

cs delete stress2
```

To get the best-fit line of the scatter plot corresponding to a stress range for a specific rock type, only the first three commands need to be modified as follows, the rest are the same.

```
crdc NHIGH1,SHIGH1 in STRESS1 := NHIGH,SHIGH in STRESS for NHIGH
                                                >= 0 & NHIGH <= 1000

crg stress1 := NHIGH1

crg stress2 := SHIGH1
```

The above described commands can be modified for a specific subset of an attribute to get the best-fit line of a scatter plot.

Histogram Plot

To get the histogram of a specific rock type, the following commands must be given.

```
crdc angle1 in ANGLE := angle in fileC for rock = "GN"

ds min(angle1),max(angle1),max(angle1)-min(angle1)

eval cat := categorize_interval(angle1,15,45,5)

eval xtab(cat) print using plot_hist
```

The first command is to create a dataset for a subset of an attribute. The second command is to display the minimum, maximum value of the attribute "angle1" and the range between these two values. The third command is to invoke the CS program "categorize_interval" for the histogram evaluation; where "15" and "45" are the corresponding minimum and maximum values of the attribute "angle1" in dataset "ANGLE". "5" is the number of intervals for the histogram and is calculated from the range between the maximum and minimum values of the "angle1". The fourth command is to ask the terminal to print the histogram. To get the histogram corresponding to formation of a specific rock type, only the first command has to be changed.

```
crdc angle2 in ANGLE2 := angle in fileC for formation = "R29"
```

The rest of the commands are the same.

The results of this thesis are the accomplishment of the above-mentioned commands. These commands may be modified to attain different objectives in data management and analysis.

CHAPTER 4

DISCUSSION OF RESULTS

Shear strength and stiffness derived from our data as well as a collection of the data from published literature are presented here. The linear regression curves and histograms of the data are presented in Appendices B through F. Discussions of friction angles are concentrated in all rock types, specific rock groups (sedimentary, metamorphic and igneous rocks), and individual rock type. The effect of water, joint type and normal stress levels are also discussed. Finally, the deformability are mentioned.

Discussion of Parameters vs. Normal Stress

Figs. B-1 through B-8 in Appendix B are the best-fit curves for peak shear stress vs. peak normal stress, residual shear stress vs. residual normal stress, peak shear stiffness, elastic shear stiffness, shear degradation distance, normal dilation distance and peak dilation rate vs. peak normal stress; the data are not related to specific rock types and joint type. Fig. B-1 shows that the peak friction angle for all rock types and joint types is about 39^{o}, while the residual friction angle is about 33.5^{o}. If results of tests on intact rocks are included, the peak friction angle is about 49^{o}. This shows that intact rocks have higher peak friction angles. Peak shear stiffness and elastic shear stiffness are normal stress dependent. They increase with increasing normal stress. Fig. B-6 shows that shear degradation distance does not vary with normal stress. However, normal dilation distance and peak dilation rate decrease

With increasing normal stress.

4.1 Discussion of Shear Strength

Appendix C through E are the best-fit curves for our data conditional on rock type and stress levels, rock type and joint type, and joint type, respectively. The corresponding peak friction angles ϕ_p and residual friction angles are summarized in Tables 4-1, 4-2, 4-3, and 4-4. The friction angles ϕ_r in these tables are then combined together with those friction angles extracted from published literature; all the values are summarized in Table 4-5.

General Range of All Rock Types

In Table 4-5, rocks are classified as sedimentary, metamorphic and igneous rocks. The peak friction angles ϕ_p for all rock types range from as low as 4^o to as high as 81^o, with the mean value equal to 36^o. The low values in this range are due to the high cohesion intercept; the high values represent as a limiting condition at extremely low normal stresses. The residual friction angles ϕ_r for all rock types range from as low as 8^o to as high as 61^o with the mean value equal to 33^o.

Ranges of Sedimentary Rocks, Metamorphic Rocks and Igneous Rocks

Table 4-6 summarizes the range, mean value and standard deviation of peak and residual friction angles for sedimentary, metamorphic and igneous rocks. For sedimentary rocks, peak friction angles range from 14^o to 77^o with the mean value equal to 47^o. The range of residual friction angles is 8^o to 61^o with the mean value equal to 33.2^o. For

Table 4-1

ϕ_p Conditional on Rock Type and Stress Levels

	Rock Type	Stress Levels ($\times 10^{-3}$ MN/m^2	ϕ_p
Sedimentary Rocks	Limestone	all levels	19
		0 - 500	48.5
		500 - 2000	26.5
		above 2000	18.5
	Sandstone	all levels	32
Metamorphic Rocks	Paragnesis	all levels	26
		0 - 100	19.5
		above 1000	26
	Amphibolite	$\tau \leq 7500$	
		all levels	33
		$\tau \leq 7500$	
		0 - 650	34
		$\tau \leq 7500$	
		650 - 3000	44
		$\tau \leq 7500$	
		650 - 8000	30
		$\tau \geq 7500$*	
		all levels	75

*Healed joints and homogenous rocks

Table 4-1 continued

	Rock Type	Stress Levels ($x10^{-3}$ MN/m^2)	ϕ_p
Metamorphic Rock	Schist	all levels	23
		0 - 1000	28.5
		1000 - 2000	28
		above 2000	25
	Phyllite	all levels	18
		0 - 500	24
		above 500	17
	Serpentine (schistose)	all levels	26
		$\tau \geq 2500$ [x]	
	Serpentine	all levels	76
		$\tau \leq 2500$	
		all levels	18
		$\tau \leq 2500$	
		0 - 500	4
		$\tau \leq 2500$	
		above 500	22
	Marble	all levels	17
		0 - 1000	31.5
		above 1000	24
	Gneiss	all levels	27
		0 - 500	30
		500 - 1000	29

[x] homogenous rocks

Table 4-1 continued

	Rock Type	Stress Levels ($x10^{-3}$ MN/m^2)	ϕ_p
Metamorphic Rock	Gneiss	1000 - 2000	29
		above 2000	32
	Gneiss(schistose)	all levels	24
		0 - 1000	32.5
		above 1000	25
	Schist(carboniferous)	all levels	26.5
		0 - 1000	35
		above 1000	27
	Schist(calcarous)	all levels	19
		0 - 2000	20
		above 2000	19.5
	Schist(sericite)	all levels	13.5
		0 - 300	7
		300 - 2000	19
		above 2000	7
Igneous Rock	Basalt	all levels	40
		0 - 2000	22.5
		above 2000	35
	Dacite	all levels	35
		0 - 1000	38
		1000 - 2000	41
		above 2000	31.5

Table 4-1 continued

	Rock Type	Stress Levels ($x10^{-3}$ MN/m^2)	ϕ_p
Igneous Rocks	Porphyry (quartzite)	all levels	31
		0 - 500	30
		above 500	32.5
	Granite	all levels	39.5
	Claystone	all levels	26
		0 - 300	27.5
		above 300	23.5
	Monzonite (quartz)	all levels	33
		0 - 1000	49
		1000 - 2000	43.5
		above 2000	26
	Tuff	all levels	21.5
		0 - 1000	18
		1000 - 3000	13
		above 3000	22
	Metashale	all levels	65
		0 - 4000	64
		above 4000	54.5
	Micro-granodiorite	all levels	29
		0 - 1000	40
		above 1000	27.5
	Monzonite	all levels	37.5

Table 4-1 continued

	Rock Type	Stress Levels ($x10^{-3}$ MN/m^2)	ϕ_p
Igneous Rock	Monzonite	0 - 200	61.5
		200 - 1000	42.5
		above 1000	36
Other	Lignite	all levels	31.5
		0 - 300	42
		above 300	37
	Sericite	all levels	28.5
	Talc	all levels	23

Table 4-2

ϕ_p Conditional on Rock Type

	Rock Type	ϕ_p
Sedimentary Rocks	Limestone	19
	Sandstone	32
Metamorphic Rocks	Amphibolite	33
		75*
	Schist	23
	Phyllite	18
	Serpentine (Schistose)	26
	Serpentine	76[x]
		18
	Marble	17
	Gneiss	27
	Gneiss (Schistose)	24
	Schist (Carboniferous)	26.5
	Schist (Calcarous)	19
	Schist (sericite)	13.5
	Paragneiss	26

* Healed Joint & Homogenous Rock Only

[x] Homogenous Rock

Table 4-2 continued

	Rock Type	ϕ_p
Igneous Rocks	Basalt	40
	Dacite	35
	Porphyry (Quarzite)	31
	Granite	39.5
	Claystone	26
	Monzonite (Quartz)	33
	Tuff	21.5
	Metashale	65
	Micro-Grandiorite	29
	Monzonite	37.5
Other	Lignite	31.5
	Sericite	29.5
	Talc	23

Table 4-3

ϕ_r, ϕ_p Conditional on Rock Type & Joint Type

	Rock Type	Discontinuity	ϕ_p	ϕ_r
Sedimentary Rocks	Limestone	Joint	20	-
		Concrete Rock Interface	14	-
		Limestone-Moraine Contact	31	-
		Bedding	27	-
	Sandstone	Break of Core Sample	26	-
Metamorphic Rocks	Paragneiss	Foliation	26	-
	Amphibolite	Joint	34	34
		Healed Joint	71	-
		Homogenous Rock	73	-
		Intact	79	-
		Sawn	32	-
		Conjugate Set	23	-
		H/W	22	-
		Foliation	31	-
	Schist	Foliation	23	-
		Separated Foliation	26	-
		Sawn	22	-
	Phyllite	Foliation	28	-
	Serpentine (Schistose)	Foliation	22	-
		Sawn	24	-

Table 4-3 continued

	Rock Type	Discontinuity	ϕ_p	ϕ_r
Metamorphic Rocks	Serpentine	Foliation	28	-
		Sawn	18	-
		Homogenous Rock	81	-
	Marble	Bedding	16	-
		Break of Test Specimen	23	-
	Gneiss	Foliation	23	-
		Joint	27	-
		Sawn	23	-
		Separated Foliation	37	-
		Fault	21	-
		Slickensided Surface	32	-
	Gneiss(Schistose)	Foliation	25	-
		Joint	16	-
		Sawn	29	-
	Schist (Carboniferous)	Fault	18	-
		Foliation	22	-
	Schist (Sericite)	Joint	15	-
Igneous Rocks	Basalt	Bedding	15	-
		Fracture	40	-
	Dacite	Sawn	37	-
		Fracture	34	-

Table 4-3 continued

	Rock Type	Discontinuity	ϕ_p	ϕ_r
Igneous Rocks	Porphyry (Quarzite)	Joint	30	-
		Foliation	31	-
	Granite	Contact of Granite & Mylonite	31	-
		Joint	41	-
	Claystone	Non-Oriented Lamination	22	10
		Oriented Lamination	25	13
	Monzonite (Quartz)	Joint	33	-
	Tuff	Bedding	22	-
		Fracture	20	-
	Metashale	Healed Joint	65	-
	Micro-Granodiorite	Artificial Grouted Joint	38	17
		Sawn Lapped w. #80 grit	-	34
	Monzonite	Artificial Grouted Joint	31	22
		Natural Grouted Joint	28	25
		Joint	39	36
		Sawn Lapped w. #80 grit	-	32
Other	Lignite	Intact	30	20
		Sawn	-	19
	Sericite	Foliation	29	-

Table 4-4A

ϕ_p Conditional on Joint Type

Joint Type	Rock Type in the Corresponding Joint Types	ϕ_p
Joint	Monzonite, Amphibolite, Quarzite Monzonite, Gneiss, Schist, Quarzite Porphyry, Schistose Gneiss, Sericite Schist, Limestone	35
Sawn	Gneiss, Serpentine, Schistose Serpentine, Schistose Gneiss, Schist, Amphibolite, Dacite	26
Intact	Lignite, Amphibolite	71
Contact Zone of Granite & Mylonite	Granite	31.5
Break of Core Sample	Sandstone	26
Fracture	Lignite, Dacite, Basalt, Tuff	37.5
Contact Between Limestone & Moraine	Limestone	32
Interface of Concrete & Rock	Limestone	15
Oriented Lamination	Claystone	25
Nonoriented Lamination	Claystone	22
Break of Test Specimen	Sandstone, Marble	23
Bedding	Marble, Limestone, Basalt, Tuff	21
Natural Grouted Joint	Monzonite	28

Table 4-4A continued

Joint Type	Rock Type in the Corresponding Joint Types	ϕ_p
Artificial Grouted Joint	Micro- granodiorite Monzonite	30
Slickensided Surface	Gneiss	31.5
Separated Foliation	Carboniferous Schist, Schist, Gneiss	33
Fault	Gneiss, Carboniferous Schist	20
Foliation	Quarzite Porphyry, Carboniferous Schist, Paragneiss, Amphibolite, Gneisss, Phyllite, Serpentine, Schistose Serpentine, Schist, Schistose Gneiss, Sericite	25
H/W Joint	Amphibolite	22
Conjugate Joint Set	Amphibolite	23
Homogenous Rock	Amphibolite, Serpentine	78
Healed Joint	Metashale, Amphibolite	51

Table 4-4B

ϕ_r Conditional on Joint Type

Joint Type	Rock Type in the Corresponding Joint Type	ϕ_r
Joint	Monzonite, Amphibolite	36
Sawn	Lignite, Amphibolite	21
Intact	Lignite	21
Sawn Joint Lapped with #80 Grit	Monzonite, Micro-Granodirote	33
Artificial Grouted Joint	Monzonite, Micro-Granodirote	20
Natural Grouted Joint	Monzonite	25
Nonoriented Lamination	Claystone	10
Oriented Lamination	Claystone	12

Table 4-5

Friction Angles of Rock Type

	Rock Type	No. of Tests*	Description of Discontinuities	Moisture	Stress σ_n (MN/m^2)	ϕ_p	ϕ_r	References
Sedimentary Rock	Chalk	-	-	wet	0-0.4	-	30	Hutchinson (1972)
			joint	dry	-	-	40	Duncan (1969)
			joint	wet	-	-	41	Duncan (1969)
	Conglomerate	-	-	dry	0.3-0.4	-	35	Krsmanovic' (1967)
	(fresh or tectonically damaged)		bedding, schistosity & fissuring	-	0.52-1.5	70	-	Kujundzi' & Colic' (1976)
	Dolomite	-	fracture	dry	-	-	39-61	Mauer (1965)
			sandblasted	dry	0.1-7.2	-	32-38	Coulson (1972)
			sandblasted	wet	0.1-7.2	-	27-35	Coulson (1972)
	(Homogenous, f.g.)	-	-	-	-	-	39	Handin & Hagen (1957)

* Numbers in this column represent the number of tests for the linear analysis.

Table 4-5 continued

	Rock Type	No. of Tests	Description of Discontinuities	Moisture	Stress σ_n (MN/m^2)	ϕ_p	ϕ_r	References
Sedimentary Rock	(Coarse to f.g.)	-	-	-	-	-	35	Handin & Hagen (1957)
	(Heterogenous f.g., calcitic)	-	-	-	-	-	40	" " "
	(Heterogenous med.-grained, calcitic)	-	-	-	-	-	35	" " "
	(Fixed grained, calcitic)	-	-	-	-	-	34	" " "
	(Homogenous, c.g. // to foliation)	-	-	dry	-	-	32	" " "
	(Homogenous, c.g. ⊥ to foliation)	-	-	dry	-	-	31	" " "
	Limestone	69	slightly rough bedding plane	-	0.21-0.6	71-77	-	Goodman (1970)
		-	rough bedding plane	-	0.31-0.68	66-72	-	Goodman (1970)
		-	joint	-	-	20	-	-

Table 4-5 continued

	Rock Type	No. of Tests	Description of Discontinuities	Moisture	Stress σ_n (MN/m^2)	ϕ_p	ϕ_r	References
Sedimentary Rock	Limestone	-	concrete-rock interface	-	-	14	-	-
		-	limestone-moraine contact	-	-	31	-	-
		-	bedding	-	-	27	-	-
		-	slightly rough bedding	-	-	36.9	29.8	Goodman (1968)
		-	rough bedding	-	-	53.5	43.2	Goodman (1968)
		-	rough sawn	dry	0-0.5	-	33-39	Patton (1966a)
		-	rough sawn	wet	0-0.5	-	33-36	Patton (1966a)
		-	sandblasted	dry	0.1-7.1	-	37-40	Coulson (1972)
		-	sandblasted	wet	0.1-7.1	-	35-38	Coulson (1972)
		-	sandblasted	dry	0.1-8.3	-	36-39	Coulson (1972)
		-	sandblasted	wet	0.1-8.3	-	35	Coulson (1972)

Table 4-5 continued

	Rock Type	No. of Tests	Description of Discontinuities	Moisture	Stress σ_n (MN/m^2)	ϕ_p	ϕ_r	References
Sedimentary Rock	Limestone	-	-	-	0-0.5	48.5	-	-
		-	-	-	0.5-2	26.5	-	-
		-	-	-	above 2	18.5	-	-
	(oolitic)	-	joint	dry	-	-	44	Duncan (1975)
	(oolitic)	-	joint	wet	-	-	48	Duncan(1969)
	(heterogenous c.g.)	-	-	-	-	-	34	Handin & Hager (1957)
	(heterogenous c.g.)	-	-	-	-	-	33	" " "
	(heterogenous f.g.)	-	-	-	-	-	35	" " "
	(massive, friable)	-	-	dry	-	-	27	" " "
		-	-	-	-	-	19	-
	Marl	-	gouge	dry	-	-	13	Goldstein, et al. (1966)
		-	gouge	wet	-	-	10	" " "

Table 5 continued

Sedimentary Rock	Sandstone	310	rough sawn	dry	0-0.5	-	26-35	Patton (1966a)
		-	rough sawn	wet	0-0.5	-	25-33	" "
		-	-	dry	0.3-3.0	-	33	Krsmanoic' (1967)
		-	-	dry	0.3-3.0	-	31	" "
		-	sandblasted	dry	0.1-7.0	-	32-34	Coulson (1972)
		-	sandblasted	wet	0.1-7.3	-	30-34	" "
		-	-	wet	0-0.3	-	29	Ripley & Lee (1962)
	(fresh or little tectonically damaged)	-	bedding, schistosity and fissuring	-	0.52-1.5	70	-	Kujundzi' & Colic' (1976)
		-	artificial, planar, polished	dry	-	-	27-32	Patton (1966a)
		-	artificial, planar, polished	wet	-	-	31-39	" "

Table 4-5 continued

Sedimentary Rock	Sandstone	-	shear fractures from failure of intact specimen	dry	10-250	-	28	Jaeger (1959)
		-	shear fractures from failure of intact specimen	wet	10-250	-	25	Jaeger (1959
		-	break of core sample	-	-	26	-	-
		-	-	-	-	32	-	-
		-	-	-	-	61	-	Obert et al. (1976)
	(massive, hard, friable, f.g., well-cemented)	-	-	-	-	-	28	Handin & Hagen (1957)
	(massive, very hard, very f. g., well-cemented)	-	-	-	-	-	45	" " "
	(massive, f.g., well-cemented)	-	-	-	-	-	37	" " "

Table 4-5 continued

Sedimentary Rock	Sandstone (massive, f.g., well-cemented // to bedding)	-	-	-	-	-	34	Hardin and Hagen (1957)
	(massive, f.g., well-cemented, ⊥ to bedding)	-	-	-	-	-	34	" " "
	Anhydrite (f.g.)	-	-	-	-	-	30	" " "
	Greywache (moderately weathered)	-	-	-	-	-	36	Martin & Millan (1974)
	Siltstone	-	minor fault, smooth, polished, chlorite coated	dry	-	-	26	Rosengren (1968)
		-	minor fault, smooth, polished, chlorite coated	wet	-	-	22	Rosengren (1968)
		-	sandblasted	dry	0.1-7.5	-	32-36	Coulson (1972)
		-	sandblasted	wet	0.1-7.2	-	27-32	Coulson (1972)

Table 4-5 continued

Sedimentary Rock	Siltstone	-	-	wet	0-0.3	-	27	Ripley & Lee (1962)
	(hard,fissile)	-	-	dry	-	-	32	Hardin & Hager (1957)
	Shale	-	-	wet	0-0.3	-	27	Ripley & Lee (1962)
		-	minor fault, smooth, polished, chlorite coated	dry	-	-	26	Rosengren (1968)
		-	minor fault, smooth, polished, chlorite coated	wet	-	-	22	Rosengren (1968)
		-	closely jointed seam in limestone	-	0.21	70	-	Goodman (1970)
	(hard calcarous, // to bedding)	-	-	-	-	-	47	Hardin & Millar (1957)
	(hard calcarous, ⊥ to bedding	-	-	-	-	-	23	" " "
	(hard, f.g.)	-	-	dry	-	-	56	" " "

Table 4-7 continued

Sedimentary Rock	Shale Breccia (waxy to earthy)	-	-	-	-	-	36-50	Deklotz et al. (1966)
	Shale (bentonitic)	-	-	-	-	-	7.5	Sinclair & Brookes (1967)
	Shale (clay)	-	-	-	-	-	28	Sinclair & Brookes (1967)
Metamorphic Rock	Amphibolite	410	discontinuities beneath natural slope	-	-	80	-	Paulding (1970)
		-	discontinuities beneath excavated slope	-	-	75	-	Paulding (1970)
		-	rough sawn	dry	0.1-4.2	-	32	Wallace et al. (1970)
		-	natural	dry	0.1-4.2	-	39	Wallace et al. (1970)
		-	-	-	0-0.65	34	-	-
		-	-	-	0.65-3	44	-	-
		-	joint	-	-	34	34	-

Table 4-5 continued

Metamorphic Rock	Amphibolite	-	healed & joint	-	-	71	-	-
		-	homogenous rock	-	-	73	-	-
		-	intact rock	-	-	79	-	-
		-	sawn	-	-	32	-	-
		-	conjugate set	-	-	23	-	-
		-	H/W set	-	-	22	-	-
		-	foliation	-	-	31	-	-
		-	-	-	-	33	-	-
		-	healed joint and homogenous rock	-	-	75	-	-
	Gneiss	450	discontinuities beneath natural slope	-	-	80	-	Paulding (1970)
		-	discontinuities beneath excavated slope	-	-	75	-	Paulding (1970)
		-	shear fractures from failure of intact specimen	dry	10-250	-	35	Jaeger (1959)

Table 4-5 continued

Metamorphic Rock	Gneiss	-	shear fractures from failure of intact specimen	wet	10-250	-	31	Jaeger (1959)
		-	natural schistose plane	dry	-	-	49	Duncan (1969)
		-	natural schistose plane	wet	-	-	44	Duncan (1969)
		-	foliation	-	-	23	-	-
		-	joint	-	-	27	-	-
		-	sawn	-	-	23	-	-
		-	separated foliation	-	-	37	-	-
		-	fault	-	-	21	-	-
		-	slickensided surface	-	-	32	-	-
		-	-	-	0-0.5	30	-	-
		-	-	-	0.5-1	29	-	-
		-	-	-	1-2.0	29	-	-

Table 4-5 continued

Metamorphic Rock	Gneiss	-	-	-	above 2.0	32	-	-
		-	-	-	-	27	-	-
	Gneiss (granitic)	-	sawn	dry	-	-	34	Jaeger (1959)
		-	fracture	dry	-	-	35	Jaeger (1959)
		-	fracture	wet	-	-	31	Jaeger (1959)
		-	fracture	-	-	40	40	Baldovin (1970)
	Gneiss (schistose)	160	sawn	dry	-	-	18-29	Deklotz et al. (1965)
		-	fracture	wet	-	-	30	Deklotz & Brown (1967)
		-	foliation	-	-	43	-	Deklotz et al. (1965)
		-	sandblasted	dry	0.1-8.1	-	25-32	Coulson (1972)
		-	sandblasted	wet	0.1-7.9	-	22-28	Coulson (1972
		-	-	-	0-1.0	32.5	-	-

Table 4-5 continued

Metamorphic Rock	Gneiss (schistose)	-	-	-	above 1.0	25	-	-
		-	foliation	-	-	25	-	-
		-	joint	-	-	24	-	-
		-	joint	-	-	16	-	-
		-	sawn	-	-	29	-	-
	(f.g.)	-	-	-	-	-	43	Deklotz et al, (1965)
	(⊥ to foliation)	-	-	-	-	-	28	Deklotz et al, (1965)
	Marble	10	joint	dry	-	-	49	Duncan & Scheerman-Chase (1965-66)
		-	joint	wet	-	-	42	Duncan & Scheerman-Chase (1965-66)
		-	bedding	-	-	16	-	-
		-	break of test specimen	-	-	23	-	-

Table 4-5 continued

Metamorphic Rock	Marble	-	shear fractures from failure of intact specimen	dry	10-250	-	32	Jaeger (1959)
		-	-	-	0-0.1	31.5	-	-
		-	-	-	above 0.1	24	-	-
		-	-	-	-	17	-	-
	(pure, f.g.)	-	-	-	-	-	29	Mogi (1964)
	(little quartz, medium-grained)	-	-	-	-	-	31	Mogi (1964)
	(pure, c.g.)	-	-	-	-	-	28	Mogi (1964)
	(med.-grained ⊥ to foliation)	-	-	-	-	-	35	Hardin & Hager (1957)
	(med.-grained // to foliation)	-	-	-	-	-	36	Hardin & Hager (1957)
	Phyllite	10	schistose plane	dry	-	-	40	Duncan (1969)
		-	schistose plane	wet	-	-	32	Duncan (1969)
		-	foliation	-	-	28	-	-

Table 4-5 continued

Metamorphic Rock	Phyllite	-	-	-	0-0.5	24	-	-
		-	-	-	above 0.5	17	-	-
		-	-	-	-	18	-	-
	Schist	270	foliation	-	-	23	-	-
		-	separated foliation	-	-	26	-	-
		-	sawn	-	-	22	-	-
		-	-	-	0-1.0	28.5	-	-
		-	-	-	1.0-2.0	28	-	-
		-	-	-	above 2.0	25	-	-
		-	-	-	-	23	-	-
	Schist (phyllitic)	-	fractures	-	-	45	40	Baldovin (1970)
	Schist (carboniferous)	20	fault	-	-	18	-	-
		-	foliation	-	-	22	-	-
		-	-	-	0-1.0	35	-	-
		-	-	-	above 1.0	27	-	-

Table 4-5 continued

Metamorphic Rock	Schist (carboniferous)	-	-	-	-	26.5	-	-
	Schist (calcarous)	6	-	-	0-2.0	20	-	-
		-	-	-	above 2.0	19.5	-	-
		-	-	-	-	19	-	-
	Schist (sericite)	22	joint	-	-	15	-	-
		-	-	-	0-0.3	7	-	-
		-	-	-	0.3-2.0	19	-	-
		-	-	-	above 2.0	7	-	-
		-	-	-	-	13.5	-	-
	Quartzite	-	discontinuities beneath natural slope	-	-	80	-	Paulding (1970)
		-	discontinuities beneath excavated slope	-	-	75	-	Paulding (1970)

Table 4-5 continued

Metamorphic Rock	Quartzite	-	-	dry	-	-	35	Jaeger & Rosengren (1969)
		-	joint	dry	-	-	44	Duncan & Schleerman-Chase (1965-66)
		-	joint	wet	-	-	24-37	" " "
		-	artificial, planar, polished	dry	-	-	23	" " "
		-	artificial, planar, polished	wet	-	-	30	" " "
	(f.g.)	-	-	-	-	-	48	Hardin & Hager (1957)
	Serpentine	33	foliation	-	-	28	-	-
		-	sawn	-	-	18	-	-
		-	homogenous rock	-	-	81	-	-
		-	-	-	0-0.5	4	-	-
		-	-	-	above 0.5	22	-	-
		-	-	-	-	18	-	-

Table 4-5 continued

Metamorphic Rock	Serpentine (schistose)	7	foliation	-	-	22	-	-
		-	sawn	-	-	24	-	-
		-	-	-	-	26	-	-
	Slate	-	-	dry	0-1.1	-	25-30	Barton (1971b)
		-	minor fault, smooth, polished, chlorite coated	dry	-	-	26	Rosengren (1968)
		-	minor fault, smooth, polished, chlorite coated	wet	-	-	22	Rosengren (1968)
	(f.g.)	-	-	-	-	-	48	Hardin & Hager (1957)
	Paragneiss	8	foliation	-	-	26	-	-
		-	-	-	0-1.0	19.5	-	-
		-	-	-	above 1.0	26	-	-
		-	-	-	-	26	-	-

Table 4-5 continued

Igneous Rock	Basalt	20	sandblasted	dry	0.1-8.5	-	35-38	Coulson (1972)
		-	sandblasted	wet	0.1-7.9	-	31-36	Coulson (1972)
		-	artificial, planar, polished	dry	-	-	33	Duncan & Scheerman-Chase (1965-66)
		-	artificial, planar, polished	wet	-	-	35	Duncan & Scheerman-Chase (1965-66)
		-	bedding	-	-	15	-	-
		-	fracture	-	-	40	-	-
		-	-	-	0-2.0	22.5	-	-
		-	-	-	above 2.0	35	-	-
		-	-	-	-	40	-	-
	Dacite	24	sawn	-	-	37	-	-
		-	fracture	-	-	34	-	-
		-	-	-	0-1.0	38	-	-

Table 4-5 continued

Igneous Rock	Dacite	-	-	-	1.0-2.0	41	-	-
		-	-	-	above 2.0	31.5	-	-
		-	-	-	-	35	-	-
	Claystone	12	non-oriented lamination	-	-	22	-	-
		-	oriented lamination	-	-	25	-	-
		-	-	-	0-0.3	27.5	-	-
		-	-	-	above 0.3	23.5	-	-
		-	-	-	-	26	-	-
	Dolerite	-	joint	dry	-	-	52	Duncan (1969)
		-	joint	wet	-	-	37	Duncan (1969)
	Gabbro	-	joint	dry	-	-	47	Patton (1966a)
		-	joint	wet	-	-	48	Patton (1966a)
		-	rough joint	dry	-	-	33	Hoskins (1968)

Table 4-5 continued

Igneous Rock	Andesite (kaolinized & tectonically damaged)	-	bedding, schisto-sity & fissuring	-	0.2-1.0	35-55	-	Kujundzi' & Colic' (1976)
	(silicified & tectonically damaged)	-	bedding, schisto-sity & fissuring	-	0.2-1.0	55	-	Kujunkzi' & Colic' (1976)
		-	closely jointed	-	-	-	34	Jaeger (1969)
	Andesite (augric)	-	-	-	-	-	28	Mogi (1964)
	Andesite (pyroxene)	-	-	-	-	-	35	Mogi (1964)
	Granite	10	rough, undulating, artificial extension fractures	-	-	72	-	Renger (1971)
			rough, undulating, artificial extension fractures	-	-	69	-	Renger (1971)
			shear fractures from failure of intact specimen	dry	-	-	35	Jaeger (1959)
			shear fractures from failure of intact specimen	wet	-	-	31	Jaeger (1959)

Table 4-5 continued

Igneous Rock	Granite	-	artificial surface	dry	-	-	38	Duncan (1969)
		-	artificial surface	wet	-	-	31	Duncan (1969)
		-	natural joints	-	-	30-50	-	Hoek & Bray (1974)
	(f.g.)	-	sandblasted	dry	0.1-7.5	-	31-36	Coulson (1972)
		-	sandblasted	wet	0.1-7.4	-	29-34	" "
	(c.g.)	-	sandblasted	dry				
	(c.g.)	-	sandblasted	dry	0.1-7.3	-	30-36	" "
		-	sandblasted	wet	0.1-7.5	-	28-34	" "
		-	contact of granite & mylomite	-	-	31	-	-
		-	joint	-	-	41	-	-
		-	-	-	-	40	-	-
		-	-	-	-	69	-	Obert et al. (1976)
	Granite (biotite)	-	-	-	-	-	48	Mogi (1964)

Table 4-5 continued

Igneous Rock	Monzonite	200	artificial grouted joint	-	-	31	-	-
		-	natural grouted joint	-	-	28	-	-
		-	joint	-	-	39	-	-
		-	sawn, lapped w. #80 grit	-	-	-	32	-
		-	-	-	0-0.2	61.5	-	-
		-	-	-	0.2-1.0	42.5	-	-
		-	-	-	above 1.0	36	-	-
		-	-	-	-	38	-	-
	Monzonite (quartz)	17	natural open joint	-	below 20	41	-	Hendron (1968)
		-	natural open joint	-	above 20	31	-	Hendron (1968)
		-	sawn	-	-	28	-	Hendron (1968)
		-	joint	-	-	33	-	-
		-	-	-	0-1.0	49	-	-

Table 4-5 continued

Igneous Rock	Monzonite (Quartz)	-	-	-	1.0-2.0	43.5	-	-
		-	-	-	above 2.0	26	-	-
	(med.-grained, porphyritic)	-	-	-	-	-	53	Deklotz & Heck (1965)
		-	-	-	-	33	-	-
	Porphyry	-	shear fracture from failure of intact specimen	dry	-	-	41	Jaeger (1959)
		-	natural joint	dry	-	39	36	Goodman (1968)
		-	-	dry	0-1.0	-	31	Barton (1971b)
		-	-	dry	4.1-13.3	-	31	Barton (1971b)
	Peridotite	-	fracture	dry	-	-	22-37	Raleigh & Patterson (1965)
	Peridotite (hornblende)	-	-	-	-	-	38	Mogi (1965)
	Porphyry (quartzite)	30	joint	-	-	30	-	-
			foliation	-	-	31	-	-

Table 4-5 continued

Igneous Rock	Porphyry (quartzite)	-	-	-	0-0.5	30	-	-
			-	-	above 0.5	33	-	-
			-	-	-	31	-	-
	Micro-granodiorite	34	artificial grouted joint	-	-	38	17	-
			sawn lapped w. #80 grit	-	-	-	34	-
		-	-	-	0-1.0	40	-	-
			-	-	above 1.0	28	-	-
			-	-	-	29	-	-
	Metashale	9	healed joint	-	-	65	-	-
			-	-	0-4.0	64	-	-
			-	-	above 4.0	55	-	-
			-	-	-	65	-	-
	Trachyte	-	rough joint	dry	-	-	30	Hoskin et al. (1968)

Table 4-5 continued

Igneous Rock	(massive, holocrystalline)		-	-	-	-	28	Mogi (1964)
	(massive, holocrystalline)		-	-	-	-	18.4	Mogi (1965)
	Tuff	24	bedding	-	-	22	10	-
			fracture	-	-	20	-	-
			-	-	-	21.5	-	-
			-	-	0-1.0	18	-	-
			-	-	1.0-3.0	13	-	-
			-	-	above 3.0	22	-	-
	Tuff (dacite pumic) (dense, finely laminated)	-	-	-	-	-	19.4	Mogi (1964)
	(dense)		-	-	-	-	29	Mogi (1964)
	(massive, slightly altered)		-	-	-	-	16	Mogi (1964)
	Diorite	-	-	dry	-	-	25	Lacy (1963)
			-	wet	-	-	20	Lacy (1963)

Table 4-5 continued

Igneous Rock	Diorite (quartz)		-	-	-	-	-	24	Mogi (1964)
	Tonalite		-	-	-	-	-	31	Saucier (1969)

Table 4-6

Mean Values of ϕ_p, ϕ_r for the Three Rock Groups

Rock Group	Range of ϕ_p	Mean ϕ_p	Std. Dev.	Range of ϕ_p	Mean ϕ_r	Std. Dev.
Sedimentary Rock	14-77	47	21.4	8-61	33.2	8.4
Metamorphic Rock	4-81	32	19.6	18-49	33.6	7.8
Igneous Rock	13-72	37	13.9	10-53	32.4	8.8

metamorphic rocks, peak friction angles range from 4^{o} to 81^{o} with mean value 32^{o}; while the residual friction angles range from 18^{o} to 49^{o} with mean value 33.6^{o}. The lower peak friction angles are due to the large cohesion intercept. For igneous rocks, peak friction angles range from 18^{o} to 72^{o} with mean value equal to 37^{o}. The residual friction angles range from 10^{o} to 53^{o} with mean value 32.4^{o}. The values of standard deviation indicate that the peak friction angles for these three groups of rocks have larger variations from the mean value than the residual friction angles. The large variation is due to the very low normal stress, healed joint, intact rocks, homogenous rocks, and the high cohesion intercept. These factors create the extreme low and high values.

Individual Major Rock Types

In Table 4-5, there are several rock types which have large ranges of peak and residual friction angles. These data represent all those calculated using the linear analysis and those from published literature. A histogram of peak or residual friction angles for the rock type with range of friction angles was plotted. These histograms are presented in Appendix F and are discussed below. Note that the number of tests for each rock type mentioned below represents those tests involved in the linear regression.

Limestone

There were about 69 tests for this rock involved in the linear regression analysis. The discontinuities are bedding plane, artificially sawn, joint, concrete-rock interface, sandblasted surface, limestone-moraine contact and joint. The stress levels are from 0.1 MN/m^2 to

8.3 MN/m^2. From the histograms, it can be seen that the peak friction angles occur mostly within the intervals of 27^o to 39^o, of 64.4^o to 77^o. The peak friction angles in the interval of 64.4^o to 77^o may be due to the effect of asperities. The residual friction angles occur frequently in the range of 35.6^o to 39.7^o.

Sandstone

For this rock, there were 30 tests involved in the regression analysis. The discontinuities are sawn, sandblasted, polished planar surface, fracture, break of core sample, bedding, and schistocity. The stress levels are from 0.1 to 250 MN/m^2. The residual friction angles occur frequently in the interval of 31.7^o to 35^o.

Siltstone

The number of tests for this rock type is not clear. The discontinuities are faults and sandblasted surfaces. The stress levels for this rock type are from 0.1 to 7.5 MN/m^2. The residual friction angles occur mostly in the range of 30.4^o to 33.2^o.

Amphibolite

There were 410 tests for this rock type in the regression analysis. The discontinuities are sawn surface, natural joint, healed joint, discontinuities underneath natural slope, conjugate joint set and foliation. The histogram shows that the peak friction angles occur from 32^o to 39.4^o and from 68.4^o to 74.2^o. The peak angles occur mostly from 27.8^o to 33.6^o. The angles occuring in the interval of 68.4^o to 74.2^o may be to the effect of asperities.

Gneiss

There were about 450 tests involved in the linear regression analysis. The discontinuities are fractures, schistose plane, foliation, joint, discontinuities beneath natural or excavated slope, sawn surface, separated foliation, fault and slickensided surface. The stress range is from 0.5 to 250 MN/m^2. The peak friction angles in the histogram are in the interval of 21^o to 36^o, and in the interval of 70.2^o to 75.1^o. The peak angles occur mostly in the range of 26^o to 31^o. The angles between 70.2^o to 75.1^o may be due to asperities.

Gneiss (schistose)

For this rock type, there were about 140 tests involved in the linear regression analysis. The discontinuities are sandblasted surface, foliation, joint and sawn surface. The stress levels are from 0.1 to 8.1 MN/m^2. Histograms show that peak friction angles occur mostly from 21.4^o to 27^o; the residual friction angles occur frequently from 22.2^o to 26^o. The residual friction angles also occur in the interval of 39^o to 43^o.

Marble

For this rock type, there were 10 tests involved in the linear regression analysis. The discontinuities are joint, bedding, fracture and break of test specimen. Stress levels are from 0.1 to 250 MN/m^2. For the histogram, residual angles occur mostly from 28^o to 33.3^o.

Schist

For schist, there were approximately 27 tests in the linear regression analysis. Discontinuities in this rock type are foliation, separated

foliation and sawn surface. Stress levels are from 1 to above 2 MN/m^2. The histogram indicates that peak friction angles occur from 22^o to 29^o, but occur mostly in the interval of 22^o to 24^o.

Quartzite

The number of tests for this rock type is not clear. The discontinuities are joint, planar polished surface and discontinuities beneath natural or excavated slope. The histogram shows that residual angles occur mostly from 23^o to 26^o.

Basalt

Basalt has approximately 20 tests involved in the linear regression analysis. The discontinuities are sandblasted surface, polished planar surface, bedding and fractures. Stress levels are from 0.1 to 8.5 MN/m^2. The residual friction angles occur mostly in the range of 34.5^o to 36.3^o.

Dacite

Dacite has about 24 tests in the linear regression analysis. Discontinuities involved in this rock type are sawn surface and fractures. Stress levels range from 1 to above 2 MN/m^2. The histogram shows that the peak friction angles occur mostly from 39.5^o to 41^o.

Granite

Granite has approximately 10 tests in the linear analysis. The discontinuities are artificial extension fractures, shear fractures, artificial surface, sandblasted surface, joint and contact of granite and mylonite. Stress levels are from 0.1 to 7.1 MN/m^2. In the range of 30^o to 55^o, the peak friction angles occur mostly in the interval of 30^o to 47^o. However, peak friction angles also occur mostly in the

range of 64^{o} to 72^{o}; this may be due to asperities. The residual angles occur mostly in the interval of 33^{o} to 36^{o}.

Monzonite

There were 200 tests involved in the linear regression analysis. Discontinuities are mainly artificial grouted or natural grouted joint, and sawn surface. The peak angles occur mostly in the interval of 35^{o} to 42^{o}. The occurence of peak angles in the interval of 55.2^{o} to 62^{o} may be due to asperities.

Monzonite (Quartz)

There were about 17 tests involved in the regression analysis. Discontinuities are sawn surface, joint and natural open joint. The stress levels range from 1 to above 2 MN/m^2. The peak angles occur mostly in the interval of 26^{o} to 32^{o}.

Porphyry

The number of tests for this rock type is not clear. The discontinuities involved in this rock type are natural joint and shear fractures. Stress levels are from 1 to 13.3 MN/m^2. The residual friction angles occur mostly in the range of 29.6^{o} to 33.4^{o}.

The range, mean value and standard deviation of the peak and residual friction angles for the above discussed rock types and the other rock types (values from regression analysis and from literature) are summarized in Table 4-7. In addition, peak friction angles and cohesion from regression analysis are included in the table. For sedimentary rocks, the range of mean ϕ_p is from 43.4^{o} to 70^{o}; the range of mean ϕ_r is

Table 4-7

Mean Values of ϕ_p, ϕ_r of Each Individual Rock Type

	Rock	No. of Test	Range of ϕ_p	Mean	St. Dev.	$\phi_{regression}$	$c_{regress.}$ ($\times 10^{-3}$ MN/m^2)	Range of ϕ_r	Mean	St. Dev.
Sedimentary Rocks	Chalk	-	-	-	-	-	-	30-41	37	6.1
	Conglomerate	-	70	70	-	-	-	35	35	-
	Dolomite	-	-	-	-	-	-	27-61	37.4	7.5
	Limestone	69	14-177	43.4	22.6	14-49	0.8-0.1	19-48	36.2	4.1
	Marl	-	-	-	-	-	-	10-13	11.5	2.1
	Sandstone	30	26-70	47.3	21.5	26-32	0.2-0.1	25-45	31.7	3.9
	Anhydrite	-	-	-	-	-	-	30	30	-
	Greywack	-	-	-	-	-	-	36	36	-
	Siltstone	-	-	-	-	-	-	22-36	30.3	3.2
	Shale	-	70	70	-	-	-	22-56	33.5	14.4
	Shale (Breccia)	-	-	-	-	-	-	36-50	43	9.9
	Shale (Bentonitic)	-	-	-	-	-	-	7.5	7.5	-
	Shale (Clay)	-	-	-	-	-	-	28	28	-

Table 4-7 continued

	Rock	No. of Test	Range of ϕ_p	Mean	St. Dev.	$\phi_{regress.}$	$c_{regress.}$	Range of ϕ_r	Mean	St. Dev.
Metamorphic Rocks	Amphibolite	410	22-80	50.4	23.2	22-75	0.3-0.12	32-39	35	3.6
	Gneiss	450	21-80	35.8	19	21-37	0.2-0.05	31-49	39.8	8.2
	Gneiss (Granitic)	-	40	40	-	-	-	31-40	35	3.7
	Gneiss (Schistose)	140	16-43	27.9	8.5	16-33	0.3-0.01	18-43	27.3	5.0
	Marble	10	16-32	22.4	6.4	16-32	0.2-0.22	28-49	35.3	7.1
	Phyllite	10	17-28	21.8	5.2	17-28	0.3-0.09	32-40	36	5.7
	Schist	270	22-29	25.1	2.7	22-29	0.3-0.13	-	-	-
	Schist (Phyllite)	-	45	45	-	-	-	40	40	-
	Schist (Carboni-ferous)	20	18-35	25.8	6.4	18-35	0.6-0.17	-	-	-
	Schist (Calcarous)	6	19-20	19.7	0.6	19-20	0.37	-	-	-
	Schist (Sericite)	22	7-19	12.4	5.3	7-19	0.6-0.2	-	-	-
	Quartzite	-	75-80	77.5	3.5	-	-	23-48	34.4	5.5

Table 4.7 continued

	Rock	No. of Test	Range of ϕ_p	Mean	St. Dev.	$\phi_{regress.}$	$c_{regress.}$	Range of ϕ_r	Mean	St. Dev.
Metamorphic Rocks	Serpentine	33	4-81	27.6	24.7	4-81	0.1-0	-	-	-
	Serpentine (Schistose)	7	22-26	24	2	22-26	0.1-0.05	-	-	-
	Slate	-	-	-	-	-	-	22-48	30.2	10.4
	Paragneiss	8	20-26	24.5	3	20-26	0.18-0.15	-	-	-
Igneous Rocks	Basalt	20	15-40	30.6	11.2	15-40	0.9-0.3	31-38	35.1	2.1
	Dacite	24	32-41	36.7	3.3	32-41	4.9-1.4	-	-	-
	Claystone	12	22-28	25	2.2	22-28	0.11-0.07	-	-	-
	Dolerite	-	-	-	-	-	-	37-52	44.5	10.6
	Gabbro	-	-	-	-	-	-	33-48	42.7	8.4
	Andesite	-	35-55	45.5	11	-	-	34	34	-
	Andesite (Augite)	-	-	-	-	-	-	28	28	-
	Andesite (Pyroxene)	-	-	-	-	-	-	35	35	-
	Granite	10	30-72	50.3	17.5	31-41	0.28-0.6	28-38	32.8	2.3

Table 4-7 continued

	Rock	No. of Test	Range of ϕ_p	Mean	St. Dev.	$\phi_{regress.}$	$c_{regress.}$	Range of ϕ_r	Mean	St. Dev.
Igneous Rocks	Granite (Biotite)	-	-	-	-	-	-	48	48	-
	Monzonite	200	28-62	39.6	11.1	28-62	0.6-0	32	32	-
	Monzonite (Quartz)	17	26-49	35.6	8.1	26-49	2.0-0	53	53	-
	Porphyry	-	39	39	-	-	-	22-41	32.3	6.0
	Peridotite	-	-	-	-	-	-	22-37	29.8	6.6
	Peridotite (Hornblende)	-	-	-	-	-	-	28	28	-
	Porphyry (Quartzite)	30	30-33	31	1.2	30-33	0.2-0.15	-	-	-
	Micro-Granodiorite	34	28-40	33.75	6.1	28-40	1.45-0.07	17-34	25.5	12.0
	Metashale	9	55-65	62.3	4.9	55-65	9-0	-	-	-
	Trachyte	-	18-30	25.3	6.4	-	-	-	-	-
	Tuff	24	13-22	19.5	3.6	13-22	0.9-1.5	10	10	-

Table 4-7 continued

	Rock	No. of Test	Range of ϕ_p	Mean	St. Dev.	$\phi_{regress.}$	$c_{regress.}$	Range of ϕ_r	Mean	St. Dev.
Igneous Rocks	Tuff (Dacite pumic)	-	-	-	-	-	-	16-29	21.3	6.8
	Diorite	-	-	-	-	-	-	20-25	22.5	3.5
	Diorite (Quartz)	-	-	-	-	-	-	24	24	-
	Tonalite	-	-	-	-	-	-	31	31	-

For igneous rocks, the reduction is from 1^{o} to 7^{o}, however, dolerite reduces its friction angle up to 15^{o}; the increase of friction angle is from 1^{o} to 8^{o}. The surface of discontinuities for those rock types that showed increase of friction angle due to water effect is mostly smooth. The increase in strength may be due to the fact that the smooth surfaces are unclean, as mentioned in Bromwell (1966) and Dickey (1966). The surface of discontinuities for those rock types that have reduction in strength is mostly rough. The reduction in strength due to water on rough surface may be related to the reduction in tensile and compressive strength of brittle material due to adverse effect of water, as indicated by Barton (1973).

Joint Type

The effect of joint type (for all rock types) on friction angles can be seen in Table 4-4. The range of ϕ_p for all the joint types is from 15^{o} to 37.5^{o} with a mean value of 26.7^{o}. The range of ϕ_r for all the joints is from 10^{o} to 36^{o} with mean value of 22.3^{o}. The joint type gives friction angles within the range of 20^{o} to 40^{o}. From Table 4-5, it can be seen that for a certain rock type, the rougher joint surfaces give higher friction angles than the smooth surfaces do, i.e., for limestone, slightly rough bedding gives peak friction angle 36.9^{o}, while rough bedding gives peak angle 53.5^{o}.

Stress Levels

Stress levels affect the friction angles. In Table 4-1, it can be seen that there is a corresponding increase or reduction in friction angle when the normal stress increases. The reduction in friction angle is due to shearing off the asperities. The increase in friction angle

from 7.5° to 37.4°. The peak angles have larger dispersion from the mean values than the residual angles do. For metamorphic rocks, the range of mean ϕ_p is from 12.4° to 77.5°; the range of mean ϕ_r is from 27.3° to 39.8°. According to the standard deviation, the variation of ϕ_p from the mean value is close to that of ϕ_r from the mean value. When compared with sedimentary rocks, the peak angles vary less from the mean values than the sedimentary rocks do. For gneiss, marble, and phyllite, the peak angles are lower than the residual angles. This can be specified by the fact that the lower peak angles account for the corresponding high cohesion as shown in the table, while most of the Mohr envelopes for the residual angles pass through the origins. For igneous rocks, the range of mean ϕ_p is from 19.5° to 50.3°; the range of mean ϕ_r is from 10° to 53°. The variation of peak angles is larger than that of residual angles. In this rock group, there are two rock types, basalt and monzonite (quartz), whose peak angles are lower than residual angles. This is due to the high cohesion intercept corresponding to the lower peak angles.

Effect of Moisture

In Table 4-5, moisture conditions are specified. The effect of water on the residual friction angles is summarized in Table 4-8. Moisture reduces the residual friction angles, but in some cases, it increases the friction angles. For sedimentary rock, the reduction of friction angles is from 1° to 5°; the increase is from 1° to 8°. For metamorphic rocks, the reduction is from 2° to 8°, with one exception that quartzite has the reduction up to 20°; the increase is about 7°.

Table 4-8

Effect of Water on Residual Friction Angles

	Rock Type	Description of Discontinuities	Dry	Wet	Reduction/ Increase	Range of Reduction/ Increase
	Reduction		ϕ_r			
Sedimentary Rock	Dolomite	sandblasted	32-38	27-35	1-5	
	Limestone	rough sawn	33-39	33-36	1-4	
		sandblasted	36-40	35-38	1-4	
		joint	44	48	4	
	Marl	gouge	13	10	3	
	Sandstone	rough sawn	26-35	25-33	1-2	1-5
		sandblasted	32-34	30-34	1-2	
		shear fracture from failure of intact specimen	28	25	3	
	Siltstone	minor fault, smooth, polished, chloride coated	26	22	4	
		sandblasted	32-36	27-32	2-5	
	Shale	minor fault, smooth, polished, chloride coated	26	22	4	

Table 4-8 continued

	Rock Type	Description of Discontinuities	Dry	Wet	Reduction/ Increase	Range of Reduction/Increase
Metamorphic Rock	Gneiss	shear fracture from failure of intact specimen	35	31	4	
		natural schistose plane	49	44	5	
	Gneiss (granite)	fracture	35	31	4	
	Gneiss (schistose)	sandblasted	25-32	22-28	2-5	2-8, 2-20
	Marble	joint	49	42	7	
	Phyllite	schistose plane	40	42	8	
	Quartzite	joint	44	24-37	7-20	
	Slate	minor fault, smooth, polished, chlorite coated	26	22	4	
Igneous Rock	Basalt	sandblasted	35-38	31-36	1-6	
	Dolerite	joint	52	37	15	
	Granite	shear fracture from failure of intact specimen	35	31	4	

Table 4-8 continued

	Rock Type	Description of Discontinuities	Dry	Wet	Reduction/ Increase	Range of Reduction/Increase
		Reduction	ϕ_r			
Igneous Rock	Granite	artificial surface	38	31	7	1-7, 1-15
	(f.g.)	sandblasted	31-36	29-34	1-6	
	(c.g.)	sandblasted	30-36	28-34	1-4	
	Diorite	-	25	20	5	
		Increase	ϕ_r			
Sedimentary Rock	Chalk	joint	40	41	1	1-8
	Sandstone	artificial, planar, polished	27-32	31-39	4-8	
Metamorphic Rock	Quartzite	artificial, planar, polished	23	30	7	7
Igneous Rock	Basalt	artificial, planar, polished	33	35	8	1-8
	Gabbro	joint	47	48	1	

with increasing normal stress may be due to the development of gouge or slickensided surface.

4.2 Discussion of Deformability

Data on deformability supplied by the sources is limited, especially, there is no data on normal stiffness. Only a small amount of data on shear stiffness was derived from tests. The values are summarized in Table 4-9. In addition, two tables, Table 4-10 and 4-11, of shear stiffness and normal stiffness were extracted from published literature. In Table 4-9, the mean value of elastic shear stiffeners varies between 0.06 to 1.5 GN/m^3; the mean value of peak shear stiffness from 0.01 to 0.35 GN/m^3. The elastic shear stiffness is larger than the peak shear stiffness. The variation of these two stiffnesses from the mean values is in the same order. In Table 4-10, (from Kulhway (1978)), the shear stiffness was determined at the yield point and peak point, with corresponding average value 3.02 GN/m^3 and 2.82 GN/m^3, respectively. The shear stiffness at yield is larger than the peak shear stiffness. In Table 4.11 (from Kulhway (1978)), the mean value of the normal stiffness is about 13.03 GN/m^3.

For all the rock types in Tables 4-9 and 4-10, the values of peak shear stiffness range from as low as 0 GN/m^3 to as high as 29.8 GN/m^3. The value of yield shear stiffness varies between 0.33 to 8.40 GN/m^3. The values of elastic shear stiffness range from 0.04 to 1.5 GN/m^3. Shear stiffness varies with rock types. From the two tables, it can be seen that for the same rock type, shear stiffness depends on joint type; the

Table 4-9

Summary of Shear Stiffness Values

Rock Type	Descrip. of Discontinuity	Range of kse ($\times 10^4$ MN/m^3)	Mean ($\times 10^4$ MN/m^3)	Standard Deviation ($\times 10^4$ MN/m^3)	Range of ksp ($\times 10^4$ MN/m^3)	Mean ($\times 10^4$ MN/m^3)	Standard Deviation ($\times 10^4$ MN/m^3)
Claystone	Oriented Lamination	0.02-0.1	0.06	0.03	0.01-0.04	0.03	0.01
	Non-Oriented Lamination	0.03-0.07	0.05	0.02	0.01-0.02	0.017	0.01
Lignite	Impact Rock	0.03-0.2	0.08	0.05	0.02-0.1	0.06	0.03
	Fracture	0.03-0.04	0.037	0.01	0-0.01	0.01	0.12
Micro-Granodi-orite	Artificial Grounded Surface	-	-	-	0.02-0.4	0.12	0.12
Amphibo-lite	Sawn	0.9-1.9	1.5	0.45	0.13-0.6	0.35	0.19
	Joint	0.2-8.9	1.12	1.08	0.04-0.85	0.19	0.13
Monzonite	Joint	0.03-1.1	0.4	0.26	0.01-0.64	0.2	0.15
	Artificial Grounded Surface	-	-	-	0.03-0.42	0.12	0.12
	Natural Grounded Surface	-	-	-	0.04-0.15	0.09	0.06

Properties of discontinuities under direct shear conditions

Discontinuity number	Test designation	Specimen description	Discontinuity thickness (cm)	Discontinuity area (cm²)	Range of initial normal stress (MN/m²)	Secant shear stiffness K_s (GN/m³) Yield Range	Yield Avg.	Peak Range	Peak Avg.	Cohesion, C (MN/m²) Maximum C	Cohesion, C (MN/m²) Residual C_r	Angle of friction φ Maximum φ	Angle of friction φ Residual ϕ_r	Curve type	Reference
DLL-1	10-14.6 run 3 — U. Illinois	Berea sandstone — dry, sawed joint	—	82	0.26	—	—	—	29.80	—	—	—	—	2a	Goodman (1968)
DLL-2	6-14.7 run 7 — U. Illinois	Limestone — dry, sawed joint	—	82	10.40	—	—	—	8.73	—	—	—	—	2a	Goodman (1968)
DLL-3	QP2 - U. C., Berkeley	Boise sandstone — dry, rough saw cut	—	6	2.43	—	—	—	1.29	—	—	—	—	3a	Goodman (1968)
DLL-4	Blackingstone — Imperial Col.	Granite — dry, rough joint from breaking beam	—	144—208	1.18— 1.42	1.26— 1.87	1.42	0.99— 1.87	1.32	—	—	—	—	3b	Goodman (1968)
DLL-5	Delgado — Imperial Col.	Slate — dry, natural cleavage surface	—	500	4.37	—	0.88	—	0.79	—	—	—	—	4a	Goodman (1968)
DLL-6	Vouglans Dam	Limestone — oolitic, compact to stylolidic	—	575	0.49	—	6.08	1.68— 4.61	2.78	—	—	—	—	4a	Goodman (1968)
DLL-7	Larouviere — 1965	Marl layers in limestone — sat.	0.1—0.3	605—730	0.47— 0.56	2.16— 3.73	2.84	0.51— 3.73	2.13	—	—	—	—	1.4a	Goodman (1968)
DL- 1	Larouviere — 1964	Marly partings in limestone — sat.	0.1—5.0	51—63	0.24— 0.77	2.16— 3.34	2.74	0.85— 5.69	2.89	—[A]	0	—[A]	38.4	1	Goodman (1968)
DL- 2	Vouglans Dam	Limestone with marly joints — dry	0.025—2.0	28—47	0.49— 1.47	—	—	2.26—23.55	9.76	0.92	0.11	46.6	37.8	1	Goodman (1968)
DL- 3	L'Aquila Meridional Apenuine	Sandstone — marl contact	—	—	0.10— 0.98	0.33— 2.08	0.84	0.11— 0.17	0.15	0.20	0.15	45.0	36.0	3	Baldwin (1970)
DL- 4	Brescia Meridional Prealps	Phyllitic schist fractures	—	—	9.20— 1.47	0.41— 0.97	0.65	0.14— 0.40	0.22	0	0	45.0	40.0	3	Baldwin (1970)
DL- 5	B-2 Sarajevo	Limestone — slightly rough bedding	—	1500	0.15— 3.63	0.83— 4.12	2.17	0.20— 1.37	0.84	1.23	0.87	36.9	29.8	3a	Goodman (1968)
DL- 6	B-3 Sarajevo	Limestone — rough bedding surfaces	—	1600	0.30— 3.36	0.33—14.90	5.93	0.26— 7.36	3.06	0.89	0.23	53.5	43.2	3a	Goodman (1968)
DL- 7	D-2 Sarajevo	Limestone — rough unfilled fractures	—	1600	1.52— 4.00	0.24—13.80	8.46	1.26— 2.61	1.98	2.69	0.88	19.0	31.8	3a	Goodman (1968)
DL- 8	Malpasset MIII8	Foliated gneiss and mylonite	4.0—5.0	10.6—24.5	0.39— 2.94	1.46— 4.71	2.55	0.69— 3.69	2.36	1.17	0	53.0	46.3	3a	Goodman (1968)
DL- 9	Delgado — Imperial Col.	Porphyry — dry, natural joint surface	—	500	3.24—10.10	0.96— 1.64	1.30	0.26— 1.94	1.02	0.74	0	39.0	35.5	3b	Goodman (1968)
DL-10	B-1 Sarajevo	Limestone — mylonite along bedding	—	1500	0.21— 2.38	1.04— 8.04	3.90	0.28— 5.69	1.25	0.51	0.29	37.3	35.5	4a	Goodman (1968)
DL-11	Vouglans Dam	Moist marly joint in limestone	1.5—3.0	980—1243	0.53— 2.99	1.18— 3.33	2.65	0.41— 4.71	1.70	0.36	0.08	26.0	25.2	4a	Goodman (1968)
DL-12	B-1 Sarajevo	Limestone — thin shale seams along bedding	—	1500	1.23— 2.80	1.56—13.90	5.96	0.32— 8.33	3.08	0.49	0.49	30.6	30.6	4b	Goodman (1968)
DL-13	Vouglans Dam	Marly joint — sat.	1.3—3.2	1030—1240	0.49— 2.94	0.09— 2.74	1.41	0.02— 1.86	0.78	0	0	23.4	23.4	4b	Goodman (1968)
DL-14	D-1 Sarajevo	Limestone — smooth unfilled fractures	—	1600	0.88— 2.40	0.41— 2.36	1.07	0.20— 1.28	0.61	0	0	38.4	36.3	4c	Goodman (1968)
DL-15	Torino Gran Paradiso Massiccio	Granitic gneiss fractures	—	—	0.20— 0.78	0.29— 0.38	0.33	0.09— 0.12	0.11	0	0	40.0	40.0	4c	Baldwin (1970)
DL-16	Vouglans Dam	Limestone with marly joints — sat.	0.025—0.2	24—40	0.49— 1.47	—	1.47	0.14—31.60	7.41	0	0	55.8	39.6	1.3a 4a,b,c	Goodman (1968)
DIS- 1	1P Krivoklat	Bedding plane in greywacke	0.5—0.8	2265	1.24	—	—	—	0.23	—	—	—	—	4b	Goodman (1968)
DIS- 2	2P Krivoklat	Bedding plane in greywacke	>0.1	3510	1.01	—	—	—	1.21	—	—	—	—	4b	Goodman (1968)
DIS- 3	3P Krivoklat	Bedding plane in greywacke	Closed, clean	3660	0.43	—	—	—	2.26	—	—	—	—	4b	Goodman (1968)
DIS- 4	Vouglans Dam	Marly sand filled joint	0.1—0.2	44000	0.98	—	—	—	2.34	—	—	—	—	4b	Goodman (1968)
DIS- 5	K1 Kurobe IV Dam	Vertical fault	Thick, uneven	—	0.37— 1.07	—	—	0.17— 0.23	0.20	—	—	—	—	4c	Goodman (1968)
DIS- 6	SLL Khajuri Dam	Closely jointed shale zone in limestone	0.2—0.5	50000	0.02[2]	—	—	0.01— 0.02	0.02	—	—	—	—	4c	Goodman (1968)
DIS- 7	SLS Khajuri Dam	Shale interbed — wet	0.2—0.5	50000	0.02— 0.03	—	—	0.01— 0.02	0.02	—	—	—	—	4c	Goodman (1968)
DIS- 8	C-2 Dolesice Dam	Schistosity plane in amphibolite	—	5000	0.12	—	—	—	0.59	—	—	—	—	—	Goodman (1968)
DIS- 9	Jupia Dam	Unbonded basalt — sandstone contact	—	307900	0.13	—	—	—	0.11	—	—	—	—	—	Goodman (1968)
	Overall summary or average		Closed — 5.0	5—307900	0.02—10.40	0.09—14.90	3.02	0.01—31.60	2.82	0.61	0.18	39.3	35.7		

DLL series — laboratory direct shear tests over limited stress range.
DL series — laboratory direct shear tests.
DIS series — in-situ block direct shear tests.

A — data too scattered and/or too little spread.

Avg. Normal stiffnesses, K_n (in GN/m³) are: 35.1 for DLL-3, 1.96 for DIS-4, 0.24 for DIS-6, 0.26 for DIS-7.

Table 4-10 Summary of shear stiffness values (from Kulhway, 1975)

Test designation (1)	Specimen description (2)	Discontinuity: Area, in square meters (3)	Discontinuity: Thickness, in millimeters (4)	Joint face roughness, in millimeters (5)	Normal stiffness, K_n, in giganewton per cubic meter (6)	Modulus of rock, E_r, in giganewton per cubic meter (7)	E_r/K_n, in meters (8)	Reference (9)
QP2	Boise sandstone with dry, rough sawed joint	5×10^{-4}	—	—	35.1	7.46	0.21	a
Vouglans Dam	Marly sand filled joint	4.4	1-2	—	1.96	—	—	b
SLL Khajuri Dam	Closely jointed shale zone in limestone	5	2-5	—	0.24	—	—	b
SLS Khajuri Dam	Shale interbed—wet	5	2-5	—	0.26	—	—	b
25	Lyon's sandstone with clay joint*	1.45×10^{-1}	2.26	1.91	5.59	2.48	0.44	c
26	"	"	1.88	1.42	5.40	"	0.46	c
28	"	"	0.25	0.20	5.40	"	0.46	c
47	"	"	0.53	0.21	5.43	"	0.46	c
69	Sierra White Granite with clay joint*	"	1.47	1.33	5.21	22.06	4.23	c
70	"	"	1.37	1.51	16.91	"	1.30	c
71	"	"	1.22	2.27	67.59	"	0.33	c
72	"	"	1.07	0.06	7.22	"	3.06	c

*Clay filled joint is saturated and has the following properties: 100% < 2μ, w_l = 57%, PI = 27.
Note: 1 GN/m³ = 3,684 lb/cu in.

(a) Mahtab (1970) (b) Goodman (1968) (c) Goodman (1972)

Table 4-11 Summary of normal stiffness values (from Kulhaway,1978)

rougher the joint surface, the higher the shear stiffness. In addition, joint width affects the shear stiffness in such a way that shear stiffness increases with decreasing discontinuity width. Filler material also affects shear stiffness. The moisture of filler material may affect the shear stiffness. Increasing wetness of filler material may decrease shear stiffness.

Table 4-11 illustrated that normal stiffness varies with rock type. However, joint type and filler material affect the normal stiffness the most. Normal stiffness increases with joint width and roughness of discontinuity surface, and it varies with different type of filler material.

It can be concluded that the variation in shear and normal stiffness depends more on joint type and filler material than on rock type. Test methods also affect the results of deformability.

CHAPTER 5

SUMMARY AND CONCLUSIONS

Summary

A model was developed to describe the stress-displacement behavior of rock joints in an organized manner and to store the values of the descriptive parameters in a large segmented database. A computer program was developed for this purpose. In addition, existing computer programs were employed for data management and statistical analysis to study the shear strength and deformability of rock joints. These shear strength and deformability results were then combined with those extracted from published literature for detailed interpretation.

Conclusions

Peak and residual friction angles of all rock types and rock groups (sedimentary, metamorphic and igneous rocks) were determined through linear regression analysis; these data were supplemented by the data extracted from published literature. The peak friction angles for all rock types have a very large range (from 12.4^{o} to 77.5^{o}). Given the fact that friction angles represent the inclination of the Mohr Envelope at certain stress levels, the low values are usually due to high cohesion, while the high values represent a limiting condition at low normal stress. Compared to the standard deviation of peak friction angles, the residual friction angles have less variability and most of the values are within a certain range (25^{o} to 35^{o}).

Considering the typical rock categories, one finds: sedimentary rocks have the highest peak friction angles, while metamorphic rocks have the lowest peak friction angles. The mean residual friction angles derived from all the information for these three rock categories are very similar, around 34^{o}.

Among all rock types, gneiss, marble, phyllite, basalt and monzonite (quartz) have peak angles lower than the residual angles. This is due to the fact that low peak angles are derived from the Mohr Envelope and influenced by the high cohesion intercept.

The effect of water can reduce the residual friction angles (no peak friction angles). The reduction may be due to the cleanliness of the joint surface. However, in a few cases water shows an increase in residual angles. This may be due to the adverse effect of water on tensile and compressive strength of brittle material.

Joint type affects the strength such that rough surfaces give higher friction angles than smooth surfaces.

Increase in normal stress can increase or reduce the friction angles. Reduction may be due to shearing off the asperities, while increasing may be due to the development of gouge or slickensided surfaces.

From the limited amount of deformability data, it can be seen that shear and normal stiffnesses depend more on joint type and filler material than on rock type. Shear stiffness and normal stiffness increase with the roughness of joint surfaces. Decreasing joint width increases shear stiffness, but decreases normal stiffness. The stiffnesses vary with different types of filler material. Wetness of filler material may affect the stiffness. Test methods also affect the stiffnesses resulting

from the deformability test.

Finally, in order to investigate the deformation behavior of rock joints, in addition to shear strength data, the stiffness data should be measured during the test.

REFERENCES

Baldovin, G. (1970), "The Shear Strength of Some Rocks by Laboratory Tests," Proceedings of the 2nd Congress Inst. Soc. Rock Mechanics, Belgrade, 1970, 2: pp. 165-172.

Barton, N.R. (1971a), "A relationship between joint roughness and joint shear strength," Proc. Int. Symp. Rock Mech. Rock Fracture, Nancy, Paper I-8.

Barton, N.R. (1971b), "Estimation of in-situ shear strength from back analysis of failed rock slopes," Proc. Int. Symp. Rock Mech. Rock Fracture, Nancy, Paper II-27.

Barton, N.R. (1972), "A Model Study of Rock-Joint Deformation," Int. J. Rock Mech. Min. Sci., Vol. 9, pp. 579-602.

Barton, N.R. (1973), "Review of a New Shear Strength Criterion for Rock Joints," Engineering Geology, Vol. 7, No. 4, pp. 287-332.

Barton, N.R. (1976), "The shear strength of rock and rock joints," International Journal of Rock Mechanics and Mining Sciences, Vol. 13, pp. 255-279.

Bromwell, L.G. (1966), "The Friction of Quartz in High Vacuum," Research Report R66-18, Department of Civil Engineering, M.I.T.

Byerlee, J.D. (1967), "Frictional Characteristics of Granite under High Confining Pressure," J. Geophys. Res. 72, pp. 3639-3648.

Byerlee, J.D. (1968), "Brittle-Ductile Transition in Rocks," J. Geophys. Res. 73, pp. 4741-4750.

Byerlee, J.D. (1975), "The Fracture Strength and Frictional Strength of Weber Sandstone," Int. J. Rock Mech. Min. Sci. & Geomech. Abstr., 12, pp. 1-4.

Coulson, J.H. (1970), "The Effects of Surface Roughness on the Shear Strength of Joints in Rock," thesis, Univ. of Illinois, U.S. Dept. Army Corps Eng., Miss. River Div., Omaha, Nebr., Tech. Rep. MRD-2-70, pp. 283.

Coulson, J.H. (1972), "Shear Strength of Flate Surfaces in Rock," Proc. 13th. Symp. on Rock Mech., Urbana, IL, pp. 77-105.

Dearman, W.R., Baynes, F.J. and Irfan, T.Y. (1978), "Engineering Grading of Weathered Granite," Engineering Geology, 12, pp. 345-374.

Deklotz, E.J., Heck, W.J., and Neff, T.L. (1965), "Tests for the Strength Characteristics of a Schistose Gneiss," Corps of Engineers MRD Laboratory Report, pp. 64-126.

Deklotz, E.J. and Heck, W.J. (1965b), "Tests for Strength Characteristics of Rock," Piledriver Project, U.S. Army Corps of Engineers, Mo. River Div., Omaha, Neb., MRD Lab., pp. 64-474.

Deklotz, E.J., Heck, W.J. and Neff, T.L., (1966), "Strength Parameters of Selected Intermediate Quality Rocks," First Interim Report, U.S. Army Corps of Engineers, Mo. River Div., Omaha, Nebr., MRD Lab., pp. 64-493.

Deklotz, E.J., and Brown, J.W. (1967), "Tests for Shear Strength Characteristics of a Schistose Gneiss, Mechanical Anisotropy," U.S. Army Corps of Engineers, Missouri River Division Technical Report No., pp. 1-67.

Dickey, J.W. (1966), "Frictional Characteristics of Quartz," S.B. Thesis, Department of Chemical Engineering, M.I.T.

Duncan, N. and Sherman-Chase, A. (1965, 1966), "Planning, Design and Construction, Rock Mechanics in Civil Engineering Works," Civil Engineering and Public Review, 60: 1751, 1755-1756, 61: 57-59, 213-215, 217, 327-330, 431, 433, 615-617, 751-753.

Duncan, N. (1969), "Engineering Geology and Rock Mechanics, 2," Leonard Hill, London, pp. 270.

Fairhurst, C. (1964), "On the Validity of Brazilian Test for Brittle Material," International Journal of Rock Mechanics and Mining Sciences, Vol. 1, pp. 535-546.

Goldstein, M., B. Goosev, N. Dyrogovsky, R. Tulinov, and A. Turovskaya (1966), "Investigation of Mechanical Properties of Cracked Rock," Proc. of the First Congress of the Int. Soc. of Rock Mechanics, Lisbon, Portugal, Vol., p. 521.

Goodman, R.E. (1968), "Effects of Joints on the Strength of Tunnels," Technical Report No. 5, U.S. Army Corps. of Engineers, Omaha District, Omaha, Neb.

Goodman, R.E. (1970), "The Deformability of Joints," Determination of the in-situ modulus of deformation of rock, ASTM, STP 477, pp. 174-196.

Goodman, R.E., Heuze, F.E. and Ohnishi, Y. (1972), "Research on Strength-Deformability-Water Pressure Relationships for Faults in Direct Shear," Final Report on ARPA Contract HO210020, Univ. of California, Berkeley, Ca.

Goodman, R.E. (1974), "The Mechanical Properties of Joints," Proc. 3rd Cong. of Int. Soc. Rock Mechanics, Denver, Vol. I-A, pp. 127-140.

Handin, J. and Hager, R.V., Jr., (1957), "Experimental Deformation of Sedimentary Rocks Under Confining Pressure: Tests at Room Temperature on Dry Samples," Bull. Am. Assoc. Pet. Geol., 41 (1), pp. 1-50.

Hendron, Jr., J.A. (1968), "Mechanical Properties of Rock," in: K.G. Stagg and O.C. ZienKiewicz (Editors), Rock Mechanics in Engineering Practice, Wiley, London, pp. 21-41.

Hoek, E. and Pentz, D.L. (1968), "The Stability of Open Pit Mines," Imperial College Rock Mechanics Research Report No. 5, Interdepartmental Rock Mechanics Project, Imperial College, London SW7, England.

Hoek, E. and Bray, J. (1974), "Rock Slope Engineering," Inst. Min. Metall., London, pp. 309.

Hoskins, E.R., Jaeger, J.C., and Rosengren, K.J. (1968), "A medium scale Direct Friction Experiment," Int. Jour. of Rock Mech. and Min. Sci., Vol. 5, pp. 143-154.

Hungr, O. and Coates, D.F. (1978), "Deformability of Points and Its Relation to Rock Foundation Settlements," Can. Geotech. J., 15, pp. 239-249.

Hutchinson, J.N. (1972), "Field and Laboratory Studies of a Fall in Upper Chalk Cliffs at Joss Bay, Isle of Thanet," Stress-strain behavior of soils, Proc. Roscoe Mem. Symp., Cambridge Univ., 1971, pp. 692-706.

Jaeger, J.C. (1959), "The Frictional Properties of Joint in Rock," Geofis. Pura Appl., Milano, 45, pp. 148-158.

Jaeger, J.C. and Rosengren, K.J., (1968), "Friction and Sliding of Joints," Anu. Conf., Broken Hill, Aust. Inst. Min. Metall. Pap. 36, p. 15.

Krsmanovic, D. (1967), "Initial and Residual Shear Strength of Hard Rocks," Geotechnique 17, pp. 145-160.

Kujundzi' and Colic', B. (1976), "Rock Mass Mechanical Characteristics in an Open Cut at Bor Copper Mine," Rock Mechanics, 8, pp. 153-167.

Kulhaway, F.H. (1975), "Stress Deformation Properties of Rock and Rock Discontinuities," Engineering Geology, 9, pp. 327-350.

Kulhaway, F.H. (1978), "Geomechanical Model for Rock Foundation Settlement," Journal of Geotechnical Engineering, pp. 213-227.

Lacy, W.C. (1963), "Quantitizing Geological Parameters, for the Prediction of Stable Slopes," Transactions of the Amer. Inst. of Mining, Metallurgical, and Petroleum Engineers, Vol. 226, p.272.

Ladanyi, B. and Archambault, G. (1970), "Simulation of Shear Behavior of a Jointed Rock Mass," Proc. 11th U.S. Symposium on Rock Mechanics, Berkeley, pp. 105-125.

Ladanyi, R. and Archambault, G. (1975), "Shear Strength and Deformability of Filled Indented Joints," Co-operative level "B" Pit Slope Project 1972-1977, Final Report on DSS Constract OSV3-0304.

Mahtab, M.A. (1970), "Three-Dimension Finite Element Analysis of Joint and Rock Slopes," thesis, Univ. of California, Berkeley.

Martin, G.R. and Millar, P.T. (1974), "Joint Strength Characteristics of a Weathered Rock," Proc. of the 3rd Cong. of the Int. Soc. of Rock Mech., Denver, Colorado, Vol. II, Part A, pp. 263-270.

Mauer, W.C. (1965), "Shear Failure of Rock Under Compression," Journal Soc. of Petroleum Engineers, Vol. 5, No. 2, p. 167.

Mogi, K. (1964), "Deformation and Fracture of Rocks under Confining Pressure: Compression Tests on Dry Rock Samples," Bull. Earthquake Res. Inst., University of Tokyo, 24 (3), pp. 491-514.

Mogi, K. (1965), "Deformation and Fracture of Rocks under Confining Pressure: Elasticity and Plasticity of Some Rocks," Bull. Earthquake Res. Inst., University of Tokyo, 43 (2), pp. 349-379.

Mogi, K. (1966), "Some Precise Measurements of Fracture Strength of Rocks under Uniform Compressive Stress," Felsmechanik und Ingenieurgeologie 4, pp. 41-55.

Morgenstern, N.R. and Noonan, D.K.J. (1974), "Fractured Coal Subjected to Direct Shear," Proc. of the 3rd Cong. of the Int. Soc. of Rock Mech., Denver, Colorado, Vol. II, Part A, pp. 282-287.

Obert, L., Brady, B.T., and Schmechel, F.W. (1976), "The Effect of Normal Stiffness on the Shear Resistance of Rock," Rock Mechanics 8,, pp. 57-72.

Patton, F.D. (1966a), "Multiple Modes of Shear Failure in Rock and Related Materials," Thesis, University of Illinois.

Patton, F.D. (1966b), "Multiple Modes of Shear Failure in Rocks," Proc. of the First Congress of the Int. Soc. of Rock Mechanics, Lisbon, Portugal, Vol. 1, pp. 509-513.

Paulding, B.W., Jr. (1970), "Coefficient of Friction of Natural Rock Surfaces," Proc. ASCE, 96, No. SM2, pp. 385-394.

Pratt, H.R., Black, A.D., Brown, W.S., and Brace, N.F. (1972), "The Effect of Specimen on the Mechanical Properties of Unjointed Diorite," Int. J. Rock Mech. Min. Sci., 9, pp. 513-529.

Pratt, H.R., Black, A.D., and Brace, W.F. (1974), "Friction and Deformation of Jointed Quartz Diorite," Proc. 3rd Cong. of Int. Soc. Rock Mech., Denver, Colorado, Vol. II, A, pp. 306-310.

Raleigh, C.B., and Paterson, M.S. (1965), "Experimental Deformation of Serpentine and its Tectnic Implications," J. Geophys. Res., 70, pp. 3965-3985.

Rengers, N. (1971), "Unebenheit under Resbungswiderstand von Gesteenstienflächen," dissertation, Tech. Hochschule Fridericiana, Karlsruhe, Ins. Bodenmech, Felsmech. Vernöff., 47, pp. 129.

Ripley, C.F. and Lee, K.L. (1962), "Sliding Friction Tests on Sedimentary Rock Specimens," Trans. 7th Int. Congr. Large Dams, Rome, 1961, Vol. 4, pp. 657-671

Rosengren, K.J. (1968), "Rock Mechanics of the Black Star Open Cut, Mount Isa.," thesis, Austr. Nat. Univ.

Ross, R.S. (1976), "A Comparison of Joint Stiffness Measurements in Direct Shear, Triaxial Compression, and In-Situ," Int. J. Rock Mech. Min. Sci. and Geomech. Abstr., Vol. 13, pp. 167-172.

Saucier, K.L. (1969), "Properties of Cedar City Tonalite," U.S. Army Corps of Engineers, Waterways Exp. Sta., Vicksburg, Miss., Misc. Pap. C-69-9.

Schneider, H.J. (1976), "The Friction and Deformation Behavior of Rock Joints," Rock Mechanics, Sept. 1976, Vol. 8, No. 3, pp. 169-184.

Wallace, G.B., Slebir, E.J., and Anderson, F.A. (1970), "Foundation Testing for Auburn Dam," Proc. 11th Symp. Rock Mech., Berkeley, pp. 461-498.

APPENDIX A

(1) Flow-Chart
(2) Computer Program
(3) Input Procedures
(4) Examples of all files

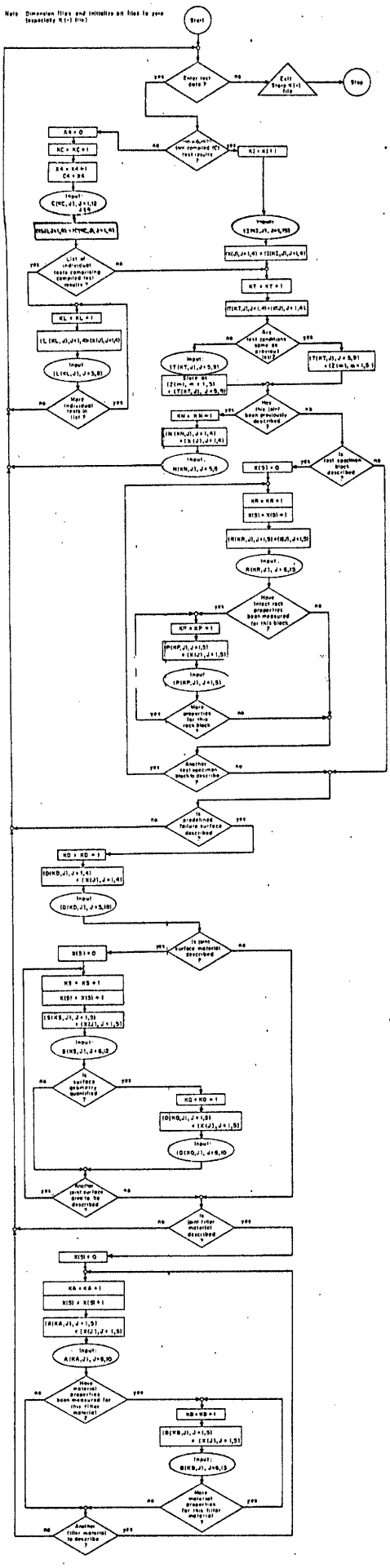

A-1 Detailed flow chart

```
                    InputR.fortran      03/22/79  2020.0 est Thu

      dimension k(12)
      integer x2,x3,x4,x5,t2,t3,t4,n2,n3,n4,r2,r3,r4,r5,p2,r3,r4,r5,d2,d3,d4,s2,s3,s4,s5,a2,a3,a4,a5,a2,a3,a4,a5,
     *b2,b3,b4,b5,c2,c3,c4,l2,l3,l4
      character*3 source,x1,t1,n1,n5,r1,p1,d1,s1,a1,a1,b1,c1,l1
      character*5 t5,t6,=1,=2,r6,r8,r9,r10,r11,r12,r13,r14,r6,r8,
     *r10,r12,d6,d8,d10,d12,d13,d14,d15,d16,d17,d18,s6,s8,s9,s10,s11,s12,
     *a7,a8,a9,a10,b6,b8,b10,b12,c12,i,j
      open(1,attach='vfile_ file1 -extend',mode='out',form='formatted')
      open(2,attach='vfile_ file2 -extend',mode='out',form='formatted')
      open(3,attach='vfile_ file3 -extend',mode='out',form='formatted')
      open(4,attach='vfile_ file4 -extend',mode='out',form='formatted')
      open(7,attach='vfile_ file7 -extend',mode='out',form='formatted')
      open(8,attach='vfile_ file8 -extend',mode='out',form='formatted')
      open(9,attach='vfile_ file9 -extend',mode='out',form='formatted')
      open(10,attach='vfile_ file10 -extend',mode='out',form='formatted')
      open(11,attach='vfile_ file11 -extend',mode='out',form='formatted')
      open(12,attach='vfile_ file12 -extend',mode='out',form='formatted')
      open(13,attach='vfile_ file13 -extend',mode='out',form='formatted')
      open(14,attach='vfile_ file14 -extend',mode='out',form='formatted')
```

Figure A-2 COMPUTER PROGRAM

```
      open(15,attach='vfile_ file%',extend'mode='out',form='formatted')
 1000 write(6,15)
   15 format(' Enter test data?')
      read(5,16)i1
   16 format(v)
      if(i1.eq.1)go to 17
      if(i1.eq.0)go to 18
   17 write(6,19)
   19 format(' Are individual test results?')
      read(5,16)i2
      if(i2.eq.1)go to 20
      if(i2.eq.0)go to 21
   20 i1=i1+i1
      write(6,130)
  130 format(' source  series no.  test no.  misc. no.  np  sp  nr  sr  kso  kap  sd  kn  md  (md/sd)=  jt type')
      read(5,16)source,i,jkk,v1,v2,w3,v4,v5,v6,w7,v8,v9,v10,iJ
      write(1,101)source,i,jkk,v1,v2,v3,v4,v5,v6,w7,v8,v9,v10,iJ
  101 format(a3,7x,i4,2(4x,i4),3x,4(f7.2,2x),2(f7.2,3x),3(f7.2,2x),f7.2,4x,a3)
      x1=source
      x2=i
      x3=J
      x4=kk
      ttest=1
      t2=2
      t3=3
      t4=4
      write(6,25)
   25 format(' Are tests conditions same as previous test?')
      read(5,16)i3
      if(i3.eq.1)go to 26
      if(i3.eq.0)go to 27
   27 write(6,131)
  131 format(' test type(basic  mod  sample area  strain rate  temperature')
      read(5,16)t5,t6,t7,t8,t9
      write(7,102)t1,t2,t3,t4,t5,t6,t7,t8,t9
  102 format(a3,9x,i4,2(6x,i4),7x,a3,5x,a3,5x,f7.2,5x,f7.2,7x,f7.2)
      z1=t5
      z2=t6
      z3=t7
      z4=t8
      z5=t9
      go to 30
   26 t5=z1
      t6=z2
      t7=z3
      t8=z4
      t9=z5
   30 write(6,32)
   32 format(' Has joint been previously described?')
      read(5,16)i4
      if(i4.eq.1)go to 33
      if(i4.eq.0)go to 34
   33 kn=knl
      n1=n1
      n2=n2
      n3=n3
      n4=n4
      write(6,132)
  132 format(' source  series no.  test no.  misc. no.')
      read(5,16)n5,n6,n7,n8
      write(4,103)n1,n2,n3,n4,n5,n6,n7,n8
  103 format(a3,9x,i4,2(6x,i4),7x,a3,9x,i4,2(6x,i4))
      go to 1000
   34 write(6,35)
   35 format(' Is intact rock described?')
```

Fig A-2 (Cont'd) COMPUTER PROGRAM

```
        read(5,16)i5
        if(i5.eq.1)go to 38
        if(i5.eq.0)go to 39
38      x5=0
49      kr=kr+1
        x5=x5+1
        r1=x1
        r2=x2
        r3=x3
        r4=x4
        r5=x5
        write(6,133)
133     format(' block   %vol.   basic composition   1st   2nd   3rd   4th   formation   anis. feature   orien. wrt test')
        read(5,16)r6,r7,r8,r9,r10,r11,r12,r13,r14,r15
        write(8,104)r1,r2,r3,r4,r5,r6,r7,r8,r9,r10,r11,r12,r13,r14,r15
104     format(a3,8x,i4,2(5x,i4),6x,i4,7x,a3,2x,f7.2,3x,a3,5(4x,a3),5x,a3,8x,f7.2)
        write(6,42)
42      format(' Have intact rock properties been measured for this rock?')
        read(5,16)i6
        if(i6.eq.1)go to 43
        if(i6.eq.0)go to 44
43      kp=kp+1
        p1=x1
        p2=x2
        p3=x3
        p4=x4
        p5=x5
        write(6,134)
134     format(' intact rock properties:para1   val   para2   val   para3   val   para4     val')
        read(5,16)p6,p7,p8,p9,p10,p11,p12,p13
        write(9,105)p1,p2,p3,p4,p5,p6,p7,p8,p9,p10,p11,p12,p13
105     format(a3,9x,i4,2(6x,i4),7x,i4,8x,a3,6x,f7.2,3(3x,a3,6x,f7.2))
        write(6,47)
47      format(' More properties for this rock?')
        read(5,16)i7
        if(i7.eq.1)go to 43
        if(i7.eq.0)go to 44
44      write(6,48)
48      format(' Another intact rock to be described?')
        read(5,16)i8
        if(i8.eq.1)go to 49
        if(i8.eq.0)go to 39
39      write(6,50)
50      format(' Is predefined failure surface described?')
        read(5,16)i9
        if(i9.eq.1)go to 51
        if(i9.eq.0)go to 1000
51      kd=kd+1
        d1=x1
        d2=x2
        d3=x3
        d4=x4
        write(6,135)
135     format(' jt orient wrt test   persistence:qual   quan   Jt width:qual   quan   corr. between surface:qual   quan
&       upper surface:basic   1st   2nd   lower surface:basic   1st   2nd   moisture')
        read(5,16)d5,d6,d7,d8,d9,d10,d11,d12,d13,d14,d15,d16,d17,d18
        write(10,106)d1,d2,d3,d4,d5,d6,d7,d8,d9,d10,d11,d12,d13,d14,d15,d16,d17,d18
106     format(a3,7x,i4,2(4x,i4),5x,f6.2,5x,a3,2(2x,f7.2,4x,a3),2x,f7.2,2x,a3,6(3x,a3))
        write(6,54)
54      format(' Is surface described in more detail?')
        read(5,16)i10
        if(i10.eq.1)go to 55
        if(i10.eq.0)go to 56
55      x5=0
65      ks=ks+1
        x5=x5+1
```

Figure A-2 (Cont'd) COMPUTER PROGRAM

```
      s1=x1
      s2=x2
      s3=x3
      s4=x4
      s5=x5
      write(6,136)
136   format(' block   % area   surface mat'l descr.:basic   1st   2nd   3rd   4th')
      read(5,16)s6,s7,s8,s9,s10,s11,s12
      write(11,107)s1,s2,s3,s4,s5,s6,s7,s8,s9,s10,s11,s12
107   format(a3,9x,i4,2(6x,i4),7x,i4,8x,a3,4x,f7.2,4x,a3,4(5x,a3))
      write(6,59)
59    format(' Is surface geometry quantified?')
      read(5,16)i11
      if(i11.eq.1)go to 60
      if(i11.eq.0)go to 61
60    ka=ka+1
      a1=x1
      a2=x2
      a3=x3
      a4=x4
      a5=x5
      write(6,137)
137   format(' asp. ht.   direction of shear:asp   dr   perpendicular:asp. incl.   dr')
      read(5,16)a6,a7,a8,a9,a10
      write(12,108)a1,a2,a3,a4,a5,a6,a7,a8,a9,a10
108   format(a3,9x,i4,2(6x,i4),7x,i4,7x,f7.2,5x,f7.2,2x,f7.2,3x,f7.2,3x,f7.2)
61    write(6,64)
64    format(' Another surface area to be described?')
      read(5,16)i12
      if(i12.eq.1)go to 65
      if(i12.eq.0)go to 56
56    write(6,66)
66    format(' Is infill material described?')
      read(5,16)i13
      if(i13.eq.1)go to 67
      if(i13.eq.0)go to 1000
67    x5=0
77    ka=ka+1
      x5=x5+1
      a1=x1
      a2=x2
      a3=x3
      a4=x4
      a5=x5
      write(6,138)
138   format(' % vol   infill mat'l:basic   1st   2nd   3rd')
      read(5,16)a6,a7,a8,a9,a10
      write(13,109)a1,a2,a3,a4,a5,a6,a7,a8,a9,a10
109   format(a3,9x,i4,2(6x,i4),7x,i4,6x,f7.2,4x,a3,3(5x,a3))
      write(6,70)
70    format(' Have properties been measured for this infill material?')
      read(5,16)i14
      if(i14.eq.1)go to 71
      if(i14.eq.0)go to 72
71    kb=kb+1
      b1=x1
      b2=x2
      b3=x3
      b4=x4
      b5=x5
      write(6,139)
139   format(' infill mat'l properties:para1   val   para2   val   para3   val   para4   val')
      read(5,16)b6,b7,b8,b9,b10,b11,b12,b13
      write(14,110)b1,b2,b3,b4,b5,b6,b7,b8,b9,b10,b11,b12,b13
110   format(a3,9x,i4,2(6x,i4),7x,i4,8x,4(a3,6x,f7.2,3x))
      write(6,75)
```

Figure A-2 (Cont'd) COMPUTER PROGRAM

```
 75    format(' More properties for this infill material?')
       read(5,16)i15
       if(i15.eq.1)go to 71
       if(i15.eq.0)go to 72
       write(6,76)
 72    format(' Another infill material  to be described?')
 76    read(5,16)i16
       if(i16.eq.1)go to 77
       if(i16.eq.0)go to 1000
       x4=0
       tc=fc11
 21    x4=x41
       c4=x4
       write(6,140)
140    format(' source   series no.   test no.   slow   which   or   Phir   Phip   (dn/ds)psave   Jt type')
       read(5,16)i16,c2,c3,c5,c6,c7,c8,c9,c10,c11,c12
111    write(2,111)c1,c2,c3,c4,c5,c6,c7,c8,c9,c10,c11,c12
       format(a3,8x,i4,2(6x,i4),6x,f7.2,4(6x,f7.2),3x,f7.2,8x,a3)
       x1=c1
       x2=c2
       x3=c3
       x4=c4
       write(6,81)
 81    format(' List of individual tests comprising series?')
       read(5,16)i17
       if(i17.eq.1)go to 82
       if(i17.eq.0)go to 83
 82    k1=k111
       11=x1
       12=x2
       13=x3
       14=x4
       write(6,141)
141    format(' test or misc. no.')
       read(5,16)15,16,17,18
       write(3,112)11,12,13,14,15,16,17,18
112    format(a3,9x,i4,2(6x,i4),7x,i4,8x,i4,3(5x,i4))
       write(6,85)
 85    format(' More individual tests in list?')
       read(5,16)i18
       if(i18.eq.1)go to 82
       if(i18.eq.0)go to 1000
       k(1) =a
       k(2)=fc
       k(3)=f1
       k(4)=fn
       k(5) =t
       k(6)=fr
       k(7)=fa
       k(8)=fd
       k(9)=fs
       k(10)=fa
       k(11)=fs
       k(12) =b
       write(15,113)k
113    format(12(5x,i4))
       close(1)
       close(2)
       close(3)
       close(4)
       close(7)
       close(8)
       close(9)
       close(10)
       close(11)
       close(12)
```

Figure A-2 (Cont'd) COMPUTER PROGRAM

```
close(13)
close(14)
close(15)
end
```

Figure A-2 (Cont) COMPUTER PROGRAM

```
Enter test data?
1
Are individual test results?
1
source   series no.   test no.   misc. no.   nP   sP   nr   sr   kse   ksP   sd   kn   nd   (nd/sd)P   Jt type
DM          3           10           2        232.4   192.3   -1  -1  -1  -1  0   -1  -7.62   0  FD
Are tests conditions same as previous test?
0
test type:basic   mod   sample area   strain rate   temperature
DST          PSB          54.81  -1 .`       -1

Has Joint been previouly described?
1
source   series no.   test no.   misc. no.
DM        3     10       1
Enter test data?
1
Are individual test results?
1
source   series no.   test no.   misc. no.   nP   sP   nr   sr   kse   ksP   sd   kn   nd   (nd/sd)P   Jt type
DM          3           10           3        404.3   286.5  -1  -1  -1  -1  0  -1  -7.62   -0.2  FD
Are tests conditions same as previous test?
0
test type:basic   mod   sample area   strain rate   temperature
DST        PSB          54.81  -1  -1
Has Joint been previouly described?
1
source   series no.   test no.   misc. no.
DM        3     10       1
```

Figure A-3 Input Procedures

source	ser no	te no	mis no	desc no	%vol	bas	1st	2nd	3rd
SWS	50	26	1	1	-1.00	SI	-	-	-
SWS	50	34	1	1	-1.00	SI	-	-	-
SWS	50	69	1	1	-1.00	CY	-	-	-
BR	2	1	1	1	-1.00	GT	-	-	-
BR	2	2	1	1	-1.00	GT	-	-	-
BR	2	3	1	1	-1.00	GT	-	-	-
BR	2	4	1	1	-1.00	GT	-	-	-
BR	2	5	1	1	-1.00	GT	-	-	-
BR	2	6	1	1	-1.00	GT	-	-	-
BR	2	7	1	1	-1.00	GT	-	-	-
BR	2	8	1	1	-1.00	GT	-	-	-
BR	2	9	1	1	-1.00	GT	-	-	-
BR	4	5	1	1	-1.00	CY	-	-	-
BR	4	6	1	1	-1.00	CY	-	-	-
OM	1	2	1	1	-1.00	CY	-	-	-
OM	4	2	1	1	-1.00	GM	-	-	-

Figure A-4 Example of File A

source	ser no	te no	mis no	desc no	aso ht	asp incl	dr	asp incl	dr
BR	1	1	1	1	6.92	-1.00	-1.00	-1.00	-1.00
BR	1	2	1	1	6.92	-1.00	-1.00	-1.00	-1.00
BR	1	3	1	1	5.72	-1.00	-1.00	-1.00	-1.00
BR	1	4	1	1	5.72	-1.00	-1.00	-1.00	-1.00

Figure A-5 Example of File Q

source	ser no	te no	desc no	nlow	nhig	cp	phip	cr	phir	(dn/ds)ave	jt
GZD	3	1	1	139.28	899.80	82.70	17.00	34.48	8.00	-1.00	NLA
GZD	3	2	1	278.56	640.55	27.58	35.50	0.00	18.50	-1.00	OLA
GZD	4	1	2	277.87	1221.11	258.56	17.30	48.27	12.50	-1.00	NLA
GZD	4	2	3	140.66	903.37	13.79	33.70	34.48	17.30	-1.00	OLA
GZD	1	1	1	69.64	151.00	68.95	50.50	24.13	24.00	-1.00	IN
GZD	1	2	1	278.56	1232.45	206.86	27.00	24.13	24.00	-1.00	IN
GZD	2	1	2	856.35	1248.69	151.69	37.00	24.13	24.00	-1.00	IN
GZD	1	3	3	275.00	8.00	903.25	0.00	25.10	0.00	-1.00	SA
GZD	13	1	4	143.42	600.56	0.00	19.70	-1.00	19.70	-1.00	FR
GZD	285	1	5	151.00	614.35	-1.00	-1.00	0.00	36.10	-1.00	SA
GZD	286	2	7	151.69	612.28	-1.00	-1.00	0.00	39.00	-1.00	SA
GZD	684	1	1	231.67	231.67	-1.00	-1.00	0.00	39.00	-1.00	CZ
GZD	714	1	1	240.64	240.64	-1.00	-1.00	0.00	59.00	-1.00	CZ
GZD	708	1	1	235.81	235.81	-1.00	-1.00	0.00	48.00	-1.00	CZ
SWS	10	1	1	273.70	1752.00	0.00	23.00	-1.00	-1.00	-1.00	FO
SWS	10	2	2	81.00	871.65	0.00	25.00	-1.00	-1.00	-1.00	FO
SWS	10	3	3	81.00	1661.00	0.00	31.50	-1.00	-1.00	-1.00	FO
SWS	10	4	4	472.43	472.43	0.00	51.50	-1.00	-1.00	-1.00	JT
SWS	10	5	5	53.86	2316.00	0.00	33.00	-1.00	-1.00	-1.00	JT
SWS	10	6	6	229.59	1377.51	0.00	30.00	-1.00	-1.00	-1.00	JT
SWS	10	7	7	0.00	610.00	0.00	32.00	-1.00	-1.00	-1.00	JT
SWS	10	8	8	106.57	266.42	0.00	31.50	-1.00	-1.00	-1.00	JT
SWS	10	9	9	76.06	2510.02	0.00	34.50	-1.00	-1.00	-1.00	JT
SWS	10	10	10	22.44	1750.43	0.00	30.00	-1.00	-1.00	-1.00	SA
SWS	10	11	11	383.23	2043.90	0.00	34.00	-1.00	-1.00	-1.00	SA
SWS	11	1	12	221.42	1372.82	0.00	26.50	-1.00	-1.00	-1.00	FO
SWS	11	2	13	88.57	1417.10	0.00	31.00	-1.00	-1.00	-1.00	FO
SWS	11	3	14	31.73	2919.39	0.00	31.00	-1.00	-1.00	-1.00	FO
SWS	11	4	15	61.51	522.80	0.00	35.00	-1.00	-1.00	-1.00	JT
SWS	11	5	16	62.28	2304.18	0.00	32.00	-1.00	-1.00	-1.00	JT
SWS	11	6	17	196.34	1570.68	0.00	33.00	-1.00	-1.00	-1.00	JT
SWS	11	7	18	69.68	2090.35	0.00	31.50	-1.00	-1.00	-1.00	JT
SWS	11	8	19	307.53	1291.63	0.00	32.00	-1.00	-1.00	-1.00	JT
SWS	11	9	20	23.50	141.00	0.00	33.00	-1.00	-1.00	-1.00	JT
SWS	11	10	21	158.16	1739.75	0.00	35.00	-1.00	-1.00	-1.00	JT
SWS	12	1	22	152.96	2228.79	0.00	11.00	-1.00	-1.00	-1.00	FO

Figure A-6 Example of File C

source	ser no	te no	mis no	jt ori	qul	qun	qul	qun	qul	qun	bas	1st	2nd	bas	1st	2nd	soils
SWS	10	1	1	-1.00	-	-1.00	-	-1.00	-	-1.00	-	-	-	-	-	-	-
SWS	11	7	1	-1.00	-	-1.00	-	-1.00	-	-1.00	-	-	-	-	-	-	-
SWS	11	10	1	-1.00	-	-1.00	-	-1.00	-	-1.00	-	-	-	-	-	-	-
SWS	12	1	1	-1.00	-	-1.00	-	-1.00	-	-1.00	-	-	-	-	-	-	-
SWS	12	10	1	-1.00	-	-1.00	-	-1.00	-	-1.00	-	-	-	-	-	-	-
SWS	12	2	1	-1.00	-	-1.00	-	-1.00	-	-1.00	-	-	-	-	-	-	-
SWS	13	10	1	-1.00	-	-1.00	-	-1.00	-	-1.00	-	-	-	-	-	-	-
SWS	13	2	1	-1.00	-	-1.00	-	-1.00	-	-1.00	-	-	-	-	-	-	-
SWS	1	1	1	-1.00	-	-1.00	-	-1.00	-	-1.00	-	-	-	-	-	-	-
SWS	1	2	1	-1.00	-	-1.00	-	-1.00	-	-1.00	-	-	-	-	-	-	-
SWS	1	3	1	-1.00	-	-1.00	-	-1.00	-	-1.00	-	-	-	-	-	-	-
SWS	2	5	1	-1.00	-	-1.00	-	-1.00	-	-1.00	-	-	-	-	-	-	-
SWS	5	4	1	-1.00	-	-1.00	-	-1.00	-	-1.00	-	-	-	-	-	-	-
SWS	5	5	1	-1.00	-	-1.00	-	-1.00	-	-1.00	-	-	-	-	-	-	-
SWS	20	1	1	-1.00	-	-1.00	-	-1.00	-	-1.00	-	-	-	-	-	-	-
SWS	20	2	1	-1.00	-	-1.00	-	-1.00	-	-1.00	-	-	-	-	-	-	-
SWS	20	3	1	-1.00	-	-1.00	-	-1.00	-	-1.00	-	-	-	-	-	-	-
SWS	20	8	1	-1.00	-	-1.00	-	-1.00	-	-1.00	-	-	-	-	-	-	-
SWS	20	9	1	-1.00	-	-1.00	-	-1.00	-	-1.00	-	-	-	-	-	-	-
SWS	20	10	1	-1.00	-	-1.00	-	-1.00	-	-1.00	-	-	-	-	-	-	-
SWS	33	1	1	-1.00	-	-1.00	-	-1.00	-	-1.00	-	-	-	-	-	-	-
SWS	33	3	1	-1.00	-	-1.00	-	-1.00	-	-1.00	-	-	-	-	-	-	-
SWS	34	1	1	-1.00	-	-1.00	-	-1.00	-	-1.00	-	-	-	-	-	-	-
SWS	34	2	1	-1.00	-	-1.00	-	-1.00	-	-1.00	-	-	-	-	-	-	-
SWS	38	2	1	-1.00	-	-1.00	-	-1.00	-	-1.00	-	-	-	-	-	-	-
SWS	38	3	1	-1.00	-	-1.00	-	-1.00	-	-1.00	-	-	-	-	-	-	-
SWS	50	25	1	-1.00	-	-1.00	-	-1.00	-	-1.00	-	-	-	-	-	-	-
SWS	50	26	1	-1.00	-	-1.00	-	-1.00	-	-1.00	-	-	-	-	-	-	-
SWS	50	29	1	-1.00	-	-1.00	-	-1.00	-	-1.00	WA	0	-	WA	0	-	-
SWS	50	30	1	-1.00	-	-1.00	-	-1.00	-	-1.00	WA	0	-	WA	0	-	-
SWS	50	31	1	-1.00	-	-1.00	-	-1.00	-	-1.00	WA	90	-	WA	90	-	-
SWS	50	32	1	-1.00	-	-1.00	-	-1.00	-	-1.00	ST	0	-	ST	0	-	-
SWS	50	34	1	-1.00	-	-1.00	-	-1.00	-	-1.00	-	-	-	-	-	-	-
SWS	50	43	1	-1.00	-	-1.00	-	-1.00	-	-1.00	-	-	-	-	-	-	-
SWS	50	69	1	-1.00	-	-1.00	-	-1.00	-	-1.00	-	-	-	-	-	-	-
SWS	50	92	1	-1.00	-	-1.00	-	-1.00	-	-1.00	CL	-	-	CL	-	-	-
SWS	50	93	1	-1.00	-	-1.00	-	-1.00	CT	1.00	-	-	-	-	-	-	-
SWS	50	94	1	-1.00	-	-1.00	-	-1.00	-	-1.00	AS	NU	-	AS	NU	-	-
BR	1	1	1	-1.00	-	-1.00	-	-1.00	-	-1.00	-	-	-	-	-	-	W
BR	1	2	1	-1.00	-	-1.00	-	-1.00	-	-1.00	-	-	-	-	-	-	D
BR	1	3	1	-1.00	-	-1.00	-	-1.00	-	-1.00	-	-	-	-	-	-	W

Figure A-7 Example of File D

source	ser no	te no	mis no	np	sp	nr	sr	kse	ksp	sd	kn	nd	(nd/sd)e	I
GZD	3	1	1	139.28	124.11	158.59	42.75	0.22	0.15	685.80	-1.00	-1.00	-1.00	LA
GZD	3	1	2	836.36	333.63	899.80	144.11	0.65	0.43	863.60	-1.00	-1.00	-1.00	LA
GZD	3	1	6	556.43	260.63	635.03	151.69	0.98	0.41	774.70	-1.00	-1.00	-1.00	LA
GZD	3	1	7	277.87	69.64	319.24	78.60	0.80	0.14	965.20	-1.00	-1.00	-1.00	LA
GZD	3	1	8	279.25	117.22	299.93	72.40	0.38	0.15	812.80	-1.00	-1.00	-1.00	LA
GZD	3	2	3	278.56	210.99	306.14	79.29	0.38	0.33	952.50	-1.00	-1.00	-1.00	LA
GZD	3	2	4	502.63	414.39	640.55	191.68	0.65	0.41	914.40	-1.00	-1.00	-1.00	LA
GZD	4	1	1	277.87	344.75	299.93	99.29	-1.00	-1.00	-1.00	-1.00	-1.00	-1.00	OLA
GZD	4	1	2	1116.30	606.37	1321.11	302.69	-1.00	-1.00	-1.00	-1.00	-1.00	-1.00	OLA
GZD	4	2	3	140.66	95.15	151.00	64.81	0.27	0.07	660.40	-1.00	-1.00	-1.00	OLA
GZD	4	2	4	568.15	401.38	602.62	239.95	0.57	0.22	685.80	-1.00	-1.00	-1.00	OLA
GZD	4	2	5	865.32	575.73	908.07	296.49	0.65	0.22	533.40	-1.00	-1.00	-1.00	OLA
GZD	1	1	5	140.66	262.70	151.00	90.33	0.33	0.25	660.40	-1.00	-1.00	-1.00	IN
GZD	1	1	4	69.64	157.90	75.16	60.68	0.30	0.24	901.70	-1.00	-1.00	-1.00	IN
GZD	1	2	1	278.56	356.47	285.95	156.52	0.62	0.47	787.40	-1.00	-1.00	-1.00	IN
GZD	1	2	2	559.19	486.10	570.22	275.80	0.54	0.54	723.90	-1.00	-1.00	-1.00	IN
GZD	1	2	6	838.43	747.42	871.53	444.04	0.98	0.84	927.10	-1.00	-1.00	-1.00	IN
GZD	1	2	3	1116.99	960.54	1232.14	276.49	0.98	0.98	965.20	-1.00	-1.00	-1.00	IN
GZD	2	1	2	856.36	788.79	896.35	381.29	0.65	-1.00	76.20	-1.00	-1.00	-1.00	IN
GZD	2	1	3	1119.75	869.90	1248.69	500.58	0.87	-1.00	76.20	-1.00	-1.00	-1.00	IN
GZD	2	1	4	1123.20	1034.25	1185.94	737.08	1.96	-1.00	812.80	-1.00	-1.00	-1.00	IN
GZD	1	3	8	-1.00	-1.00	141.01	51.03	-1.00	-1.00	-1.00	-1.00	-1.00	-1.00	SA
GZD	1	3	7	-1.00	-1.00	889.46	390.26	-1.00	-1.00	-1.00	-1.00	-1.00	-1.00	SA
GZD	1	3	6	-1.00	-1.00	141.01	37.58	-1.00	-1.00	-1.00	-1.00	-1.00	-1.00	SA
GZD	1	3	5	-1.00	-1.00	859.81	121.36	-1.00	-1.00	-1.00	-1.00	-1.00	-1.00	SA
GZD	13	1	2	143.42	179.27	157.90	142.04	0.30	0.08	685.80	-1.00	-1.00	-1.00	FR
GZD	13	1	3	574.35	200.00	604.56	196.58	0.43	0.09	533.40	-1.00	-1.00	-1.00	FR
GZD	285	1	1	-1.00	-1.00	364.76	169.62	-1.00	-1.00	-1.00	-1.00	-1.00	-1.00	SA
GZD	285	1	2	-1.00	-1.00	614.35	372.33	-1.00	-1.00	-1.00	-1.00	-1.00	-1.00	SA
GZD	285	1	3	-1.00	-1.00	151.00	78.60	-1.00	-1.00	-1.00	-1.00	-1.00	-1.00	SA
GZD	286	2	1	-1.00	-1.00	151.69	106.18	-1.00	-1.00	-1.00	-1.00	-1.00	-1.00	SA
GZD	286	2	2	-1.00	-1.00	302.69	233.74	-1.00	-1.00	-1.00	-1.00	-1.00	-1.00	SA
GZD	286	2	3	-1.00	-1.00	612.28	482.65	-1.00	-1.00	-1.00	-1.00	-1.00	-1.00	SA

Figure A-8 Example of File I

source	ser no	te no	desc no	te or mis no			
GZD	3	1	1	1	2	6	7
GZD	3	1	1	8	-1	-1	-1
GZD	3	2	1	3	4	-1	-1
GZD	4	1	2	1	2	-1	-1
GZD	4	2	3	3	4	5	-1
GZD	1	1	1	4	5	-1	-1
GZD	1	2	1	1	2	3	6
GZD	2	1	2	2	3	4	-1
GZD	1	3	3	7	7	8	8
GZD	13	1	4	2	3	-1	-1
GZD	285	1	5	4	4	4	-1
GZD	286	2	7	1	2	3	-1
GZD	684	1	1	1	-1	-1	-1
GZD	714	1	1	1	-1	-1	-1
GZD	708	1	1	1	-1	-1	-1
SWS	1	1	1	1	2	3	0
SWS	1	2	2	1	2	3	0
SWS	1	3	3	1	2	0	0
SWS	1	4	4	1	0	0	0
SWS	1	5	5	1	2	3	0
SWS	1	6	6	1	2	0	0
SWS	1	7	7	1	2	0	0
SWS	1	8	8	1	2	0	0
SWS	1	9	9	1	2	3	0
SWS	1	10	10	1	2	0	0
SWS	1	11	11	1	2	3	0
SWS	11	1	12	1	2	3	0
SWS	11	2	13	1	2	3	0
SWS	11	3	14	1	2	3	0
SWS	11	4	15	1	2	0	0
SWS	11	5	16	1	2	3	0
SWS	11	6	17	1	2	3	0
SWS	11	7	18	1	2	3	0
SWS	11	8	19	1	2	0	0
SWS	11	9	20	1	2	0	0

Figure A-9 Example of File L

source	ser no	te no	mis no	source	ser no	te no	mis no
GZD	3	1	2	GZD	3	1	1
GZD	3	1	7	GZD	3	1	1
GZD	3	1	8	GZD	3	1	1
GZD	3	2	4	GZD	3	2	3
GZD	4	1	2	GZD	4	1	1
GZD	4	2	3	GZD	4	1	1
GZD	4	2	4	GZD	4	1	1
GZD	4	2	5	GZD	4	1	1
GZD	1	1	4	GZD	1	1	5
GZD	1	2	2	GZD	1	2	1
GZD	1	2	6	GZD	1	2	1
GZD	1	2	3	GZD	1	2	1
GZD	2	1	3	GZD	2	1	2
GZD	2	1	4	GZD	2	1	2
GZD	1	3	7	GZD	1	3	8
GZD	1	3	6	GZD	1	3	8
GZD	1	3	5	GZD	1	3	8
GZD	13	1	3	GZD	13	1	2
GZD	285	1	2	GZD	285	1	1
GZD	285	1	3	GZD	285	1	1
GZD	286	2	2	GZD	286	2	1
GZD	286	2	3	GZD	286	2	1
SWS	10	1	2	SWS	10	1	1
SWS	10	1	3	SWS	10	1	1
SWS	10	2	1	SWS	10	2	1
SWS	10	2	3	SWS	10	2	1
SWS	10	3	2	SWS	10	3	1
SWS	10	5	2	SWS	10	5	1
SWS	10	5	3	SWS	10	5	1
SWS	10	6	2	SWS	10	6	1
SWS	10	7	2	SWS	10	7	1
SWS	10	8	2	SWS	10	8	1
SWS	10	9	2	SWS	10	9	1
SWS	10	9	3	SWS	10	9	1
SWS	10	10	2	SWS	10	10	1
SWS	10	11	2	SWS	10	11	1
SWS	10	11	3	SWS	10	11	1

Figure A-10 Example of File N

source	ser no	te no	mis no	desc no	para 1	val	para 2	val	para 3	val	para 4	val
GZD	3	1	1	1	-	-1.00	-	-1.00	LL	74.00	PL	30.00
GZD	3	1	2	1	DN	1422.49	WN	33.90	LL	80.00	PL	30.00
GZD	3	1	6	1	DN	1487.76	WN	24.90	LL	80.00	PL	39.30
GZD	3	1	7	1	DN	1673.99	WN	21.80	LL	71.00	PL	34.90
GZD	3	1	8	1	DN	1486.56	WN	27.60	LL	67.00	PL	33.30
GZD	3	2	3	1	DN	1517.00	WN	27.90	LL	75.00	PL	31.00
GZD	3	2	4	1	DN	1587.48	WN	21.30	LL	75.00	PL	30.00
GZD	4	2	1	1	DN	1606.71	WN	22.20	-	-1.00	-	-1.00
GZD	4	2	2	1	DN	1656.37	WN	22.50	-	-1.00	-	-1.00
GZD	4	2	3	1	DN	1699.62	WN	17.20	-	-1.00	-	-1.00
GZD	4	2	4	1	DN	1657.97	WN	20.30	-	-1.00	-	-1.00
GZD	4	2	5	1	DN	1636.74	WN	19.80	-	-1.00	-	-1.00
GZD	1	1	5	1	DN	841.00	WN	49.20	-	-1.00	-	-1.00
GZD	1	1	4	1	DN	873.04	WN	43.30	-	-1.00	-	-1.00
GZD	1	2	1	1	DN	917.49	WN	42.10	-	-1.00	-	-1.00
GZD	1	2	2	1	DN	929.10	WN	43.00	-	-1.00	-	-1.00
GZD	1	2	6	1	DN	900.27	WN	41.90	-	-1.00	-	-1.00
GZD	1	2	3	1	DN	901.87	WN	44.90	-	-1.00	-	-1.00
GZD	2	1	2	1	DN	906.68	WN	40.20	-	-1.00	-	-1.00
GZD	2	1	3	1	DN	906.68	WN	40.20	-	-1.00	-	-1.00
GZD	2	1	4	1	DN	1334.83	WN	29.60	-	-1.00	-	-1.00
GZD	1	3	8	1	DN	903.47	WN	32.50	-	-1.00	-	-1.00
GZD	1	3	7	1	DN	903.47	WN	32.50	-	-1.00	-	-1.00
GZD	1	3	6	1	DN	903.47	WN	32.50	-	-1.00	-	-1.00
GZD	1	3	5	1	DN	903.47	WN	32.50	-	-1.00	-	-1.00
GZD	13	1	2	1	DN	909.88	WN	35.60	-	-1.00	-	-1.00
GZD	13	1	3	1	DN	946.72	WN	37.00	-	-1.00	-	-1.00
GZD	285	1	1	1	DN	828.18	WN	51.30	-	-1.00	-	-1.00
GZD	285	1	2	1	DN	828.18	WN	51.30	-	-1.00	-	-1.00
GZD	285	1	3	1	DN	828.18	WN	51.30	-	-1.00	-	-1.00
GZD	286	2	1	1	DN	808.96	WN	50.70	-	-1.00	-	-1.00
GZD	286	2	2	1	DN	808.96	WN	50.70	-	-1.00	-	-1.00
GZD	286	2	3	1	DN	808.96	WN	50.70	-	-1.00	-	-1.00
GZD	714	1	1	1	-	-1.00	WN	22.00	LL	30.00	PL	22.00
GZD	708	1	1	1	-	-1.00	WN	21.90	LL	40.00	PL	18.00
GZD	684	1	1	1	-	-1.00	WN	17.70	LL	35.00	PL	16.00
SWS	12	3	1	1	W	3.70	-	-1.00	-	-1.00	-	-1.00
SWS	12	4	1	1	W	0.00	-	-1.00	-	-1.00	-	-1.00
SWS	60	1	1	1	SCP	43.25	SCP	16.70	E10	9.81	E50	25.50
SWS	60	2	1	1	SCP	43.25	SCP	16.70	E10	9.81	E50	25.50

Figure A-11 Example of File P

source	ser no	te no	sis no	desc no	blk	%vol	bas	1st	2nd	3rd	4th	form	anis feat	ori
GZD	3	1	1	1	-	-1.00	CS	CR	-	-	-	TX	LA	-1.
GZD	3	2	3	1	-	-1.00	CS	CR	-	-	-	TX	LA	-1.
GZD	4	1	1	1	-	-1.00	CS	CR	-	-	-	TX	OLA	-1.
GZD	1	1	5	1	-	-1.00	LN	-	-	-	-	TX	-	-1.
GZD	1	2	1	1	-	-1.00	LN	-	-	-	-	TX	-	-1.
GZD	2	1	2	1	-	-1.00	LN	-	-	-	-	TX	-	-1.
GZD	1	3	8	1	-	-1.00	LN	-	-	-	-	TX	-	-1.
GZD	13	1	2	1	-	-1.00	LN	-	-	-	-	TX	-	-1.
GZD	285	1	1	1	-	-1.00	LN	-	-	-	-	NDA	-	-1.
GZD	286	2	1	1	-	-1.00	LN	-	-	-	-	NDA	-	-1.
GZD	684	1	1	1	-	-1.00	GT	SS	-	-	-	NDA	-	-1.
GZD	714	1	1	1	-	-1.00	PSS	SDR	-	-	-	NDA	-	-1.
GZD	708	1	1	1	-	-1.00	GT	PST	-	-	-	NDA	-	-1.
SWS	10	1	1	1	-	-1.00	GN	BI	MU	PL	CH	R22	FO	-1.
SWS	10	2	1	1	-	-1.00	PH	SR	-	-	-	R22	FO	-1.
SWS	10	3	1	1	-	-1.00	GN	FG	MU	PL	BI	R22	FO	-1.
SWS	10	4	1	1	-	-1.00	GN	FG	MU	PL	BI	R22	-	-1.
SWS	10	5	1	1	-	-1.00	GN	FG	MU	PL	BI	R22	-	-1.
SWS	10	6	1	1	-	-1.00	GN	FG	MU	PL	BI	R22	-	-1.
SWS	10	7	1	1	-	-1.00	GN	FG	MU	PL	BI	R22	-	-1.
SWS	10	8	1	1	-	-1.00	GN	FG	MU	PL	BI	-	LI	-1.
SWS	10	9	1	1	-	-1.00	GN	FG	MU	PL	BI	-	LI	-1.
SWS	10	10	1	1	-	-1.00	GN	FG	MU	PL	BI	R22	FO	-1.
SWS	10	11	1	1	-	-1.00	GN	FG	MU	PL	BI	R22	FO	-1.
SWS	11	1	1	1	-	-1.00	GN	FG	SR	BI	-	R22	FO	-1.
SWS	11	2	1	1	-	-1.00	GN	FG	MU	BI	-	R22	FO	-1.
SWS	11	3	1	1	-	-1.00	GN	FG	PL	MU	BI	R22	FO	-1.
SWS	11	4	1	1	-	-1.00	GN	FG	PL	MU	BI	R22	-	-1.
SWS	11	5	1	1	-	-1.00	GN	FG	PL	MU	BI	R22	-	-1.
SWS	11	6	1	1	-	-1.00	GN	FG	PL	MU	BI	R22	-	-1.
SWS	11	7	1	1	-	-1.00	GN	FG	PL	MU	BI	R22	-	-1.
SWS	11	8	1	1	-	-1.00	GN	FG	PL	MU	BI	R22	-	-1.
SWS	11	9	1	1	-	-1.00	GN	FG	PL	MU	BI	R22	-	-1.

Figure A-12 Example of File R

source	ser no	te no	mis no	bas	mod	samp area	strain rate	temp
GZD	3	1	1	OST	-	-1.00	1016.00	-1.00
GZD	3	1	2	OST	-	-1.00	1016.00	-1.00
GZD	3	1	6	OST	-	-1.00	1016.00	-1.00
GZD	3	1	7	OST	-	-1.00	1016.00	-1.00
GZD	3	1	8	OST	-	-1.00	1016.00	-1.00
GZD	3	2	3	OST	-	-1.00	1016.00	-1.00
GZD	3	2	4	OST	-	-1.00	1610.00	-1.00
GZD	4	1	1	OST	-	-1.00	1610.00	-1.00
GZD	4	1	2	OST	-	-1.00	1610.00	-1.00
GZD	4	2	3	OST	-	-1.00	1610.00	-1.00
GZD	4	2	4	OST	-	-1.00	1610.00	-1.00
GZD	4	2	5	OST	-	-1.00	1610.00	-1.00
GZD	1	1	5	OST	-	-1.00	1610.00	-1.00
GZD	1	1	4	OST	-	-1.00	1610.00	-1.00
GZD	1	2	1	OST	-	-1.00	1610.00	-1.00
GZD	1	2	2	OST	-	-1.00	1610.00	-1.00
GZD	1	2	6	OST	-	-1.00	1610.00	-1.00
GZD	1	2	3	OST	-	-1.00	1610.00	-1.00
GZD	2	1	2	OST	-	-1.00	1610.00	-1.00
GZD	2	1	3	OST	-	-1.00	1610.00	-1.00
GZD	2	1	4	OST	-	-1.00	1610.00	-1.00
GZD	1	3	8	OST	-	-1.00	1610.00	-1.00
GZD	1	3	7	OST	-	-1.00	1610.00	-1.00
GZD	1	3	6	OST	-	-1.00	1610.00	-1.00
GZD	1	3	5	OST	-	-1.00	1610.00	-1.00
GZD	13	1	2	OST	-	-1.00	1610.00	-1.00
GZD	13	1	3	OST	-	-1.00	1610.00	-1.00
GZD	285	1	1	OST	-	-1.00	1610.00	-1.00
GZD	285	1	2	OST	-	-1.00	1610.00	-1.00
GZD	285	1	3	OST	-	-1.00	1610.00	-1.00
GZD	286	2	1	OST	-	-1.00	1610.00	-1.00
GZD	286	2	2	OST	-	-1.00	1610.00	-1.00
GZD	286	2	3	OST	-	-1.00	1610.00	-1.00
GZD	684	1	1	OST	-	-1.00	1610.00	-1.00
GZD	714	1	1	OST	-	-1.00	1610.00	-1.00

Figure A-13 Example of File T

source	ser no	te no	mis no	desc no	blk	%area	bas	1st	2nd	3rd	4th
SWS	10	1	1	1	-	-1.00	CH	SR	-	-	-
SWS	11	7	1	1	-	-1.00	SL	-	-	-	-
SWS	11	10	1	1	-	-1.00	SL	-	-	-	-
SWS	12	1	1	1	-	-1.00	SO	NP	-	-	-
SWS	12	10	1	1	-	-1.00	SO	NP	-	-	-
SWS	12	2	1	1	-	-1.00	SO	NP	-	-	-
SWS	13	10	1	1	-	-1.00	UD	-	-	-	-
SWS	13	2	1	1	-	-1.00	SR	-	-	-	-
SWS	1	1	1	1	-	-1.00	GA	-	-	-	-
SWS	1	2	1	1	-	-1.00	GA	-	-	-	-
SWS	1	3	1	1	-	-1.00	GA	-	-	-	-
SWS	2	5	1	1	-	100.00	MI	-	-	-	-
SWS	5	4	1	1	-	100.00	MI	-	-	-	-
SWS	5	5	1	1	-	100.00	MI	-	-	-	-
SWS	2	1	1	1	-	-1.00	NS	-	-	-	-
SWS	20	2	1	1	-	-1.00	NS	-	-	-	-
SWS	20	3	1	1	-	-1.00	NS	-	-	-	-
SWS	20	8	1	1	-	-1.00	NS	-	-	-	-
SWS	20	9	1	1	-	-1.00	NS	-	-	-	-
SWS	20	10	1	1	-	-1.00	NS	-	-	-	-
SWS	33	1	1	1	-	-1.00	NS	-	-	-	-
SWS	33	3	1	1	-	-1.00	NS	-	-	-	-
SWS	34	1	1	1	-	-1.00	NS	-	-	-	-
SWS	34	2	1	1	-	-1.00	MI	-	-	-	-
SWS	38	2	1	1	-	-1.00	MI	-	-	-	-
SWS	38	3	1	1	-	-1.00	NS	-	-	-	-
SWS	50	25	1	1	-	-1.00	GO	-	-	-	-
SWS	50	32	1	1	-	-1.00	SL	-	-	-	-
BR	1	1	1	1	B	-1.00	-	-	-	-	-
BR	1	2	1	1	B	-1.00	-	-	-	-	-
BR	1	3	1	1	B	-1.00	-	-	-	-	-
BR	1	4	1	1	B	-1.00	-	-	-	-	-
BR	2	2	1	1	B	-1.00	-	-	-	-	-
BR	3	1	1	1	B	-1.00	EP	AL	BM	HE	MNO
BR	3	2	1	1	B	-1.00	EP	AL	BM	HE	MNO
BR	3	3	1	1	B	-1.00	EP	AL	BM	HE	MNO
BR	7	1	1	1	-	-1.00	CA	-	-	-	-
BR	7	1	10	1	-	-1.00	CA	-	-	-	-
DM	1	2	1	1	-	-1.00	SL	-	-	-	-
DM	2	6	1	1	-	-1.00	OX	-	-	-	-
DM	2	9	1	1	-	-1.00	SL	-	-	-	-

Figure A-14 Example of File S

APPENDIX B

Descriptive parameters vs. normal stress

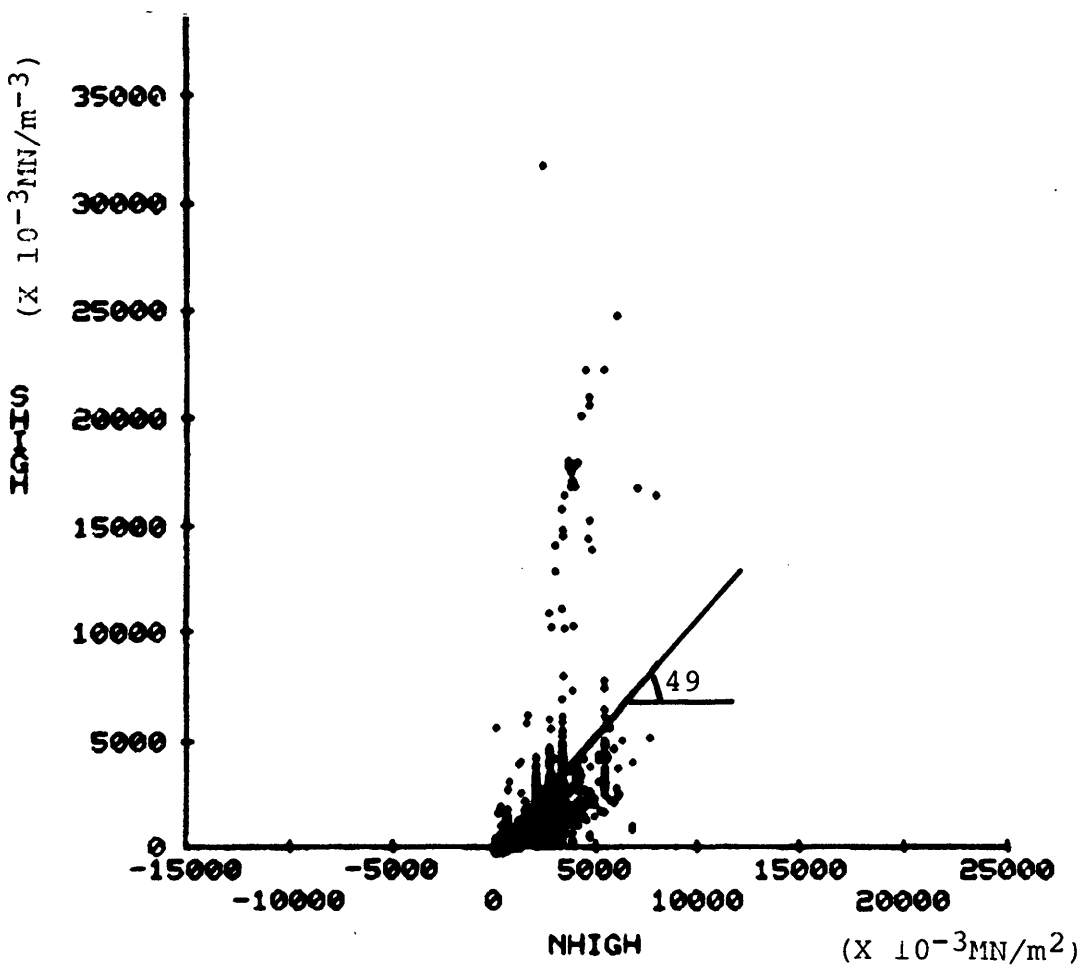

Figure B-1 Peak friction angle of all rock types

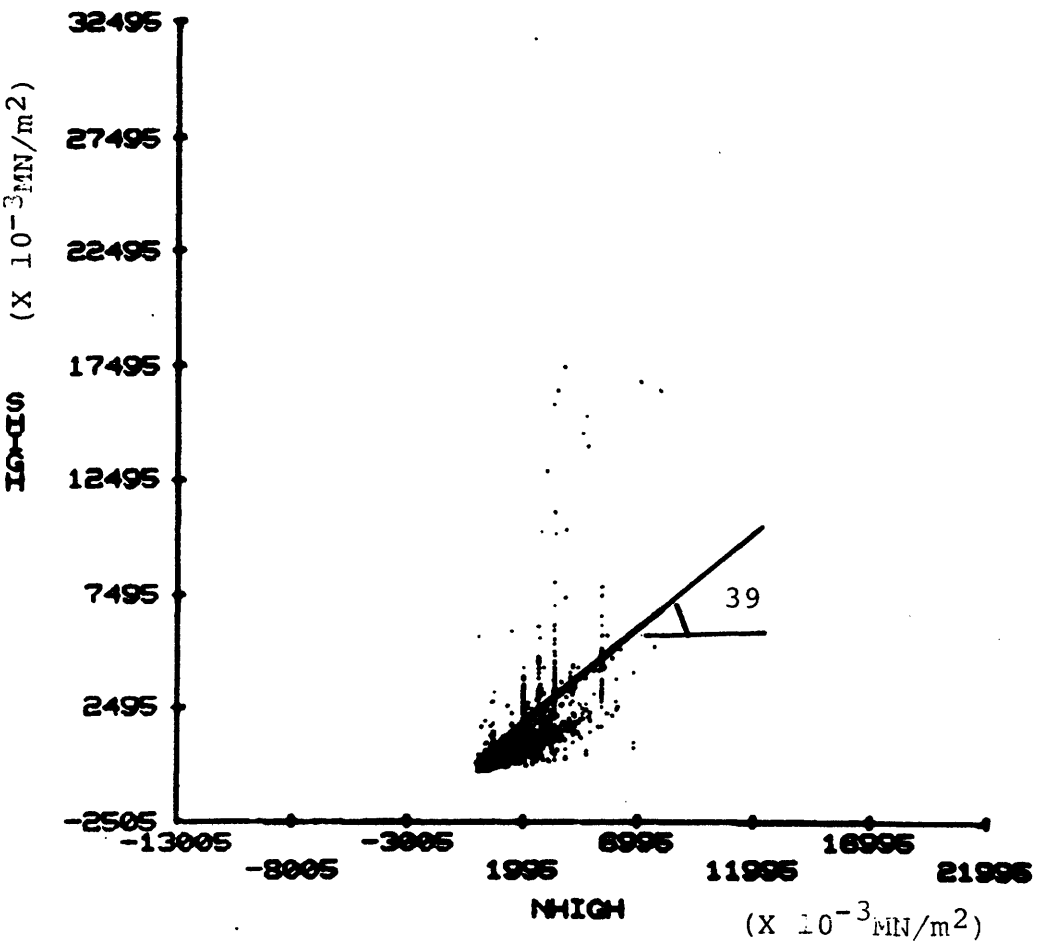

Figure B-2 Peak friction angle of all rock types (without intact rocks)

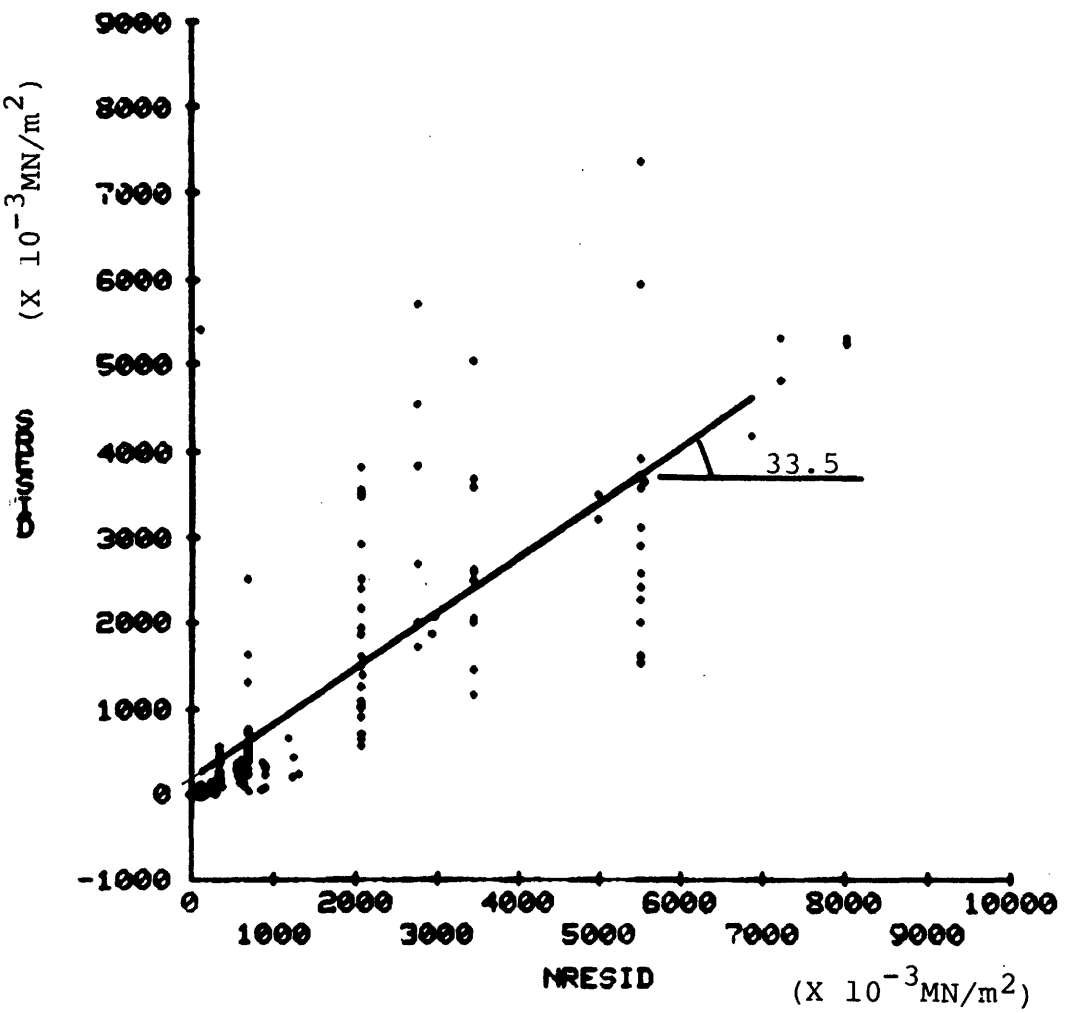

Figure B-3 Residual friction angle of all rock types

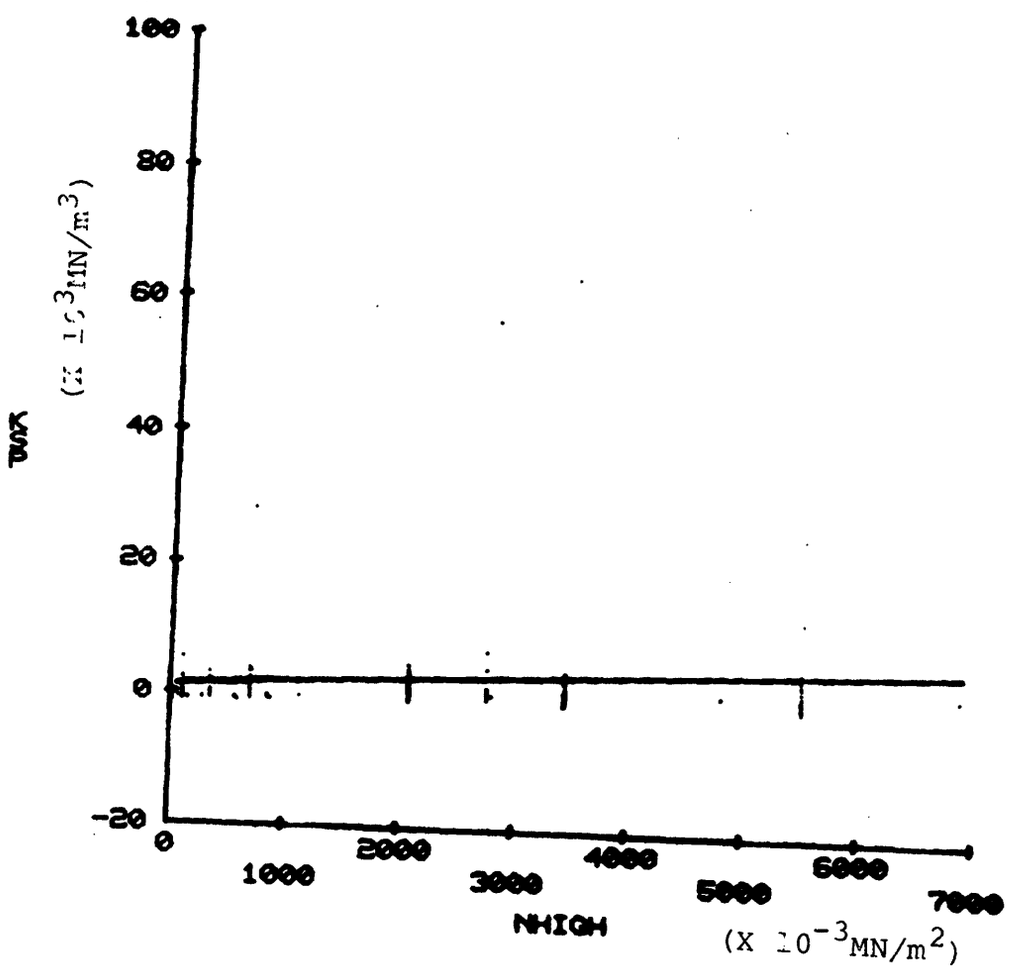

Figure B-4 Peak shear stiffness vs. normal stress

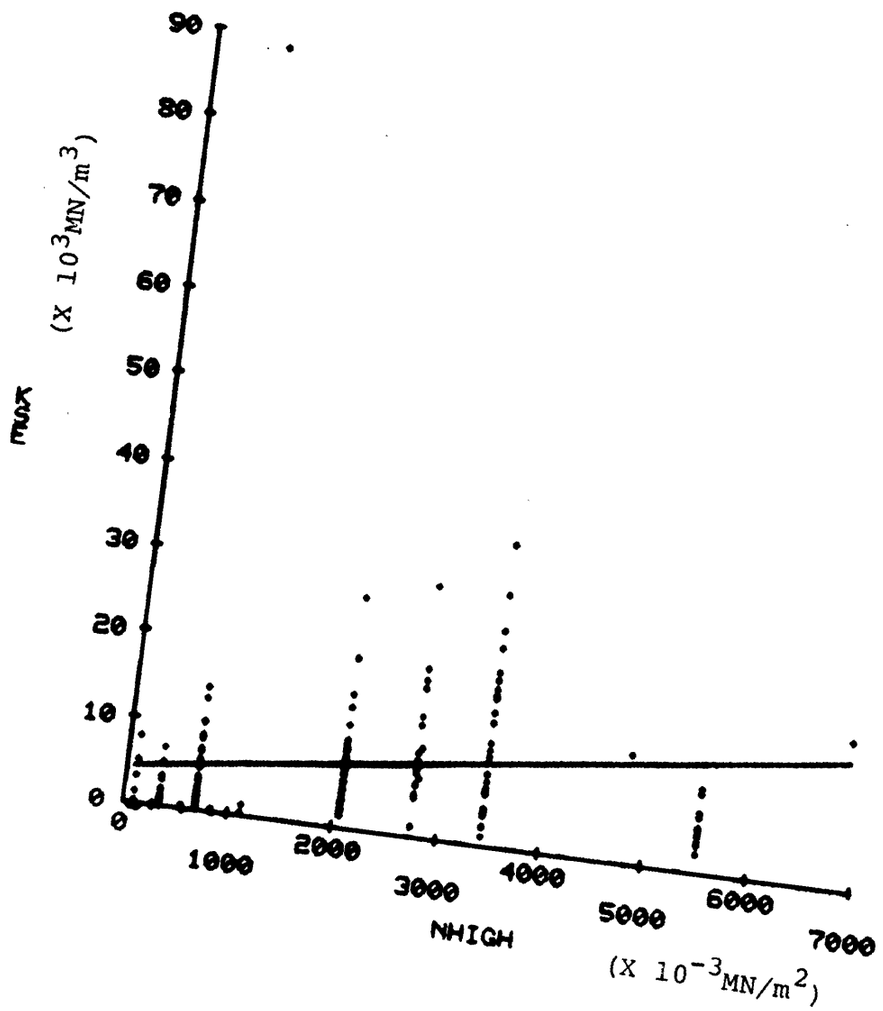

Figure B-5 Elastic shear stiffness vs. normal stress

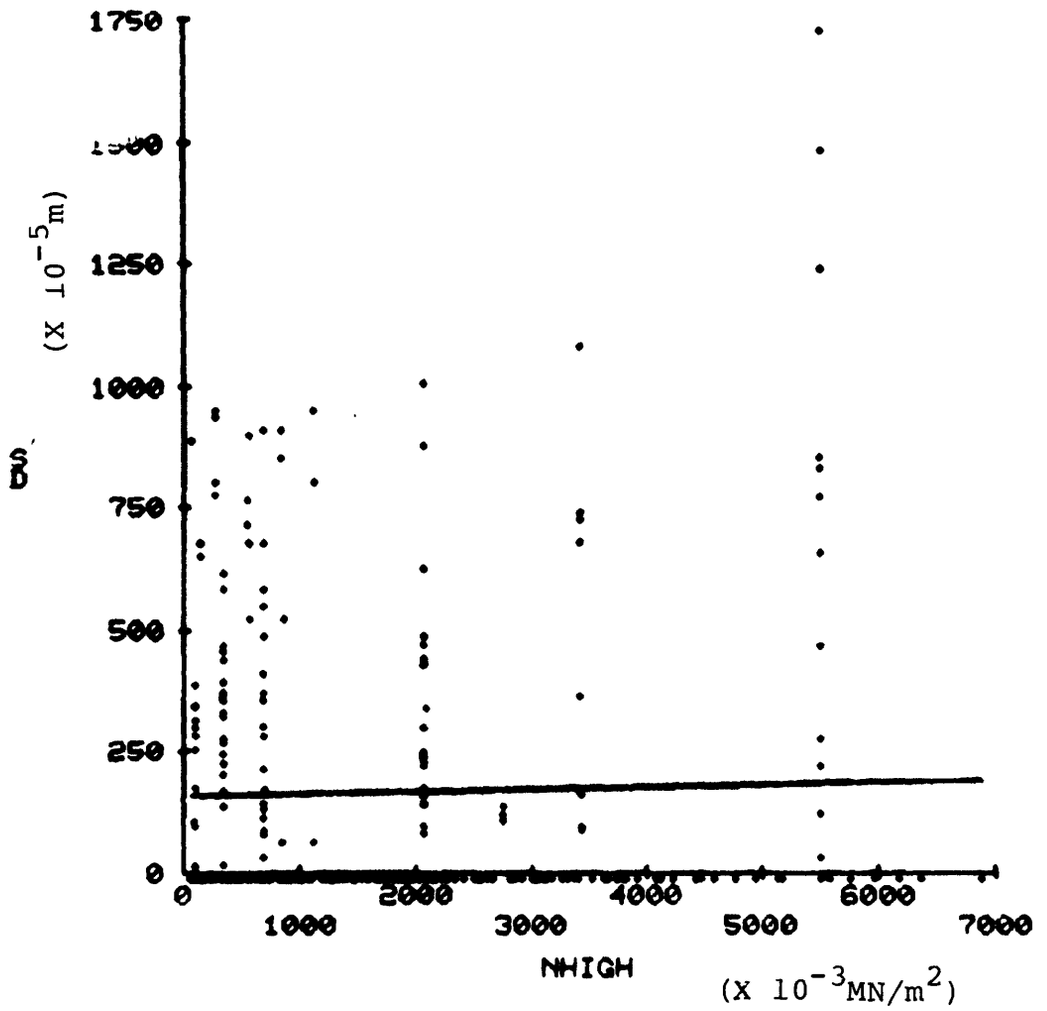

Figure B-6 Shear degradation distance vs. normal stress

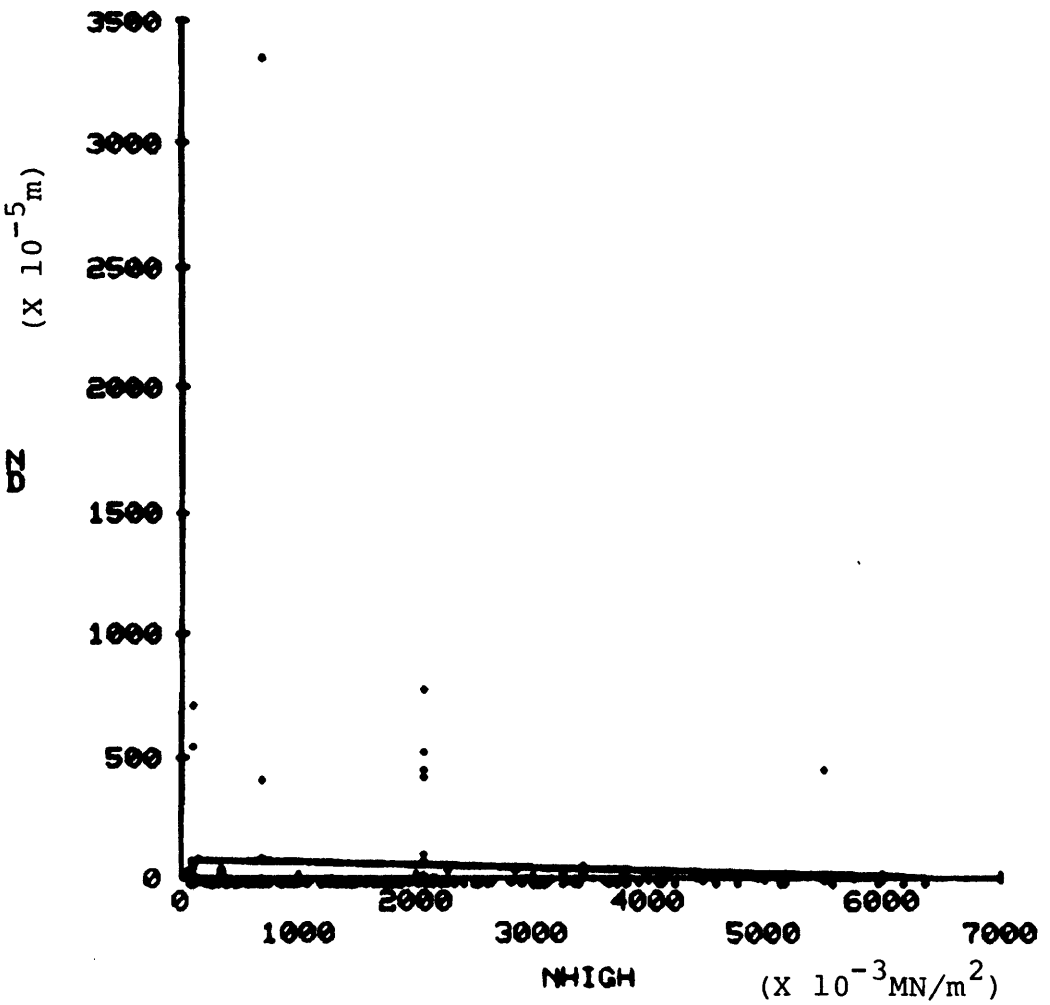

Figure B-7 Normal dilation distance vs. normal stress

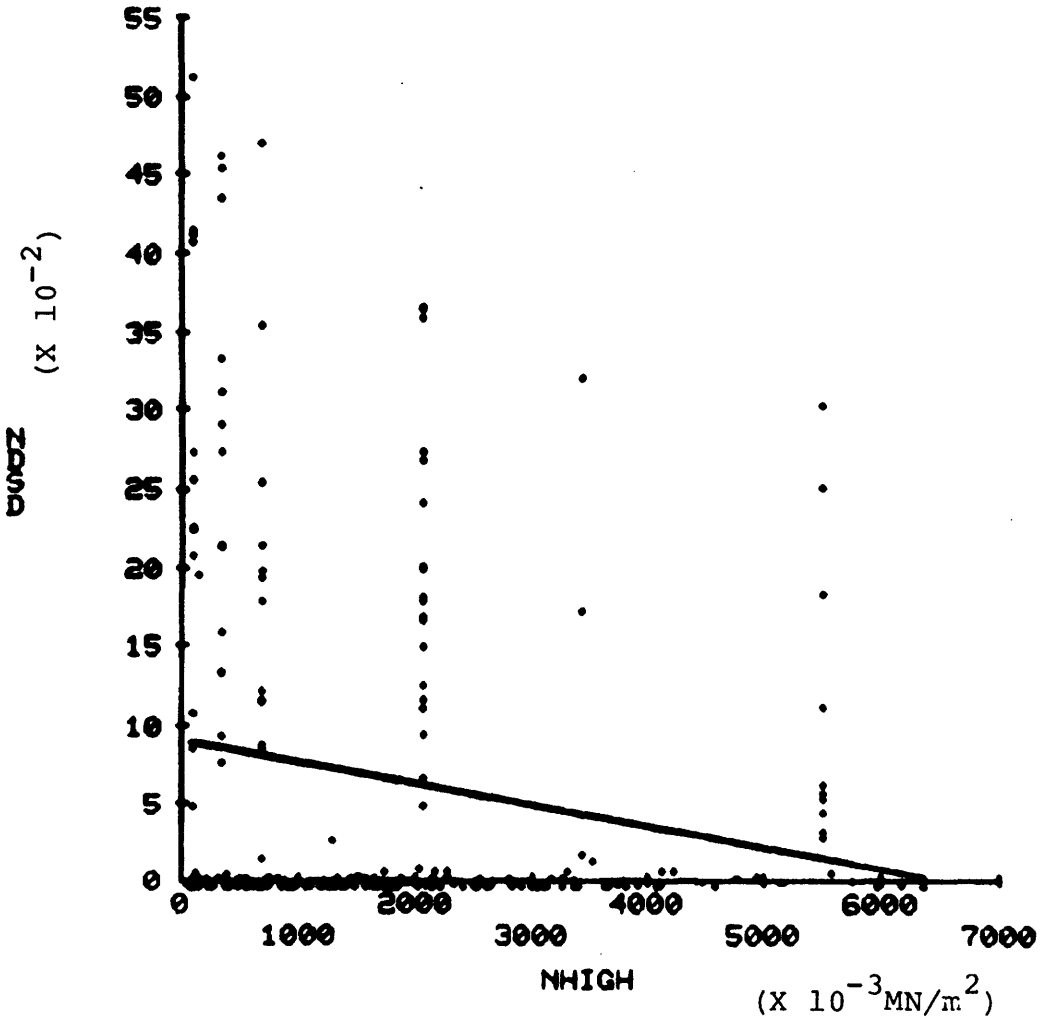

Figure B-8 Peak dilation rate vs. normal stress

APPENDIX C

Peak friction angles of rock types for different stress levels

Note: All units on the horizontal and vertical axes are $X10^{-3}MN/m^2$

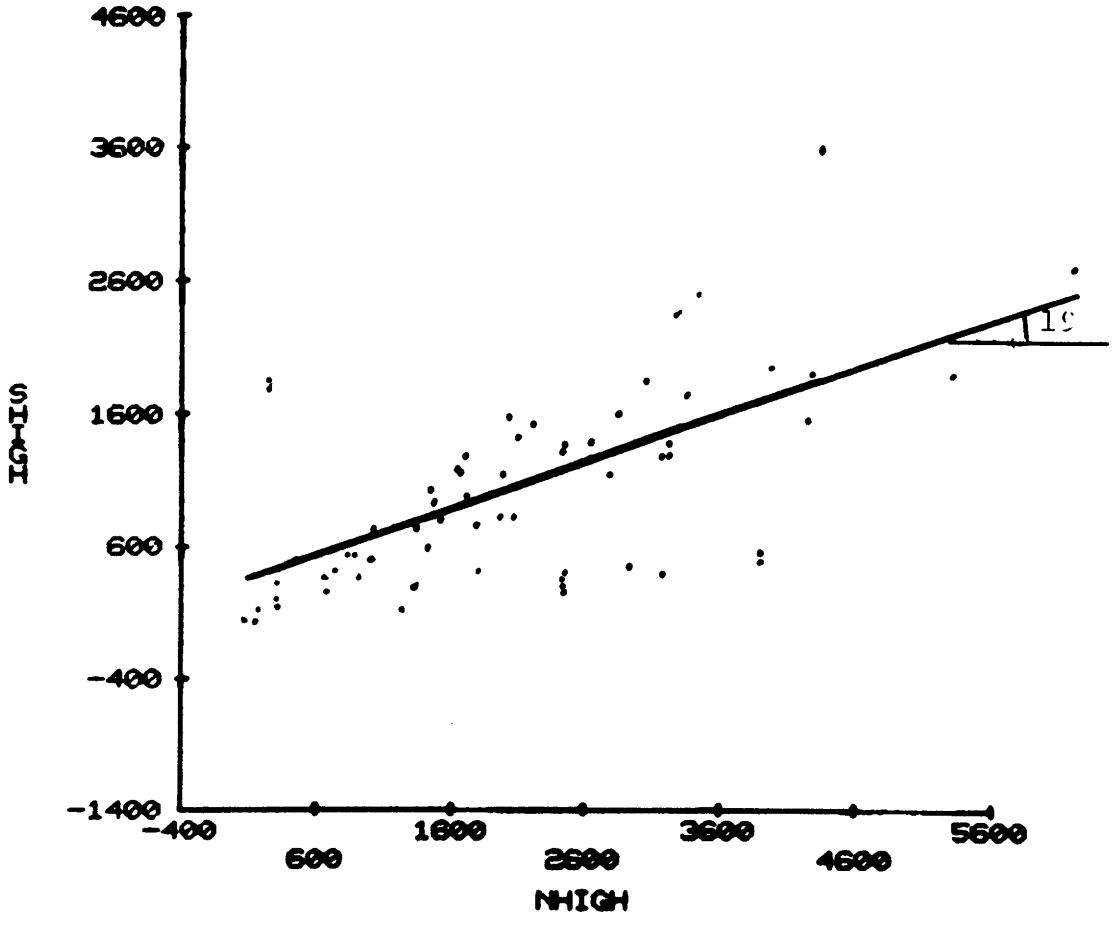

Figure C-1 Peak friction angle of limestone for all stress levels

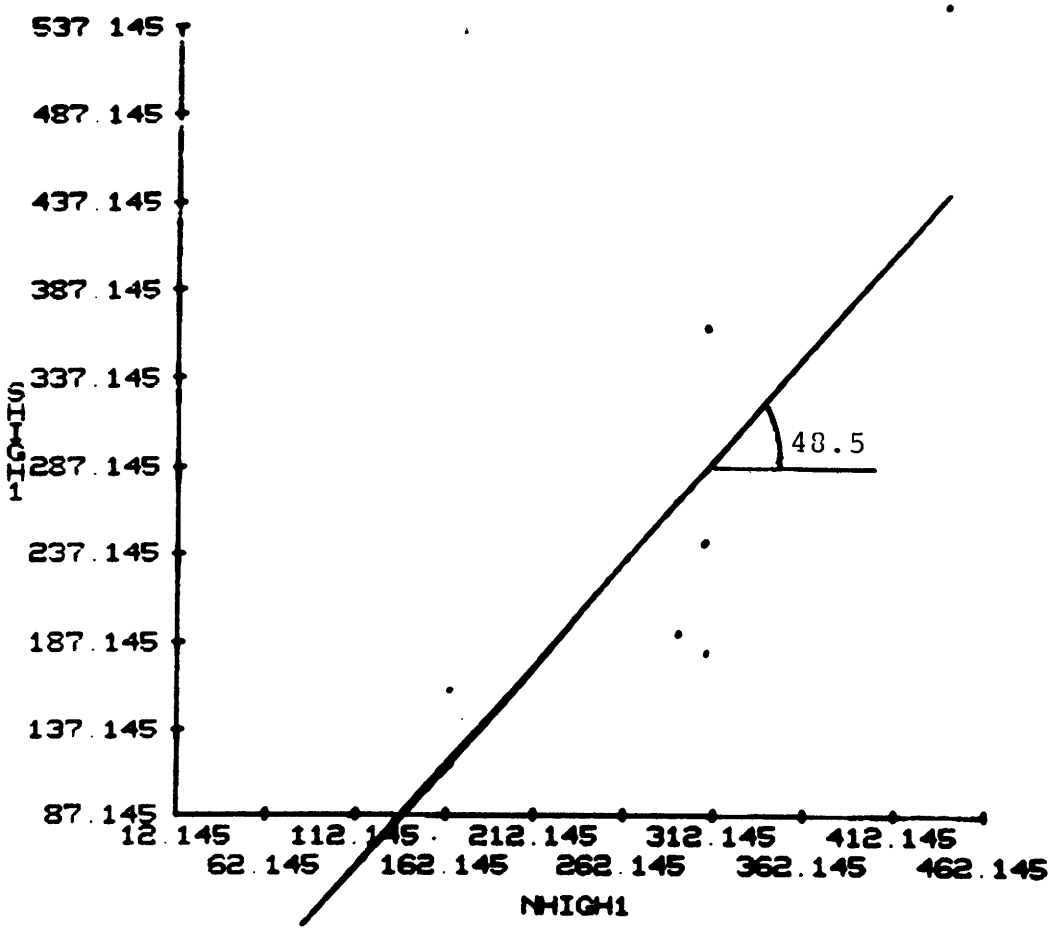

Figure C-2 Peak friction angle of limestone for normal stress below 0.5 MN/m^2

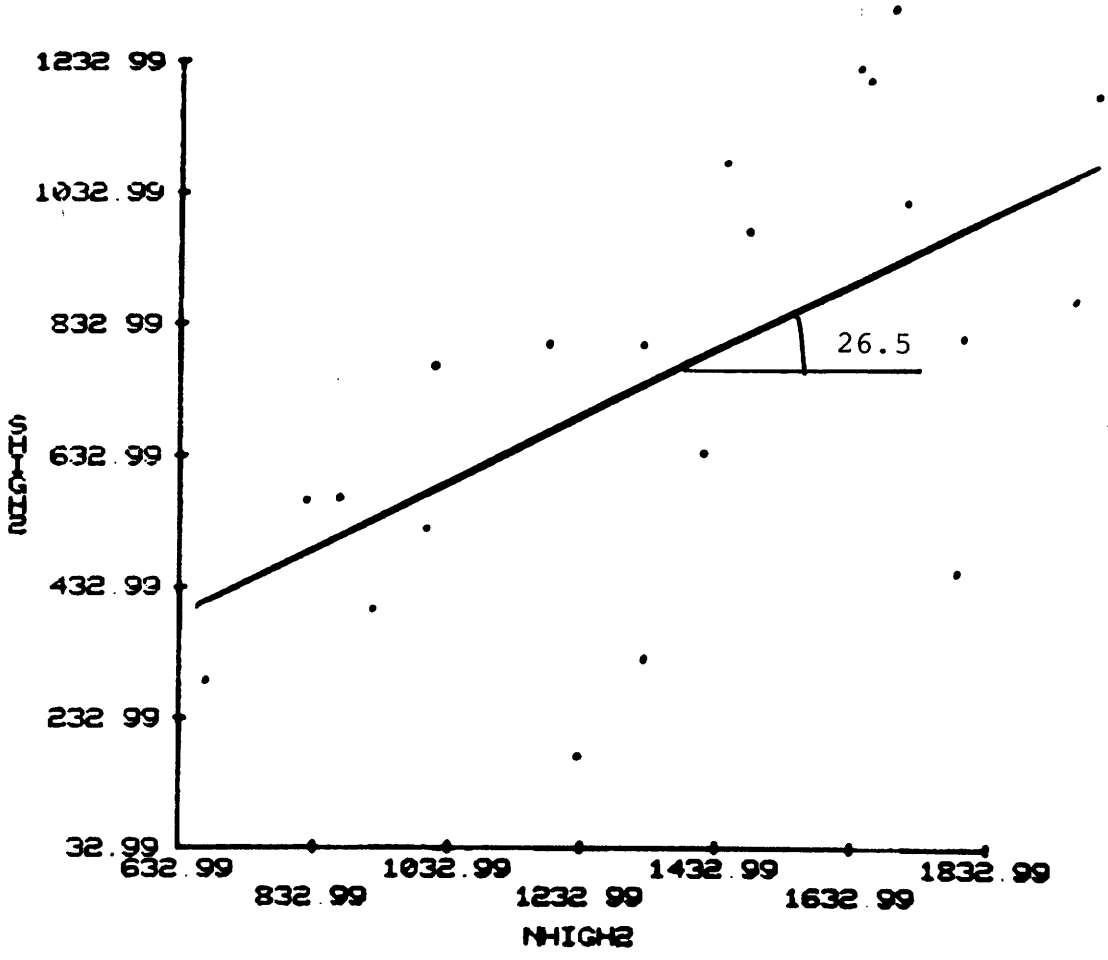

Figure C-3 Peak friction angle of limestone for normal stress between 0.5 and 2 MN/m^2

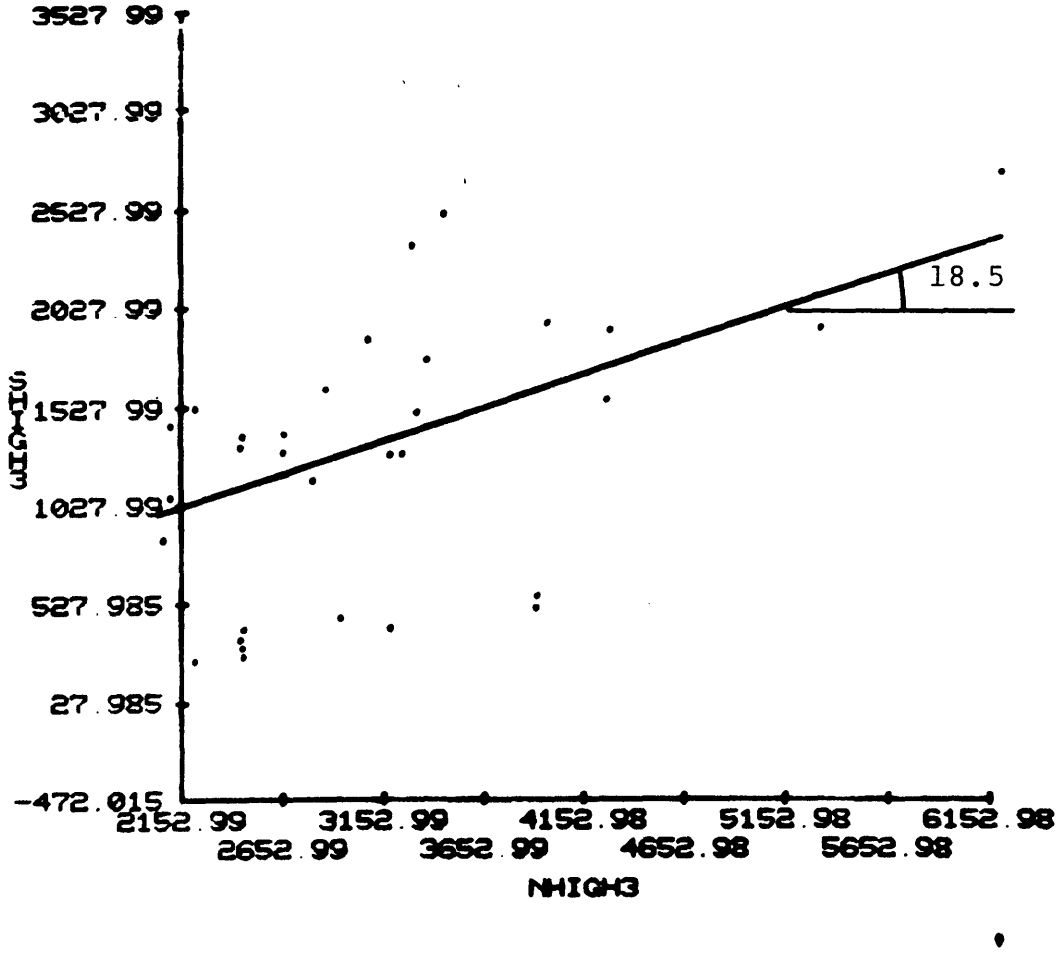

Figure C-4 Peak friction angle of limestone for normal stress above 2 MN/m^2

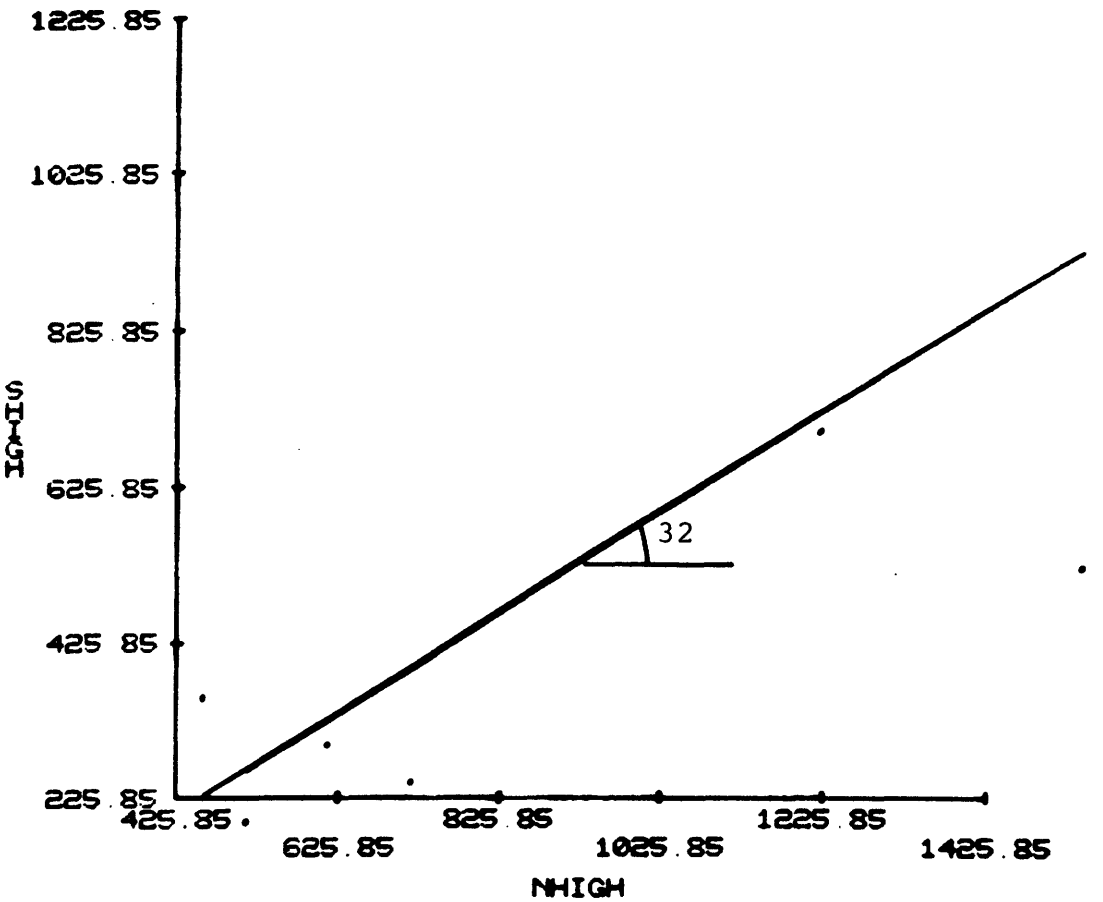

Figure C-5 Peak friction angle of sandstone for all normal stress levels

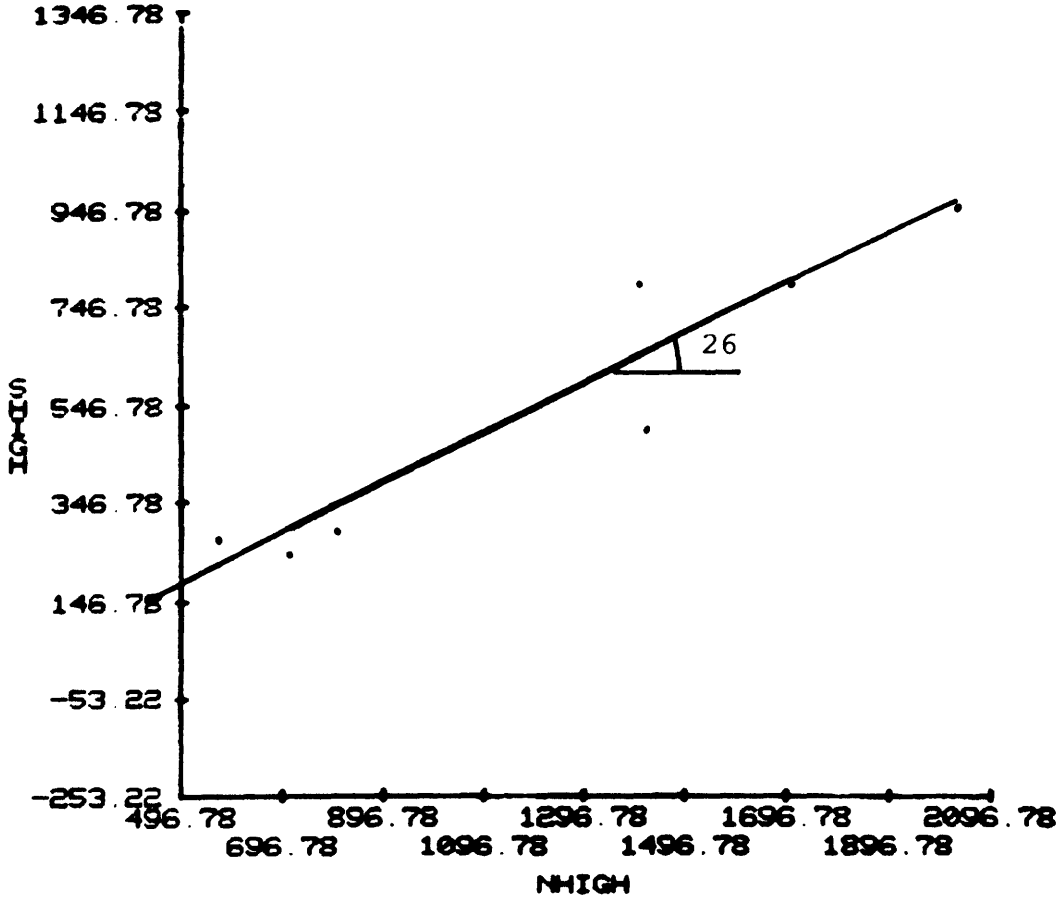

Figure C-6 Peak friction angle of paragneiss for all normal stress levels

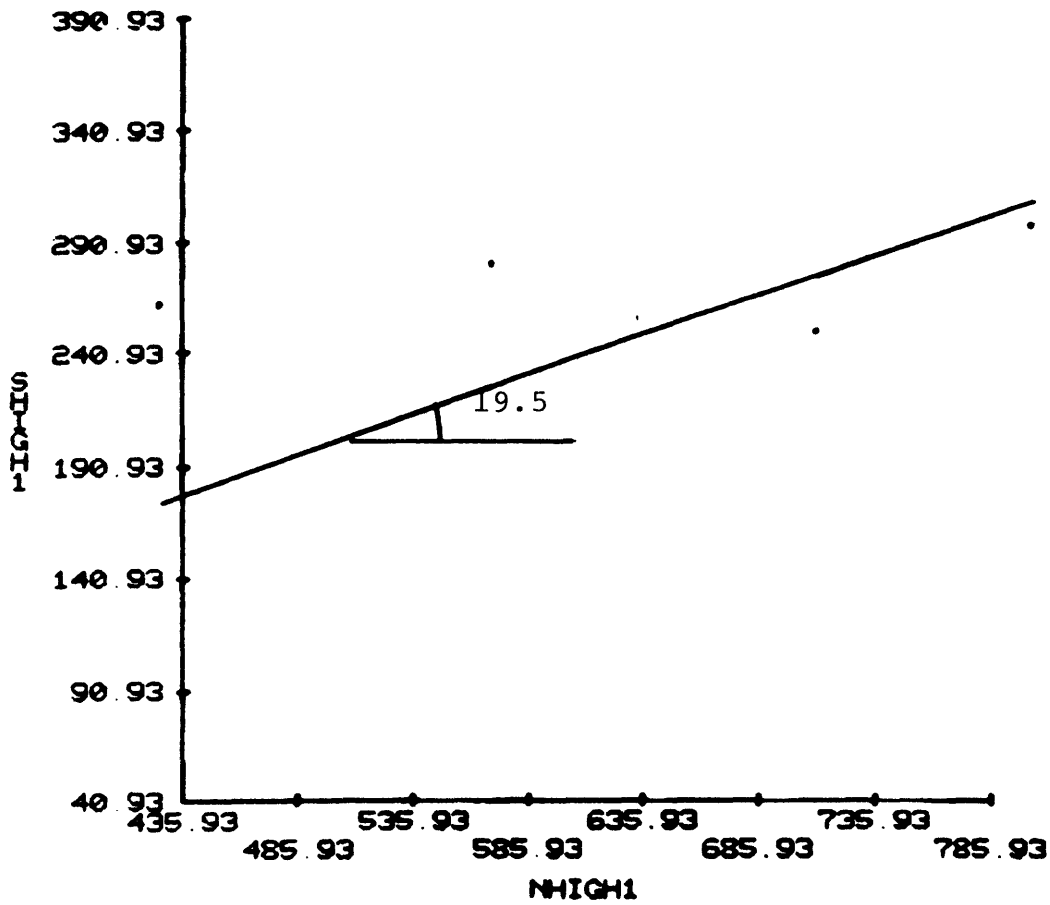

Figure C-7 Peak friction angle of paragneiss for normal stress below 1 MN/m^2

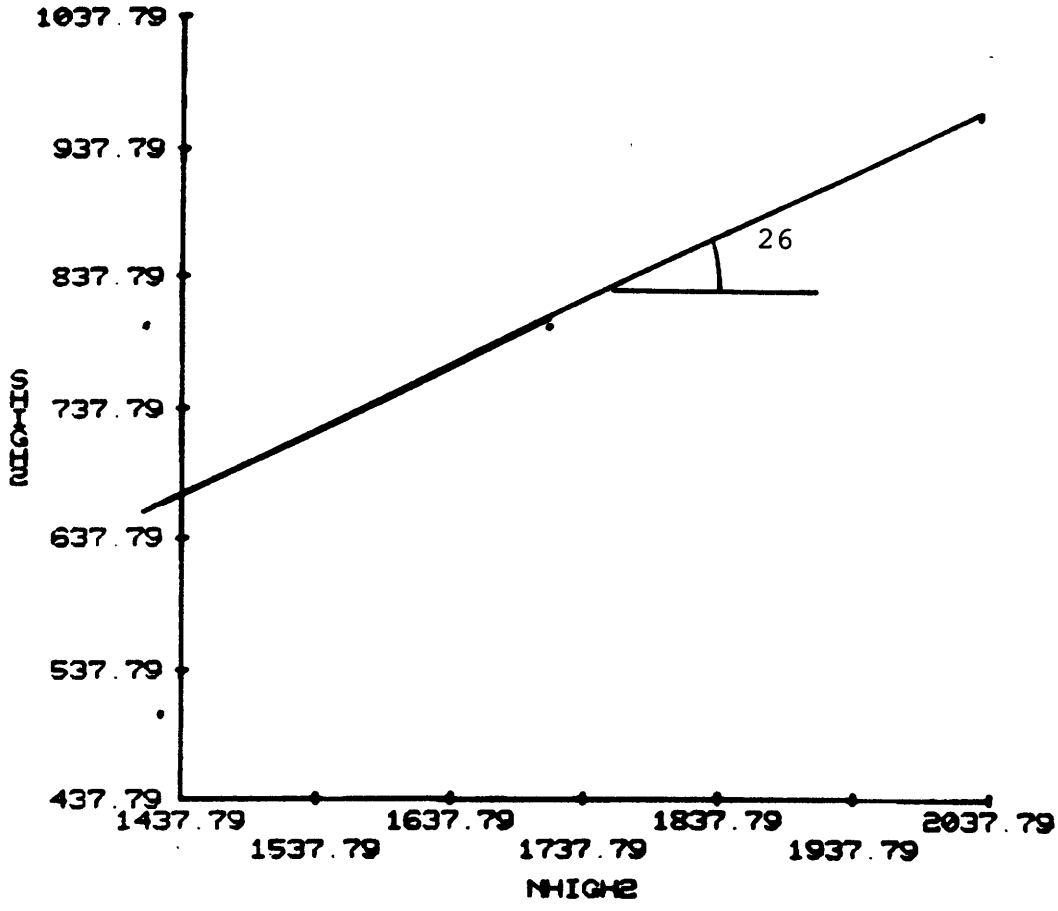

Figure C-8 Peak friction angle of paragneiss for normal stress above 1 MN/m^2

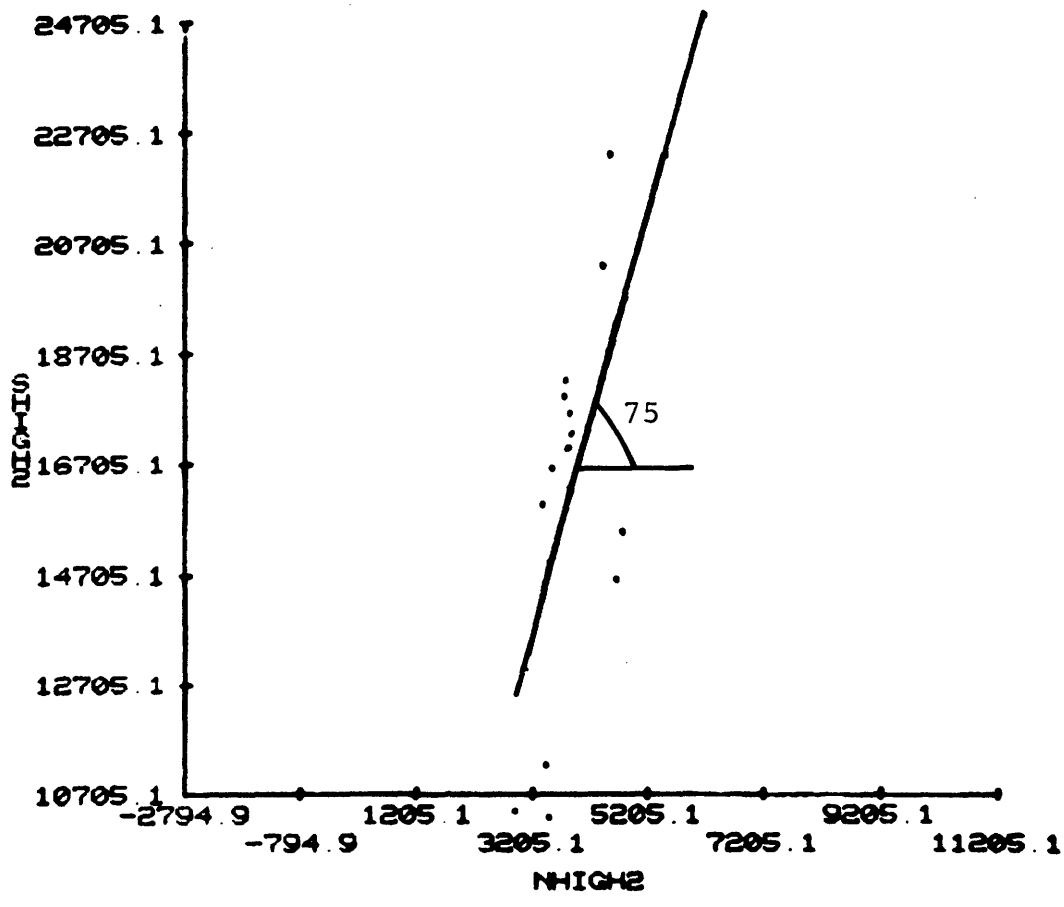

Figure C-9 Peak friction angle of amphibolite (intact and homogeneous) for all normal stress levels

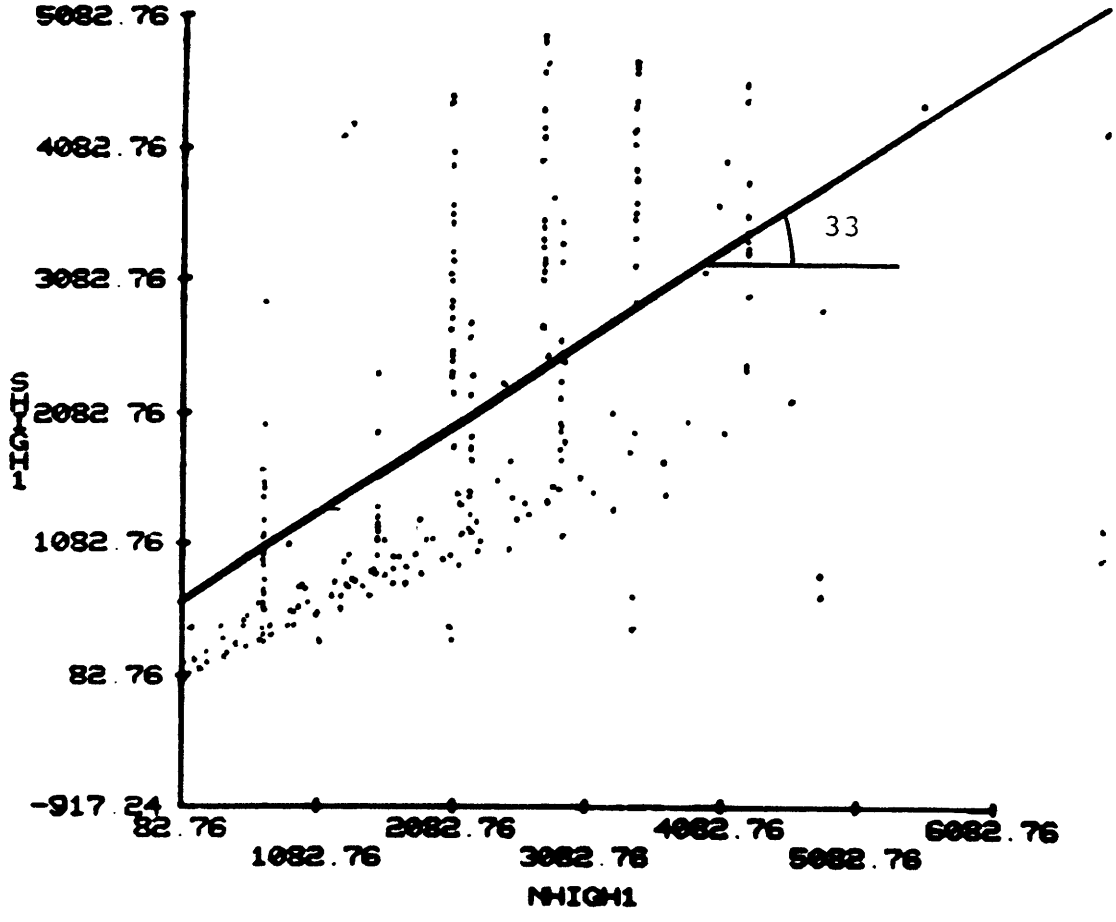

Figure C-10 Peak friction angle of amphibolite for all normal stress levels

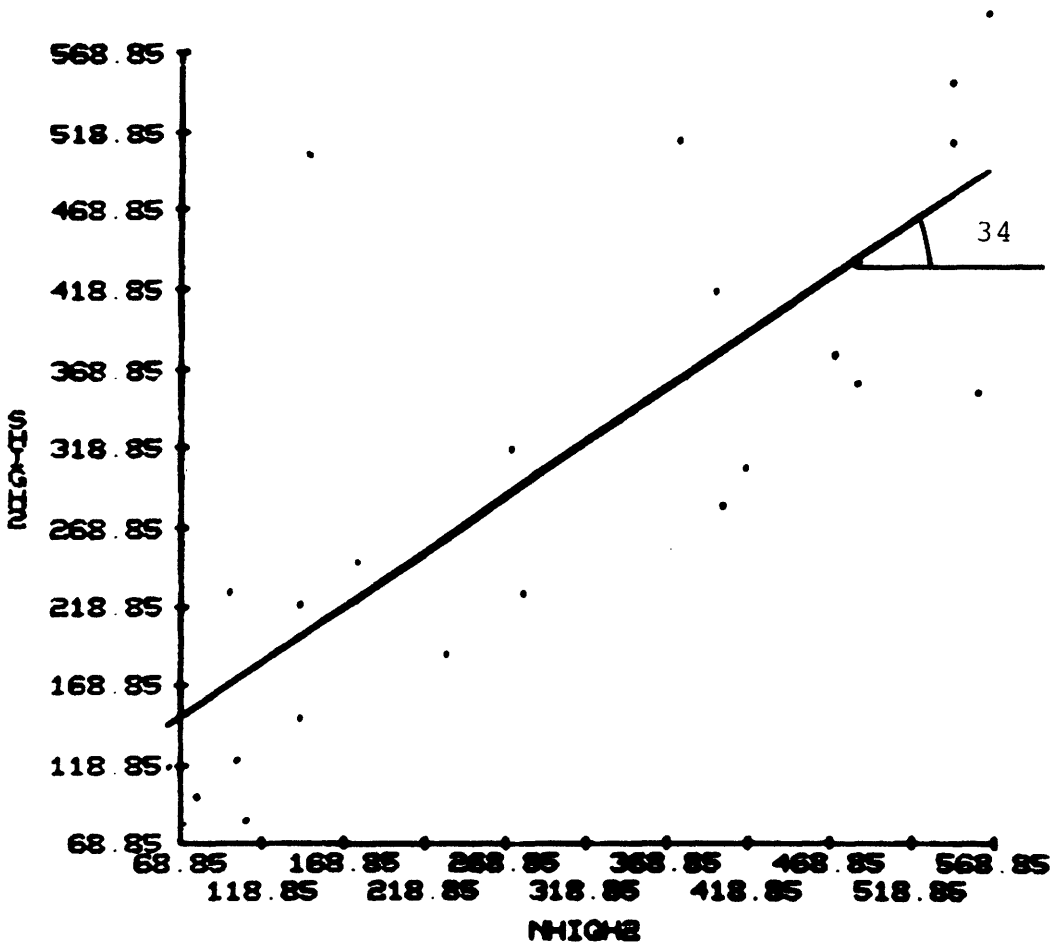

Figure C-11 Peak friction angle of amphibolite for normal stress below 0.65 MN/m^2

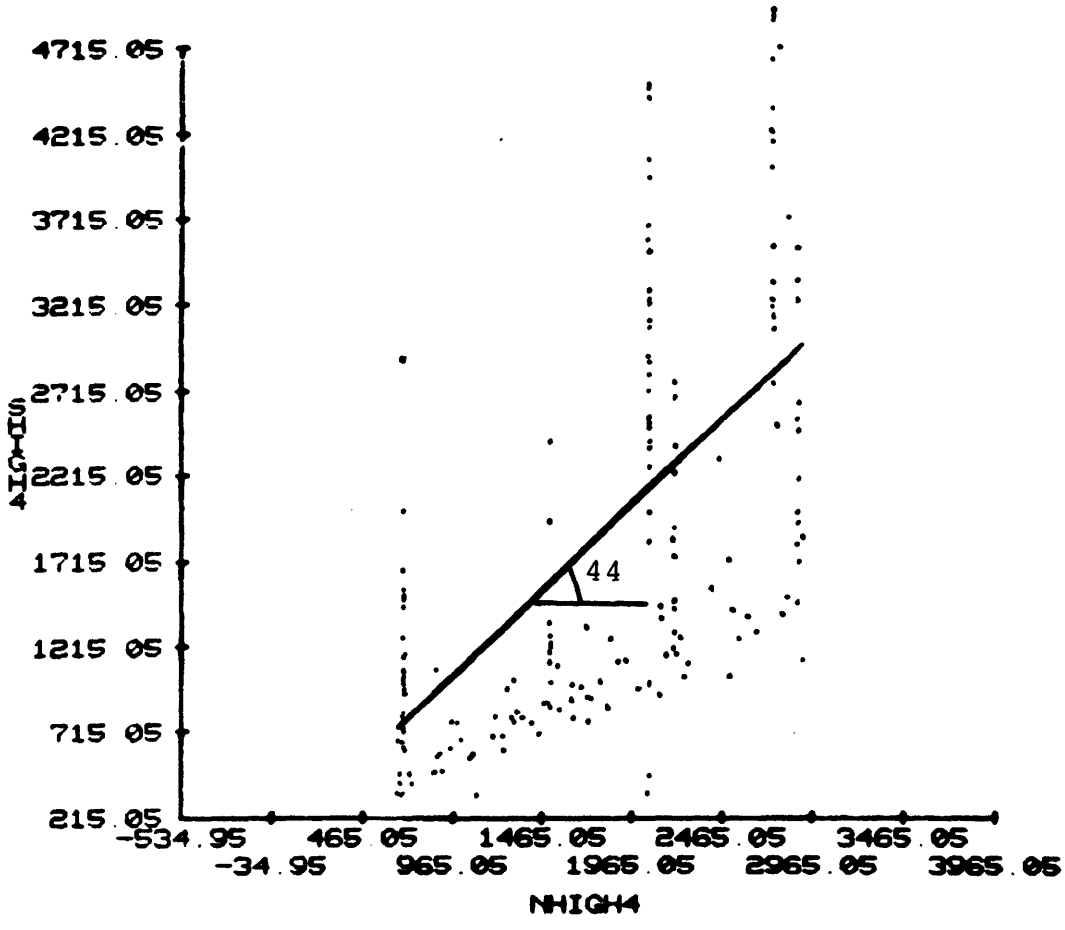

Figure C-12 Peak friction angle of amphibolite for normal stress between 0.65 and 3 MN/m^2

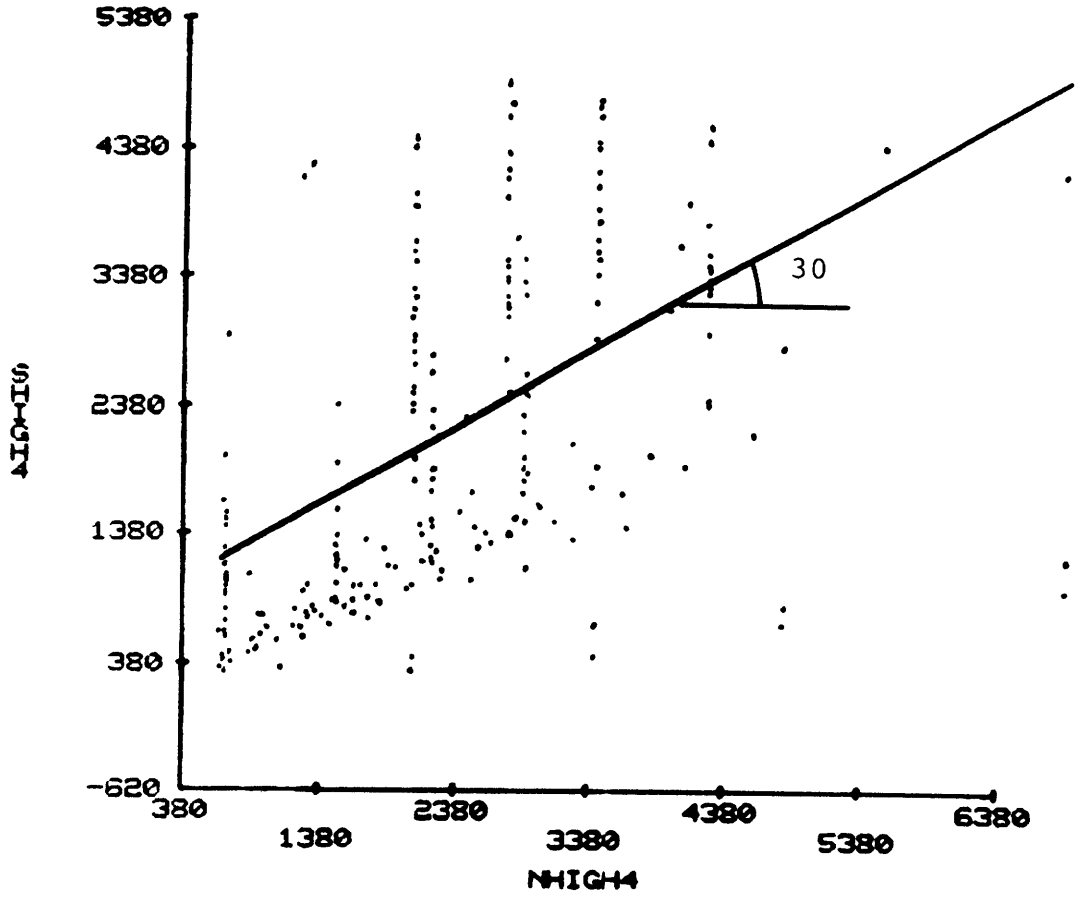

Figure C-13 Peak friction angle of amphibolite for normal stress between 0.65 and 8 MN/m^2

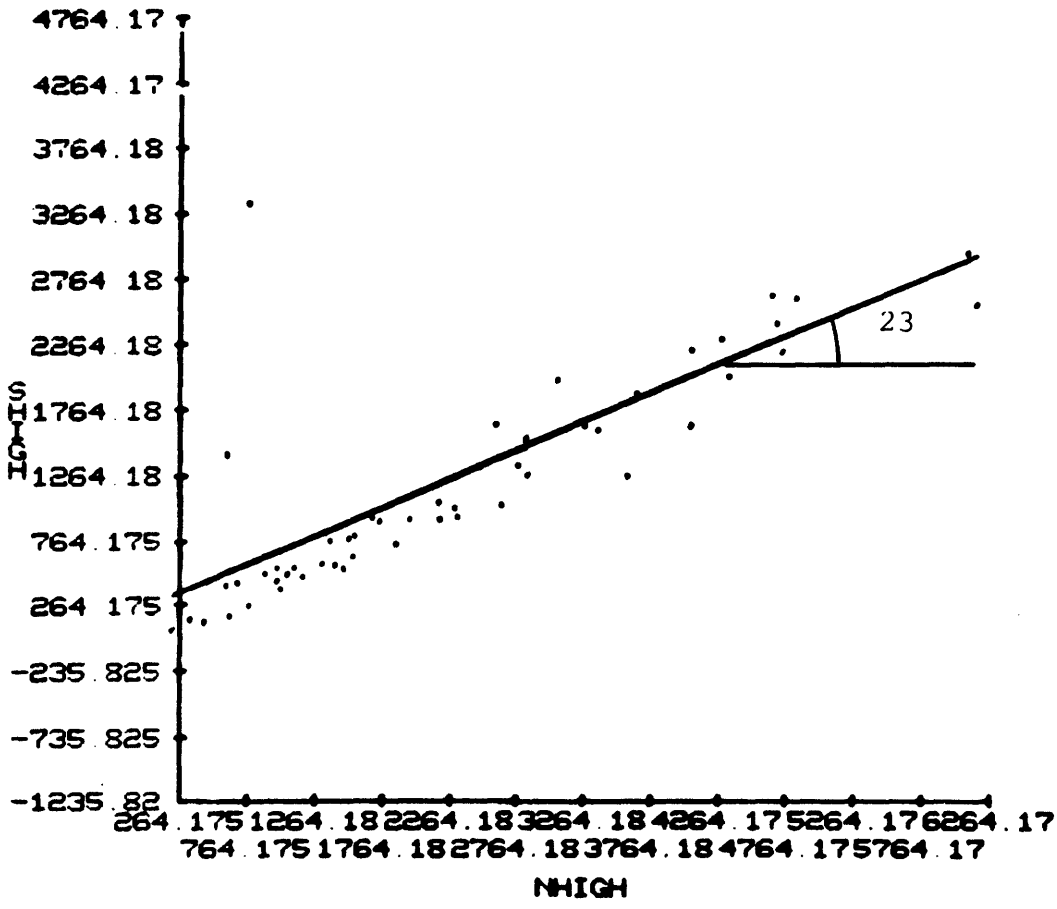

Figure C-14 Peak friction angle of schist for all normal stress levels

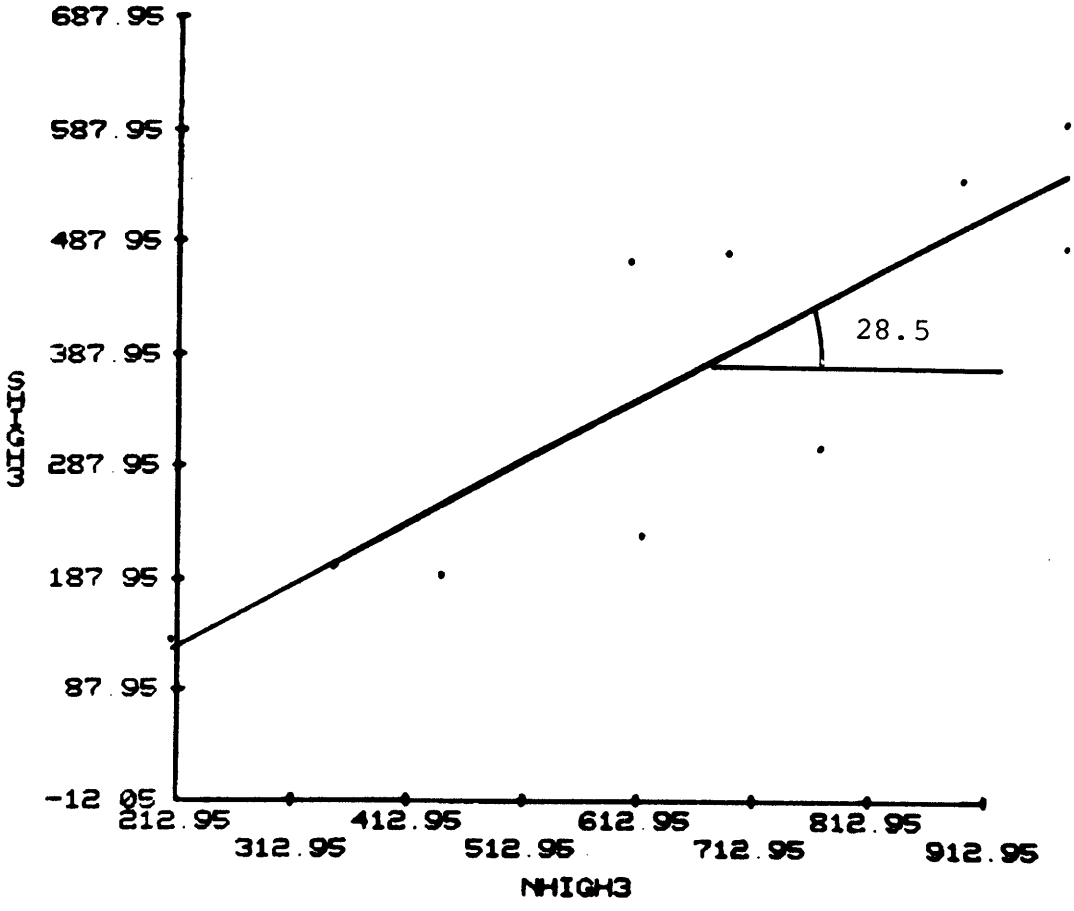

Figure C-15 Peak friction angle of schist for normal stress below 1 MN/m^2

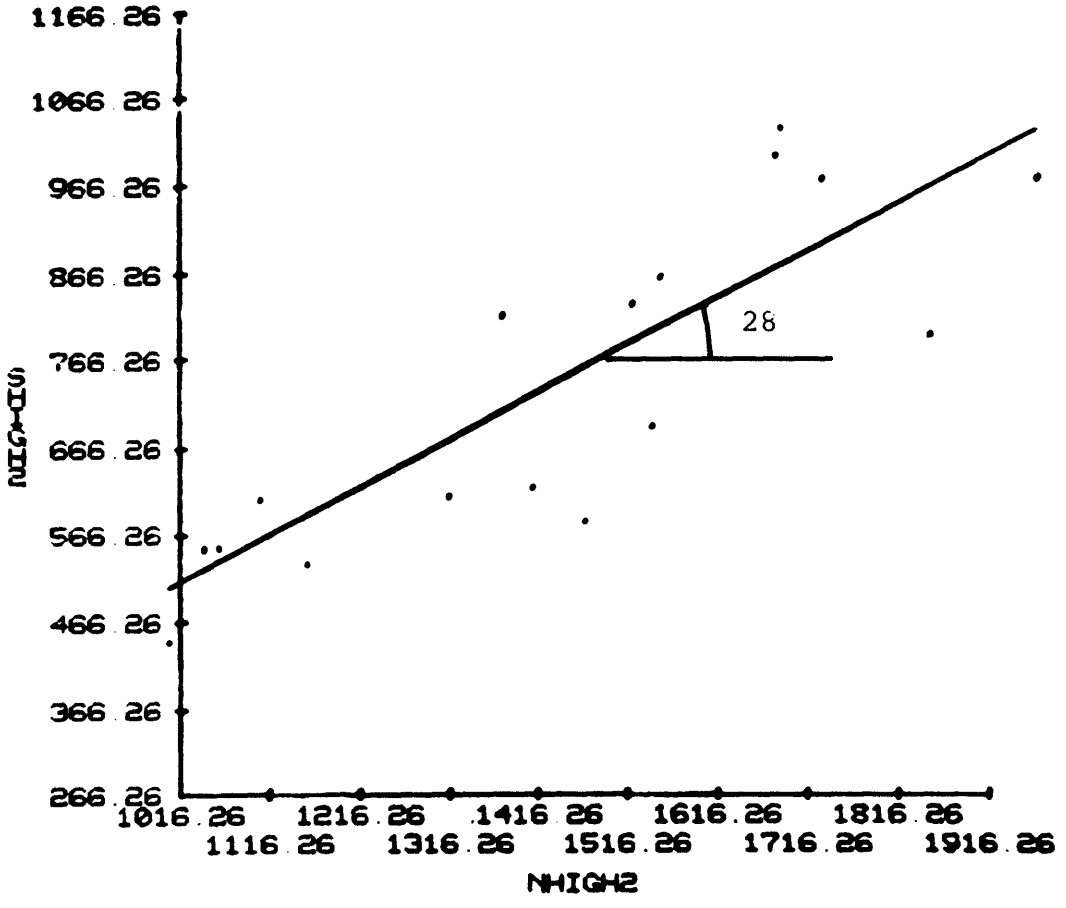

Figure C-16 Peak friction angle of schist for normal stress between 1 and 2 MN/m^2

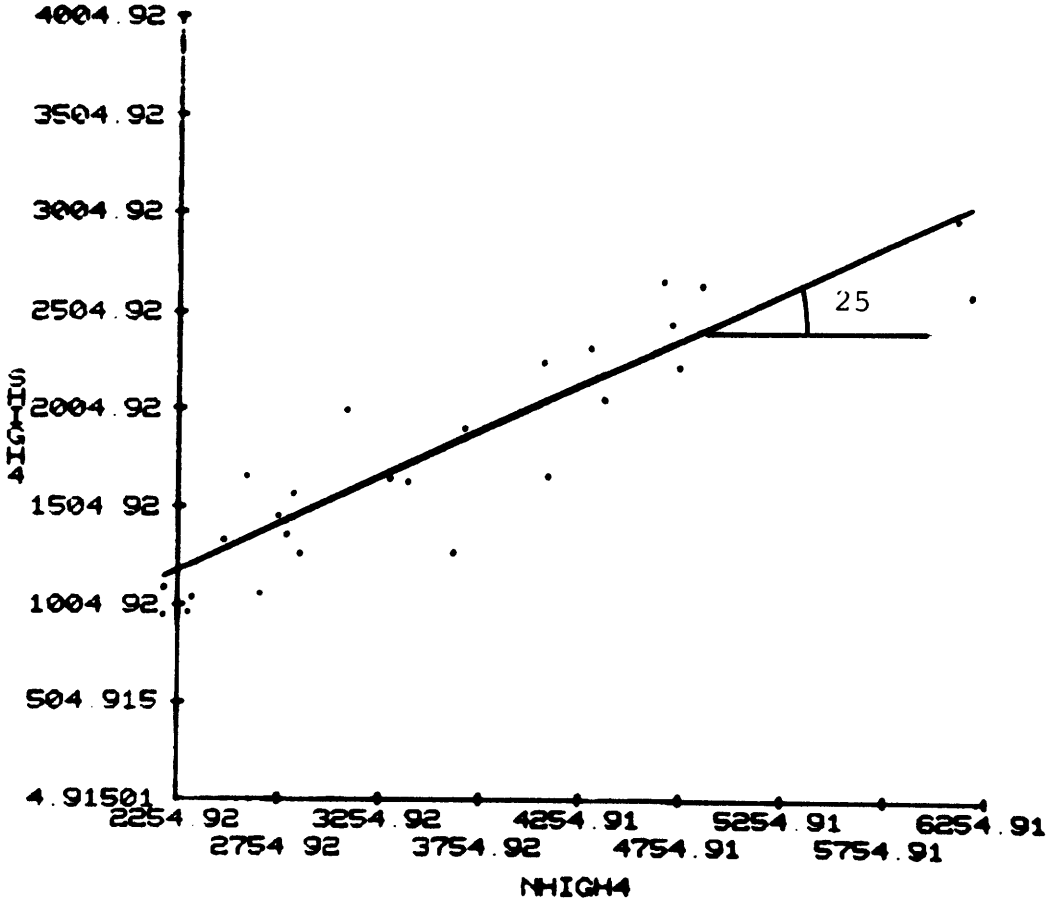

Figure C-17 Peak friction angle of schist for normal stress above 2 MN/m^2

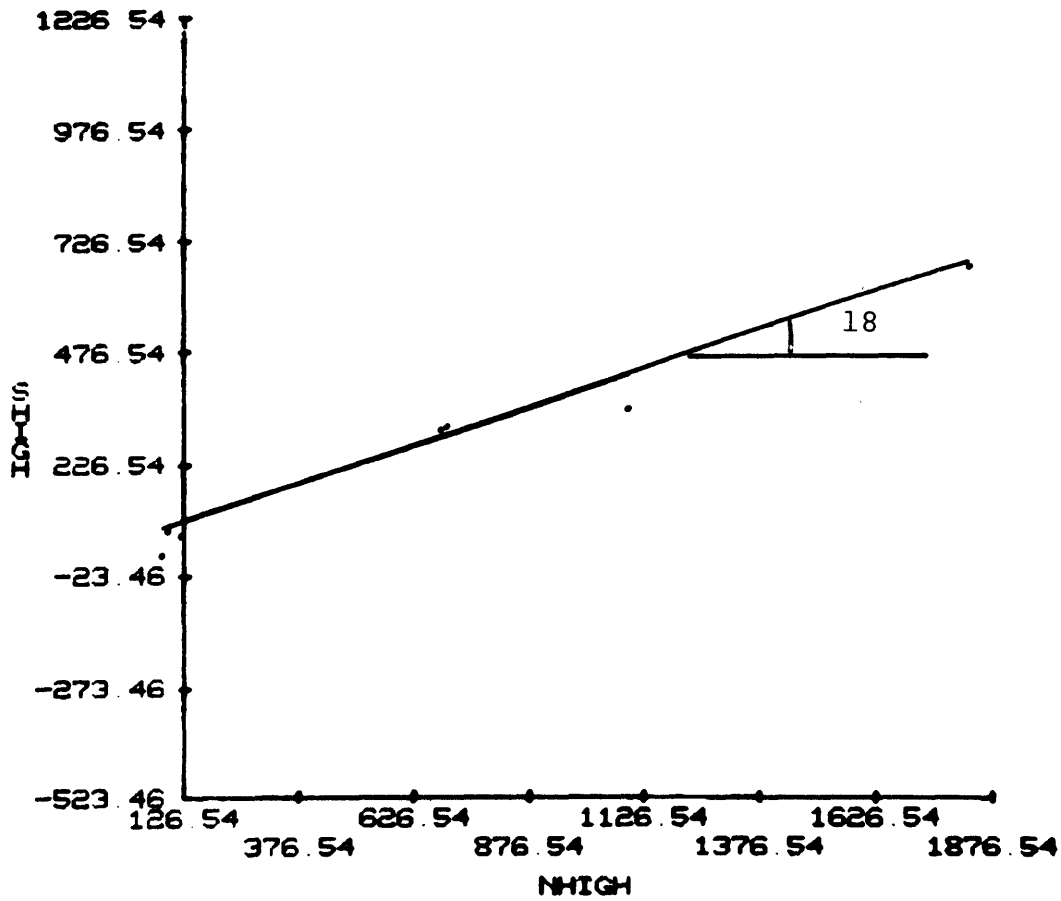

Figure C-18 Peak friction angle of phyllite for all normal stress levels

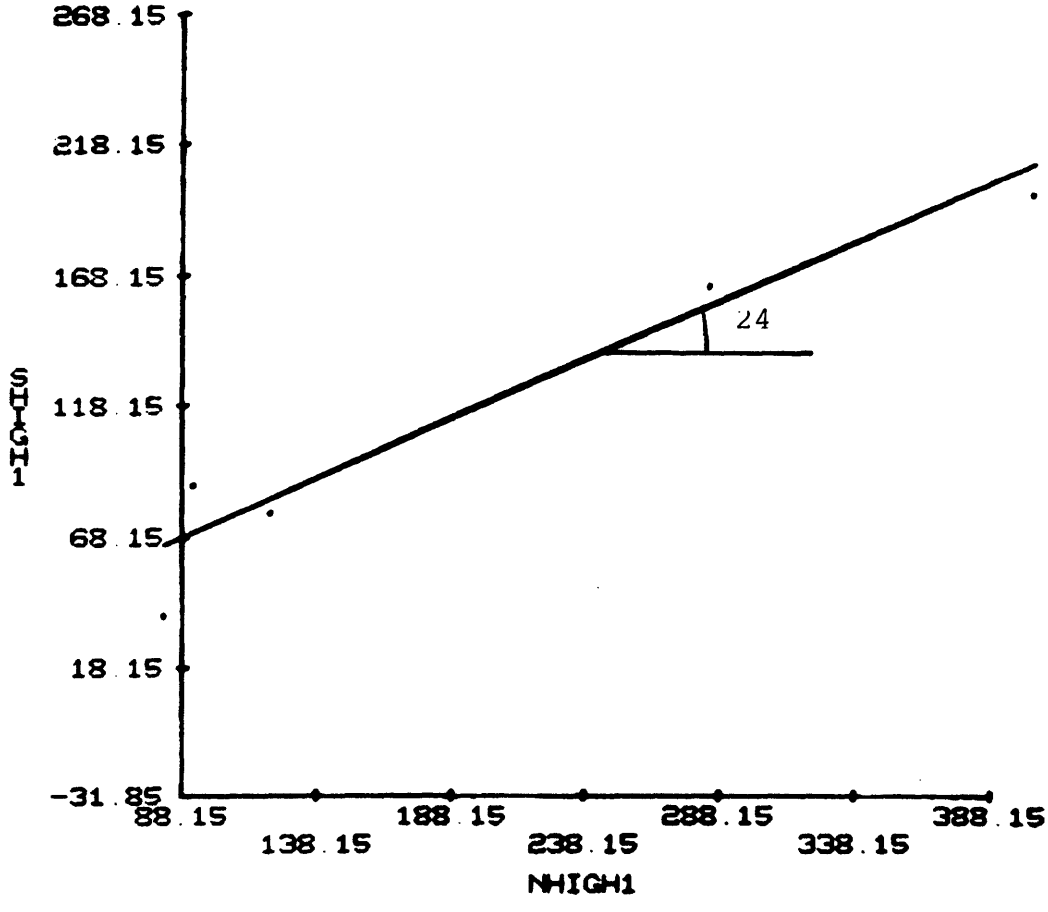

Figure C-19 Peak friction angle os phyllite for normal stress below 0.5 MN/m^2

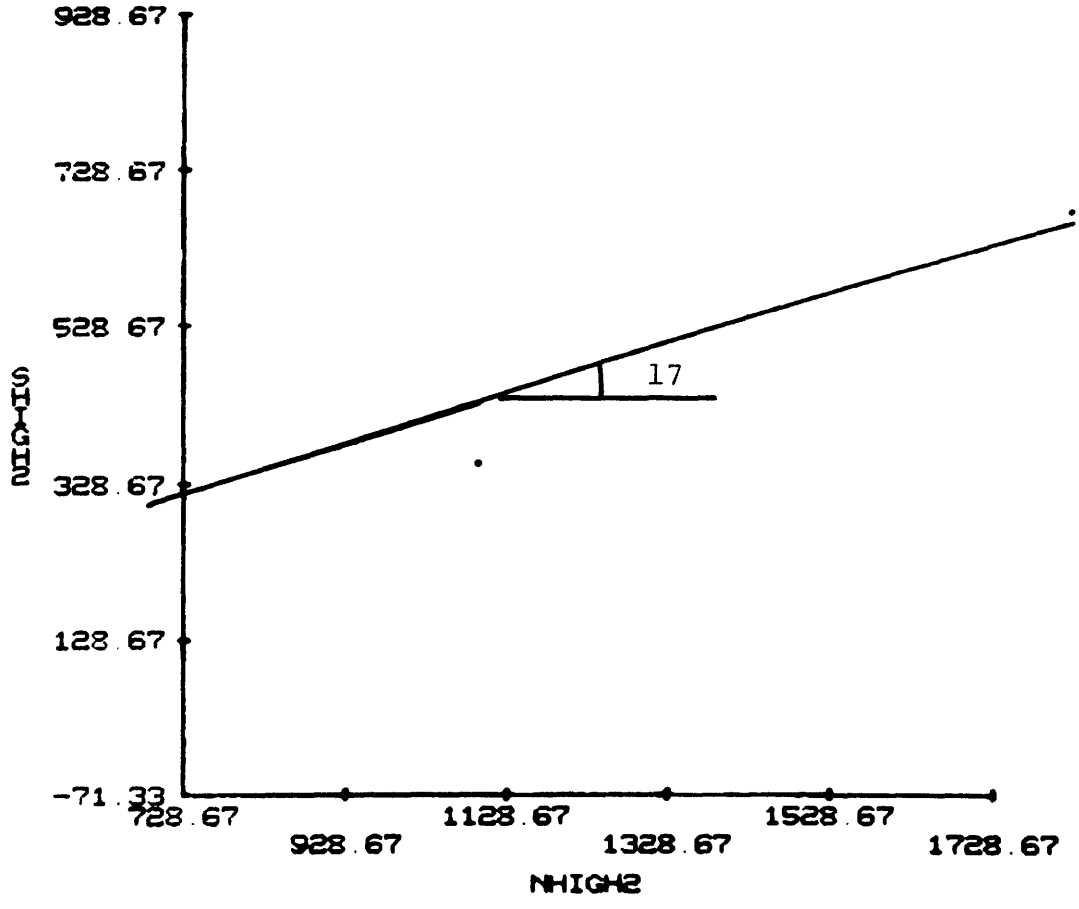

Figure C-20 Peak friction angle of phyllite for normal stress above 0.5 MN/m^2

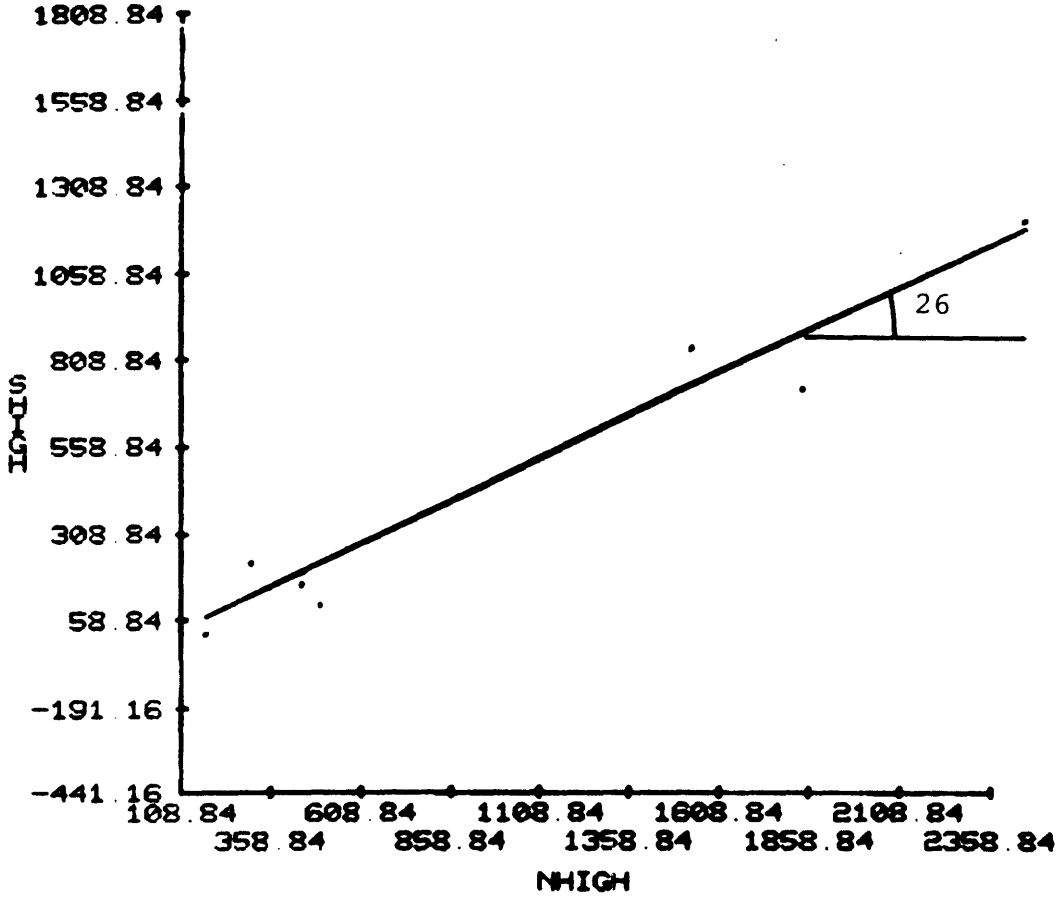

Figure C-21 Peak friction angle of serpentine (schistose) for all normal stress levels

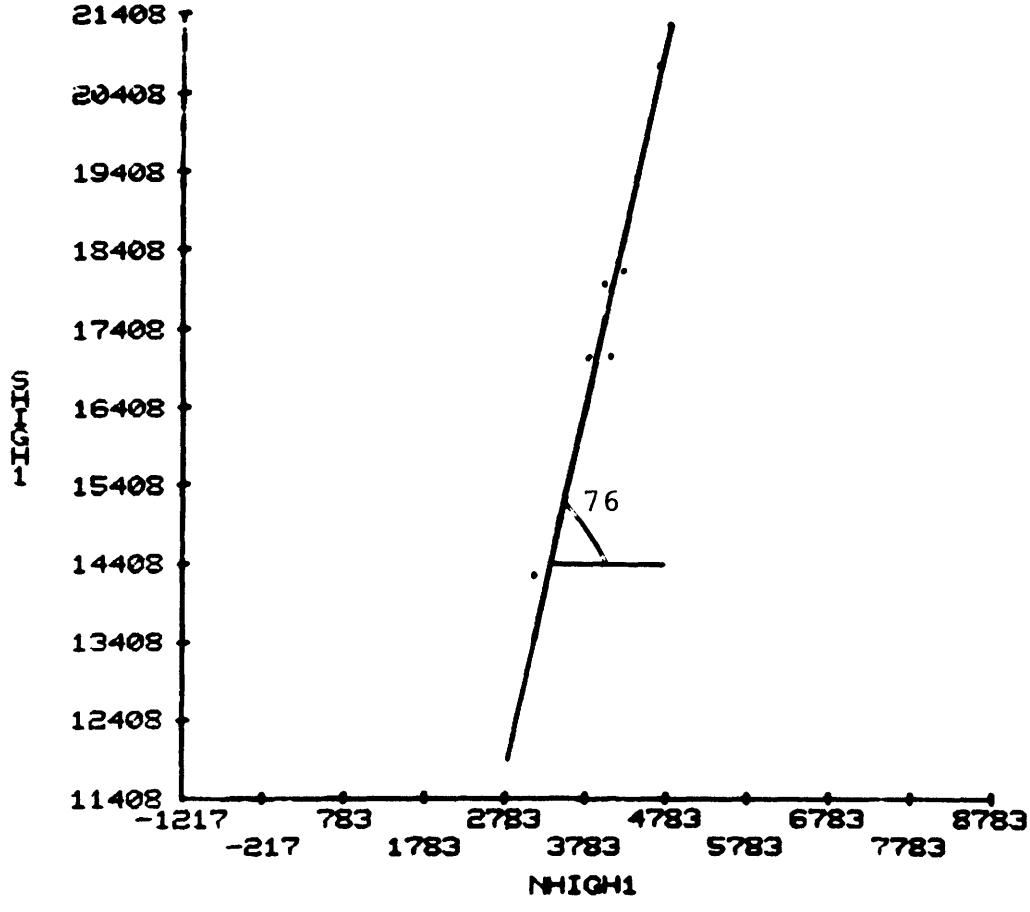

Figure C-22 Peak friction angle of homogeneous serpentine for all normal stress levels

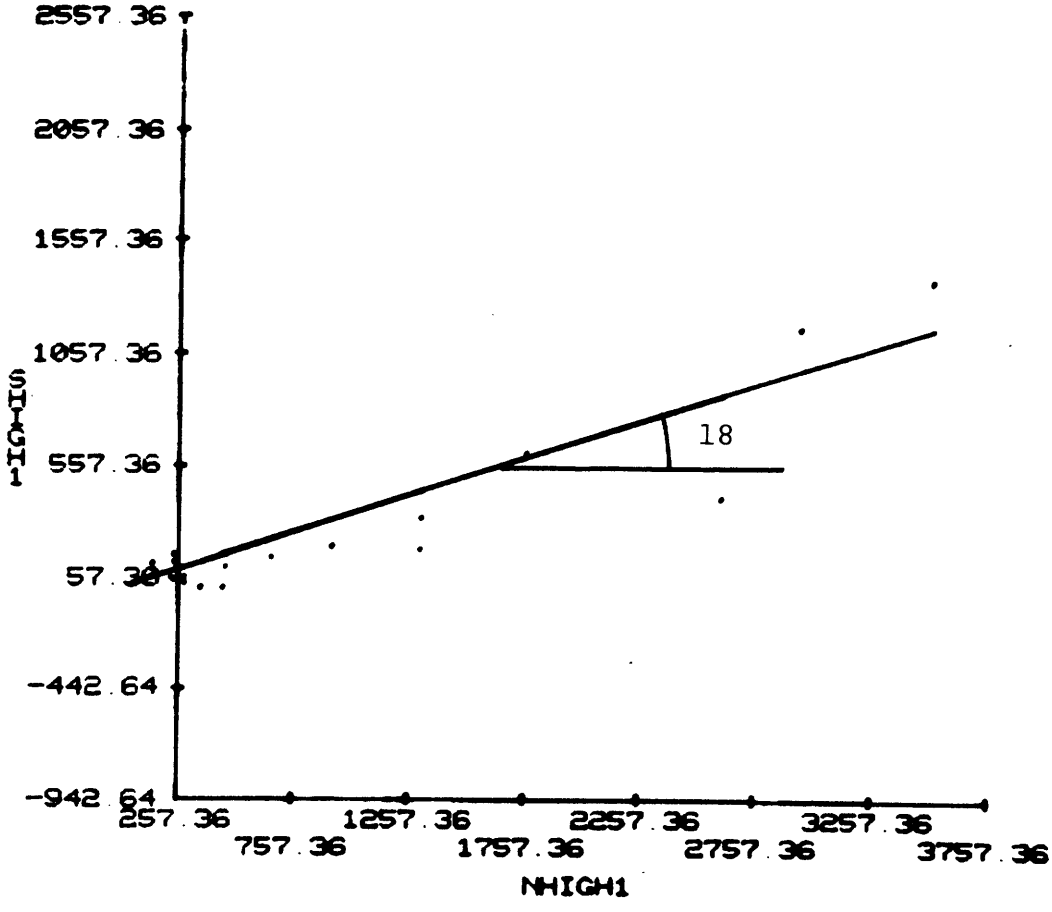

Figure C-23 Peak friction angle of serpentine for all normal stress levels

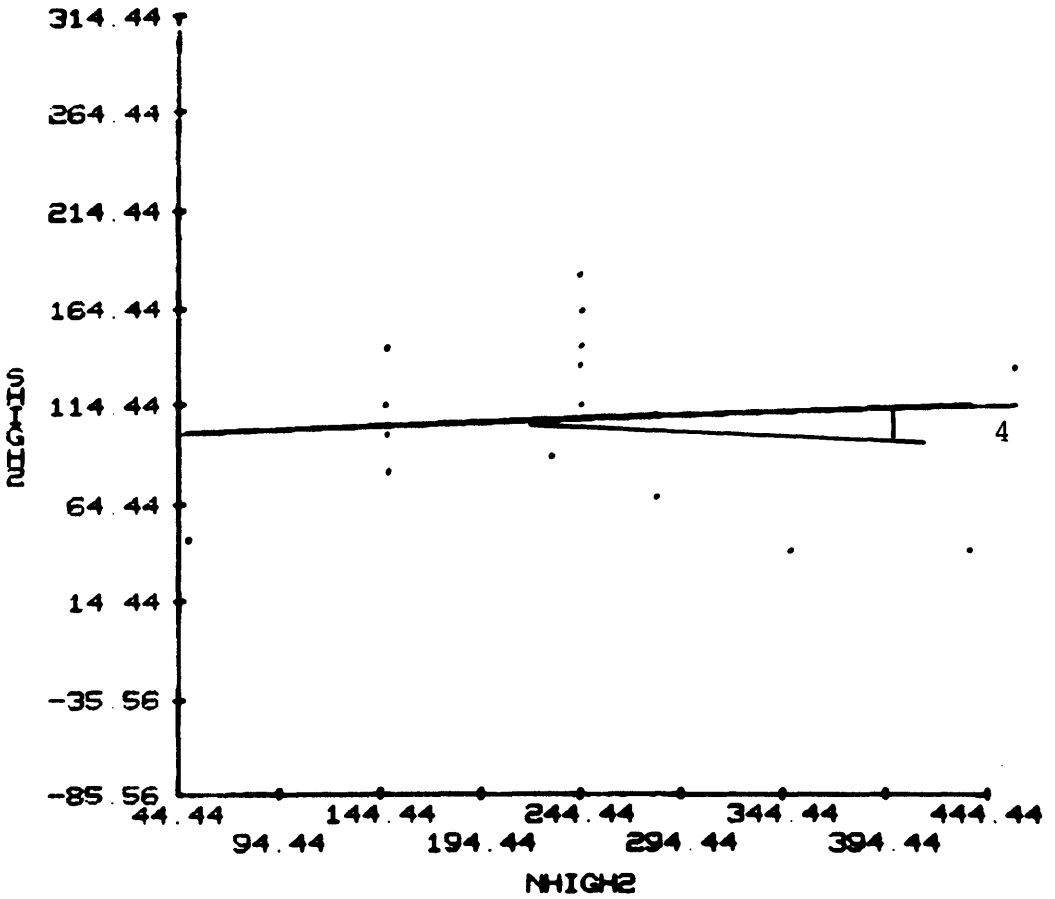

Figure C-24 Peak friction angle of serpentine for normal stress below 0.5 MN/m^2

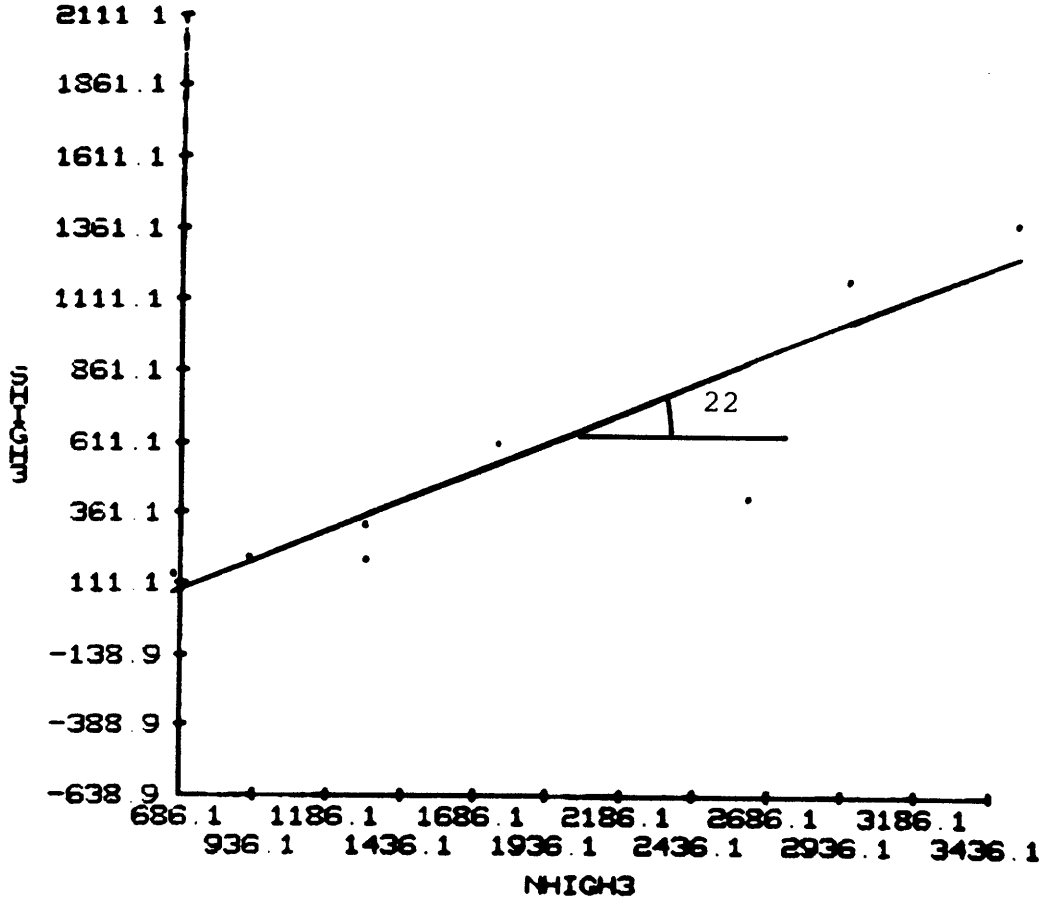

Figure C-25 Peak friction angle of serpentine for normal stress above 0.5 MN/m^2

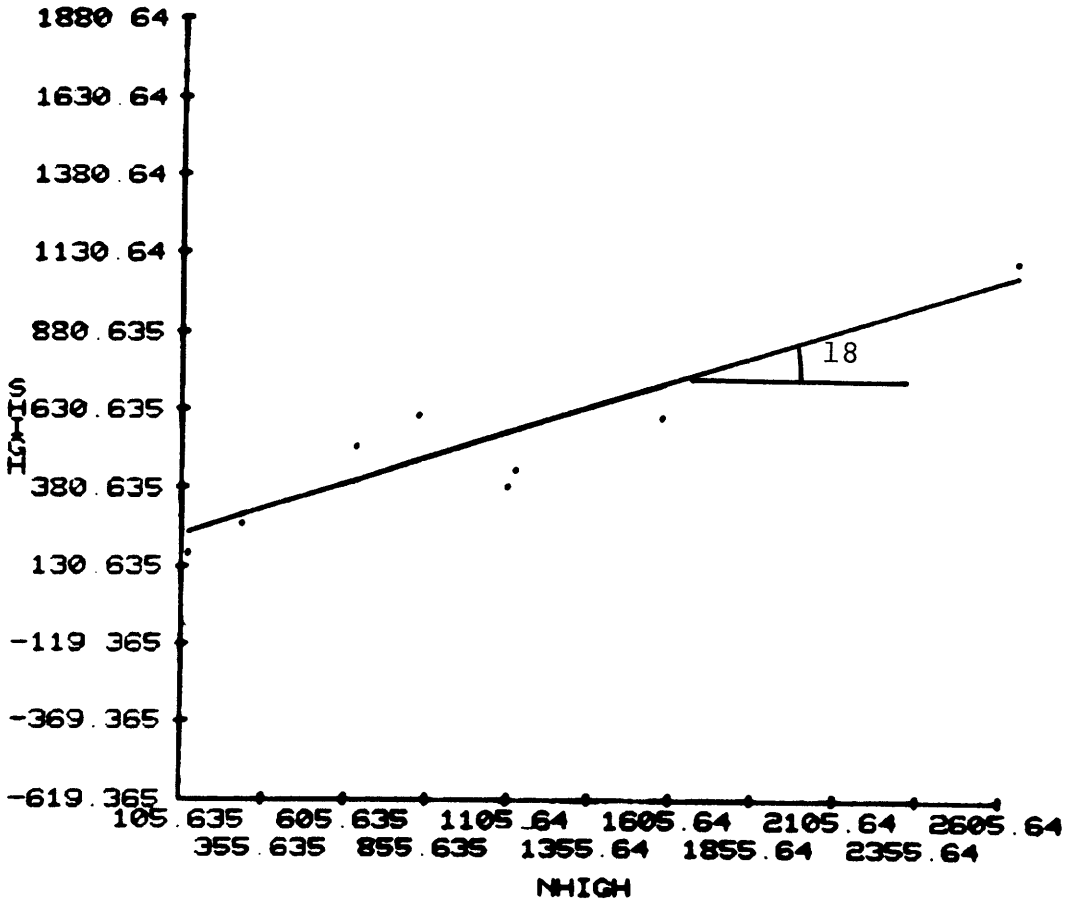

Figure C-26 Peak friction angle of marble for all normal stress levels

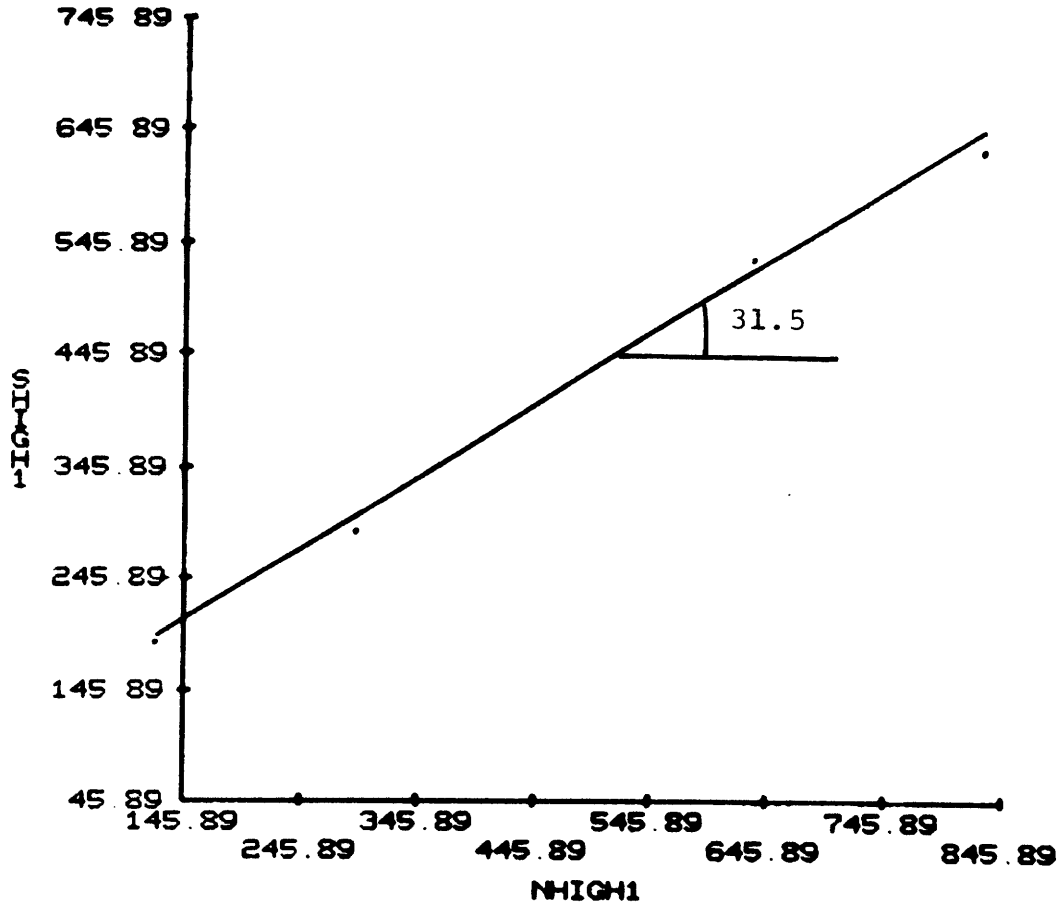

Figure C-27 Peak friction angle of marble for normal stress below 1 MN/m^2

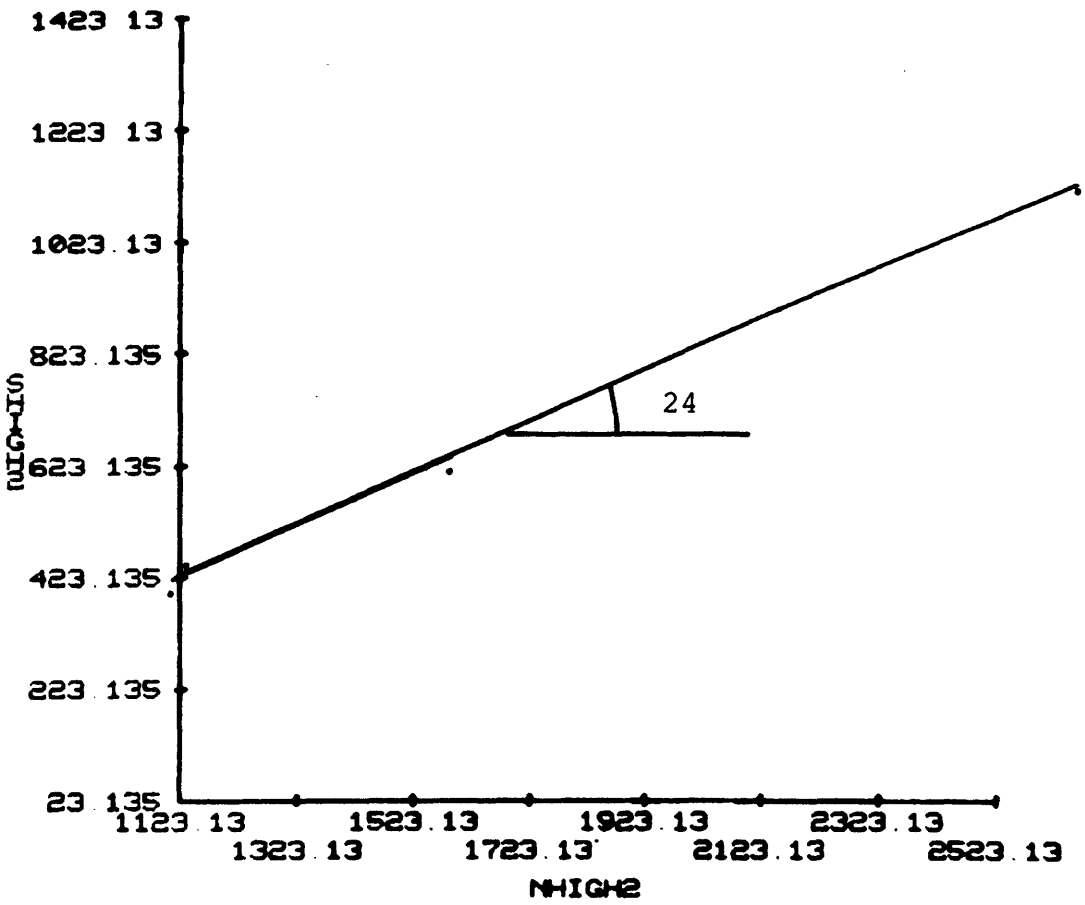

Figure C-28 Peak friction angle of marble for normal stress above 1 MN/m^2

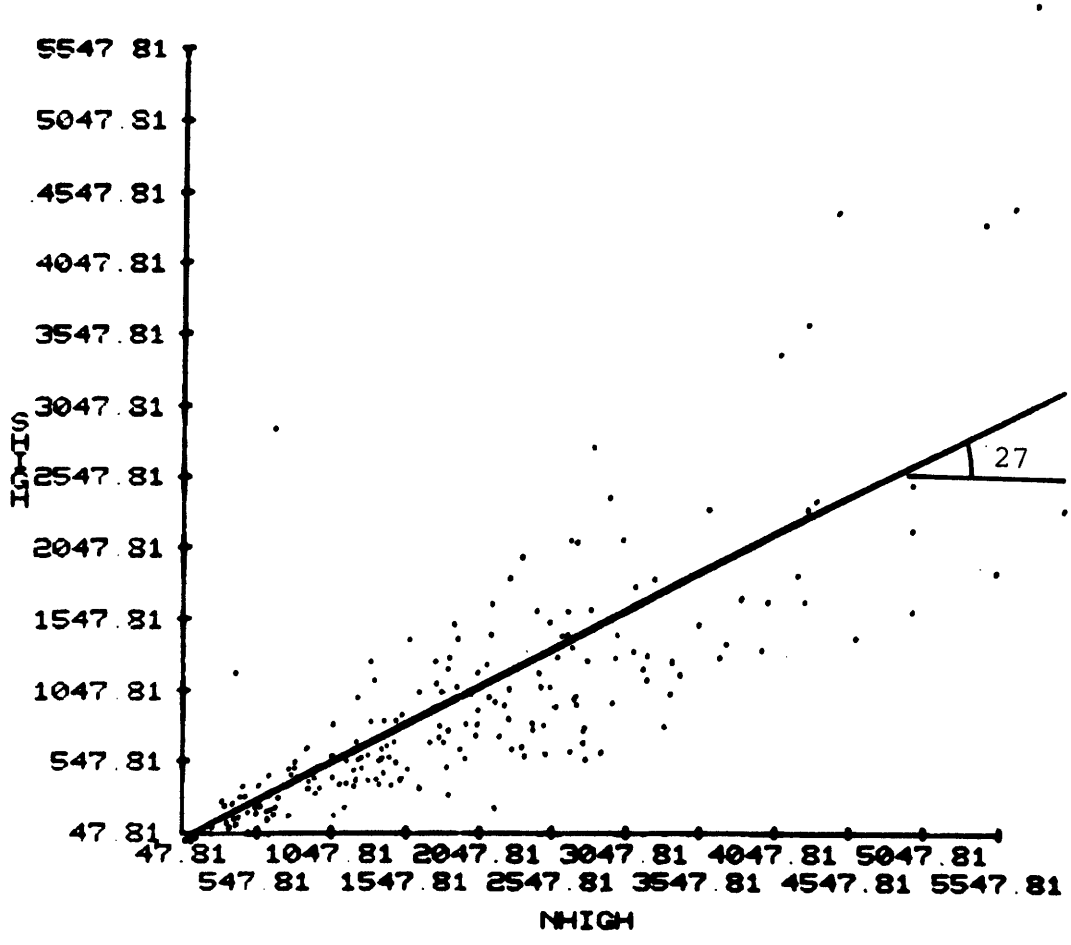

Figure C-29 Peak friction angle of gneiss for all normal stress levels

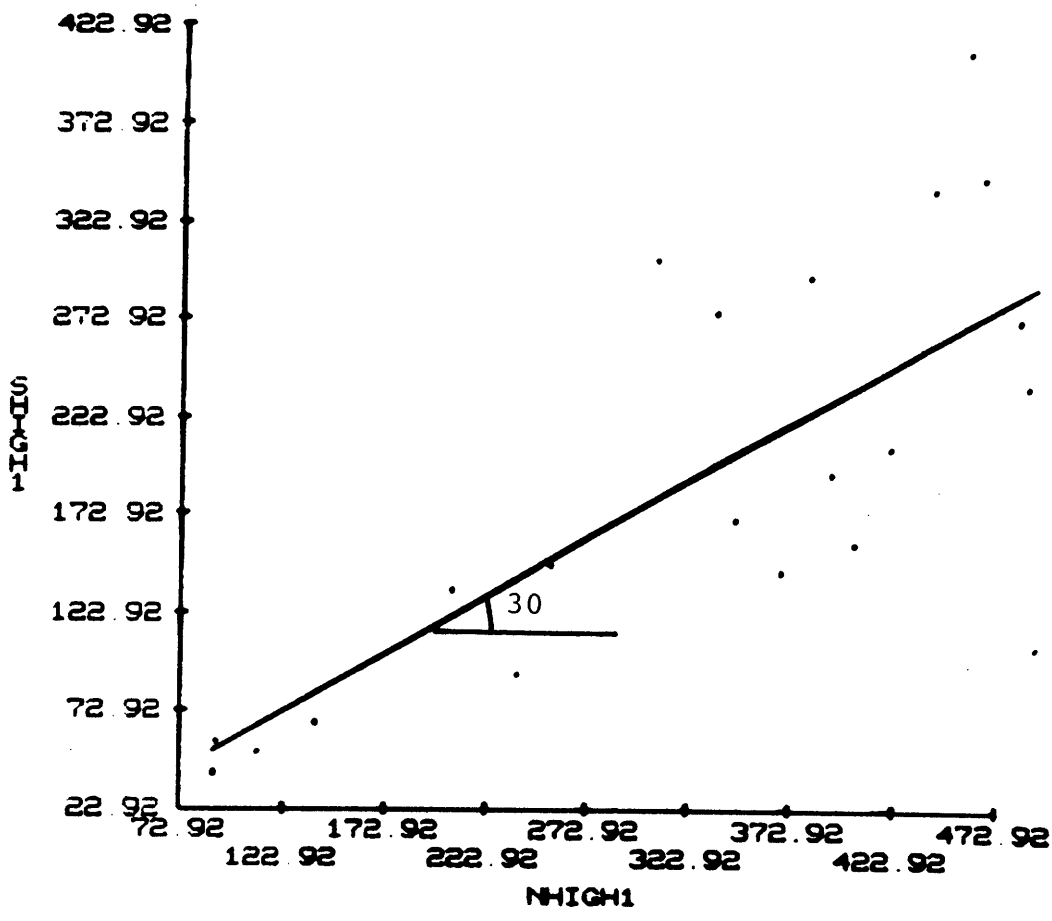

Figure C-30 Peak friction angle of gneiss for normal stress below 0.5 MN/m^2

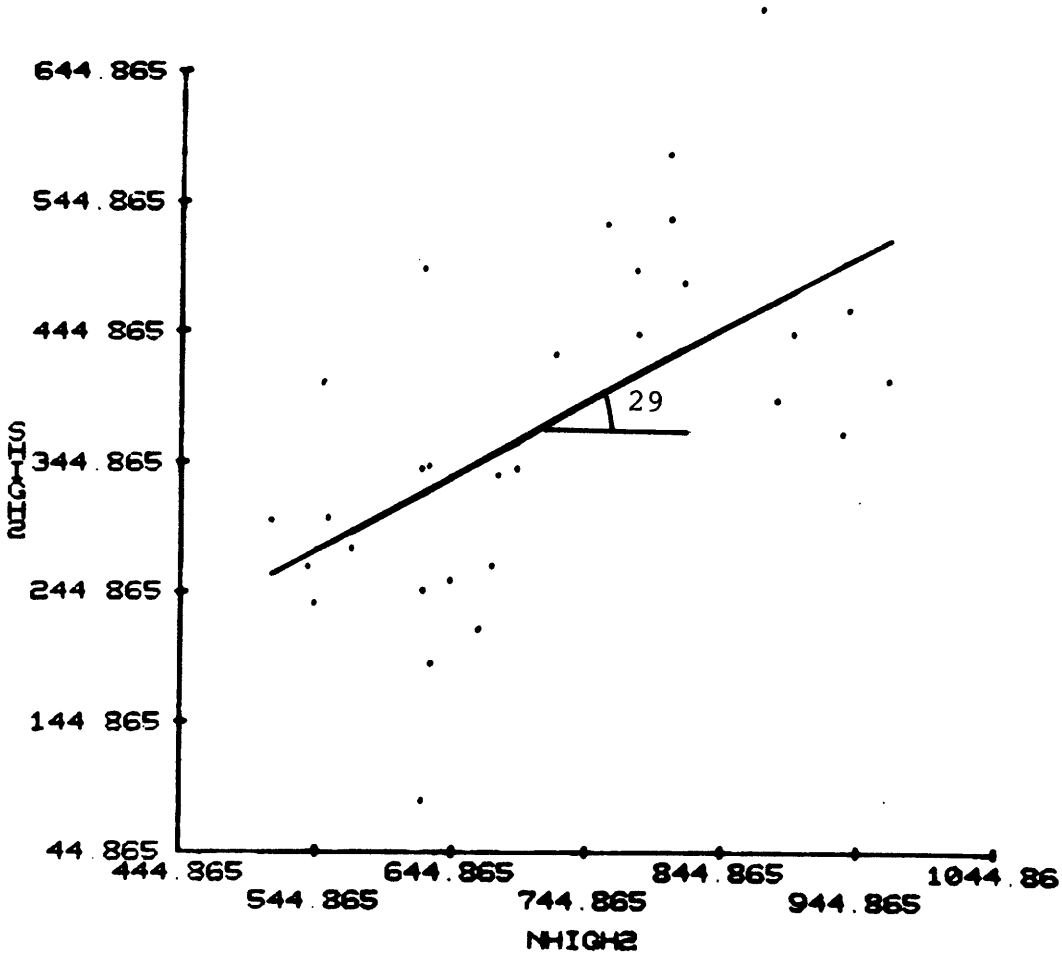

Figure C-31 Peak friction angle of gneiss for normal stress between 0.5 and 1 MN/m^2

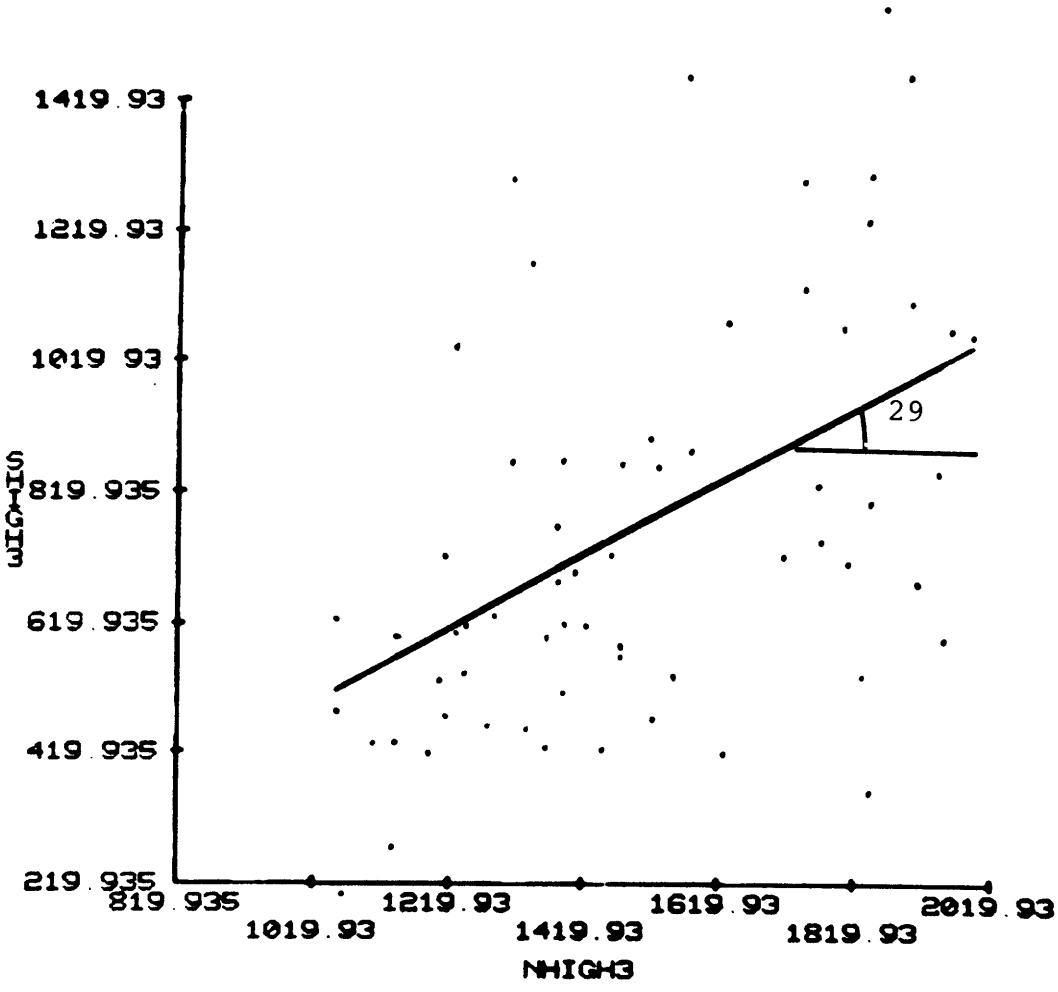

Figure C-32 Peak friction angle of gneiss for normal stress between 1 and 2 MN/m^2

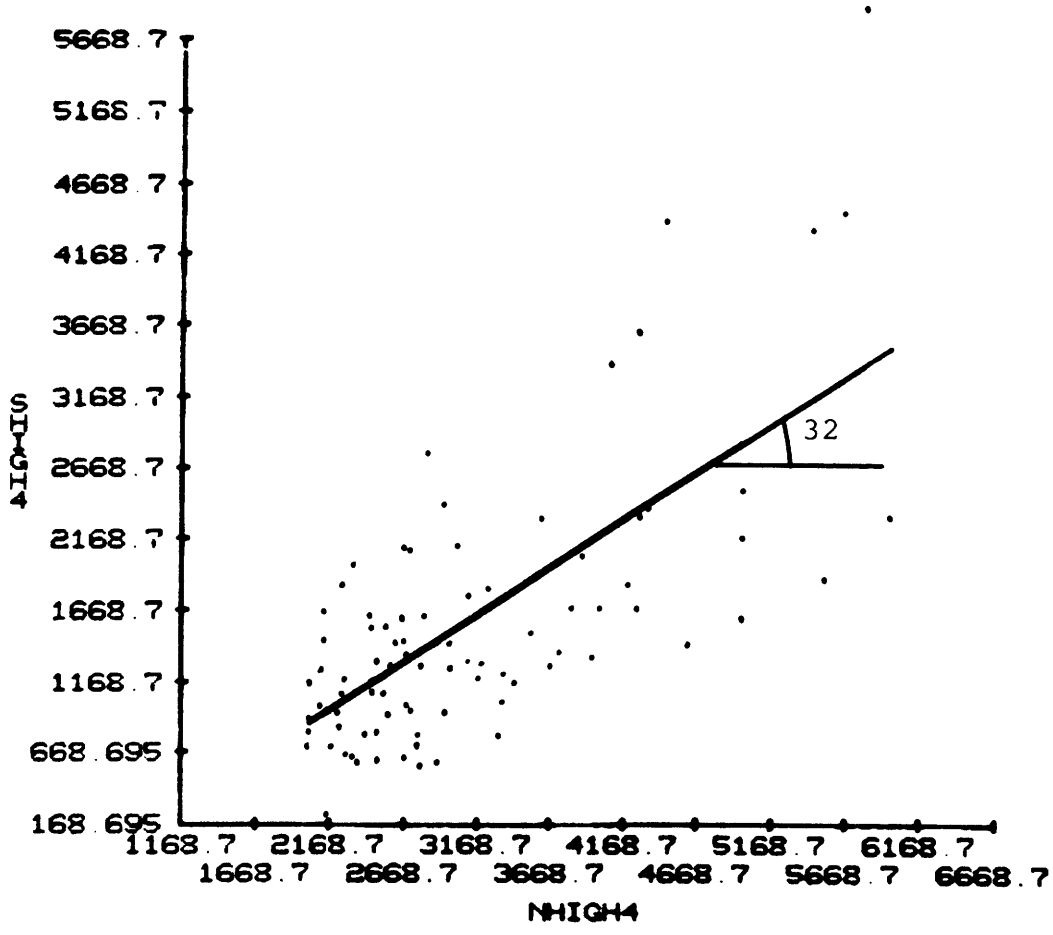

Figure C-33 Peak friction angle of gneiss for normal stress above 2 MN/m^2

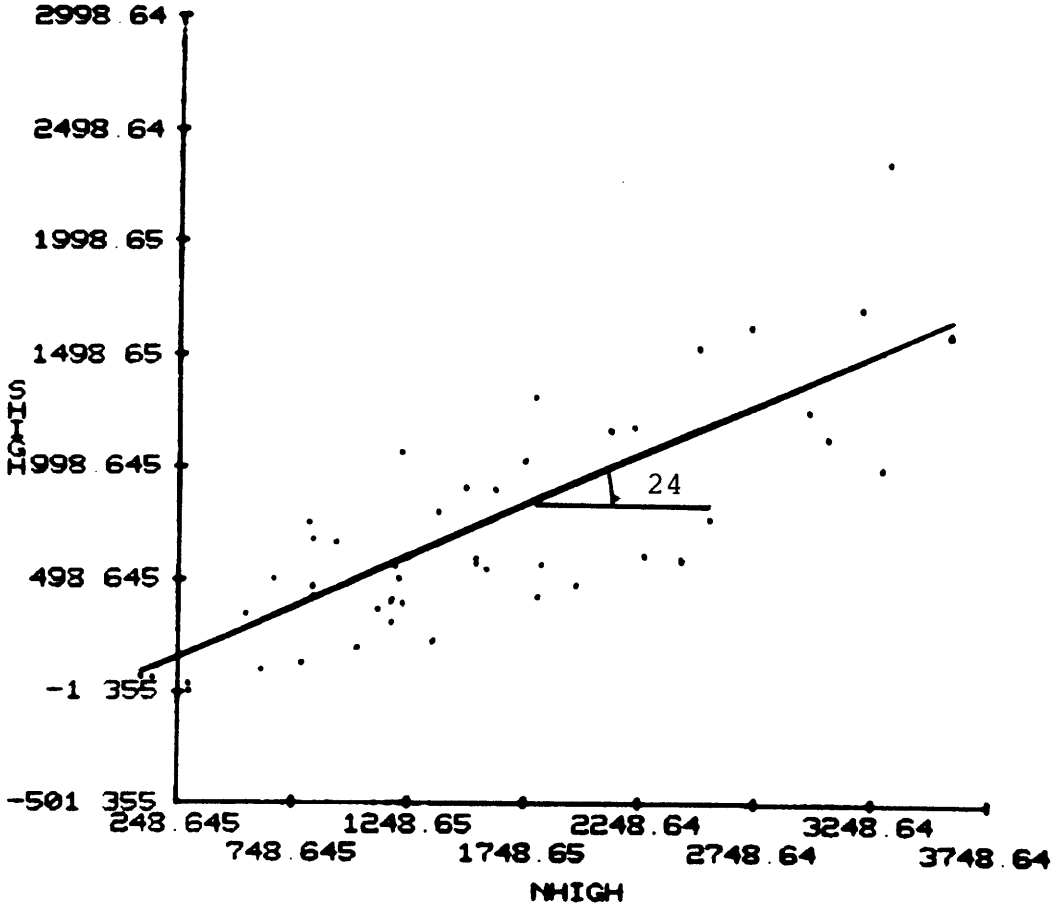

Figure C-34 Peak friction angle of gneiss (schistose) of all normal stress levels

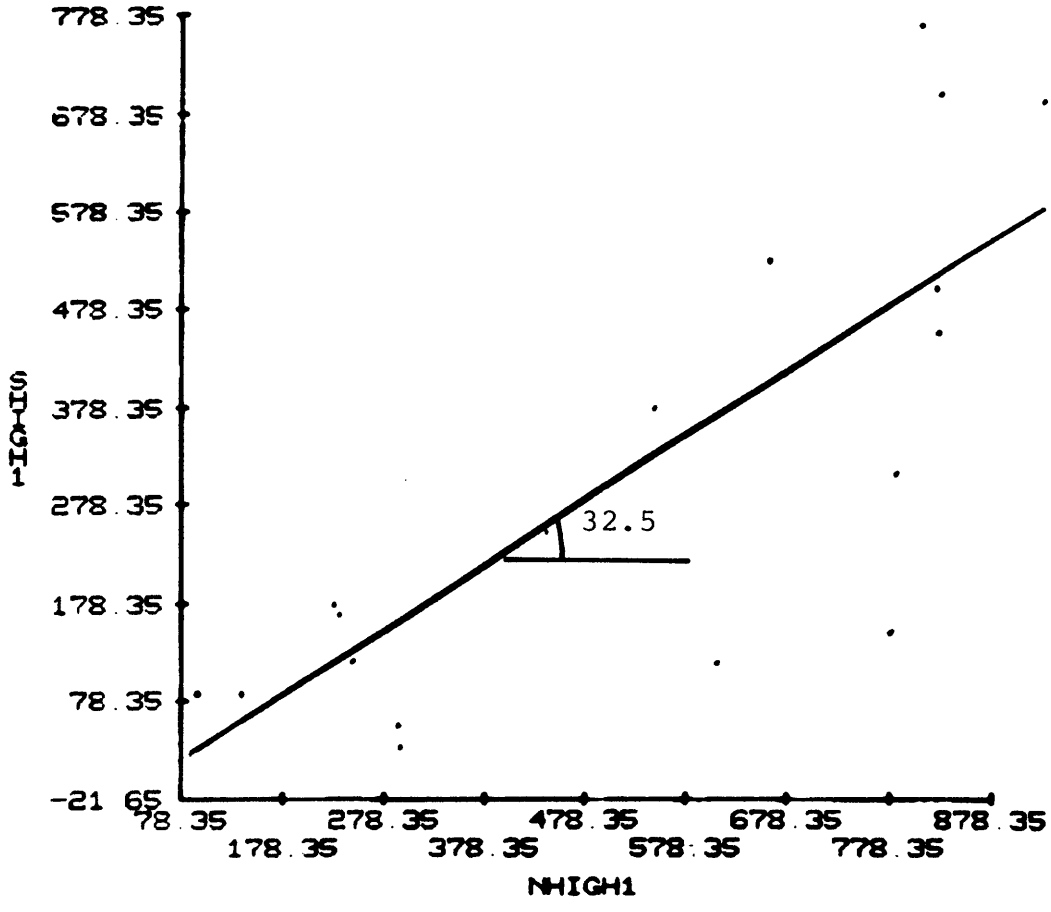

Figure C-35 Peak friction angle of gneiss (schistose) for normal stress below 1 MN/m^2

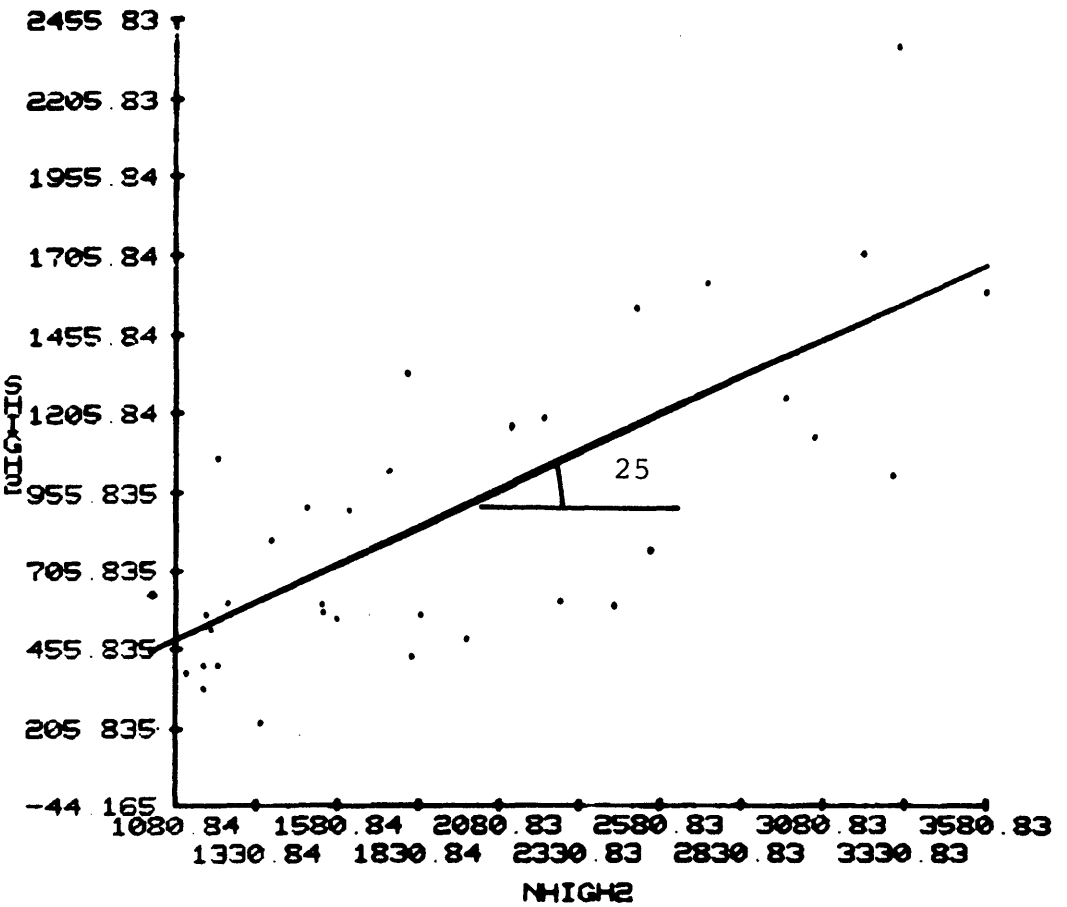

Figure C-36 Peak friction angle of gneiss (schistose) for normal stress above 1 MN/m^2

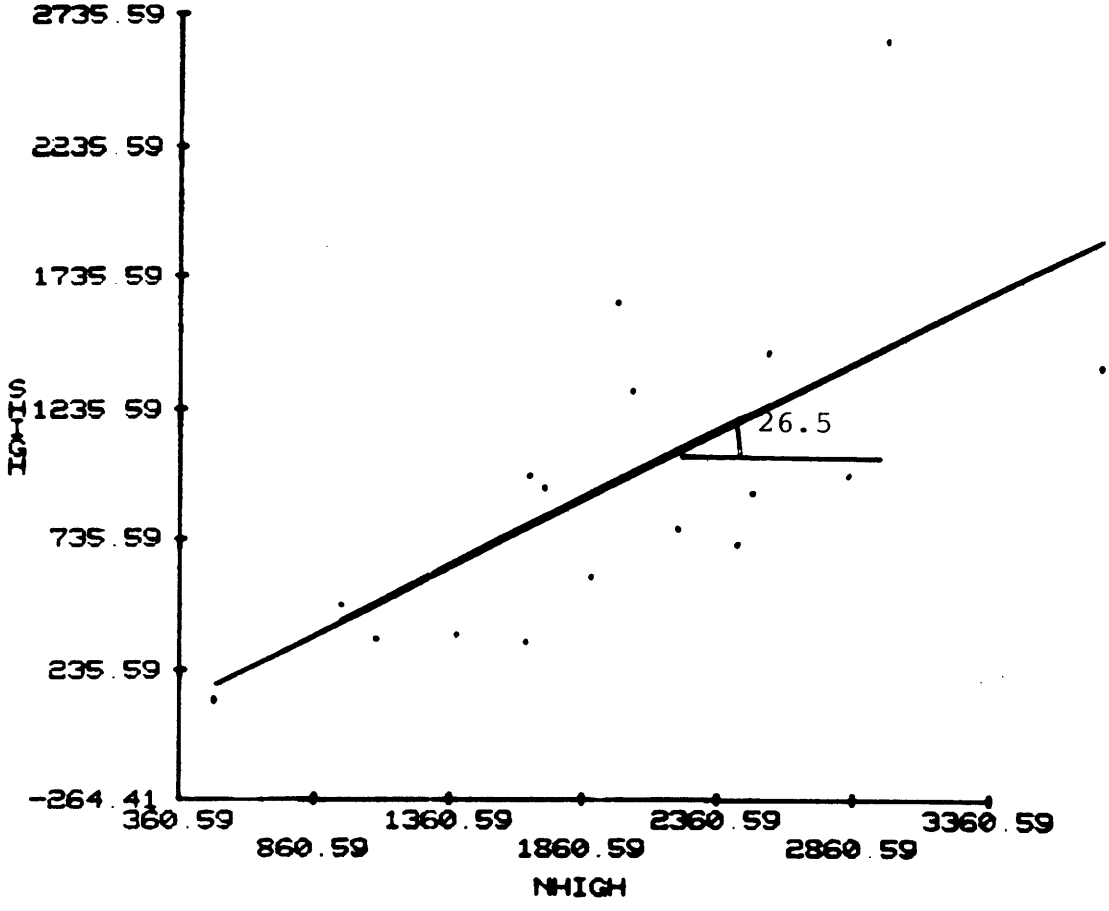

Figure C-37 Peak friction angle of schist (carboniferous) for all normal stress levels

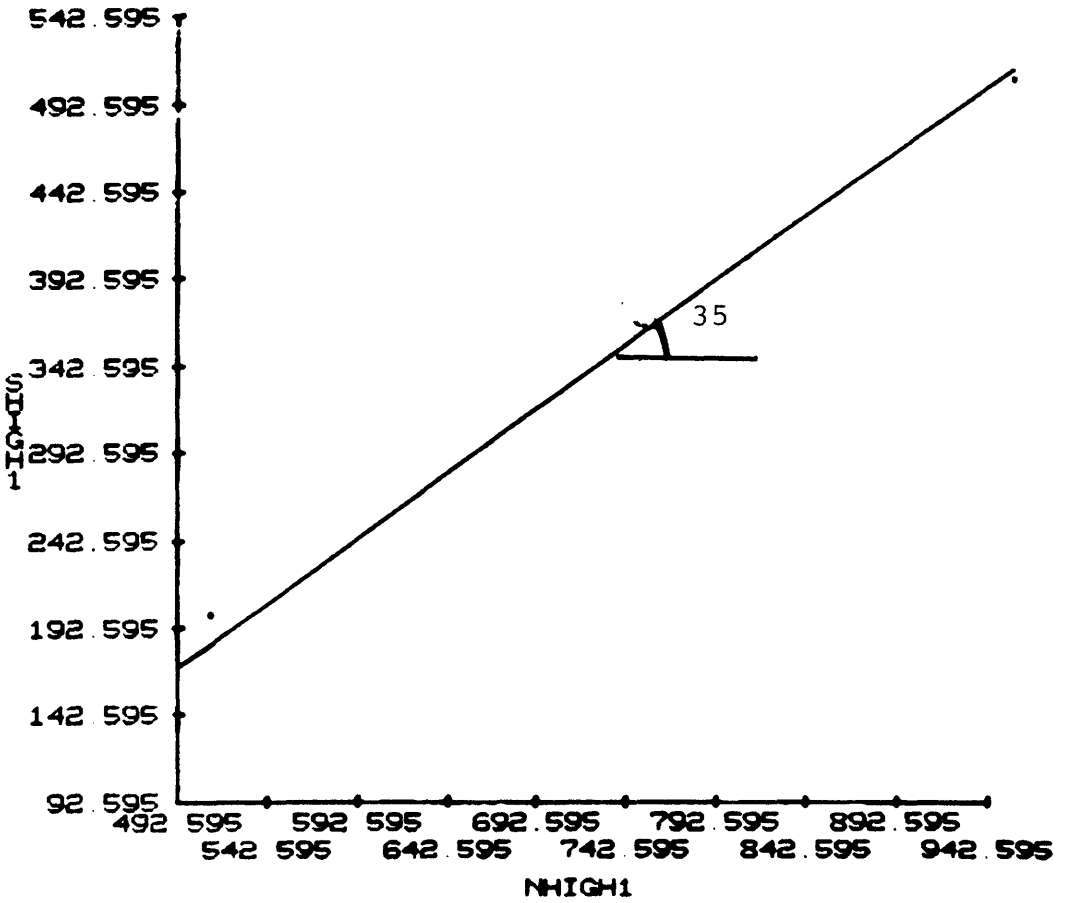

Figure C-38 Peak friction angle of schist (carboniferous) for normal stress below 1 MN/m^2

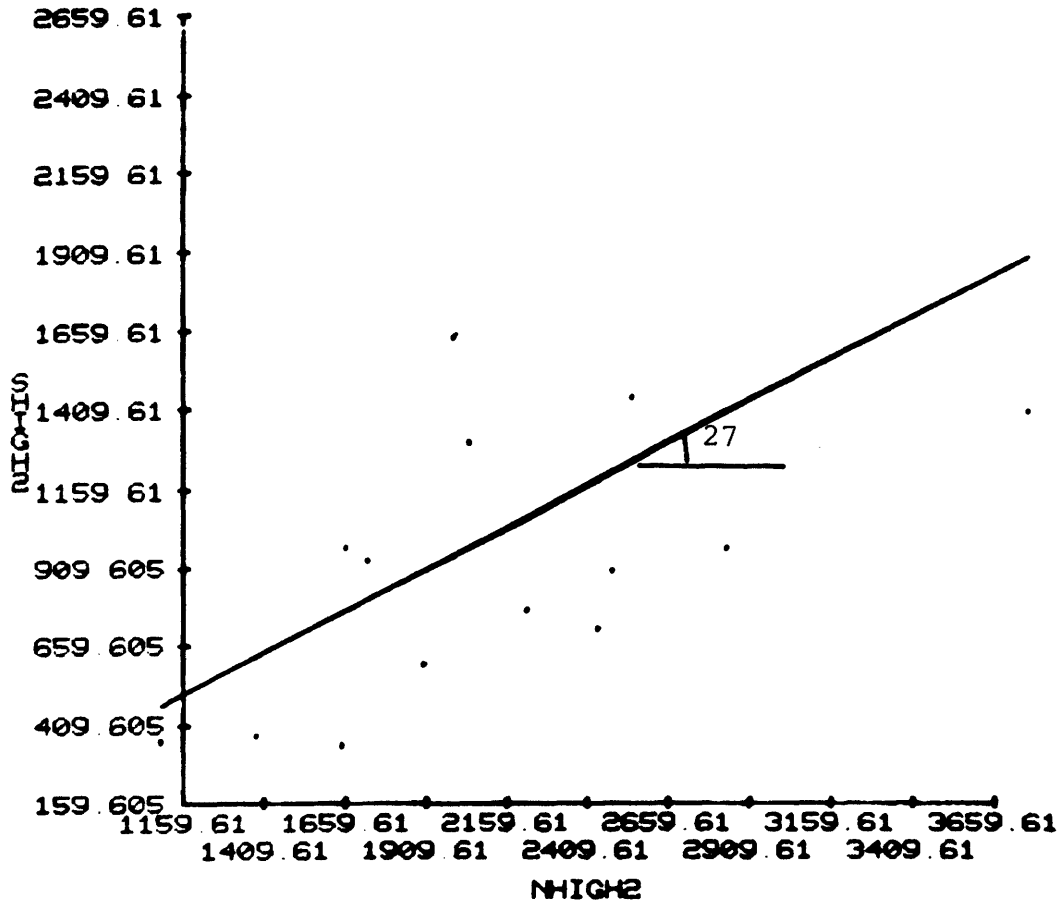

Figure C-39 Peak friction angle of schist (carboniferous) for normal stress above 1 MN/m^2

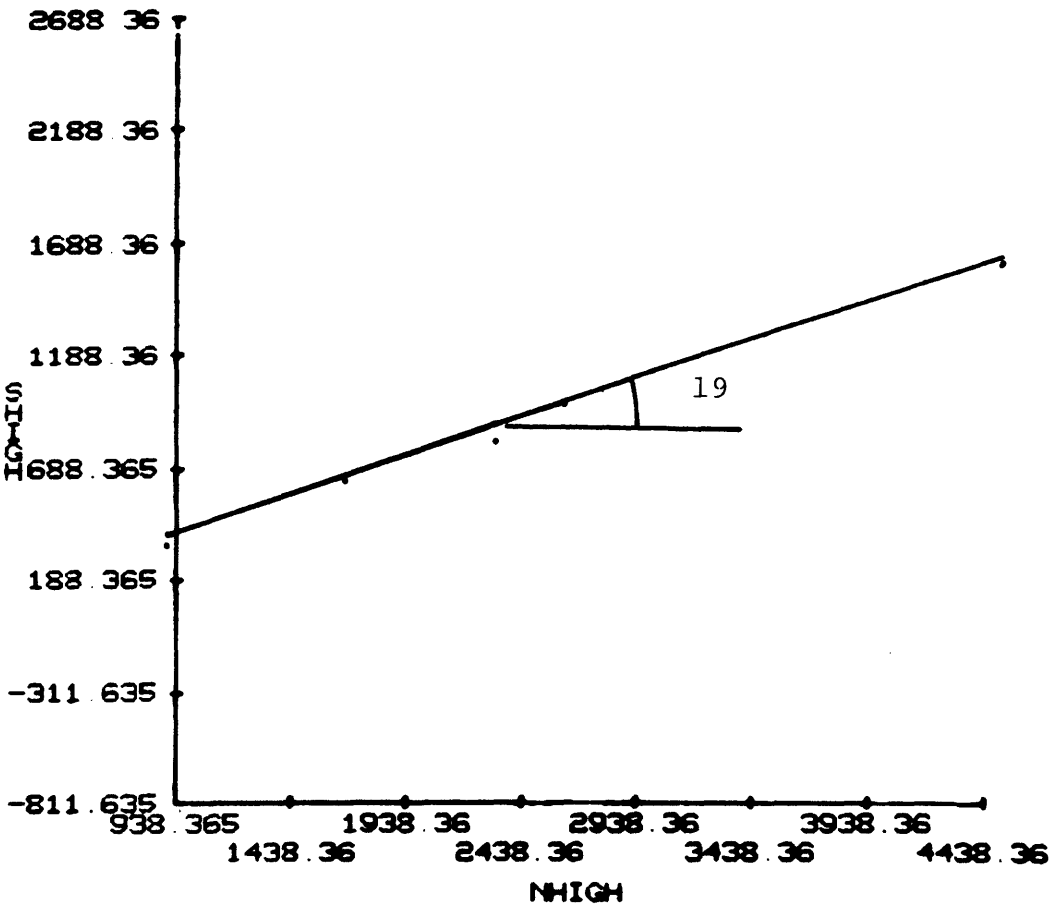

Figure C-40 Peak friction angle of schist (calcarous) for all normal stress levels

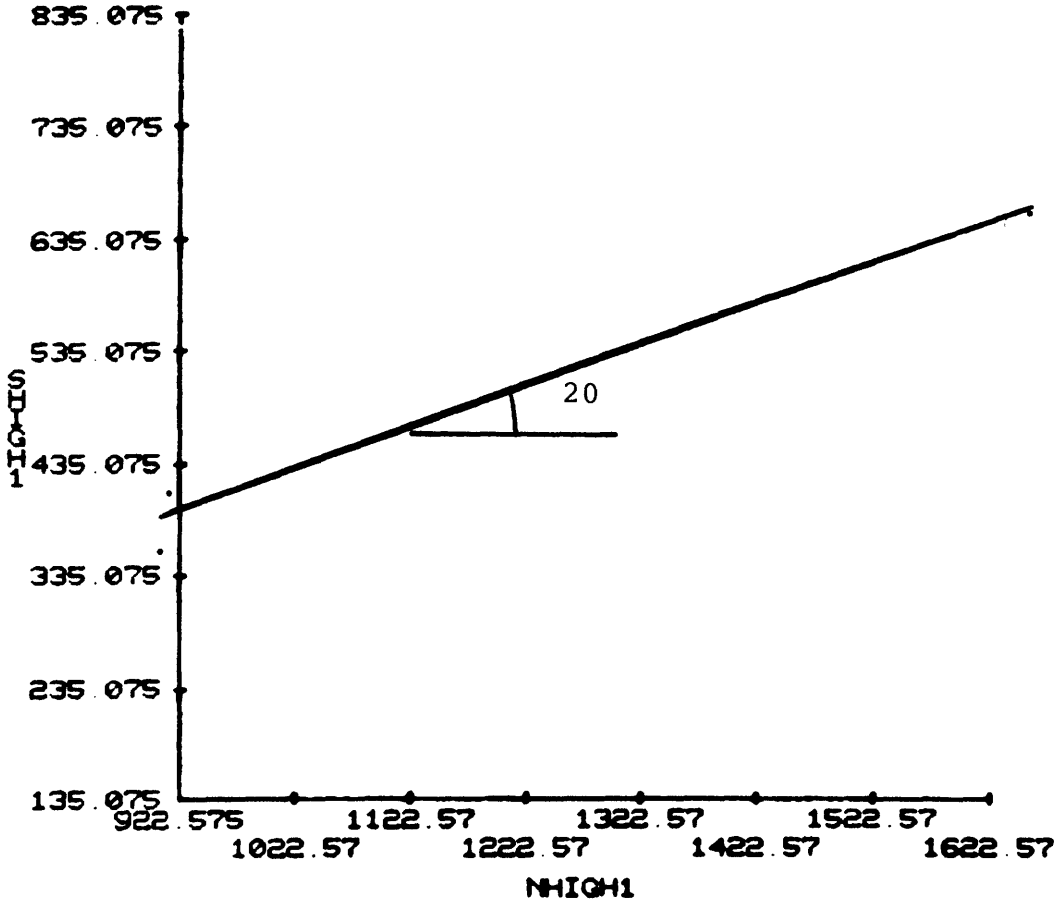

Figure C-41 Peak friction angle of schist (calcarous) for normal stress below 2 MN/m^2

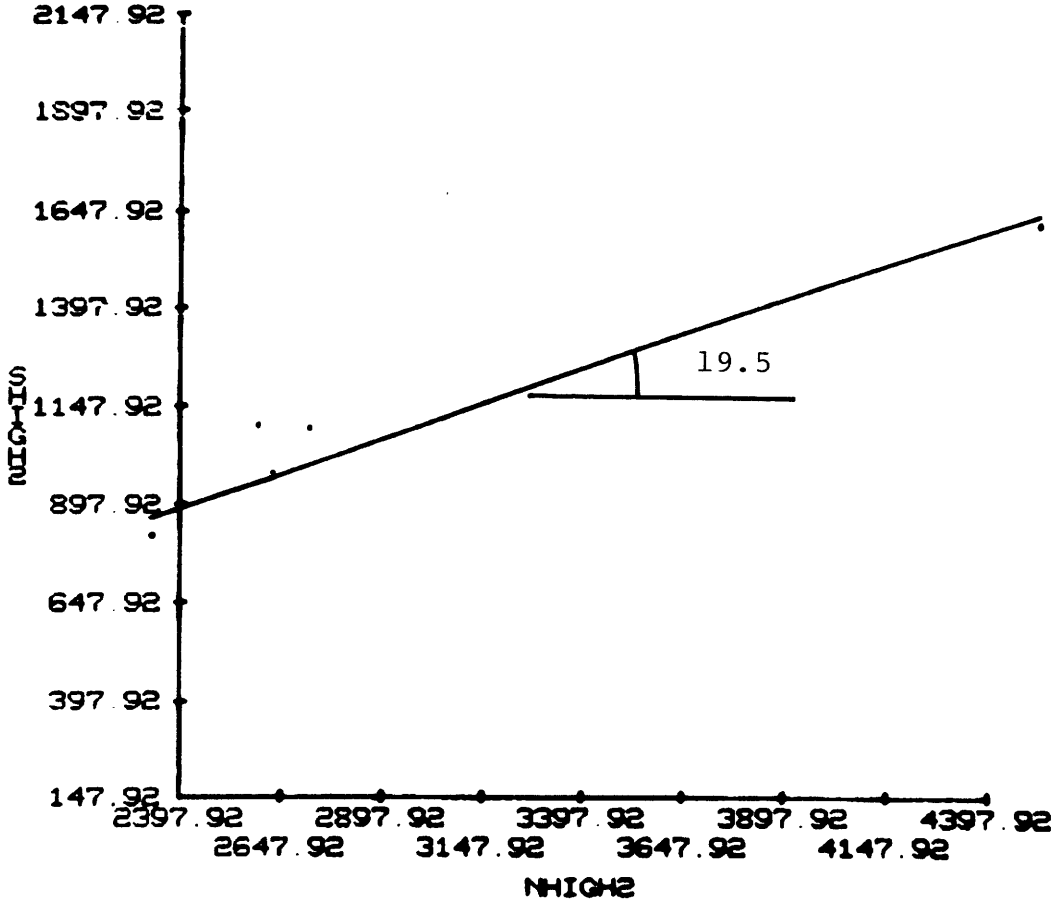

Figure C-42 Peak friction angle of schist (calcarous) for normal stress above 2 MN/m^2

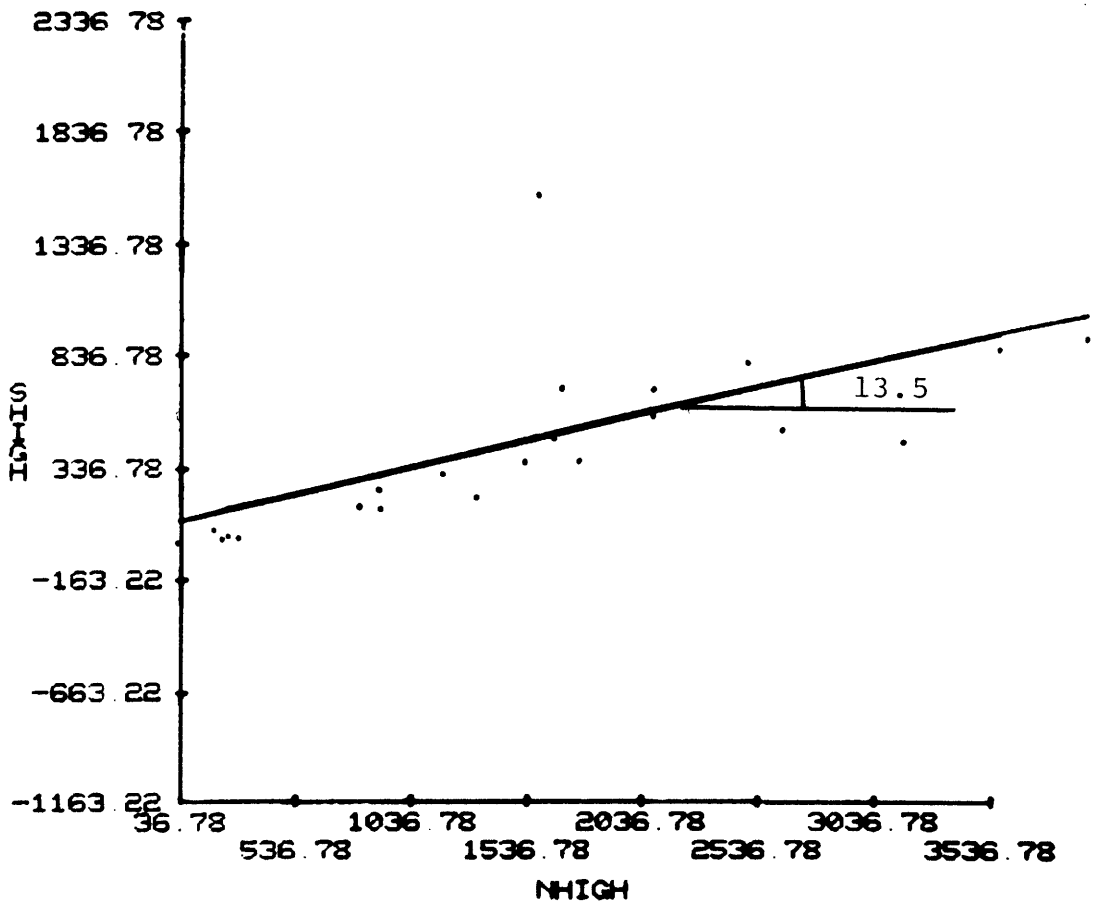

Figure C-43 Peak friction angle of schist (sericite) for all normal stress levels

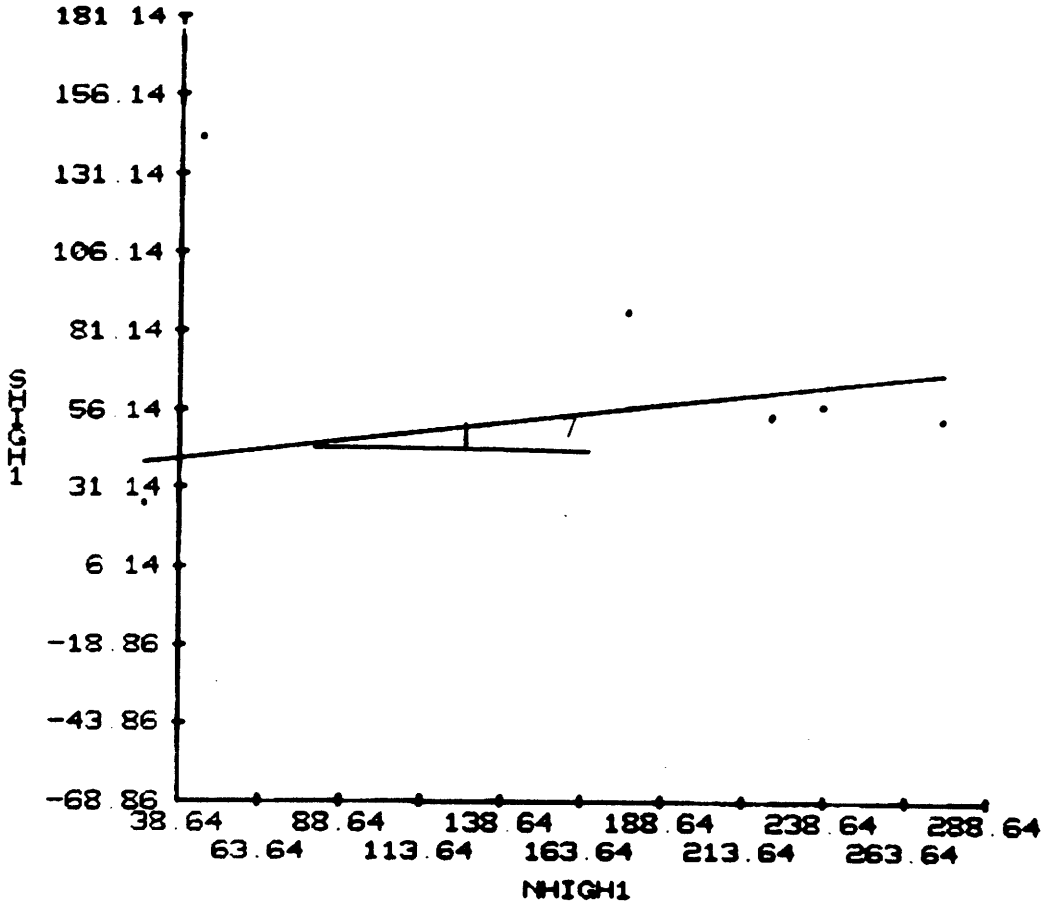

Figure C-44 Peak friction angle of schist (sericite) for normal stress below 0.3 MN/m^2

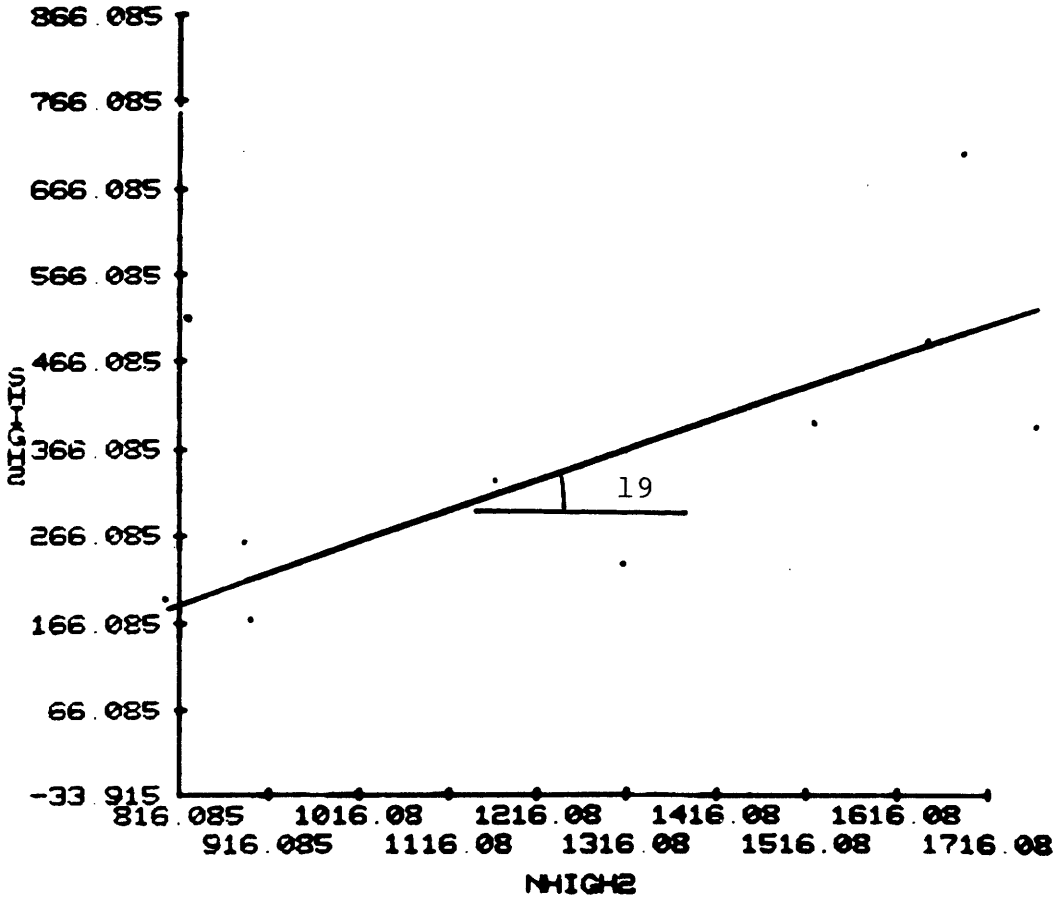

Figure C-45 Peak friction angle of schist (sericite) for normal stress between 0.3 and 2 MN/m^2

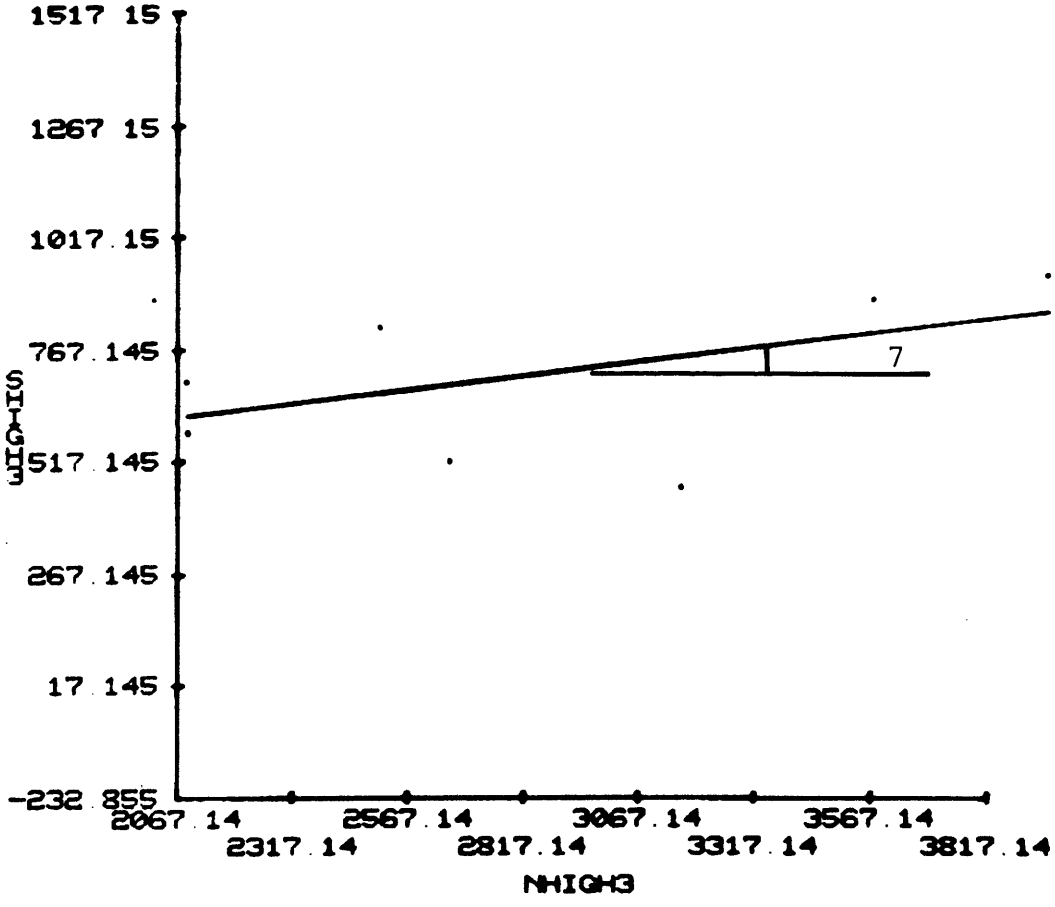

Figure C-46 Peak friction angle of schist (sericite) for normal stress above 2 MN/m^2

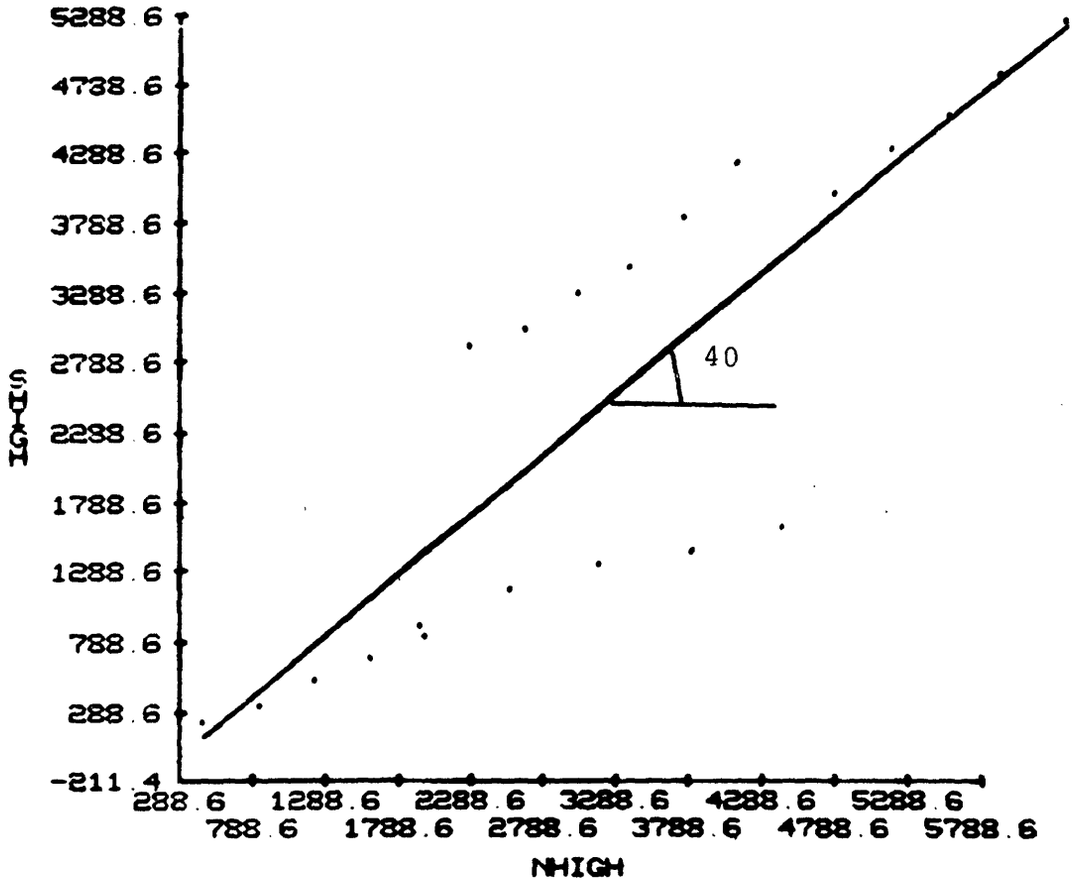

Figure C-47 Peak friction angle of basalt for all normal stress levels

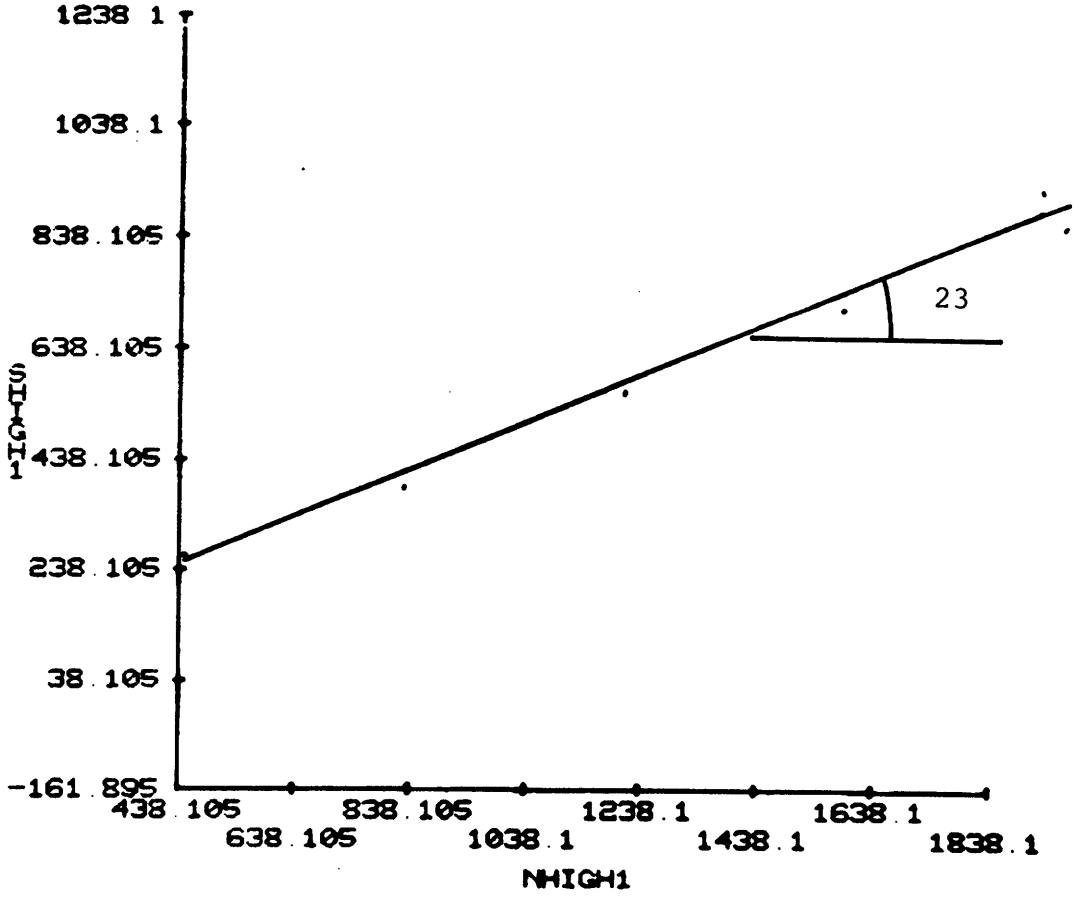

Figure C-48 Peak friction angle of basalt for normal stress below 2 MN/m^2

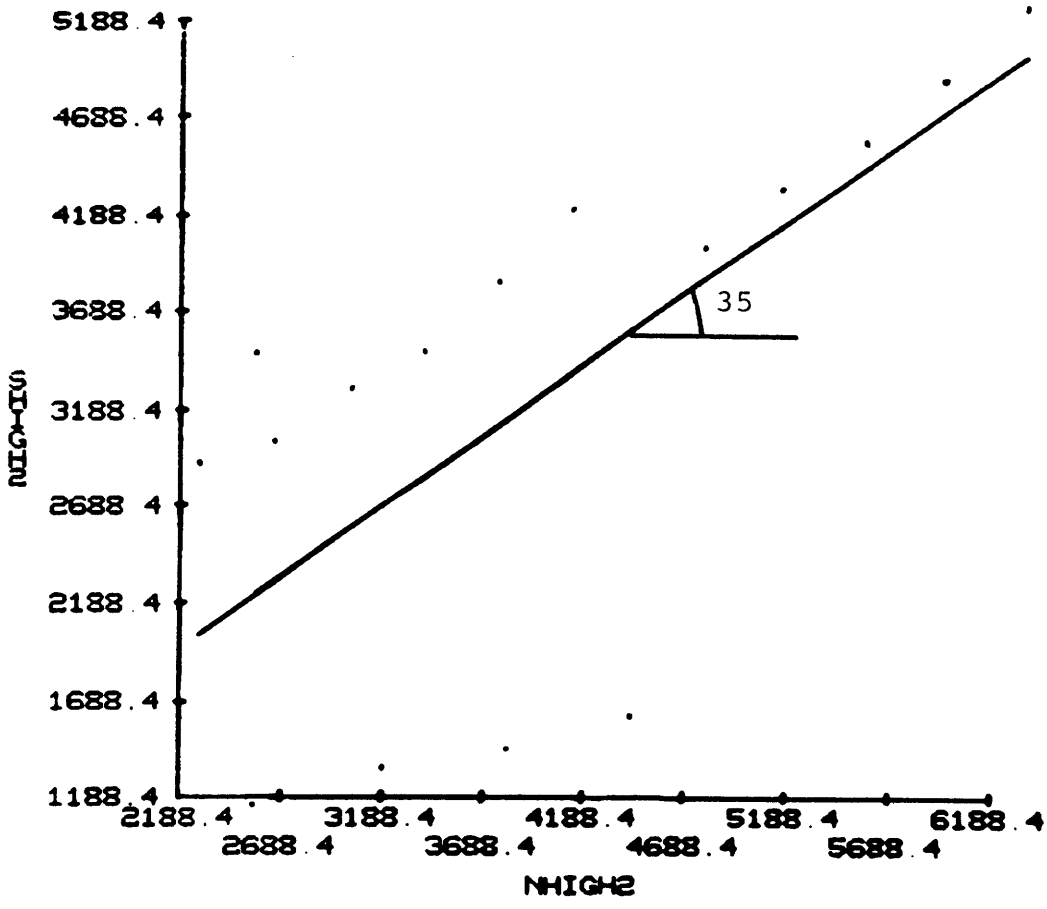

Figure C-49 Peak friction angle of basalt for normal stress above 2 MN/m^2

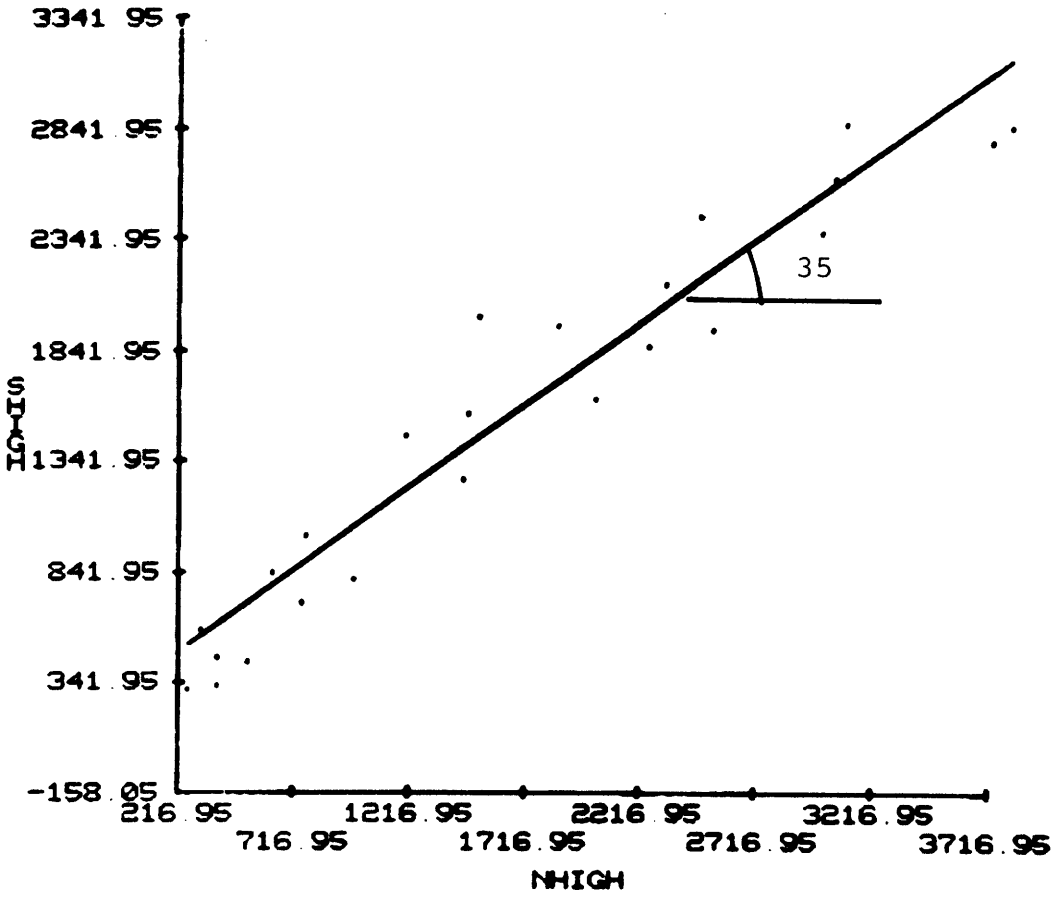

Figure C-50 Peak friction angle of dacite for all normal stress levels

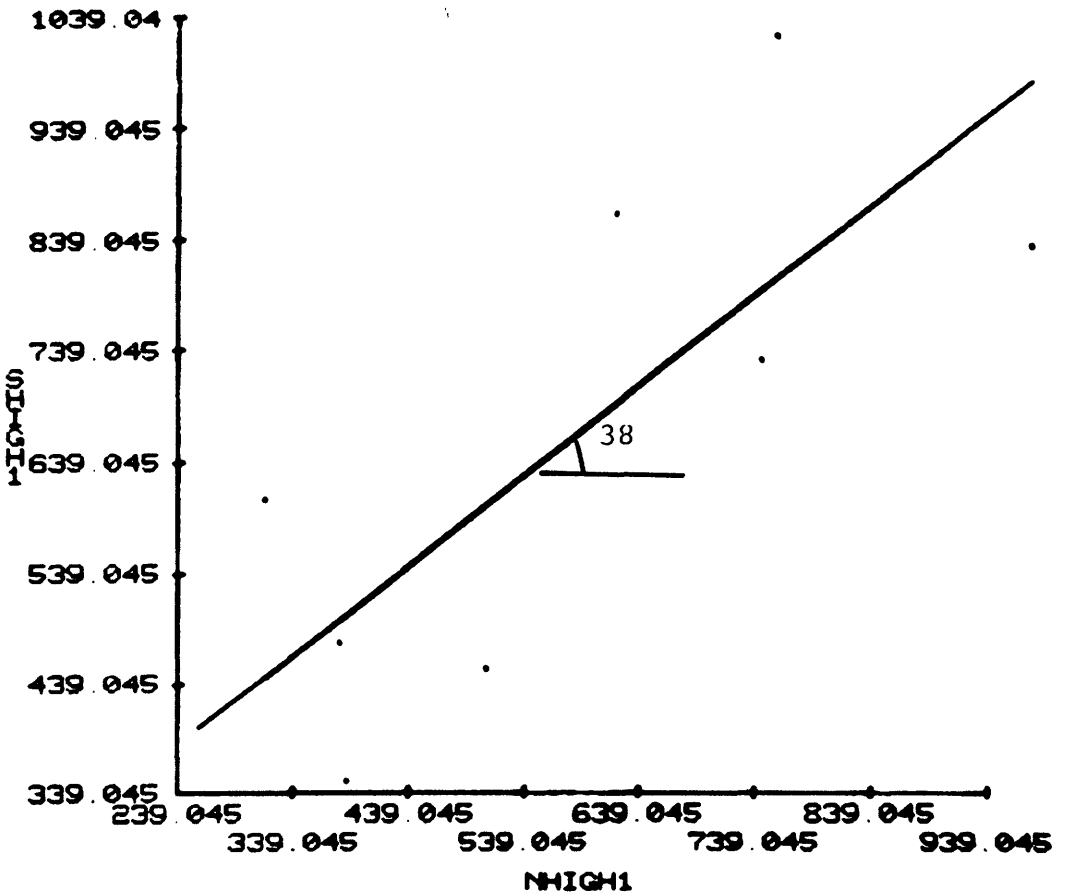

Figure C-51 Peak friction angle of dacite for normal stress below 1 MN/m^2

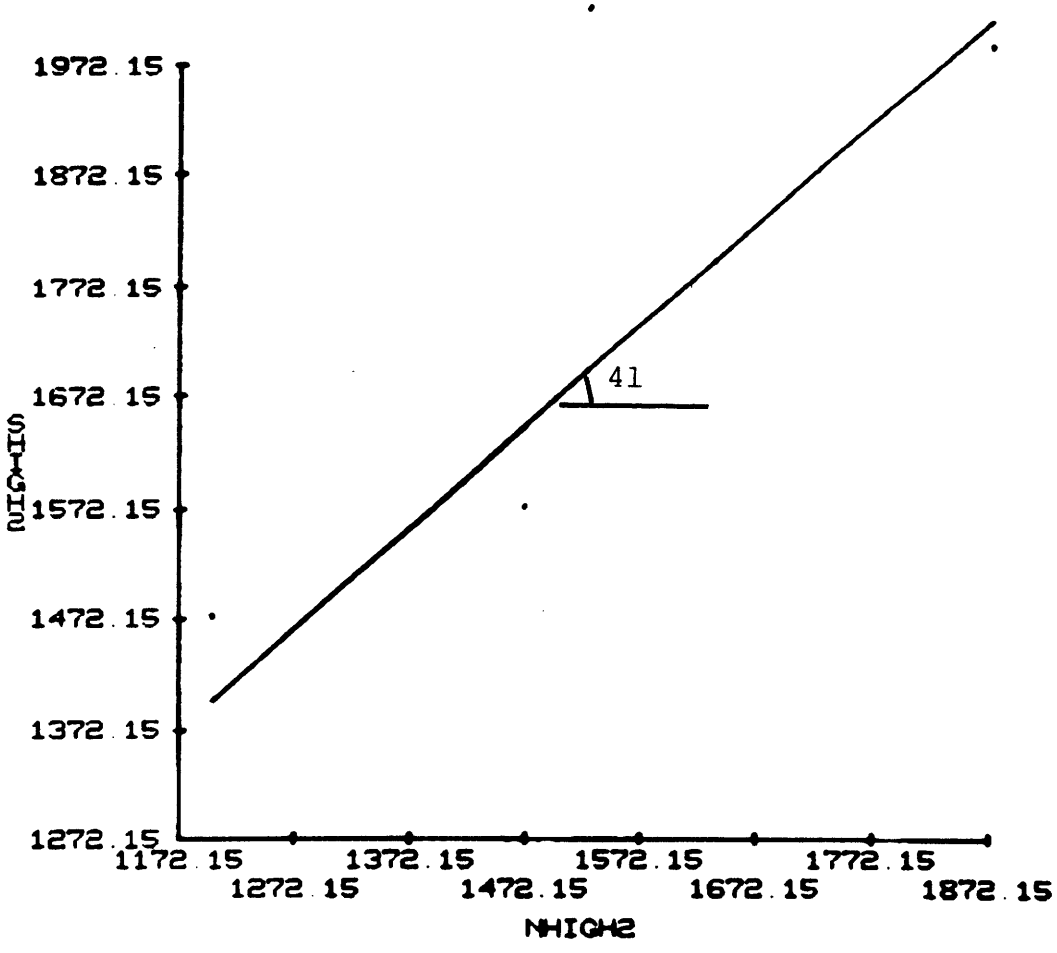

Figure C-52 Peak friction angle of dacite for normal stress between 1 and 2 MN/m^2

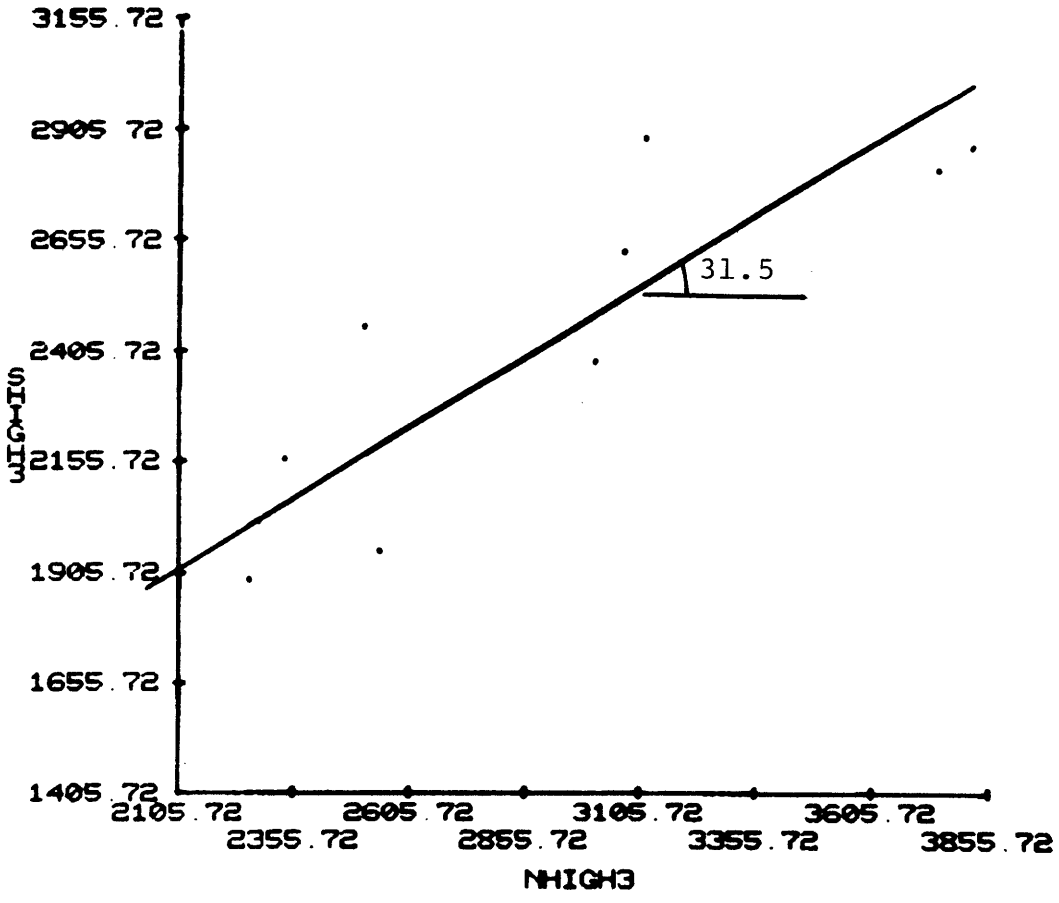

Figure C-53 Peak friction angle of dacite for normal stress above 2 MN/m^2

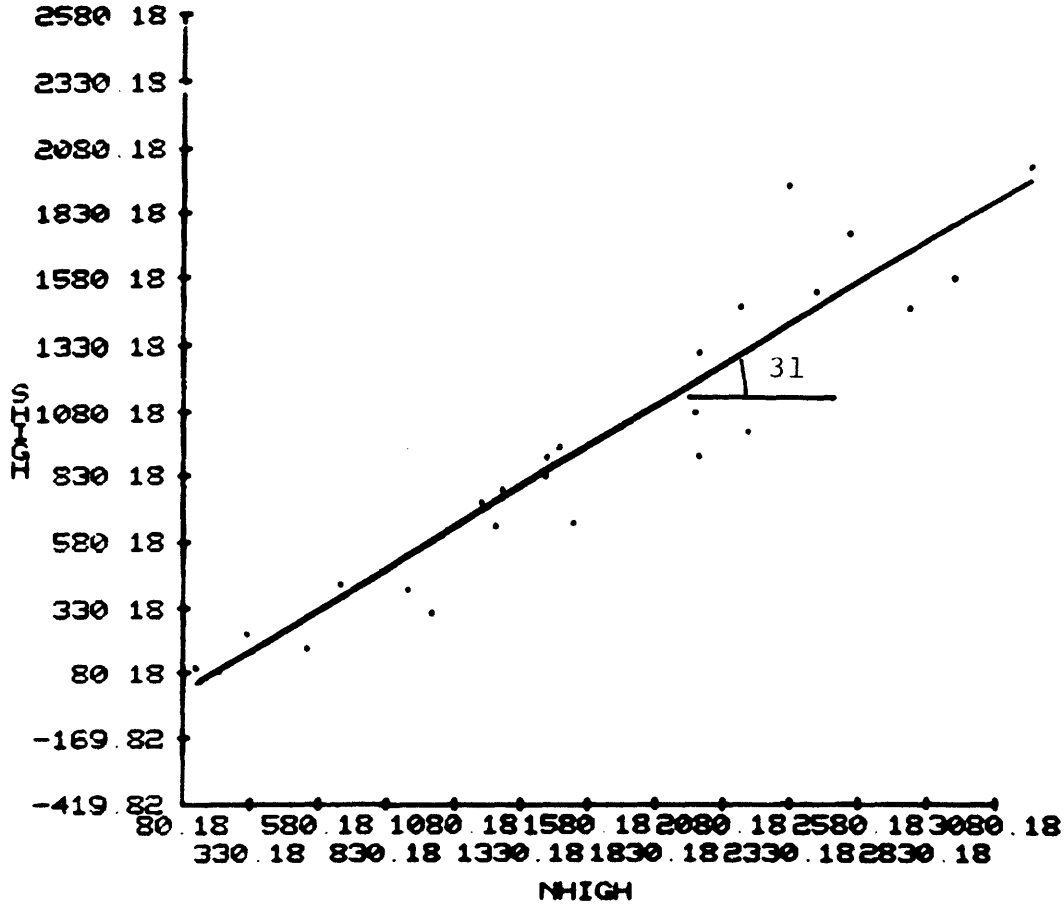

Figure C-54 Peak friction angle of porphyry (quarzite) for all normal stress levels

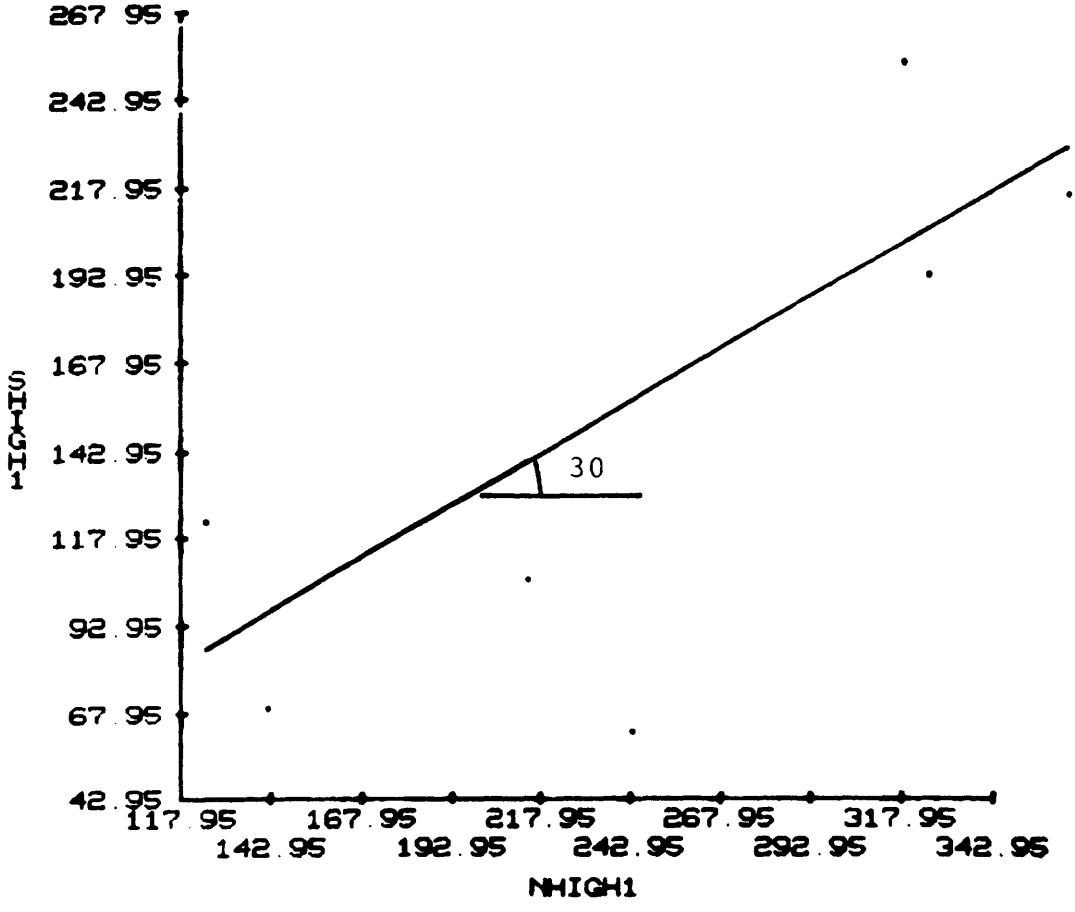

Figure C-55 Peak friction angle of porphy (quarzite) for normal stress below 0.5 MN/m^2

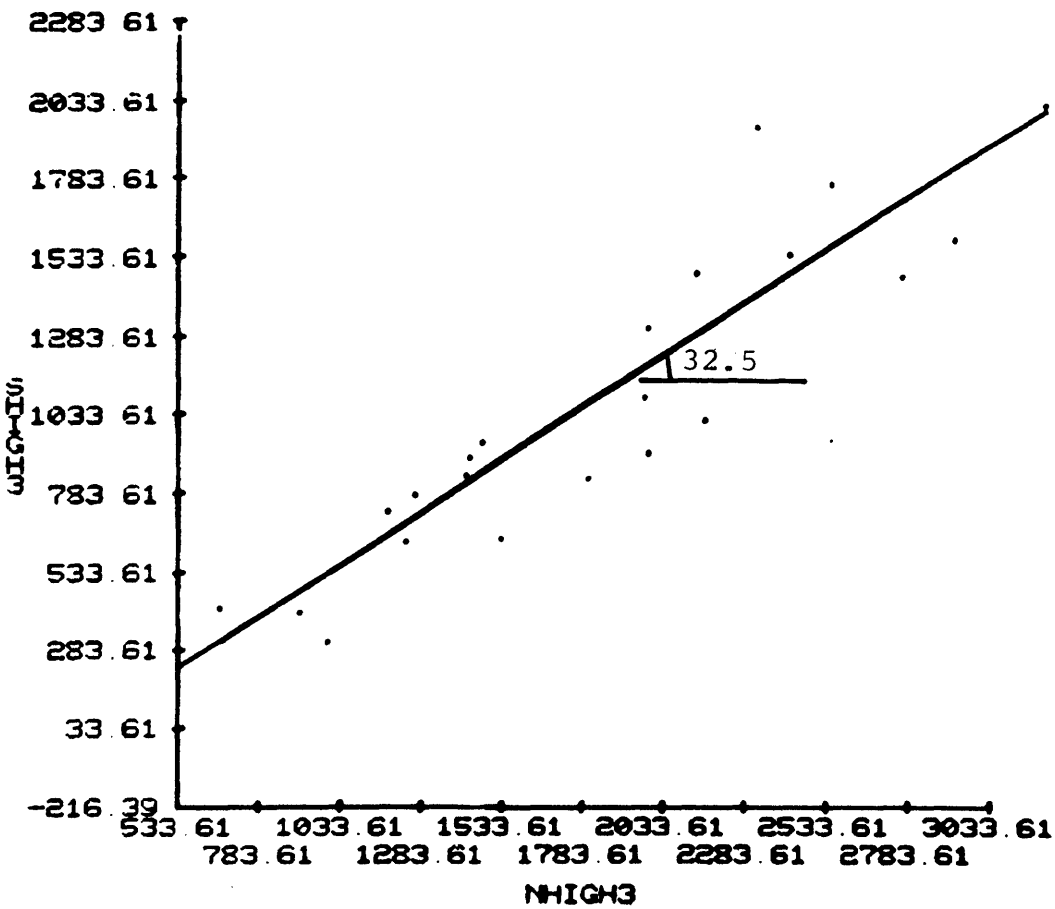

Figure C-56 Peak friction angle of porphyry (quarzite) for normal stress above 0.5 MN/m^2

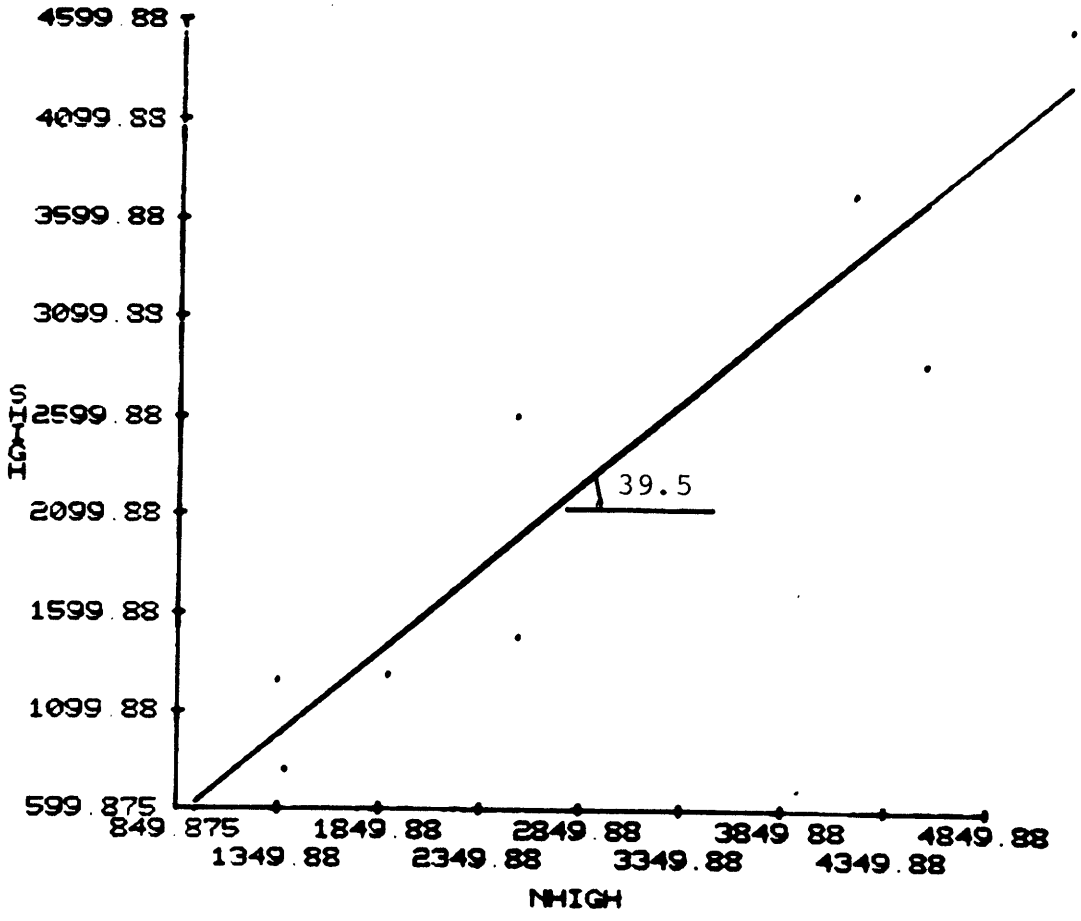

Figure C-57 Peak friction angle of granite for all normal stress levels

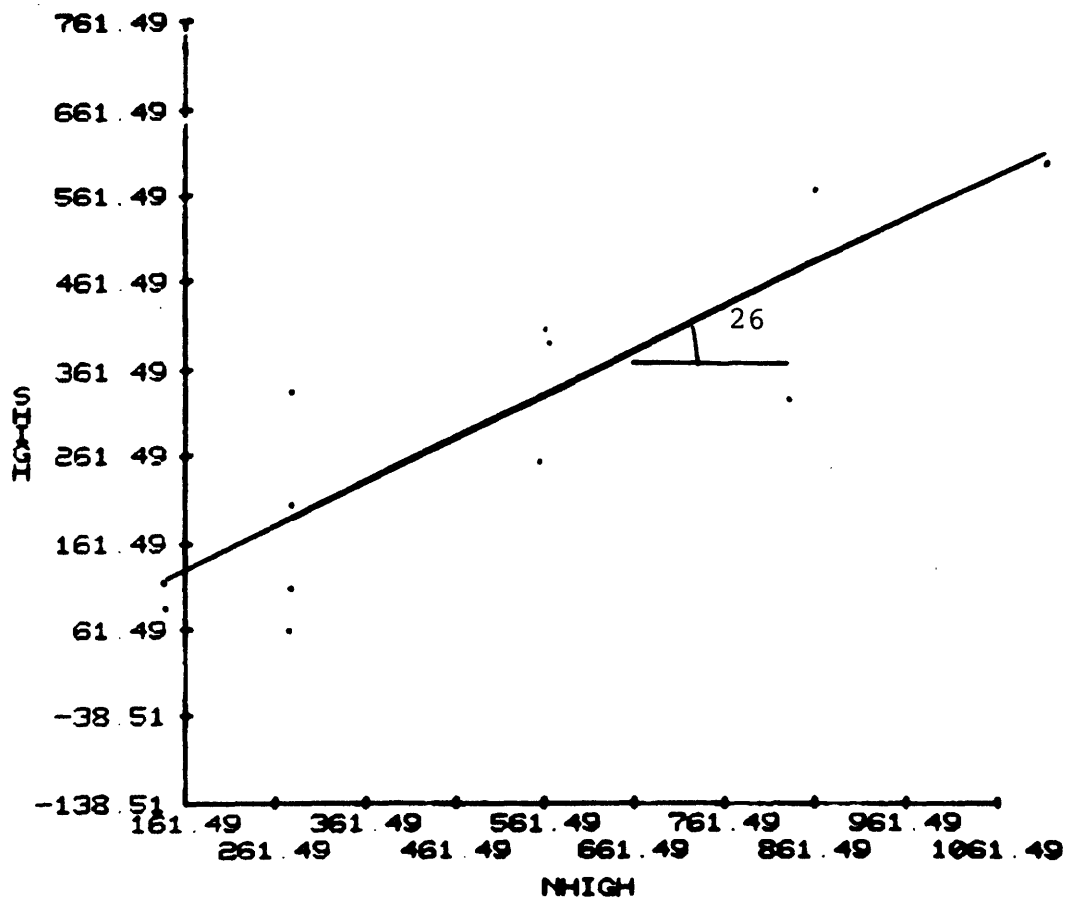

Figure C-58 Peak friction angle of claystone for all normal stress levels

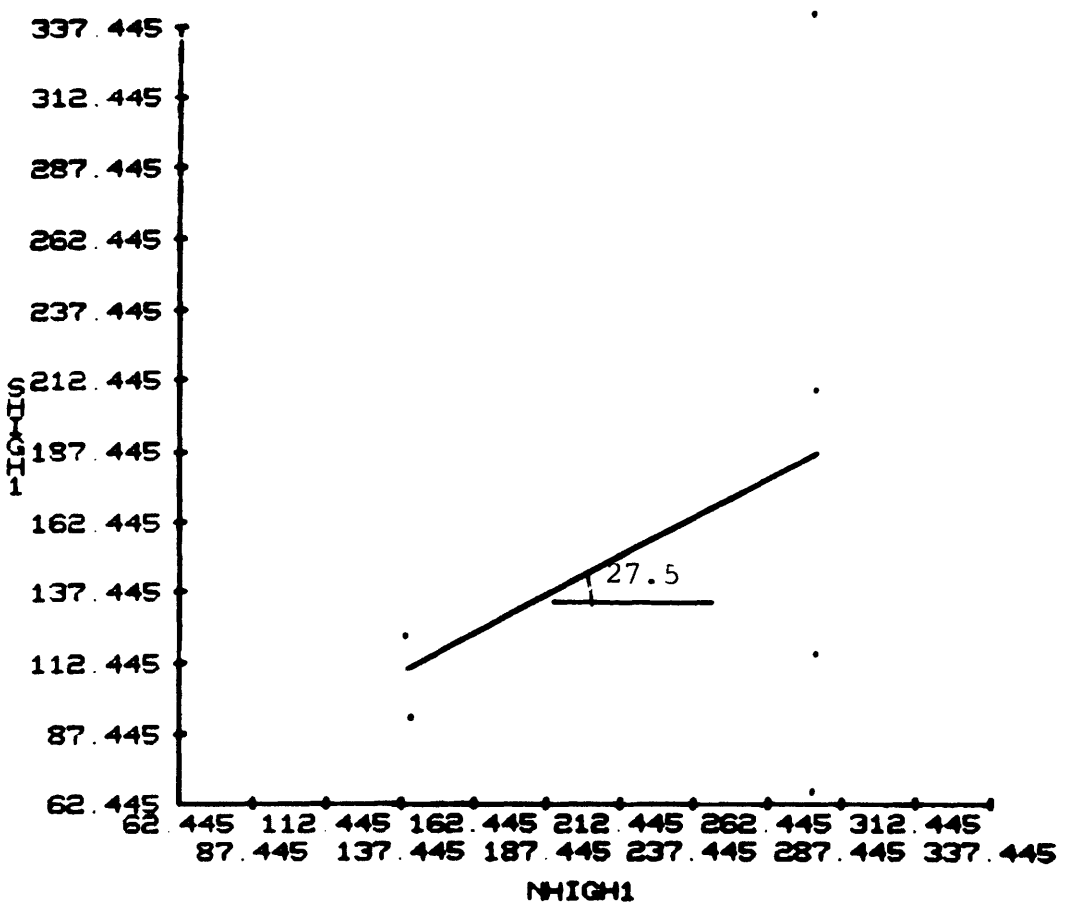

Figure C-59 Peak friction angle of claystone for nformal stress below 0.3 MN/m^2

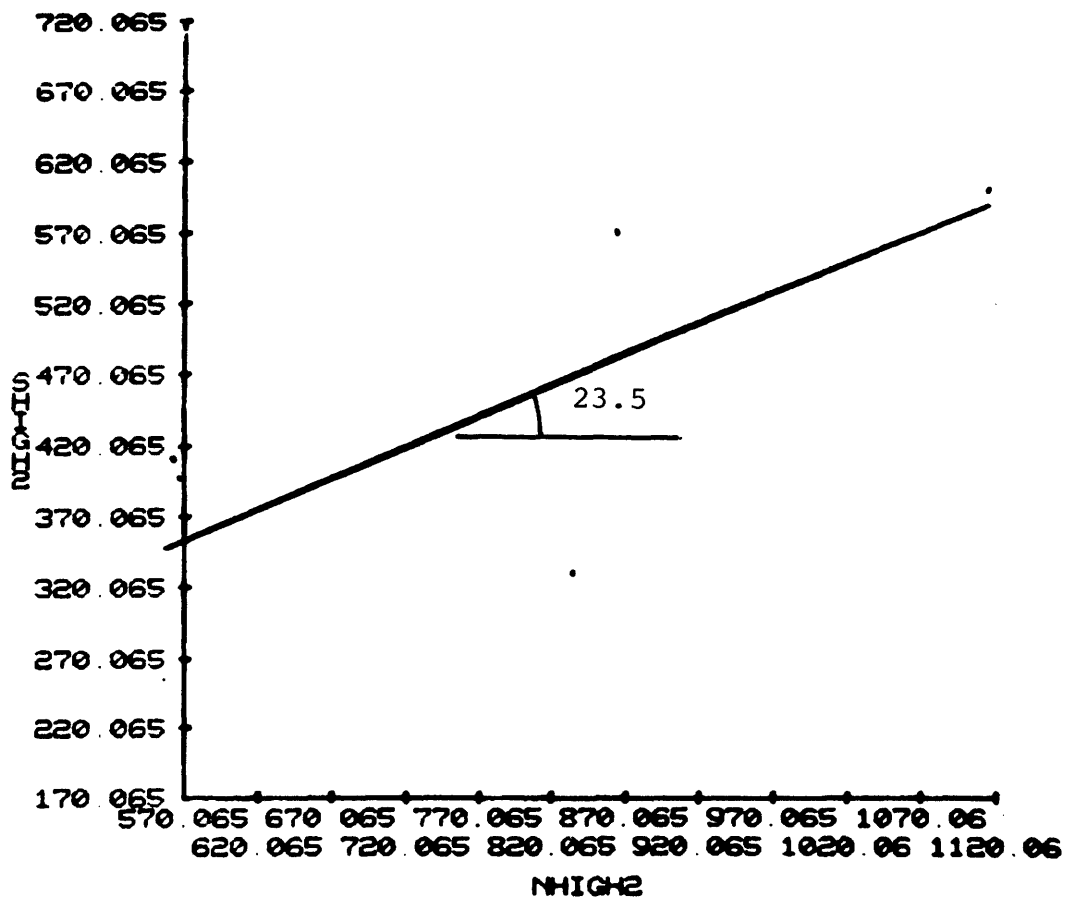

Figure C-60 Peak friction angle of claystone for normal stress above 0.3 MN/m^2

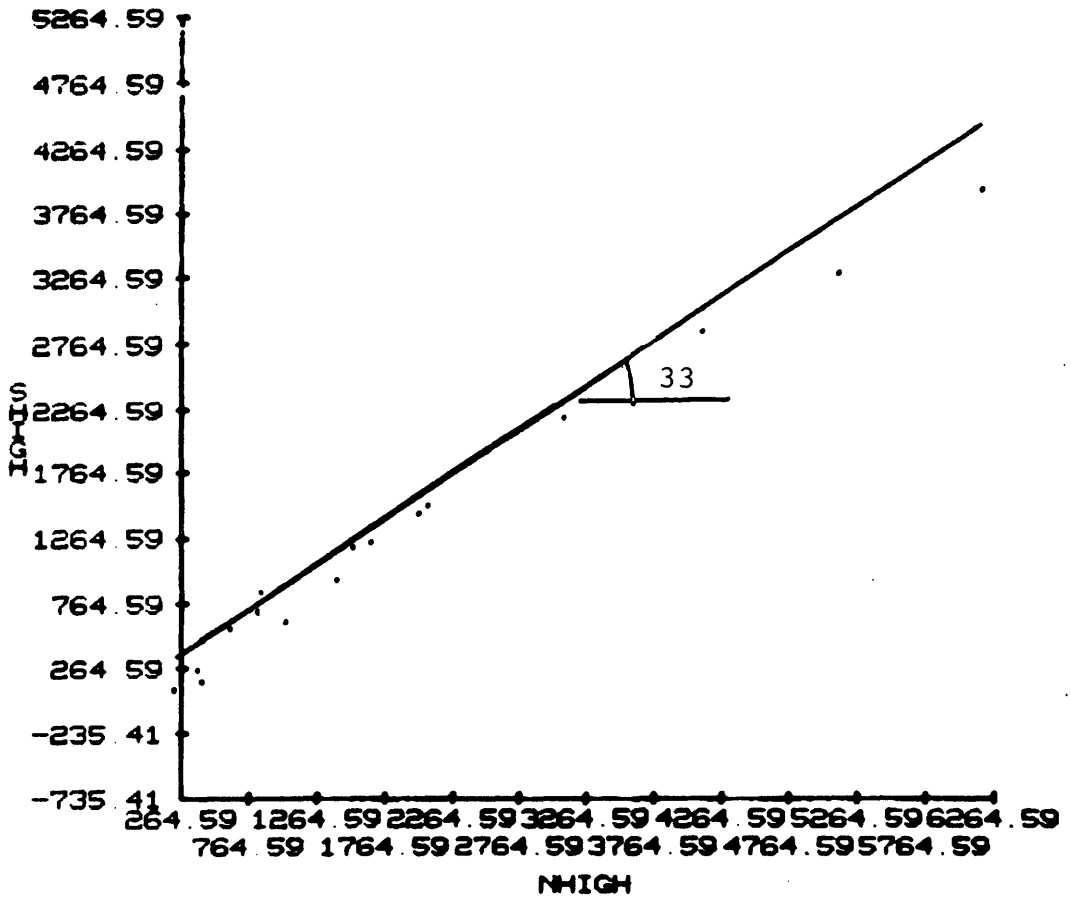

Figure C-61 Peak friction angle of monzonite (quarz) for all normal stress levels

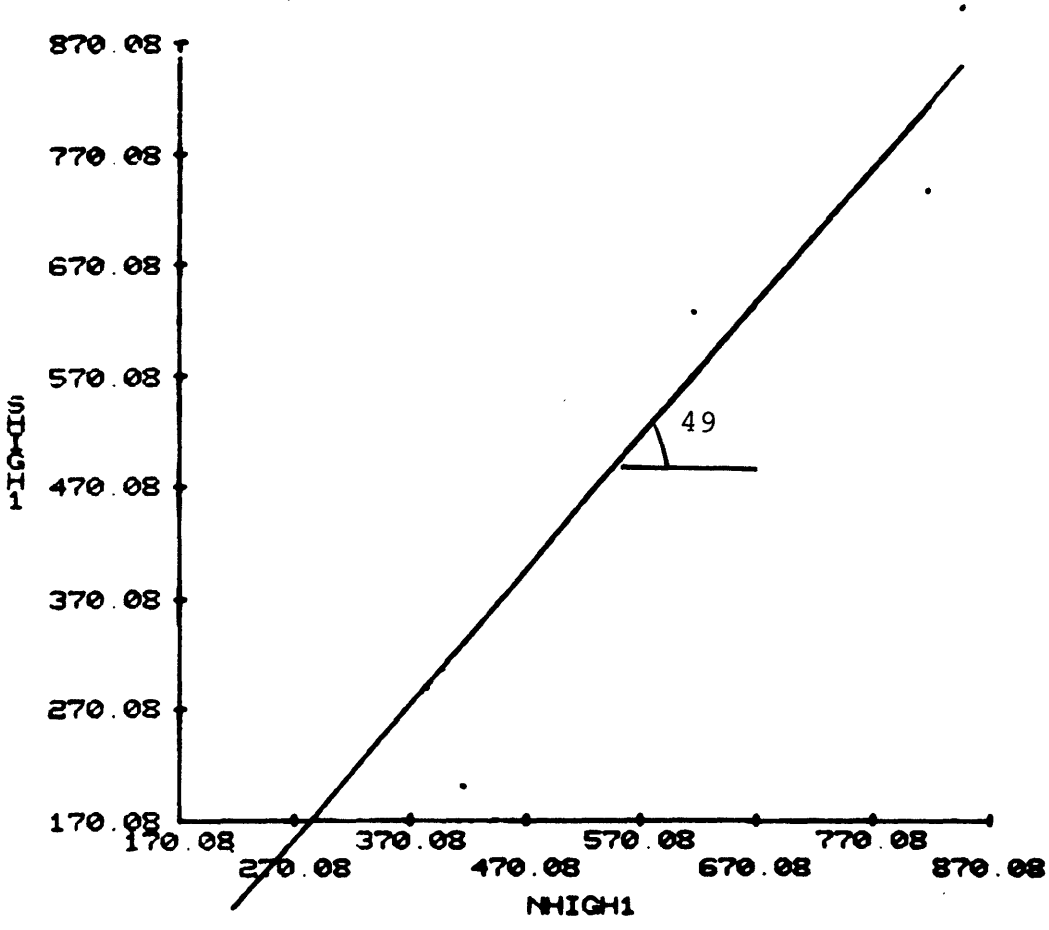

Figure C-62 Peak friction angle of monzonite (quarz) for normal stress below 1 MN/m^2

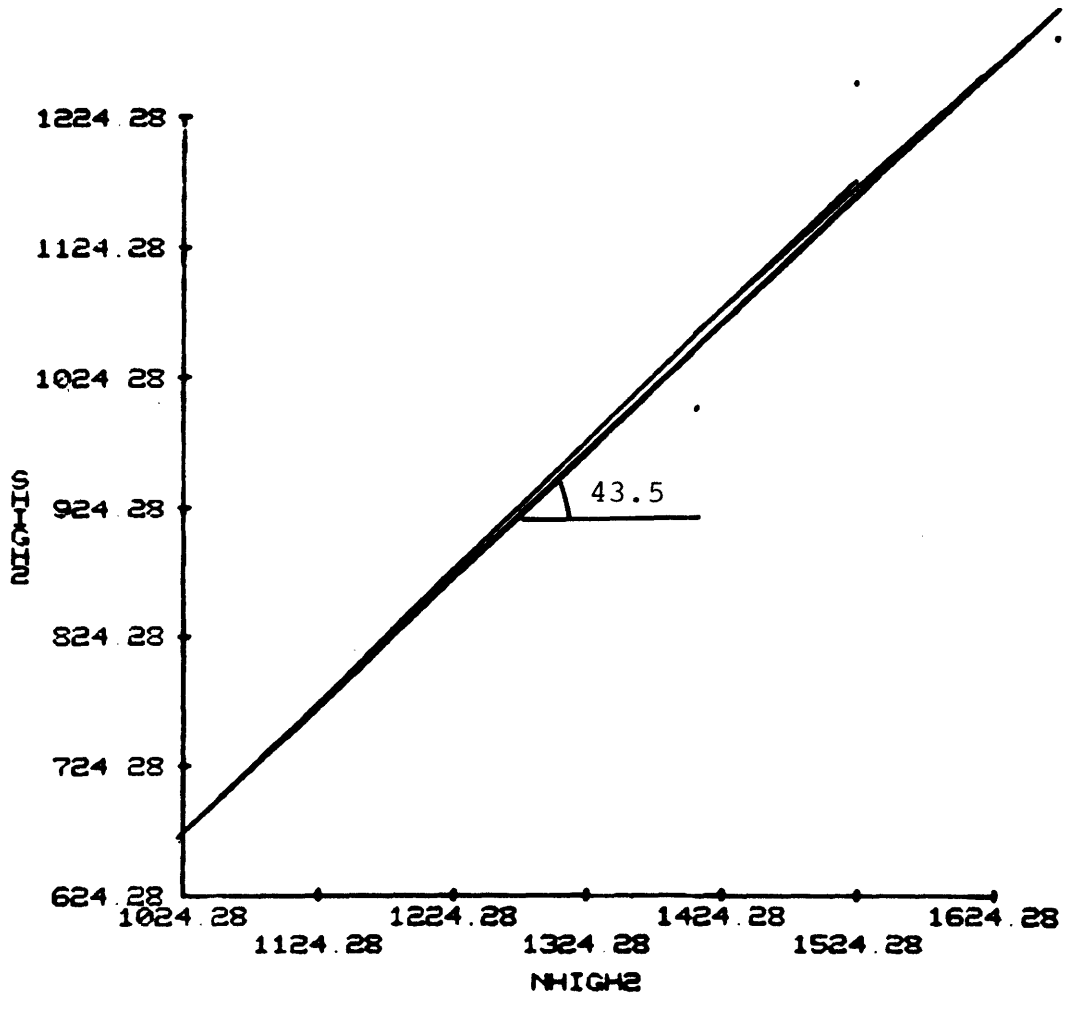

Figure C-63 Peak friction angle of monzonite (quarz) for normal stress between 1 and 2 MN/m^2

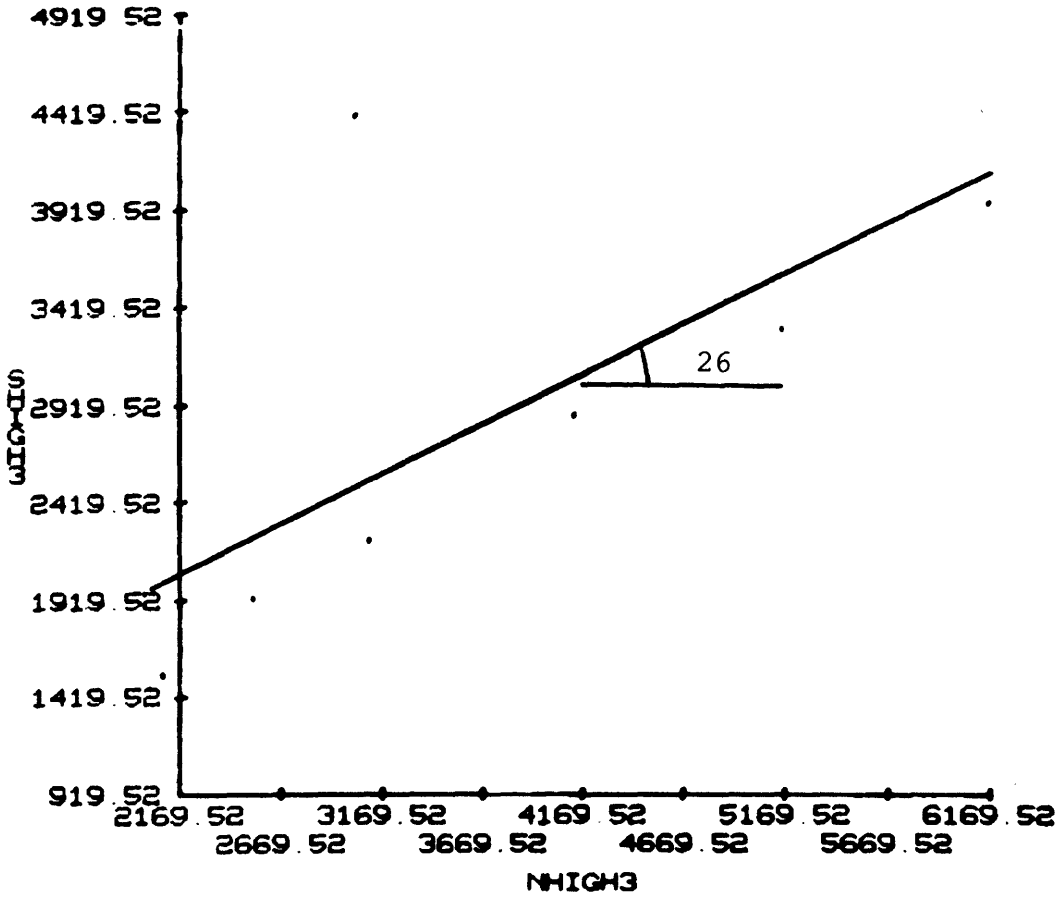

Figure C-64 Peak friction angle of monzonite (quarz) for normal stress above 2 MN/m^2

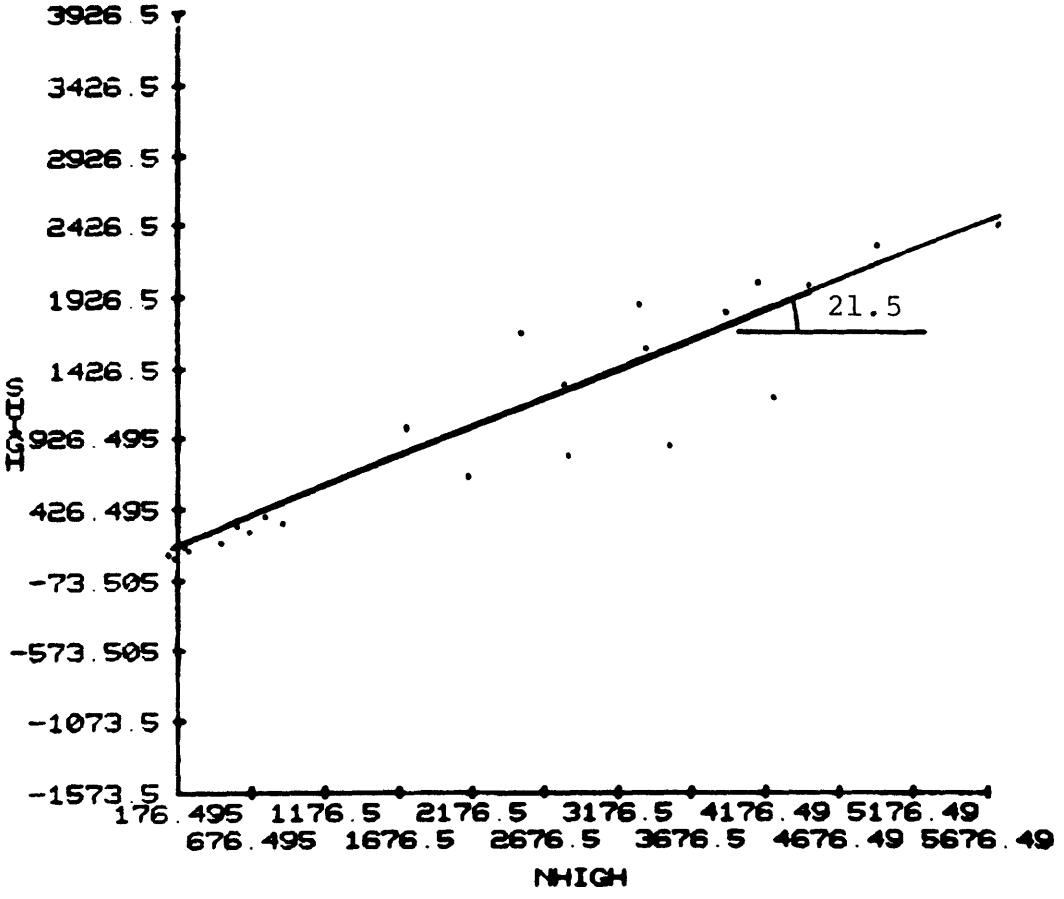

Figure C-65 Peak friction angle of tuff for all normal stress levels

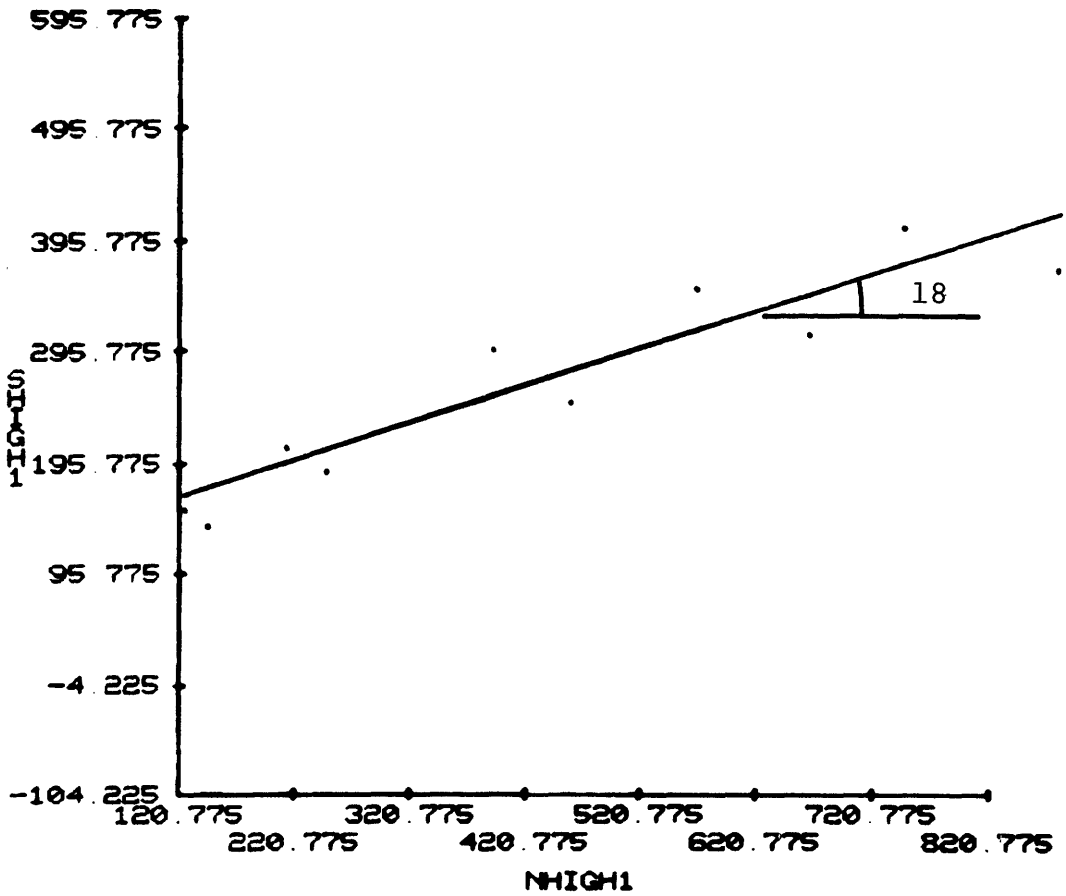

Figure C-66 Peak friction angle of tuff for normal stress below 1 MN/m^2

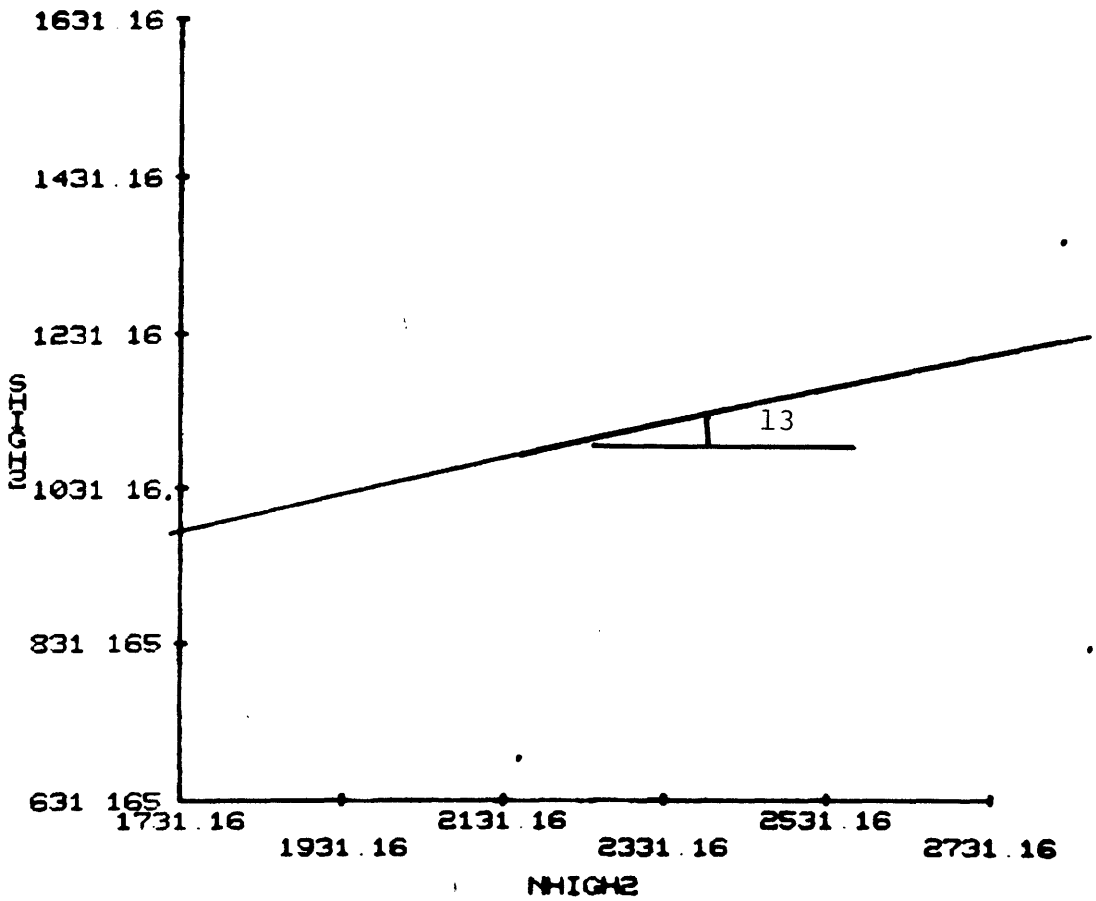

Figure C-67 Peak friction angle of tuff for normal stressbetween 1 and 3 MN/m^2

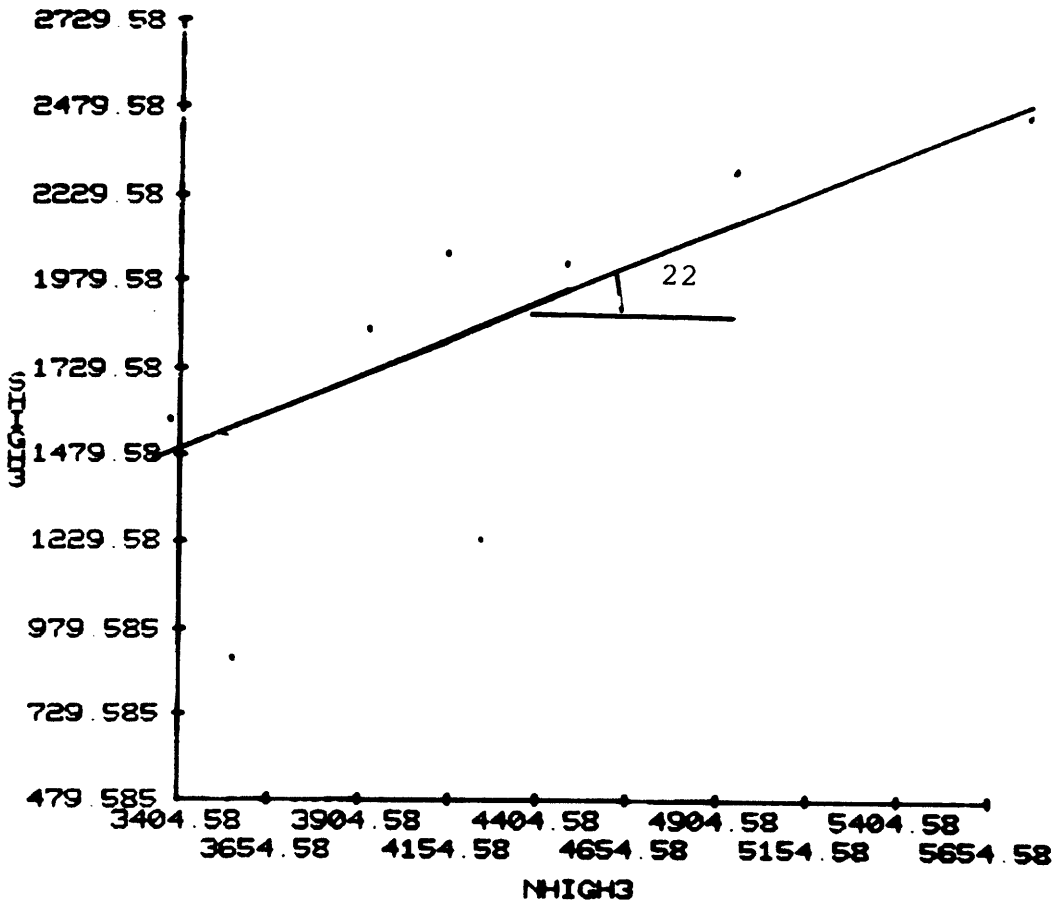

Figure C-68 Peak friction angle of tuff for normal stress above 3 MN/m^2

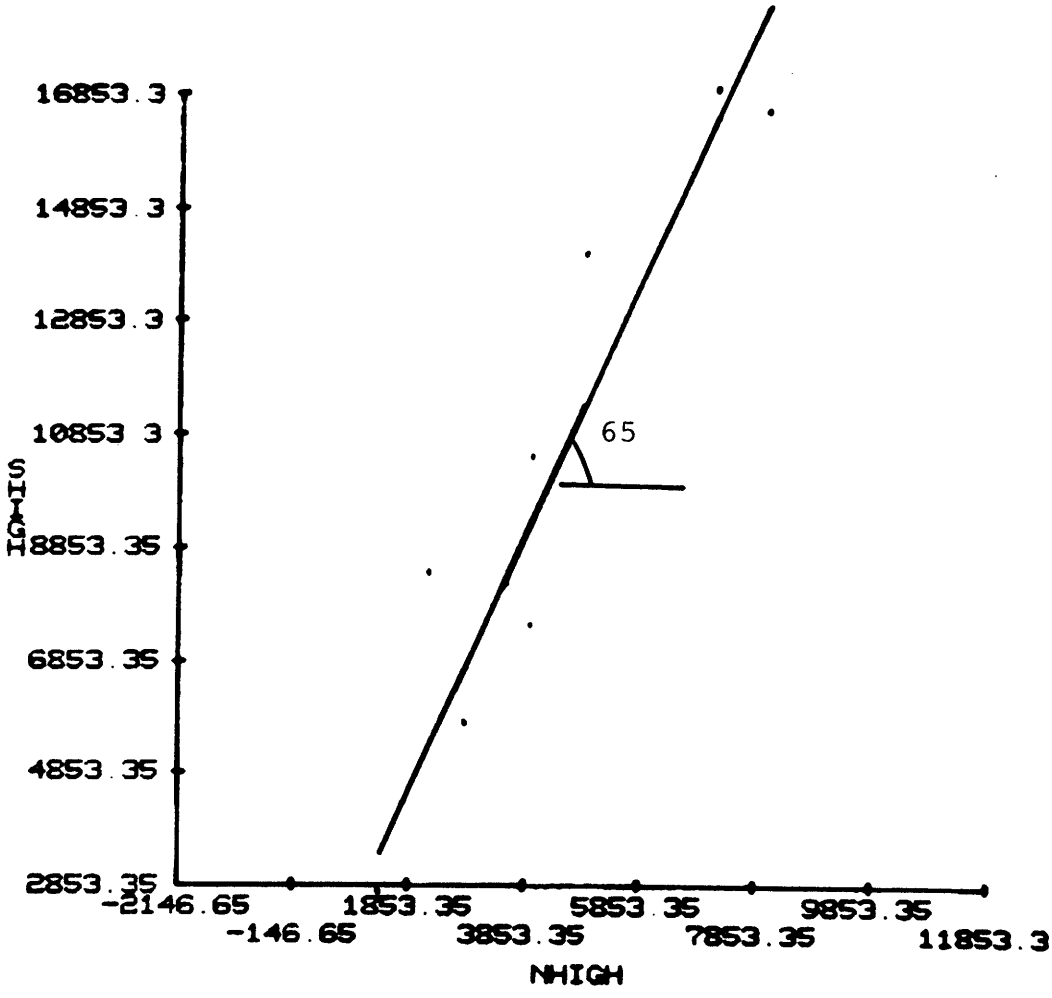

Figure C-69 Peak friction angle of metashale for all normal stress levels

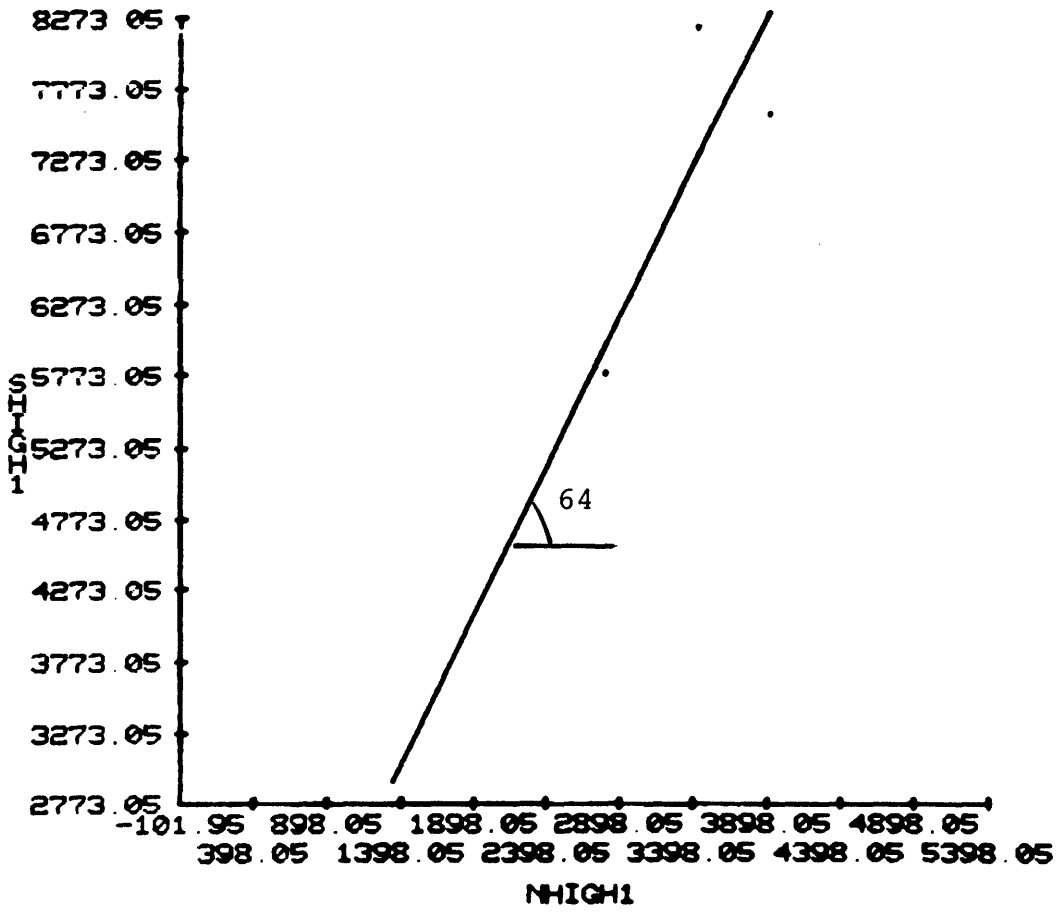

Figure C-70 Peak friction angle of metashale for normal stress below 4 MN/m^2

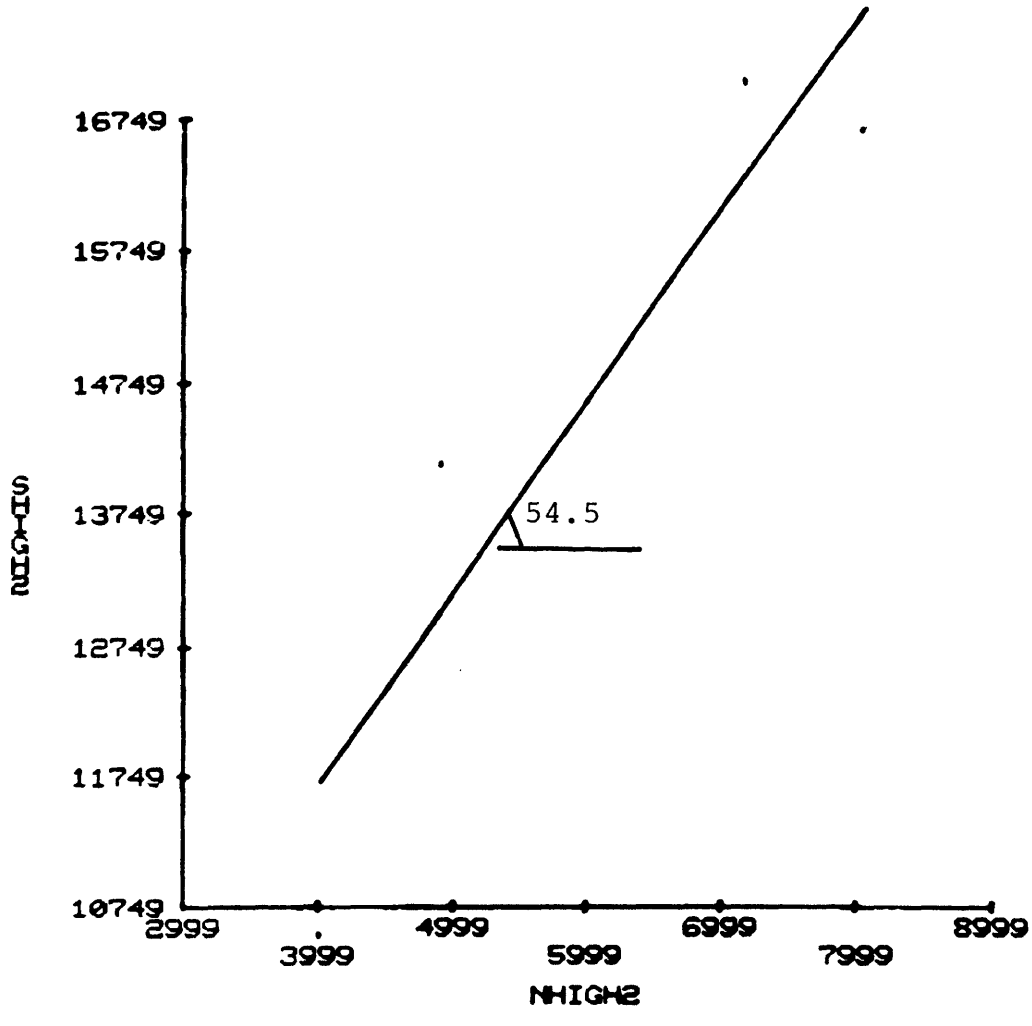

Figure C-71 Peak friction angle of metashale for normal stress above 4 MN/m^2

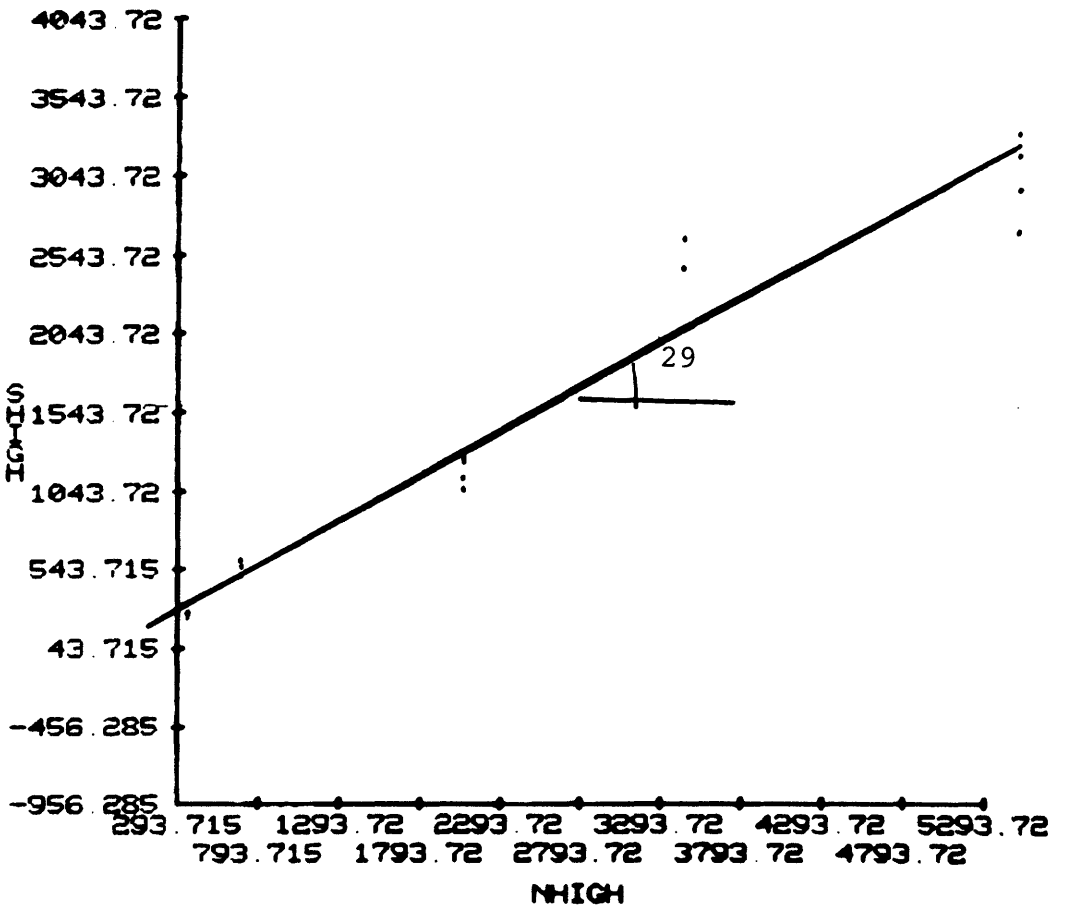

Figure C-72 Peak friction angle for micro-granodiorite for all normal stress levels

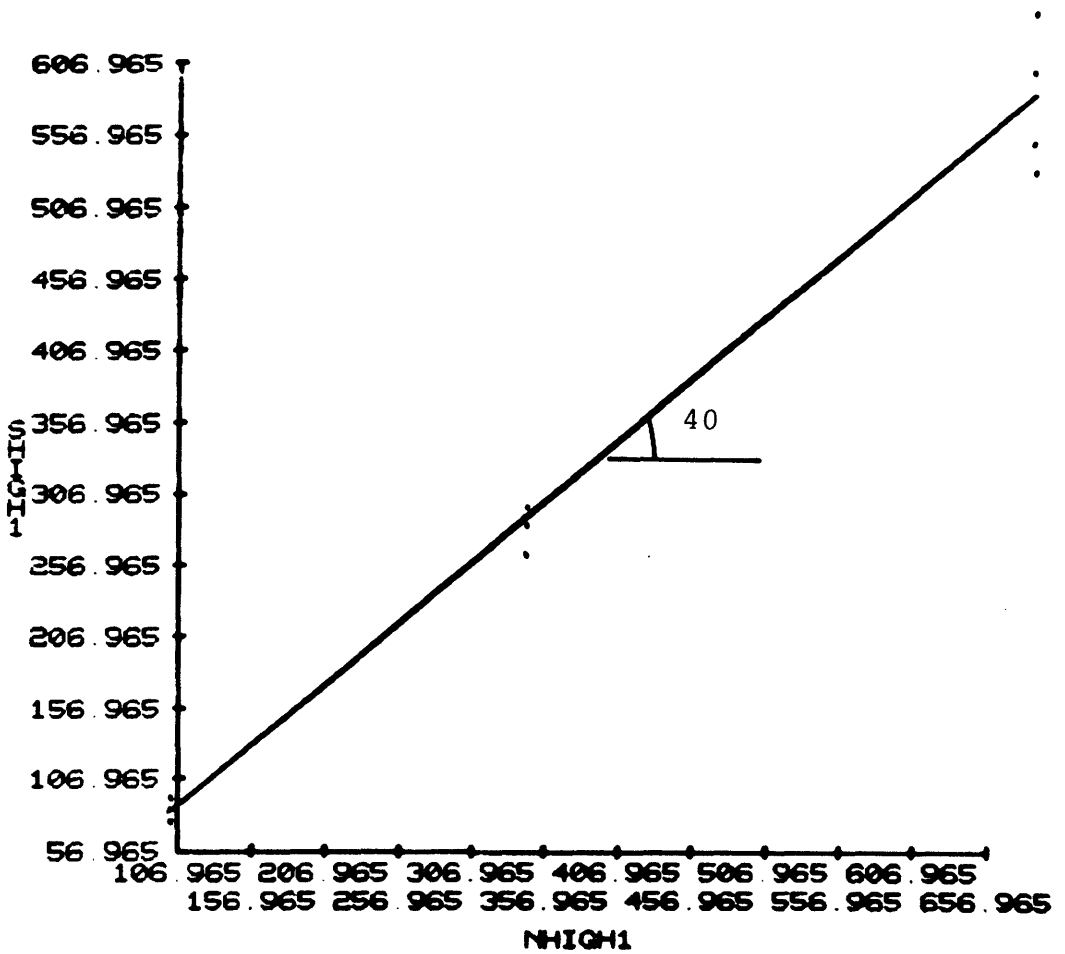

Figure C-73 Peak friction angle of micro-granodiorite for normal stress below 1 MN/m2

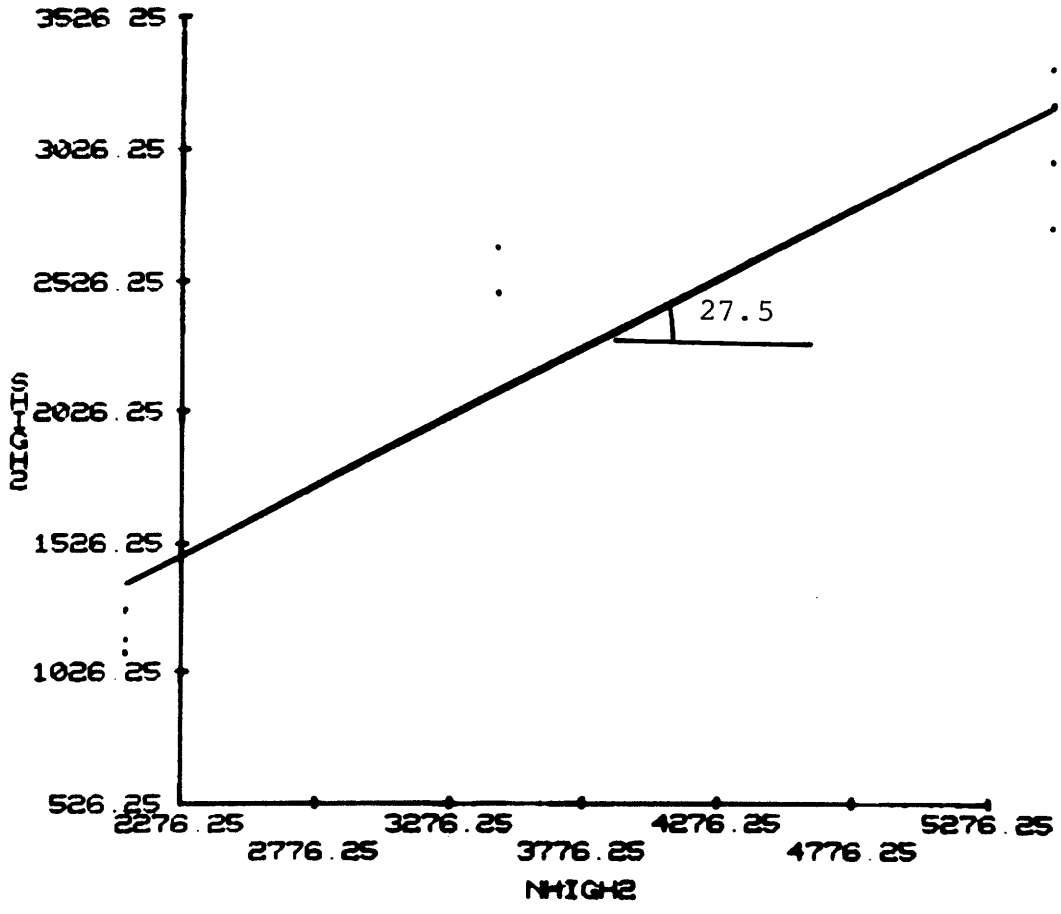

Figure C-74 Peak friction angle of micro-granodiorite for normal stress above 1 MN/m^2

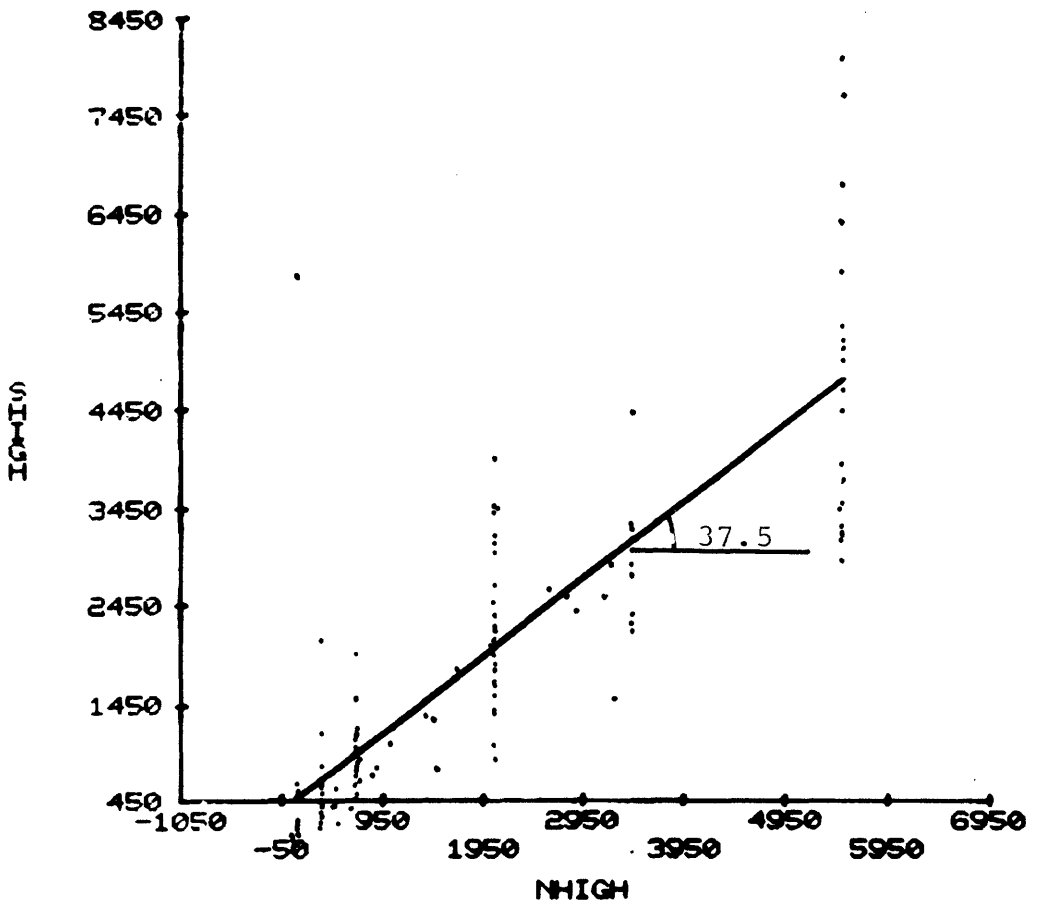

Figure C-75 Peak friction angle of monzonite for all normal stress levels

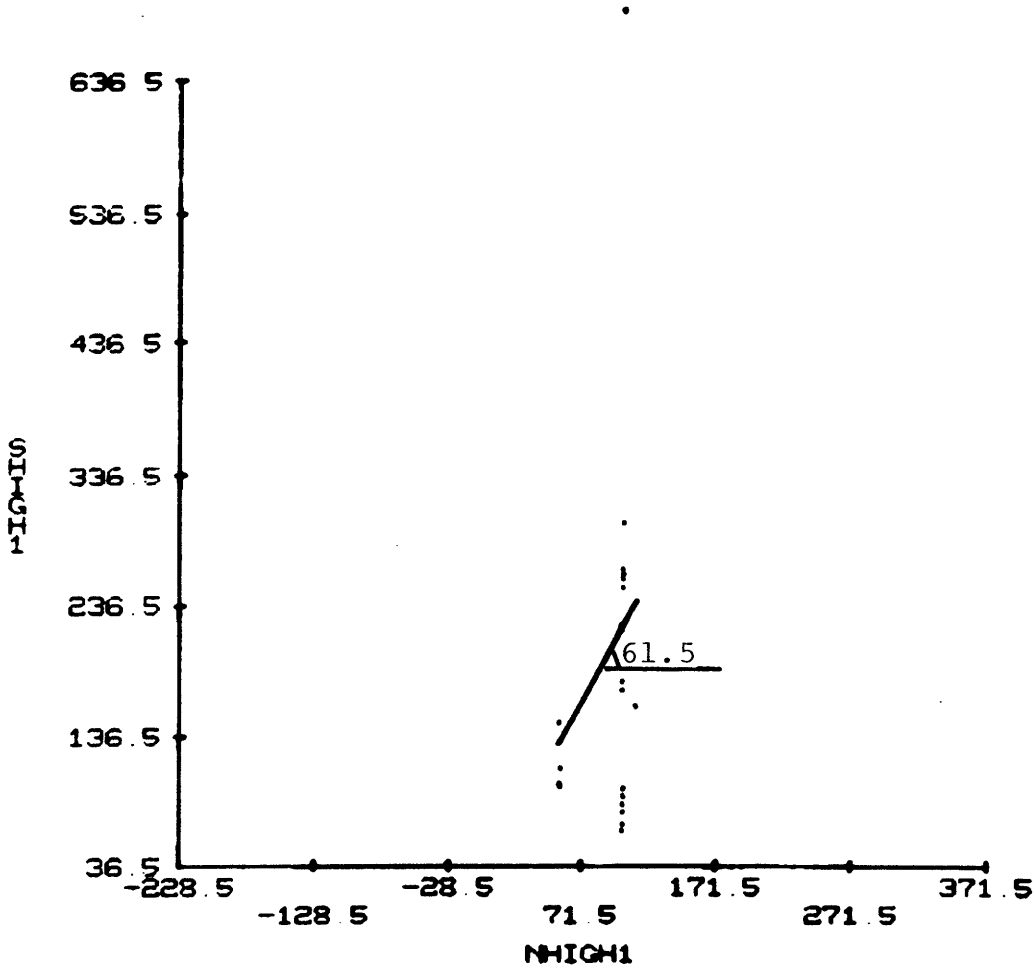

Figure C-76 Peak friction angle of monzonite for normal stress below 0.2 MN/m^2

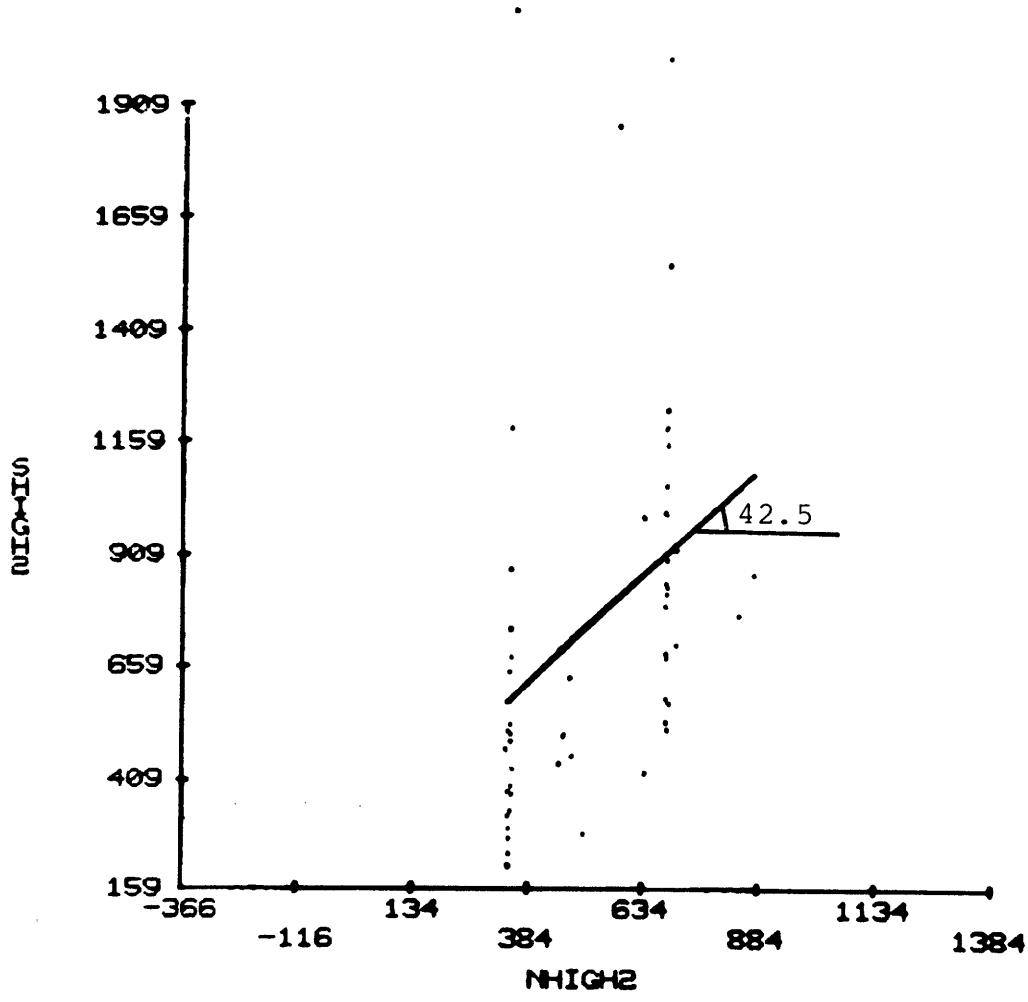

Figure C-77 Peak friction angle of monzonite for normal stress between 0.3 and 1 MN/m^2

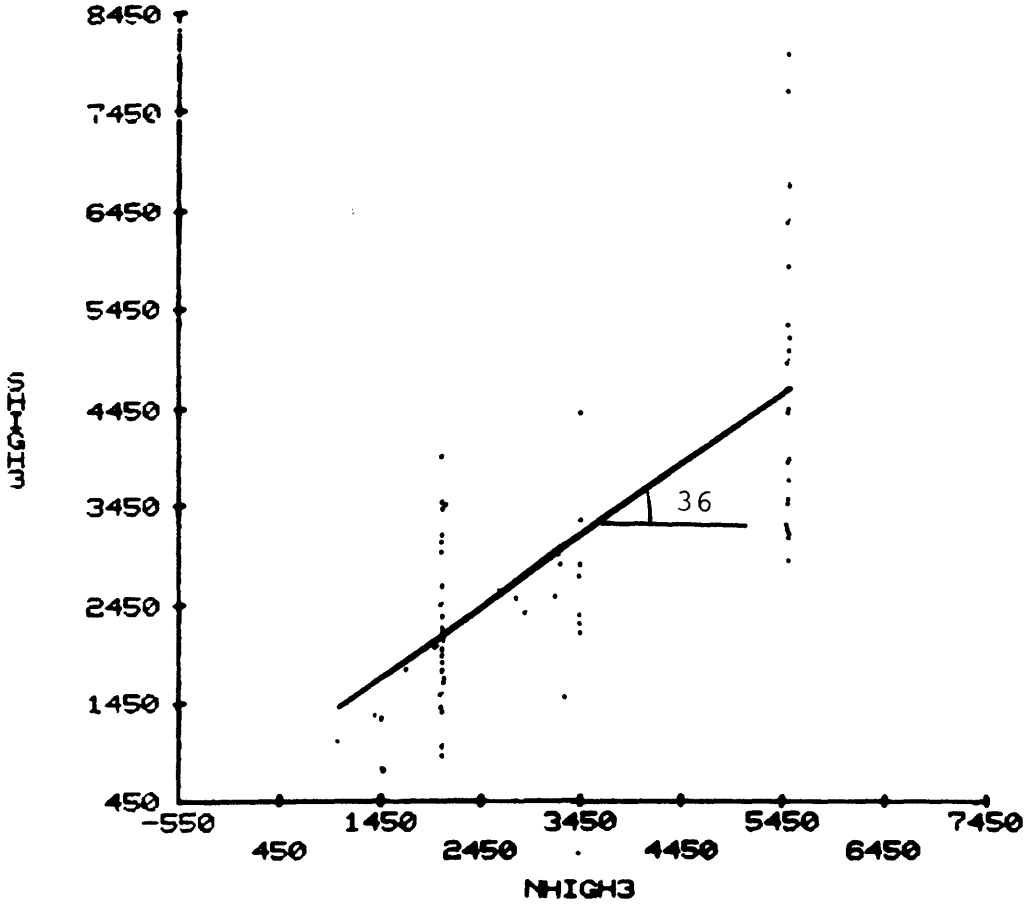

Figure C-78 Peak friction angle of monzonite for normal stress above 1 MN/m^2

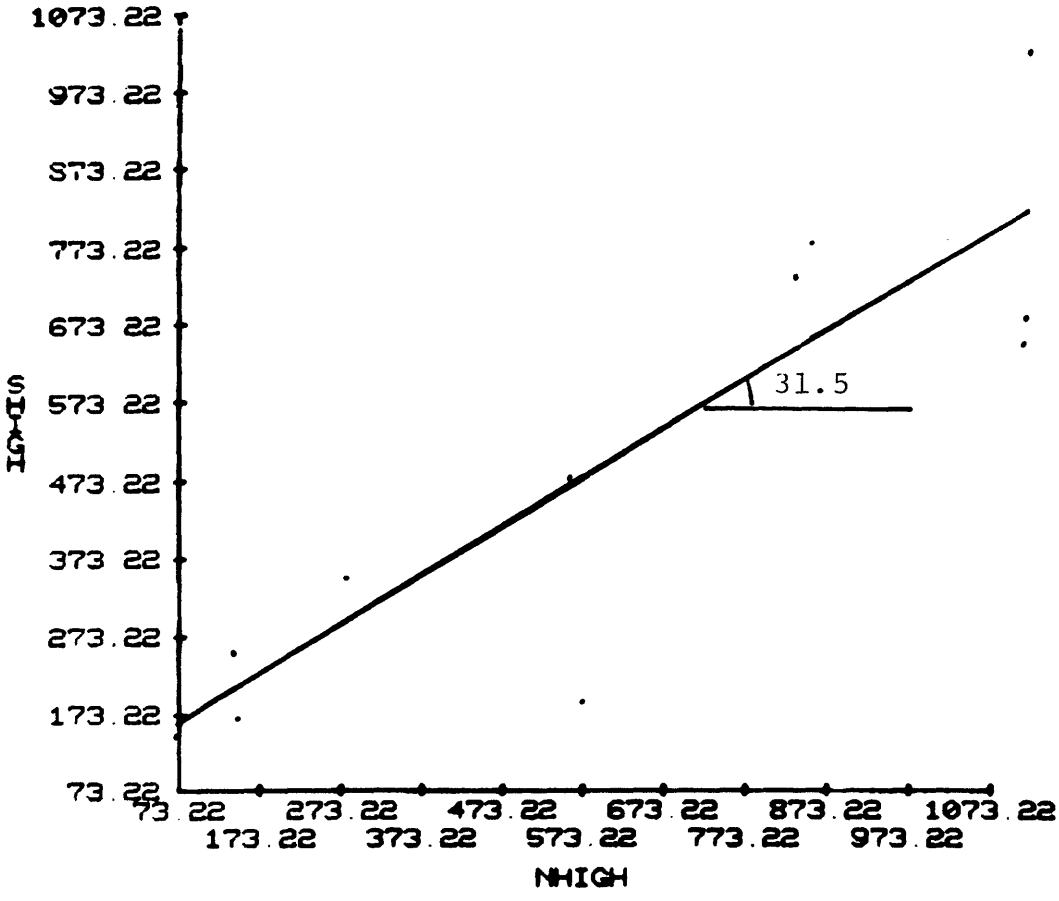

Figure C-79 Peak friction angle of lignite for all normal stress levels

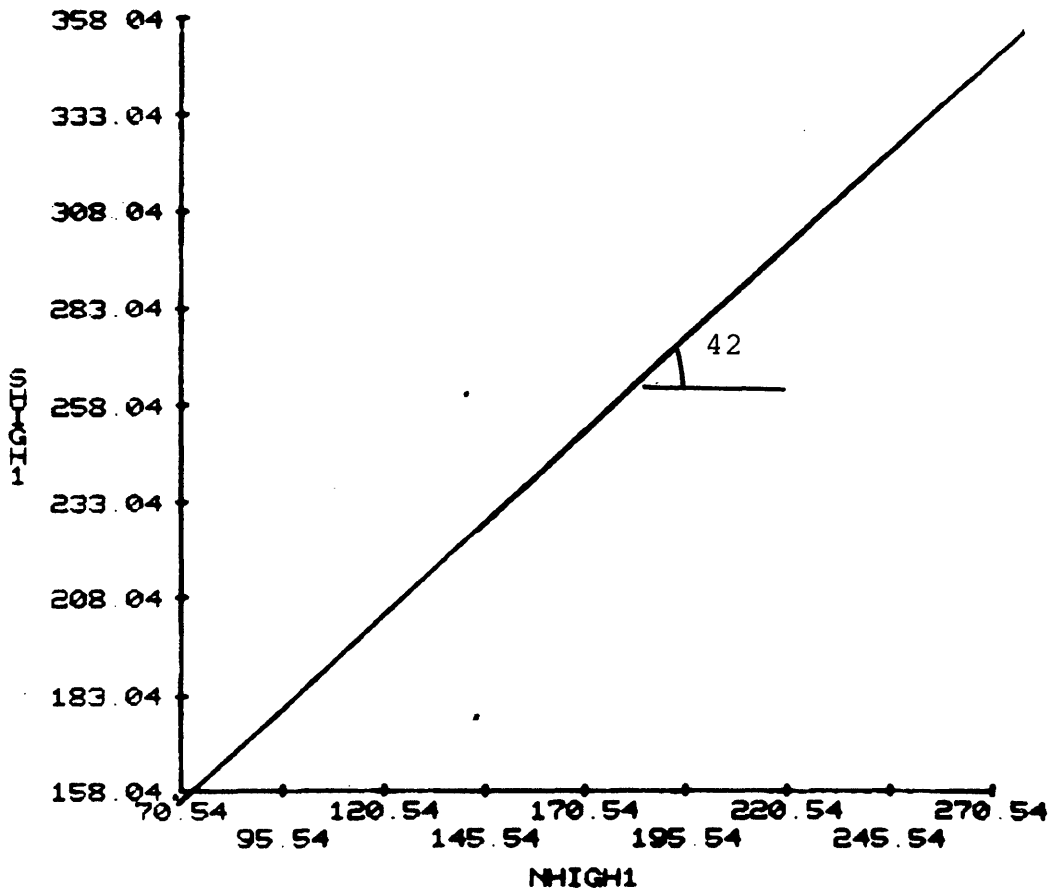

Figure C-80 Peak friction angle of lignite for normal stress below 0.3 MN/m^2

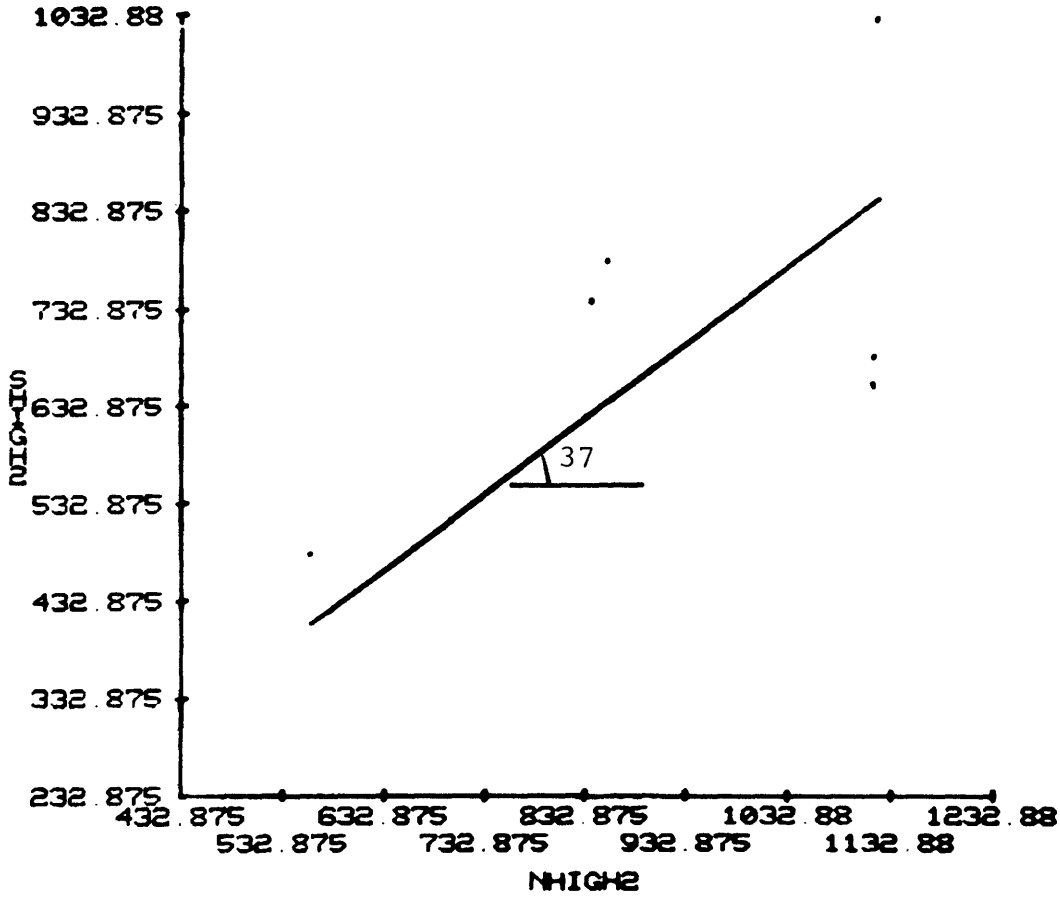

Figure C-81 Peak friction angle of lignite for normal stress above 0.3 MN/m^2

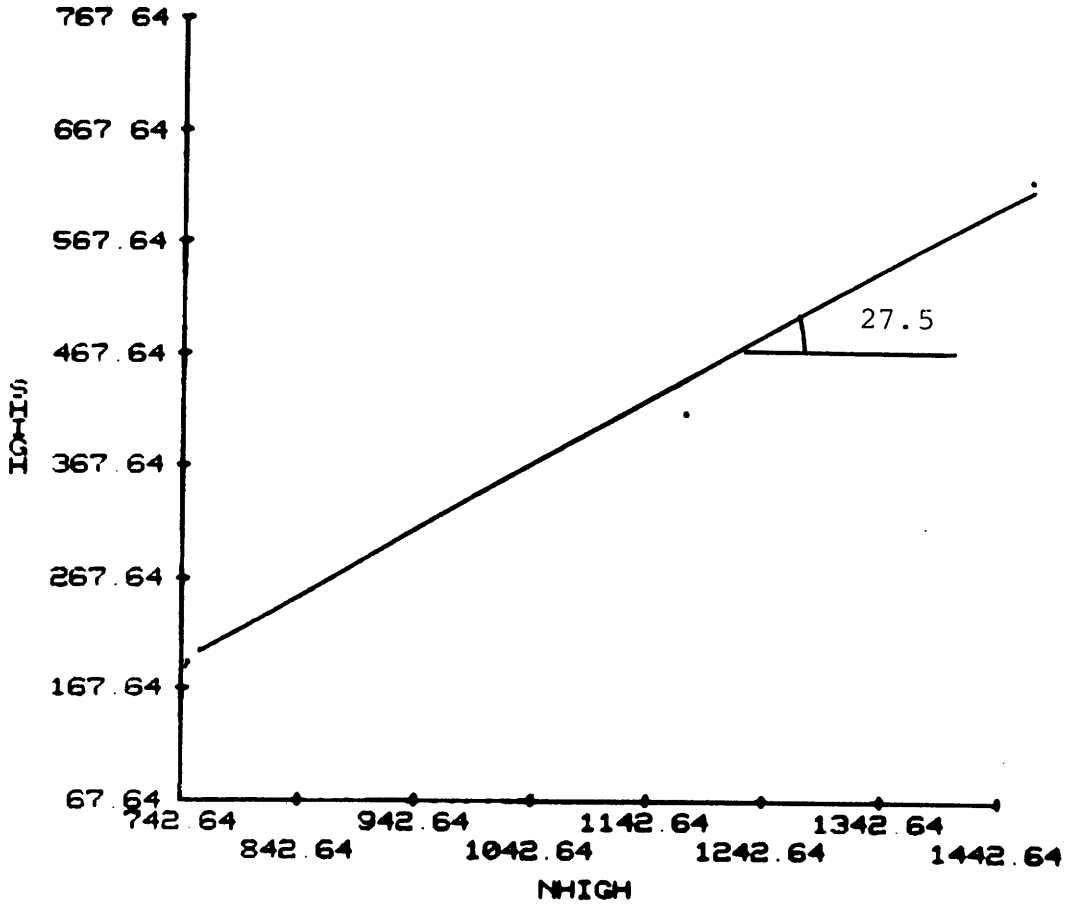

Figure C-82 Peak friction angle of sericite for all normal stress levels

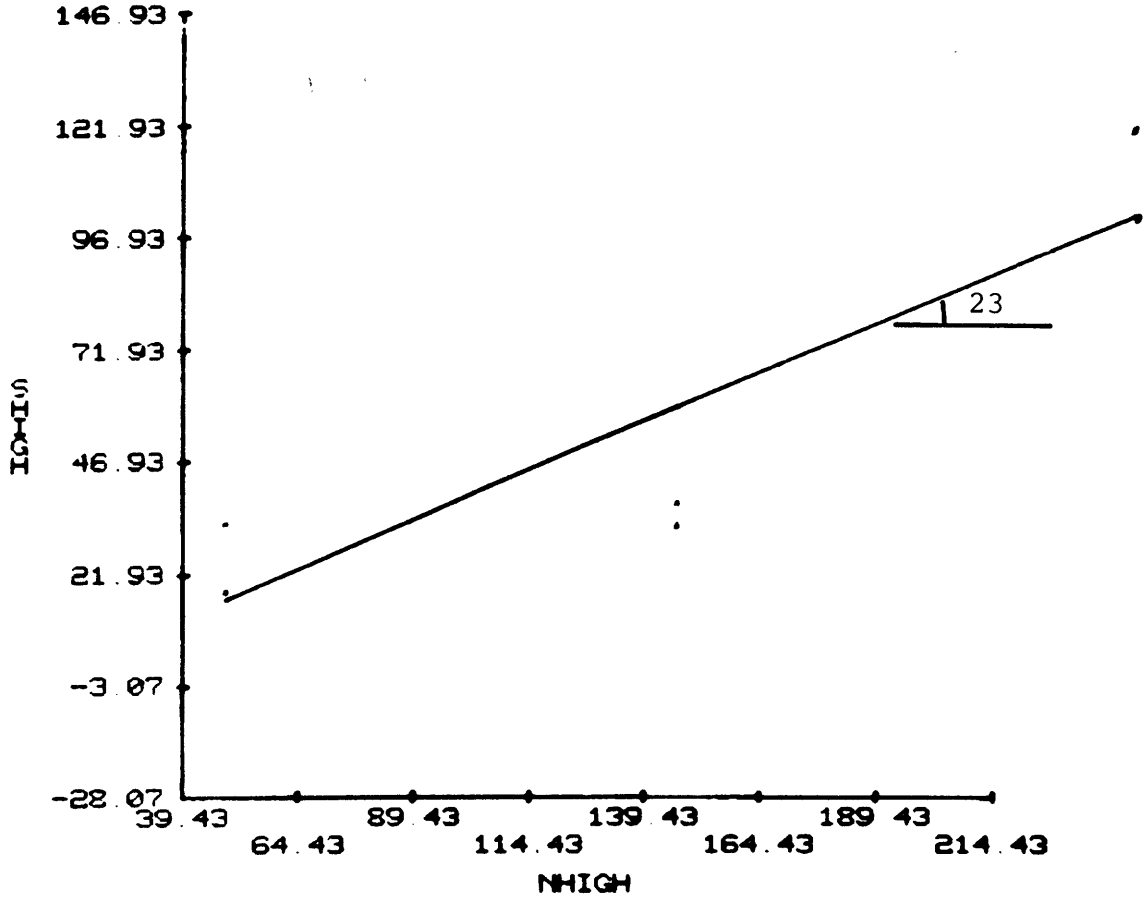

Figure C-83 Peak friction angle of talc for all normal stress levels

APPENDIX D

Peak and residual friction angles of rock types with description of discontinuities

Note: Units on the horizontal and vertical axes are X $10^{-3} MN/m^2$

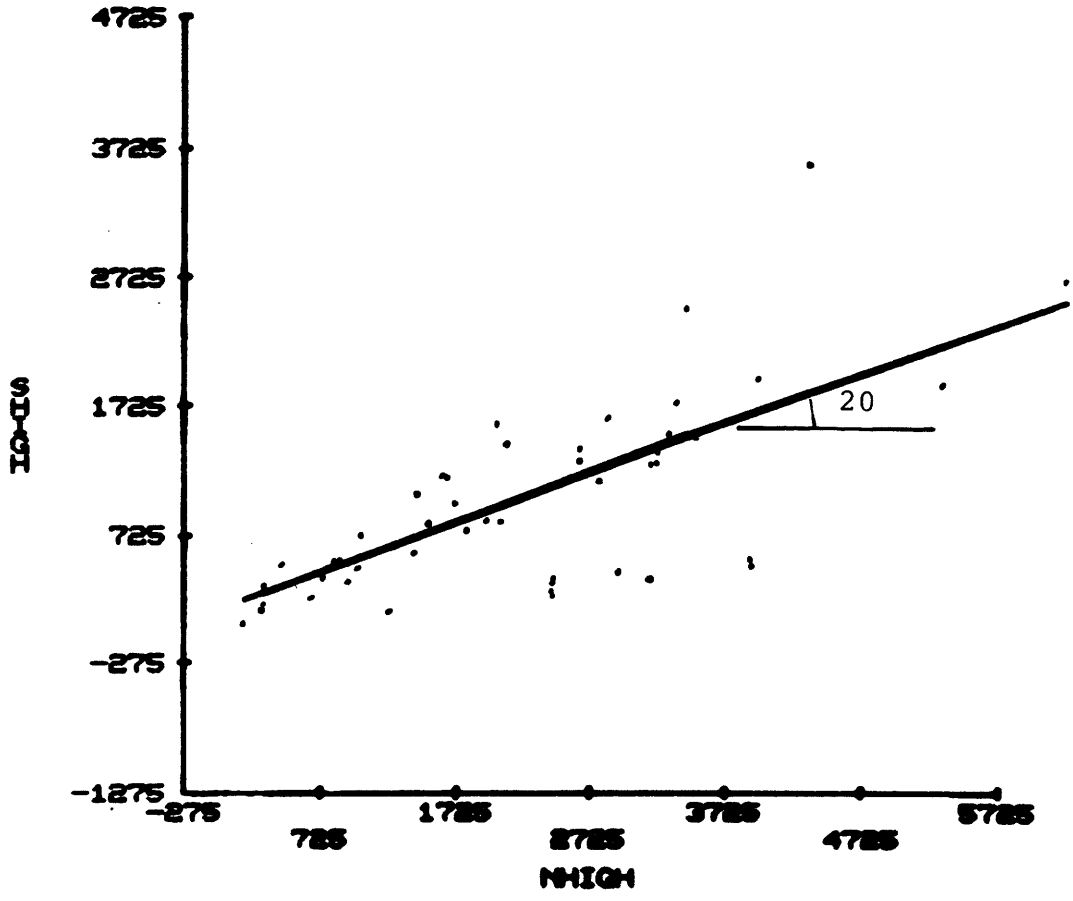

Figure D-1 Peak friction angle of limestone with joint surface

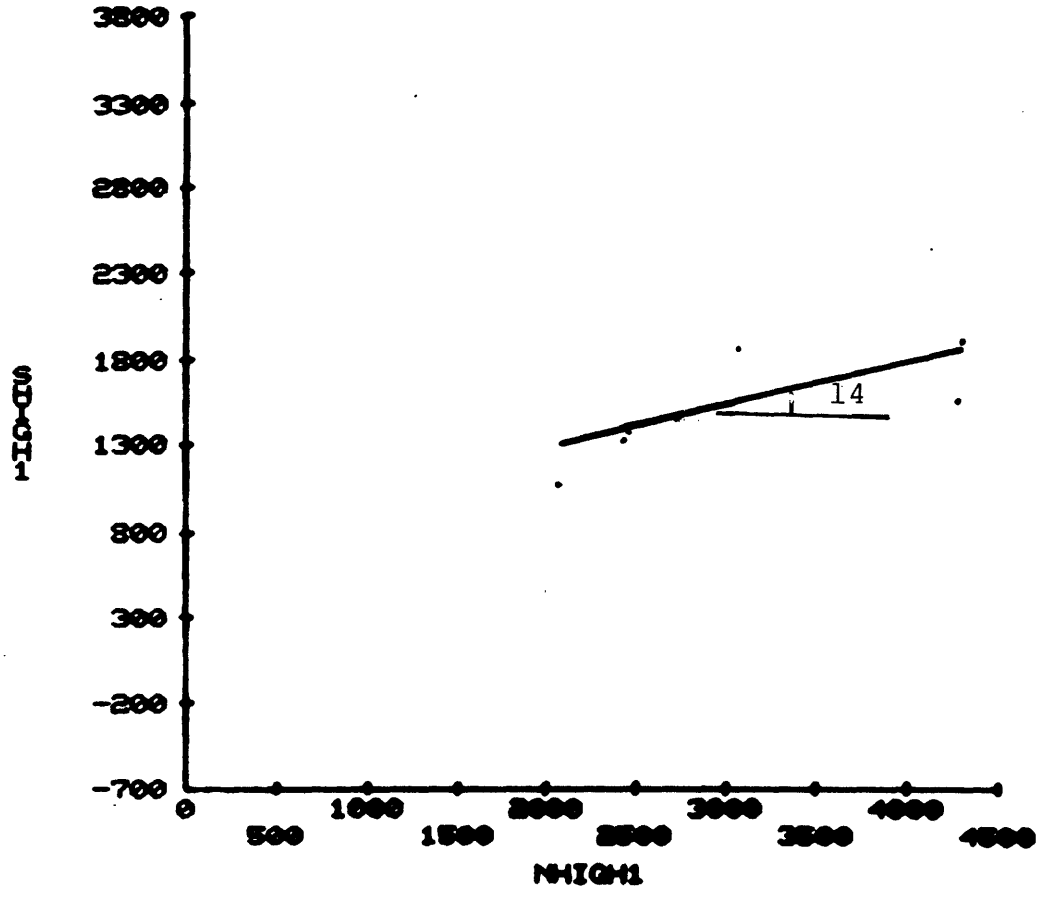

Figure D-2 Peak friction angle of limestone with concrete-limestone interface

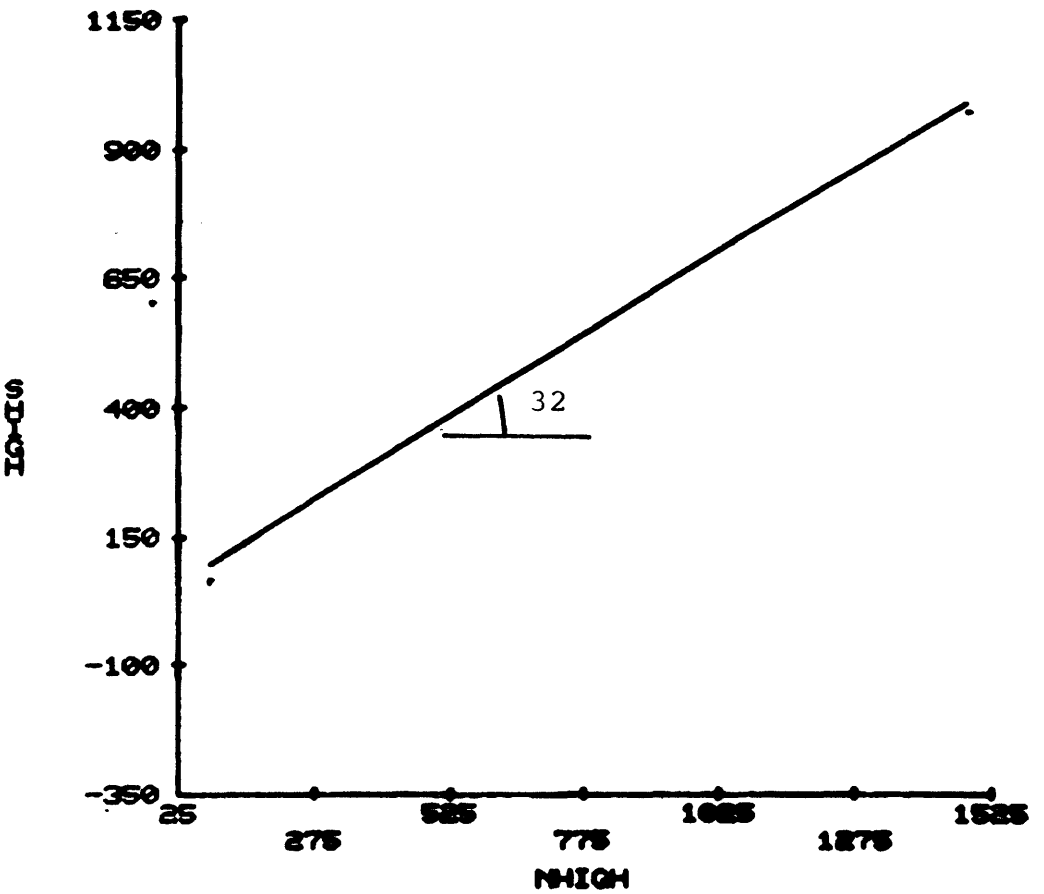

Figure D-3 Peak friction angle of limestone with contact between limestone and moraine

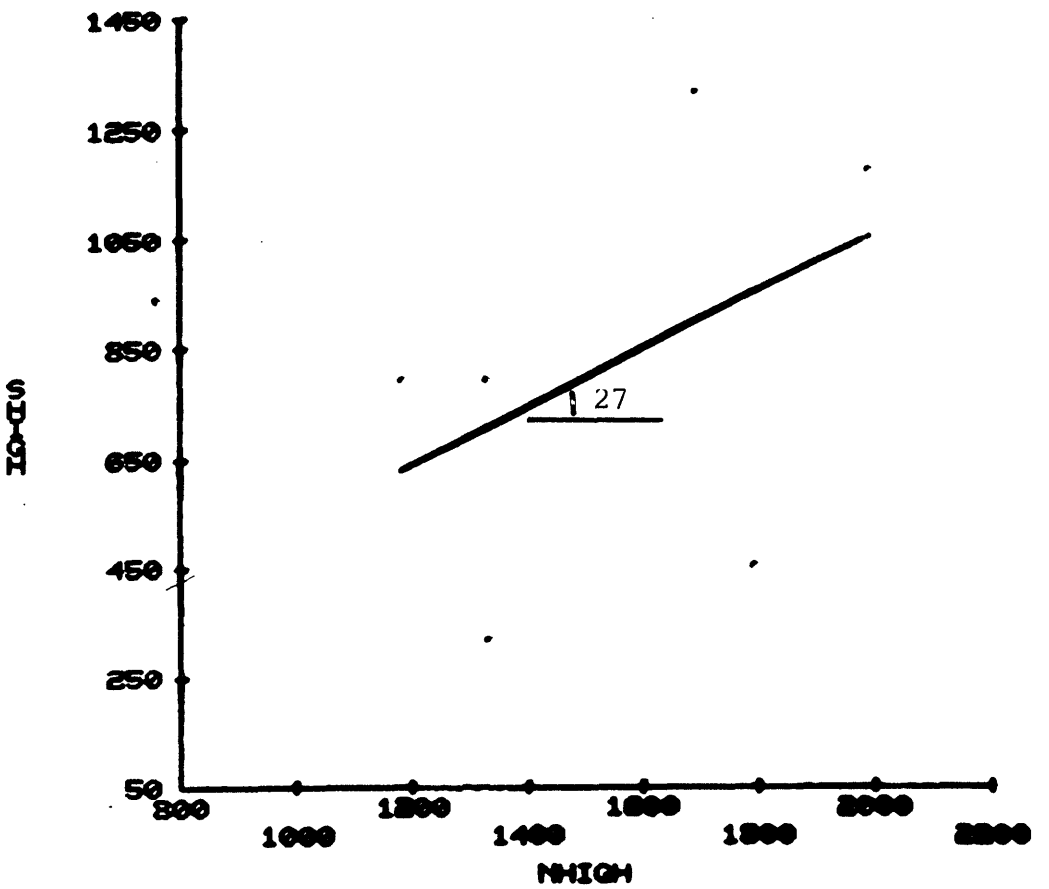

Figure D-4 Peak friction angle of limestone with bedding

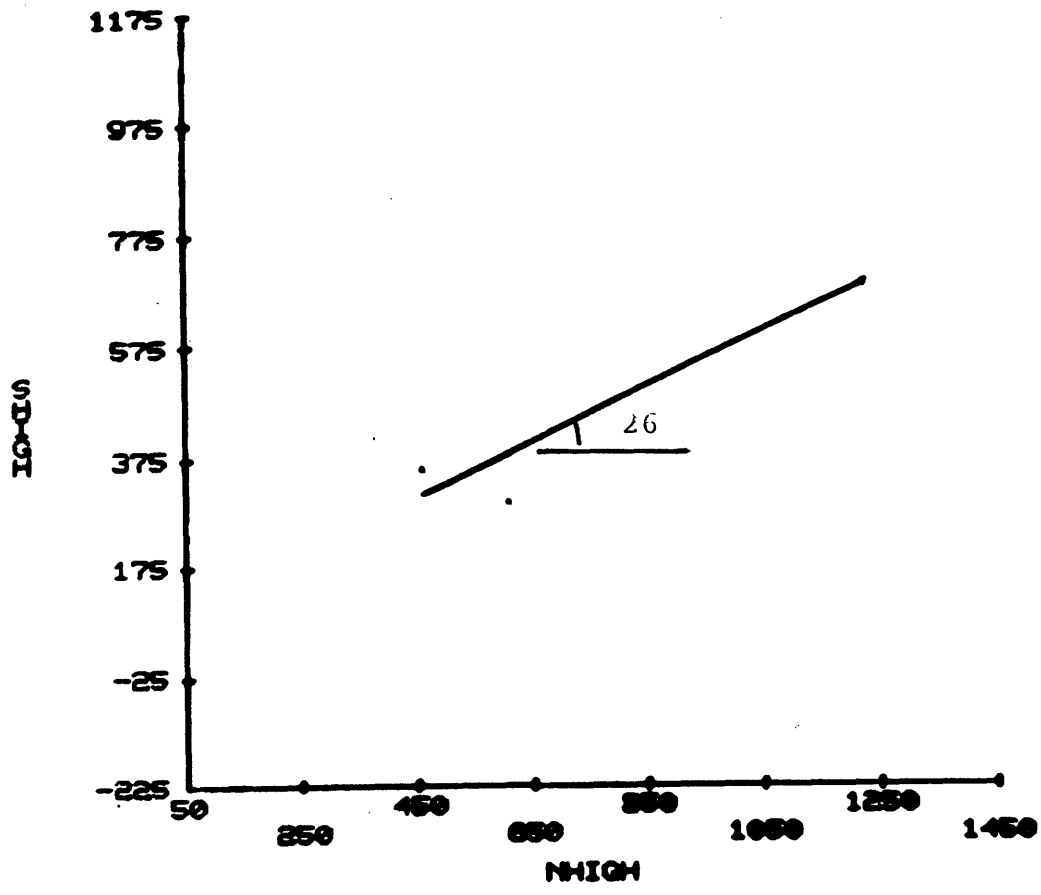

Figure D-5 Peak friction angle of sandstone with break of core sample

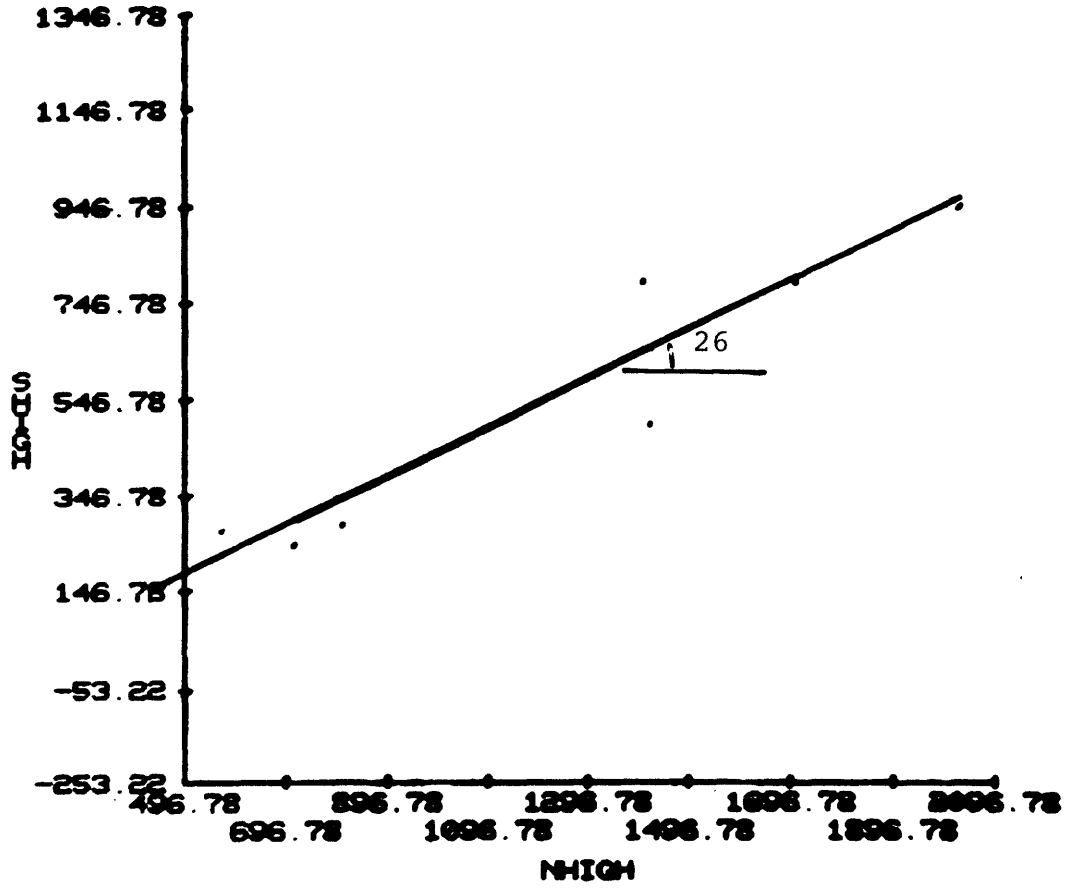

Figure D-6 Peak friction angle of paragneiss with foliation

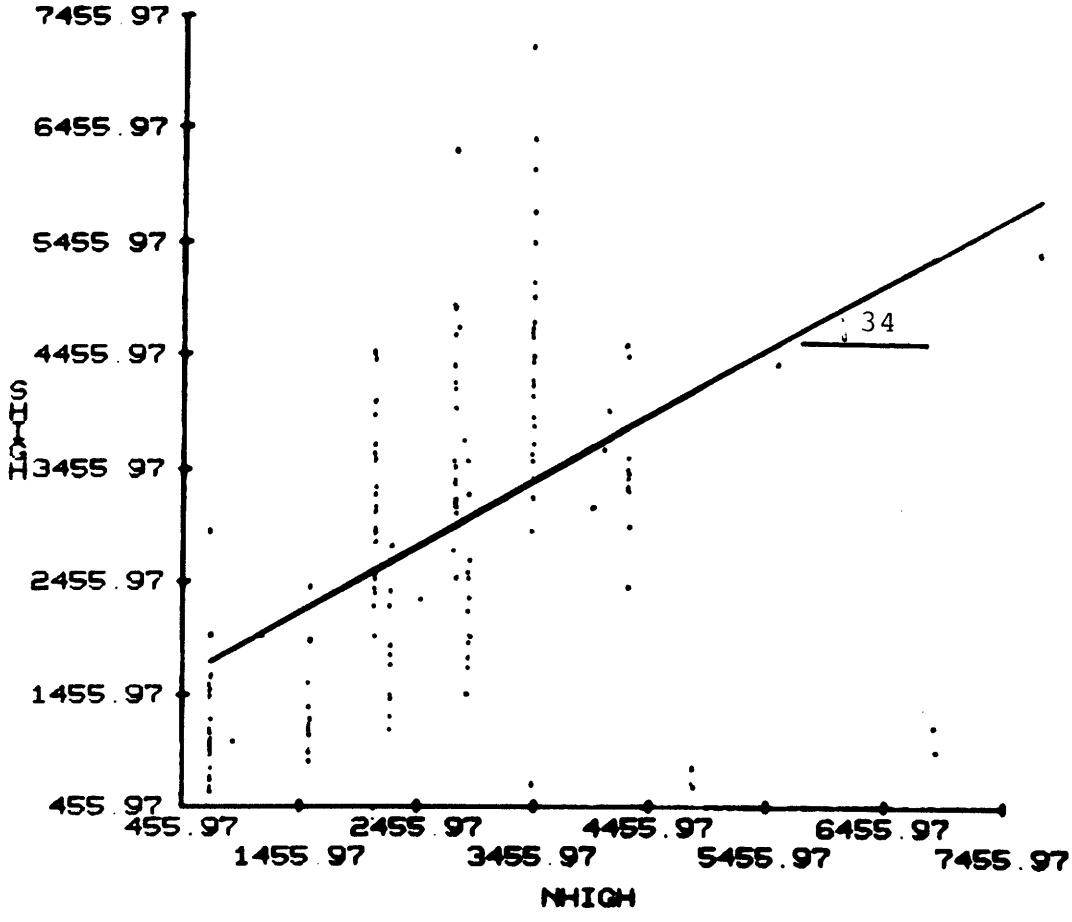

Figure D-7 Peak friction angle of amphibolite with joint surface

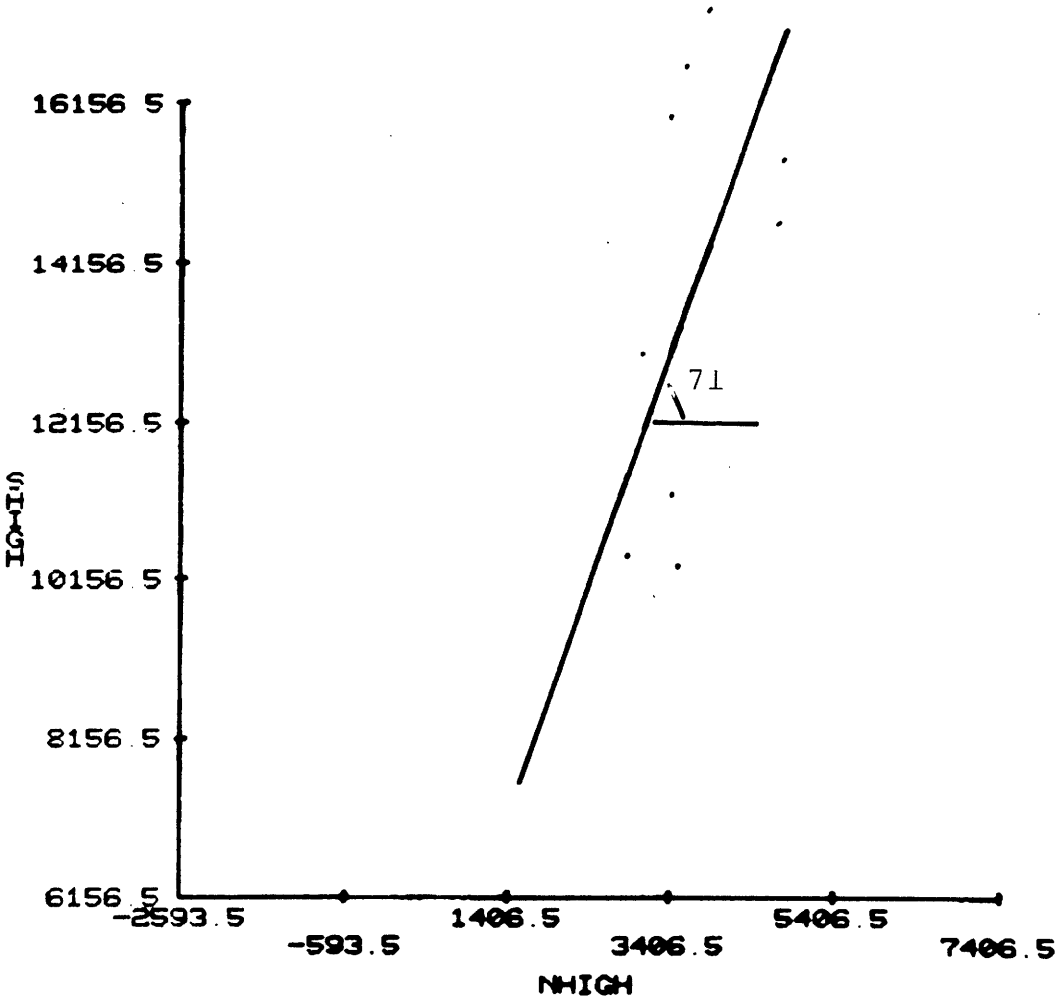

Figure D-8 Peak friction angle of amphibolite with healed joint

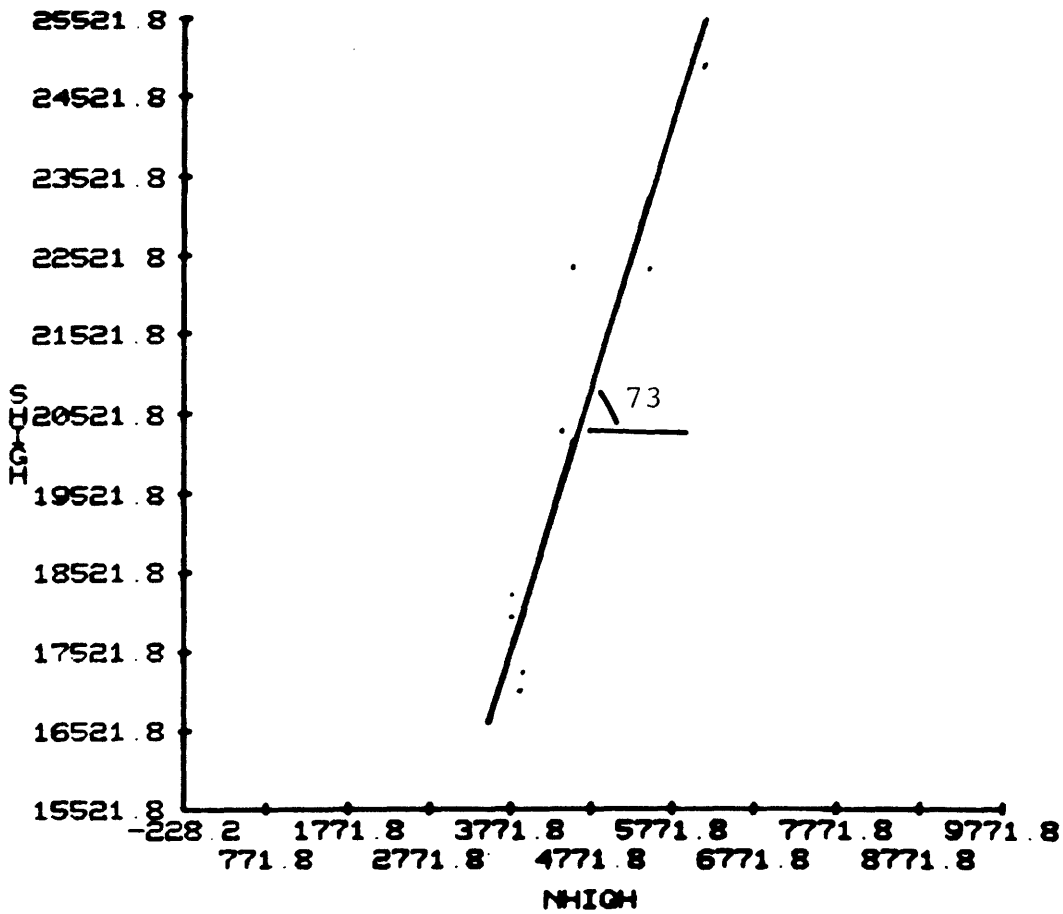

Figure D-9 Peak friction angle of homogeneous amphibolite

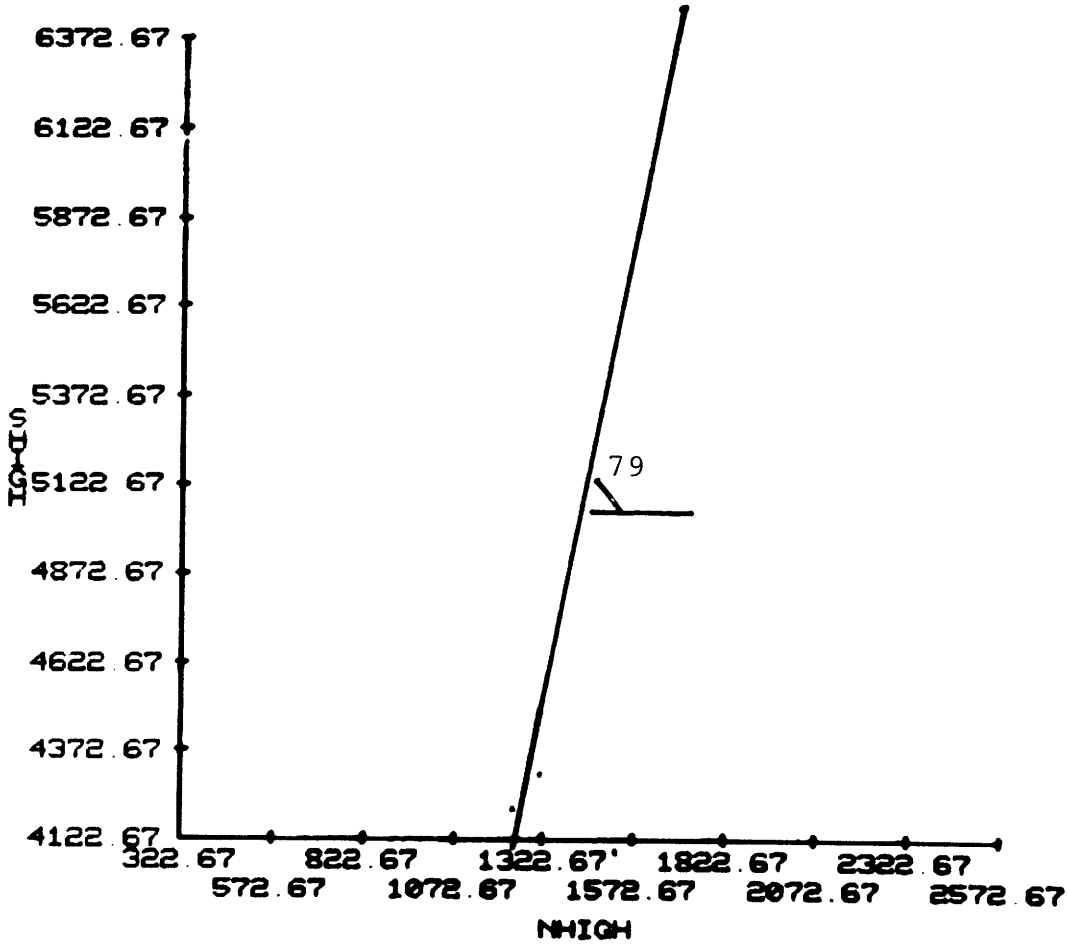

Figure D-10 Peak friction angle of intact amphibolite

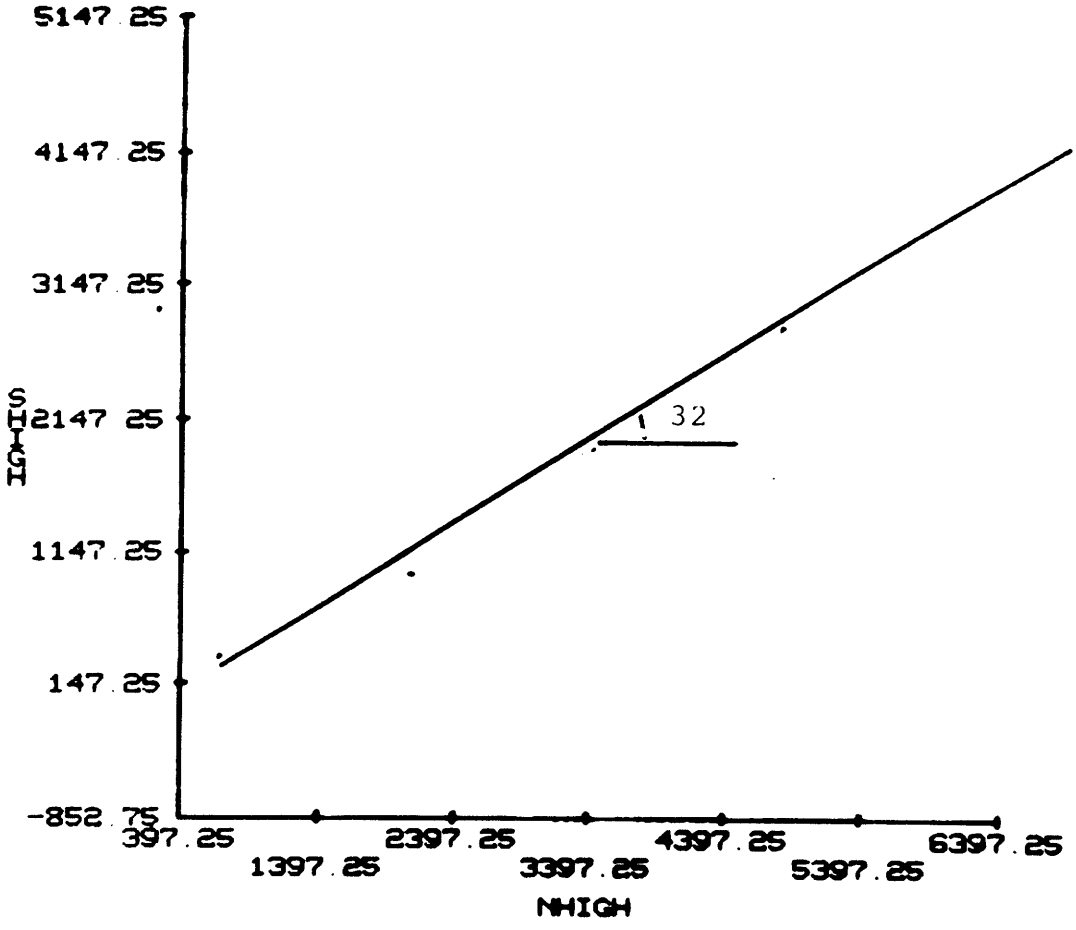

Figure D-11 Peak friction angle of amphibolite with sawn surface

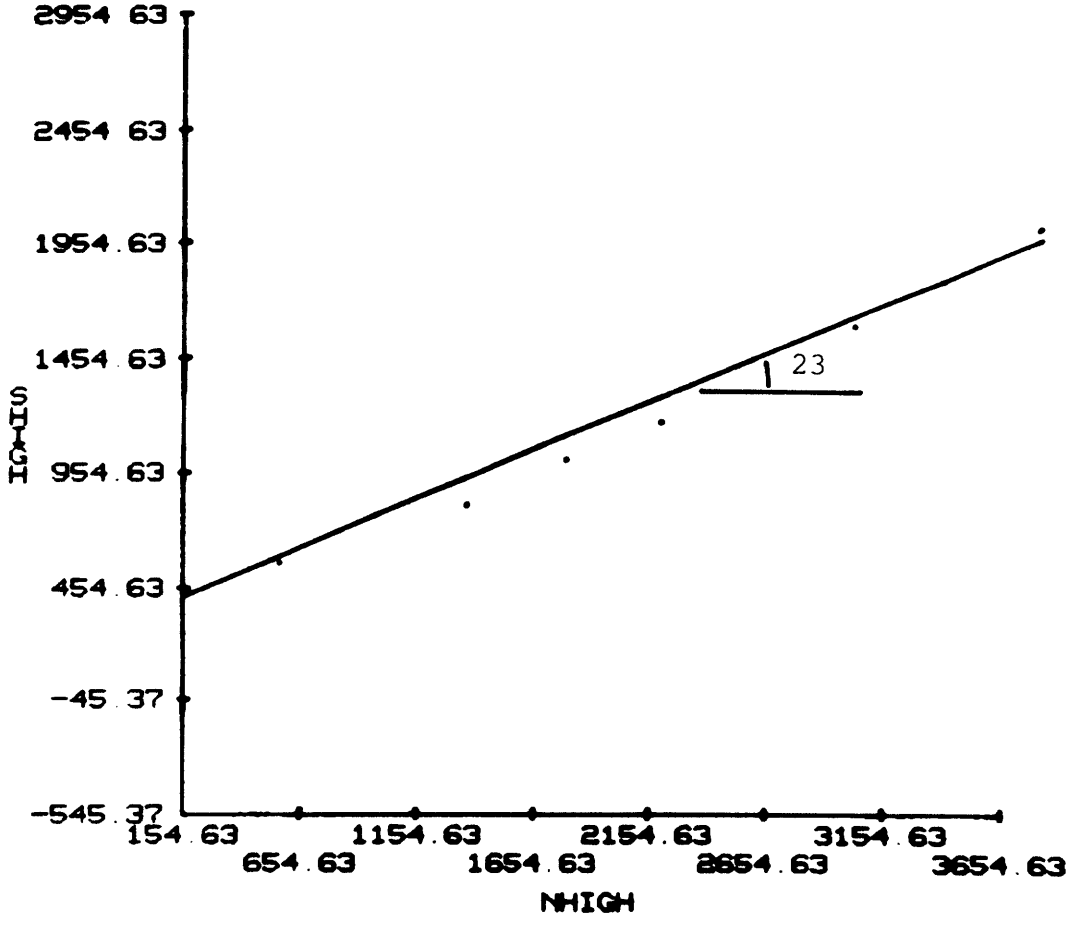

Figure D-12 Peak friction angle of amphibolite with conjugate joint set

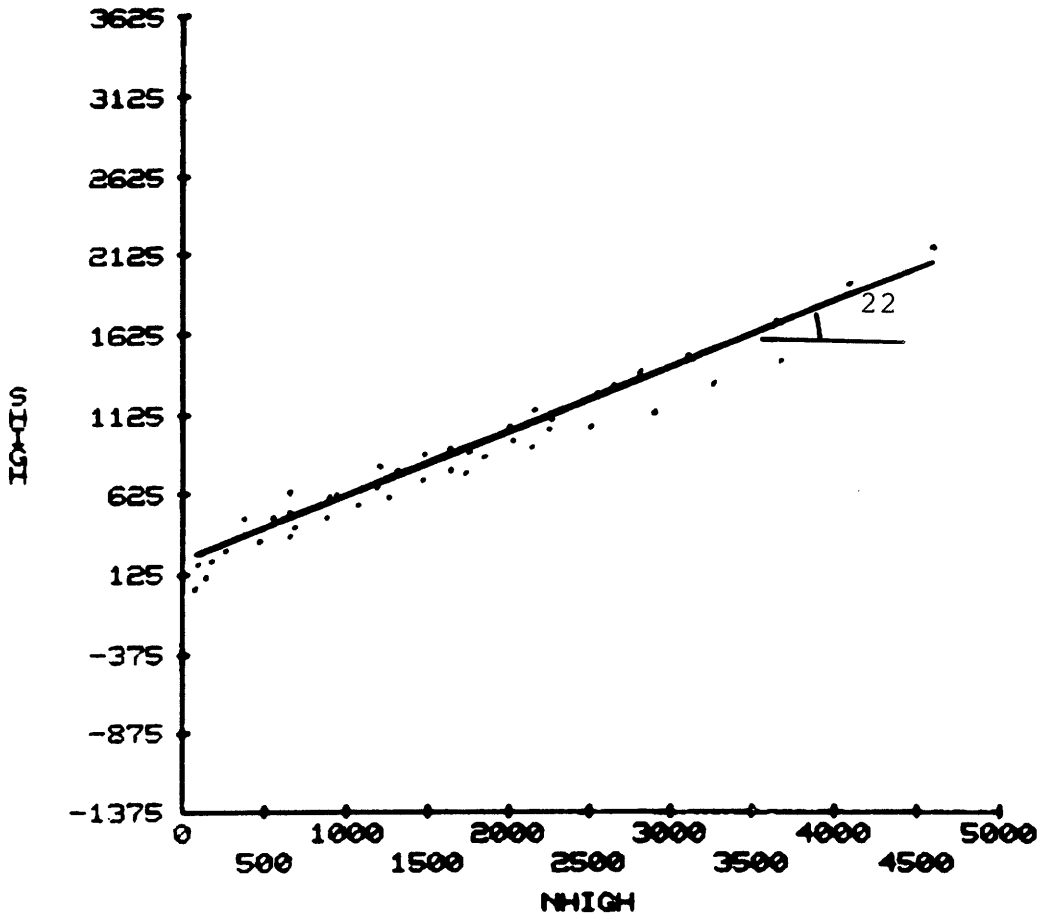

Figure D-13 Peak friction angle of amphibolite with H/W joint set

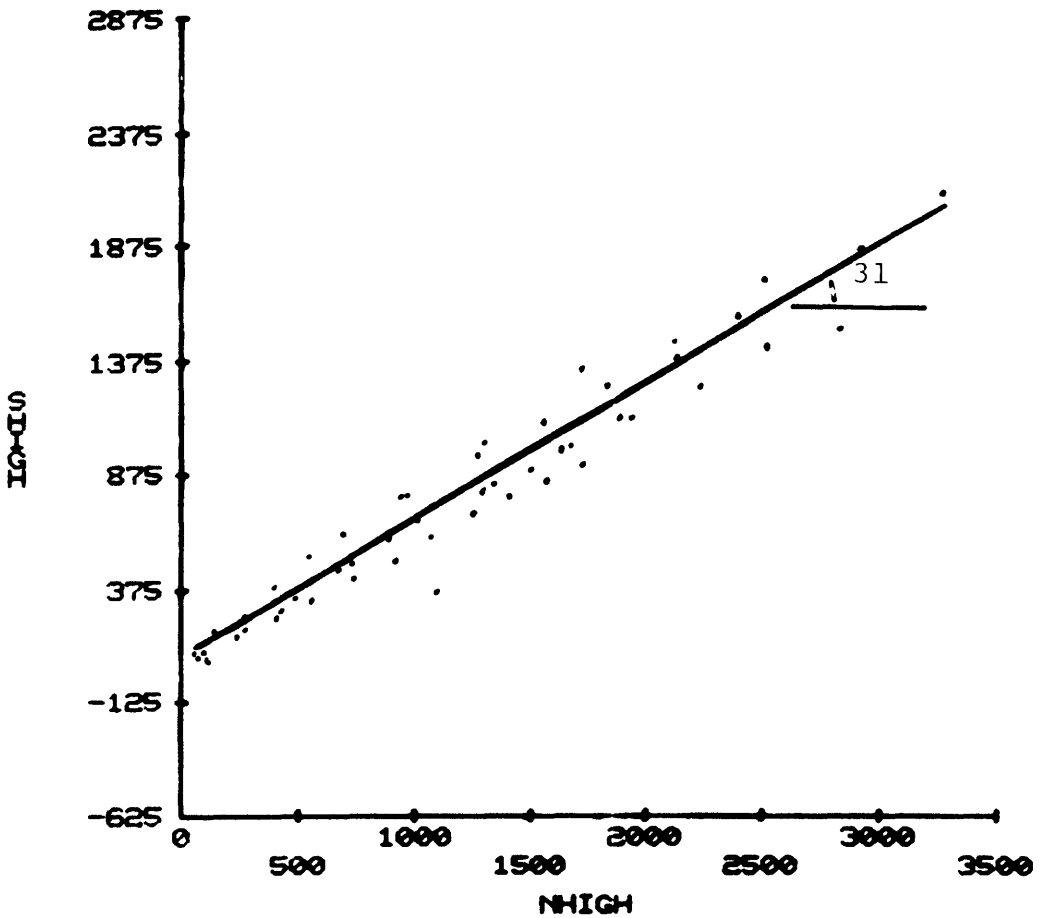

Figure D-14 Peak friction angle of amphibolite with foliation

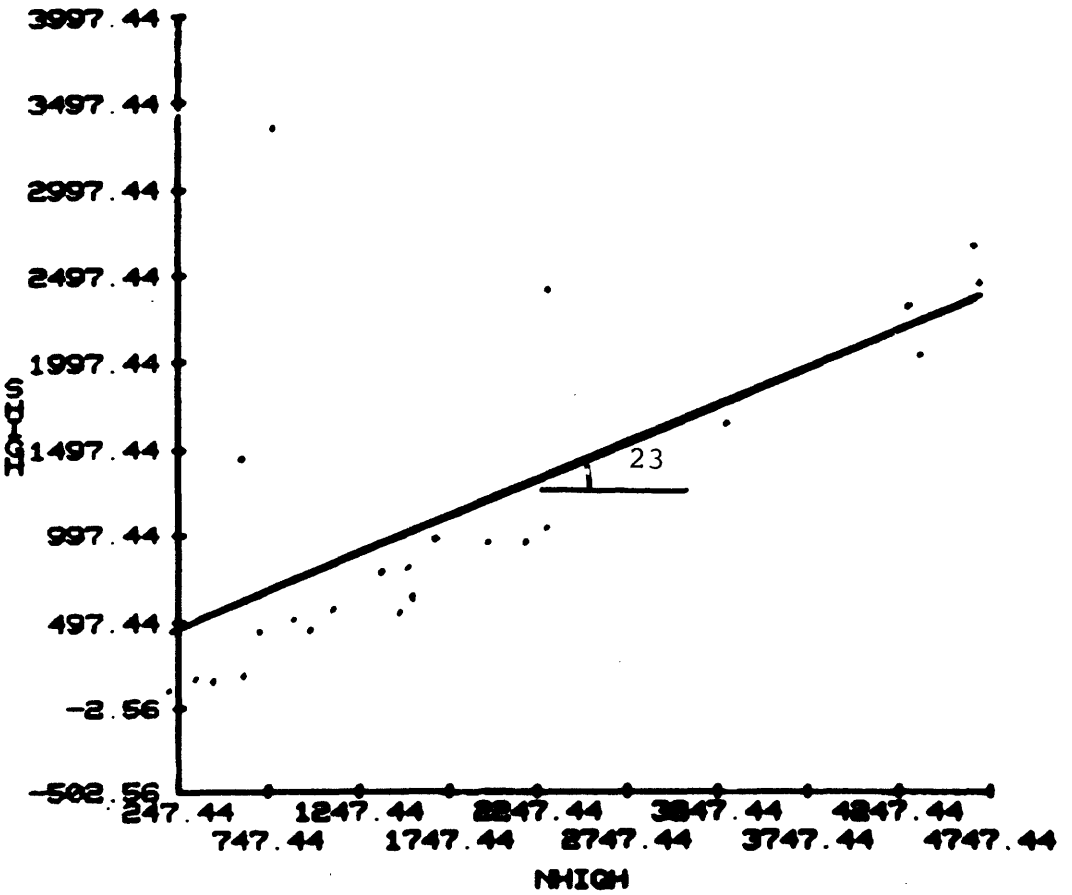

Figure D-15 Peak friction angle of schist with foliation

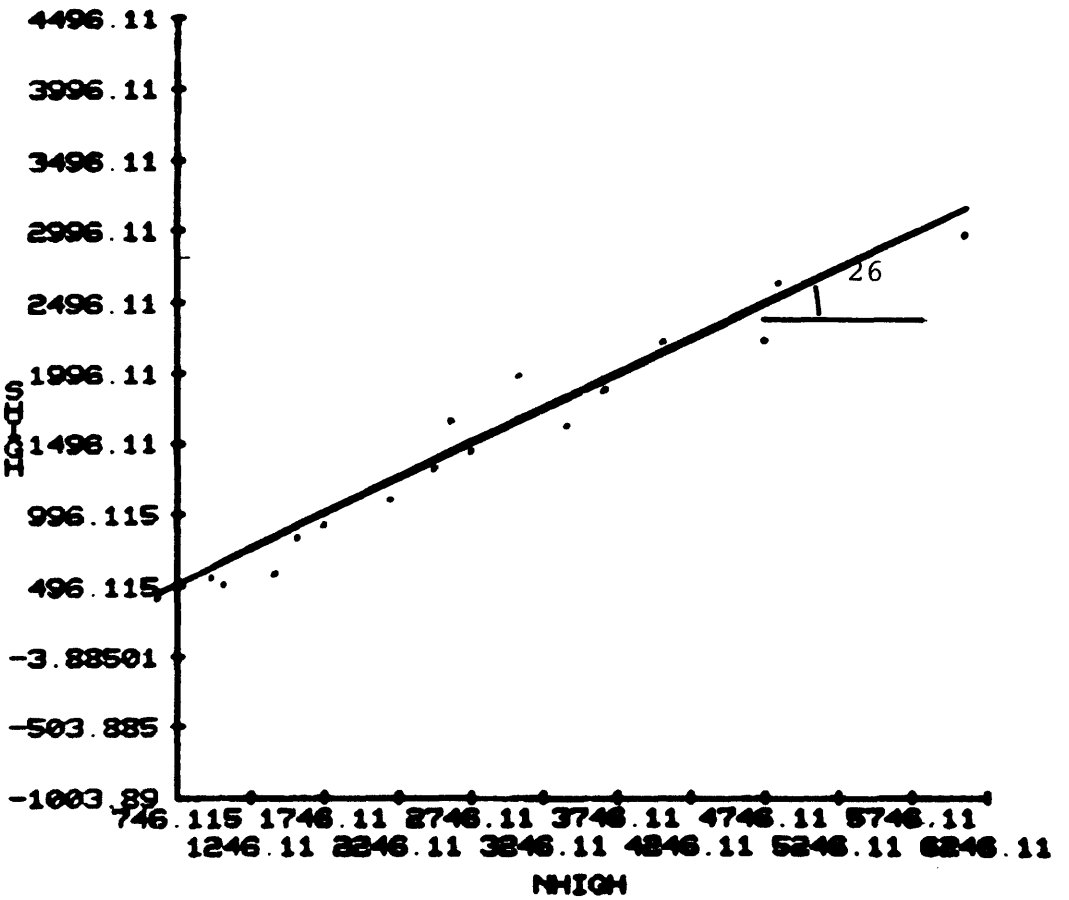

Figure D-16 Peak friction angle of schist with separated foliation

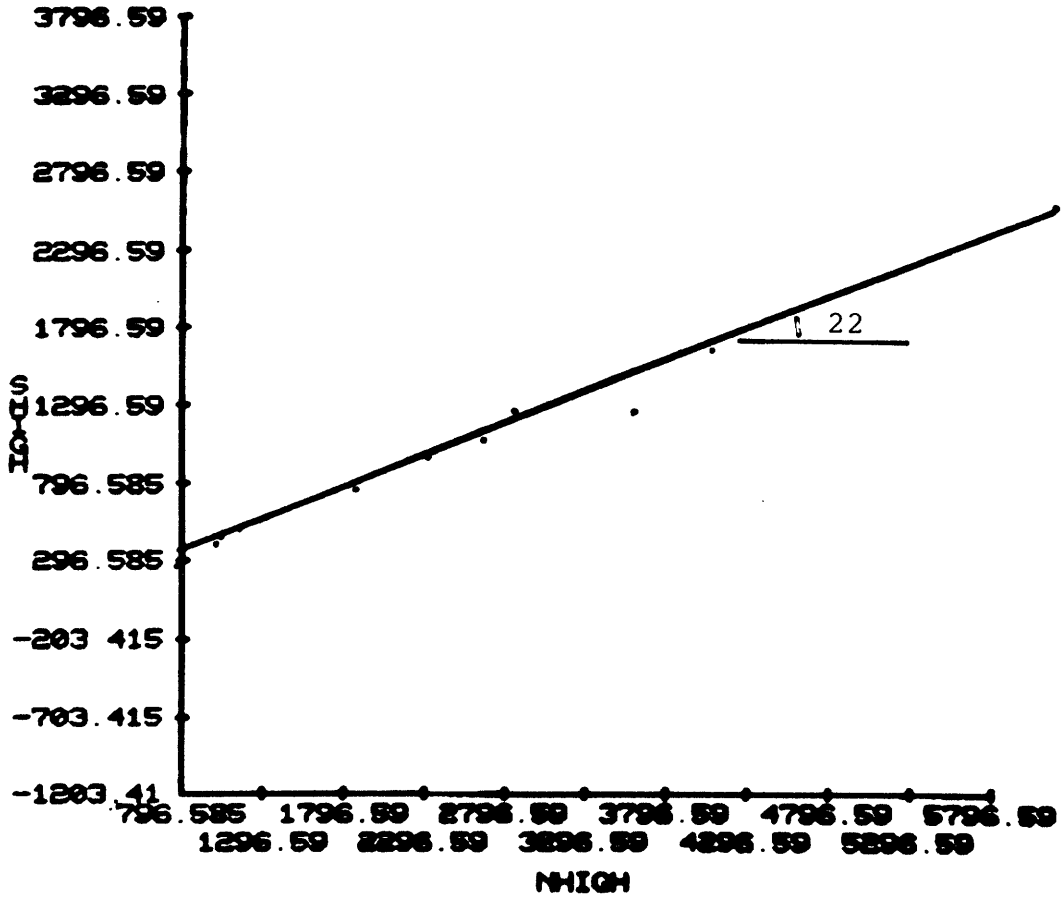

Figure D-17 Peak friction angle of schist with sawn surface

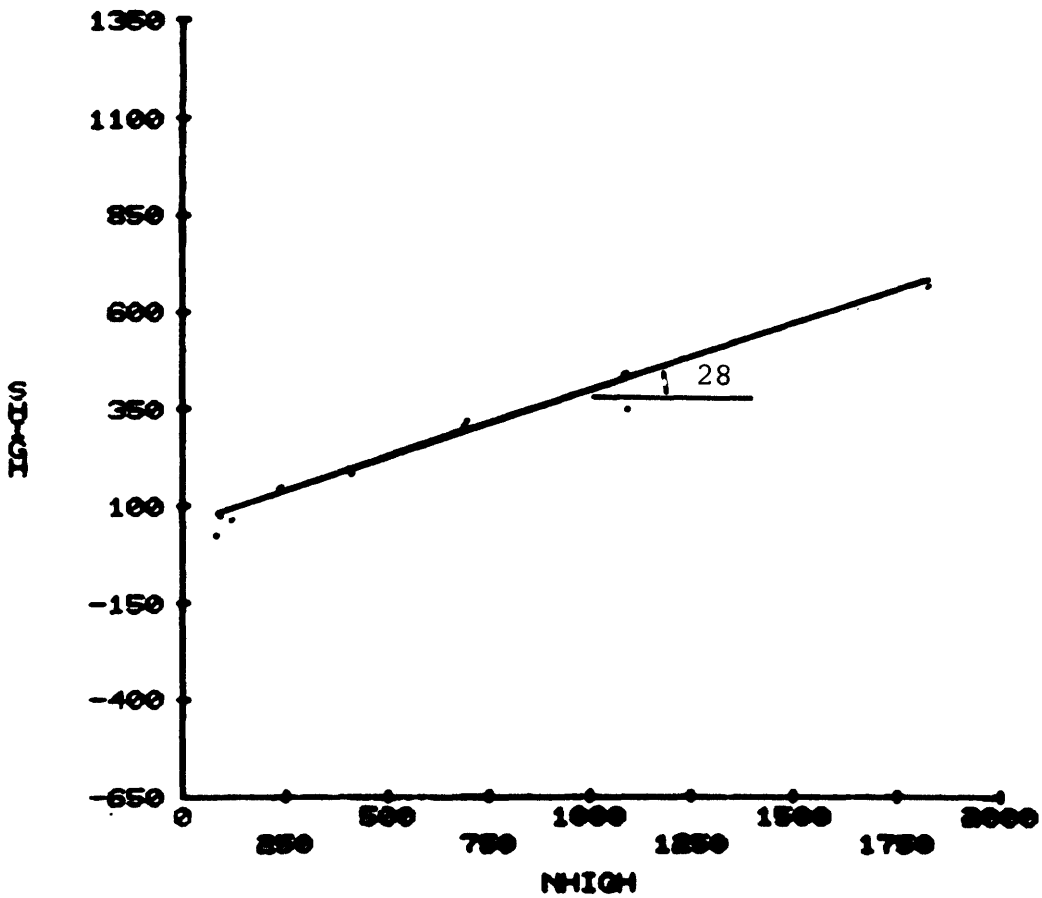

Figure D-18 Peak friction angle of phyllite with foliation

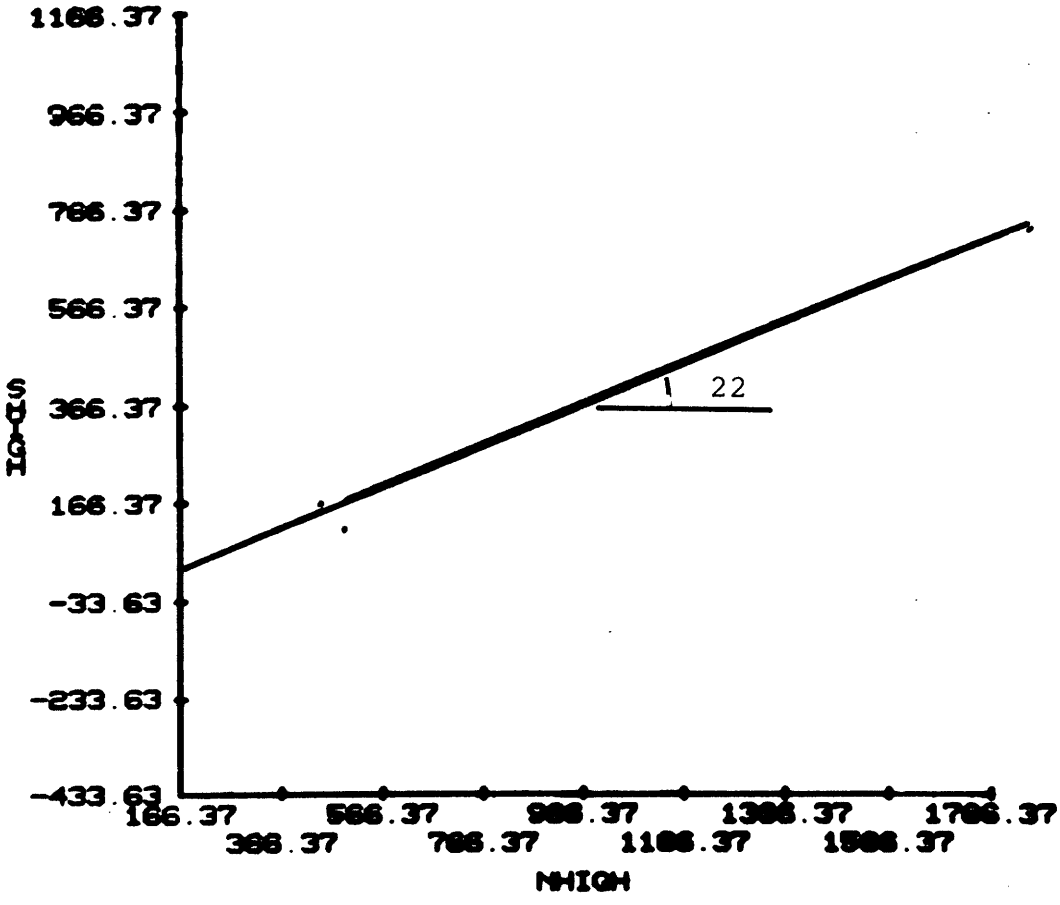

Figure D-19 Peak friction angle of serpentine (schistose) with foliation

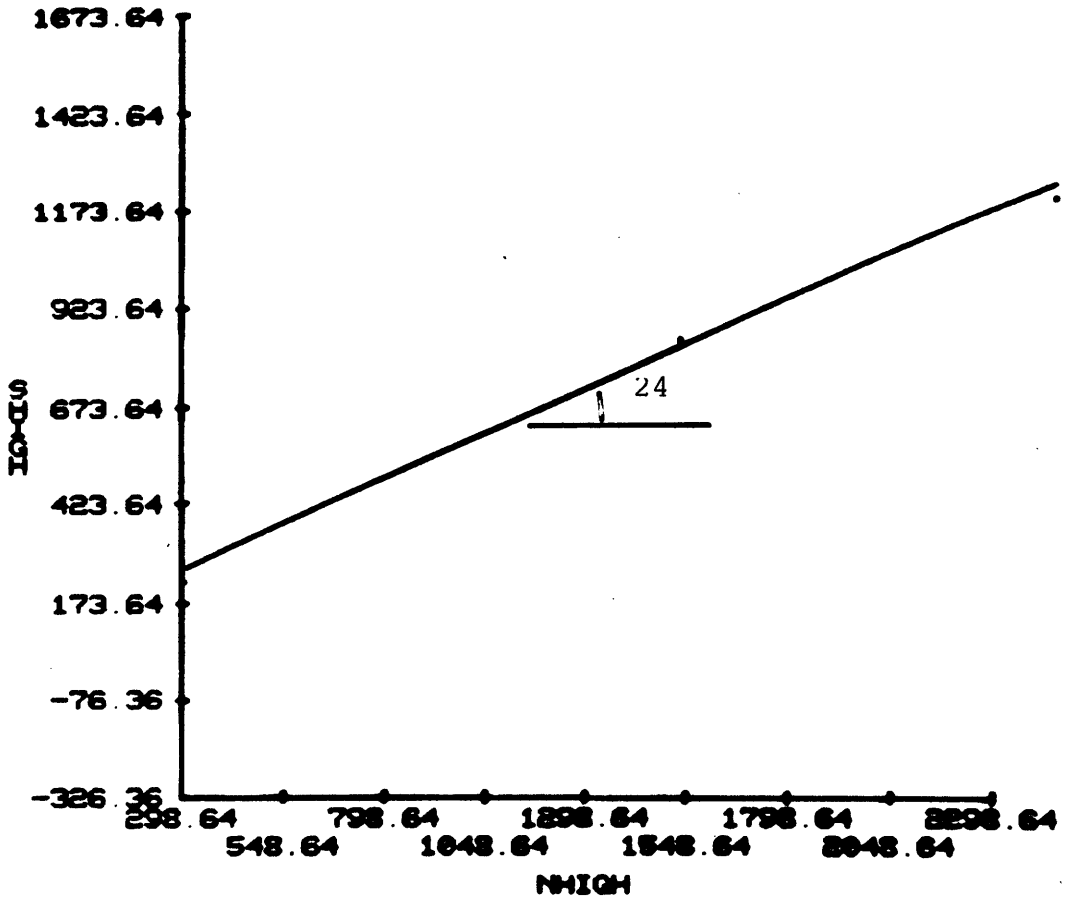

Figure D-20 Peak friction angle of serpentine (schistose) with sawn surface

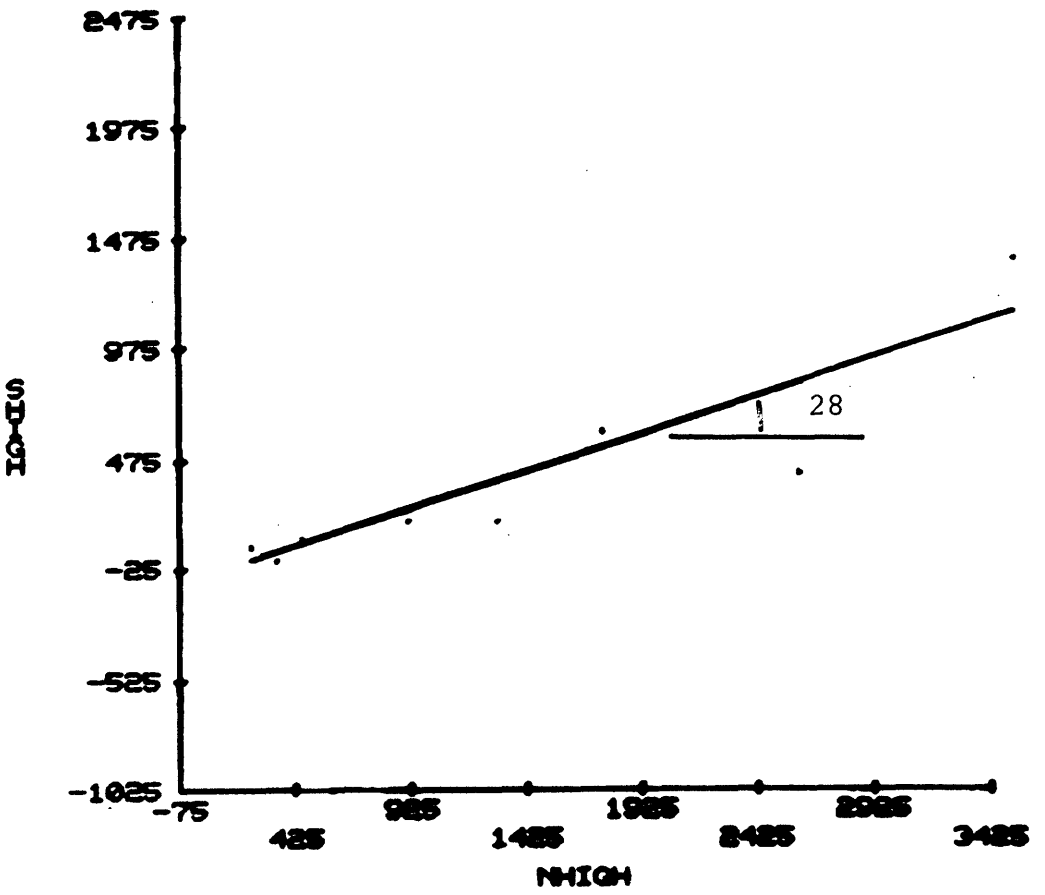

Figure D-21 Peak friction angle of serpentine with foliation

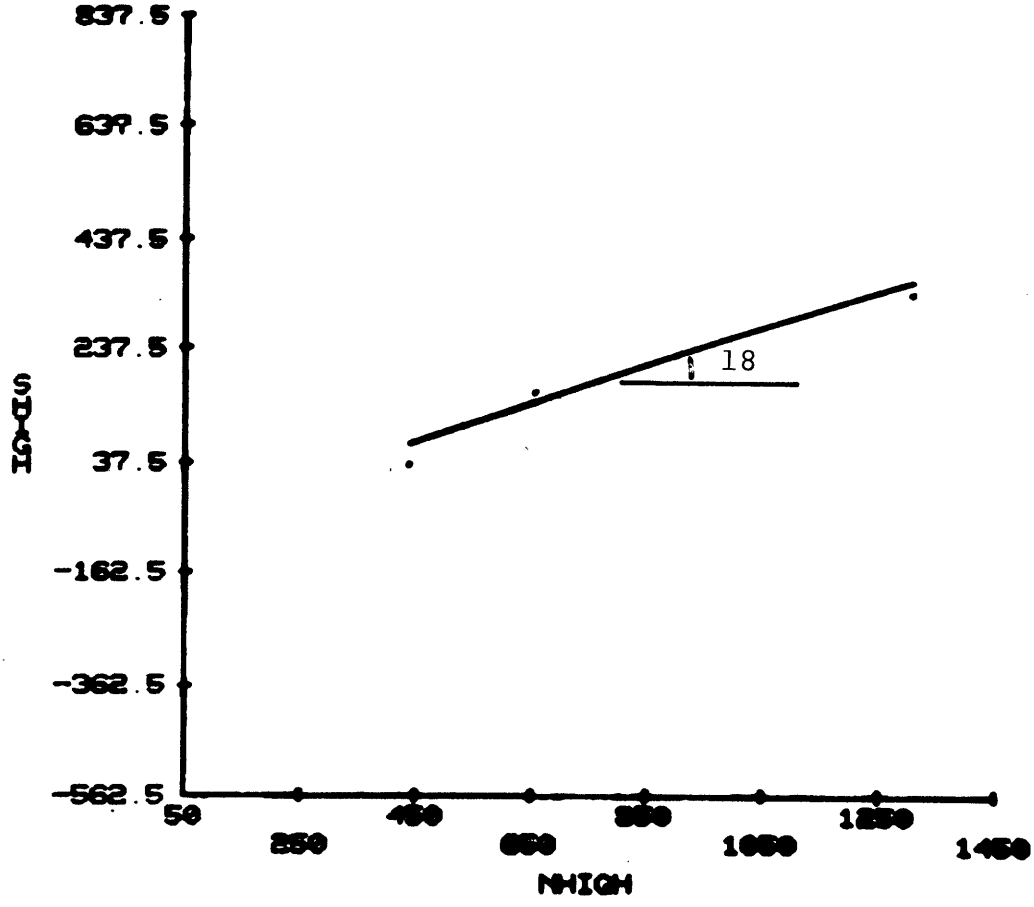

Figure D-22 Peak friction angle of serpentine with sawn surface

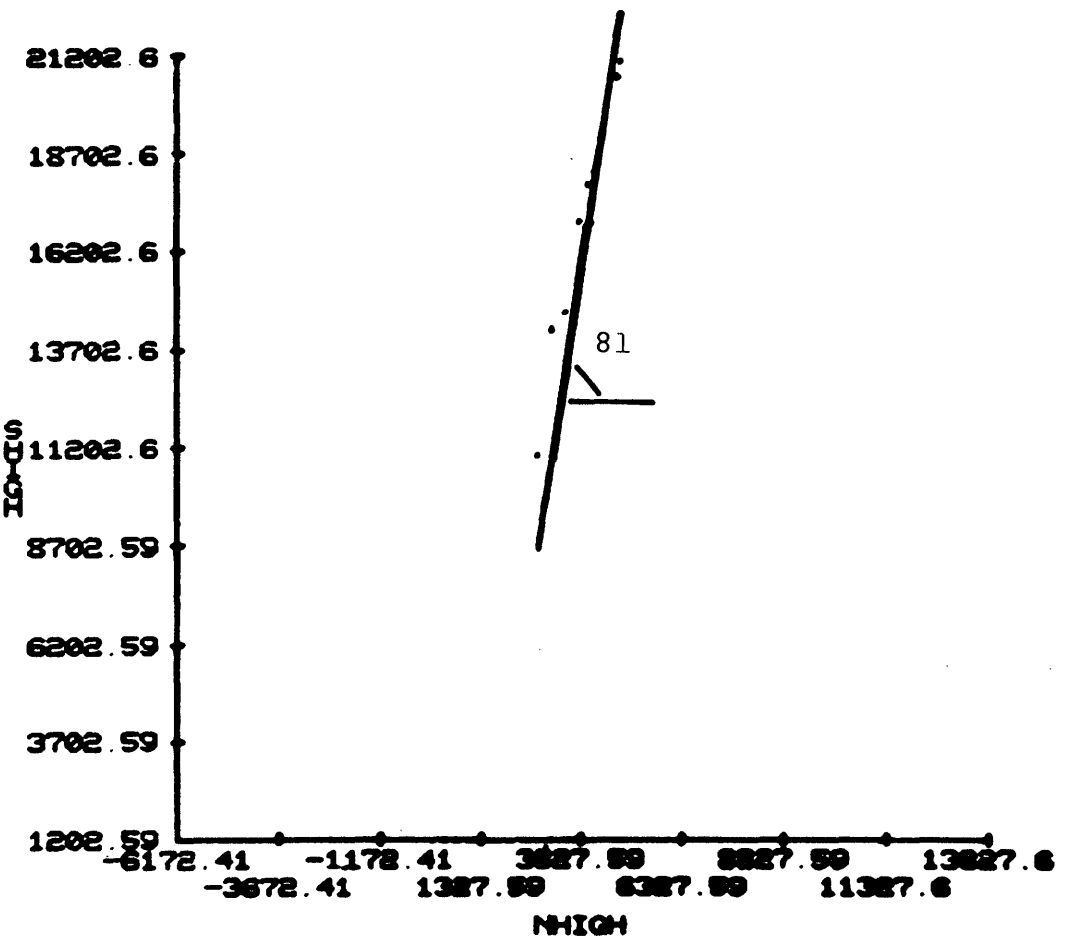

Figure D-23 Peak friction angle of homogeneous serpentine

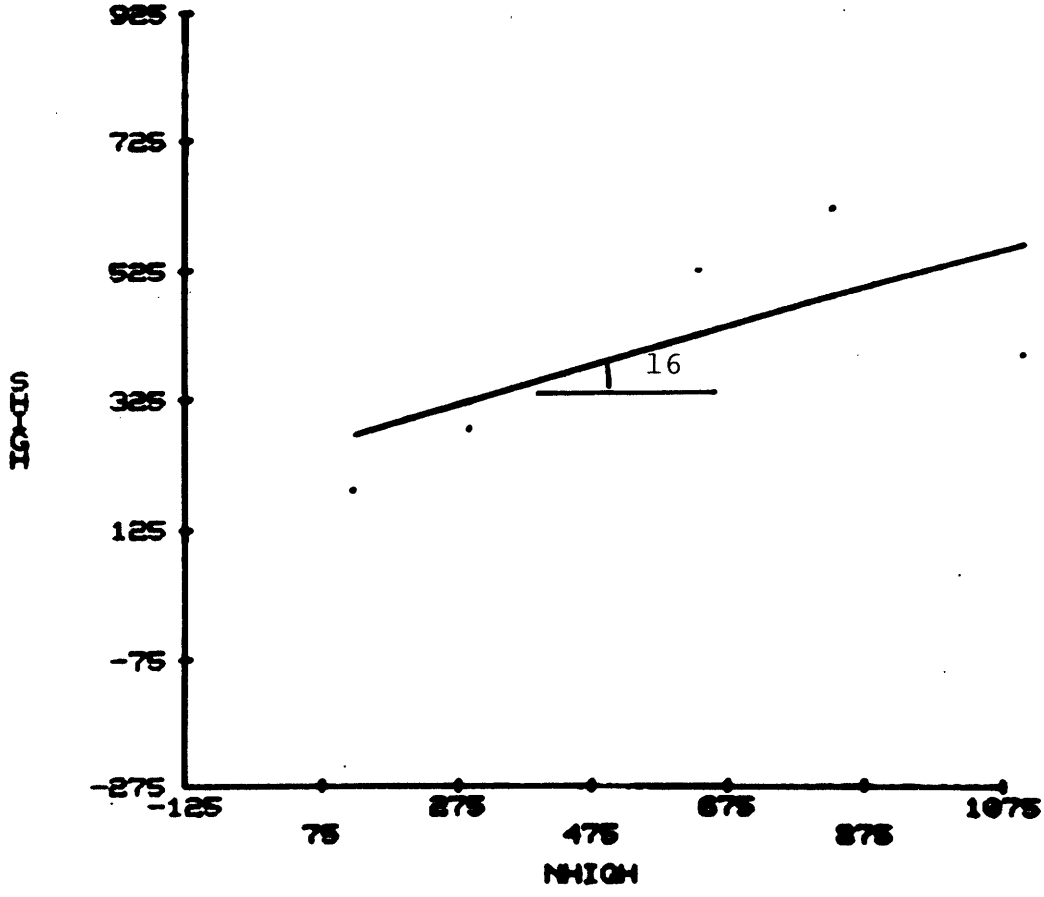

Figure D-24 Peak friction angle of marble with bedding

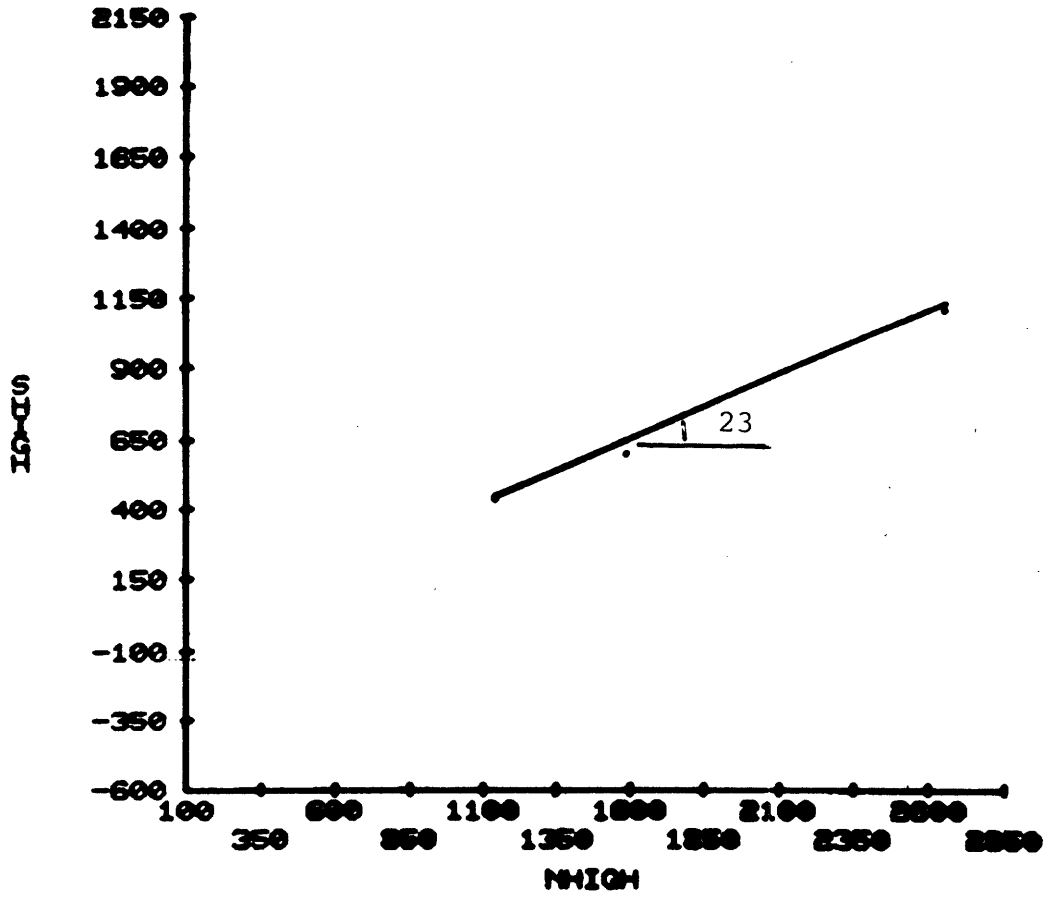

Figure D-25 Peak friction angle of marble with break of test specimen

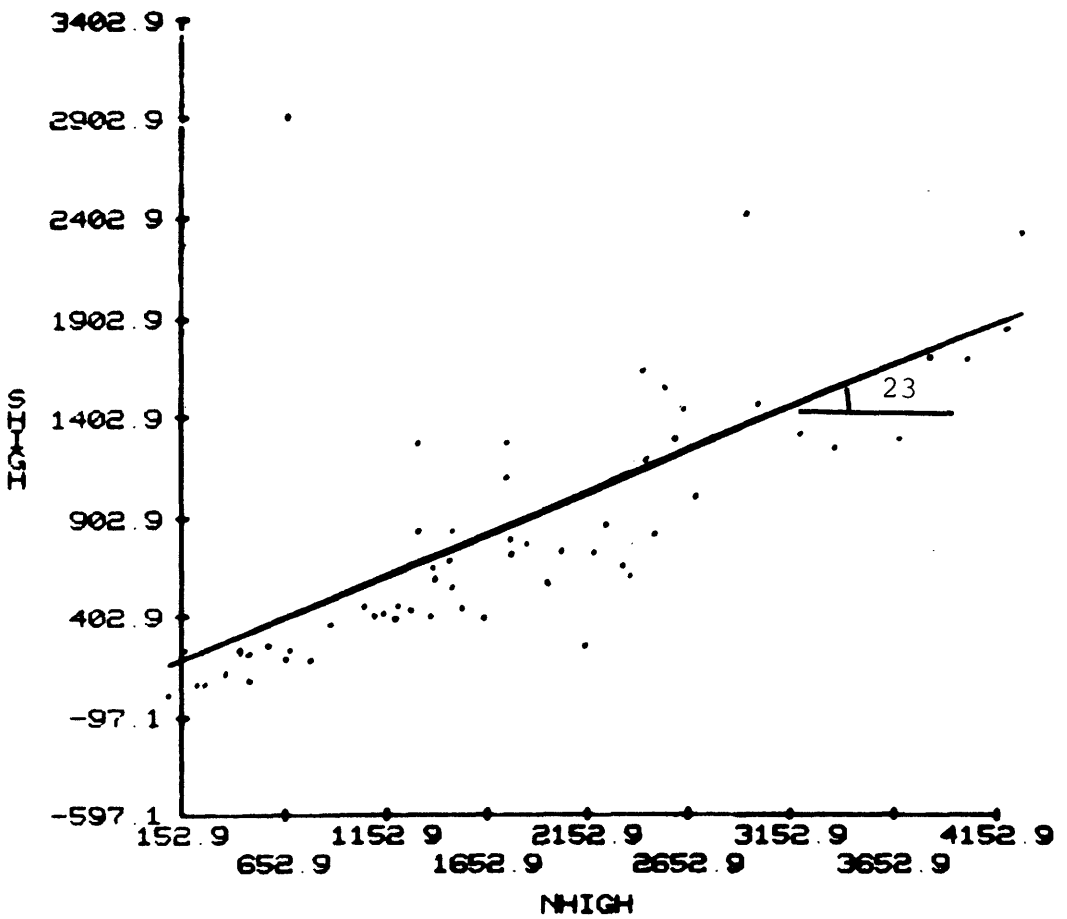

Figure D-26 Peak friction angle of gneiss with foliation

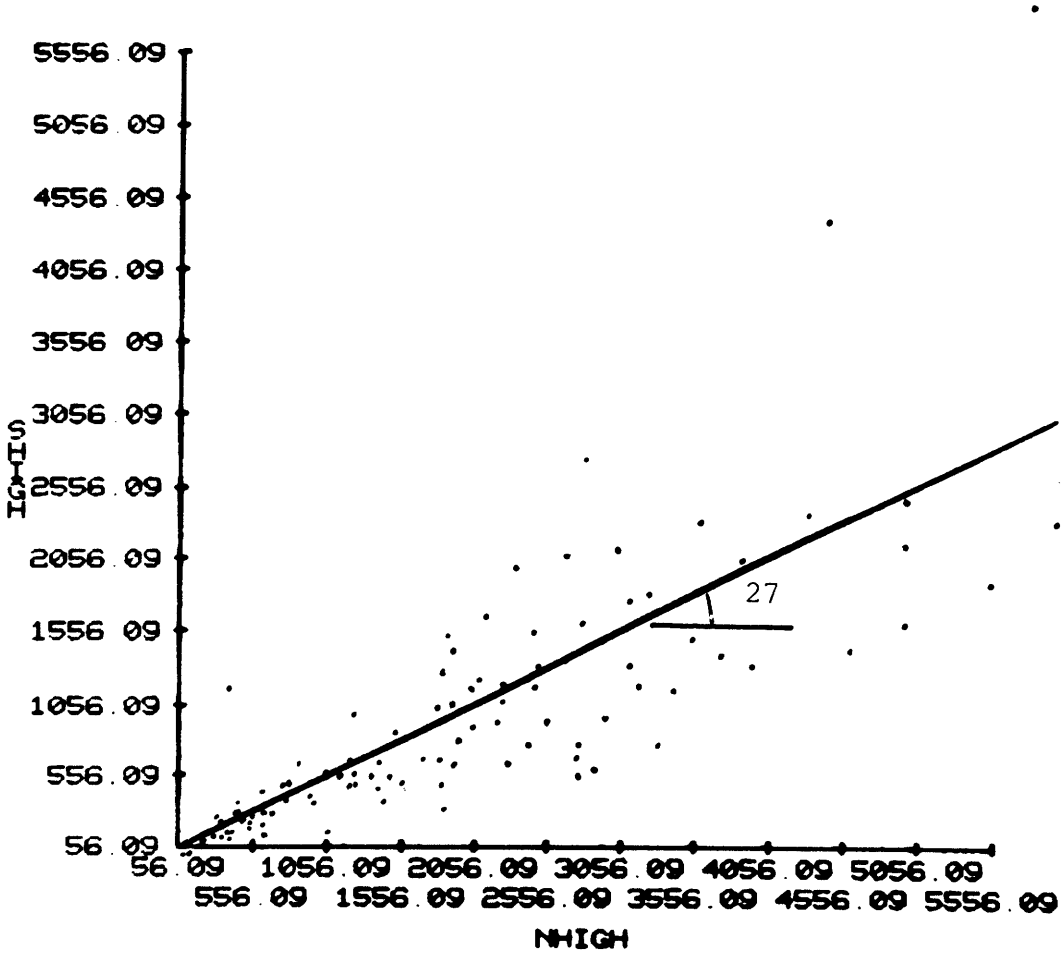

Figure D-27 Peak friction angle of gneiss with joint surface

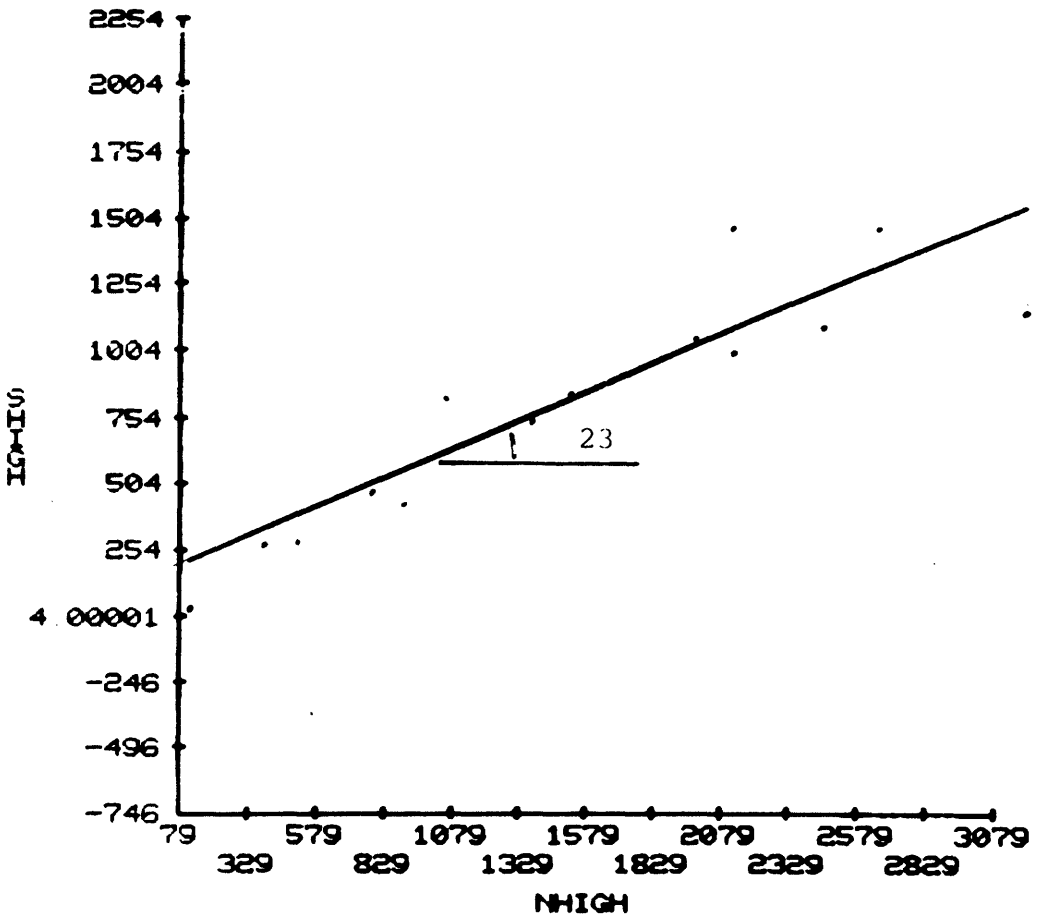

Figure D-28 Peak friction angle of gneiss with sawn surface

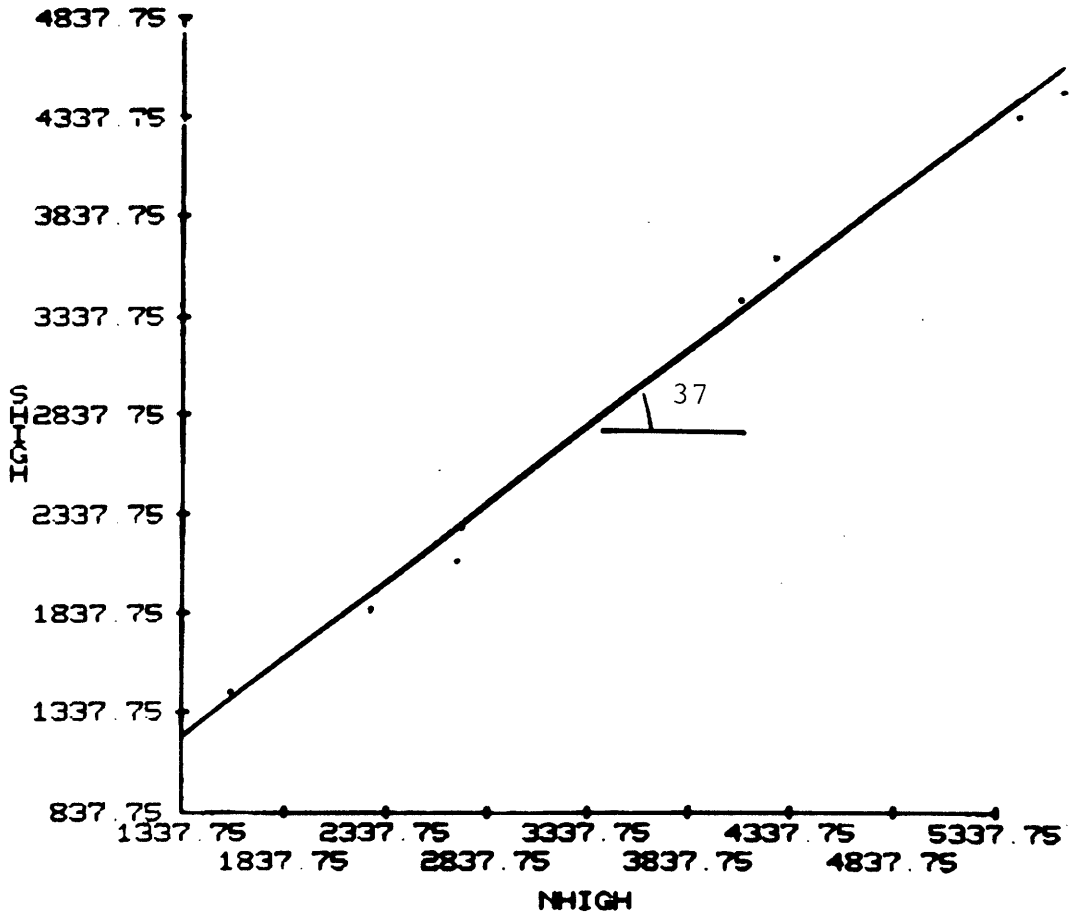

Figure D-29 Peak friction angle of gneiss with separated foliation

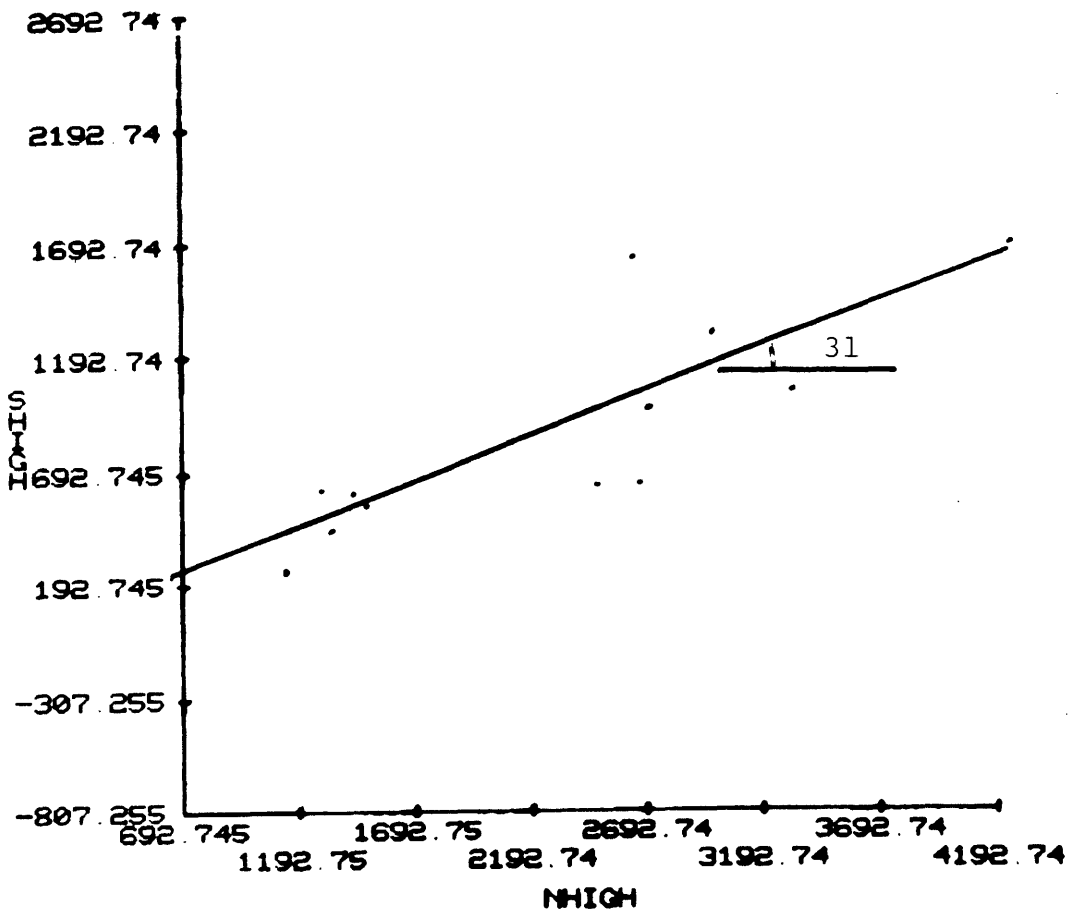

Figure D-30 Peak friction angle of gneiss with fault

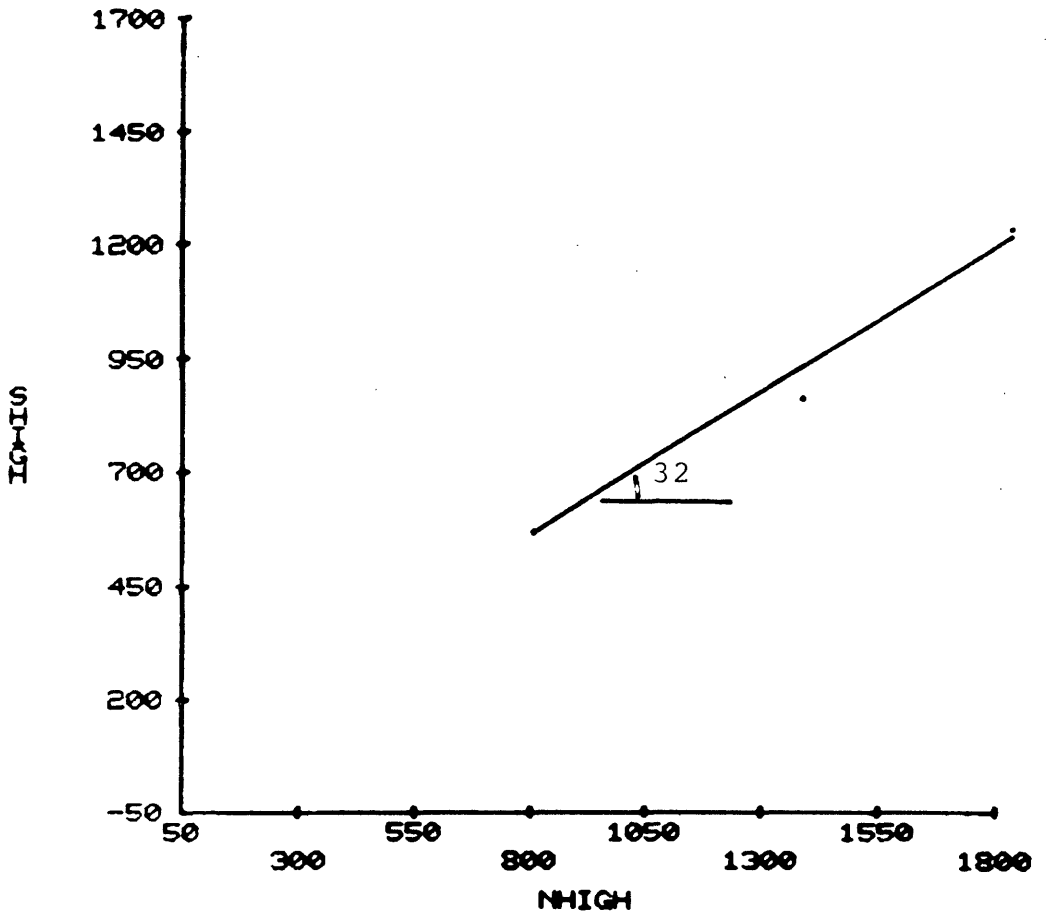

Figure D-31 Peak friction angle of gneiss with slickensided surface

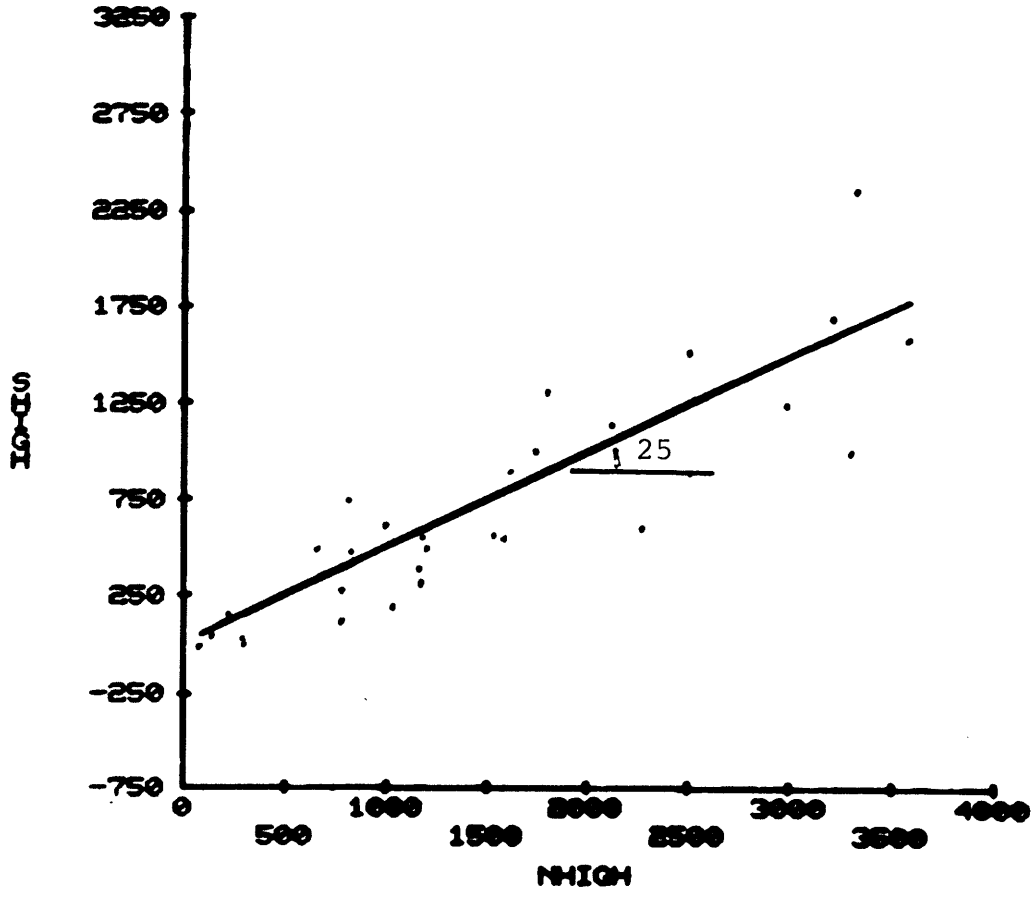

Figure D-32 Peak friction angle of gneiss(schistose) with foliation

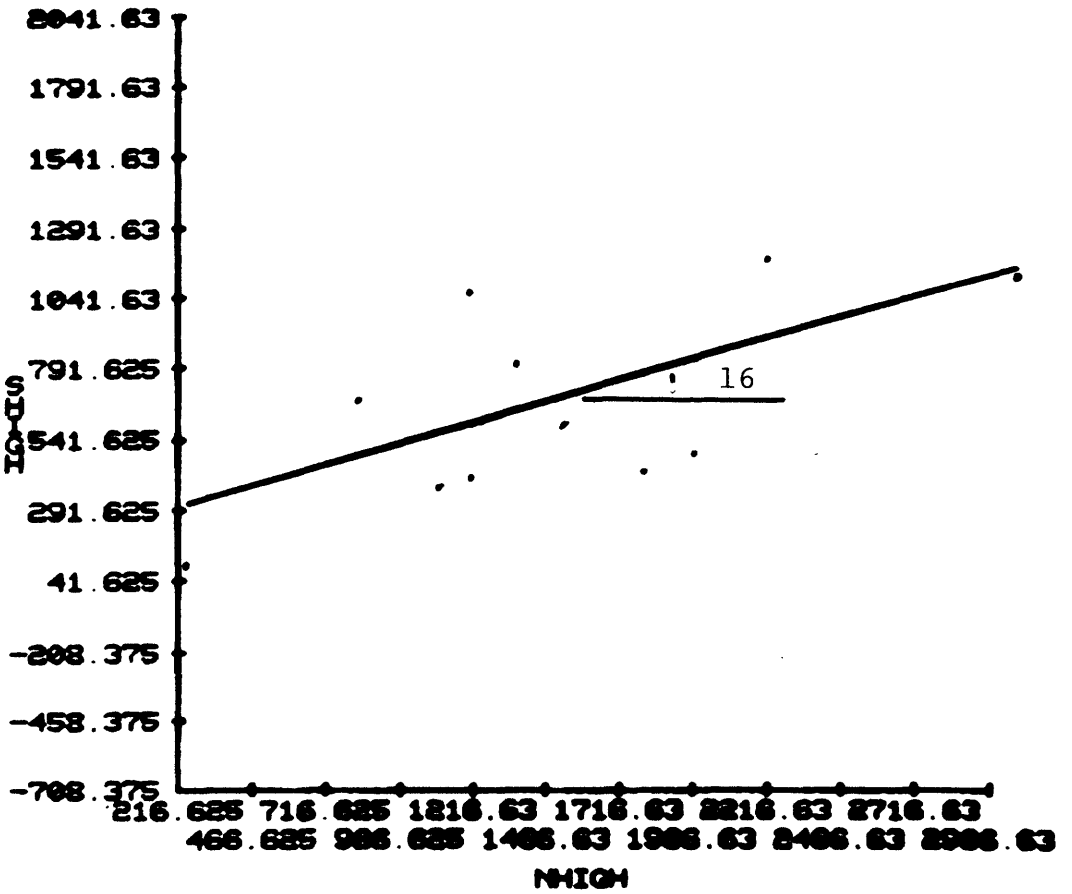

Figure D-33 Peak friction angle of gneiss (schistose) with joint surface

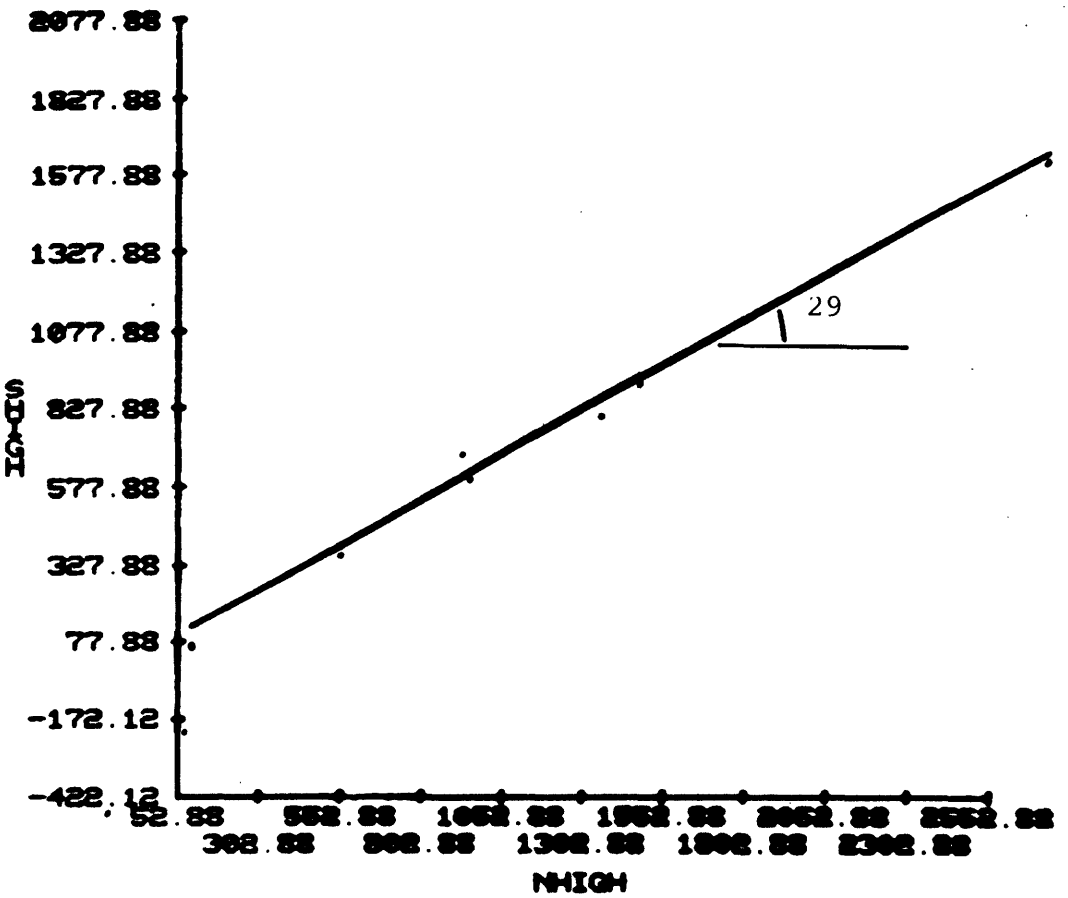

Figure D-34 Peak friction angle of gneiss (schistose) with sawn surface

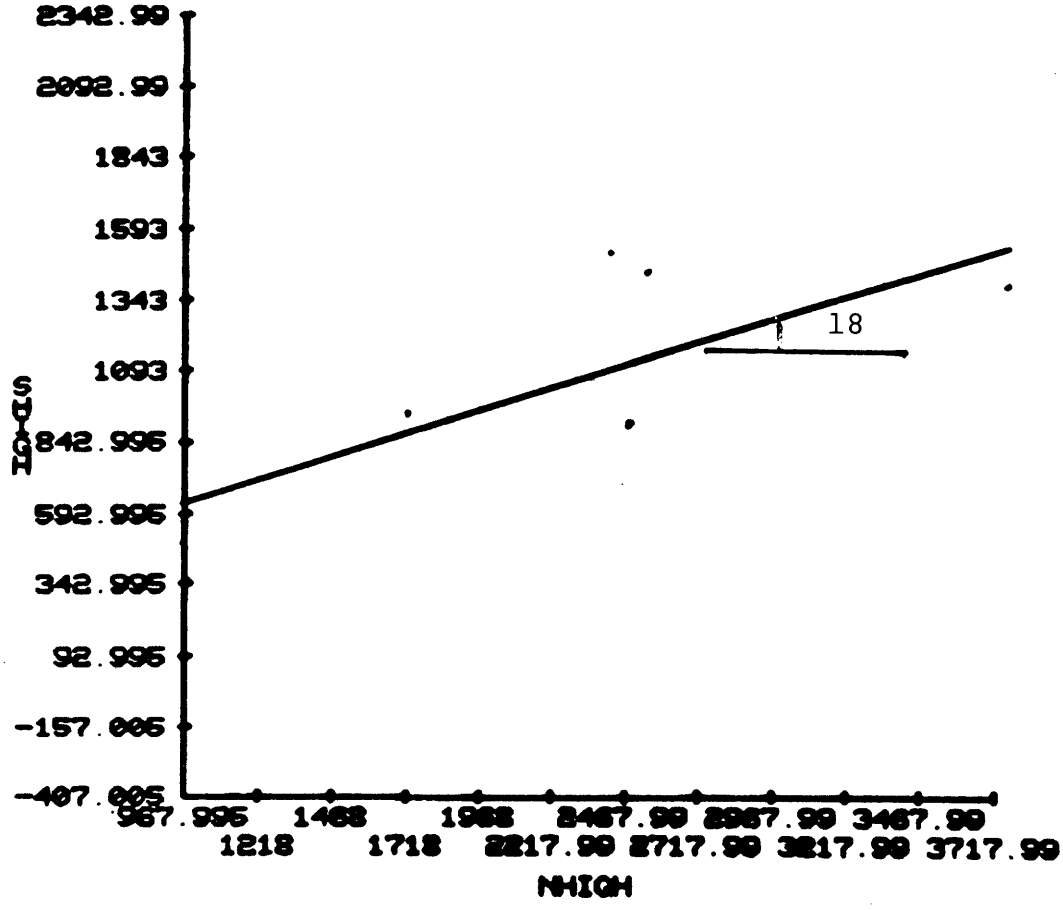

Figure D-35 Peak friction angle of schist (carboniferous) with fault

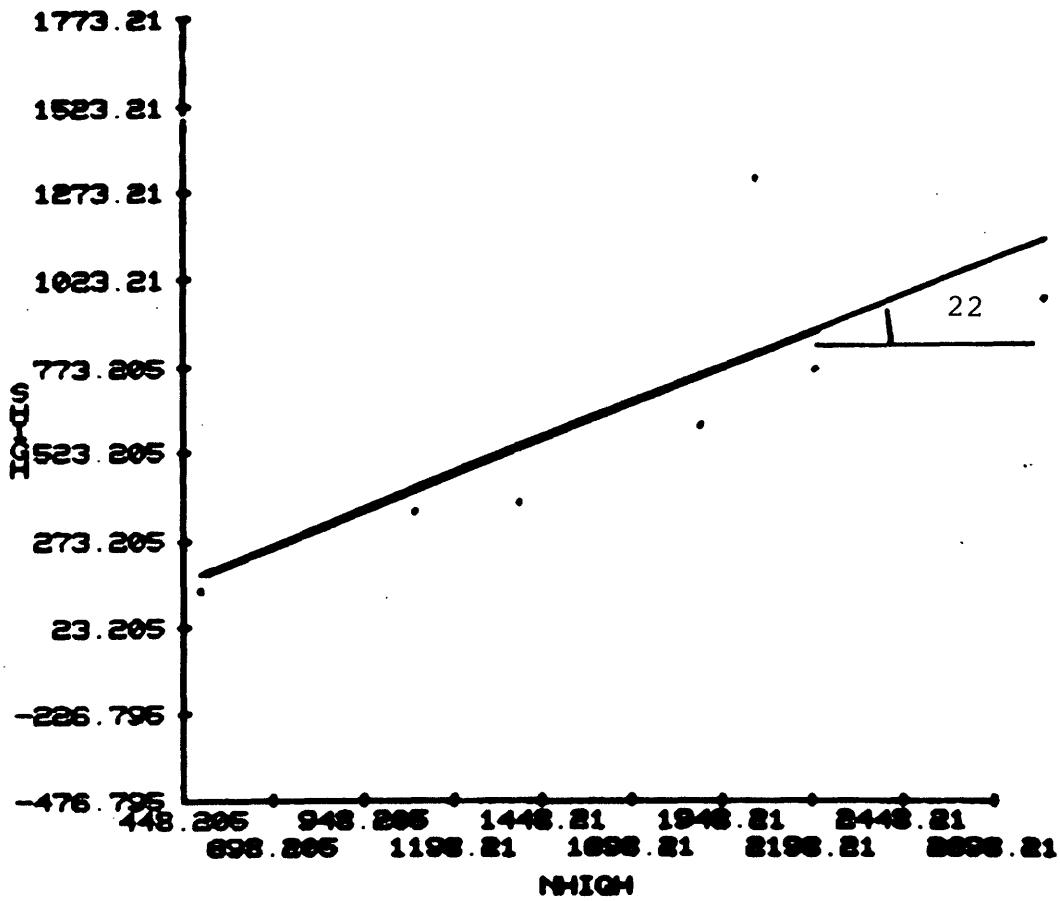

Figure D-36 Peak friction angle of schist (carboniferous) with foliation

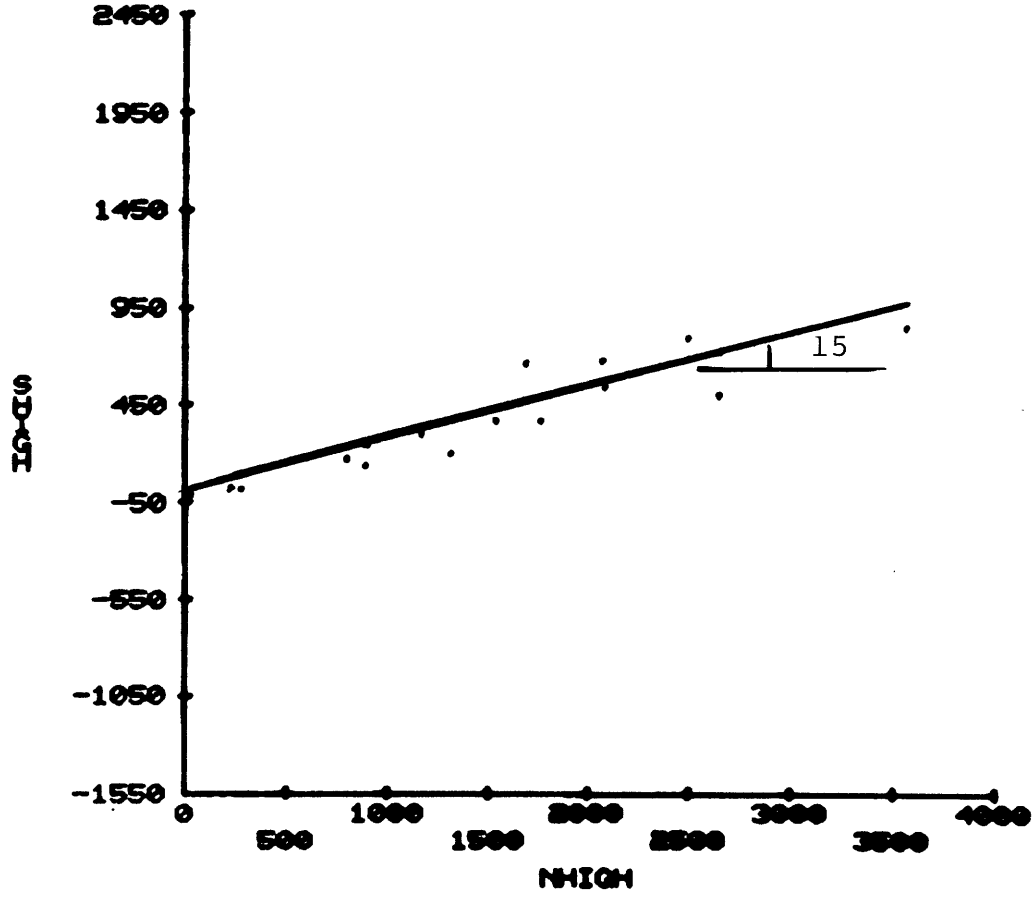

Figure D-37 Peak friction angle of schist(sericite) with joint surface

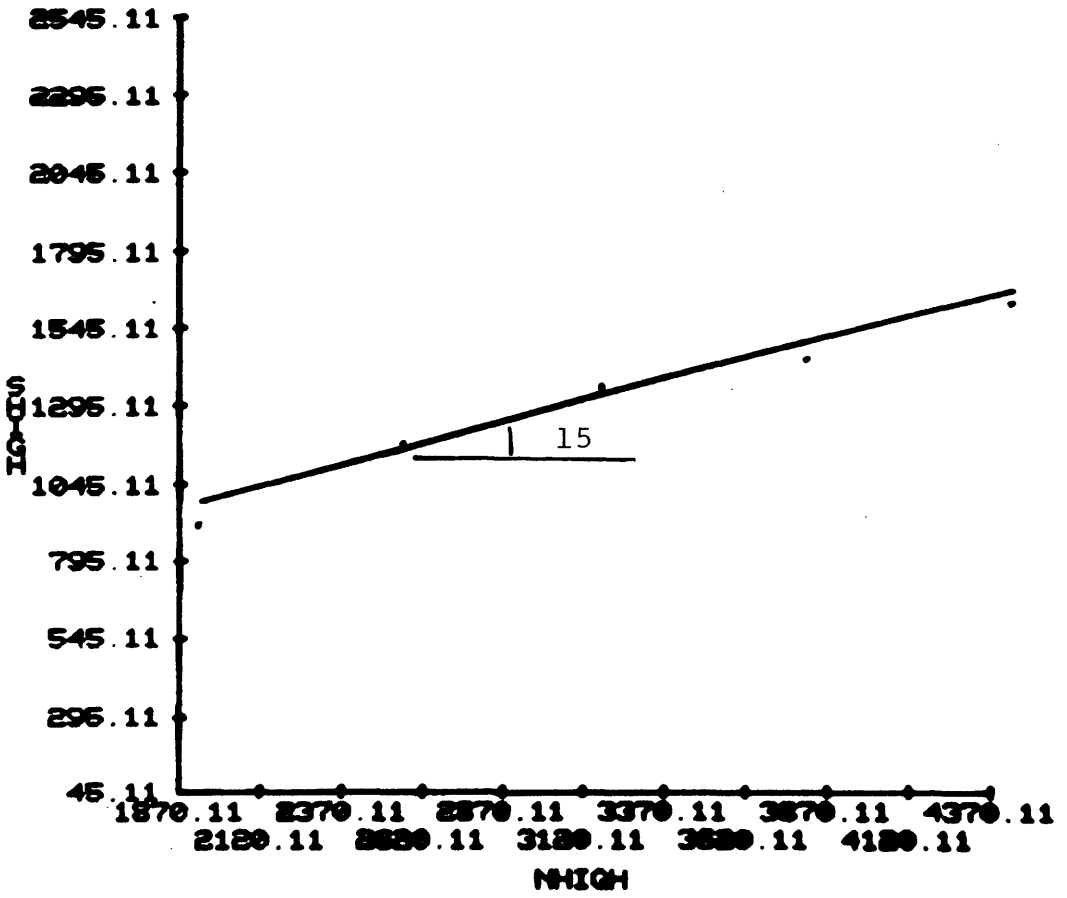

Figure D-38 Peak friction angle of basalt with bedding

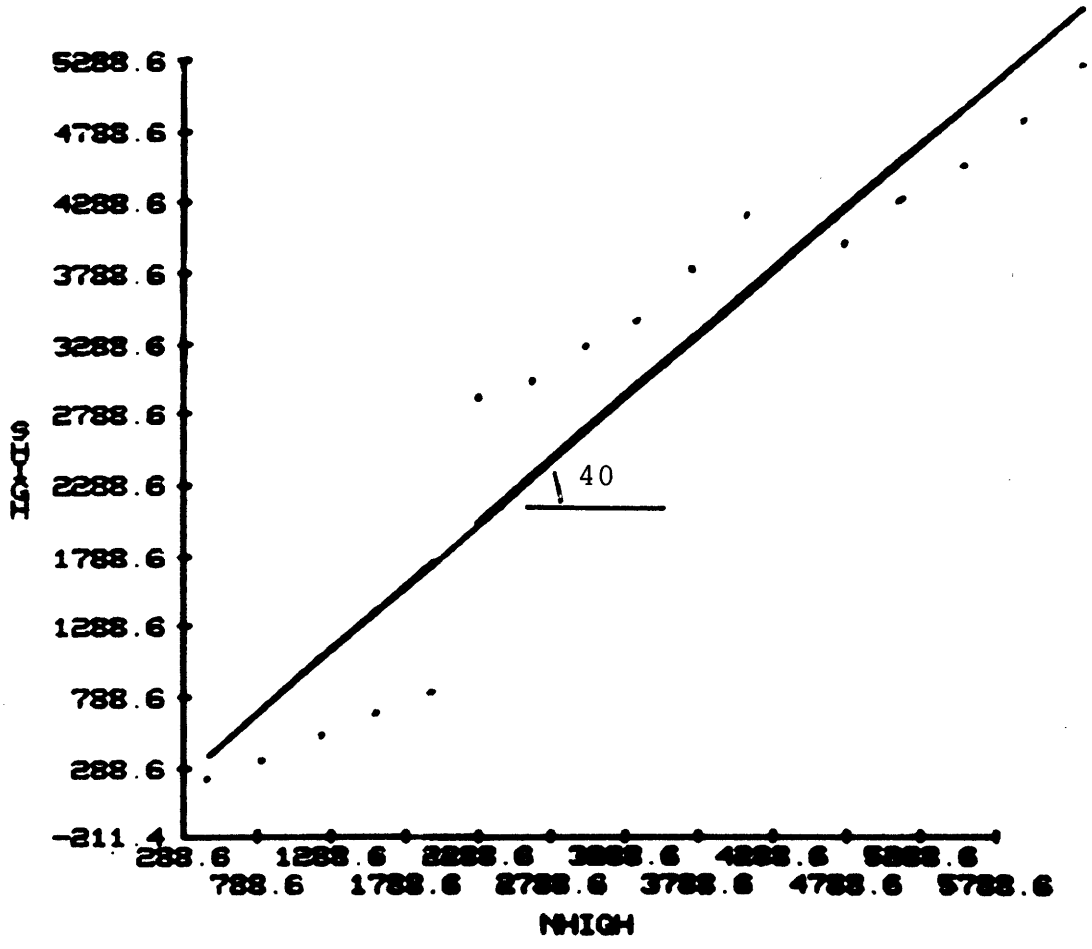

Figure D-39 Peak friction angle of basalt with fractures

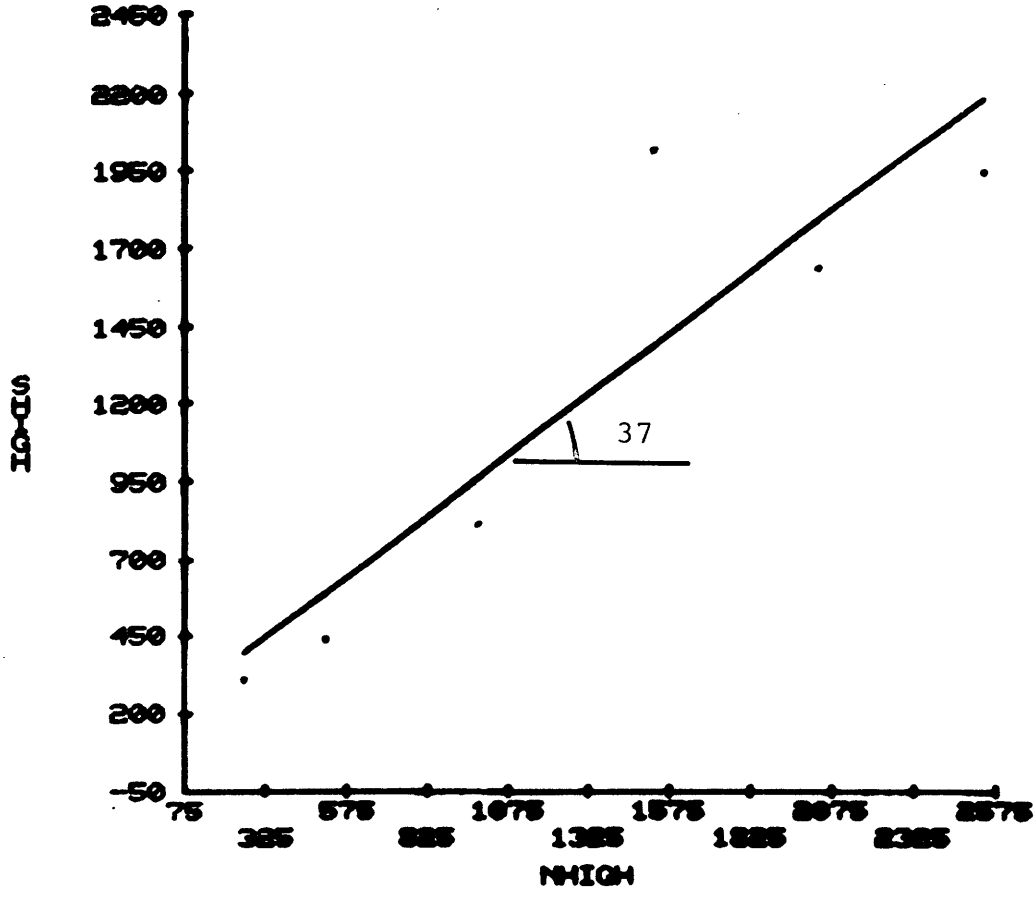

Figure D-40 Peak friction angle of dacite with sawn surface

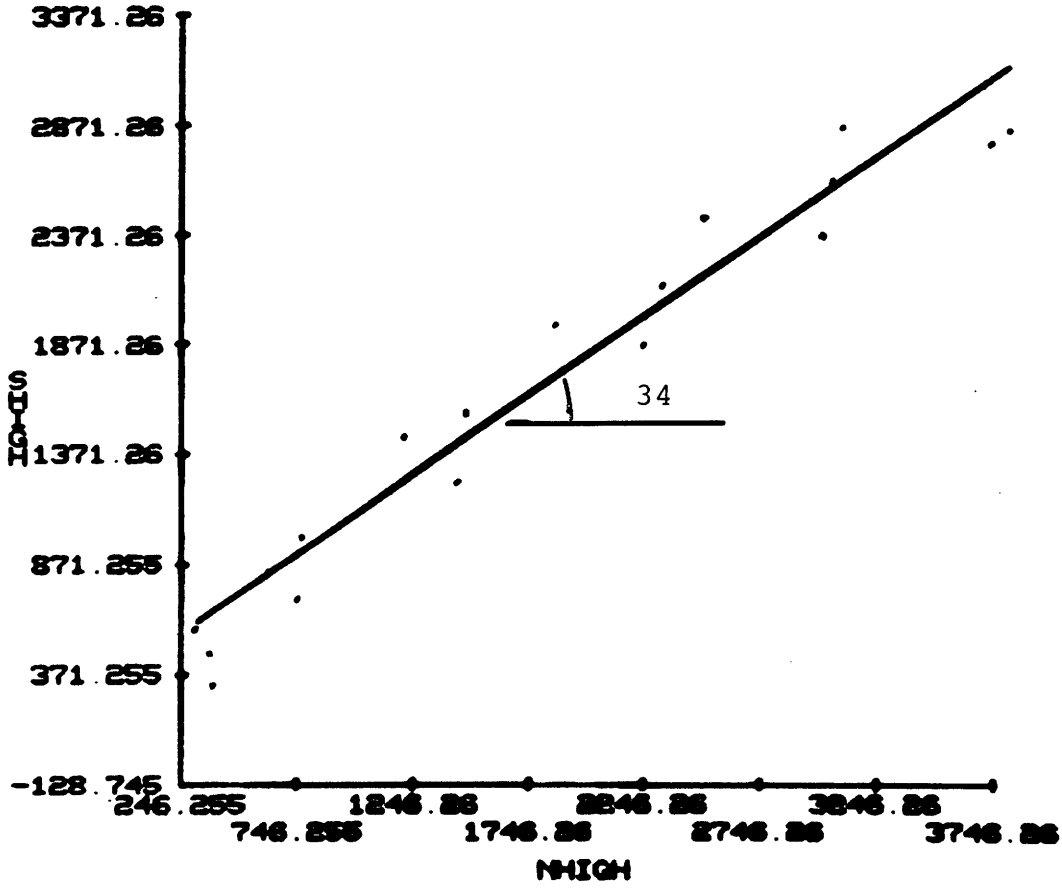

Figure D-41 Peak friction angle of dacite with fractures

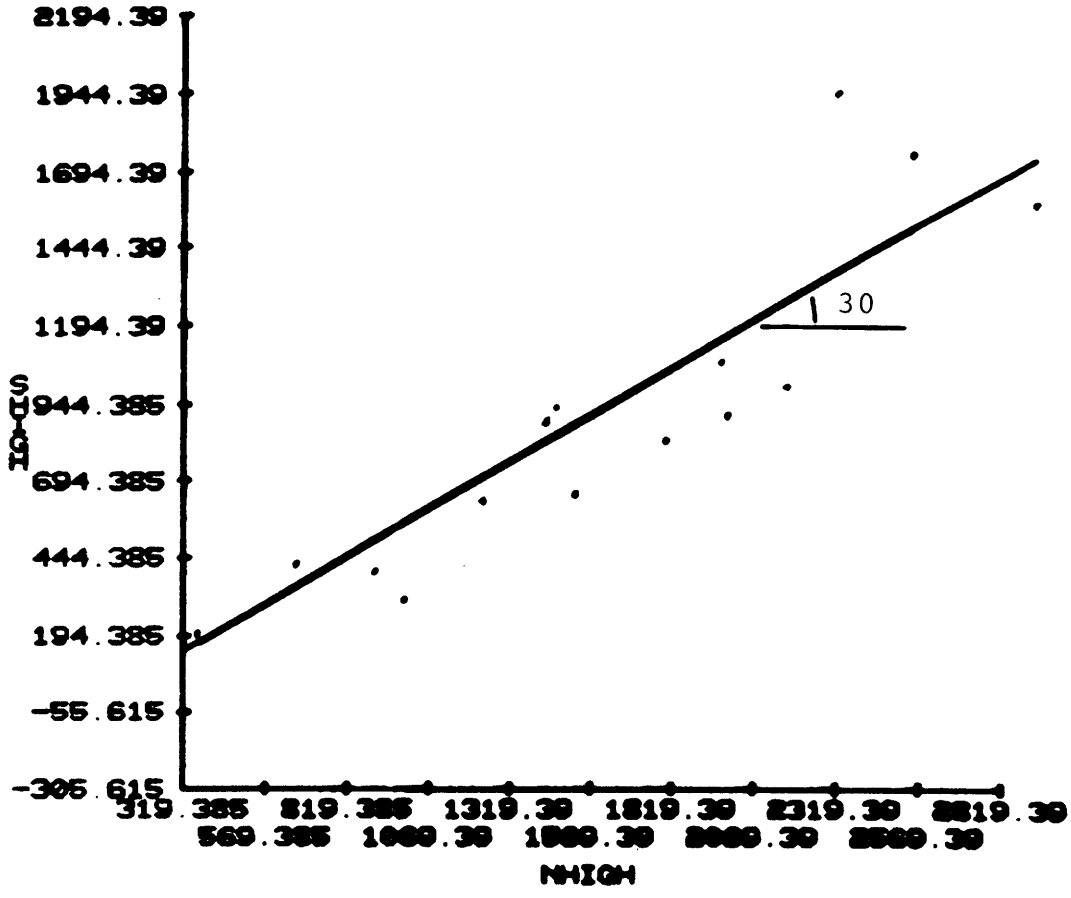

Figure D-42 Peak friction angle of porphyry (quarzite) with joint surface

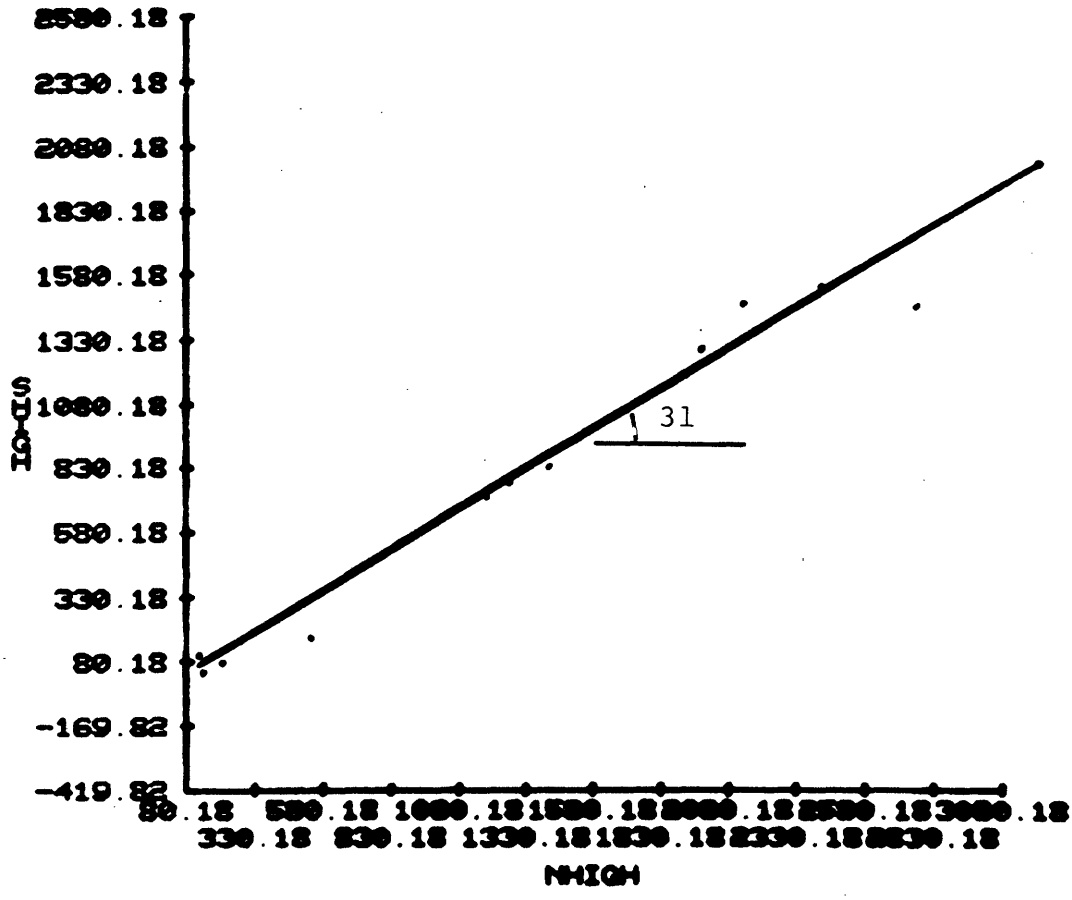

Figure D-43 Peak friction angle of porphyry (quarzite) with foliation

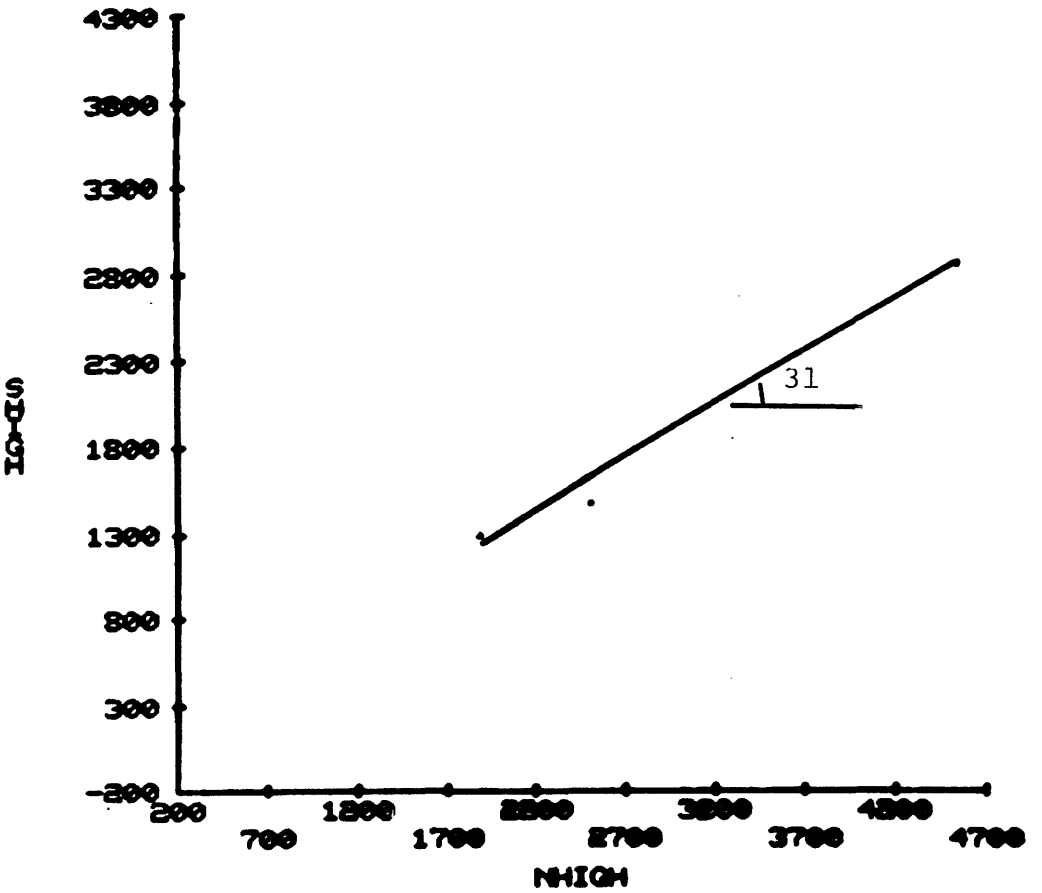

Figure D-44 Peak friction angle of granite with contact between granite and mylonite

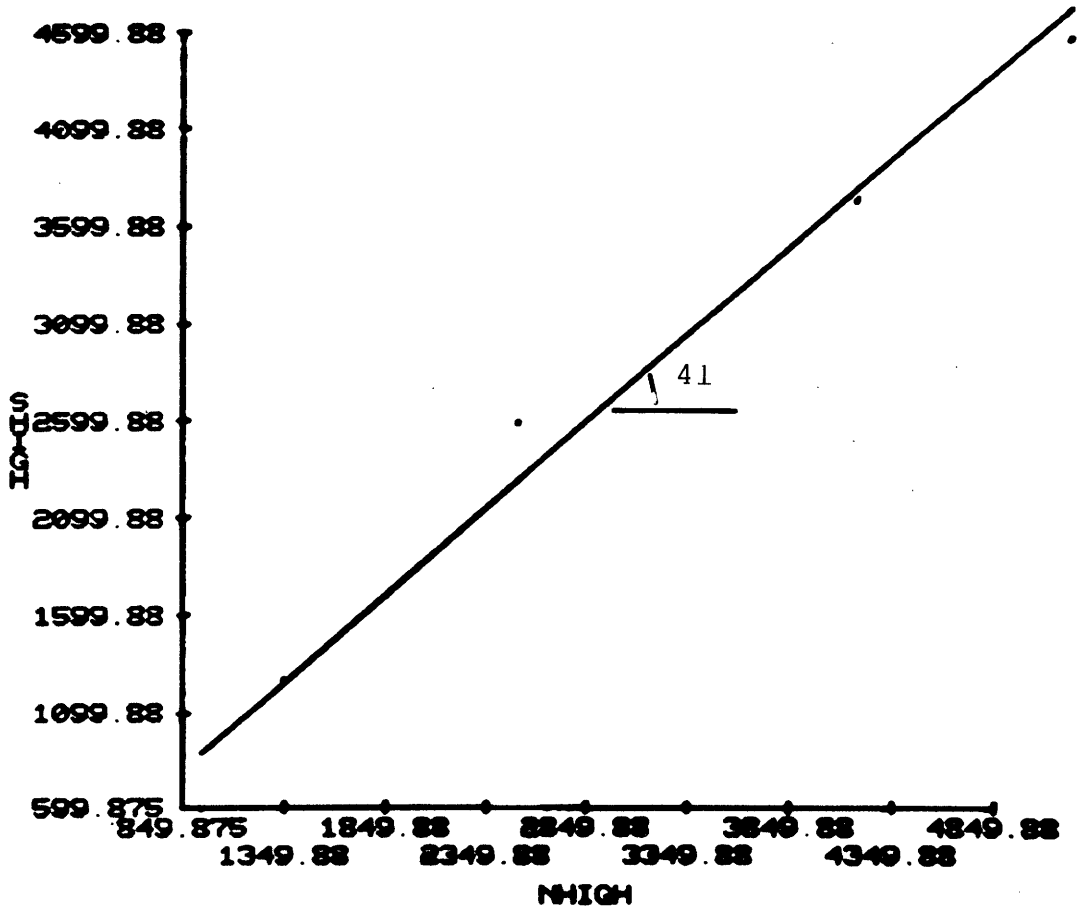

Figure D-45 Peak friction angle of granite with joint surface

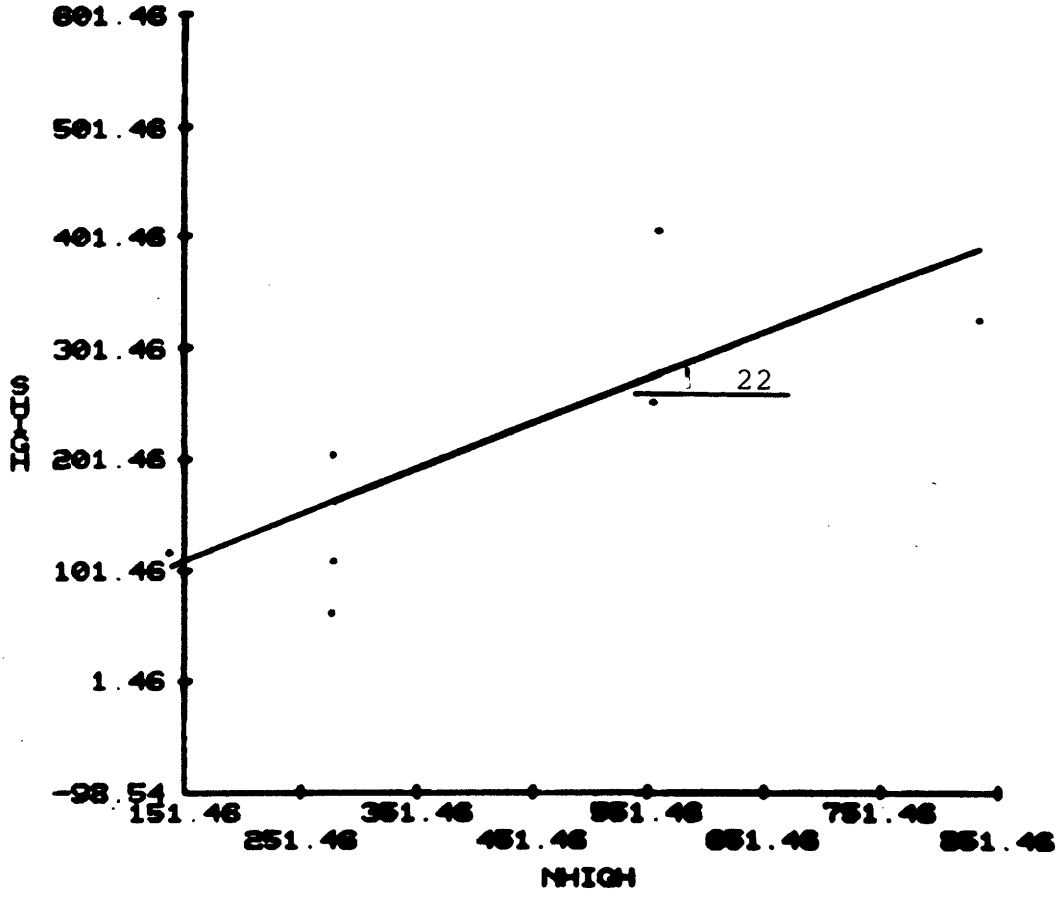

Figure D-46 Peak friction angle of claystone with non-oriented lamination

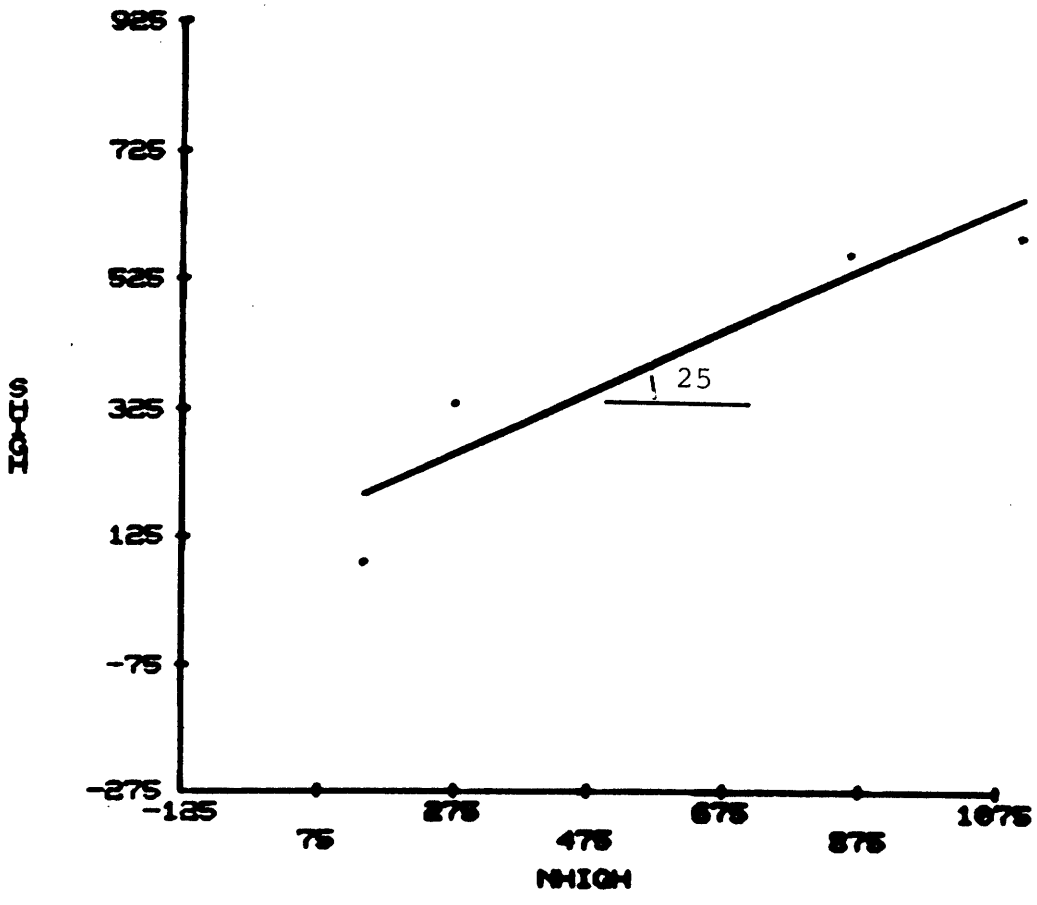

Figure D-47 Peak friction angle of claystone with oriented lamination

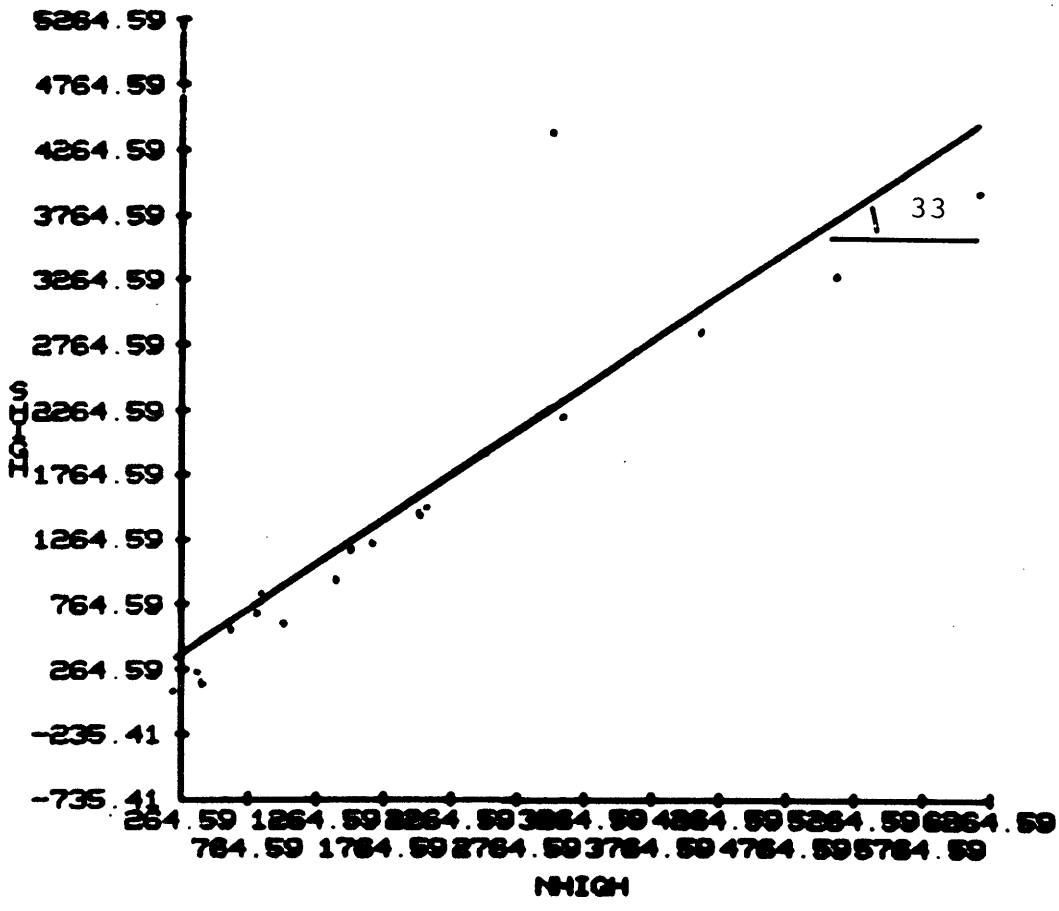

Figure D-48 Peak friction angle of monzonite (quarz) with joint surface

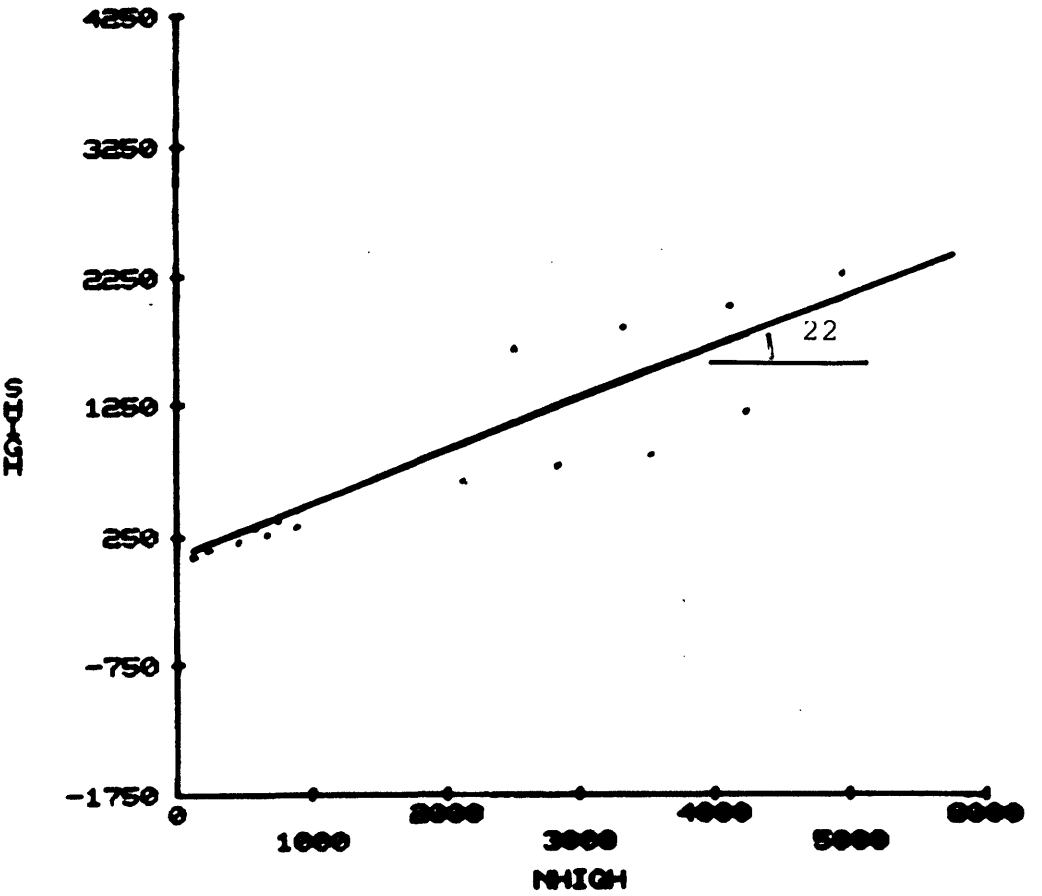

Figure D-49 Peak friction angle of tuff with bedding

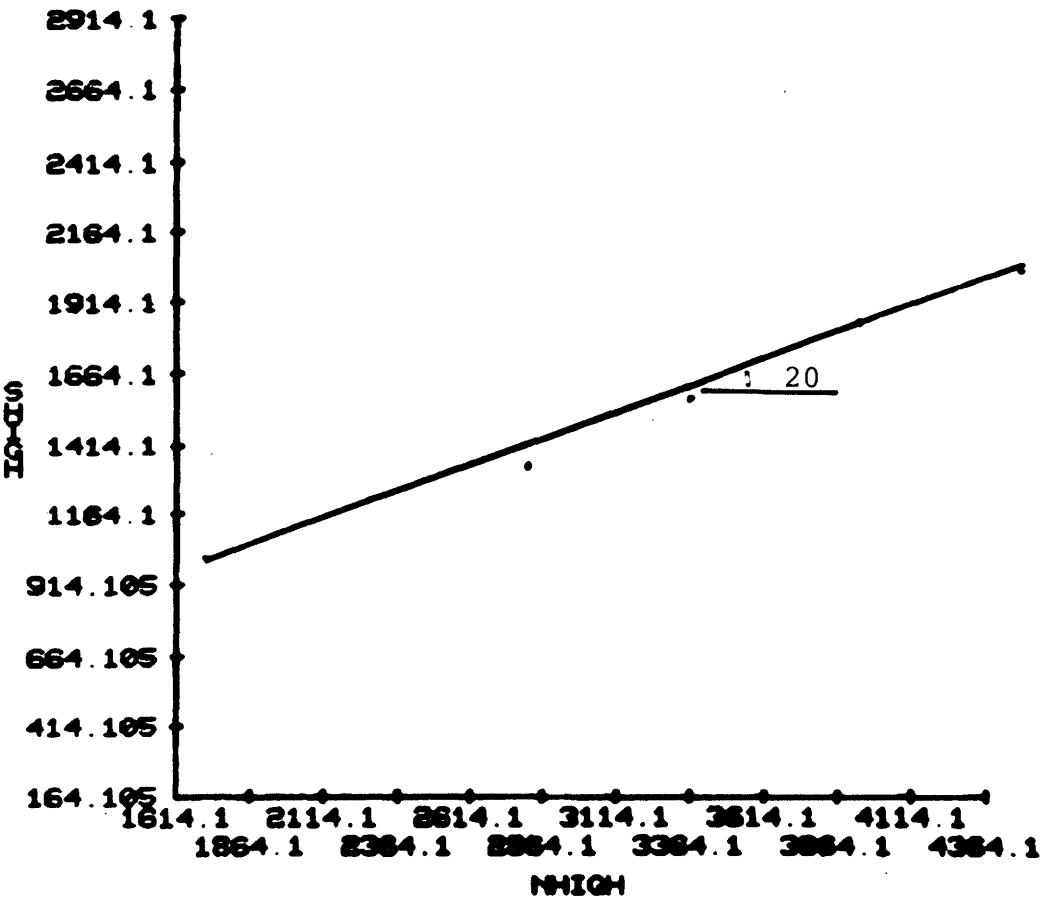

Figure D-50 Peak friction angle of tuff with fractures

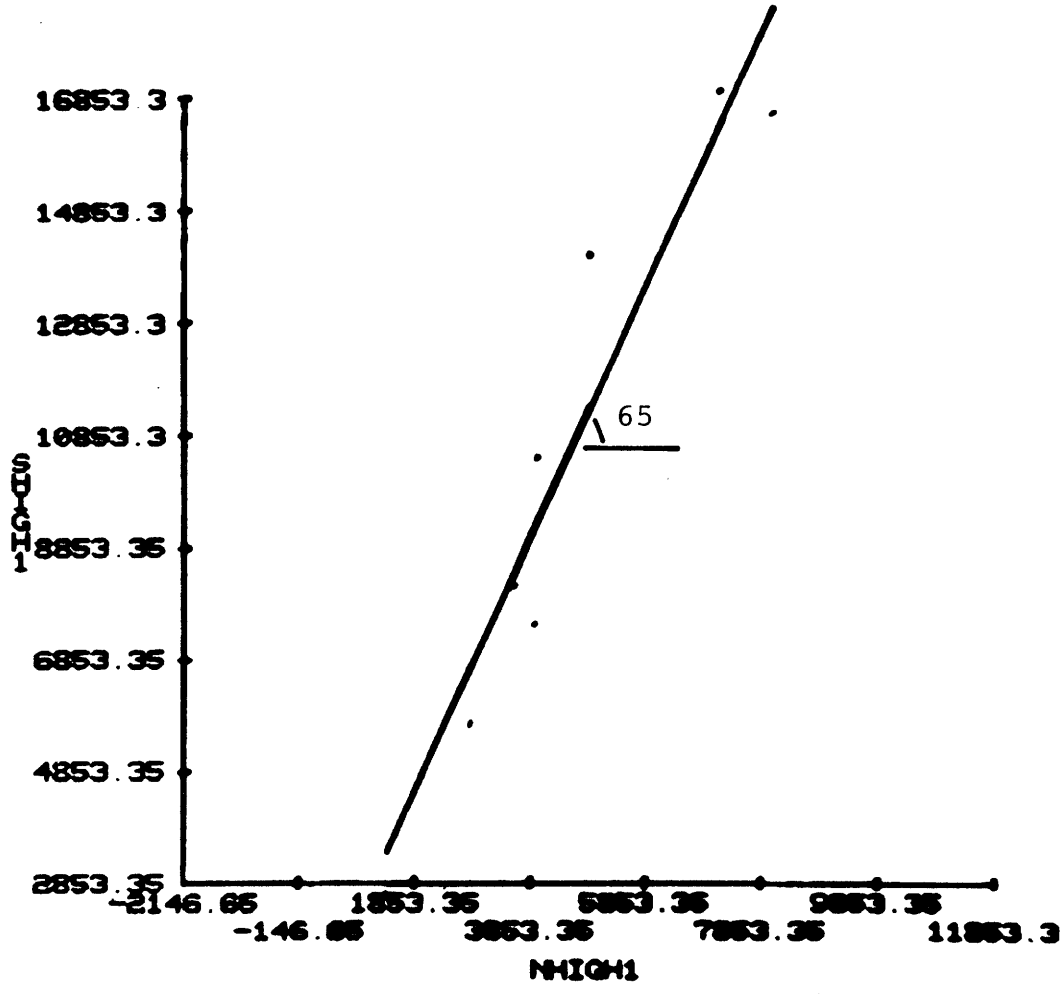

Figure D-51 Peak friction angle of metashale with healed joint

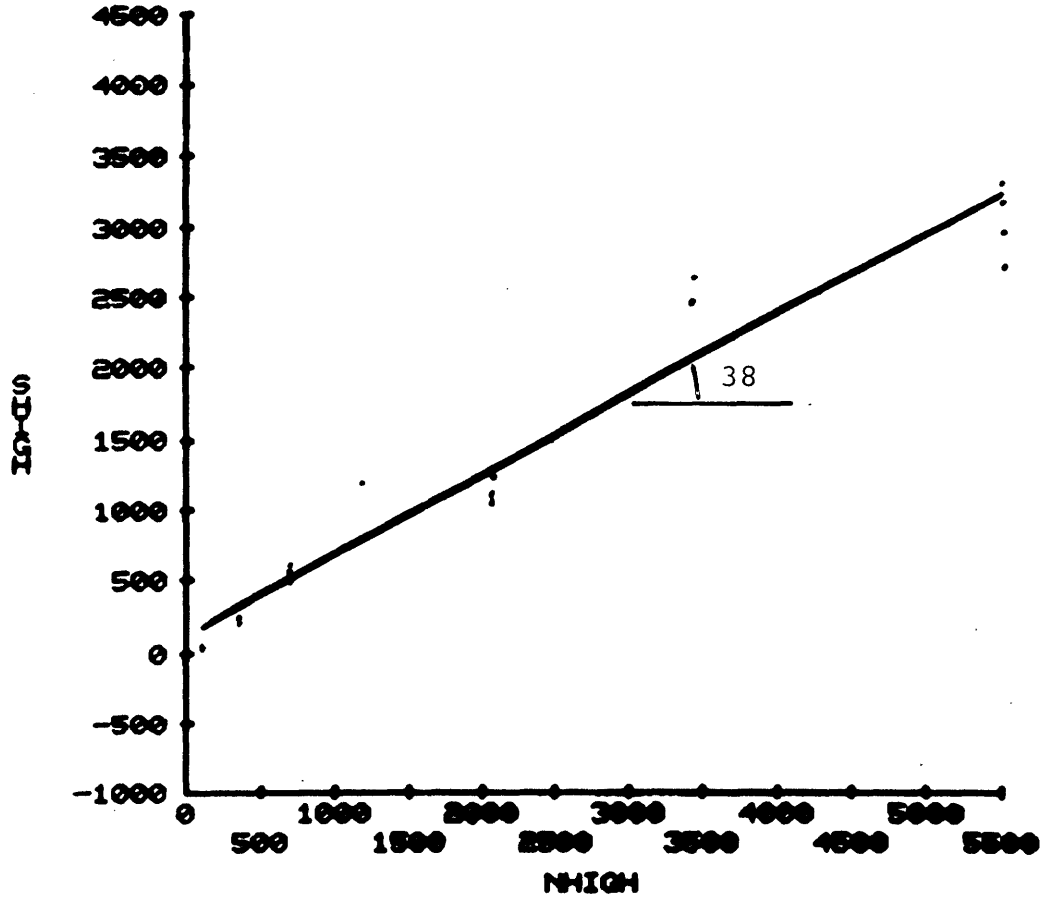

Figure D-52 Peak friction angle of micro-granodiorite with artificial grouted joint

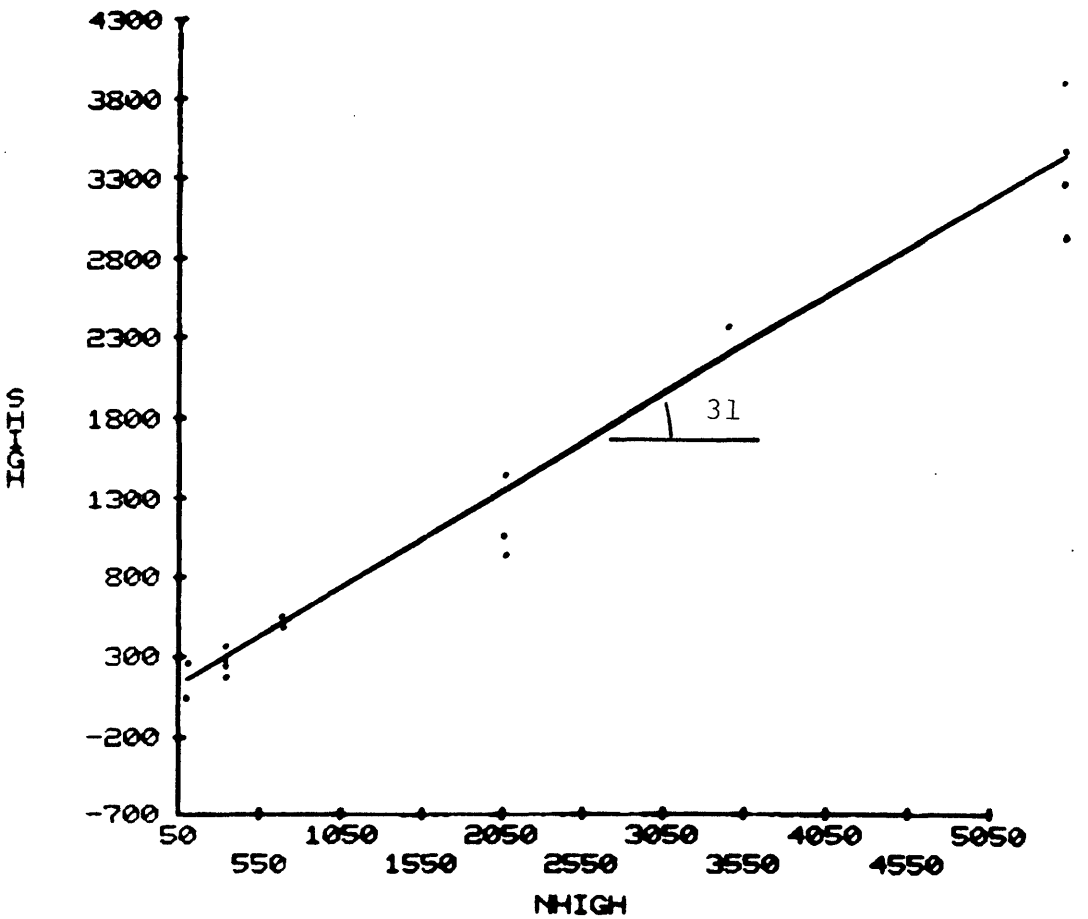

Figure D-53 Peak friction angle of monzonite with artificial grouted joint

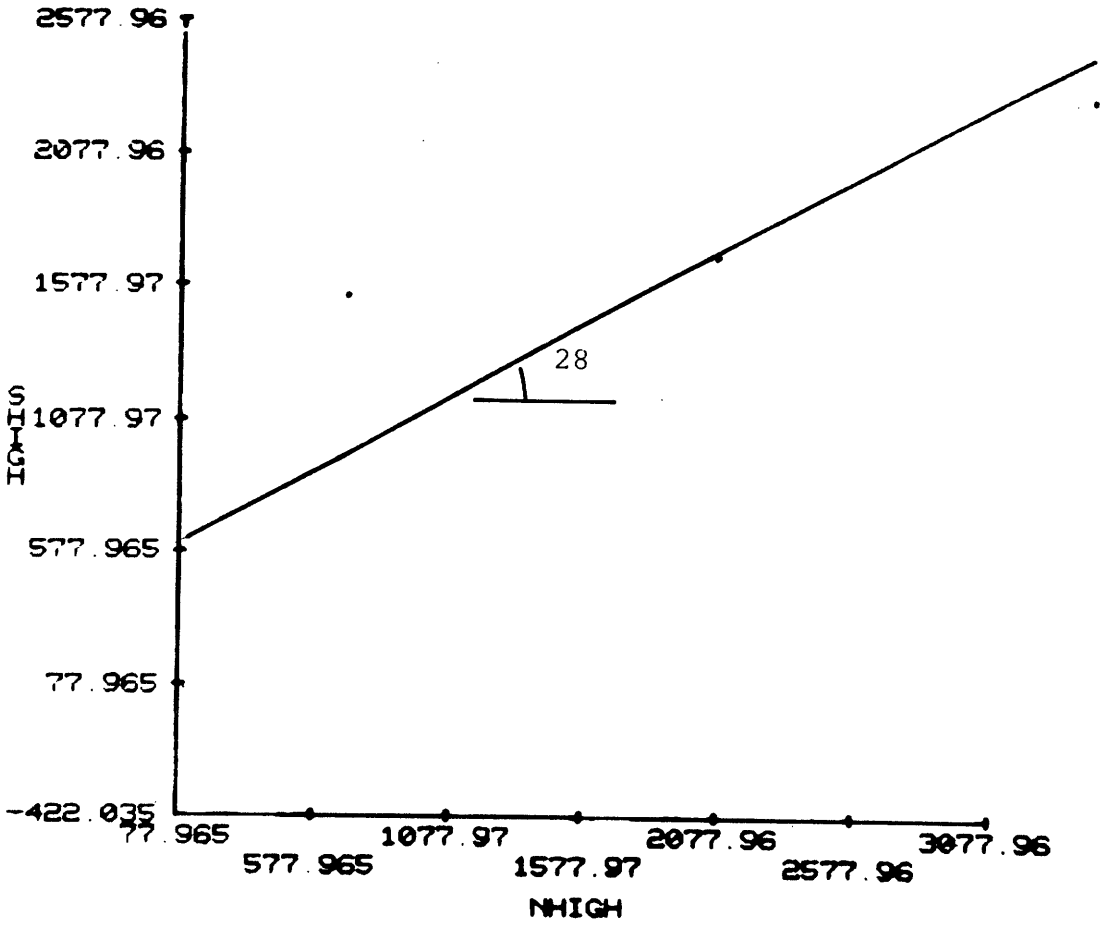

Figure D-54 Peak friction angle of monzonite with natural grouted joint

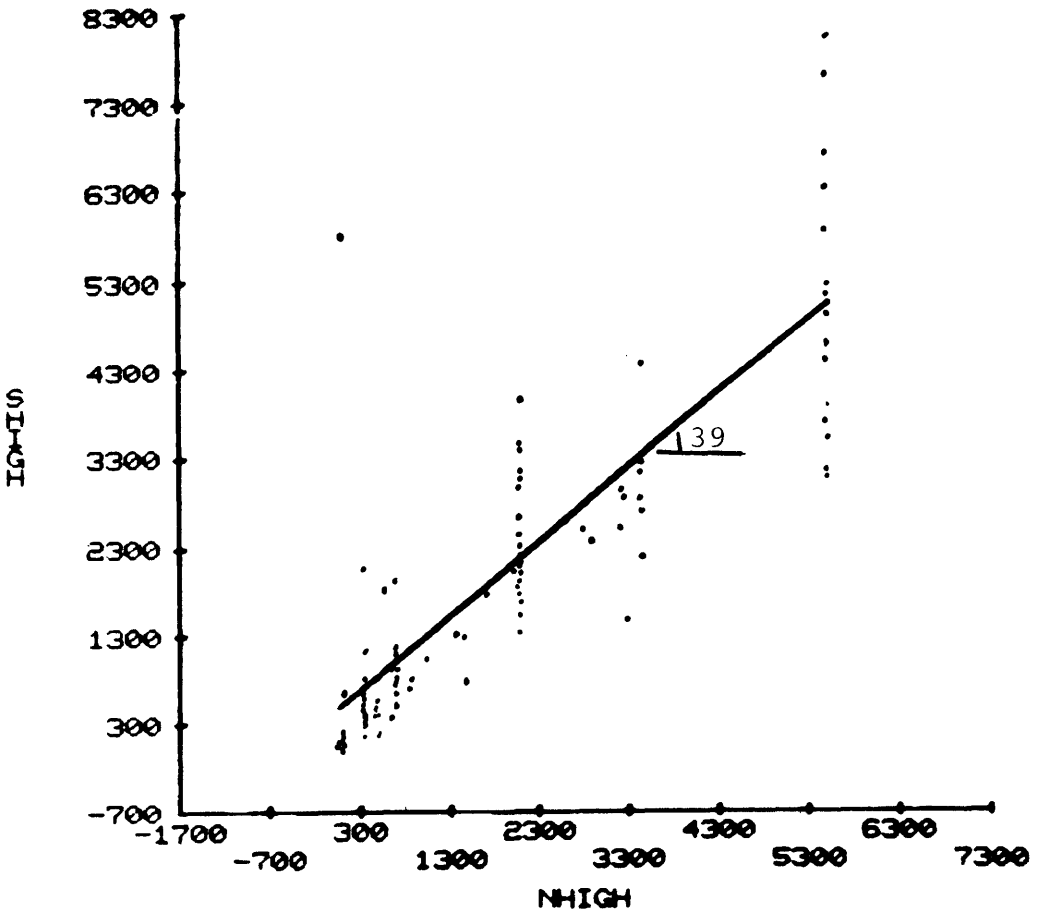

Figure D-55 Peak friction angle of monzonite with joint surface

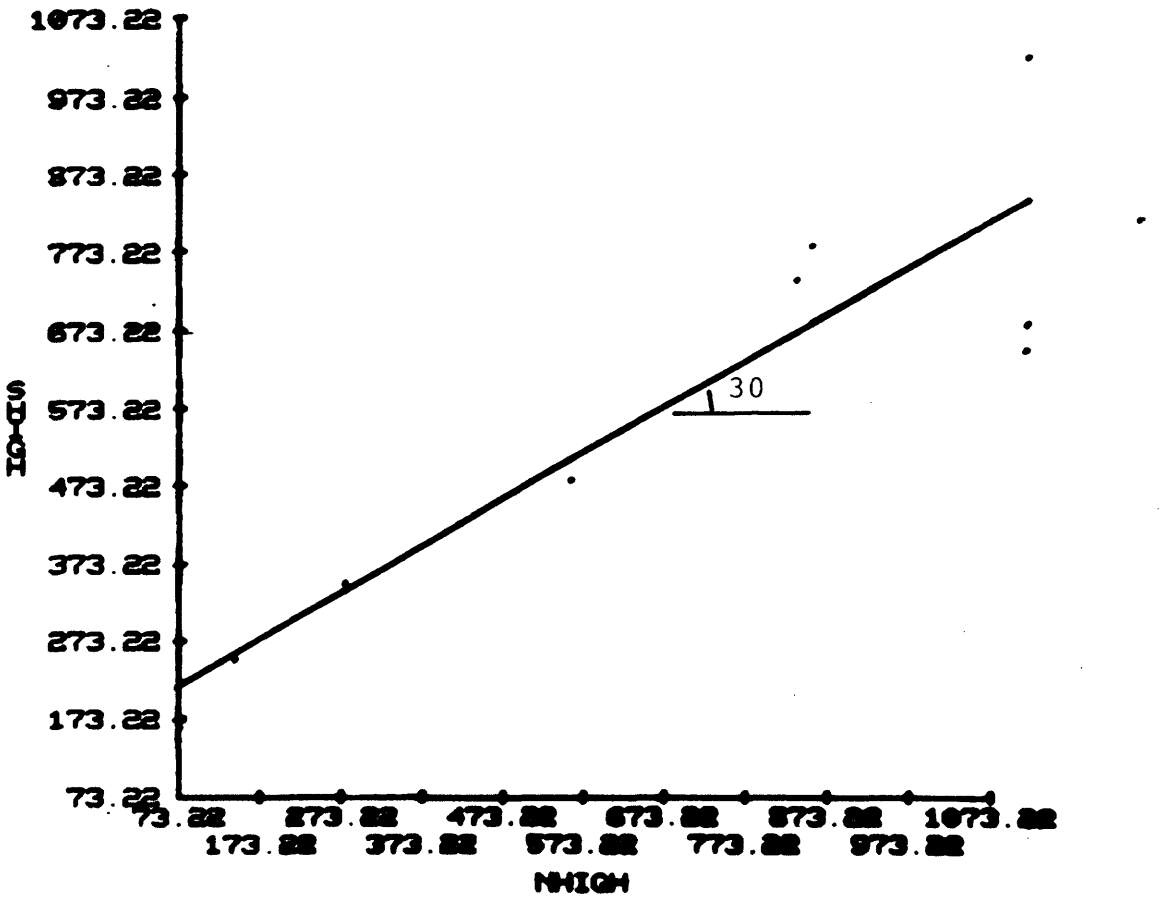

Figure D-56 Peak friction angle of intact lignite

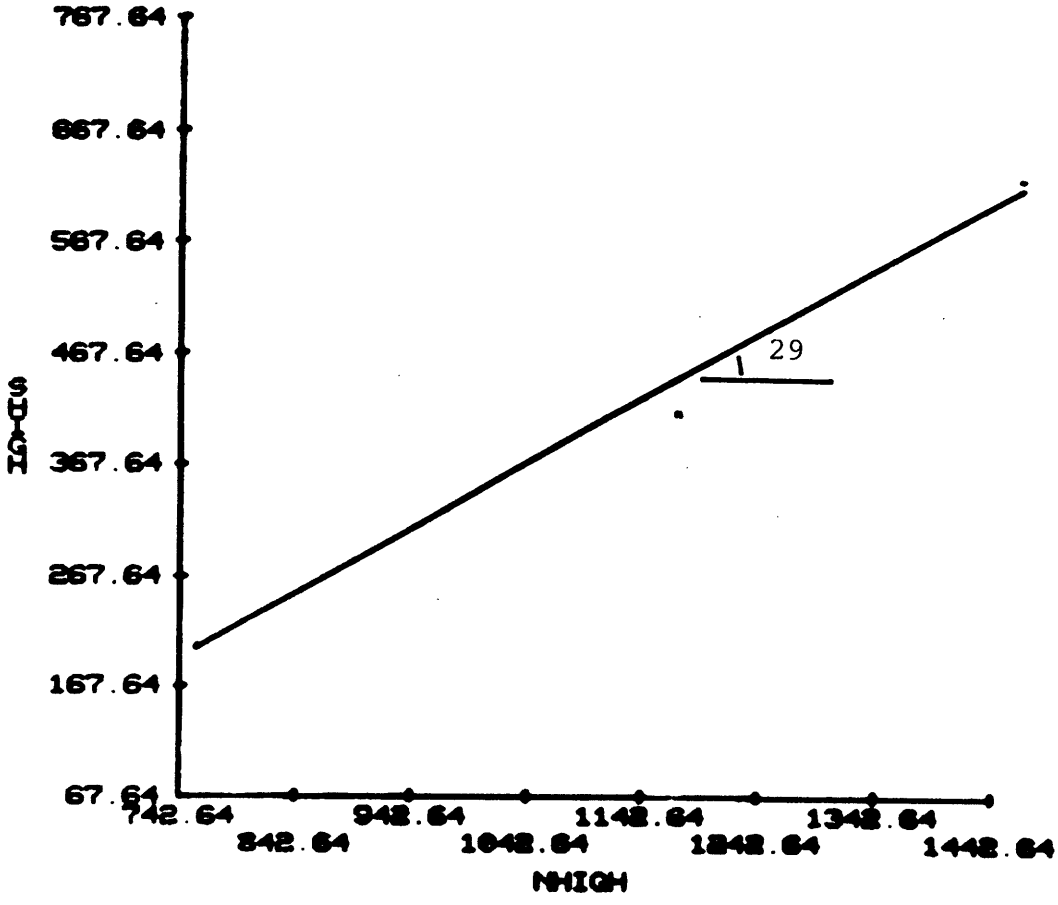

Figure D-57 Peak friction angle of sericite with foliation

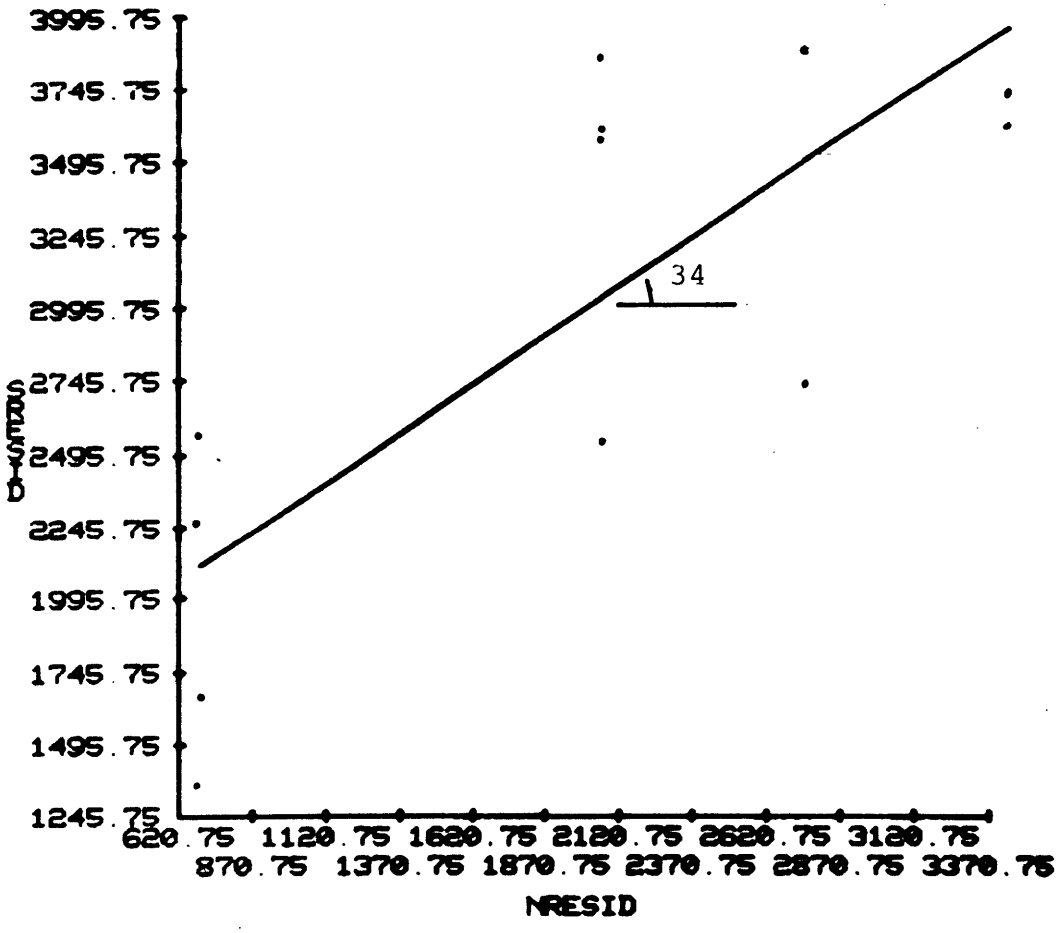

Figure D-58 Residual fr_ction angle of amphibolite with joint surface

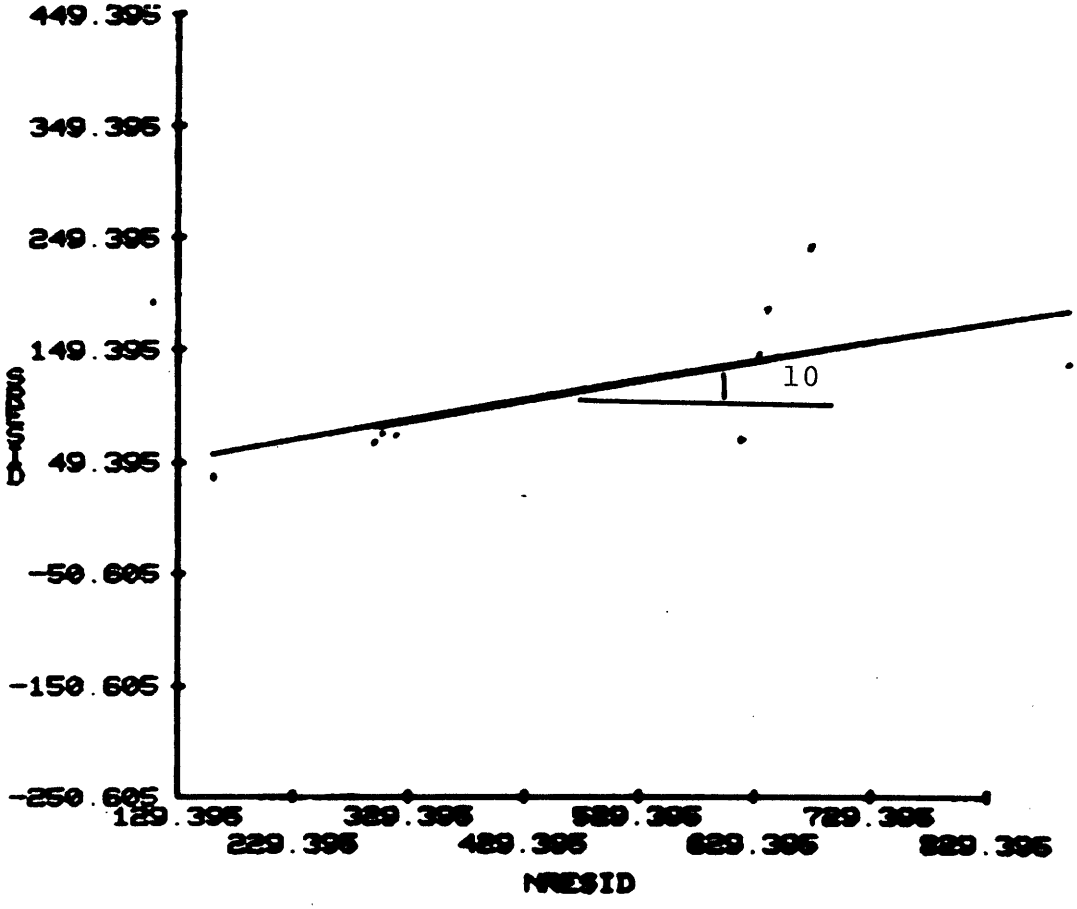

Figure D-59 residual friction angle of claystone with non-oriented lamination

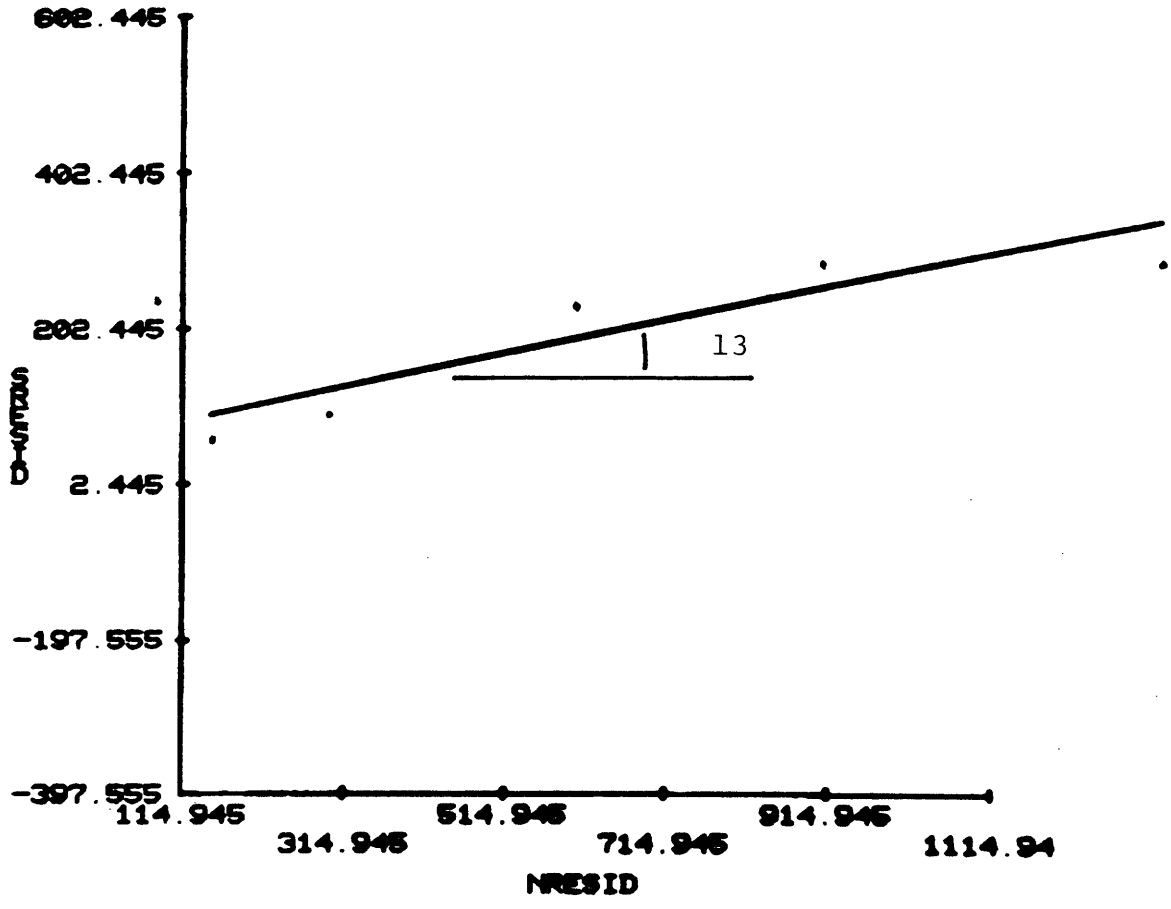

Figure D-60 Residual friction angle of claystone with oriented lamination

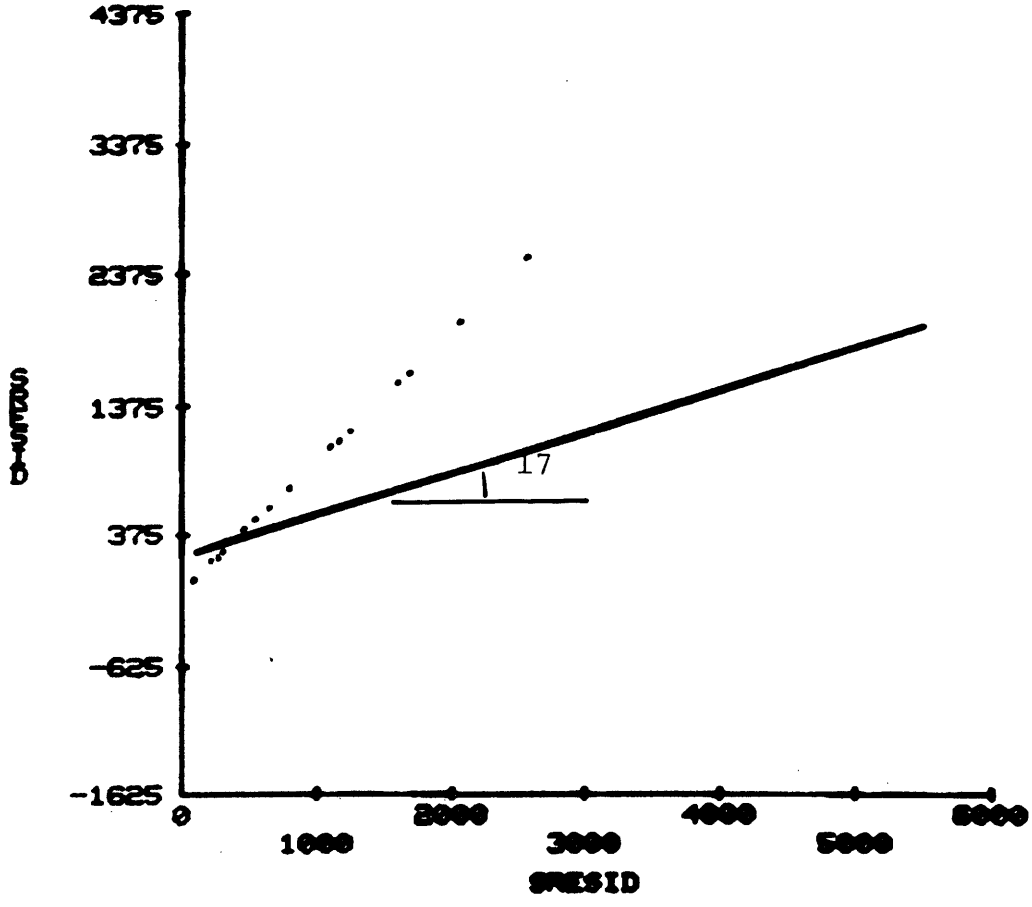

Figure D-61 Residual friction angle of micro-granodiorite with artificial grouted joint

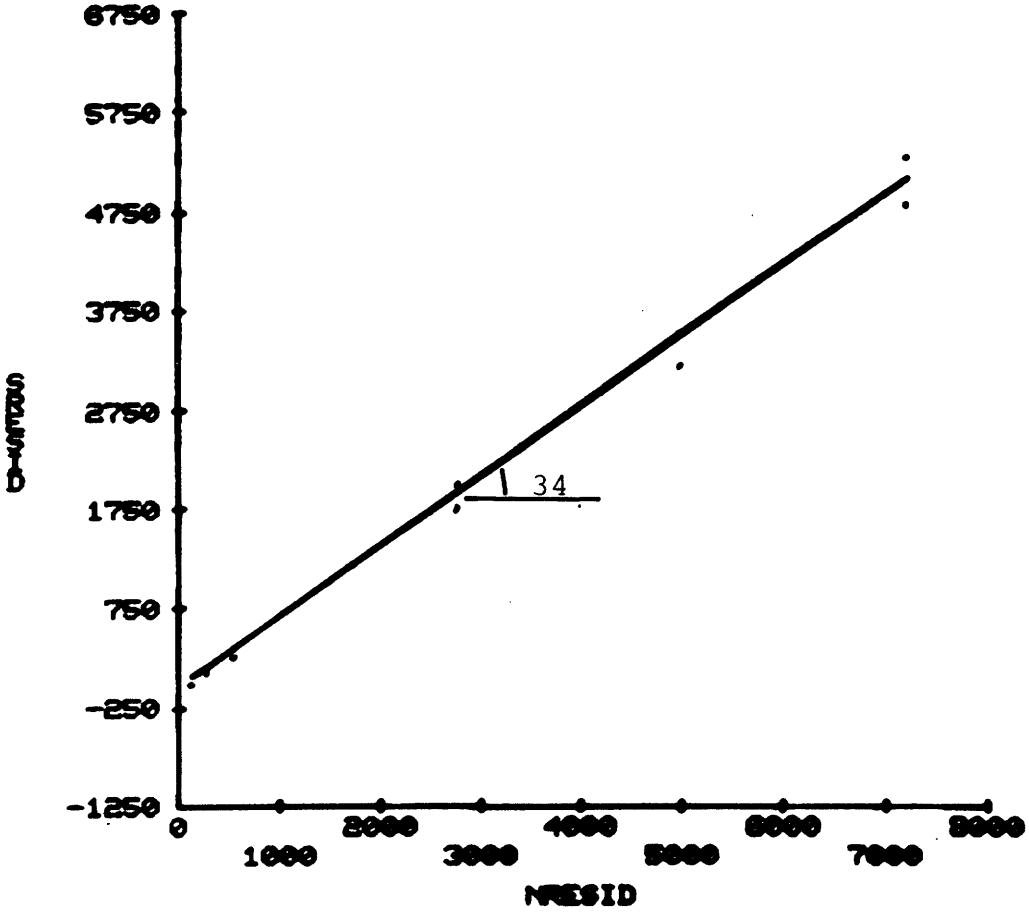

Figure D-62 Peak friction angle of micro - granodiorite with sawn surface lapped with #80 grit

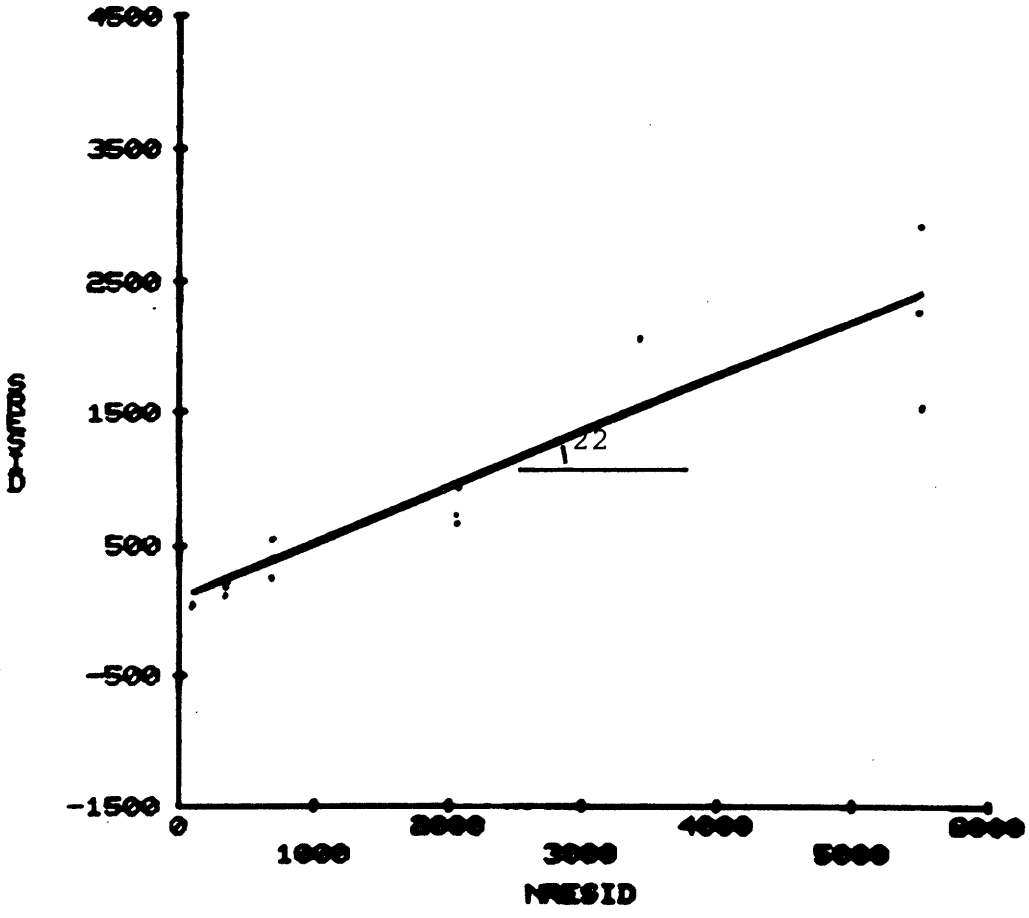

Figure D-63 Residual friction angle of monzonite with artificial grouted joint

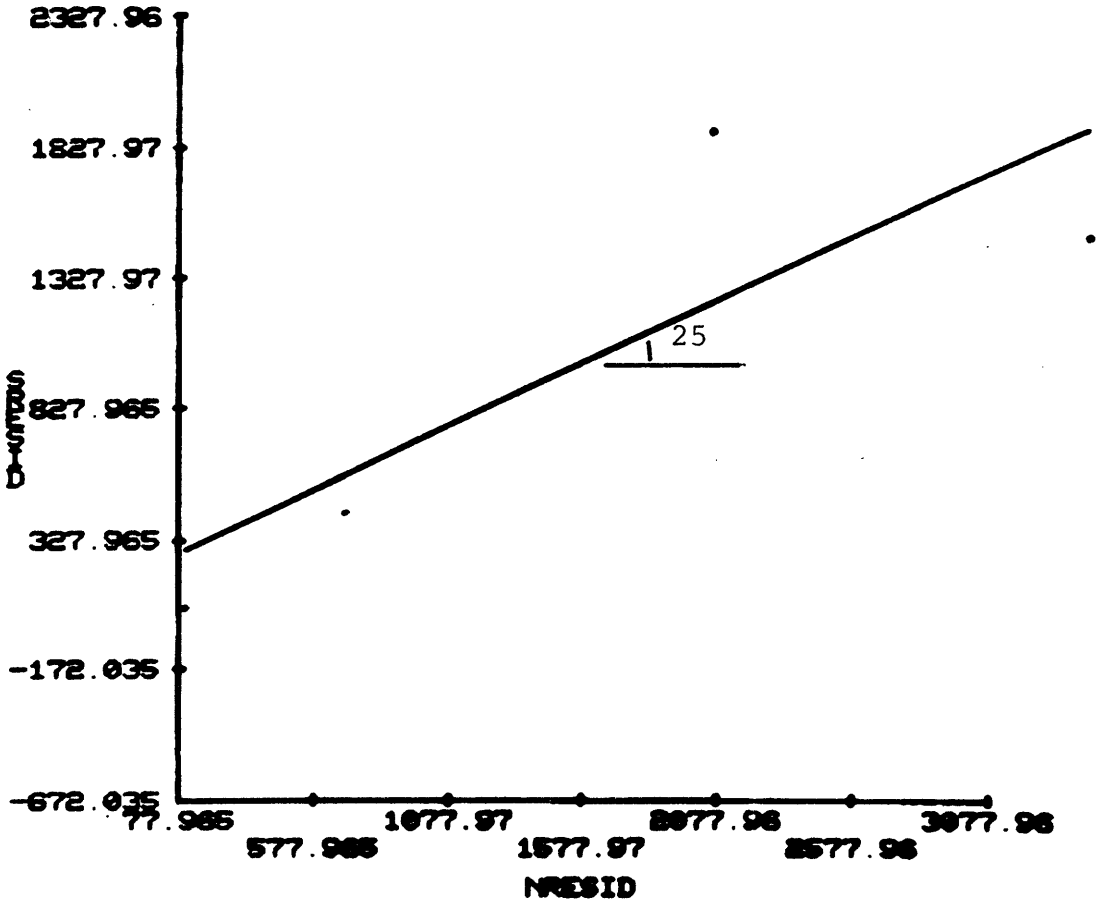

Figure D-64 Residual friction angle of monzonite with natural grouted joint

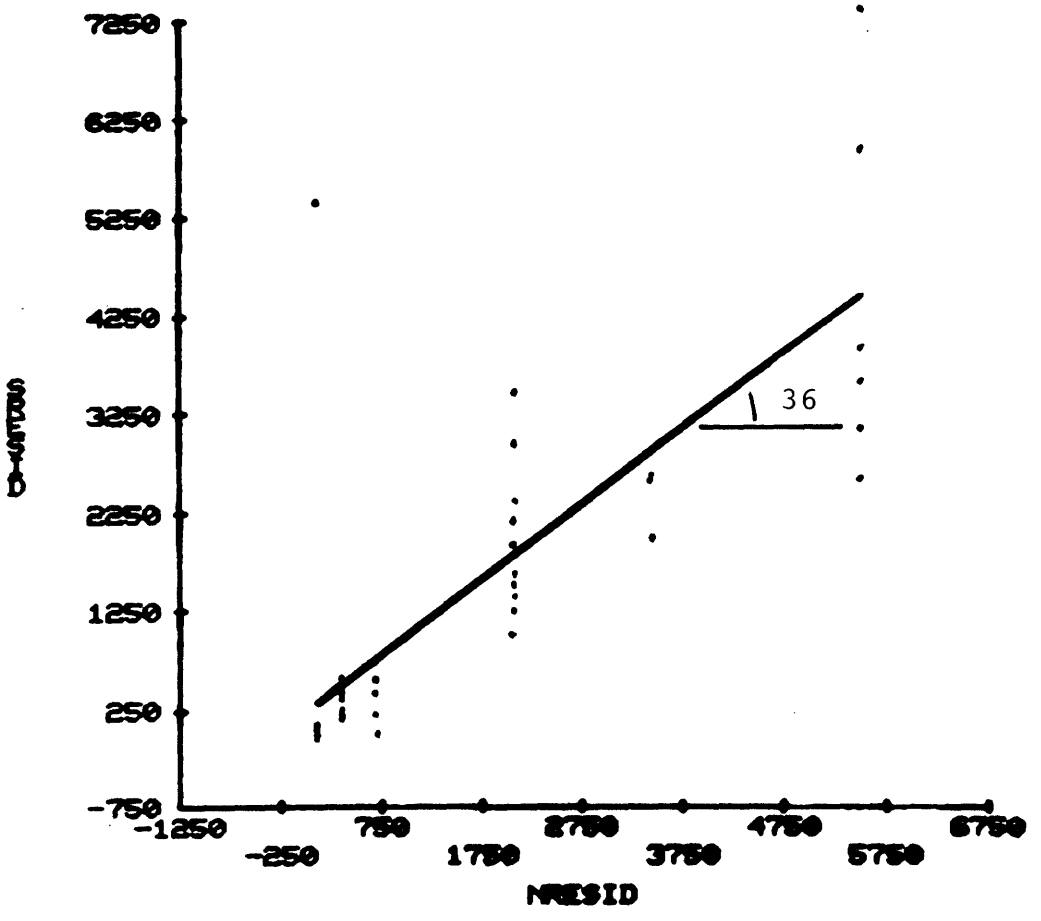

Figure D-65 Residual friction angle of monzonite with joint surface

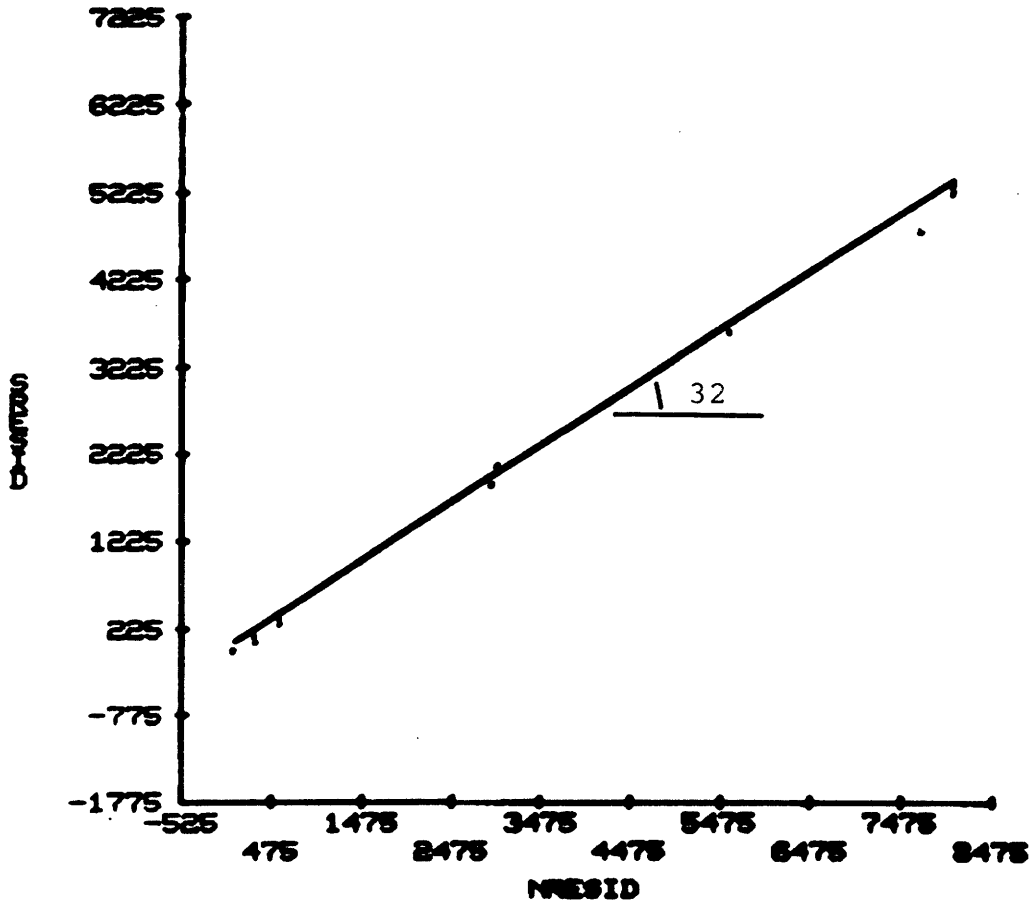

Figure D-66 Residual friction angle of monzonite with sawn surface lapped with #80 grit

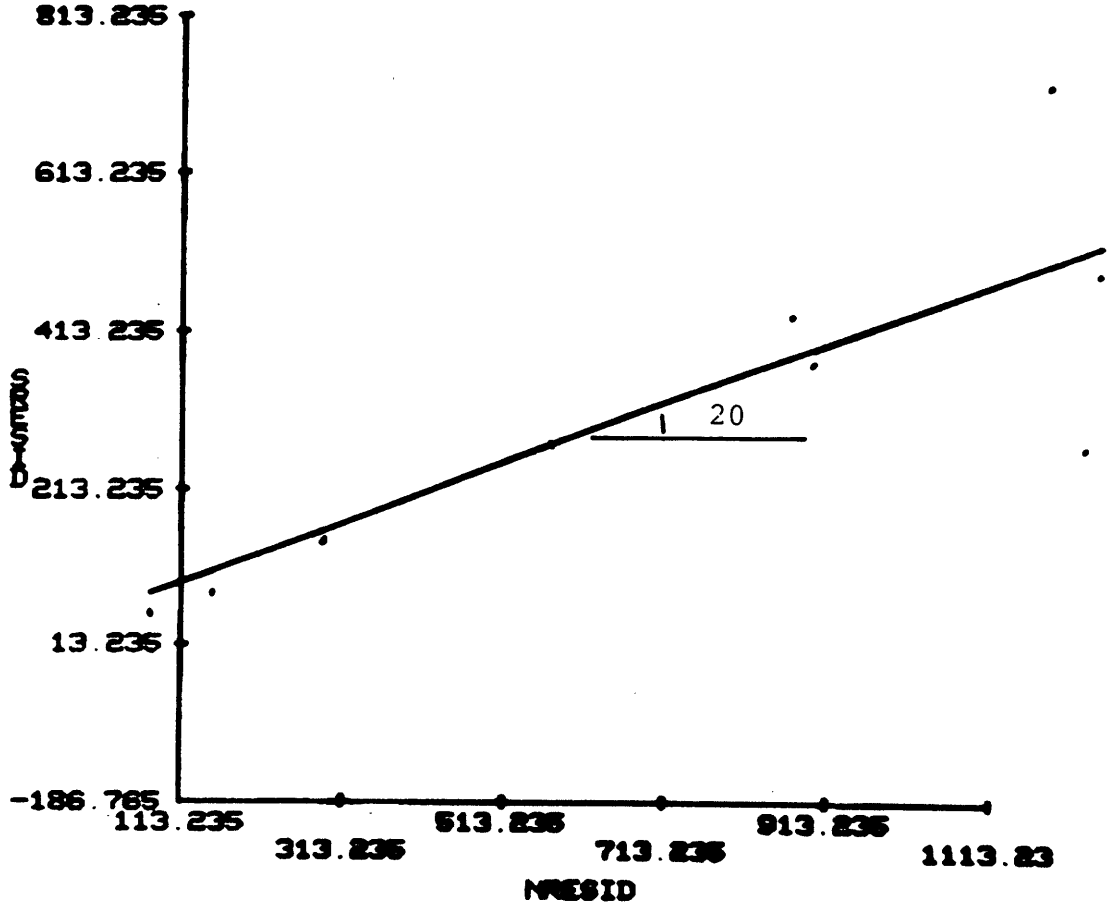

Figure D-67 Residual friction angle of intact lignite

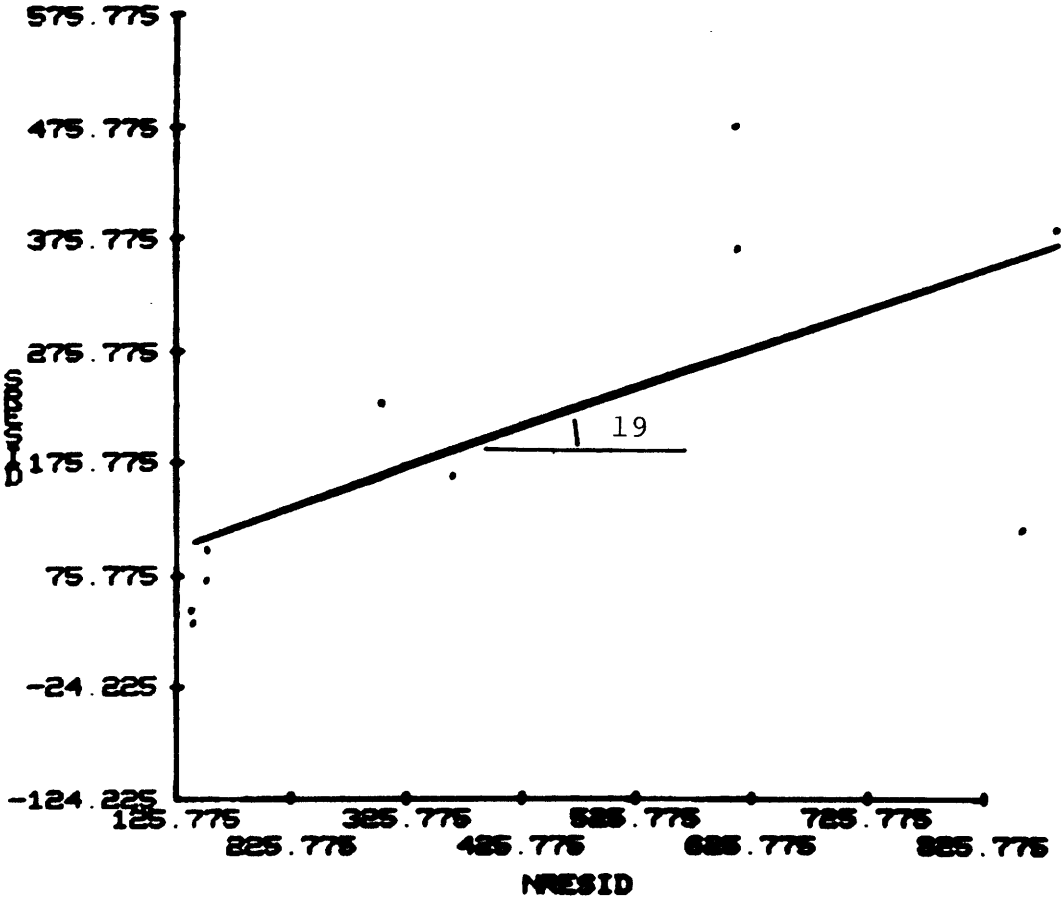

Figure D-68 Residual friction angle of lignit with sawn surface

APPENDIX E

Peak and residual friction angles conditional on discontinuities

Note: Units on the horizontal and vertical axes are X $10^{-3} MN/m^2$

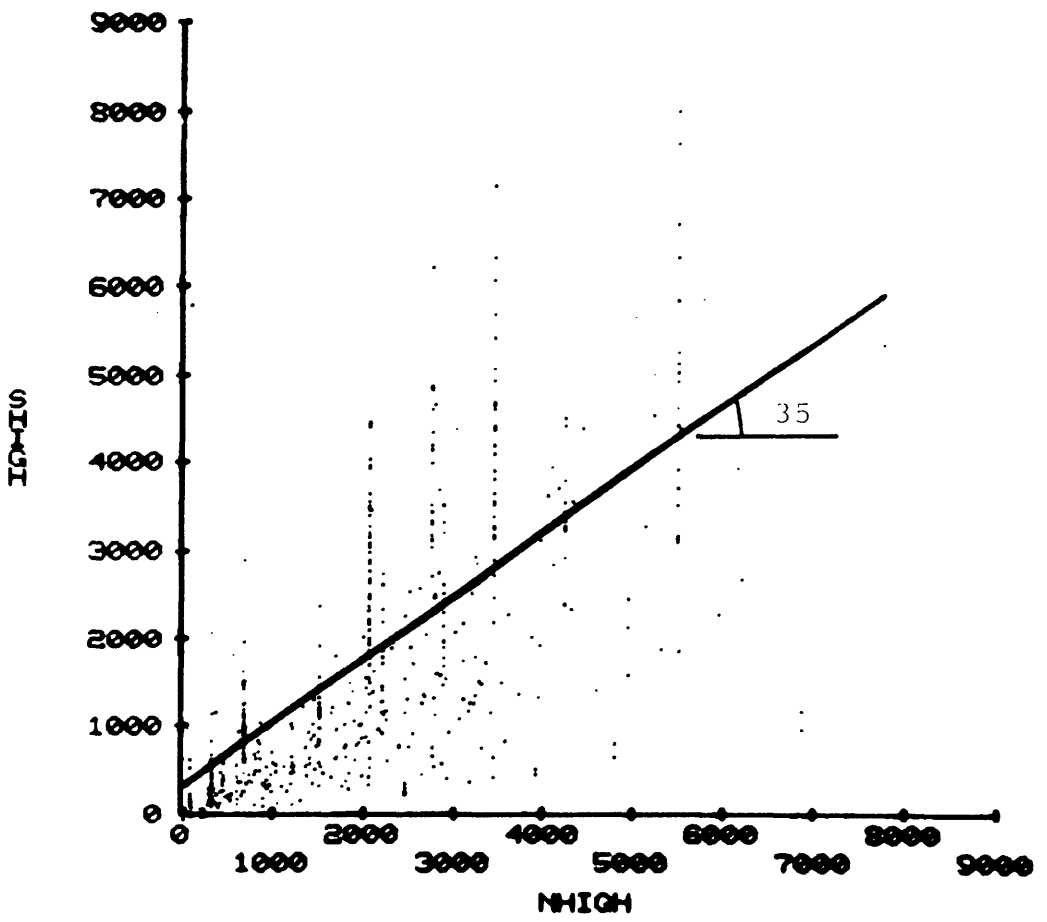

Figure E-1 Peak friction angle conditional on joint surface

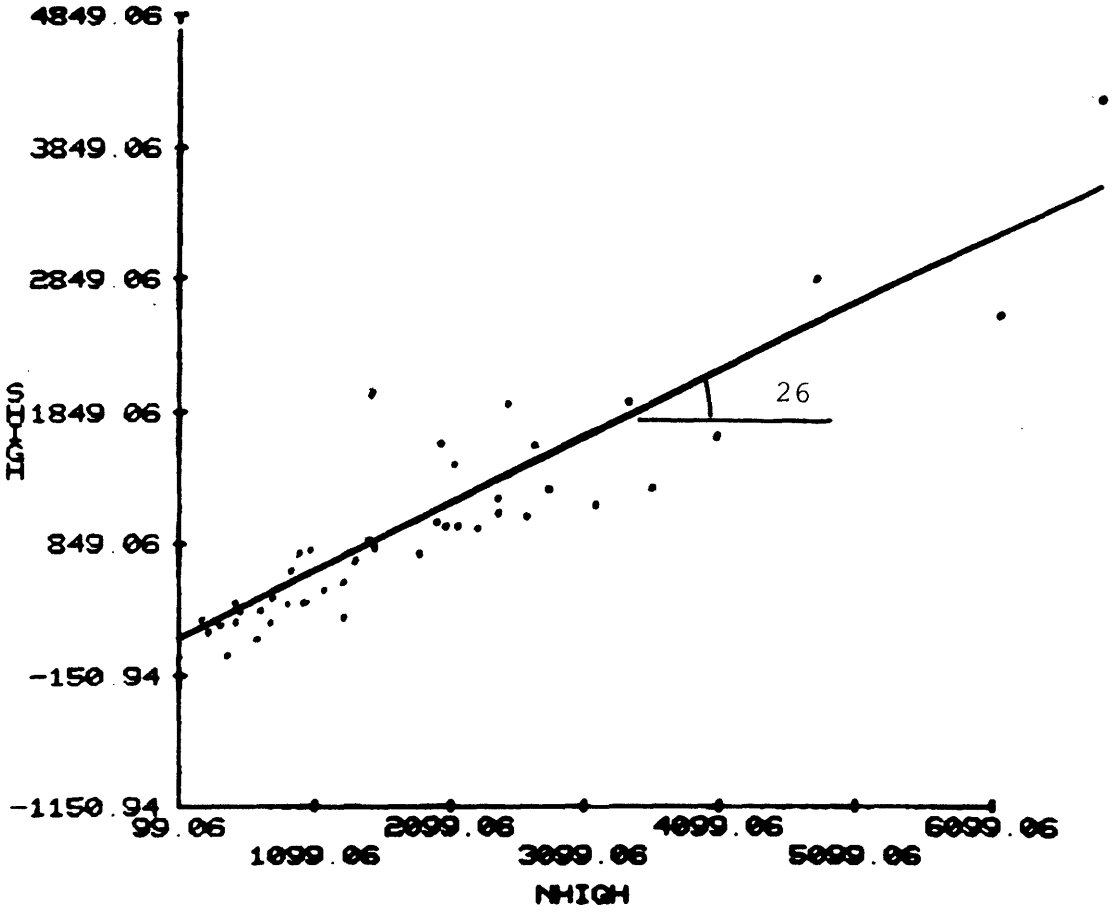

Figure E-2 Peak friction angle conditional on sawn surface

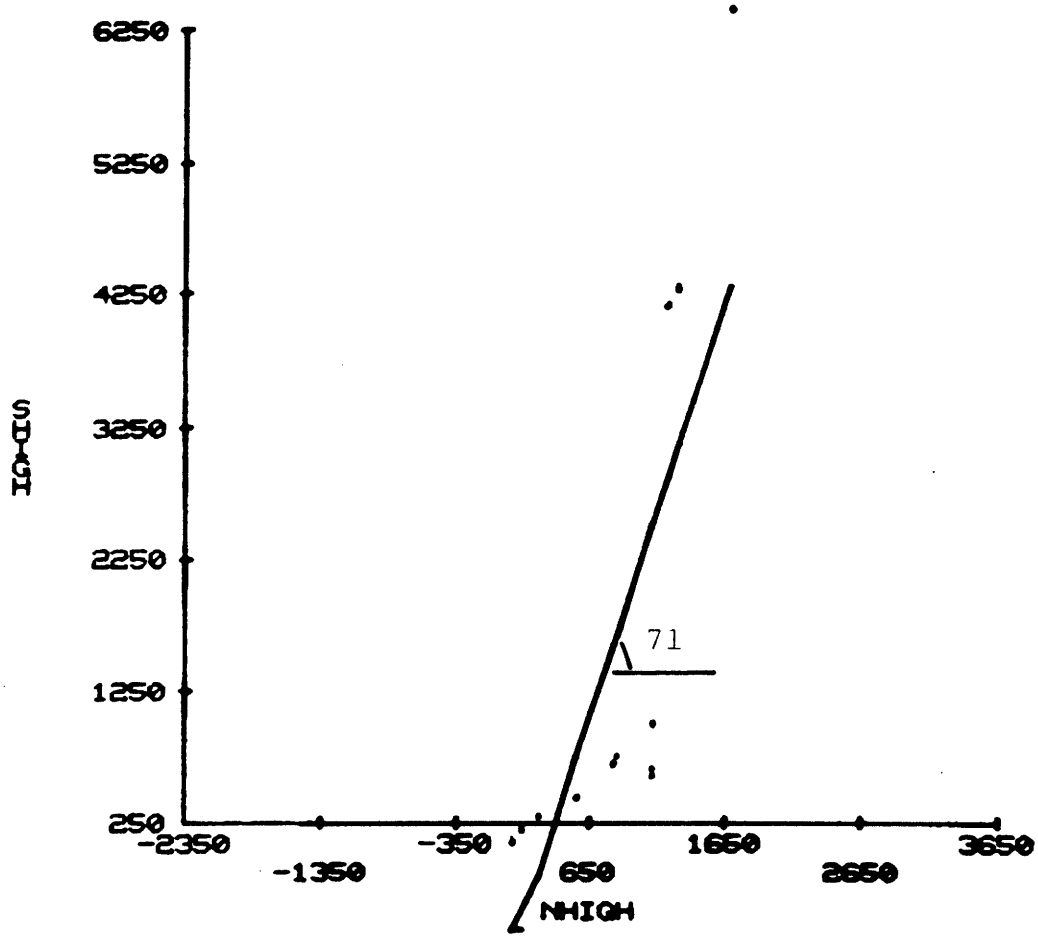

Figure E-3 Peak friction angle conditional on all intact rocks

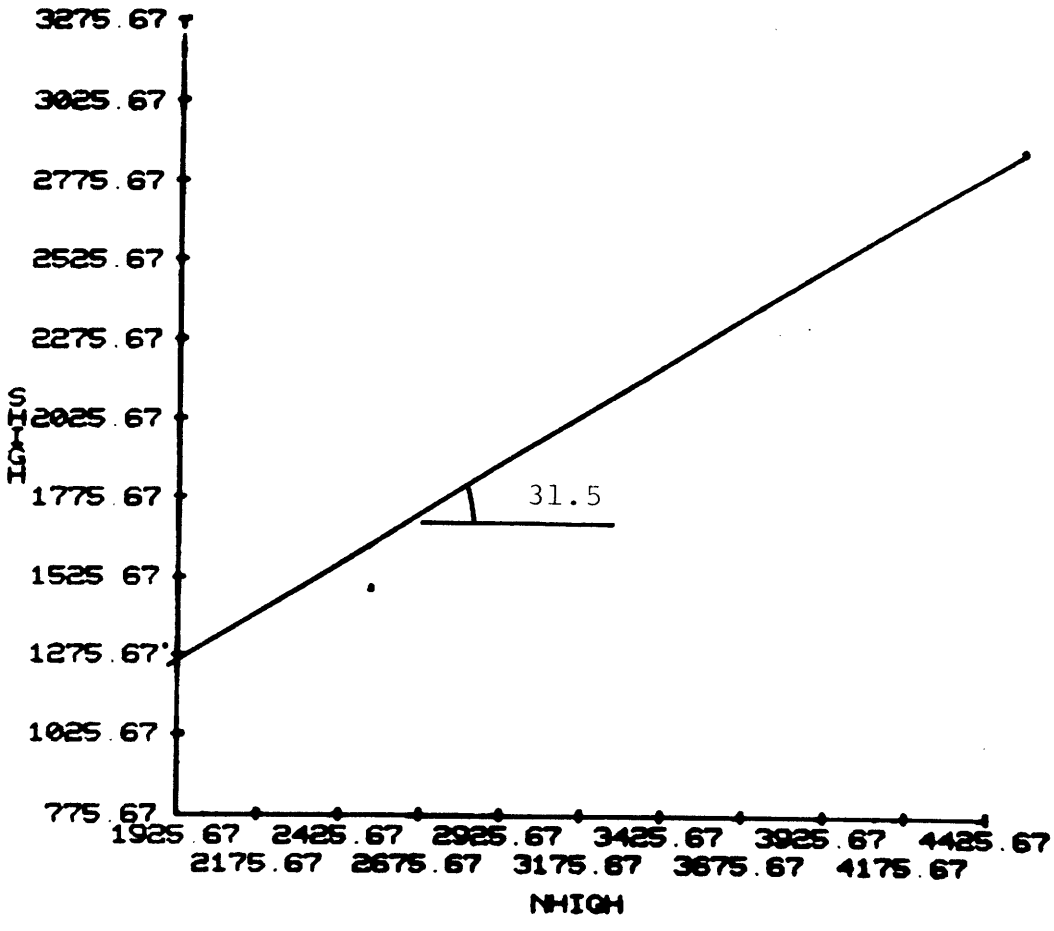

Figure E-4 Peak friction angle conditional on contact between granite and mylonite

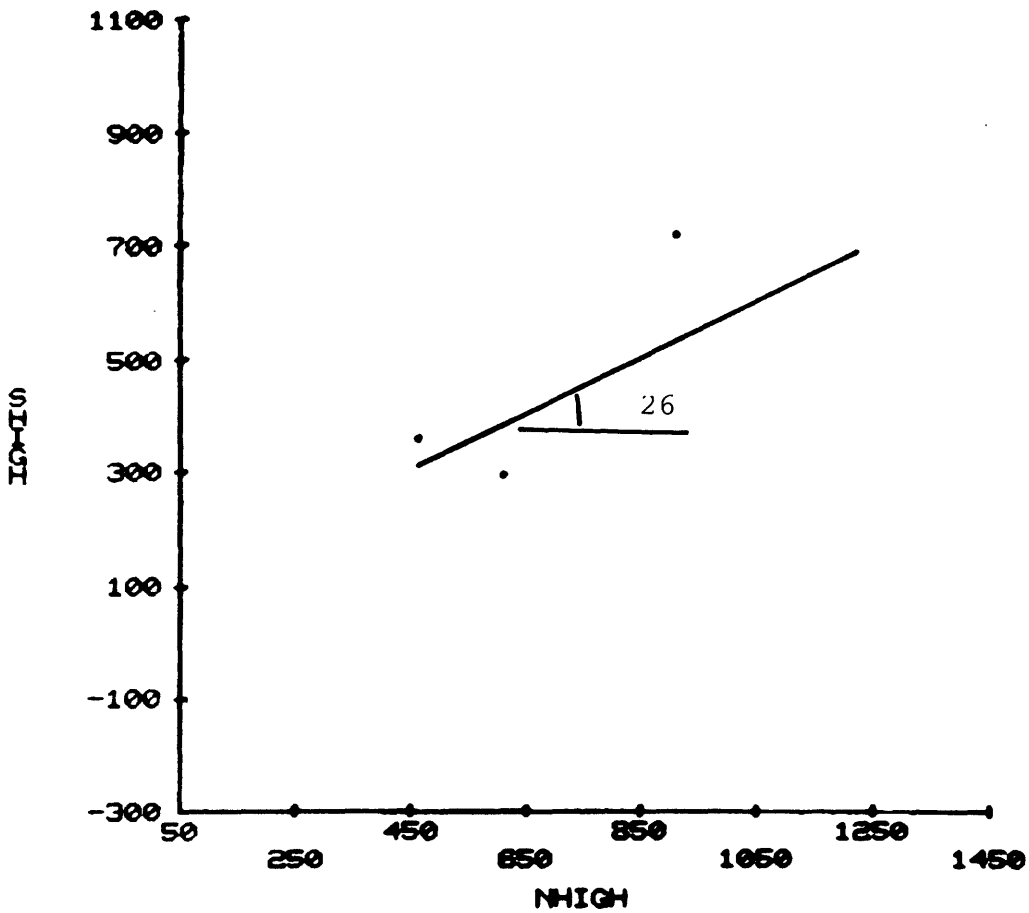

Figure E-5 Peak friction angle conditional on break of core sample

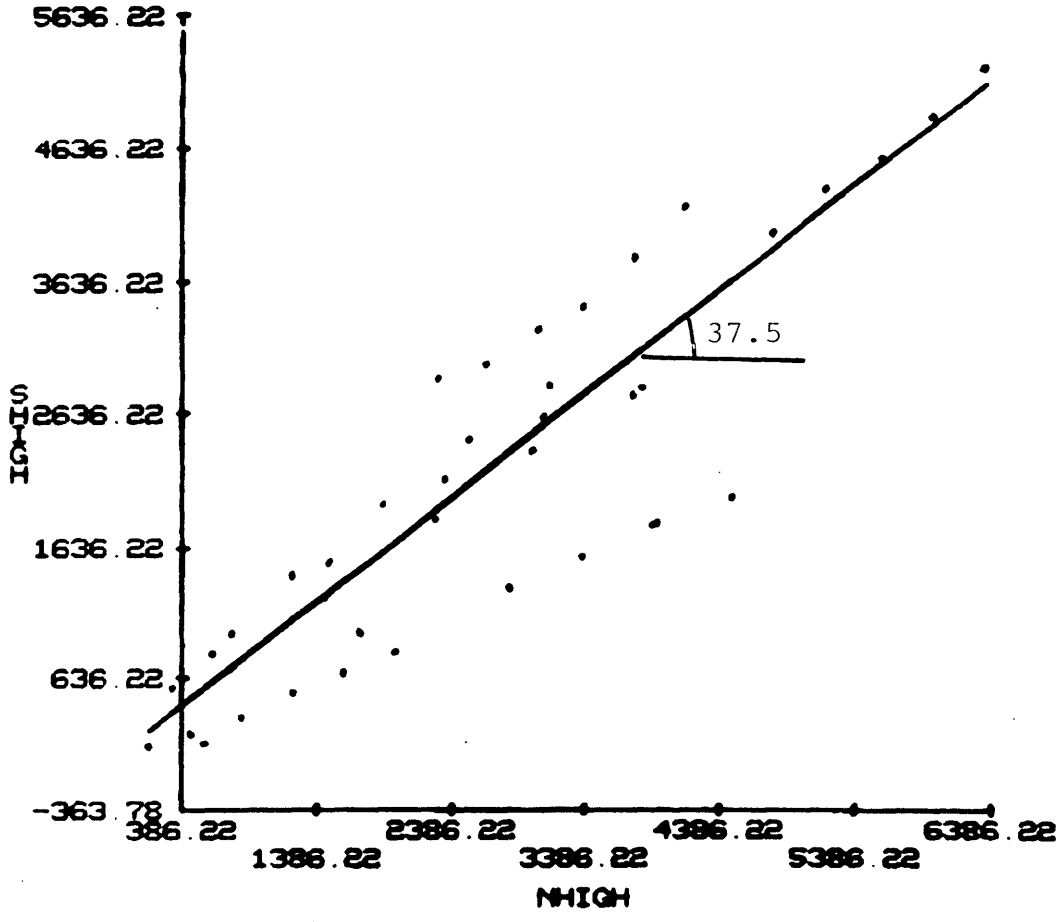

Figure E-6 Peak friction angle conditional on fractures

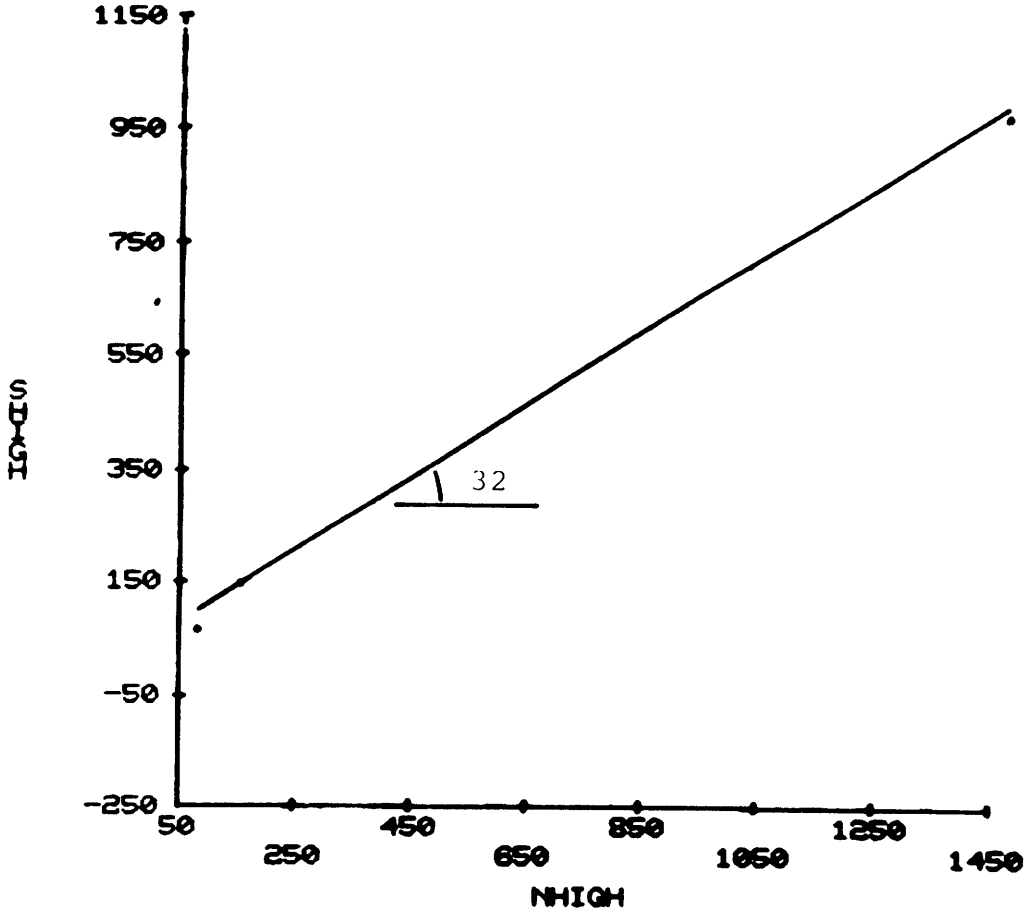

Figure E-7 Peak friction angle condit ional on contact between limestone and moraine

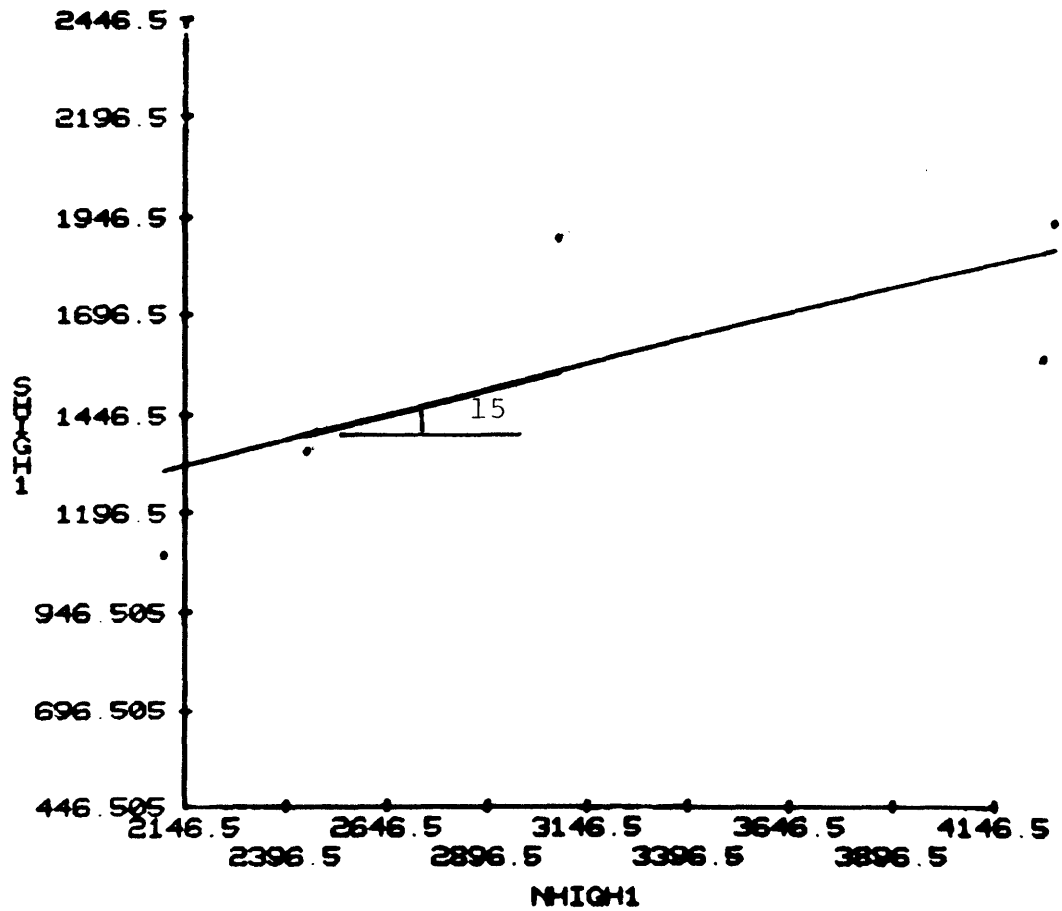

Figure E-8 Peak friction angle conditional on concrete-limestone interface

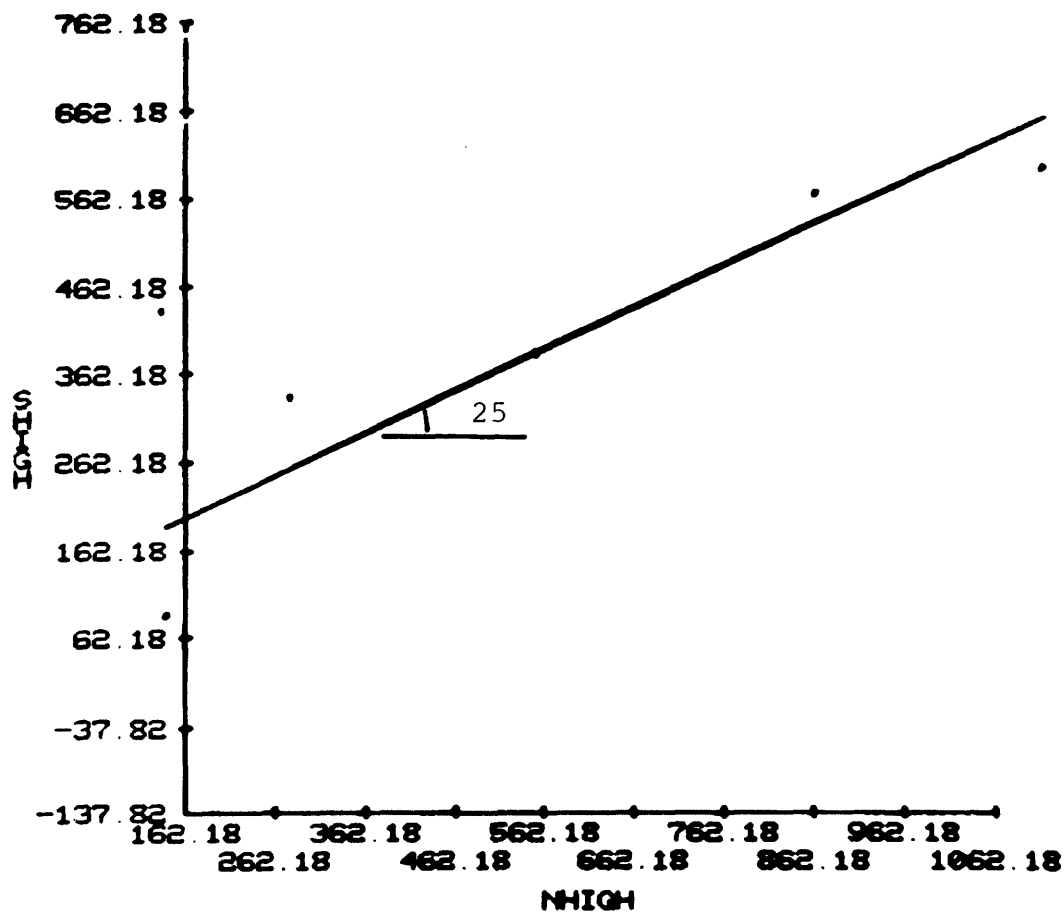

Figure E-9 Peak friction angle conditional on oriented lamination

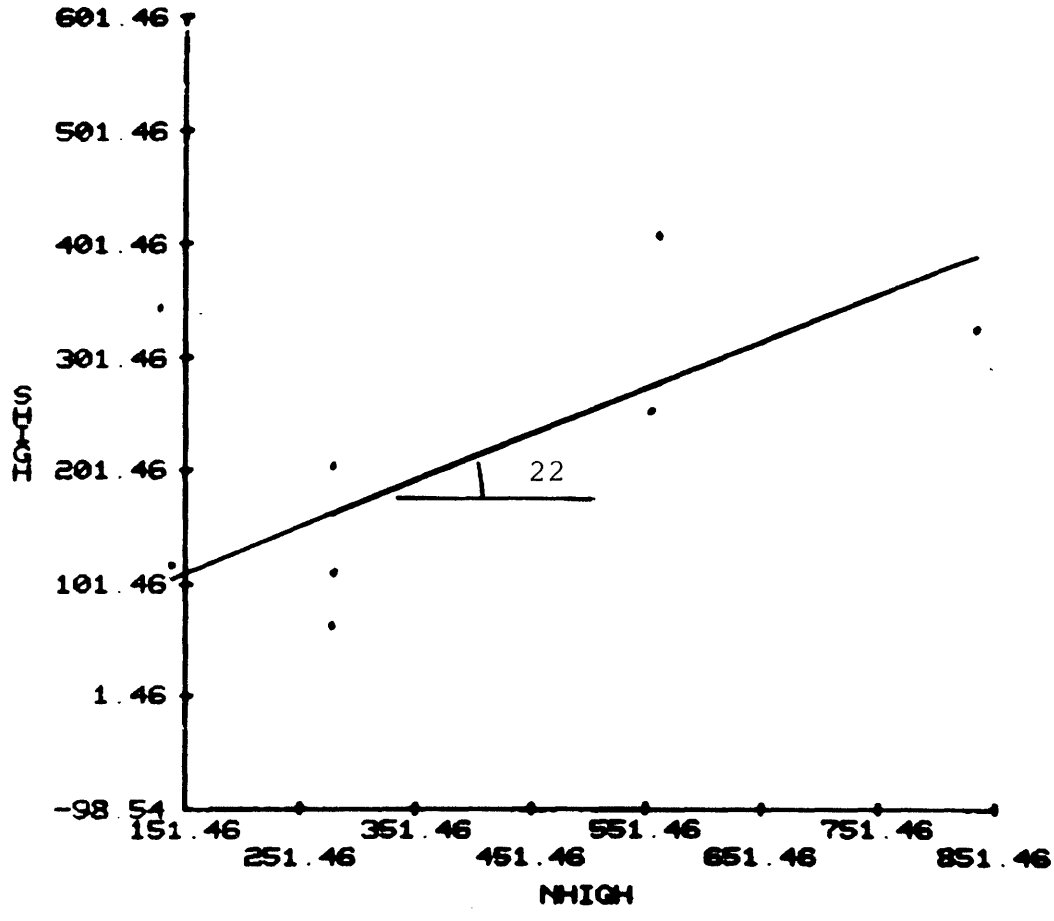

Figure E-10 Peak friction angle conditional on non-oriented lamination

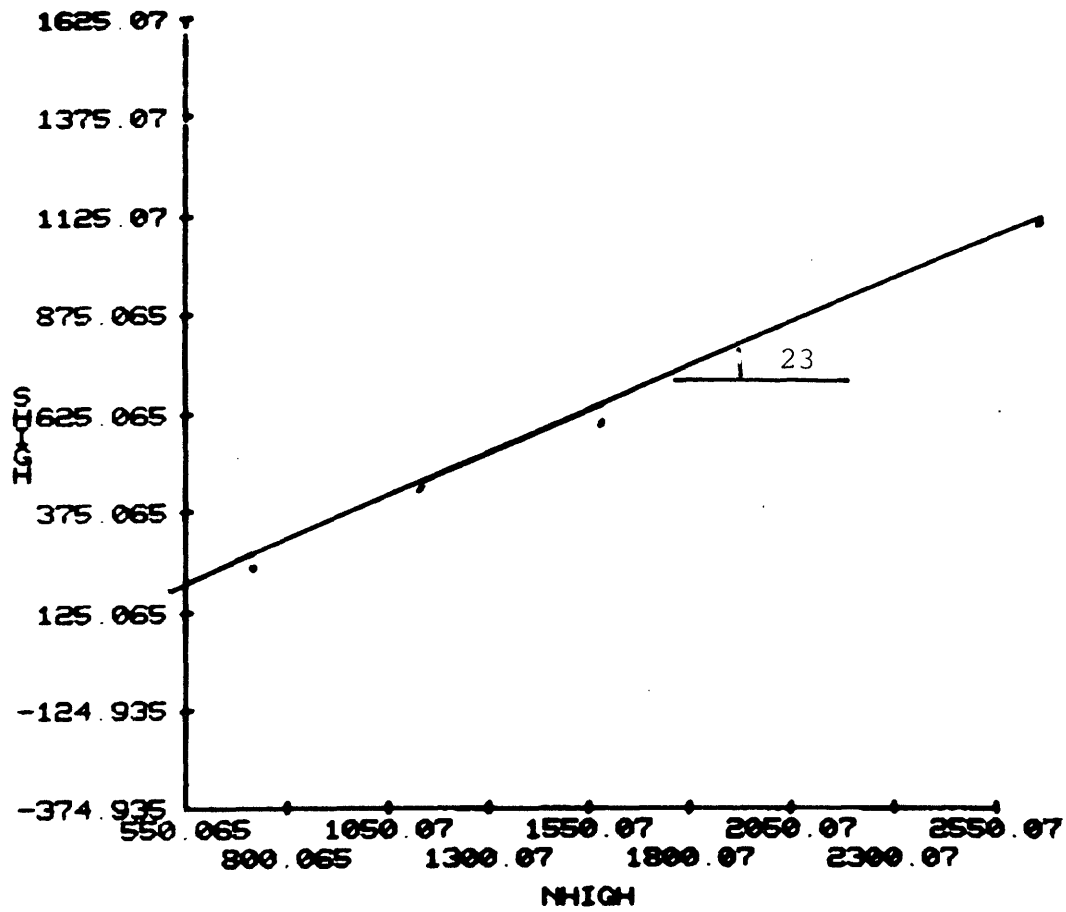

Figure E-11 Peak friction angle conditional on break of test specimen

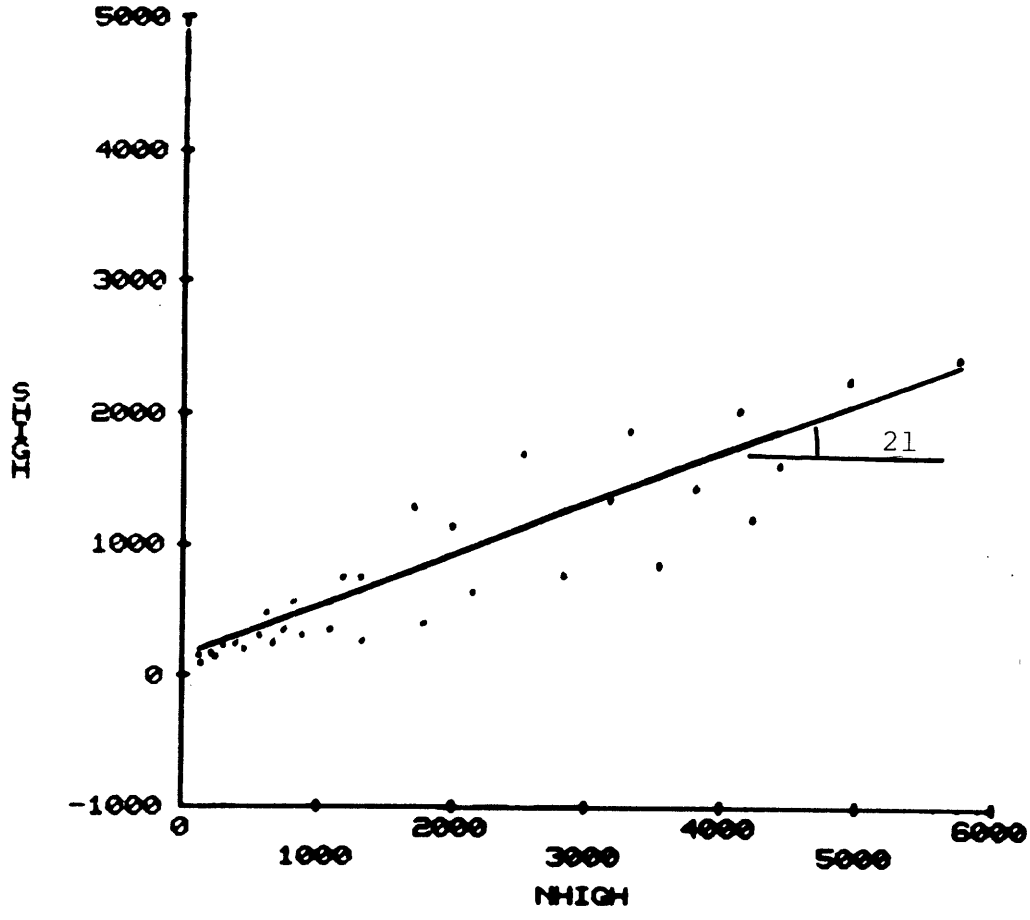

Figure E-12 Peak friction angle conditional on bedding

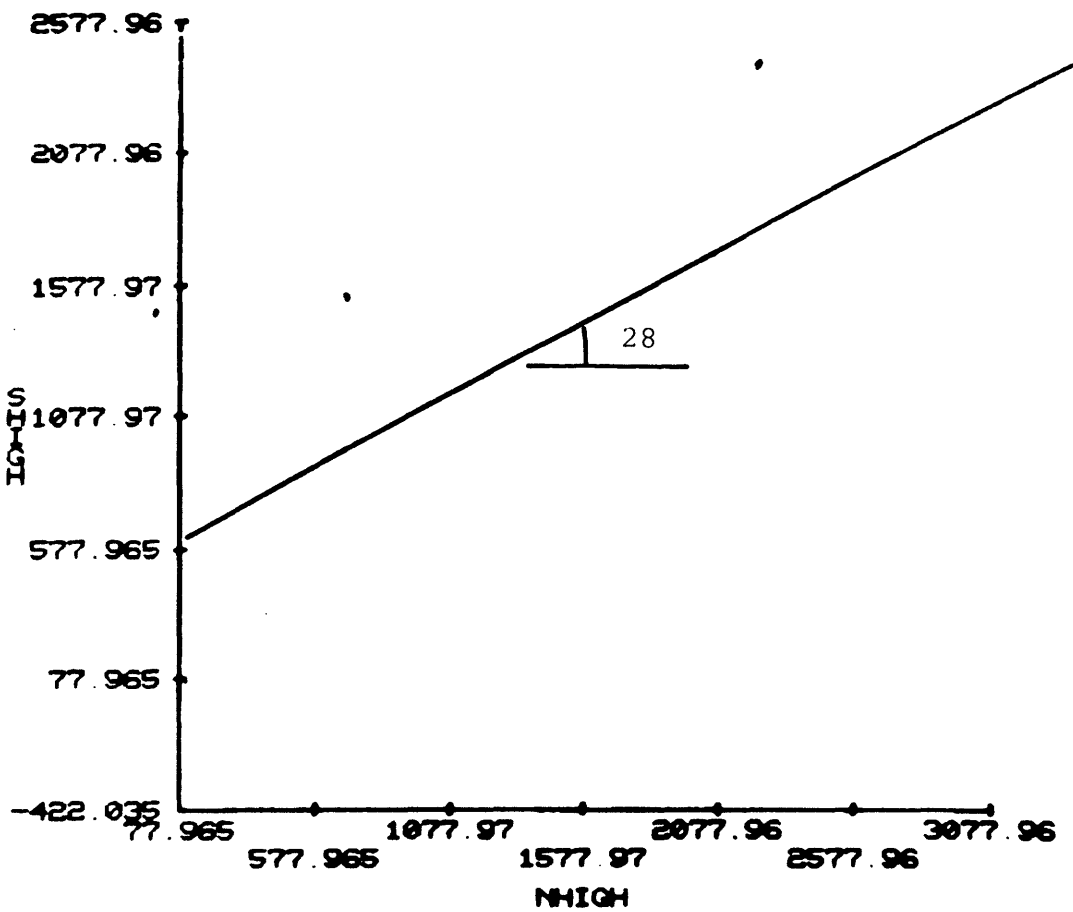

Figure E-13 Peak friction angle conditional on natural grouted joint

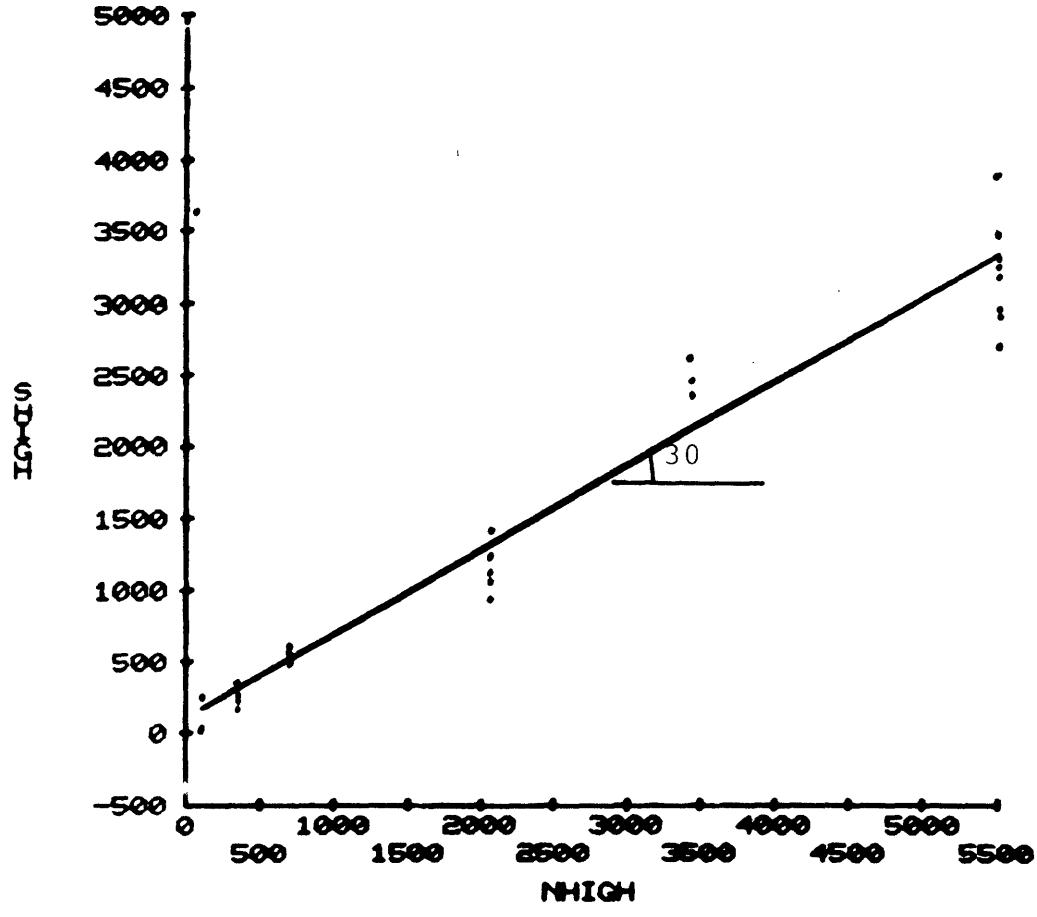

Figure E-14 Peak friction angle conditional on artificial grouted joint

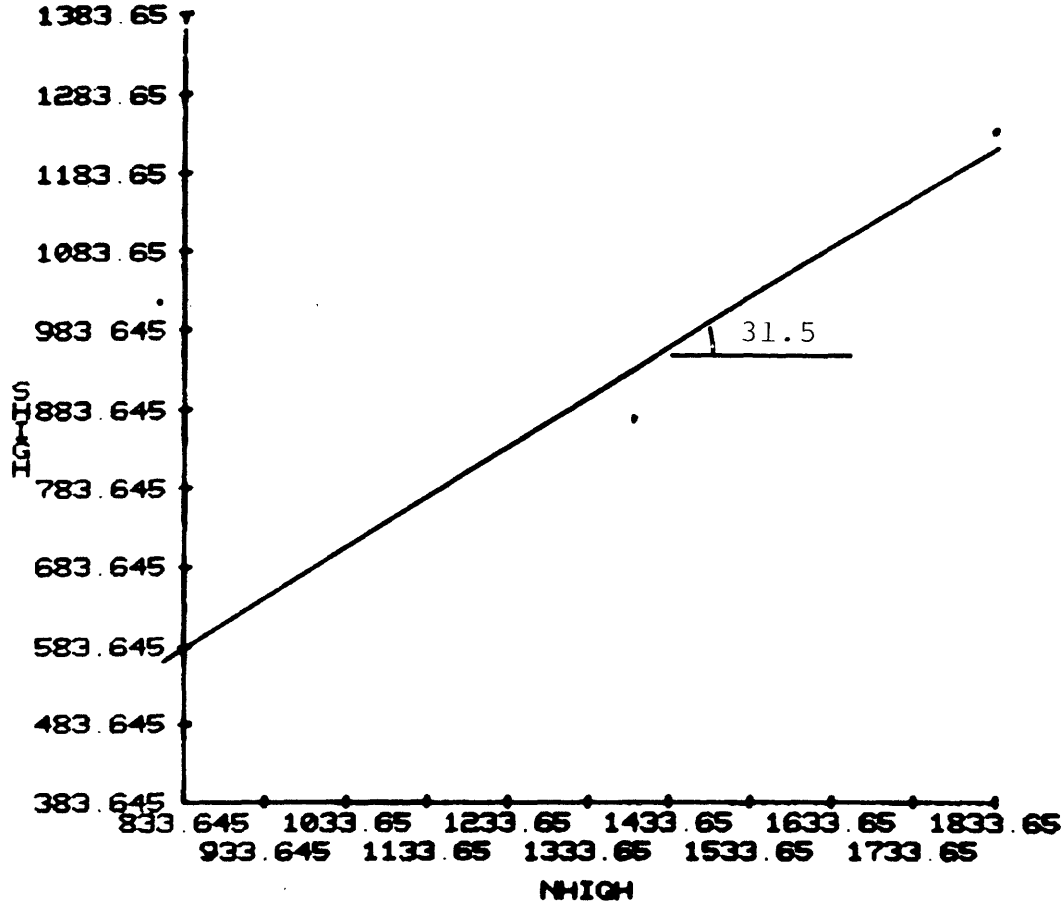

Figure E-15 Peak friction angle conditional on slickensided surface

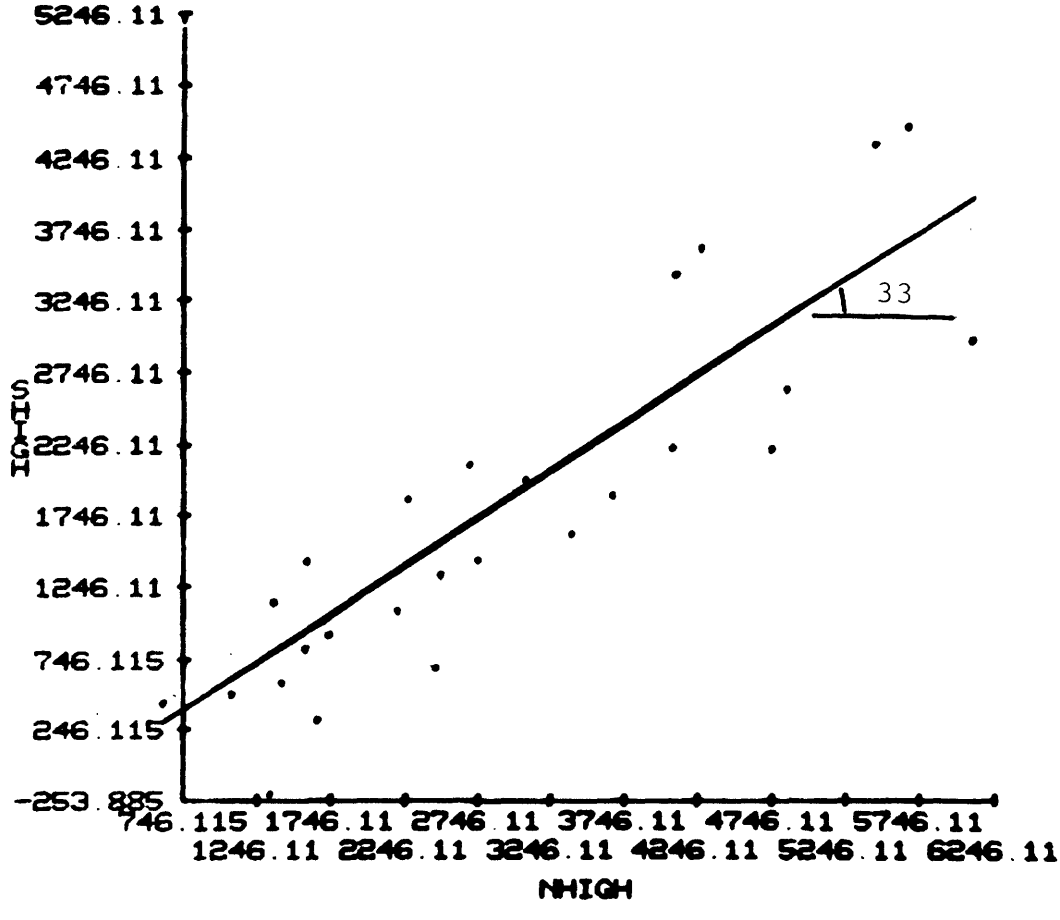

Figure E-16 Peak friction angle conditional on separated foliation

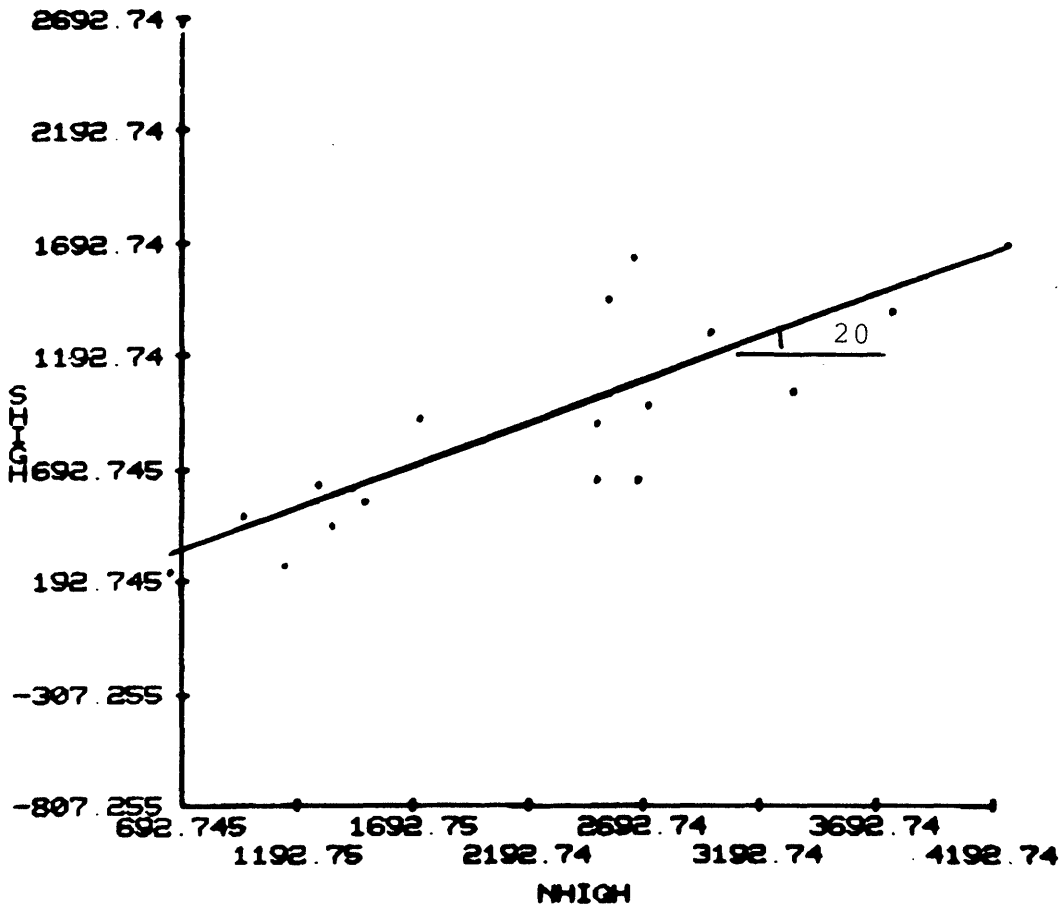

Figure E-17 Peak friction angle conditional on fault

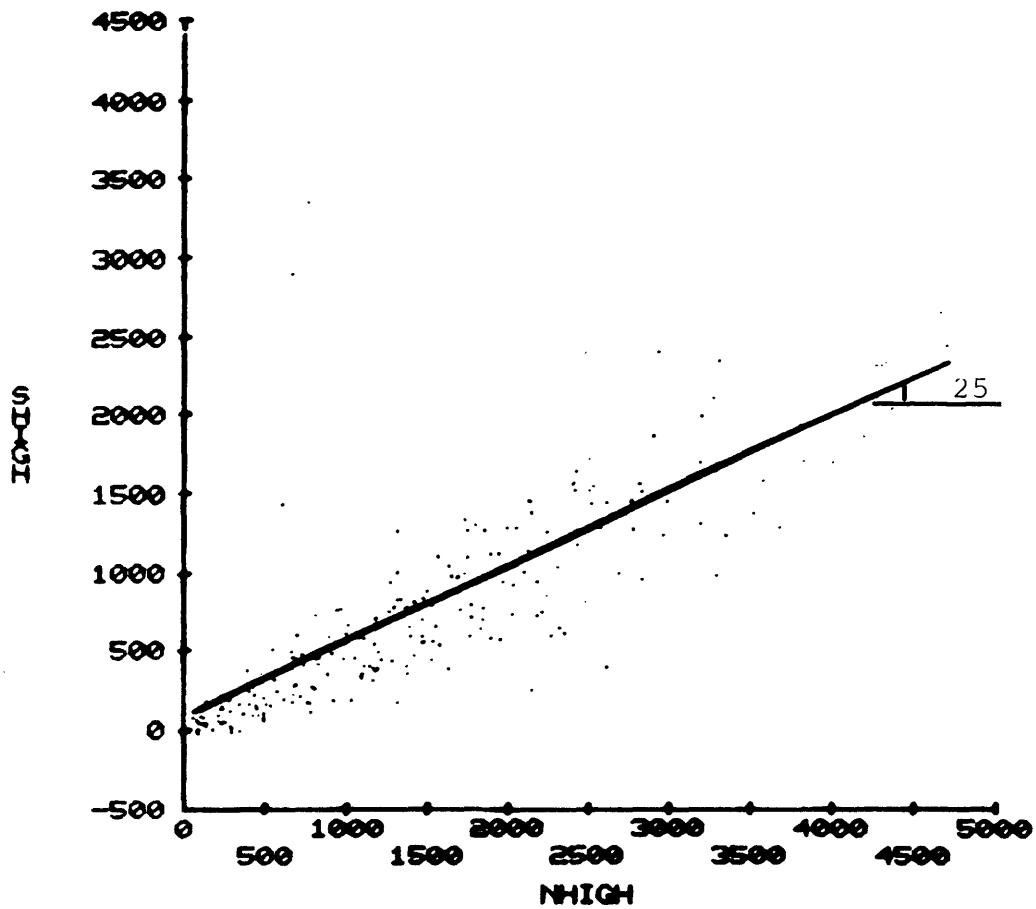

Figure E-18 Peak friction angle conditional on foliation

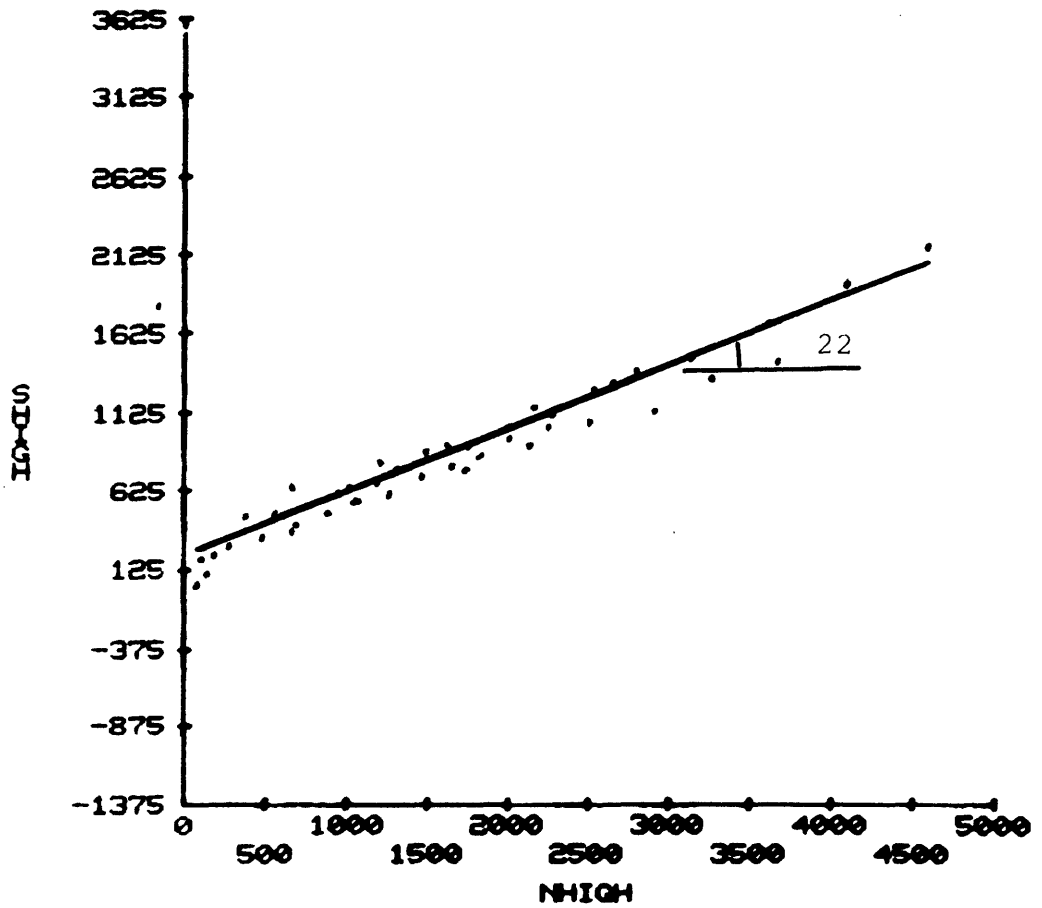

Figure E-19 Peak friction angle conditional on H/W joint set

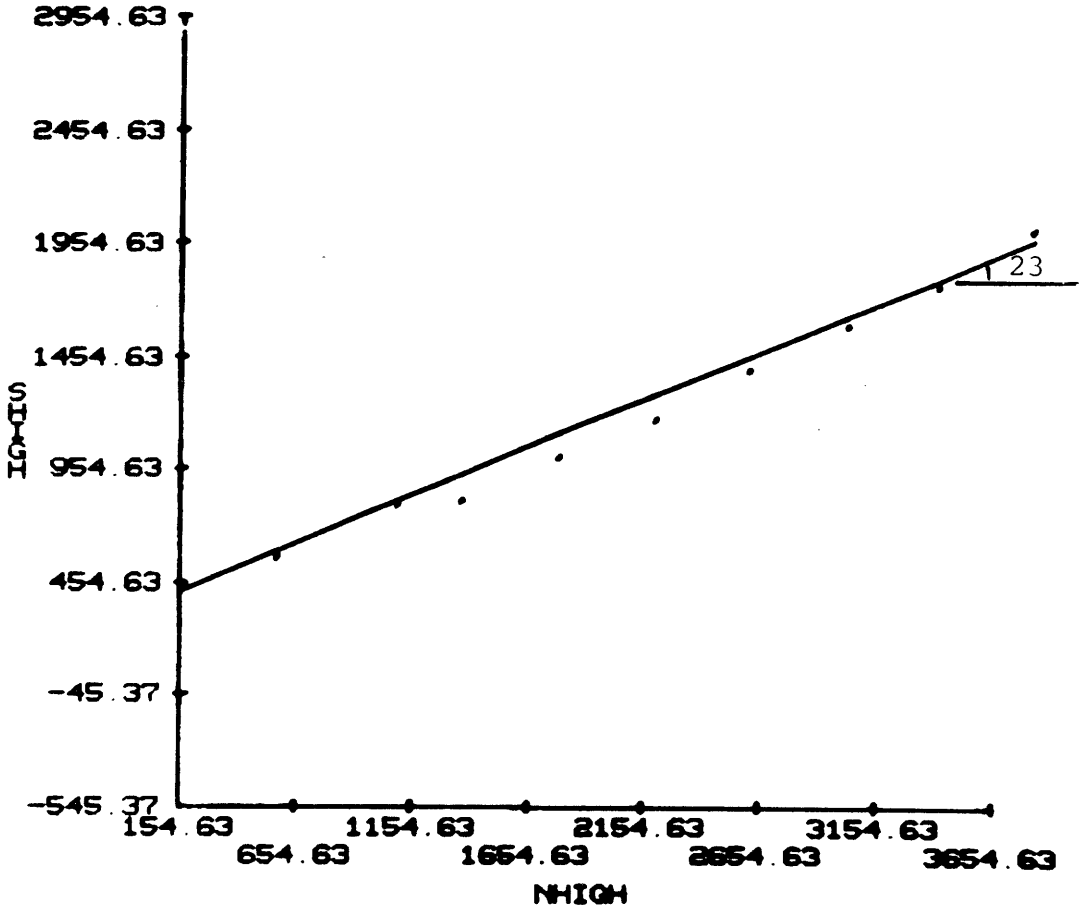

Figure E-20 Peak friction angle conditional on conjugate joint set

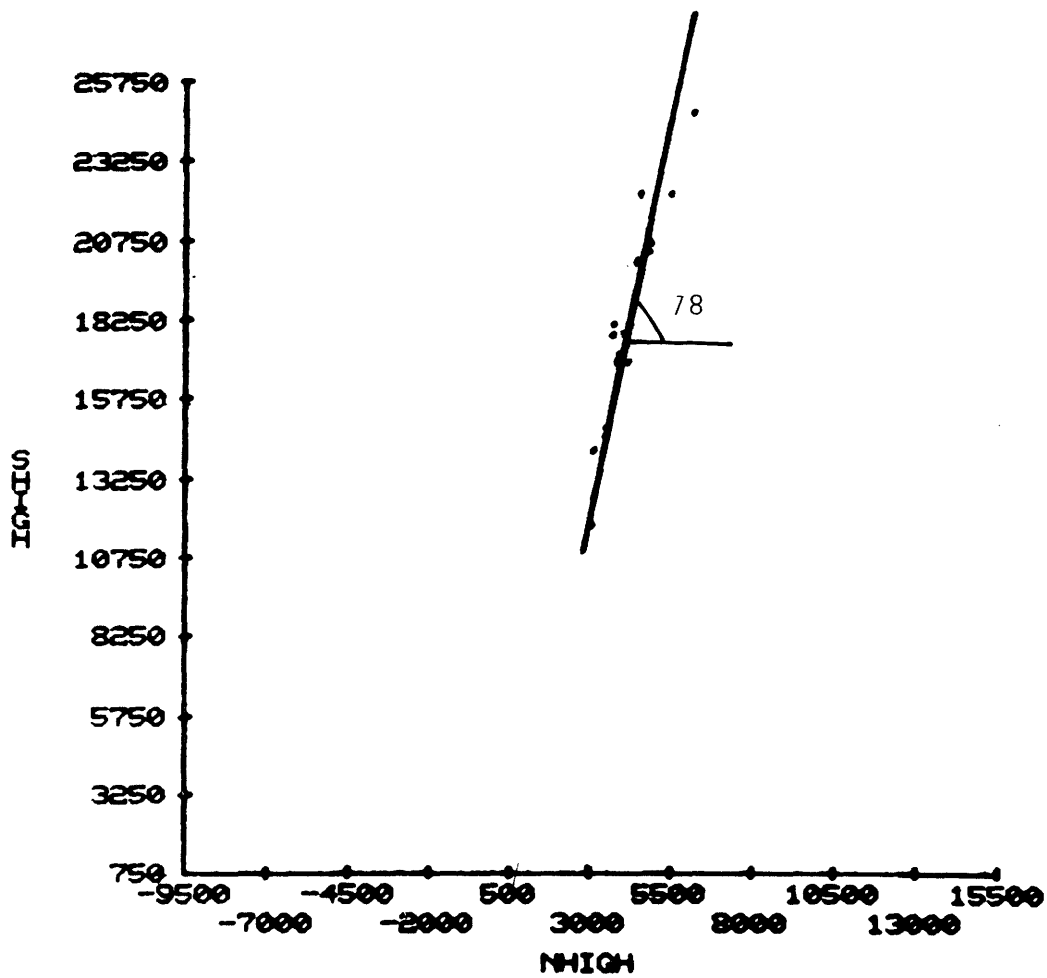

Figure E-21 Peak friction angle conditional on homogeneous rock

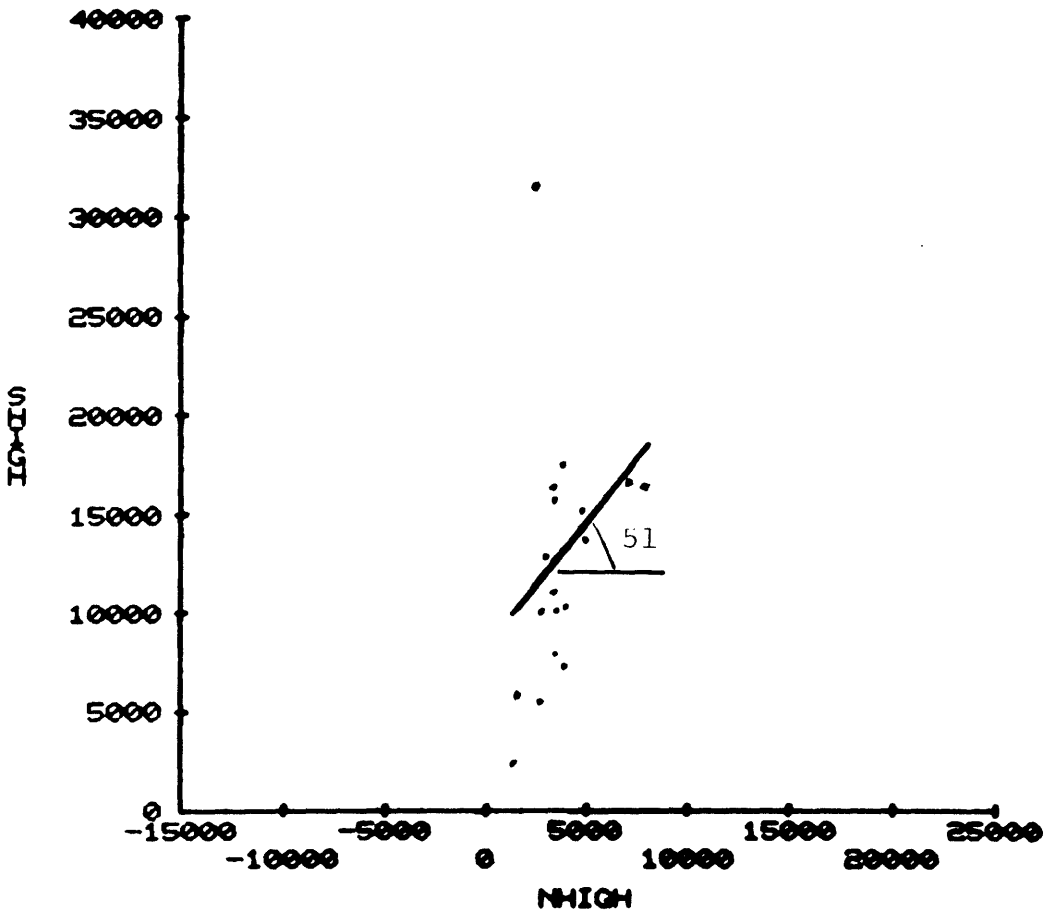

Figure E-22 Peak friction angle conditional on healed joint

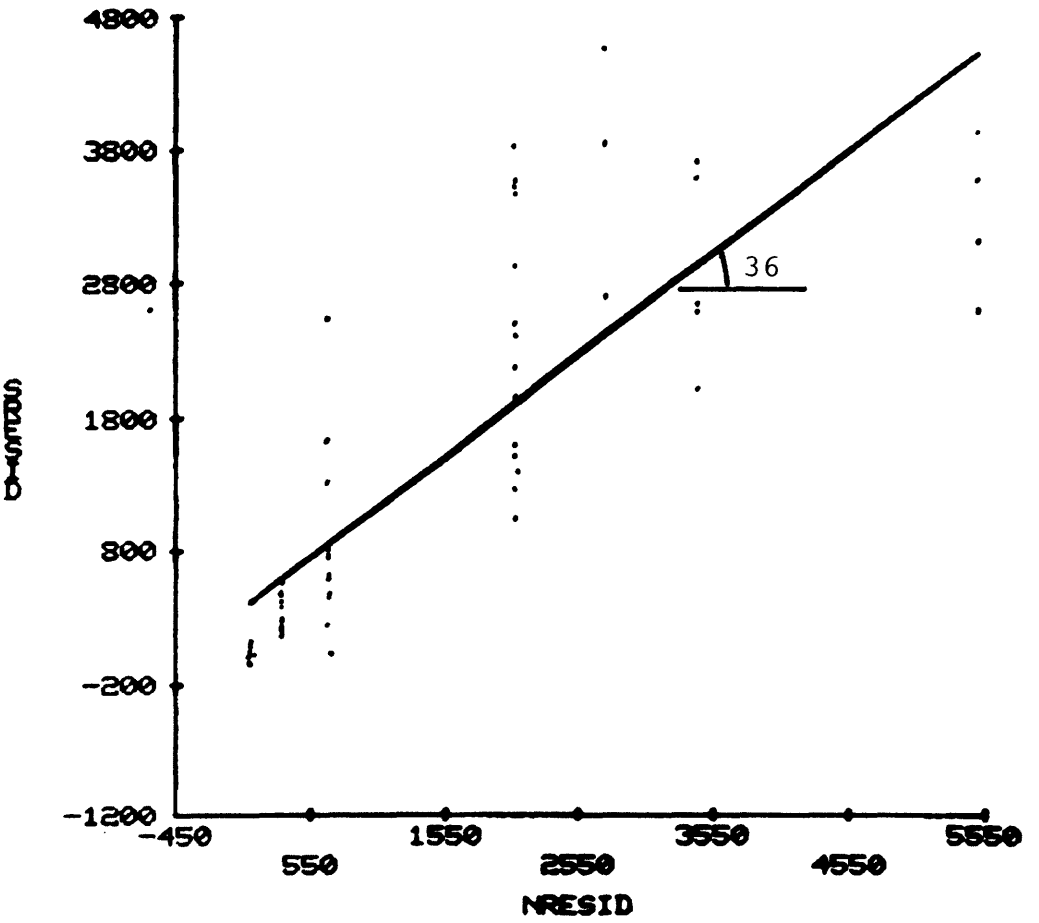

Figure E-23 Residual friction angle conditional on joint surface

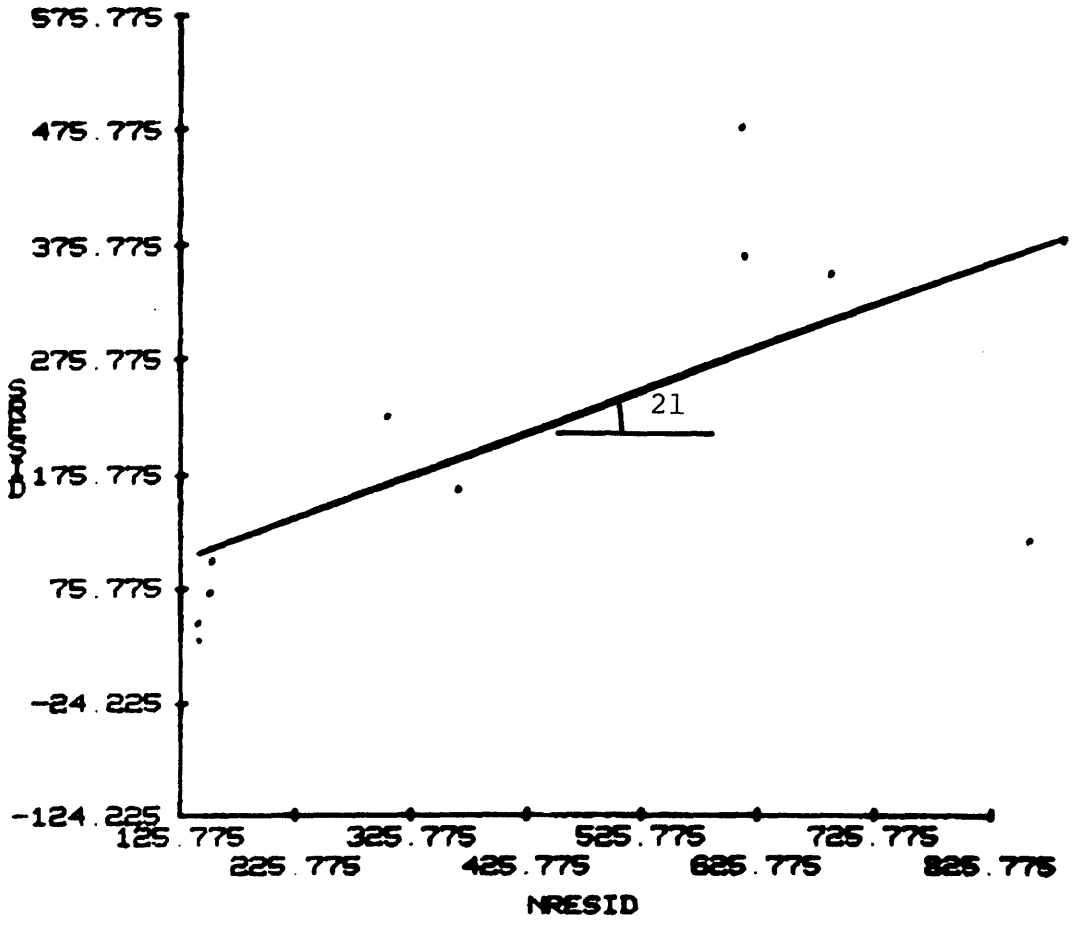

Figure E-24 Residual friction angle conditional on sawn surface

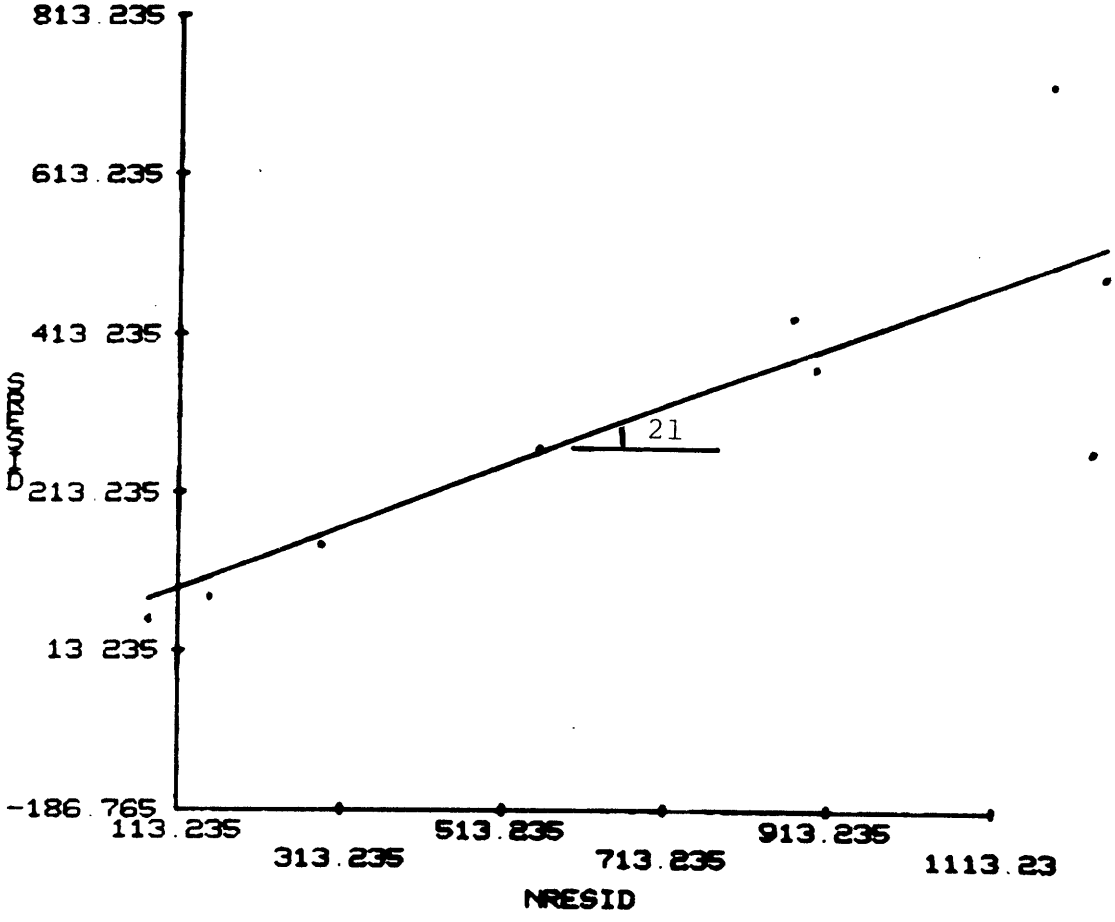

Figure E-25 Residual friction angle conditional on intact rocks

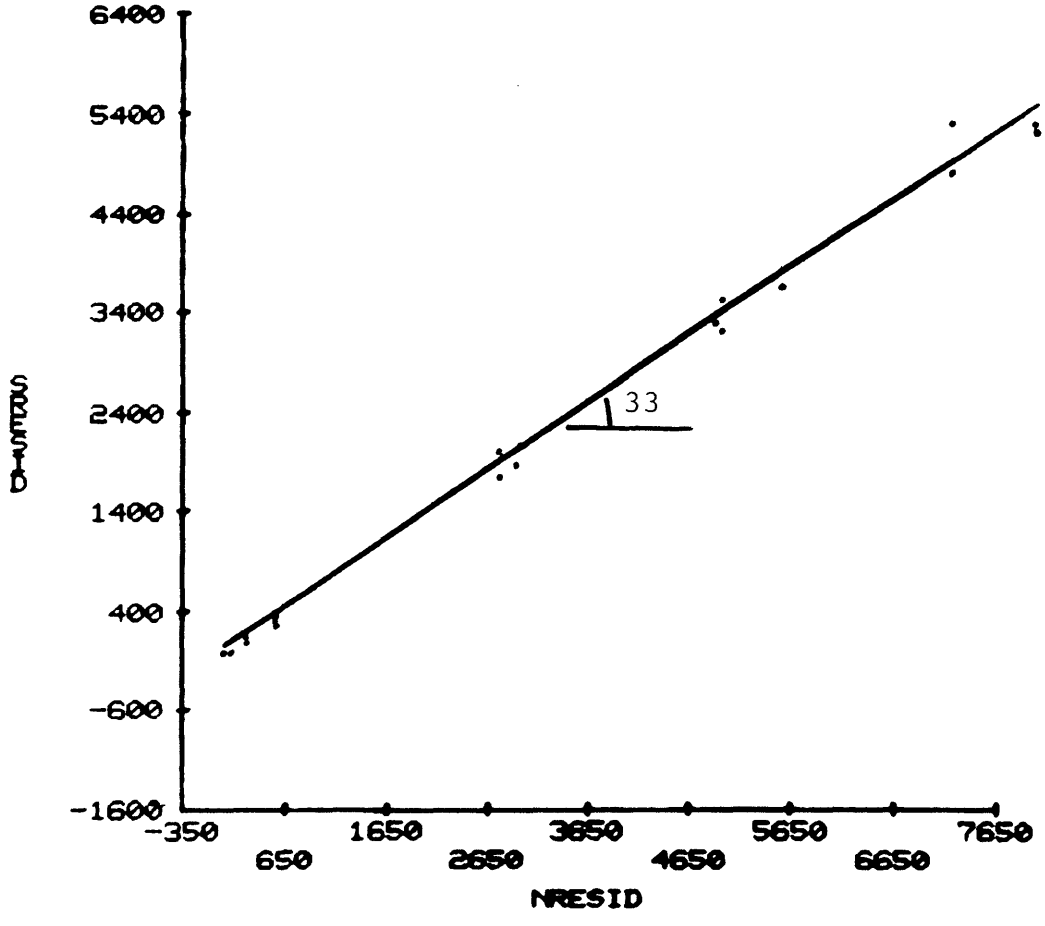

Figure E-26 Residual friction angle conditional on sawn joint lapped with #80 grit

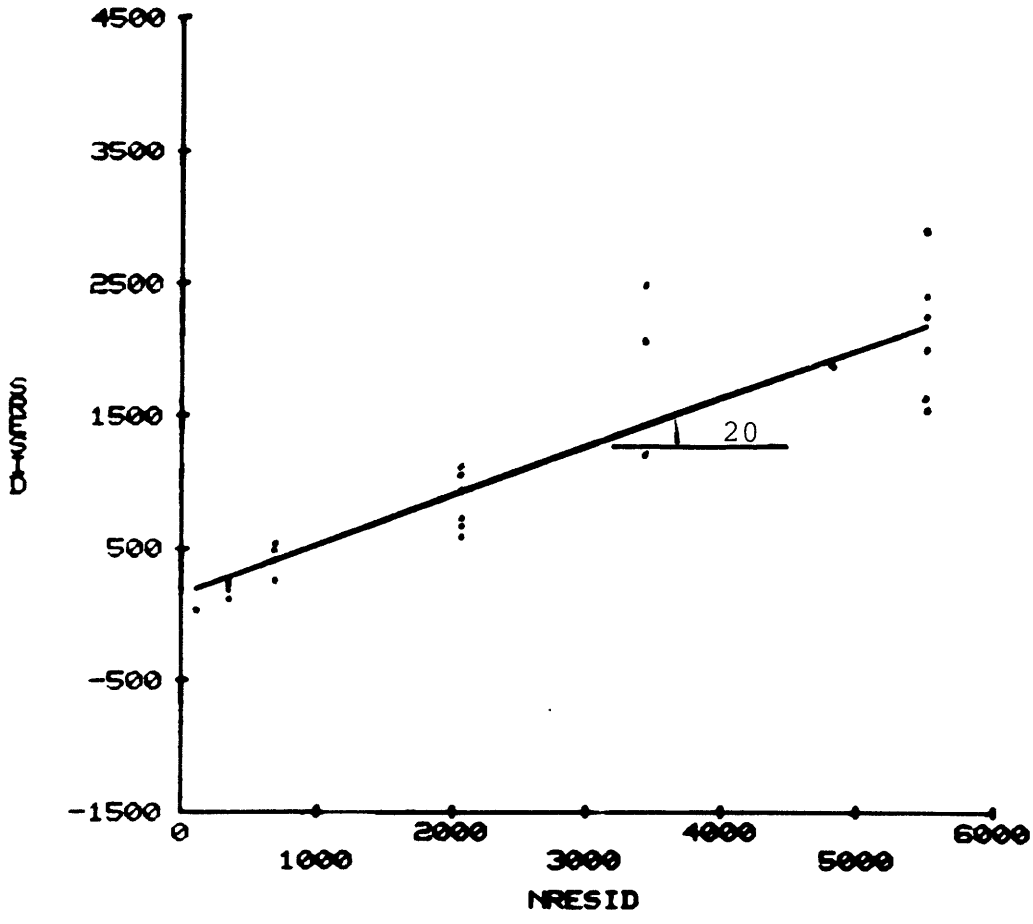

Figure E-27 Residual friction angle conditional on artificial grouted surface

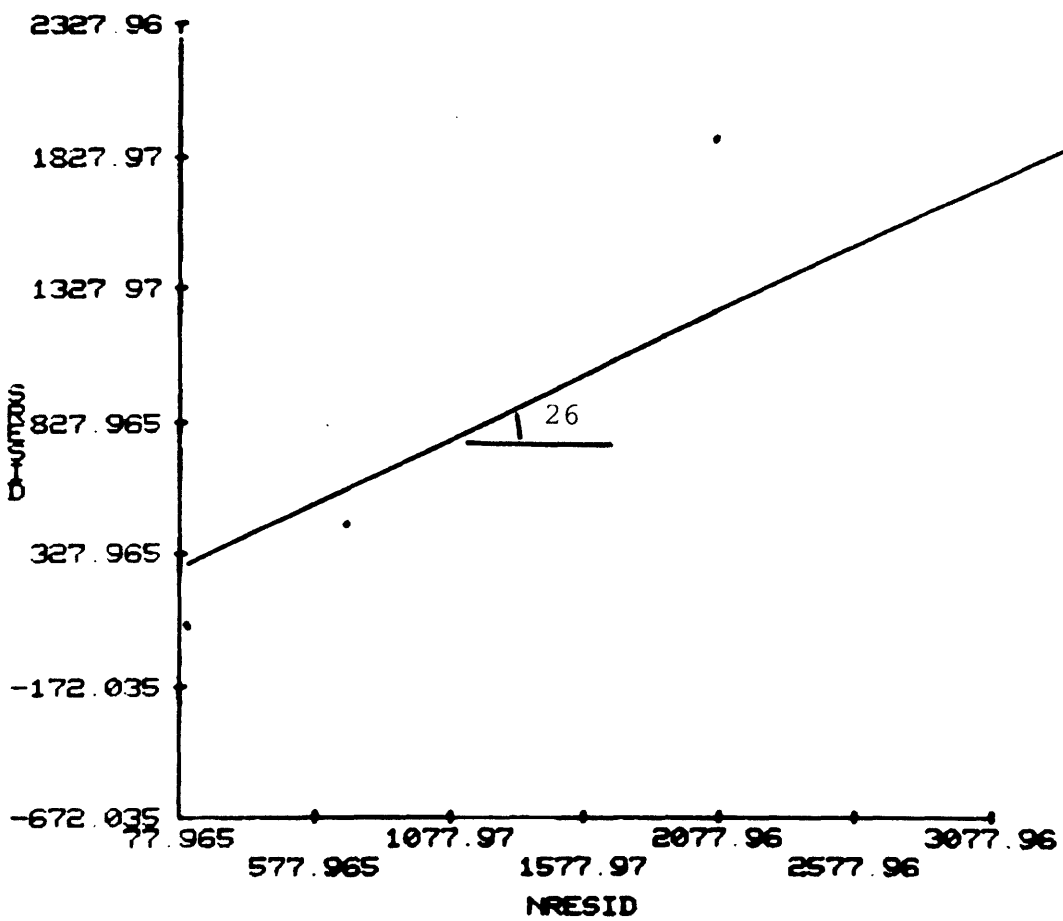

Figure E-28 Residual friction angle conditional on natural grouted joint

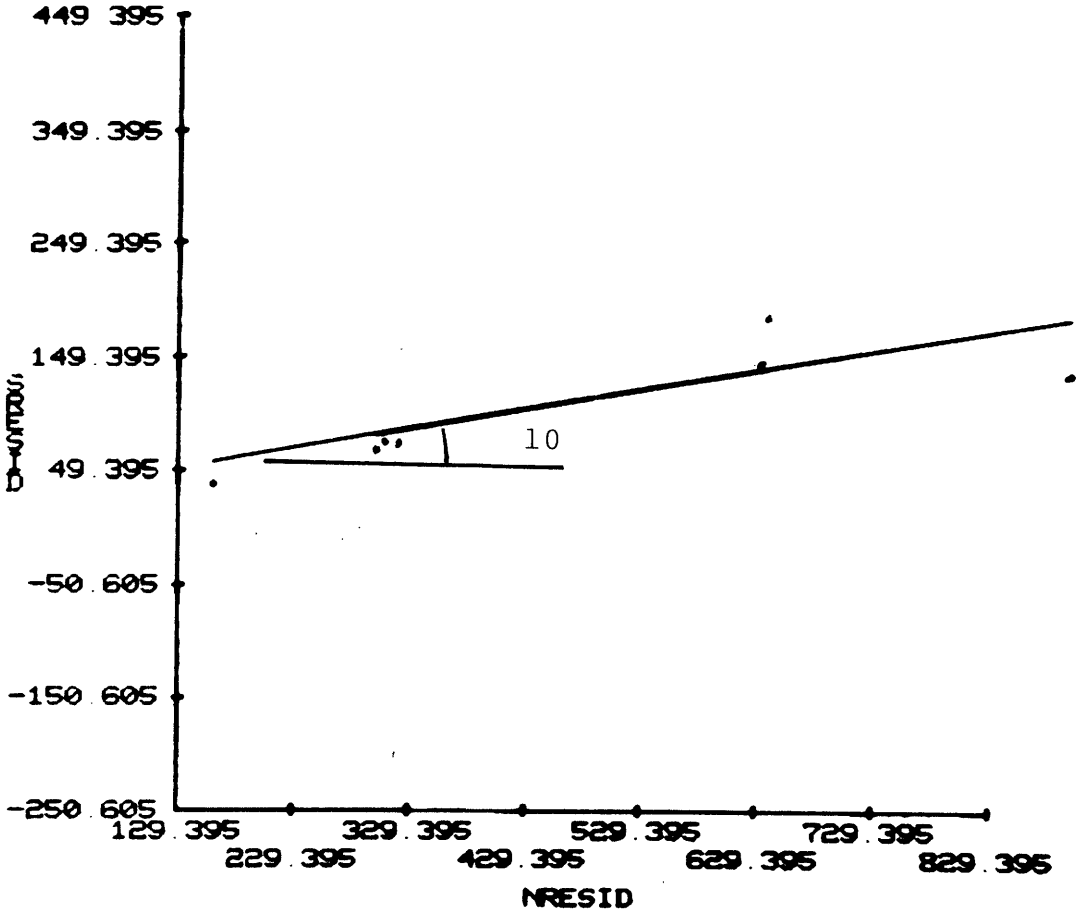

Figure E-29 Residual friction angle conditional on non-oriented lamination

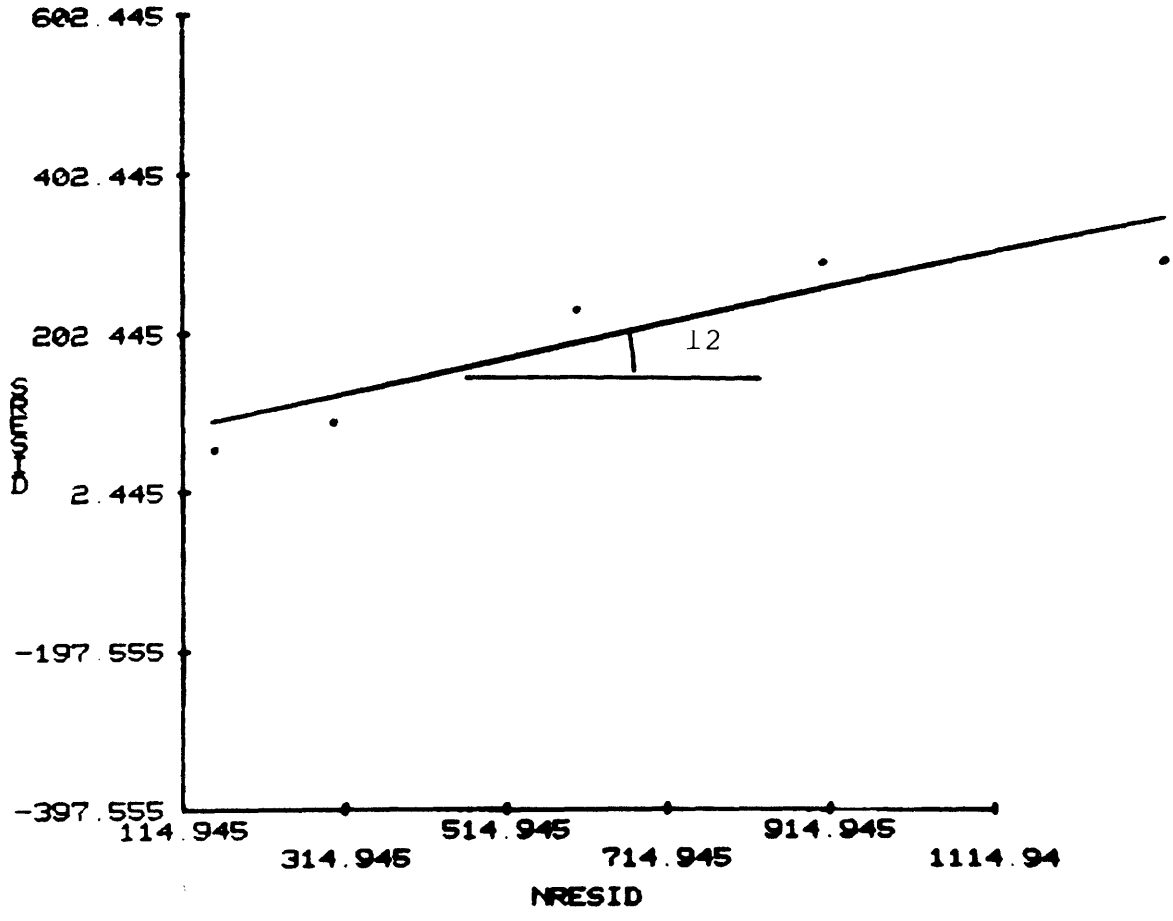

Figure E-30 Residual friction angle conditional on oriented lamination

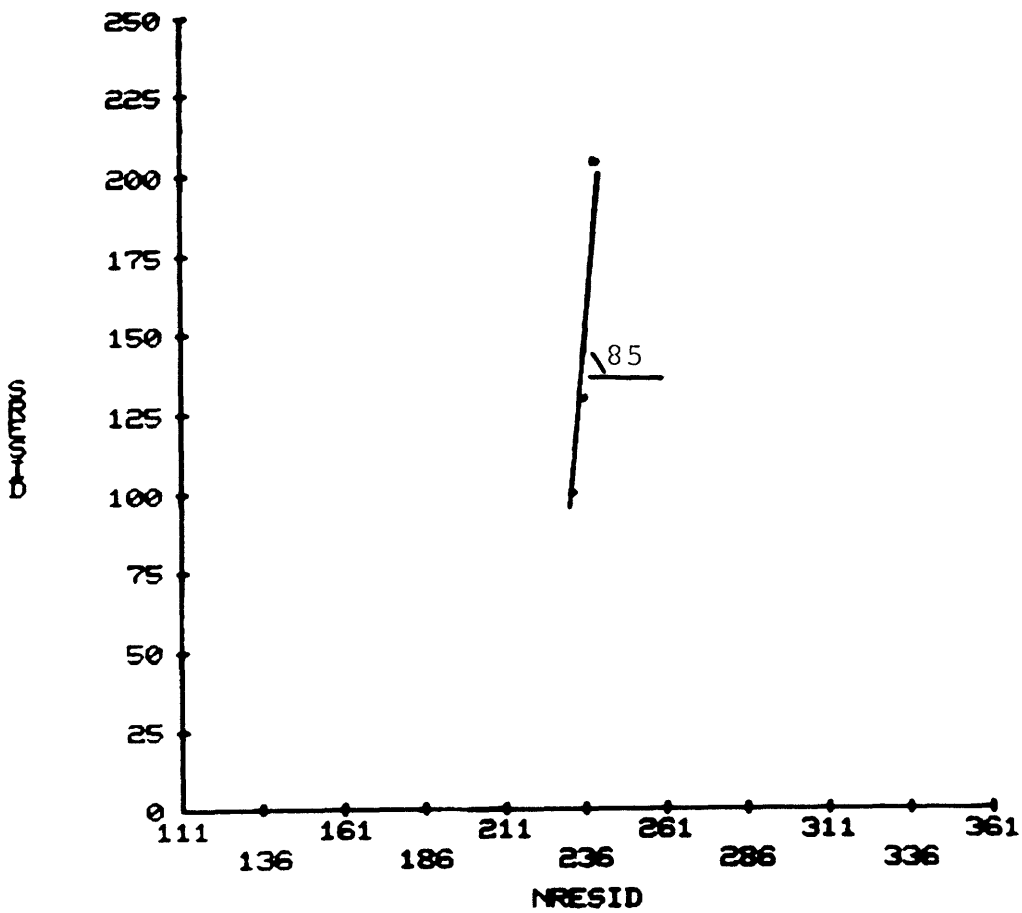

Figure E-31 Residual friction angle conditional on contact between granite and mylonite

APPENDIX F

Histograms of peak and residual friction angles of individual rock types

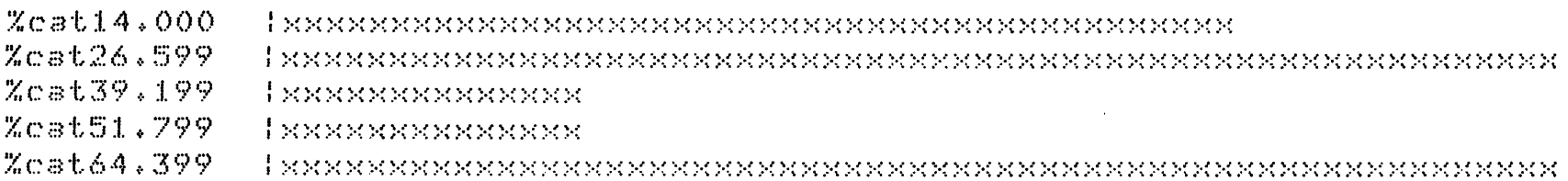

Figure F-1 Histogram of peak friction angle of limestone

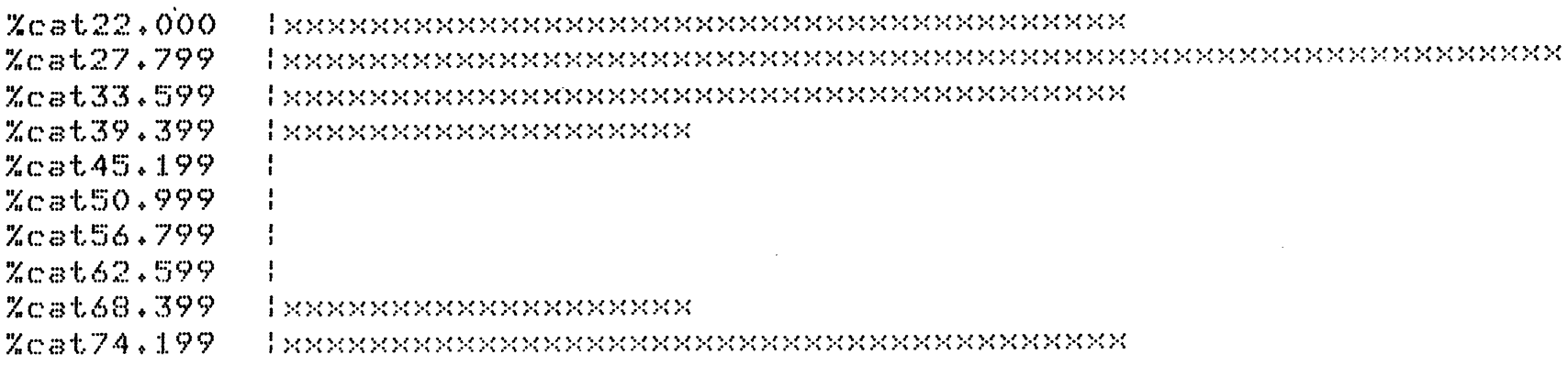

Figure F-2 Histogram of peak friction angle of amphibolite

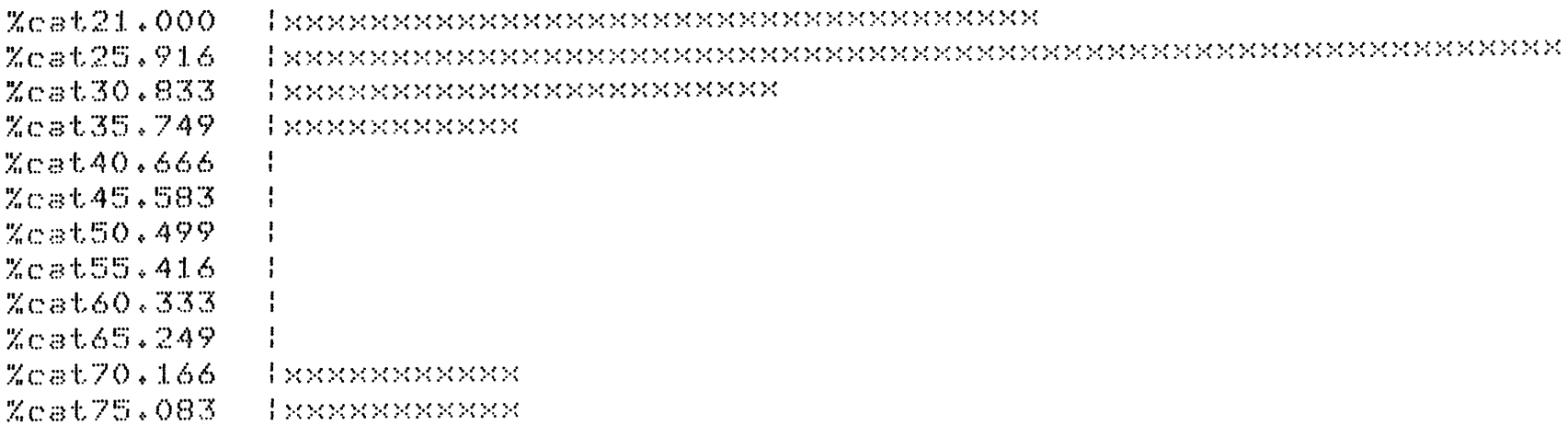

Figure F-3 Histogram of peak friction angle of gneiss

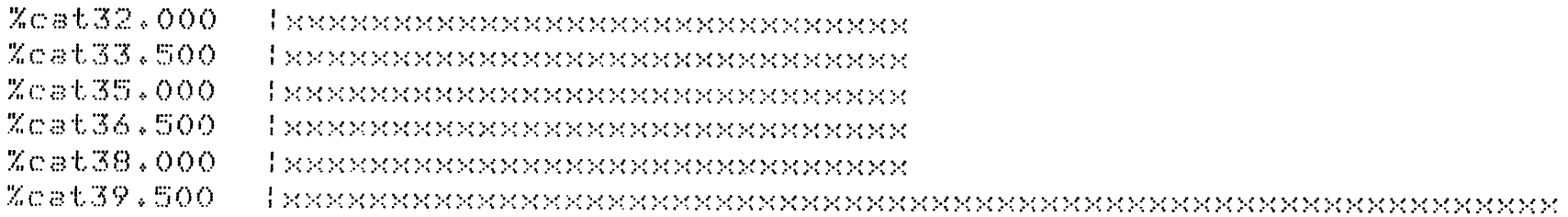

Figure F-4 Histogram of peak friction angle of dacite

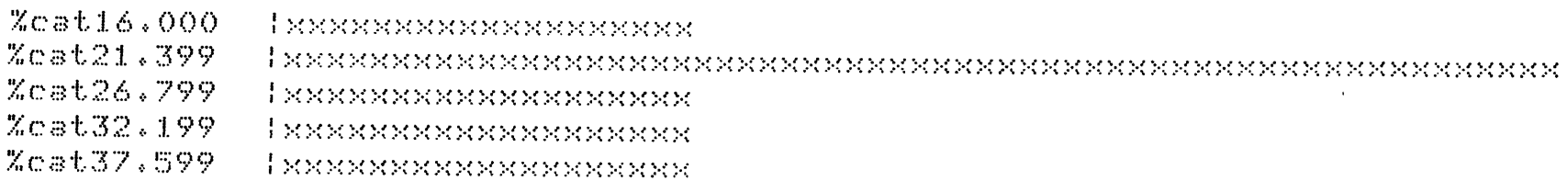

Figure F-5 Histogram of peak friction angle of gneiss(schistose)

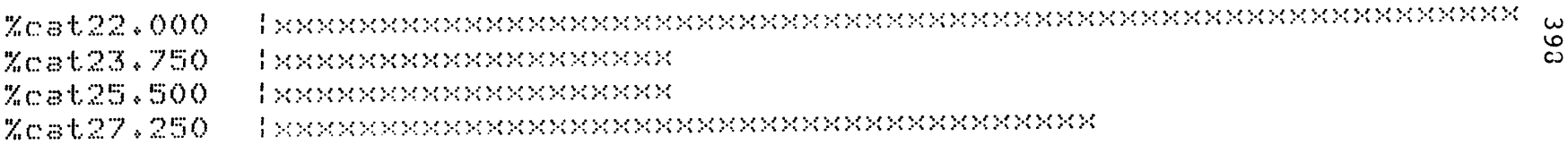

Figure F-6 Histogram of peak friction angle of schist

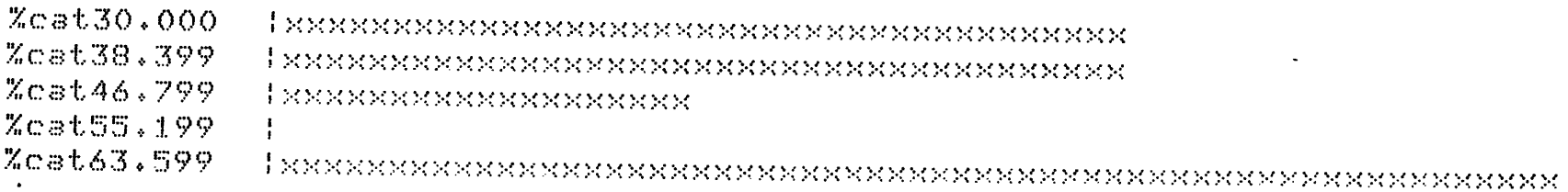

Figure F-7 Histogram of peak friction angle of granite

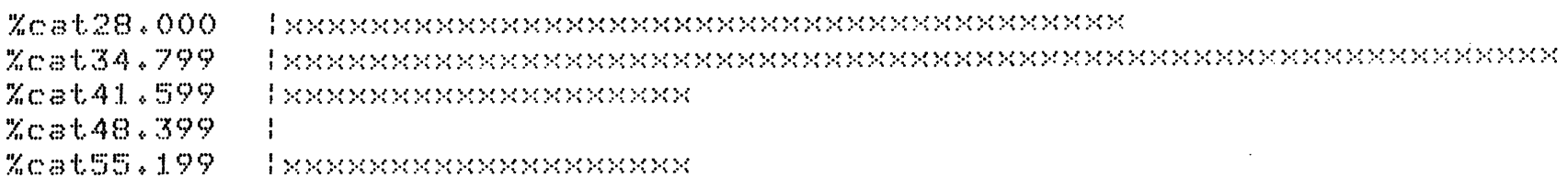

Figure F-8 Histogram of peak friction angle of monzonite

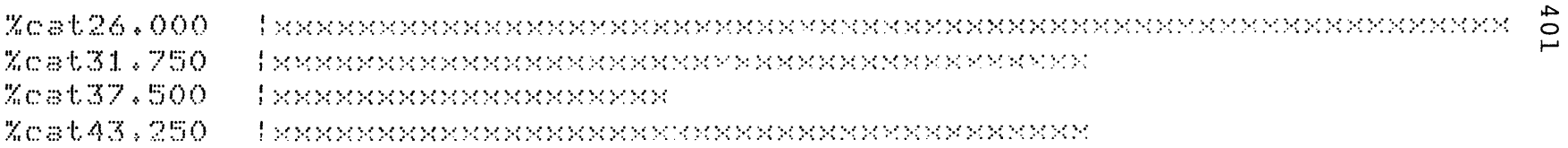

Figure F-9 Histogram of peak friction angle of monzonite(quartz)

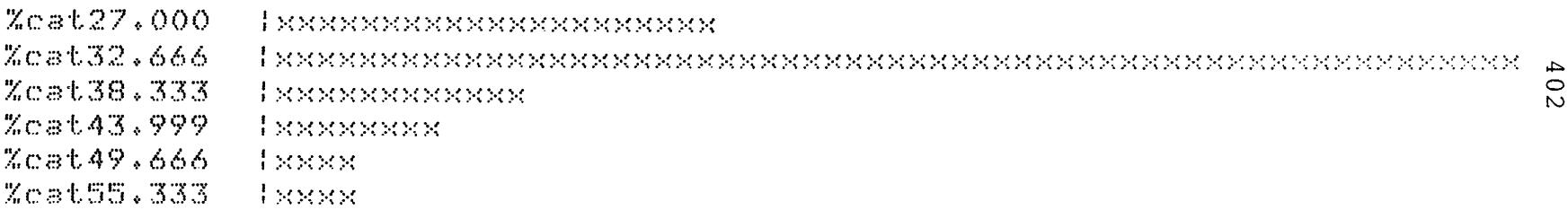

Figure F-10 Histogram of residual friction angle of dolomite

```
%cat19.000  |XX
%cat23.142  |XX
%cat27.285  |XX
%cat31.428  |XXXXXXXXXXXXXXXXXXXXXXXXXXXXXXXXXX
%cat35.571  |XXXXXXXXXXXXXXXXXXXXXXXXXXXXXXXXXXXXXXXXXXXXXXXXXXXXXXXXXXX
%cat39.714  |XXXXXX
%cat43.857  |XXXX
```

Figure F-11   Histogram of residual friction angle of limestone

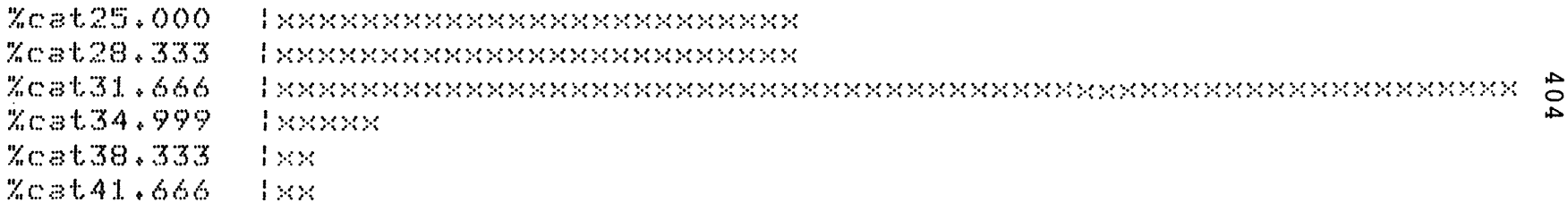

Figure F-12 Histogram of residual friction angle of sandstone

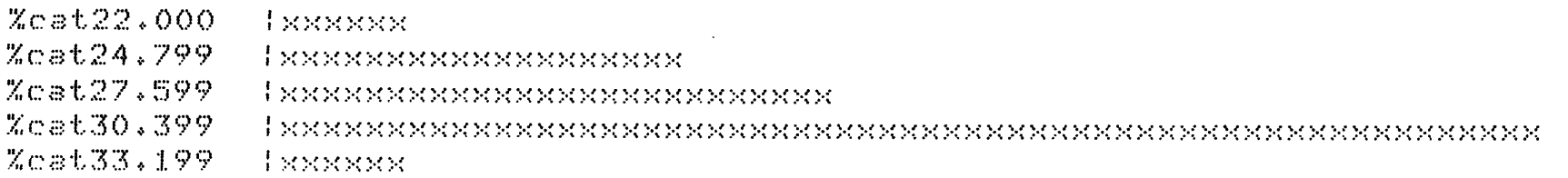

Figure F-13 Histogram of residual friction angle of siltstone

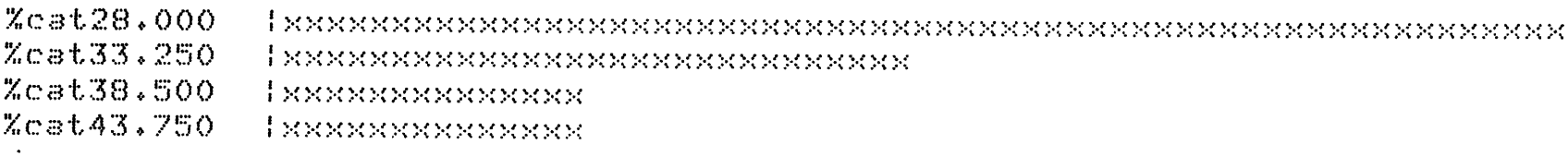

Figure F-14 Histogram of residuals friction angle of marble

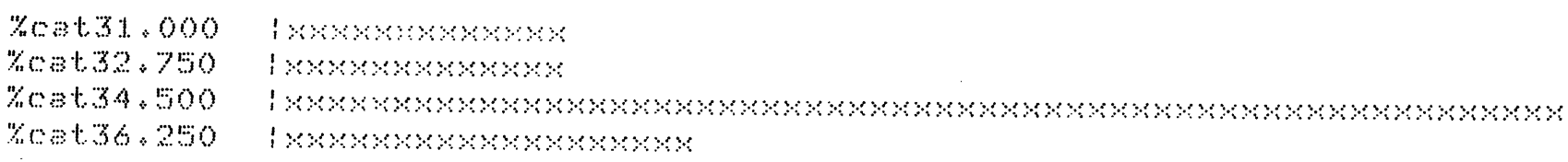

Figure F-15 Histogram of residual friction angle of basalt

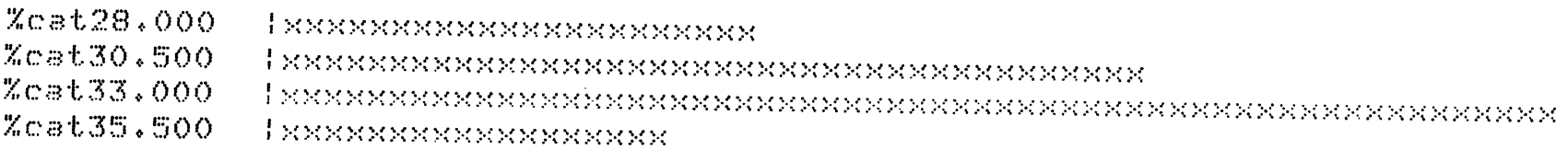

Figure F-16 Histogram of residual friction angle of granite

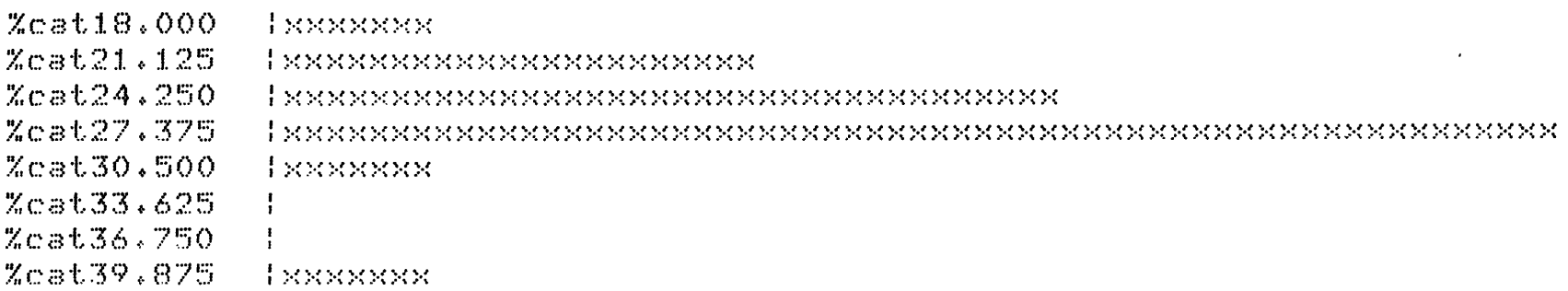

Figure F-17 Histogram of residual friction angle of gneiss(schistose)

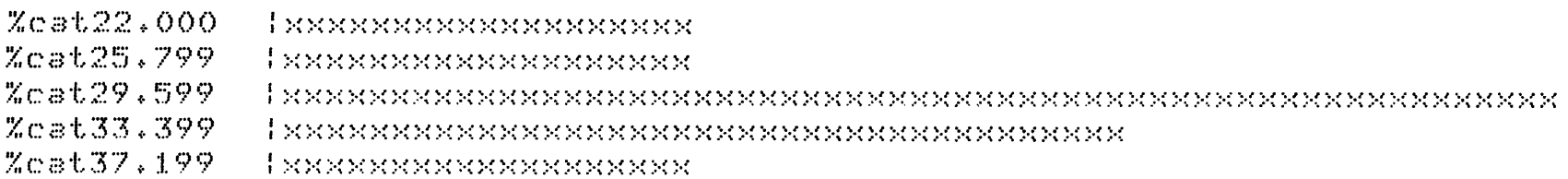

Figure F-18 Histogram of residual friction angle of porphyry

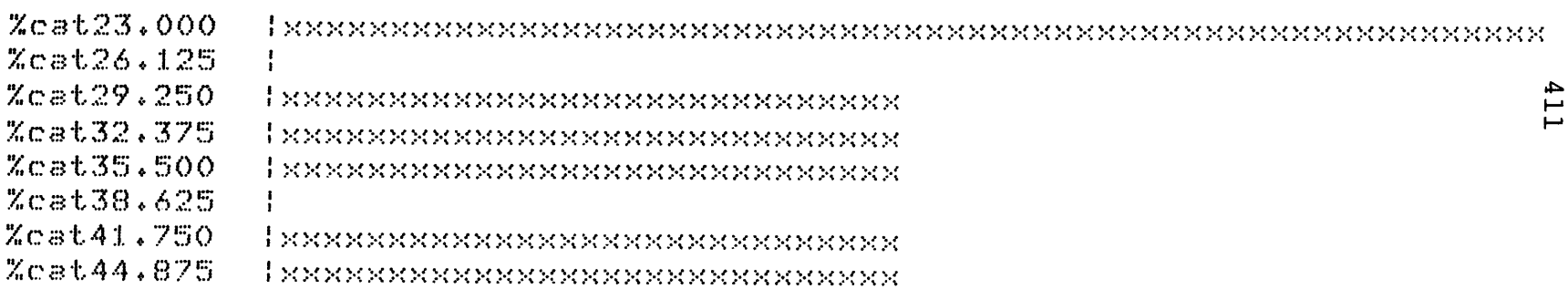

Figure F-19 Histogram of residual friction angle of quarzite